World Journal of Gastroenterology ®

Volume 11 Number 48
December 28, 2005

Supported by NSFC
2005-2006

National Journal Award
2005

ELSEVIER

The WJG Press and Elsevier Inc.

The WJG Press, Apartment 1066 Yishou Garden, 58 North
Langxinzhuang Road, PO Box 2345, Beijing 100023, China
Telephone: +86-(0)10-85381901-1023
Fax: +86-10-85381893
E-mail: wjg@wjgnet.com
http: //www.wjgnet.com

ISSN 1007-9327 CN 14-1219/R Local Post Offices Code No. 82-261

World Journal of Gastroenterology
www.wjgnet.com
Volume 11
Number 48
Dec 28
2005

ISSN 1007-9327
CN 14-1219/R

WJG

World Journal of Gastroenterology ®

Indexed and Abstracted in:
Index Medicus, MEDLINE, PubMed, Chemical Abstracts, EMBASE/Excerpta Medica, Abstracts Journals, Nature Clinical Practice Gastroenterology and Hepatology, CAB Abstracts and Global Health.

Volume 11 Number 48
December 28, 2005

World J Gastroenterol
2005 December 28; 11(48): 7555-7718
Online Submissions
www.wjgnet.com/wjg/index.jsp
www.wjgnet.com
Printed on Acid-free Paper

ELSEVIER

A Weekly Journal of Gastroenterology and Hepatology

ELSEVIER

World Journal of Gastroenterology®

Supported by NSFC 2005-2006

Volume 11 Number 48
December 28, 2005

National Journal Award 2005

Contents

World Journal of Gastroenterology®
Volume 11 **Number** 48 **December 28**, 2005

Contents

World Journal of Gastroenterology®
Volume 11 **Number** 48 **December 28**, 2005

Contents

Editorial Coordinator for this issue: Anitha Kumaran

World Journal of Gastroenterology (*World J Gastroenterol , WJG*), a leading international journal in gastroenterology and hepatology, has an established reputation for publishing first class research on esophageal cancer, gastric cancer, liver cancer, viral hepatitis, colorectal cancer, and *Helicobacter pylori* infection, providing a forum for both clinicians and scientists, and has been indexed and abstracted in Index Medicus, MEDLINE, PubMed, Chemical Abstracts, EMBASE, Abstracts Journals, Nature Clinical Practice Gastroenterology and Hepatology, CAB Abstracts and Global Health. *WJG* is a weekly journal published jointly by The *WJG* Press and Elsevier Inc. The publication date is on 7th, 14th, 21st, and 28th every month. The *WJG* is supported by The National Natural Science Foundation of China, No. 30224801 and No.30424812, which was founded with a name of *China National Journal of New Gastroenterology* on October 1,1995, and renamed as *WJG* on January 25, 1998.

PUBLISHED JOINTLY BY
The WJG Press and Elsevier Inc.

PRINTING GROUP
Printed in Beijing on acid-free paper by Beijing Kexin Printing House

 Print ISSN 1007-9327 CN 14-1219/R.

EDITORIAL OFFICE
Editor: *World Journal of Gastroenterology*,
The WJG Press, Apartment 1066 Yishou Garden, 58 North Langxinzhuang Road, PO Box 2345, Beijing 100023, China
Telephone: +86-(0)10-85381901-1023
Fax: +86-10-85381893
E-mail: wjg@wjgnet.com
http://www.wjgnet.com

Public Relationship Manager
Jing Wang
The WJG Press, Apartment 1066 Yishou Garden, 58 North Langxinzhuang Road, PO Box 2345, Beijing 100023, China
Telephone: +86-(0)10-85381901-1023
Fax: +86-10-8538 1893
E-mail: s.y.guo@wjgnet.com
http://www.wjgnet.com

SUBSCRIPTION INFORMATION
Foreign
Elsevier (Singapore) Pte Ltd, 3 Killiney Road
#08-01, Winsland House I, Singapore 239519
Telephone: +65-6349 0200
Fax: +65-6733 1817
E-mail: r.garcia@elsevier.com
http://asia.elsevierhealth.com
Institutional Rates Print-2005 rates: USD1 500.00
Personal Rates Print-2005 rates: USD700.00

Domestic
Local Post Offices Code No. BM 82-261

Author Reprints
The WJG Press, Apartment 1066 Yishou Garden, 58 North Langxinzhuang Road, PO Box 2345, Beijing 100023, China
Telephone: +86-(0)10-85381901-1023
Fax: +86-10-85381893
E-mail: wjg@wjgnet.com
http://www.wjgnet.com

ADVERTISING
Rosalia Da Carcia
Elsevier Science
Journals Marketing & Society Relations Health Science Asia
3 Killiney Road #08-01, Winsland House 1
Singapore 239519
Telephone: +65-6349 0200
Fax +65- 6733 1817
E-mail: r.garcia@elsevier.com
http://asia.elsevierhealth.com

INSTRUCTIONS TO AUTHORS
Full instructions are available online at http://www.wjgnet.com/wjg/help/instructions.jsp If you do not have web access please contact the editorial office.

PO Box 2345, Beijing 100023, China
www.wjgnet.com
wjg@wjgnet.com

ELSEVIER

World J Gastroenterol 2005;11(48):7555-7559
World Journal of Gastroenterology ISSN 1007-9327

• *GASTRIC CANCER* •

Effect of pseudolaric acid B on gastric cancer cells: Inhibition of proliferation and induction of apoptosis

Ke-Shen Li, Xue-Feng Gu, Ping Li, Yong Zhang, Ya-Shuang Zhao, Zhen-Jiang Yao, Nai-Qiang Qu, Bin-You Wang

Ke-Shen Li, Ya-Shuang Zhao, Zhen-Jiang Yao, Nai-Qiang Qu, Bin-You Wang, Department of Epidemiology, Harbin Medical University, Harbin 150086, Heilongjiang Province, China
Xue-feng Gu, Ping Li, Yong Zhang, Department of Biotechnology and Engineering, Harbin Institute of Technology, Harbin 150001, Heilongjiang Province, China
Supported by the National Natural Science Foundation of China, No. 30371243
Correspondence to: Dr Bin-You Wang, Department of Epidemiology, Harbin Medical University, Harbin 150086, Heilongjiang Province, China. wangby@public.hr.hl.cn
Telephone: +86-451-86842915 Fax: +86-451-86842915
Received: 2005-04-29 Accepted: 2005-07-12

Abstract

AIM: To examine the effect of pseudolaric acid B on the growth of human gastric cancer cell line, AGS, and its possible mechanism of action.

METHODS: Growth inhibition by pseudolaric acid B was analyzed using MTT assay. Apoptotic cells were detected using Hoechst 33258 staining, and confirmed by DNA fragmentation analysis. Western blot was used to detect the expression of apoptosis-regulated gene Bcl-2, caspase 3, and cleavage of poly (ADP-ribose) polymerase-1 (PARP-1).

RESULTS: Pseudolaric acid B inhibited the growth of AGS cells in a time- and dose-dependent manner by arresting the cells at G_2/M phase, which was accompanied with a decrease in the levels of cdc2. AGS cells treated with pseudolaric acid B showed typical characteristics of apoptosis including chromatin condensation and DNA fragmentation. Moreover, treatment of AGS cells with pseudolaric acid B was also associated with decreased levels of the anti-apoptotic protein Bcl-2, activation of caspase-3, and proteolytic cleavage of PARP-1.

CONCLUSION: Pseudolaric acid B can dramatically suppress the AGS cell growth by inducing apoptosis after G_2/M phase arrest. These findings are consistent with the possibility that G_2/M phase arrest is mediated by the down-regulation of cdc2 levels. The data also suggest that pseudolaric acid B can trigger apoptosis by decreasing Bcl-2 levels and activating caspase-3 protease.

Key words: Pseudolaric acid B; Apoptosis; AGS cells

Li KS, Gu XF, Li P, Zhang Y, Qu NQ, Yao ZJ, Zhao YS, Wang BY. Effect of pseudolaric acid B on gastric cancer cells: Inhibition of proliferation and induction of apoptosis. *World J Gastroenterol* 2005; 11(48): 7555-7559
http://www.wjgnet.com/1007-9327/11/7555.asp

INTRODUCTION

Extracts from the root and trunk barks of the Chinese tree *Pseudolarix kaempferi* containing pseudolaric acids are used in traditional Chinese medicine for the treatment of fungal infections[1]. Pseudolaric acid B is the major cell-permeable constituent that displays potent antifungal, antifertil, and anti-angiogenic properties[2-7]. Pseudolaric acid B has cancer chemopreventive activity and inhibits *in vitro* growth of a number of human cancer cell lines, including KB, A-549, HCT-8, P-388, and L-1210 tumor cells[8]. However, no information is at present available on the chemopreventive potentials of pseudolaric acid B on gastric carcinoma.

Apoptosis, a mode of cell death, is a physiologic event that regulates cell number and eliminates damaged cells. Recent studies implicated that apoptosis is a common mechanism through by which chemotherapeutic agents exert their cytotoxicity and that the efficiency of anti-tumor agents is related to the intrinsic propensity of target tumor cells to respond to these agents by apoptosis[9]. *In vitro* studies have shown that pseudolaric acid B treatment can induce apoptosis in human HeLa cells via the activation of c-Jun N-terminal kinase and caspase-3[10]. In order to exploit the chemotherapeutic potentials of pseudolaric acid B on gastric carcinoma, we treated human gastric cancer cell line, AGS, with pseudolaric acid B to examine its antiproliferative effect and apoptosis-inducing activity. Our results suggest that pseudolaric acid B can inhibit the growth of AGS human gastric cancer cells by inducing cell cycle arrest, which correlates with a marked decrease in the expression of key G_2/M-regulating proteins cdc2. The data also suggest that pseudolaric acid B can trigger apoptosis by decreasing Bcl-2 levels and activating caspase-3 protease. Pseudolaric acid B may be used as an effective chemotherapeutic agent against gastric carcinoma.

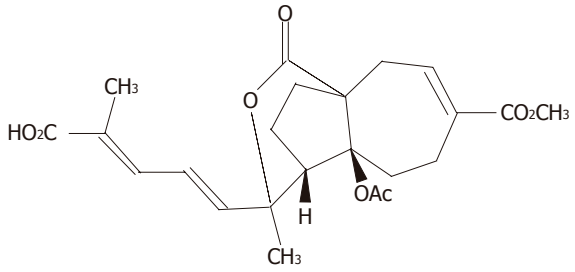

Figure 1 Chemical structure of pseudolaric acid B ($C_{23}H_{28}O_8$, MW = 432.5).

MATERIALS AND METHODS

Materials

Gastric adenocarcinoma cell line (AGS) was obtained from the Shanghai Institute of Cancer Research. Pseudolaric acid B was purchased from Calbiochem Company (La Jolla, CA, USA). The chemical structure of pseudolaric acid B is shown in Figure 1. Hoechst 33258, RNase A, proteinase K and MTT [3'-(4,5-dimethylthiazol-2-yl)-2,5-diphenyl tetrazolium bromide] were purchased from Sigma Chemical Company (St. Louis, USA). Monoclonal antibodies to Cdc2, Bcl-2, caspase-3, and PARP were purchased from Santa Cruz Biotechnology Incorporation (Santa Cruz, CA, USA). PVDF membrane was obtained from Bio-Rad (CA, USA).

Cell culture and treatment with pseudolaric acid B

AGS was maintained in RPMI 1640 supplemented with 10% fetal calf serum, penicillin G (100 kU/L) and kanamycin (0.1 g/L) in a humidified atmosphere of 95% air and 50 mL/L CO_2 at 37 °C. The medium was changed twice a week. A 10 mmol/L stock solution of pseudolaric acid B was prepared in DMSO and stored at -20 °C. Final concentrations of pseudolaric acid B used for different experiments were prepared by diluting the stock with DMEM.

Assay for cell proliferation inhibition (MTT assay)

AGS cells were subcultured in a 96-well plate with 1×10^4 cells/well in 100 μL medium. After 24-h incubation at 37 °C, the medium in each well was discarded and replaced with a fresh medium at various concentrations of pseudolaric acid B in a final volume of 200 μL. Cells were incubated at 37 °C for 6, 12, 24, and 48 h, respectively. At the end of incubation, 50 μL of PBS solution containing 1 mg/mL MTT was added to each well, and further incubated for 4 h. The cell suspension was then centrifuged at 720 r/min for 5 min, and the formazan precipitate in each well was dissolved in 100 μL DMSO for optical density reading at 570 nm.

Flow cytometric analysis

Control and pseudolaric acid B-treated cells were harvested by trypsinization (0.5% trypsin/2.6 mmol/L EDTA), washed twice with ice-cold PBS and fixed in methanol/PBS (9/1, v/v) at 22 °C for at least 30 min. The fixed cells were then washed twice with ice-cold PBS and stained with 50 mg/mL of propidium iodide in the presence of 25 mg/mL of RNase A. Cell cycle phase distribution was determined by flow cytometry (FACSCalibur, Becton Dickinson) and the data were analyzed by multicycle DNA content and cell cycle analysis software (Modfit LT 2.0).

Nuclear damage observed with Hoechst 33258 staining

After being treated with pseudolaric acid B, AGS cells were collected by centrifugation at 1 000 r/min for 5 min and washed twice with PBS. The cells were fixed with 3.7% paraformaldehyde at room temperature for 2 h, centrifuged and washed with PBS, stained with Hoechst 33258 (167 μmol/L) for 30 min at 37 °C. At the end of incubation, the cells were washed and resuspended in PBS for the observation of nuclear morphology under fluorescence microscope (Nikon, Japan).

DNA fragmentation analysis

After being treated with pseudolaric acid B for 12, 24, or 48 h, the cells were harvested and incubated in 0.2 mL lysis buffer containing 10 mmol/L Tris–HCl (pH 8.0), 1 mmol/L EDTA, 1% sodium dodecyl sulfate, and 100 μg/mL proteinase K at 37 °C for 24 h. RNase A (0.5 mg/mL) was added and further incubated at 55 °C for 18 h. Genomic DNA was extracted by phenol/chloroform, precipitated with ethanol and dissolved in TE. Integrity of the DNA was analyzed by electrophoresis on 1.7% agarose gels with ethidium bromide staining.

Western blot analysis

After being treated with pseudolaric acid B for the indicated periods, the cells were washed with PBS and lysed in a buffer containing 20 mmol/L Tris–HCl, 150 mmol/L NaCl, 1% Triton X-100, 1.5 mmol/L $MgCl_2$, 1 mmol/L $NaVO_3$, 100 mmol/L NaF, 10% glycerol, 1 mmol/L EGTA, 10 mmol/L sodium pyrophosphate, and 1 mmol/L phenylmethylsulfonyl fluoride, pH 7.5. Cell lysates were centrifuged at 12 000 *g* for 125 min at 4 °C. The protein concentrations were determined using Bio-Rad protein assay (Bio-Rad Laboratories, USA). After SDS-PAGE, proteins were transferred to PVDF membranes for 2 h at 80 mA. Blots were probed with mouse monoclonal antihuman anti-Bcl-2, anti-caspase-3, and rabbit monoclonal anti-human anti-PARP antibodies. Immunoreactivity was detected using either an anti-mouse (Santa Cruz) or an anti-rabbit (Amersham) peroxidase-conjugated secondary immunoglobulin G antibody followed by enhanced chemiluminescence (ECL, Amersham). Experiments were repeated at least thrice.

Statistical analysis

Data analysis was performed using Student's *t* test. $P<0.05$ was considered statistically significant.

RESULTS

Pseudolaric acid B inhibited AGS cell proliferation

The effects of pseudolaric acid B on cell growth in AGS cell lines were tested. As shown in Figure 2, pseudolaric

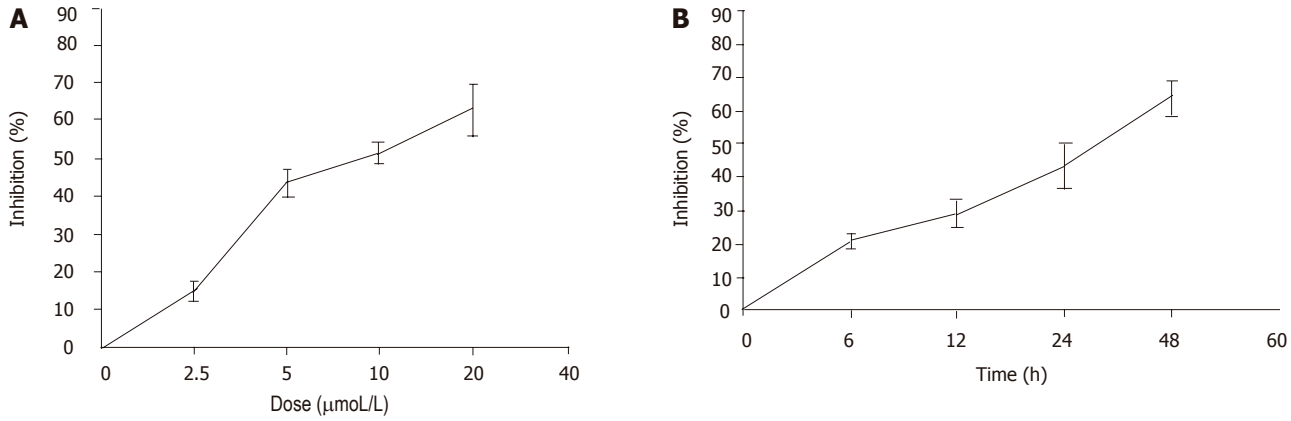

Figure 2 Dose- and time-dependent inhibitory effect of pseudolaric acid B on growth of AGS cells. **A:** AGS cells were treated with various doses of pseudolaric acid B for 24 h; **B**: AGS cells were treated with 5 μmol/L pseudolaric acid B for various time periods. Each point indicates mean±SD of three independent experiments.

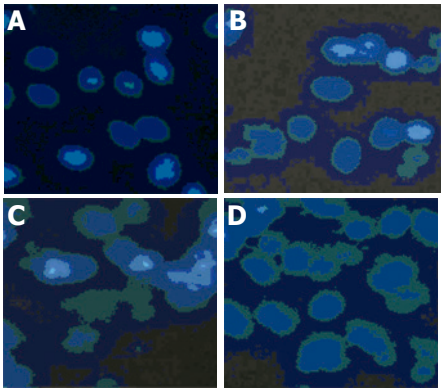

Figure 3 Time-dependent effect of 5 μmol/L pseudolaric acid B on morphological changes in AGS cells. **A:** 0; **B:** 12; **C:** 24; **D:** 48 h.

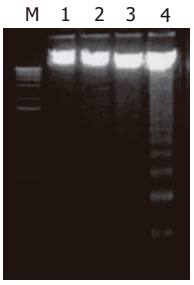

Figure 4 Time-dependent effect of 5 μmol/L pseudolaric acid B on internucleosomal DNA fragmentation in AGS cells. M: Marker; lane 1: 0 h; lane 2: 12 h; lane 3: 24 h; lane 4: 48 h.

acid B inhibited AGS cell proliferation in a time- and dose-dependent manner. Only a minor inhibition of AGS cell growth was observed in the presence of 2.5 μmol/L pseudolaric acid B. Growth was inhibited by more than 40% in cells exposed to 5 μmol/L pseudolaric acid B after 24 h. A concentration of 5 μmol/L pseudolaric acid B was used in all further experiments.

Changes of cell cycle detected by flow cytometric analysis

We further investigated the effects of pseudolaric acid B on the progression of AGS cells throughout the cell cycle. AGS cells were cultured for various lengths of time in the presence or absence of 5 μmol/L pseudolaric acid B and analyzed by flow cytometry. As shown in Table 1, pseudolaric acid B induced a time-dependent accumulation of AGS cells in the G_2/M phase accompanied with a decreased percentage of cells in S and G_0/G_1 phases of the cell cycle.

Table 1 Time course analysis of the cell cycle in pseudolaric acid B-treated cells

Time (h)	G_0/G_1 (%)	S (%)	G_2/M (%)
0 (control)	56.23	33.42	10.35
12	50.64	31.49	17.87[a]
24	43.56	30.81	25.63[b]
48	33.54	28.45	38.01[b]

[a]P<0.05 , [b]P<0.01 *vs* control. Results were representative of three independent experiments.

Morphological changes and DNA fragmentation in AGS cells

To determine the mode of cell death induced by pseudolaric acid B, morphologic alterations in the AGS cells after treatment with 5 μmol/L pseudolaric acid B for up to 48 h were examined under fluorescent microscope after Hoechst 33342 staining. In the control group, AGS cells were round in shape and stained homogeneously. After 24 h of treatment with pseudolaric acid B, blebbing nuclei and granular apoptotic bodies appeared (Figure 3). We analyzed chromosomal DNA from control and pseudolaric acid B-treated cells. Compared to DNA from control cells, treatment with pseudolaric acid B induced apoptosis, as shown by the formation of distinct internucleosomal DNA fragments (Figure 4). The intensity of the DNA banding ladder progressively increased in a time-dependent manner. An early DNA fragmentation was observed after 12 h of incubation with pseudolaric acid B.

Down-regulation of cdc2 levels in response to pseudolaric acid B

Because pseudolaric acid B arrested AGS cells at the

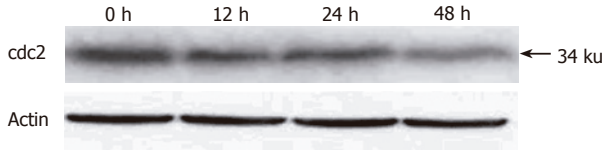

Figure 5 cdc2 levels in AGS cells down-regulated by pseudolaric acid B treatment.

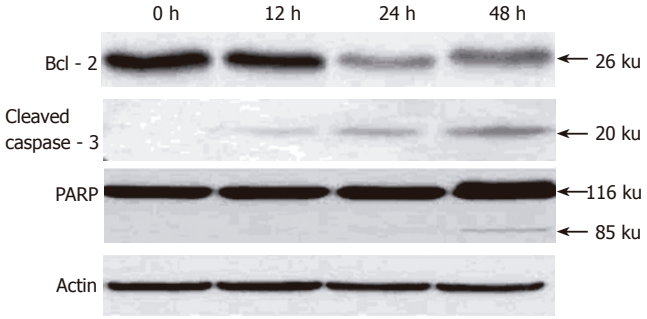

Figure 6 Time-dependent down-regulation of Bcl-2, activation of caspase-3, and PARP cleavage in cultured AGS cells induced by pseudolaric acid B.

G_2/M phase, it was of interest to test the effect of this compound on cdc2 levels, which plays an important role in the G_2 to M progression of the cell cycle. A time-dependent reduction in cdc2 protein level was evident in cells treated with pseudolaric acid B for 48 h (Figure 5).

Down-regulation of Bcl-2, activation of caspase-3, and cleavage of PARP induced by pseudolaric acid B treatment

To investigate the mechanism underlying apoptosis induced by pseudolaric acid B, we tested the effect of this compound on Bcl-2 level, an important regulator of apoptotic signaling pathways[19]. As shown in Figure 5, Western blot analysis revealed that pseudolaric acid B treatment decreased Bcl-2 protein levels. We also found that pseudolaric acid B induced proteolytic processing of caspase-3 in a time-dependent manner. Activation of caspase-3 led to the cleavage of a number of proteins, including PARP-1. Pseudolaric acid B treatment also induced a time-dependent proteolytic cleavage of PARP-1, with concomitant accumulation of the 85 ku and the disappearance of the full-size 116 ku molecule (Figure 6). These findings suggested that pseudolaric acid B could induce apoptosis by down-regulating Bcl-2 and activating caspase-3.

DISCUSSION

Gastric cancer is the second most common cause of cancer death worldwide. Though extensive clinical research has been carried out with numerous combinations of cytotoxic agents, the overall prognosis of advanced gastric cancer still remains poor[11]. Thus, there is considerable interest in identifying more effective cancer chemotherapeutic agents. Pseudolaric acid B, the diterpenoid isolated from the root and trunk bark of *Pseudolarix kaempferi* Gordon tree, has been recently reported to exert an antiproliferative effect on several cancer cell lines[10,12,13]. Since there is no report about its effect on human gastric cancer, we treated human gastric cancer cell line, AGS, with pseudolaric acid B to examine its antiproliferative effect and apoptosis-inducting activity. MTT assay showed that pseudolaric acid B could significantly inhibit growth of AGS cells in a dose- and time-dependent manner. In addition, flow cytometric analysis further revealed that pseudolaric acid B induced a time-dependent accumulation of AGS cells in the G_2/M phase which was coupled with a parallel depletion of the S and G_0/G_1 phase. To further analyze the molecular mechanism by which pseudolaric acid B causes cell cycle arrest, we evaluated cdc2 protein levels. The cdc2/cyclin B complex is one of the major regulatory elements governing the G_2 to M progression[14]. Cdc2 is activated by phosphorylation of and binding to cyclin B, which is synthesized during the S and G_2 phases of the cell cycle[15]. In our study, pseudolaric acid B treatment reduced cdc2 protein levels, suggesting that cell cycle arrest is mediated by the limitation of the supply of cdc2 to cdc2/cyclin B complex formation, which is an essential step in regulating passage into mitosis.

Cell cycle checkpoints are activated to ensure orderly and timely completion of critical events such as DNA replication and chromosome segregation. It is widely accepted that activation of checkpoints in response to DNA damage leads to cell cycle arrest, but in the case of severe damage, the cell cycle arrest leads to cell apoptosis[16,17]. The effects of pseudolaric acid B are compatible with this model. Our present investigation clearly demonstrated that pseudolaric acid B could induce apoptosis of AGS cells, which appears to account for its growth inhibitory and antiproliferative activities. The induction of cell apoptosis was accompanied with characteristic morphological changes, such as chromatin condensation and nuclear fragmentation. Internucleosomal DNA fragmentation as determined by agarose gel electrophoresis also supported the progress of apoptosis of pseudolaric acid B-treated AGS cells.

Apoptosis is a closely regulated process, involving changes in the expression of distinct genes. One of the major genes involved in regulating apoptosis is the protooncogene Bcl-2 encoding a 26-ku mitochondria-associated protein[18,19]. Bcl-2 functions as an intracellular apoptosis suppressor by controlling the mitochondrial membrane permeability with its pro-apoptotic relative, Bax. Diminished expression of Bcl-2 has been observed in certain types of cells undergoing apoptosis[20]. In line with these findings, pseudolaric acid B treatment decreased Bcl-2 protein levels in AGS cells, suggesting that down-regulation of Bcl-2 may be required for AGS cell apoptosis induced by pseudolaric acid B, thus increasing mitochondrial permeability and cytochrome *c* release, which initiates the progress of apoptosis. In addition, involvement of caspase 3 was also examined in pseudolaric acid B-induced AGS cell apoptosis. Caspase-3, a cysteine protease that exists as an inactive proenzyme in cells, is activated by proteolytic processing at internal aspartic

acid residue when cells receive an apoptosis-inducing signal[21]. Activation of caspase-3 leads to degradation and inactivation of key cellular proteins such as DNA repair, signaling, and structural proteins[22,23]. Among these, the cleavage of PARP represents a well described response of cells undergoing caspase-mediated apoptosis[24]. AGS cells treated with pseudolaric acid B exhibited time-dependent activation of caspase-3 and proteolytic cleavage of PARP, indicating that apoptosis of AGS cells is induced by pseudolaric acid B and caspase cascade process.

In conclusion, naturally occurring diterpenoid, pseudolaric acid B, is a potent inhibitor of the growth of human gastric cancer cells. Growth inhibition of the compound is highly related to the induction of cell cycle arrest and apoptosis.

REFERENCES

1 **Li E,** Clark AM, Hufford CD. Antifungal evaluation of pseudolaric acid B, a major constituent of Pseudolarix kaempferi. *J Nat Prod* 1995; **58:** 57-67

2 **Yang SP,** Dong L, Wang Y, Wu Y, Yue JM. Antifungal diterpenoids of Pseudolarix kaempferi, and their structure-activity relationship study. *Bioorg Med Chem* 2003; **11:** 4577-4584

3 **Wang WC,** Lu RF, Zhao SX, Zhu YZ. [Antifertility effect of pseudolaric acid B] *Zhongguo Yao Li Xue Bao* 1982; **3:** 188-192

4 **Zhang YL,** Lu RZ, Yan AL. [Inhibition of ova fertilizability by pseudolaric acid B in hamster] *Zhongguo Yao Li Xue Bao* 1990; **11:** 60-62

5 **Wang WC**, Gu ZP, Koo A, Chen WS. Effects of pseudolaric acid B on blood flows of endometrium and myometrium in pregnant rats. *Zhongguo Yao Li Xue Bao* 1991; **12:** 423-425

6 **Tan WF,** Zhang XW, Li MH, Yue JM, Chen Y, Lin LP, Ding J. Pseudolarix acid B inhibits angiogenesis by antagonizing the vascular endothelial growth factor-mediated anti-apoptotic effect. *Eur J Pharmacol* 2004; **499:** 219-228

7 **Li MH,** Miao ZH, Tan WF, Yue JM, Zhang C, Lin LP, Zhang XW, Ding J. Pseudolaric acid B inhibits angiogenesis and reduces hypoxia-inducible factor 1alpha by promoting proteasome-mediated degradation. *Clin Cancer Res* 2004; **10:** 8266-8274

8 **Pan DJ,** Li ZL, Hu CQ, Chen K, Chang JJ, Lee KH. The cytotoxic principles of Pseudolarix kaempferi: pseudolaric acid-A and -B and related derivatives. *Planta Med* 1990; **56:** 383-385

9 **Kim R,** Tanabe K, Uchida Y, Emi M, Inoue H, Toge T. Current status of the molecular mechanisms of anticancer drug-induced apoptosis. The contribution of molecular-level analysis to cancer chemotherapy. *Cancer Chemother Pharmacol* 2002; **50:** 343-352

10 **Gong X,** Wang M, Wu Z, Tashiro S, Onodera S, Ikejima T. Pseudolaric acid B induces apoptosis via activation of c-Jun N-terminal kinase and caspase-3 in HeLa cells. *Exp Mol Med* 2004; **36:** 551-556

11 **Parkin DM,** Pisani P, Ferlay J. Estimates of the worldwide incidence of 25 major cancers in 1990. *Int J Cancer* 1999; **80:** 827-841

12 **Gong XF,** Wang MW, Tashiro S, Onodera S, Ikejima T. Pseudolaric acid B induces human melanoma A375-S2 cell apoptosis in vitro. *Zhongguo Zhong Yao Za Zhi* 2005; **30:** 55-57

13 **Gong XF,** Wang MW, Tashiro S, Onodera S, Ikejima T. Pseudolaric acid B induces apoptosis through p53 and Bax/Bcl-2 pathways in human melanoma A375-S2 cells. *Arch Pharm Res* 2005; **28:** 68-72

14 **Nurse P.** Universal control mechanism regulating onset of M-phase. *Nature* 1990; **344:** 503-508

15 F**ang F,** Newport JW. Evidence that the G1-S and G2-M transitions are controlled by different cdc2 proteins in higher eukaryotes. *Cell* 1991; **66:** 731-742

16 **Orren DK**, Petersen LN, Bohr VA. Persistent DNA damage inhibits S-phase and G2 progression, and results in apoptosis. *Mol Biol Cell* 1997; **8:** 1129-1142

17 **Smith ML**, Fornace AJ Jr. Mammalian DNA damage-inducible genes associated with growth arrest and apoptosis. *Mutat Res* 1996; **340:** 109-124

18 **Adams JM**, Cory S. The Bcl-2 protein family: arbiters of cell survival. *Science* 1998; **281:** 1322-1326

19 **Burlacu A**. Regulation of apoptosis by Bcl-2 family proteins. *J Cell Mol Med* 2003; **7:** 249-257

20 **Oltvai ZN,** Milliman CL, Korsmeyer SJ. Bcl-2 heterodimerizes in vivo with a conserved homolog, Bax, that accelerates programmed cell death. *Cell* 1993; **74:** 609-619

21 **Nicholson DW**. Caspase structure, proteolytic substrates, and function during apoptotic cell death. *Cell Death Differ* 1999; **6:** 1028-1042

22 **Wolf BB,** Schuler M, Echeverri F, Green DR. Caspase-3 is the primary activator of apoptotic DNA fragmentation via DNA fragmentation factor-45/inhibitor of caspase-activated DNase inactivation. *J Biol Chem* 1999; **274:** 30651-30656

23 **Enari M**, Sakahira H, Yokoyama H, Okawa K, Iwamatsu A, Nagata S. A caspase-activated DNase that degrades DNA during apoptosis, and its inhibitor ICAD. *Nature* 1998; **391:** 43-50

24 **Kaufmann SH,** Desnoyers S, Ottaviano Y, Davidson NE, Poirier GG. Specific proteolytic cleavage of poly(ADP-ribose) polymerase: an early marker of chemotherapy-induced apoptosis. *Cancer Res* 1993; **53:** 3976-3985

Science Editors Wang XL and Guo SY **Language Editor** Elsevier HK

PO Box 2345, Beijing 100023, China
www.wjgnet.com
wjg@wjgnet.com

ELSEVIER

World J Gastroenterol 2005;11(48):7560-7563
World Journal of Gastroenterology ISSN 1007-9327

Effects of six months losartan administration on liver fibrosis in chronic hepatitis C patients: A pilot study

Silvia Sookoian, María Alejandra Fernández, Gustavo Castaño

Silvia Sookoian, Cardiología Molecular, Instituto de Investigaciones Médicas A. Lanari, University of Buenos Aires, Buenos Aires, Argentina
María Alejandra Fernández, Cathedra of Physiopathology, School of Pharmacy and Biochemistry, University of Buenos Aires, Buenos Aires, Argentina
Gustavo Castaño, Gastroenterology Section, Hospital José M. Penna. & Consejo de Investigación, Government of the City of Buenos Aires, Buenos Aires, Argentina
Correspondence to: Silvia Sookoian, MD, PhD, Instituto de Investigaciones Médicas, A Lanari. Cardiología Molecular, Combatientes de Malvinas 3150, Buenos Aires 1427, Argentina. ssookoian@intramed.net
Telephone: +54-11-45148701-04 Fax: +54-11-45238947
Received: 2005-03-28 Accepted: 2005-04-30

Abstract

AIM: To evaluate the safety and efficacy of chronic administration of losartan on hepatic fibrosis in chronic hepatitis C patients.

METHODS: Fourteen patients with chronic hepatitis C non-responders (n = 10), with contraindications (n = 2) or lack of compliance (n = 2) to interferon plus ribavirin therapy and liver fibrosis were enrolled. Liver and renal function test, clinical evaluation, and liver biopsies were performed at baseline and after losartan administration at a dose of 50 mg/d during the 6 mo. The control group composed of nine patients with the same inclusion criteria and paired liver biopsies (interval 6-14 mo). Histological activity index (HAI) with fibrosis stage was assessed under blind conditions by means of Ishak's score. Subendothelial fibrosis was evaluated by digital image analyses.

RESULTS: The changes in the fibrosis stage were significantly different between losartan group (decrease of 0.5±1.3) and controls (increase of 0.89±1.27; P<0.03). In the treated patients, a decrease in fibrosis stage was observed in 7/14 patients *vs* 1/9 control patients (P<0.04). A decrease in sub-endothelial fibrosis was observed in the losartan group. No differences were found in HAI after losartan administration. Acute and chronic decreases in systolic arterial pressures (P<0.05) were observed after the losartan administration, without changes in mean arterial pressure or renal function.

CONCLUSION: Chronic AT-II type 1 receptor (AT1R) blockade may reduce liver fibrosis in patients with chronic hepatitis C.

Key words: Hepatitis C; Liver fibrosis; Losartan; AT1R; Chronic liver disease; Angiotensin II

Sookoian S, Fernández MA, Castaño G. Effects of six months losartan administration on liver fibrosis in chronic hepatitis C patients: A pilot study. *World J Gastroenterol* 2005; 11(48):7560-7563
http://www.wjgnet.com/1007-9327/11/7560.asp

INTRODUCTION

The hepatitis C virus (HCV) is one of the leading causes of chronic hepatitis, liver cirrhosis, and hepatocellular carcinoma. Although major progress has been made in the treatment of chronic HCV infection, the current treatment regimens, including Peginterferons in association with ribavirin, appear capable of eradicating HCV in only 30-50% of the treated patients[1]. In this scenario, alternative medical strategies to reduce hepatic fibrosis are under investigation, since drugs with antifibrotic effects may be an option in the treatment of patients with chronic hepatitis C who do not respond to the standard antiviral therapy.

Much evidence suggests that hepatic stellate cells (HSCs) play important roles in the pathogenesis of liver fibrosis, since they were shown to undergo a transformation during the injury that is termed as activation[2]. Furthermore, *in vitro* studies have shown that angiotensin II (ANGII) is a mitogenic protein for a number of cell types and between them the HSCs undergo a MAPK-dependent pathway. In these cells, ANGII upregulates the transforming growth factor beta 1 expression *via* AT-II type 1 receptor (AT1R) *in vitro*. Additionally, proliferation of activated HSCs was found in chronic liver diseases taking part in the development of liver fibrosis[3]. The fact that the actions of ANGII are mediated through AT1R is related to the therapeutic interventions, since AT1R can be completely blocked by losartan, a specific ANGII receptor antagonist. For instance, ANGII stimulated mRNA expression of TGF-beta and fibronectin can be reversed by saralasin and losartan, a nonselective and specific antagonists for AT1R receptors, respectively[4]. Lastly, in animal

Table 1 Presenting features of the studied patients

	Treated group (n = 14)		Untreated group (n = 9)	
	Baseline	Post losartan	Baseline	Second biopsy
Females/males	4/14		1/8	
Age (yr)	49.6±13		51.4±9.6	
Hematocrit	45.2±3.59	44.1±3.85	48.8±4.66	47.8±4.15
White blood cells (K/mm^3)	6.66±1.41	6.71±1.67	5.98±0.95	5.78±1.19
Platelets (K/mm^3)	227±80.8	246±90.7[b]	223±68	209±78.4
Glucose (g/L)	0.99±0.38	1±0.29	0.95±0.1	1.01±0.06
Blood urea nitrogen (g/L)	0.31±0.06	0.32±0.06	0.28±0.07	0.25±0.04
Creatinine (mg/dL)	0.88±0.07	0.95±0.11	0.99±0.07	0.96±0.12
Total bilirubin (mg/dL)	1±0.53	1.08±0.63	1.35±0.58	1.19±0.58
Alkaline phosphatase (IU/L)	253±118	269±68.9	264±93.4	349±134
Alanine aminotransferase (IU/L)	90.5±66	91.9±47.6	264±167[a]	169±124
Aspartate aminotransferase (IU/L)	65.3±41	67±40.9	161±97.8[a]	130±84.5
Cholesterol (mg/dL)	157±36.4	161±42.6	166±38.1	169±39.2
Albumin (g/dL)	4.12±0.32	4.43±0.24[b]	4.32±0.56	4.32±0.5
Globulins (g/dL)	3.64±0.53	3.77±0.45	3.74±0.63	3.91±0.63
G glutamyl transpeptidase (IU/ L)	63.2±47.9	74.5±53.7	194±178[a]	217±214
Prothrombin time (%)	103±19.3	106±17.4	107±8.19	97±9.83
KPTT (s)	32.6±3.38	39.6±18.7	37.8±6.99	34.5±2.38

Results are expressed as mean±SD. [a]P<0.05 in comparison with baseline measurements in the treated group. [b]P<0.01 in comparison with baseline measurements in the treated group.

models of fibrosis, chronic administration of losartan prevented the development of hepatic fibrosis and portal hypertension[3,5,6].

The purpose of this study was to investigate the safety and efficacy of chronic administration of losartan on hepatic fibrosis in chronic hepatitis C patients.

MATERIALS AND METHODS

Fourteen outpatients (10 men and 4 women) aged 49.6±13 years, with both chronic hepatitis C infection and biopsy proven liver fibrosis, were enrolled in a pilot study.

Ten patients were previous non-responders to a 12-mo combined therapy of interferon and ribavirin, two had contraindications and two showed lack of compliance to the mentioned treatment.

In the control group, nine sex- and age-matched untreated chronic hepatitis C patients with the same inclusion and exclusion criteria who underwent paired liver biopsies (interval 6-14 mo) were included. No patient had a previous history of autoimmune disease, alcohol intake, current intravenous drug use or other chronic liver diseases. All were negative for hepatitis B surface antigen and anti-human immunodeficiency virus. Their clinical characteristics are shown in Table 1.

Written informed consent was obtained from all patients, and the local ethical committee approved the study protocol, based on the 1975 Declaration of Helsinki.

Systolic, diastolic, and mean arterial blood pressures were taken by an automatic sphygmomanometer (VR 12, Electronics for Medicine). Liver and renal function tests and liver biopsies were performed at baseline and after the losartan administration at a dose of 50 mg/d during 6 mo (Losacor, kindly donated by Roemmers, Buenos Aires, Argentina). During the losartan administration, patients did not receive any other medication. Clinical and biochemical follow-ups were assessed and blood pressure was monitored during the first hours, at 1 wk and monthly after the losartan administration.

Liver histology

Ultrasound-assisted liver biopsy was performed using modified Menghini needle of 1.4 mm diameter (Hepafix, Braun, Germany). Liver specimens, previously fixed in formalin, were stained with hematoxylin and eosin, Masson trichrome, silver impregnation for reticular fibers, Perls blue and Prussian blue, and examined by a liver pathologist who was blinded to the clinical data of the patients. Histological activity index (HAI) and fibrosis stage were assessed by means of Ishak's score.

Digital image analysis

Selected areas for fibrosis quantification included the hepatic lobule but without the portal, periportal, septal, and pericentral vein areas. Histological slides stained for reticular fibers were evaluated for sub-endothelial deposit of types III collagen[7] by a digital image analysis. A previous study of our group using this method showed a high correlation between image analysis and fibrosis stage[8]. Images were obtained using a video camera (Sony CCD Iris camera) attached to a light microscope and converted to digital format on a computer by CAP VIEW Leadtek Winfast 2000 PAL device (Leadtek Research Inc.). Standardization of the images was performed with software Adobe Photoshop 7.0 (Adobe Systems Inc.). The quantification of the selected color areas of the digitalized, standardized, and processed images was performed in a 256 gray tones scale with software Scion image for Windows (2000 Scion Corporation), and expressed in pixels/inch^2.

Statistical analysis

Results were expressed as mean±SD. Differences between

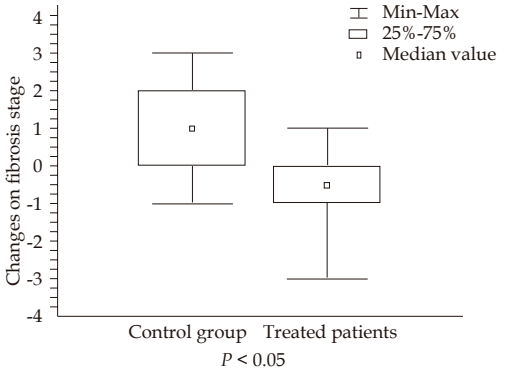

Figure 1 Changes in fibrosis stage in control group and treated patients.

Table 2 Histological changes in liver biopsies

	Treated group (n = 14)		Untreated group (n = 9)	
	Baseline	Post losartan	Baseline	Second biopsy
Histology activity index	8.08±2.56	8.54±1.51	7.0±2.12	7.6±2.3
Fibrosis stage	3.29±1.44	2.64±1.22	2.67±2	3.56±2.13
Sub-endothelial fibrosis (pixels/inch^2)	2.48±1.04	1.00±0.53[a]	1.65±0.43	1.55±0.27

Results are expressed as mean±SD. [a]P<0.01 *vs* baseline.

Table 3 Changes in arterial pressure after losartan administration

	Baseline	3 h	1 mo
Systolic arterial pressure (mmHg)	134±22.7	125±17.4[a]	124±18.1[a]
Diastolic arterial pressure (mmHg)	80.8±14	81.2±14.2	82.5±13.7
Mean arterial pressure (mmHg)	98.4±16.3	95.7±14.8	100±15.8

Results are expressed as mean±SD. [a]P<0.05 *vs* baseline.

Table 4 Orthostatic variations in arterial pressure after losartan administration

	Supine position	Sitting position	
Baseline (10:00 am)			
Systolic arterial pressure (mmHg)	132.7±22.1	132.2±16.8	
Diastolic arterial pressure (mmHg)	80.7±13.4	87.8±8.93	(P<0.0001)
Mean arterial pressure (mmHg)	98±15.7	102.6±11.1	(P<0.01)
Three hours post losartan			
Systolic arterial pressure (mmHg)	124. 7±17.4	127.3±14.9	
Diastolic arterial pressure (mmHg)	81.1±14.2	83.5±11.1	
Mean arterial pressure (mmHg)	95. 7±14.8	98.1±12	

proportions were analyzed by χ^2 test and the Fisher's exact test. Differences between the groups were analyzed by paired and unpaired Student's t- test, by Mann–Whitney U or Wilcoxon matched paired tests, according to the distribution and the scale of measurement. Spearman's ρ coefficient was utilized for correlations. Significance was established at P<0.05.

RESULTS

Effects of losartan

The changes in fibrosis stage were significantly different between losartan group and controls (a decrease of 0.64± 1.3 *vs* an increase of 0.89±1.27, respectively; P<0.02) (Table 2). In the treated patients, a decrease in fibrosis stage was observed in 7/14 patients *vs* 1/9 control patients (P<0.04). Three of the seven patients showed a reduction of two or more points in fibrosis stage. No differences were observed in HAI after losartan administration. Sub-endothelial fibrosis evaluated by image analysis of lobular areas was significantly reduced after losartan administration, without changes in the control group (Table 2 and Figure 1). A significant correlation was found between fibrosis stage and sub-endothelial fibrosis (Spearman's ρ 0.36, P<0.03). A significant increase was observed in albumin level and platelet counts in the treated patients.

Additionally, no significant differences were found in any clinical or biochemical parameters between responders and non-responders to losartan, except that patients who responded to losartan had higher baseline serum alkaline phosphatase than non-responders (309±132 IU/L *vs* 194± 25 IU/L, P = 0.009).

Safety

Acute (3 h) and chronic (1 mo) decreases in systolic arterial pressures in supine position, and a loss of physiologic increase in diastolic pressures from supine to sitting position were observed after losartan administration (Tables 3 and 4). Nevertheless, only one treated patient had a single episode of mild orthostatic hypotension. No differences were observed in renal function tests after losartan administration.

DISCUSSION

It is well known that, at present, the most effective therapy for treating hepatic fibrosis is the removal of the causative agent. In chronic hepatitis C, this goal may be achieved with standard antiviral therapy in a great proportion of patients. Nevertheless, non-responder patients may obtain a benefit from the emerging antifibrotic therapies.

Since renin-angiotensin system blockers are promising drugs in reducing the accumulation of scar tissue in experimental models of chronic liver injury, we performed a pilot study with chronic losartan administration in 14 chronic HCV non-responder patients or with contraindications to interferon plus ribavirin regimen.

Liver biopsy is considered the gold-standard method for the assessment of liver fibrosis[9]. In our study, paired biopsy specimens taken at baseline and at the study completion were compared by means of the standard Ishak score and by an image analysis method for quantification of liver fibrosis. Histopathological scores showed that losartan had an inhibitory effect on the progression of hepatic fibrosis stage. Subendothelial fibrosis evaluated by image analysis of lobular areas was significantly decreased after losartan administration in comparison with the untreated control group.

Regarding biochemical evaluation of the patients, liver

and renal function tests, and blood cells content did not change in either group, except for the platelet content and the albumin concentration in the losartan treated patients, who evidenced a significant improvement in comparison with the control group. Additionally, serum HCV-RNA levels had no change after the study in both groups (data not shown).

Several authors, including us, demonstrated in randomized controlled trials that losartan had equal or greater effects in lowering portal pressure than propranolol, without serious adverse effects[10-13]. The effects of losartan on portal pressure may be explained by the effect of the blockade of AT1R on the contractility of hepatic activated stellate cells, by means of a decrease in intrahepatic vascular resistance. In addition to these events, antifibrotic effects of AT1 blockade may have actions on the structural component of portal hypertension.

With regard to the safety of this treatment, no serious side effects were noted during the study. Nonetheless, an overall decrease was observed in systolic arterial pressures in supine position.

The pathogenesis of HCV-induced liver fibrosis is poorly understood due to the lack of a rodent model of persistent HCV infection. However, since liver fibrosis is the excessive accumulation of extracellular matrix proteins including collagen, it is rational to assume that any chronic damage of the liver may lead to the same final outcome.

Experimental and human studies have consistently shown that ANGII is involved in the development of fibrosis in cardiac and renal tissues in conditions associated with chronic inflammation. Besides, *in vivo* studies have shown that ACE inhibitors and AT1 receptors antagonists can limit the progression of cardiac, renal and pulmonary fibrosis.

In human beings, their efficacy has been tested in a few preliminary pilot studies in patients with NASH[14] and in chronic HCV infection[15], suggesting that renin–angiotensin blocking agents may have beneficial effects on fibrosis progression.

In conclusion, this study shows that administration of an AT1R antagonist may improve liver scores of fibrosis stage in patients with chronic hepatitis C, suggesting that losartan may provide an effective new approach to the treatment of non-responders to antiviral therapy. However, a randomized, controlled trial seems to be necessary in order to confirm the benefit of AT1R blocking for hepatic fibrosis in chronic HCV infection. Lastly, one may speculate that the combination treatment of the clinically used Peginterferons and AT1R blocker may provide a new strategy for anti-liver fibrosis treatment in HCV.

REFERENCES

1 NIH Consensus Statement on Management of Hepatitis C: 2002. *NIH Consens State Sci Statements 2002*; **19**: 1-46

2 **Bataller R**, Sancho-Bru P, Gines P, Lora JM, Al-Garawi A, Sole M, Colmenero J, Nicolas JM, Jimenez W, Weich N, Gutierrez-Ramos JC, Arroyo V, Rodes J. Activated human hepatic stellate cells express the renin-angiotensin system and synthesize angiotensin II. *Gastroenterology* 2003; **125**: 117-125

3 **Yoshiji H**, Kuriyama S, Yoshii J, Ikenaka Y, Noguchi R, Nakatani T, Tsujinoue H,Fukui H. Angiotensin-II type 1 receptor interaction is a major regulator for liver fibrosis development in rats. *Hepatology* 2001; **34**: 745-750

4 **Leung PS**, Suen PM, Ip SP, Yip CK, Chen G, Lai PB. Expression and localization of AT1 receptors in hepatic Kupffer cells: its potential role in regulating a fibrogenic response. *Regul Pept* 2003; **116**: 61-69

5 **Croquet V**, Moal F, Veal N, Wang J, Oberti F, Roux J, Vuillemin E, Gallois Y, Douay O, Chappard D, Cales P. Hemodynamic and antifibrotic effects of losartan in rats with liver fibrosis and/or portal hypertension. *J Hepatol* 2002; **37**: 773-780

6 **Yoshiji H**, Noguchi R, Kuriyama S, Yoshii J, Ikenaka Y. Combination of interferon and angiotensin-converting enzyme inhibitor, perindopril, suppresses liver carcinogenesis and angiogenesis in mice. *Oncol Rep* 2005; **13**: 491-495

7 **Ushiki T**. Collagen fibers, reticular fibers and elastic fibers. A comprehensive understanding from a morphological viewpoint. *Arch Histol Cytol* 2002; **65**: 109-126

8 **Fernadez A**, Castano G, Sookoian S, Lemberg A, Amante M, Parisi C,Perazzo J. A new image analysis method for quantification of liver fibrosis. *J Hepatol* 2003; **38**: 216-Abs .

9 Afdhal NH, Nunes D. Evaluation of liver fibrosis: a concise review. *Am J Gastroenterol* 2004; **99**: 1160-1174

10 **Schneider AW**, Kalk JF,Klein CP. Effect of losartan, an angiotensin II receptor antagonist, on portal pressure in cirrhosis. *Hepatology* 1999; **29**: 334-339

11 **Castano G**, Viudez P, Frider B, Sookoian S. Discussion on randomized comparison of long-term losartan versus propranolol in lowering portal pressure in cirrhosis. *Gastroenterology* 2002; **122**: 1544-1545

12 **Sookoian S,** Castano G, Garcia SI, Viudez P, Gonzalez C, Pirola CJ. A1166C angiotensin II type 1 receptor gene polymorphism may predict hemodynamic response to losartan in patients with cirrhosis and portal hypertension. *Am J Gastroenterol* 2005; **100**: 636-642

13 **De BK**, Bandyopadhyay K, Das TK, Das D, Biswas PK, Majumdar D, Mandal SK, Ray S, Dasgupta S. Portal pressure response to losartan compared with propranolol in patients with cirrhosis. *Am J Gastroenterol* 2003; **98**: 1371-1376

14 **Yokohama S**, Yoneda M, Haneda M, Okamoto S, Okada M, Aso K, Hasegawa T, Tokusashi Y, Miyokawa N, Nakamura K. Therapeutic efficacy of an angiotensin II receptor antagonist in patients with nonalcoholic steatohepatitis. *Hepatology* 2004; **40**: 1222-1225

15 **Terui Y**, Saito T, Watanabe H, Togashi H, Kawata S, Kamada Y, Sakuta S. Effect of angiotensin receptor antagonist on liver fibrosis in early stages of chronic hepatitis C. *Hepatology* 2002; **36**: 1022

Science Editor Ma JY and Guo SY **Language Editor** Elsevier HK

PO Box 2345, Beijing 100023, China
www.wjgnet.com
wjg@wjgnet.com

ELSEVIER

World J Gastroenterol 2005;11(48):7564-7568
World Journal of Gastroenterology ISSN 1007-9327

Tumor necrosis factor-α-induced protein 1 and immunity to hepatitis B virus

Marie C Lin, Nikki P Lee, Ning Zheng, Pai-Hao Yang, Oscar G Wong, Hsiang-Fu Kung, Chee-Kin Hui, John M Luk, George Ka-Kit Lau

Marie C Lin, Pai-Hao Yang, Oscar G Wong, Hsiang-Fu Kung, Institute of Molecular Biology, The University of Hong Kong, Hong Kong SAR, China
Nikki P Lee, John M Luk, Department of Surgery, The University of Hong Kong, Hong Kong SAR, China
Nikki P Lee, John M Luk, George Ka-Kit Lau, Center for the Study of Liver Diseases, The University of Hong Kong, Hong Kong SAR, China
Ning Zheng, Chee-Kin Hui, George Ka-Kit Lau, Department of Medicine, The University of Hong Kong, Hong Kong SAR, China
Correspondence to: George KK Lau, M.D. , Department of Medicine Rm 1838, Queen Mary Hospital 102 Pokfulum Road, Hong Kong SAR, China. gkklau@netvigator.com
Fax: +852-28184030
Received: 2004-10-06 Accepted: 2005-01-05

Abstract

AIM: To compare the gene expression profile in a pair of HBV-infected twins.

METHODS: The gene expression profile was compared in a pair of HBV-infected twins.

RESULTS: The twins displayed different disease outcomes. One acquired natural immunity against HBV, whereas the other became a chronic HBV carrier. Eighty-eight and forty-six genes were found to be up- or down-regulated in their PBMCs, respectively. Tumor necrosis factor-alpha-induced protein 1 (TNF-αIP1) that expressed at a higher level in the HBV-immune twins was identified and four pairs of siblings with HBV immunity by RT-PCR. However, upon HBV core antigen stimulation, TNF-αIP1 was downregulated in PBMCs from subjects with immunity, whereas it was slightly upregulated in HBV carriers. Bioinformatics analysis revealed a K+ channel tetramerization domain in TNF-αIP1 that shares a significant homology with some human, mouse, and *C elegan* proteins.

CONCLUSION: TNF-αIP1 may play a role in the innate immunity against HBV.

Key words: TNF-α; HBV; Immunity

Lin MC, Lee NP, Zheng N, Yang PH, Wong OG, Kung HF, Hui CK, Luk JM, Lau GKK. Tumor necrosis factor-α-induced protein 1 and immunity to hepatitis B virus. *World J Gastroenterol* 2005;11(48):7564-7568
http://www.wjgnet.com/1007-9327/11/7564.asp

INTRODUCTION

Though substantial advances have been made in understanding of the pathogenesis of hepatitis B virus (HBV), HBV infection remains a global health threat with currently more than 350 million carriers and causes about one million deaths worldwide. The situation is particularly severe in high-endemic areas like southeastern Asia. For instance, a study of 16 334 subjects in 1978-1979 in Hong Kong suggested that 43% of the local population have evidence of past infection and 10% are HBs Ag carriers[1].

The major spread mode of HBV in most high endemic areas, such as Hong Kong and China, is perinatal transmission, which accounts for 40%-50% of chronic HBV infection[2,3]. The reason for the preponderance of perinatal transmission among Orientals is at least in part related to the high prevalence of HBV infection among the Asian carriers of reproductive age[2]. Though the incidence of perinatal transmission is high in China, not all siblings in the same family with HBV-infected mothers remain persistently infected with HBV as some acquired natural immunity against the virus. We are among the first group to demonstrate that the use of HLA-matched donor marrow from siblings with natural immunity could enable serological clearance of HBV in their HBsAg positive recipient siblings[4-7]. This indicates that the transfer of certain molecules from the donor's immune system is sufficient to confer the recipient immunity against HBV. However, the identities of these molecules are unknown.

In this study, Affymetrix cDNA mircroarray was employed to investigate the differential gene expression patterns in PBMCs in an identical twin pair who had different outcomes to HBV infection. Use of the twin pair could eliminate the potential confounding factors like age, gender, and living environment, etc. A novel cytokine signaling-related gene, TNF-αIP1, is significantly downregulated in chronic HBV carriers. Moreover, we have confirmed that this gene is indeed differentially expressed in several groups of HBV-infected siblings who display different disease outcomes by reverse transcription-polymerase chain reaction (RT-PCR). We also found that upon HBcAg stimulation, TNF-αIP1 exhibited different

responses between PBMC isolated from subjects with immunity and chronic infection. These results suggest that TNF-αIP1 may be involved in immunity against HBV infection. An understanding of the immunological and genetic differences in PBMCs of these sibling pairs should provide insight into the molecular mechanisms of the protection and enable a more rationale design of therapeutic regimen for chronic HBV infection in Chinese.

MATERIALS AND METHODS

Patient sample information

Eight groups of HLA-A, B and DR identical Chinese siblings (including pair of identical twins) who differed in their outcomes to HBV infection were used in this study. RNA was isolated from PBMC of the siblings with spontaneous recovery (anti-HBs and anti-HBc positive) and their corresponding HLA-matched HBV-infected siblings (HBsAg positive).

PBMC preparation, RNA extraction, and labeling

Heparinized venous blood was collected and PBMC was separated by density-gradient centrifugation over Ficoll-Hypaque. Total RNA was extracted from PBMC using RNeasy kit (Qiagen, Valencia, CA, USA) following manufacturer's instructions. For each sample, 60 mg of total RNA was reverse transcribed using Superscript II (Invitrogen, Carlsbad, CA, USA) according to manufacturer's instructions.

DNA microarray

Generation of antisense RNA (aRNA) probe for cDNA microarray analysis was carried out as described previously[8]. Briefly, mRNA was amplified using two or three rounds of cDNA synthesis followed by aRNA synthesis. T7-promoter-oligo-dT [5'-GCCAGTGAATTGTAATAC GACTCACTATAGGGAGGCGG-$(dT)_{24}$-3'] was used for cDNA synthesis and T7 RNA polymerase was used for aRNA synthesis. Ten micrograms of starting total RNA was used to obtain 10 mg of final aRNA. During the process of the final aRNA synthesis, biotinylated UTP and CTP were used for labeling purpose (Enzo, Farmingdale, NY, USA). Detection of the hybridized probe using streptavidin-phycoerythrin fluorescent conjugate was done according to manufacturer's protocol (Molecular Probes, Eugene, OR, USA).

The labeled aRNA probe from PBMC was hybridized to a HU 95A gene chip representing 12 000 full-length human genes (Affymetrix, Santa Clara, CA, USA). The threshold for significant up- or down-regulation was 2.0- and 0.5-fold, respectively. Hybridizations were typically carried out for 16 h at 45 ℃ followed by washing, staining and using Affymetrix fluidic stations. Stained arrays were scanned in the G2500 A Hewlett-Packard Gene Array Scanner (Hewlett-Packard, Palo Alto, CA, USA) at the excitation wavelength of 488 nm. The amount of emitted light was proportional to the bound target at each location on the probe arrays.

RT-PCR

Total RNA was reverse transcribed using the Superscript II (Invitrogen) according to the manufacturer's instructions. PCR conditions for pre-B-cell colony-enhancing factor (PBEF), IL-18 receptor accessory protein (IL-18 RAP), TNF-αIP1 and GADPH were as follows: at 94 ℃ for 30 s, at 57 ℃ for 30 s, at 72 ℃ for 1 min for 35, 35, 35, and 32 cycles, respectively. The primer sequences of the genes tested were PBEF (sense: 5'-AAAAGCTGTTCCTGAGG GCTTTG-3'; anti-sense: 5'-TGACCACAGATACAGGCA CTGATG-3'); IL-18RAP (sense 5'-CCAGAGCCACAGA AATCACATTTC-3'; anti-sense 5'-CAAGAAATAGAGCC AGTGCTCCCA-3'); TNF-αIP1 (sense: 5'- TTACCTCCG AGATGACACCATCAC-3'; anti-sense: 5'-TCCTCATCTT CACTGGGGGAA-3').

RESULTS AND DISCUSSION

Perinatal transmission is the most common spread mode of hepatitis B infection in Chinese. Yet not all the siblings infected with HBV from mothers become chronic HBV carriers. It appears that different disease outcomes of these siblings represent success and failure of their immune systems in controlling HBV infection. In this study, we attempted to explore this phenomenon by investigating gene expression profiles in PBMCs of two identical twins who displayed diverse disease outcomes.

The differences in PBMC gene expression between two identical twins were analyzed using a DNA microarray chip containing 12 000 human expressed genes. Eighty-eight genes were expressed at a higher level and 46 genes were expressed at a lower level in twins with immunity (HBV resistant) compared to the HBV carrier twins [HBV susceptible). These genes were grouped on the basis of their predicted functions into 12 major groups (metabolism, cell signaling, transcription, transport physiology, growth, and differentiation, immune system, cell adhesion, house keeping, cell cycle, translation, apoptosis, and unknown genes (ESTs)] (Figure 1). We found that genes with unknown functions represented the major portion of genes with altered expression levels in the HBV immune twin.

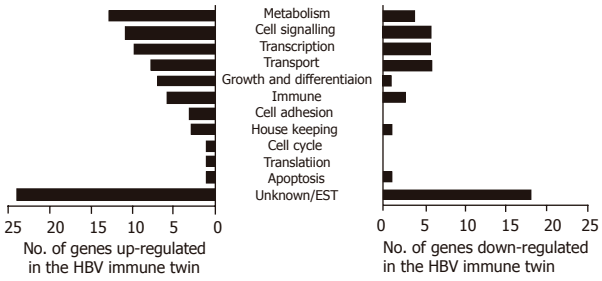

Figure 1 Number of genes upregulated or downregulated in the immune twin compared to the HBV carrier twin. PBMCs from two HBV infected twins with different disease outcomes were analyzed for gene expression using DNA microarray. Eighty-eight genes were identified as upregulated and 46 downregulated. They were further divided into 12 groups based on their presumed functions.

Table 1 Differential expression of immunity-related genes in PBMCs of HBV identical twin patients

UniGene ID	Gene name	Known function(s)	Fold change
Hs.244613	Signal transducer and activator of transcription 5b (STAT 5b)	Signal transducer of IL-2, IL-4, CSF1, and different growth hormones. I mportant for TCR signaling, apoptosis, adult mammary gland development, and sexual dimorphism of liver gene expression	–4.2
Hs.239138	Pre-B-cell colony-enhancing factor (PBEF)	A cytokine that increases the expression of IL-6 and IL-8 in fetal membrane and may be important in both normal spontaneous labor and infection-induced preterm labor	2.2
Hs.158315	Interleukin 18 receptor accessory protein (IL-18RAP)	An accessory subunit of the heterodimeric receptor for IL-18 enhances the IL-18 binding a ligand binding subunit of IL-18 receptor. The coexpression of IL-18R1 and this protein is required for the activation of NF-κB and MAPK8 (JNK) in response to IL-18	3.0
Hs.76090	Tumor necrosis factor-alpha-induced protein 1 (endothelial) (TNF-αIP1)	Unknown	2.3
Hs.225948	Chemokine (C-C motif) ligand 27 (CCL27)	Cytokine that plays a role in mediatinghoming of lymphocytes to cutaneous sites. It specifically binds to chemokine receptor 10 (CCR10). Studies of murine protein indicate that these protein-receptor interactions have a pivotal role in T-cell-mediated skin inflammation	-2.5
Hs.301921	C-C chemokine receptor type 1 (C-C CKR-1)	Cytokine receptor important for host protection from inflammatory response and susceptibility to virus and parasite	-2.7
Hs.57735	Scavenger receptor class F, member 1 (SCARF1)	Scavenger receptor that has roles in the binding and degradation of acetylated low density lipoprotein and may be involved in atherosclerosis	-2.2
Hs.4930	Low density lipoprotein receptor-related protein 4 (LRP4)	A membrane protein which may be involved in calcium ion binding	-2.8

[1]Fold changes between the HBV immune twin pair. Positive number indicates upregulation, whereas negative number denotes downregulation.

We are interested in the immune system-related genes that are putative candidates for conferring HBV immunity. Among the up- or down-regulated genes, eight genes were related to immune responses including several cytokine/chemokine signaling-related genes (Table 1). Three genes, namely cytokine PBEF, interleukin IL-18 receptor (R) accessory protein and TNF-αIP1 were upregulated in the immunity twin. PBEF is a cytokine transcribed in human bone marrow, liver tissue and muscle[9,10] and synergized with stem cell factor (SCF) and IL-7 activating pre-B-cell colony formation[11]. IL-18R accessory protein enhances the IL-18 binding activity of IL-18R1 and is required for the activation of nuclear factor-kappa B (NF-κB) and mitogen-activated protein kinase 8 (MAPK 8) in response to IL-18. TNF-αIP1 is first identified as a primary response gene in human umbilical vein endothelial cells towards TNF-α stimulation[12], but yet with no known function.

Five genes were downregulated in the HBV-immuned twins. They are the signal transducer and activator of transcription 5b (Stat5b), which is crucial for normal immune function and T-cell-mediated mitogenic signals and is a key signal transducer of T-cell receptor[13]. The chemokine (C-C motif) ligand 27 (CCL27) and C-C chemokine receptor type 1 (C-C CKR-1) are important for host inflammatory response. We also observed the downregulation of the scavenger receptor class F member 1 (SCARF1) and low-density lipoprotein receptor-related protein 4. Scavenger receptors encompass a broad range of molecules involved in receptor-mediated endocytosis of selected polyanionic ligands, including modified low-density lipoproteins (LDL)[14]. Further investigating the role of these genes and the molecular differences between immune siblings and HBV chronic carrier siblings may help us in designing therapeutic measures that modulate the immune system of patients in controlling HBV infection.

Of the eight immune system-related genes, TNF-αIP1 demonstrated the highest frequency of differential expression among the other groups of HBV-infected HLA-matched siblings with different disease outcomes as determined by semi-quantitative RT-PCR (Figure 2A). As shown in Figure 2B, the expression level of TNF-αIP1 was

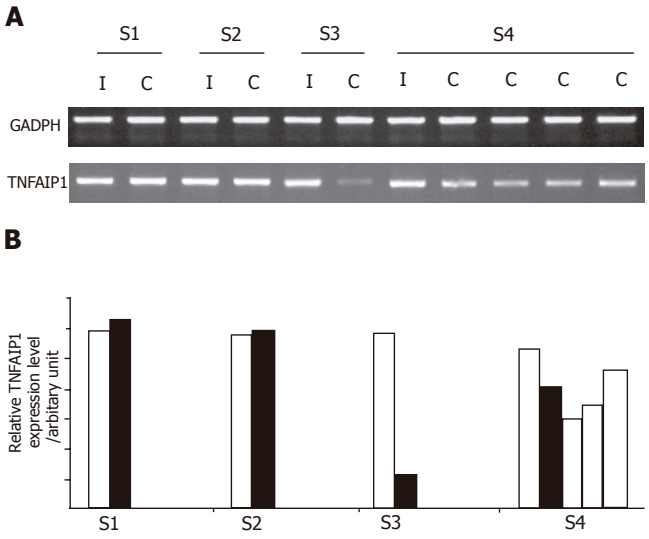

Figure 2 Expression levels of TNF-αIP1 gene in HBV-infected siblings with different disease outcomes. **A:** RT-PCR analysis of TNF-αIP1 in four sibling pairs; **B:** Fold changes of band intensity of TNF-αIP1 in different sibling groups. Open bar: HBV immune patients; black or patterned bars: HBV carrier; S1: sibling group 1; S2: sibling group 2; S3: sibling group 3; S4: sibling group 4.

lower in HBV carriers than in their HBV immune siblings in two siblings groups. Noticeably, the expression of TNF-αIP1 was significantly downregulated in HBV carrier siblings of group 3 and all four carrier siblings displayed down-regulation of TNF-αIP1. Suggesting that TNF-αIP1 may be a gene differentially expressed in PBMCs of HBV immune and carrier patients.

Recent studies suggest that cytokine response plays an important role in successful host defense against HBV infection. In transgenic mouse and chimpanzee model, cytotoxic T lymphocytes do not directly kill HBV-infected hepatocytes, but inhibit the viral replication through the actions of TNF-α and interferon (IFN-γ)[15,16]. Romero and Lavine[17] demonstrated that TNF-α and IFNs can downregulate the activity of HBV core/pregenomic (C/P) promoter, hence contributing to viral clearance. Moreover, activated intrahepatic antigen-presenting cells can inhibit liver HBV replication by secreting IL-12 and TNF-α[18]. One of the downstream mechanisms of how TNF-α modulates HBV infection is via the activation of NF-κB, which can inhibit HBV replication[19]. Interestingly, we have shown that TNF-αIP1 (a TNF-α inducible gene) expresses at a higher level in HBV immunized twin. TNF-αIP1 was first identified as an endothelial primary response gene towards TNF-α (then named B12), which induces TNF-αIP1 expression rapidly and transiently. Biochemical characterization suggests that TNF-αIP1 is a 36 ku protein, which may play a regulatory role and locate intracellularly[12]. The role of TNF-αIP1 in TNF-α-mediated NF-κB activation and HBV replication inhibition is of interest for further study.

Phylogenetic analysis showed that TNF-αIP1 could evolve into human and mouse endothelial protein 1 (Edp1), reflecting the fact that Edp1 is likely the mouse ortholog of TNF-αIP1 (Figure 3A). Predicted from the

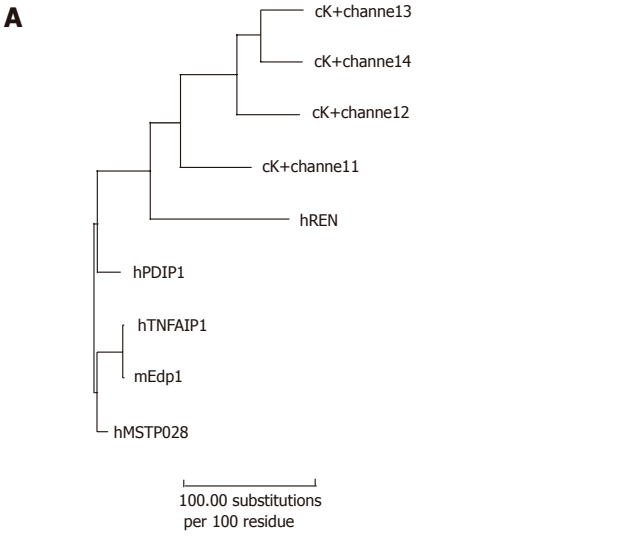

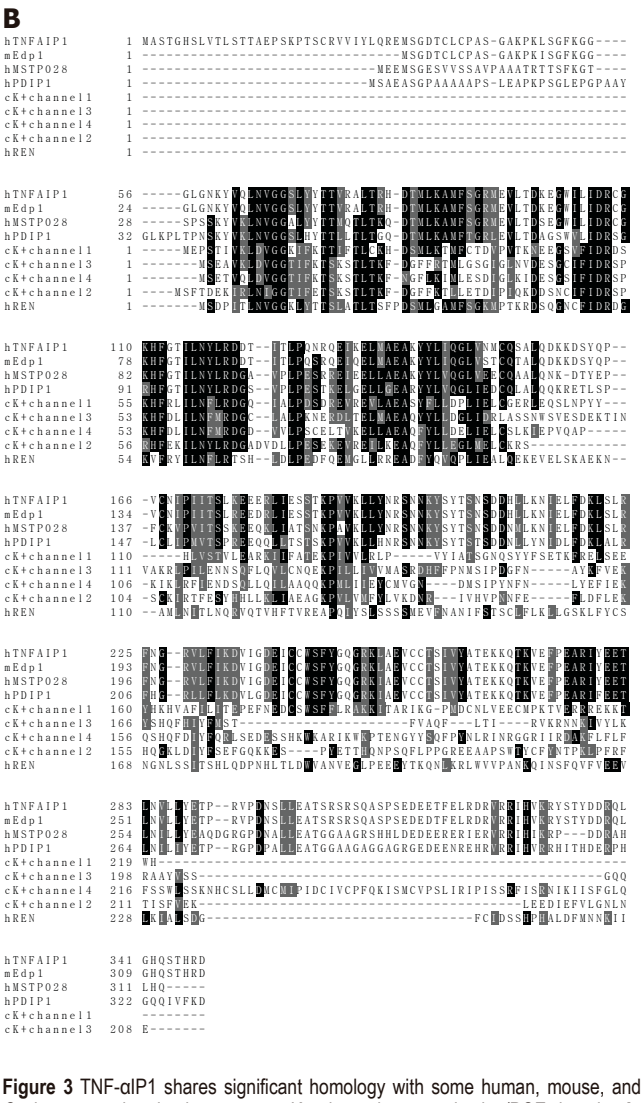

Figure 3 TNF-αIP1 shares significant homology with some human, mouse, and *C elegan* proteins, having common K+ channel tetramerization/POZ domain. **A:** Phylogenetic analysis of evolutionary distance of the protein sequences. The protein sequences were analyzed by the Growtree program provided by the GCG package. Kimura distance was adopted as the distance correction method. **B:** Amino acid sequence alignment of TNF-αIP1 (A41784) with mouse Edp1 protein (AAC78826), human MSTP028 protein (NP_114160), PDIP1 (AAL14962), human REN protein (XP_208568), and four C elegan K+ channel family members and with highest homology to TNF-αIP1 (NP_499312, NP_494320, NP_494476 and NP_494315). Black line: K+ channel tetramerization/POZ domain.

amino acid sequence of TNF-αIP1 (A41784), there is a K+ channel tetramerization domain in the middle of the sequence. This N-terminal, cytoplasmic tetramerization domain (T1) of voltage-gated K+ channels encodes molecular determinants for subfamily-specific assembly of alpha-subunits into functional tetrameric channels[20]. It is distantly related to the BTB/POZ domain which plays an oligomerization role in the function of this protein. Interestingly, the K+ channel tetramerization domain is the common domain feature shared by many TNF-α inducible proteins. For instance, mouse TNF-α inducible proteins such as Edp1 share high homology with the entire amino acid sequence of TNF-αIP1 (97% identity) (Figures 3A and B). It is also noticed that there was a group of C elegan proteins containing the K+ channel tetramerization domain. However, the function of this group of proteins is unknown.

Among the proteins containing K+ channel tetramerization domain, polymerase delta-interacting protein 1 (PDIP1) is best characterized[21]. PDIP1 is a TNF-α inducible protein and plays a role in linking cytokine activation and DNA replication in the liver as well as in other tissues. It localizes inside the nuclei and interacts with DNA polymerase δ small subunit (p50) and proliferating cell nuclear antigen (PCNA). In addition, it modulates DNA polymerase δ activity in a PCNA dependent manner. Importantly, it shares high homology (62% identity) with TNF-αIP1 (B12). PDIP1 is involved in TNF-α-mediated hepatocyte regeneration and stimulates hepatocyte proliferation upon TNF-α signal[21]. It is of interest to know whether this is also true for TNF-αIP1 using cell proliferation assay.

REFERENCES

1 **Yeoh EK,** Chang WK, Kwan JPW. Epidemiology of viral hepatitis B infection in Hong Kong. In Lam SK, Lai CL, Yeoh EK (editors): Viral hepatitis B infection: Vaccine and control. Singapore: *World Scientific* **1984:** 33-41

2 **Lok AS,** Lai CL, Wu PC, Wong VC, Yeoh EK, Lin HJ. Hepatitis B virus infection in Chinese families in Hong Kong. *Am J Epidemiol* 1987; **126:** 492-499

3 **Stevens CE,** Beasley RP, Tsui J, Lee WC. Vertical transmission of hepatitis B antigen in Taiwan. *N Engl J Med* 1975; **292:** 771-774

4 **Lok AS,** Liang RH, Chung HT. Recovery from chronic hepatitis B. *Ann Intern Med* 1992; **116:** 957-958

5 **Lau GK,** Lok AS, Liang RH, Lai CL, Chiu EK, Lau YL, Lam SK. Clearance of hepatitis B surface antigen after bone marrow transplantation: role of adoptive immunity transfer. *Hepatology* 1997; **25:** 1497-1501

6 **Lau GK,** Liang R, Lee CK, Yuen ST, Hou J, Lim WL, Williams R. Clearance of persistent hepatitis B virus infection in Chinese bone marrow transplant recipients whose donors were anti-hepatitis B core- and anti-hepatitis B surface antibody-positive. *J Infect Dis* 1998; **178:** 1585-1591

7 **Lau GK,** Lie AKW, Kwong YL, Lee CK, Hou J, Lau YL, Lim WL, Liang R. A case-controlled study on the use of HBsAg-positive donors for allogeneic hematopoietic cell transplantation. *Blood* 2000; **96:** 452-458

8 **Luo L,** Salunga RC, Guo H, Bittner A, Joy KC, Galindo JE, Xiao H, Rogers KE, Wan JS, Jackson MR, Erlander MG. Gene expression profiles of laser-captured adjacent neuronal subtypes. *Nat Med* 1999; **5:** 117-122

9 **Samal B,** Sun Y, Stearns G, Xie C, Suggs S, McNiece I. Cloning and characterization of the cDNA encoding a novel human pre-B-cell colony-enhancing factor. *Mol Cell Biol* 1994; **14:** 1431-1437

10 **Ognjanovic S,** Bryant-Greenwood GD. Pre-B-cell colony-enhancing factor, a novel cytokine of human fetal membranes. *Am J Obstet Gynecol* 2002; **187:** 1051-1058

11 **Rongvaux A,** Shea RJ, Mulks MH, Gigot D, Urbain J, Leo O, Andris F. Pre-B-cell colony-enhancing factor, whose expression is up-regulated in activated lymphocytes, is a nicotinamide ph osphoribosyltransferase, a cytosolic enzyme involved in NAD biosynthesis. *Eur J Immunol* 2002; **32:** 3225-3234

12 **Wolf FW,** Marks RM, Sarma V, Byers MG, Katz RW, Shows TB, Dixit VM. Characterization of a novel tumor necrosis factor-a-induced endothelial primary response gene. *J Biol Chem* 1992; **267:** 1317-1326

13 **Welte T,** Leitenberg D, Dittel BN, al-Ramadi BK, Xie B, Chin YE, Janeway Jr CA, Bothwell ALM, Bottomly K, Fu XY. STAT5 interaction with the T cell receptor complex and stimulation of T cell proliferation. *Science* 1999; **283:** 222-225

14 **Peiser L,** Mukhopadhyay S, Gordon S. Scavenger receptors in innate immunity. *Curr Opin Immunol* 2002; **14:** 123-128

15 **Guidotti LG,** Ishikawa T, Hobbs MV, Matzke B, Schreiber R, Chisari FV. Intracellular inactivation of the hepatitis B virus by cytotoxic T lymphocytes. *Immunity* 1996; **4:** 25-36

16 **Guidotti LG,** Rochford R, Chung J, Shapiro M, Purcell R, Chisari FV. Viral clearance without destruction of infected cells during acute HBV infection. *Science* 1999; **284:** 825-829

17 **Romero R,** Lavine JE. Cytokine inhibition of the hepatitis B virus core promoter. *Hepatology* 1996; **23:** 17-23

18 **Kimura K,** Kakimi K, Wieland S, Guidotti LG, Chisari FV. Activated intrahepatic antigen-presenting cells inhibit hepatitis B virus replication in the liver of transgenic mice. *J Immunol* 2002; **169:** 5188-5195

19 **Biermer M,** Puro R, Schneider RJ. Tumor necrosis factor alpha inhibition of hepatitis B virus replication involves disruption of capsid integrity through activation of NF-kB. *J Virol* 2003; **77:** 4033-4042

20 **Bixby KA,** Nanao MH, Shen NV, Kreusch A, Bellamy H, Pfaffinger PJ, Choe S. Zn2+-binding and molecular determinants of tetramerization in voltage-gated K+ channels. *Nat Struct Biol* 1999; **6:** 38-43

21 **He H,** Tan CK, Downey KM, So AG. A tumor necrosis factor a-and interleukin 6-inducible protein that interacts with the small subunit of DNA polymerase d and proliferating cell nuclear antigen. *PNAS* 2001; **98:** 11979-11984

Science Editors Wang XL and Guo SY **Language Editor** Elsevier HK

PO Box 2345, Beijing 100023, China
www.wjgnet.com
wjg@wjgnet.com

ELSEVIER

World J Gastroenterol 2005;11(48):7569-7578
World Journal of Gastroenterology ISSN 1007-9327

High affinity mouse-human chimeric Fab against Hepatitis B surface antigen

Biplab Bose, Navin Khanna, Subrat K Acharya, Subrata Sinha

Biplab Bose, Subrata Sinha, Department of Biochemistry, All India Institute of Medical Sciences, New Delhi, India
Navin Khanna, International Center for Genetic Engineering and Biotechnology, New Delhi, India
Subrat K. Acharya, Department of Gastroenterology, All India Institute of Medical Sciences, New Delhi, India
Supported by the Department of Biotechnology (DBT), Govt. of India, NO. BT/PR2540/PID/25/101/2001
Correspondence to: Professor Subrata Sinha, Department of Biochemistry, All India Institute of Medical Sciences, Ansari Nagar, New Delhi, PIN-110029,
India. sub_sinha2004@yahoo.co.in
Telephone: +91-11-26594483
Fax: +91-11-26588663 / +91-11-26588641
Received: 2005-04-06 Accepted: 2005-04-26

Abstract

AIM: Passive immunotherapy using antibody against hepatitis B surface antigen (HBsAg) has been advocated in certain cases of Hepatitis B infection. We had earlier reported on the cloning and expression of a high affinity scFv derived from a mouse monoclonal (5S) against HBsAg. However this mouse antibody cannot be used for therapeutic purposes as it may elicit anti-mouse immune responses. Chimerization by replacing mouse constant domains with human ones can reduce the immunogenicity of this antibody.

METHODS: We cloned the V_H and V_L genes of this mouse antibody, and fused them with CH1 domain of human IgG1 and C_L domain of human kappa chain respectively. These chimeric genes were cloned into a phagemid vector. After initial screening using the phage display system, the chimeric Fab was expressed in soluble form in *E. coli*.

RESULTS: The chimeric Fab was purified from the bacterial periplasmic extract. We characterized the chimeric Fab using several *in vitro* techniques and it was observed that the chimeric molecule retained the high affinity and specificity of the original mouse monoclonal. This chimeric antibody fragment was further expressed in different strains of *E. coli* to increase the yield.

CONCLUSION: We have generated a mouse-human chimeric Fab against HBsAg without any significant loss in binding and epitope specificity. This chimeric Fab fragment can be further modified to generate a full-length chimeric antibody for therapeutic uses.

Key words: Chimeric Fab; Hepatitis B surface antigen; Phage display

Bose B, Khanna N, Acharya SK, Sinha S. High affinity mouse-human chimeric Fab against Hepatitis B surface antigen. *World J Gastroenterol* 2005; 11(48): 7569-7578
http://www.wjgnet.com/1007-9327/11/7569.asp

INTRODUCTION

Hepatitis B virus (HBV) infection is the 10th leading cause of death worldwide, with 2 billion people infected by it and 350 million suffering from chronic HBV infection[1]. Protective antibodies that appear after natural infection are mostly directed against the major antigenic 'a'determinant of Hepatitis B surface antigen (HBsAg)[2]. The immunodominant 'a' epitope is a part of a large antigenic area of HBsAg, called the major hydrophilic region[3] and this epitope is present in all serotypes[4]. Antibodies against HBsAg are thus advocated for passive immunotherapy against Hepatitis B infection in cases of accidental needle stick injuries, for liver transplant patients and to prevent vertical transfer of HBV infection from mother to child[5-8]. Presently, human anti-HBs immune globulin (HBIG) collected from the blood of hyperimmune donors is used for postexposure prophylaxis. Being a blood derived product anti-HBs HBIG is costly and can cause cross-contamination. Therefore a recombinant antibody to HBsAg can be a suitable alternative to such a practice.

Although several recombinant antibodies against HBsAg have been reported in literature, none is available for clinical use[9–12]. In our previous work we had expressed and characterized a recombinant anti-HBs scFv cloned from a mouse monoclonal 5S[13]. This antibody binds to HBsAg with high affinity (K_D = 0.889 nmol/L). It tested positive in an *in vitro* surrogate test for seroconversion and protective antibodies (Hepanostika anti-HBs kit, Organon Teknika, The Netherlands). The scFv generated from this hybridoma retained the high affinity and epitope specificity[13]. However this mouse monoclonal cannot be used for therapeutic purposes as it may trigger human anti-mouse antibody response, especially when multiple infusions are required to obtain therapeutic efficacy[14,15]. It is well known that immunogenic reactions are predominantly directed towards constant domains of

Table 1 Oligonucleotide primers used for generation of the chimeric Fd and light chain

Primer	Sequence
5′ primer for V_H (5H23M)	5′- AG GTC CAG CTT CTC GAG CCC GGG GC -3′
3′ primer for V_H (Fd3)	5′-CGA TGG GCC CTT GGT GGA GGC TGA AGA GAC AGT GAC TGA GGT TCC-3′
5′ primer for C_H1 of human IgG1 (Fd5)	5′-GGA ACC TCA GTC ACT GTC TCT TCA GCC TCC ACC AAG GGC CCA TCG-3′
3′ primer for C_H1 of human IgG1 (CG1Z)	5′- GCA TGT ACT AGT TTT GTC ACA AGA TTT GGG -3′
5′ primer for V_L (5L35)	5′-CCA GAT GTG AGC TCG TGA TGA CCC AGA CTC CA-3′
3′ primer for V_L (K3)	5′-CAG ATG GTG CAG CCA CAG TCC GTT TGA GTT CCA GCT TGG-3′
5′ primer for C_L of human κ chain (K5)	5′-CCA AGC TGG AAC TCA AAC GGA CTG TGG CTG CAC CAT CTG-3′
3′ primer for C_L of human κ chain (Ck1d)	5′- GCG CCG TCT AGA ATT AAC ACT CTC CCC TGT TGA AGC TCT TTG TGA CGG GCG AAC TCA G -3′

Primer names are given in parenthesis. Sites for restriction enzymes are shown as underlined. Complementary overhangs are shown in bold letters.

murine antibodies[16]. Problems associated with the HAMA response can be reduced by creating mouse-human chimeric antibodies, where mouse constant regions are replaced by human ones[17-19].

The exact mechanisms of antibody-mediated virus neutralization are not clear till date. A few of the principal mechanisms, which have been postulated for virus neutralization, are virus aggregation, inhibition of attachment of virus to cell receptors and inhibition of events after attachment to cell receptors[20,21]. Though high affinity binding to viral epitopes is a pre-requisite for antibody-mediated virus neutralization, the importance of antibody constant domains is not clear. Apart from full-length antibodies, antibody Fab fragments have been shown to neutralize viruses[22-26]. It has been shown that $F(ab)_2$ fragments derived from HBIG is effective for the prevention of vertical transfer of HBV infection in neonates[27]. In comparison to a full-length antibody, a Fab fragment can be easily expressed in bacterial expression systems[28]. A recombinant Fab can be further modified for increase in affinity[29], for chimerization/humanization[30] and can be linked with antibody Fc region to generate a full-length antibody[31,32].

In the present work, we have fused the variable regions of the mouse monoclonal 5S (IgG1/κ) with the corresponding human constant regions (C_H1 of IgG1/C_L of κ) to generate a mouse-human chimeric Fab. This chimeric Fab was expressed using a phage display expression system. After initial screening of functional clones, the chimeric Fab was expressed in *E. coli* in soluble form. It was purified by affinity chromatography and characterized for antigen binding. We observed that the chimeric Fab fragment retained the high affinity binding and epitope specificity of the original mouse monoclonal. This chimeric molecule can be further modified for generation of a therapeutically useful full-length chimeric antibody.

MATERIALS AND METHODS

Materials

The phagemid vector pCOMB3H was provided by The Scripps Research Institute, La Jolla, USA. Shanta Biotech (India) provided purified recombinant HBsAg expressed in a *Pichia* system. *E. coli* XL1-Blue and TG1 cells and helper phage M13 KO7 were obtained from MRC, Cambridge, UK. *E. coli* strains AD494 and BL 21 CodonPlus were procured from Novagen. 5S hybridoma cells were maintained in RPMI (Sigma, USA) with 10% FCS (Sigma, USA). Anti-M13 mouse antibody was provided by Dr. Vijay Chaudhary, University of Delhi, South Campus, New Delhi, India.

Construction of the chimeric light chain and Fd fragment

The strategy for generation of the chimeric Fd and light chain is shown in Figure 1. The variable region genes of 5S hybridoma were amplified by reverse transcription followed by PCR. Primers used for all reverse transcriptions and PCRs are listed in Table 1. Total RNA was isolated from 5S cells using TRI reagent (Sigma, USA) and cDNAs for the V_H and V_L fragments were generated by reverse transcription using Omniscript RTase (Qiagen). Primers used for reverse transcriptions were Fd3 and K3 for V_H and V_L respectively. These primers have overhangs complementary to the 5' regions of the respective human constant domains. The V_H fragment was further amplified by PCR using primers 5H23M and Fd3. Similarly, the V_L fragment was amplified by PCR using primers 5L35 and K3. Conditions for both the PCRs were: 30 cycles at 94 °C for 1 min, 50 °C for 1 min, 72 °C for 2 min, followed by a final extension for 10 min at 72 °C.

For amplification of human constant domains, RNA was isolated from human peripheral blood lymphocytes (PBLs) using TRI reagent. cDNAs for the C_H1 region of human IgG1 and the C_L region of human kappa chain were generated by reverse transcription using Omniscript RTase (Qiagen). Primers used for reverse transcriptions were CG1Z and Ck1d for C_H1 and C_L respectively. The C_H1 fragment was further amplified by PCR using primers Fd5 and CG1Z. Human C_L was amplified by PCR using primers K5 and Ck1d. Fd5 and K5 carry overhangs complementary to the 3' end of variable regions of 5S. Conditions for both these PCRs were: 30 cycles at 94 °C for 1 min, 60 °C for 1 min, 72 °C for 2 min, followed by a final extension for 10 min at 72 °C.

PCR amplified fragments were resolved in 1.5% agarose gel and respective bands were eluted out using QIAquick gel extraction kit (Qiagen). PCR amplified C_H1 (human IgG1) and mouse V_H were used as templates for generation of the chimeric Fd by overlap PCR. Initial assembly of equimolar amounts of the mouse V_H and human C_H1 was done by PCR for 20 cycles at 94 °C for

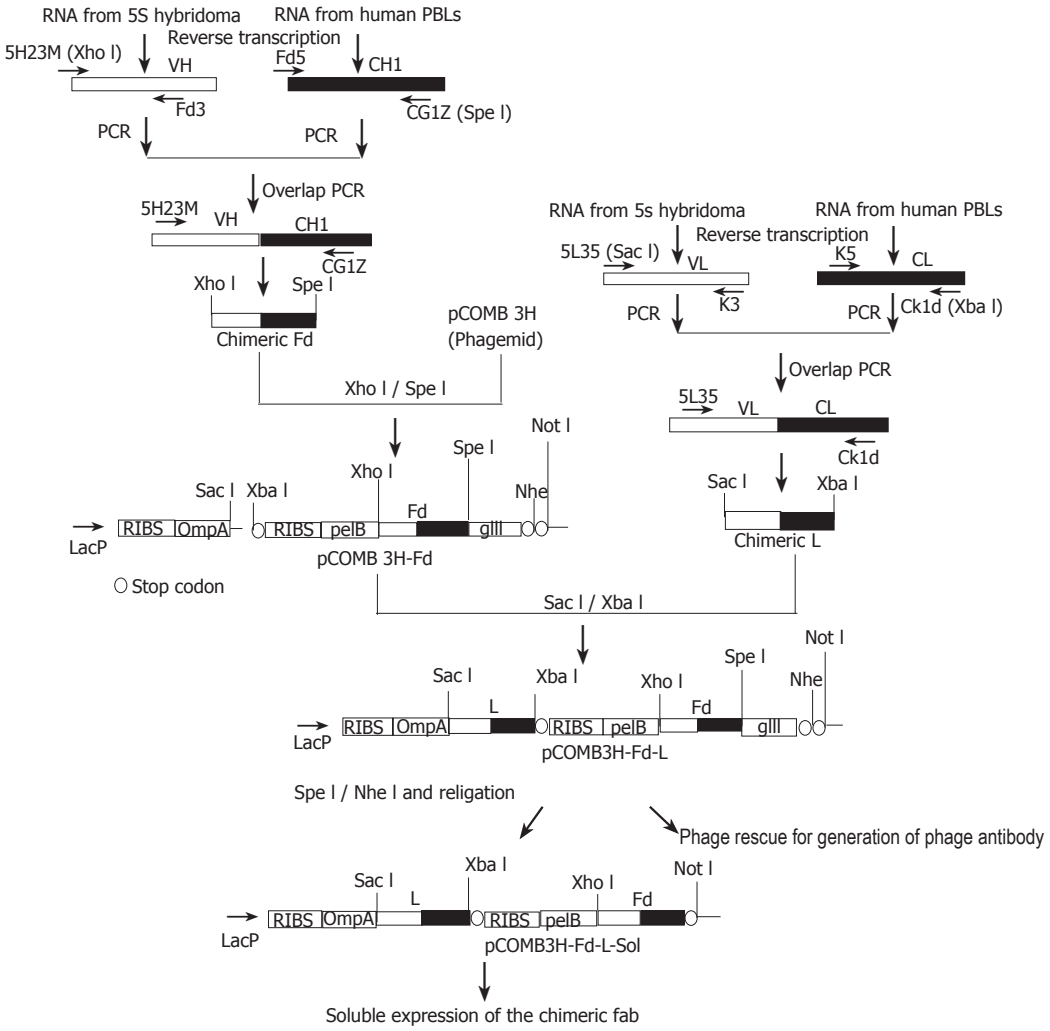

Figure 1 Schematic representation of the strategy for cloning and expression of the anti-HBs chimeric Fab. The V_H and V_L fragments of 5S hybridoma were fused with human C_H1 and C_L by overlap PCR. The resulting chimeric fragments were cloned in the bi-cistronic phagemid vector pCOMB3H. Both the fragments are under the control of a single *LacZ* promoter. *ompA* and *pelB* are two leader sequences, provided for directing the light chain and Fd fragment to the bacterial periplasm. Two ribosome-binding sites are present in the vector for stable expression of both the fragments. The Fd fragment was cloned upstream to the phage gIII sequence, for surface display of the chimeric Fab. This *gIII* fragment was removed by digestion with *Spe I/Nhe I* and after self-ligation of the vector, the Fab fragment was expressed in soluble form.

1 min, 60 °C for 1 min and 72 °C for 2 min, followed by final extension of 10 min at 72 °C. The product of the initial assembly reaction was diluted 10 times and used as the template for pull through PCR using primers 5H23M and CG1Z. Similarly human kappa C_L and mouse V_L fragment were joined to generate the chimeric light chain. Primers used for this reaction were 5L35 and Ck1d.

Construction of the phagemid construct

We used the bi-cistronic phagemid vector pCOMB3H, a variant of the phagemid pComb3[33], for the expression of the chimeric Fab. The essential features of this vector system and our cloning strategy are shown in Figure 1. The chimeric Fd was digested with *Xho1* and *Spe1* and cloned into the phagemid vector pCOMB3H. The resulting construct (pCOMB3H-Fd) was transformed into chemically competent *E. coli* XL1-Blue cells by standard chemical method ($CaCl_2$/heat shock)[34]. Transformed cells were grown on Amp-Agar plates. Colonies were picked up after overnight incubation and screened for the presence of the insert by colony PCR and restriction digestion (*Xho1*/*Spe1*). The recombinant phagemid pCOMB3H-Fd was isolated by alkali-lysis method and digested with *Sac1* and *Xba1*. The chimeric light chain digested with these two enzymes was cloned into pCOMB3H-Fd to generate the phagemid construct pCOMB3H-Fd-L. This construct was transformed into chemically competent XL1-Blue cells by standard chemical transformation method and after overnight incubation, recombinant clones were checked for the presence of the chimeric light chain by colony PCR and by restriction digestion (*Sac1*/*Xba1*).

Expression of the phage antibody and selection of antigen binding clones

Cells transformed with the construct pCOMB3H-Fd-L were used for expression of the chimeric Fab on phage surface. Phage displaying chimeric Fab was rescued by infection with helper phage M13-KO7 as described by

Barbas *et al*.[33]. Phage was precipitated from the culture supernatant by incubating with PEG/NaCl (20% PEG/2.5 mol/L NaCl) for 8 h on ice. After centrifugation, precipitated phage was resuspended in PBS and titrated to determine phage concentration[35].

Clones displaying functional Fab fragment were selected by biopanning over antigen-coated plates. The method for biopanning has been discussed in detail in our earlier article[13]. Essentially this method involves incubation of phage in uncoated ELISA plate followed by incubation of unbound phage in antigen-coated plate. After thorough washing, bound phage was eluted out at low pH. Eluted phage was passed through two more rounds of selection over coated and uncoated wells with increasing number of washing.

Identification of antigen binding clones by phage-ELISA

Phage obtained after three rounds of selection, was reinfected in XL1-Blue cells and amplified by standard phage rescue protocol as mentioned earlier. Antigen binding clones were identified by phage-ELISA. Maxisorp ELISA plates were coated with HBsAg (250 ng/well) in bicarbonate buffer (pH 9.5). After blocking with 2% non-fat milk in PBS (MPBS), phage (~10^{12}/well) was added and incubated for 1 h at room temperature. Bound phage was detected by incubation with 1:1 000 dilution of anti-M13 mouse antibody for 1 h at room temperature, followed by 1 h incubation with 1:2 000 dilution of anti-mouse antibody-HRP conjugate (Promega, USA). ELISA was developed by using 100 μL of 0.4 mg/mL *o*-phenylenediamine and 0.8 μL/mL of H_2O_2 in citrate-phosphate buffer (pH 5). The same amount of helper phage (M13-KO7) was used as negative control in phage-ELISA.

The phagemid construct was isolated from the clone showing maximum binding and the nucleotide sequences of the chimeric Fd and light chain were determined by sequencing using ABI-Prism automatic DNA sequencer. Primers used for sequencing the light chain were 5'-ATGAAAAAGACAGCTATCGC-3' and 5'-TAATAAC AATCCAGCGGCTG-3'. Primers used for sequencing the Fd fragment were 5'-TCTTTTCATAATCAAAATCACC G-3' and 5'-AAATGAAATACCTATTGCC-3'.

Soluble expression of the chimeric Fab

The antigen binding clone selected by phage ELISA was further processed for soluble expression of the anti-HBs chimeric Fab. For soluble expression of the chimeric Fab, the phage *gIII* sequence was removed from the recombinant phagemid construct pCOMB3H-Fd-L by double digestion with *Spe I* and *Nhe I*. Digestion by these two enzymes provides compatible ends for self-ligation of the vector. Double digested phagemid was self-ligated to generate the construct pCOMB3H-Fd-L-Sol and transformed in chemically competent XL1-Blue cells. For soluble expression of recombinant chimeric Fab, 1 L Super Broth with 20 mmol/L $MgCl_2$ and ampicillin (100 μg/mL) was inoculated with 10 mL of overnight culture of the recombinant clone and grown at 37 °C till the A_{600} reached approximately 0.6, when overexpression of the chimeric Fab was induced by 1 mmol/L IPTG. After overnight growth at 30 °C, cells were harvested by centrifugation at 4 000 r/min. Cell pellet was re-suspended in 20 mL PBS/ 1 mmol/L EDTA and kept on ice for 40 min. Clarified periplasmic extract was obtained by centrifugation of the re-suspended product at 10 000 *g*. The same method was used to express the soluble chimeric Fab in three other *E. coli* strains (AD494, BL21 CodonPlus and TG1).

Purification of the recombinant chimeric Fab

The periplasmic extract was concentrated (~10 times) using Centriprep YM-30 centrifugal filter (Millipore, USA). The recombinant chimeric Fab was purified from the periplasmic extract by affinity chromatography using HiTrap Protein G HP column (Amersham) as per the manufacturer's protocol. In brief, the protein G column (1 mL) was washed thoroughly with double distilled water (five column volumes) and equilibrated with five column volumes of equilibration buffer (pH 7.0). The concentrated periplasmic extract was allowed to pass through the column using a syringe at a speed of 2 mL/min. The column was washed thoroughly by 10 volume of equilibration buffer and bound chimeric Fab was eluted out by 5 volume of elution buffer (pH 2.7). Eluted fractions were immediately neutralized using neutralization buffer (77 μL/mL, pH 9). The eluted fractions were concentrated by Centriprep YM-30 centrifugal filter and checked on SDS-PAGE.

Electrophoresis and Western blot analysis

The purified chimeric Fab was resolved by 12% SDS-PAGE, separately in reducing (with βME) and non-reducing conditions (without βME or DTT). The resolved protein was stained by silver staining.

For Western blot analysis, the concentrated periplasmic extract was resolved by 12% SDS-PAGE in non-reducing conditions and electroblotted on nitrocellulose membrane. After blocking with 4% MPBS for 2 h, the chimeric Fab was detected by Rabbit anti-Human IgG-HRP conjugate (1:1 000 dilution; Dako). The blot was developed using DAB/H_2O_2 system. An equal amount of concentrated periplasmic extract of untransformed XL1-Blue cells was used as the negative control for the Western blot experiment. A separate Western blot experiment was performed under reducing conditions for the detection of the monomeric Fd and light chain. Whenever required, intensity of bands in Western blots was measured densitometrically using ChemiImager 4400 (Alpha Innotech Corp., USA).

Antigen binding assays for the chimeric Fab

Binding of the chimeric Fab was checked by solid phase ELISA. Maxisorp ELISA plate was coated with 250 ng/well of HBsAg in bicarbonate buffer (pH 9.5). After blocking with 4% MPBS, different dilutions of the chimeric Fab was added to antigen coated wells and bound antibodies were detected by Rabbit anti-Human IgG-HRP conjugate (1:2 000 dilution; Dako). Hybridoma supernatant of the original mouse monoclonal 5S was

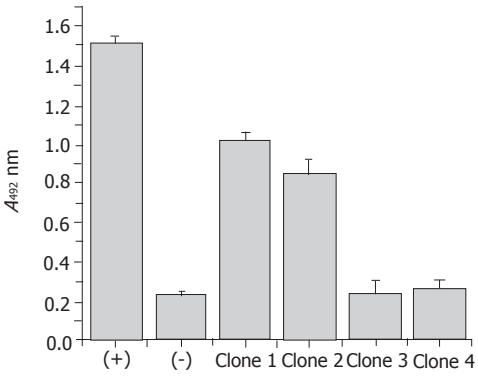

Figure 2 Phage ELISA to identify antigen binding clones. After three rounds of biopanning, selected phage was rescued and antigen-binding clones were detected by phage ELISA. In this experiment 5S hybridoma supernatant and helper phage M13 KO7 were used as positive (+) and negative (–) control respectively. Clone 1 was used for soluble expression of the chimeric Fab.

used as a positive control for this experiment. The extract of untransformed XL1-Blue cells was used as a negative control and corresponding readings were deducted from the readings of the chimeric Fab. This ELISA method was also used to study the levels of expression the chimeric Fab in different *E. coli* strains.

For competitive ELISA, plates were coated with HBsAg (100 ng/well) in bicarbonate buffer and blocked with 4% MPBS. Different amounts of the chimeric Fab were mixed with 1:80 dilution of 5S hybridoma supernatant and added to antigen-coated wells. After one hour incubation at room temperature, bound mouse antibody was detected by anti-mouse-HRP conjugate (Bangalore Genei, India). Periplasmic extract of untransformed XL1-Blue cells was used as the negative control and binding of the mouse monoclonal in its presence was taken as the maximum binding to calculate the percent inhibition.

Determination of the dissociation constant of the chimeric Fab

The dissociation constant (K_D) of HBsAg and chimeric Fab interaction was determined in solution phase by an ELISA method as described by Friguet *et al*.[36]. Essentially the technique involves incubation of a fixed amount of the antibody with different amounts of the antigen in solution phase for a prolonged period so that the equilibrium is reached. This is followed by detection of unbound antibody by conventional ELISA. This ELISA data is then used to calculate the K_D value, by using an equation derived from the law of mass action. The advantage of this technique is that it can be used to determine the affinity of an antibody without prior purification.

For this experiment we used crude periplasmic extract of the clone expressing the chimeric Fab in soluble form. A fixed amount of the periplasmic extract (1:300 dilution, in 100 μL of 4% MPBS) was incubated with varying concentrations of HBsAg (3-10 nmol/L) for 16 h at 4 °C. This equilibrated solution was incubated in antigen coated ELISA plates (250 ng antigen/well) for 20 min at room temperature to capture the free Fab. Bound chimeric Fab was detected by Rabbit anti-human IgG-HRP conjugate (Dako).

Protein estimation

Protein concentrations were estimated by Bradford assay[37].

RESULTS

Generation of a phagemid construct for the expression of phage antibody: Variable regions of the light chain and heavy chain of the mouse monoclonal 5S were amplified by RT-PCR. The $C_{H}1$ region of human IgG1 and C_L of human kappa chain were amplified by RT-PCR using RNA extracted from human PBLs. After the fusion of the mouse V_H and human $C_{H}1$, resulting chimeric Fd was cloned into the phagemid vector pCOMB3H to generate the recombinant construct pCOMB3H-Fd. Similarly, the chimeric light chain, generated by joining the mouse V_L and human C_L, was cloned into pCOMB3H-Fd to generate the recombinant construct pCOMB3H-Fd-L. This construct was transformed in XL1-Blue cells and phage displaying the chimeric Fab was generated by phage rescue using helper phage.

Selection of antigen binding clones and phage ELISA: The anti-HBs chimeric Fab was first expressed as phage antibody and antigen-binding clones were enriched by bio-panning over antigen coated plate. Selection was done on uncoated and antigen coated wells alternatively, thereby removing plastic binding clones, which can interfere in subsequent ELISAs. After three rounds of selection, functional clones were amplified and rescued to generate phage particles displaying the chimeric Fab and antigen-binding clones were detected by phage ELISA (Figure 2). As shown in Figure 2, clone 1 had the maximum binding and was used for soluble expression of the chimeric Fab. Nucleotide sequences of the chimeric Fd and light chain of this clone were submitted to the EMBL Nucleotide Sequence Database (EMBL accession numbers: AJ878860 and AJ878861). Sequence analysis indicated that the variable regions in these chimeric genes are identical to the variable regions of the mouse monoclonal 5S (data not shown).

Soluble expression of the chimeric Fab: Phage *gIII* sequence was removed from pCOMB3H-Fd-L for soluble expression of the chimeric Fab. The anti-HBs chimeric Fab was expressed in *E. coli* XL1-Blue cells by inducing overnight with 1 mmol/L IPTG. The leader sequences, present upstream to the chimeric genes, drag both the chains to the bacterial periplasm, where they form inter- and intra-chain disulphide bonds. The periplasmic extract was concentrated and the chimeric Fab was purified using Protein G column. Yield of the purified chimeric Fab when expressed in XL1-Blue cells was ~40 μg/L of culture. The purified product was resolved by SDS-PAGE in non-reducing (without βME/DTT) as well as in reducing conditions (with βME). As shown in Figure 3A, the chimeric Fab is expressed as a heterodimer (~50 ku) of the chimeric Fd and light chain. In reducing conditions, both the chains were detected in monomeric form (~25 ku).

Expression of the heterodimeric chimeric Fab was further confirmed by Western blot in non-reducing

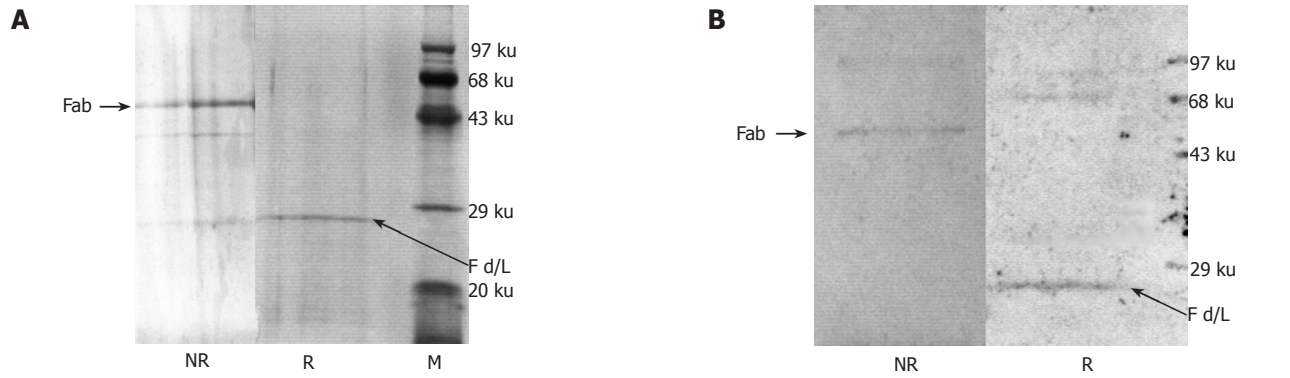

Figure 3 SDS-PAGE (**A**) and Western Blot (**B**) analysis of the chimeric Fab. The purified chimeric Fab was resolved in 12% SDS-PAGE under reducing (R) and non-reducing conditions (NR). In non-reducing conditions the Fab is a heterodimer of molecular weight ~50 ku. In reducing conditions the heterodimer dissociates into chimeric light chain (~25 ku) and Fd (~25 ku). Both the gels were stained by silver staining. M is the lane for the protein marker. Similar observations were made in Western Blots (**B**) of the chimeric Fab in reducing (R) and non-reducing (NR) conditions. Electroblotted antibody fragments were detected by Rabbit anti-Human IgG-HRP conjugate (1:1 000 dilution; Dako).

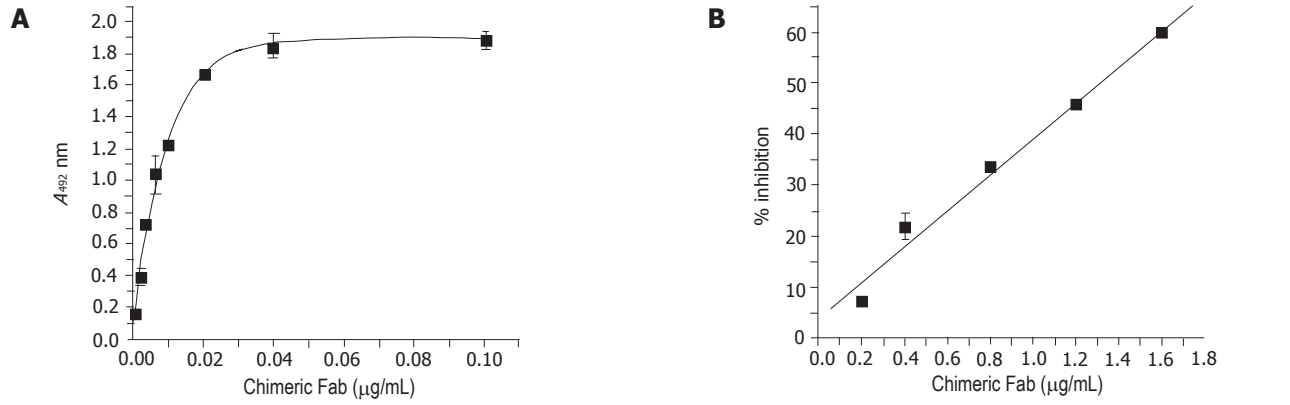

Figure 4 Binding properties of the anti-HBs chimeric Fab. 1 Solid phase ELISA was performed with different dilutions of the soluble chimeric Fab. The result of the competitive ELISA between the chimeric Fab and the mouse monoclonal 5S is shown in Figure (**B**). Different amounts of the chimeric Fab were allowed to compete with 1:80 dilution of the 5S-hybridoma culture supernatant for binding to HBsAg. Bound mouse monoclonal was detected with anti-mouse HRP and the % inhibition of binding was calculated.

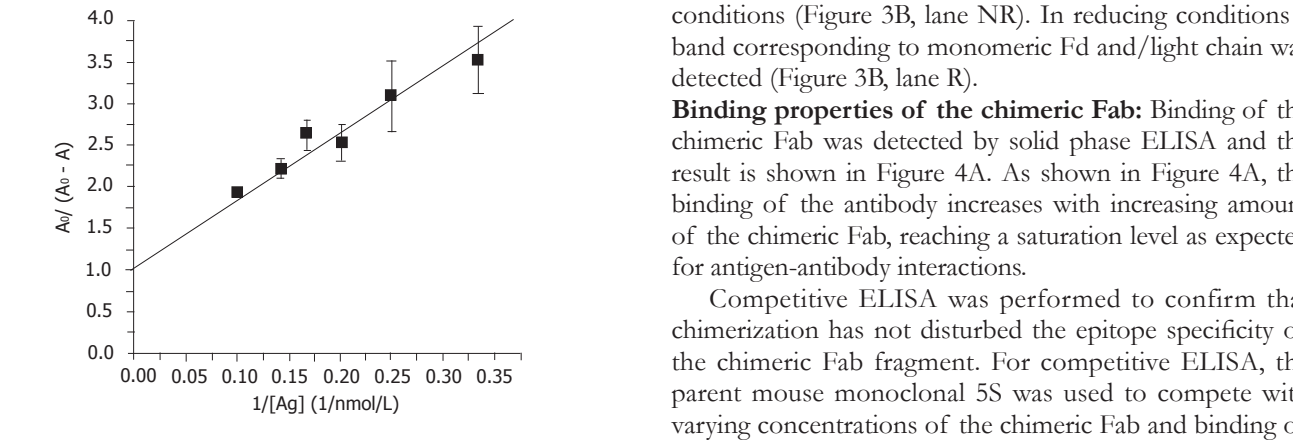

Figure 5 Dissociation constant (K_D) of the chimeric Fab. The K_D was determined using an ELISA based method. Different amounts of HBsAg were incubated with concentrated periplasmic extract of the clone expressing the anti-HBs chimeric Fab for 16 h and unbound antibody was detected by ELISA using rabbit anti-human antibody-HRP (Dako). The data was fitted to the equation $A_0/(A_0–A) = K_D*1/[Ag]+1$, where Ao = absorbance when the antibody was incubated without any antigen, A = absorbance corresponding to free antibody after incubation with the antigen. Dissociation constant of the chimeric Fab was determined from the slope of the straight line (K_D = 8.166±0.14 nmol/L).

conditions (Figure 3B, lane NR). In reducing conditions a band corresponding to monomeric Fd and/light chain was detected (Figure 3B, lane R).

Binding properties of the chimeric Fab: Binding of the chimeric Fab was detected by solid phase ELISA and the result is shown in Figure 4A. As shown in Figure 4A, the binding of the antibody increases with increasing amount of the chimeric Fab, reaching a saturation level as expected for antigen-antibody interactions.

Competitive ELISA was performed to confirm that chimerization has not disturbed the epitope specificity of the chimeric Fab fragment. For competitive ELISA, the parent mouse monoclonal 5S was used to compete with varying concentrations of the chimeric Fab and binding of the mouse antibody was detected using anti-mouse-HRP conjugate. Figure 4B shows that the chimeric Fab inhibits the binding of the mouse antibody, indicating that both of these bind to the same epitope.

Dissociation constant of the chimeric Fab: The dissociation constant of the chimeric Fab in solution phase was determined using an ELISA based technique developed by Friguet *et al.*[36]. As calculated from the slope

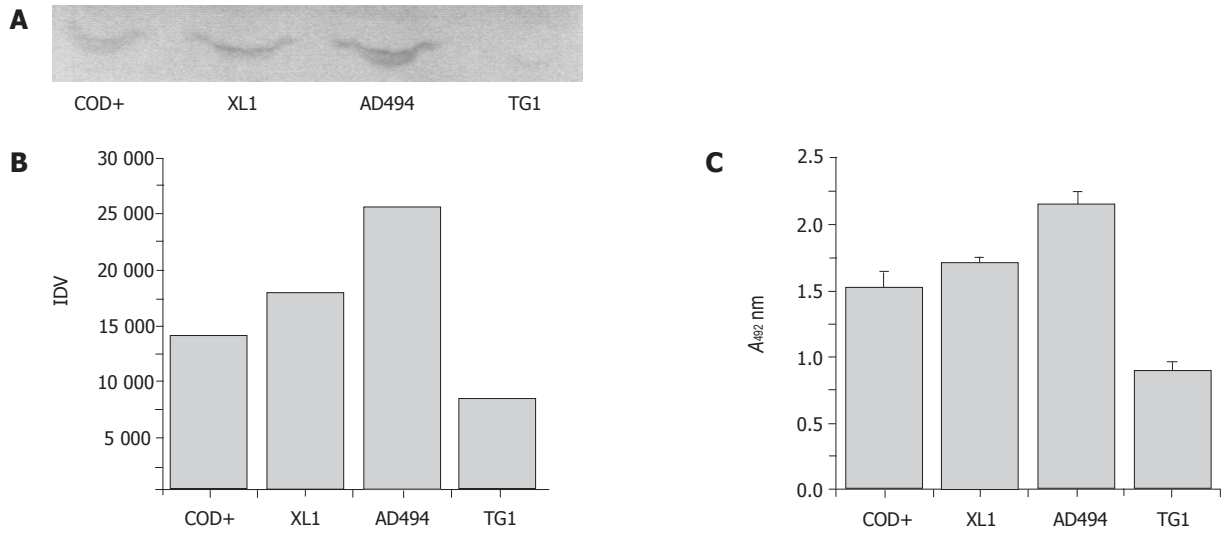

Figure 6 Expression profile of the chimeric Fab in different strains of *E. coli*. The chimeric Fab was expressed in soluble form in different *E. coli* strains in identical conditions. Levels of expression of the chimeric Fab were checked by Western blot in non-reducing conditions (**A**). Intensities of bands were measured densitometrically (**B**). Levels of expression were also checked by ELISA (**C**). Equal amount of the periplasmic extracts were allowed to bind to HBsAg coated on ELISA plate and bound chimeric Fab was detected. (XL1 = XL1-Blue, AD494 = AD494, COD+ = BL21 Codon Plus, TG1 = TG1, IDV = integrated density value).

Table 2 Yields of the anti-HBs chimeric Fab in different *E. coli* strains

E. coli strain	Yield (μg/L)[1]
XL1-Blue	40
AD494	62
BL21 Codon Plus	40
TG1	8

[1]Estimated by Bradford assay, after purification by protein G column

of the line in Figure 5, the K_D of the chimeric anti-HBs Fab is 8.166±0.14 nmol/L, (r^2 = 0.914).

Expression of the chimeric Fab in different *E.coli* strains: Yield of this chimeric Fab in *E. coli* XL1-Blue cells was found to be low (~40 μg/L). The recombinant construct pCOMB3H-Fd-L-Sol was transformed into three other strains of *E. coli*, (AD494, BL21 CodonPlus and TG1) to check the yield of the chimeric Fab in soluble form. The chimeric Fab was expressed in these cells in the same fashion as stated above for XL1-Blue cells. The levels of expression of the chimeric Fab in different *E. coli* strains were checked by Western Blot and compared densitometrically (Figures 6A and B). The levels of expression of the chimeric Fab in different strains of *E. coli* were further confirmed by ELISA using crude periplasmic extracts. The result of the ELISA is shown in Figure 6C. Yields of the purified chimeric Fab expressed in different *E. coli* strains are shown in Table 2. As shown in Figure 6 and Table 2, maximum yield of the chimeric Fab was observed in case of *E. coli* AD494 cells.

DISCUSSION

5S is a mouse monoclonal that binds to HBsAg with high affinity[13]. However, like any other mouse monoclonal, this antibody can give rise to HAMA response and cannot be used clinically. HAMA may neutralize the injected mouse antibody directly by immune complex formation, which could lead to rapid clearance or to hypersensitivity reactions[38,39]. As immunogenic reactions are predominantly directed towards the Fc region of murine antibodies[16], creation of mouse-human chimeric antibodies by swapping murine constant regions with the human ones can address the problem of HAMA response, at least in part[17-19]. But such domain swapping can alter the immunological and pharmacokinetic properties of an antibody, making the task of generation of chimeric antibodies quite tricky[40].

One of the crucial aspects in generation of chimeric antibodies is the selection of human isotypes for domain swapping. Effector functions of antibody constant domains are broadly dependent on the antibody classes and subclasses[41]. Usually human IgG1 is the preferred choice for chimeric antibodies in situations where activation of effector functions is the desired outcome[42]. Rath and Devey[43] had observed that the subclasses of antibodies associated with HBsAg in circulating immune complexes of patients with either acute or chronic HBV infections were predominantly IgG1 and IgG4. A study involving children, who have recovered from acute hepatitis B, has shown that after natural seroconversion, specific antibodies were highly restricted to IgG1[44]. It has also been observed that anti-HBs IgG1 is predominant after vaccination with recombinant vaccines[44,45].

Apart from being important for effector functions, the choice of isotype can also affect the antigen binding of a chimeric molecule. It has been observed that changes in constant domains can affect the functional affinity and specificity of antibodies[46]. Pritsch *et al*.[47] have shown that Fab fragments of antibodies sharing identical variable regions but C_H1 of different isotypes have significant differences in affinities. A molecular dynamic study

involving anti-HEL Fab has shown that, the interactions between C_L and C_H1 domains may have influence not only around the local interface between C_L and C_H1 but also around the interacting regions between HEL and Fv[48].

In the present work, the variable region genes of 5S (IgG1/κ) were fused with the C_H1 region of human IgG1 and human kappa chain constant region, to generate a mouse-human chimeric Fab. The C_H1 region of IgG1 and kappa C_L were amplified using RNA extracted from human PBLs and linked with respective variable regions of 5S hybridoma by overlap PCR. The chimeric fragments were subsequently cloned into the phagemid vector pCOMB3H and phage antibodies were expressed. Functional clones were selected by biopanning over antigen coated plate and selected clones were checked for binding by phage ELISA. It is well known that cloning of antibody genes by PCR may introduce mutations and may amplify truncated antibody genes, generating clones that are non-functional[49,50]. Use of a phagemid expression system allows the initial expression of antibody molecules as phage antibodies, which can be easily selected for antigen binding and then be further processed for soluble expression. As shown in Figure 2, two of the four clones checked by phage ELISA after three rounds of biopanning showed high binding. Clone 1 was further processed for soluble expression of the chimeric Fab. SDS-PAGE and Western blot in both reducing and non-reducing conditions confirmed that the chimeric Fab was expressed in the form of a heterodimer (Figures 3A and B). The chimeric Fab was further characterized by ELISA and competitive ELISA. Competitive ELISA confirmed that the chimeric Fab and the original mouse monoclonal bind to the same epitope (Figure 4B). The dissociation constant of the chimeric Fab as determined by the ELISA based method was found to be high (8.166±0.14 nmol/L). The dissociation constant for the original mouse monoclonal is 0.8899 nmol/L[13]. Given the level of accuracy of the method used for the determination of K_D values, one can consider both of these values to be in the same broad range. An anti-human antibody was used in the ELISA to calculate the K_D of the chimeric Fab; whereas an anti-mouse antibody was used in case of the mouse monoclonal. Such a difference in experimental setup can also be attributed for the difference in K_D values.

Though it seems simple, high yield expression of heterologous proteins in bacterial systems sometimes proves to be problematic. Multiple factors like codon usage[51], DNA/RNA/Protein interaction[52], regulatory factors for transcription and translation and nucleotide usage in the leader peptide[53] affect the yield of heterologous proteins in bacteria. The yield of Fab depends upon the relative levels of expression of the light chain and Fd. The light chain-heavy chain balance depends upon codon usage in the signal peptides and 5' sequence of coding regions[54]. In this present work, the yield of soluble recombinant Fab in XL1-Blue cells was low (~40 μg/L). Such a low yield of Fab fragment expressed in *E. coli* using pCOMB3H vector system has been reported earlier[55]. To optimize the yield of the soluble chimeric Fab, the recombinant construct was transformed in different *E. coli* strains — TG1, AD 494 and BL21 CodonPlus. *E. coli* BL21 CodonPlus-RP (Novagen) cells contain extra copies of the *argU* and *proL* genes. These genes encode tRNAs that recognize the arginine codons AGA, AGG and the proline codon CCC, respectively. *E. coli* BL21 has been used for high-level expression of several antibody fragments[56,57]. *E. coli* AD494 cells are thioredoxin negative (*trxB*$^-$), thereby providing an oxidizing environment in the cytoplasm. Proper folding and assembly of antibody domains require inter- and intra-chain disulphide bond formation. Therefore bacterial periplasm is suitable for the assembly of functional Fab fragments. An oxidizing environment in the cytoplasm may also help to increase the yield of properly folded soluble antibody fragments. We expressed the anti-HBs chimeric Fab in soluble form in different *E. coli* strains under identical conditions. As shown in Figure 6 and Table 2, there was a slight increase in the expression of the chimeric Fab in AD494 cells; whereas the expression in BL21 was equivalent to that in XL1-Blue cells. Though Raffai *et al*.[55] had observed increased yield of soluble Fab fragment in TG1 in comparison to XL1-Blue cells, we could not detect any such increase in yield.

Though chimerization and humanization are essential to reduce immunogenicity of non-human antibodies before they can be used clinically such genetic engineering can alter functional capabilities of the molecule, often leading to loss of binding or reduction in affinity. Our results show that the chimerization of the 5S mouse monoclonal did not disturb its binding to the antigen and the chimeric Fab binds to the same epitope as that of the original mouse monoclonal. Though chimeric and monovalent in nature, the affinity of the recombinant chimeric Fab remained in the same range as the mouse monoclonal 5S. The high affinity binding of this chimeric Fab fragment indicates that it can be further modified to generate a clinically applicable full-length chimeric anti-HBs antibody, with out any significant loss of binding affinity.

ACKNOWLEDGMENTS

We are thankful to Dr. Dennis R. Burton and The Scripps Research Institute, La Jolla, USA for providing the vector pCOM3H. We thank Dr. Vijay Chaudhary for his gift of anti-M13 antibody. We are also thankful to M/s. Mathura Prasad and Satish for their technical and secretarial assistance.

REFERENCES

1 **Lavanchy D**. Hepatitis B virus epidemiology, disease burden, treatment, and current and emerging prevention and control measures. *J Viral Hepat* 2004; **11:** 97-107
2 **Chisari FV**, Ferrari C. Hepatitis B virus immunopathology. *Springer Semin Immunopathol* 1995; **17:** 261-281
3 **Milich DR**, Chen M, Schodel F, Peterson DL, Jones JE, Hughes JL. Role of B cells in antigen presentation of the hepatitis B core. *Proc Natl Acad Sci USA* 1997; **94:** 14648-14653
4 **Magnius LO**, Norder H. Subtypes, genotypes and molecular epidemiology of the hepatitis B virus as reflected by sequence

variability of the S-gene. *Intervirology* 1995; **38:** 24-34
5 **Prince AM**, Szmuness W, Woods KR, Grady GF. Antibody against serum-hepatitis antigen. Prevalence and potential use as immune serum globulin in prevention of serum-hepatitis infections. *N Engl J Med* 1971; **285:** 933-938
6 **Karasu Z**, Ozacar T, Akyildiz M, Demirbas T, Arikan C, Kobat A, Akarca U, Ersoz G, Gunsar F, Batur Y, Kilic M, Tokat Y. Low-dose hepatitis B immune globulin and higher-dose lamivudine combination to prevent hepatitis B virus recurrence after liver transplantation. *Antivir Ther* 2004; **9:** 921-927
7 **Beasley RP**, Hwang LY, Lee GC, Lan CC, Roan CH, Huang FY, Chen CL. Prevention of perinatally transmitted hepatitis B virus infections with hepatitis B virus infections with hepatitis B immune globulin and hepatitis B vaccine. *Lancet* 1983; **2:** 1099-1102
8 **Li XM**, Yang YB, Hou HY, Shi ZJ, Shen HM, Teng BQ, Li AM, Shi MF, Zou L. Interruption of HBV intrauterine transmission: a clinical study. *World J Gastroenterol* 2003; **9:** 1501-1503
9 **Li YW**, Lawrie DK, Thammana P, Moore GP, Shearman CW. Construction, expression and characterization of a murine/human chimeric antibody with specificity for hepatitis B surface antigen. *Mol Immunol* 1990; **27:** 303-311
10 **Zheng W**, Tan H, Song S, Lu H, Wang Y, Yu Y, Yin R. The construction and expression of a fusion protein consisting anti-HBsAg antibody fragment Fab and interferon-a in E.coli. *World J Gastroenterol* 2000; **6(Suppl 3):** tk 83a
11 **Sanchez L**, Ayala M, Freyre F, Pedroso I, Bell H, Falcon V, Gavilondo JV. High cytoplasmic expression in E. coli, purification, and in vitro refolding of a single chain Fv antibody fragment against the hepatitis B surface antigen. *J Biotechnol* 1999; **72:** 13-20
12 **Maeda F**, Nagatsuka Y, Ihara S, Aotsuka S, Ono Y, Inoko H, Takekoshi M. Bacterial expression of a human recombinant monoclonal antibody fab fragment against hepatitis B surface antigen. *J Med Virol* 1999; **58:** 338-345
13 **Bose B**, Chugh DA, Kala M, Acharya SK, Khanna N, Sinha S. Characterization and molecular modeling of a highly stable anti-Hepatitis B surface antigen scFv. *Mol Immunol* 2003; **40:** 617-631
14 **Schroff RW**, Foon KA, Beatty SM, Oldham RK, Morgan AC Jr. Human anti-murine immunoglobulin responses in patients receiving monoclonal antibody therapy. *Cancer Res* 1985; **45:** 879-885
15 **Shawler DL**, Bartholomew RM, Smith LM, Dillman RO. Human immune response to multiple injections of murine monoclonal IgG. *J Immunol* 1985; **135:** 1530-1535
16 **Spiegelberg HL**, Weigle WO. Studies on the catabolism of gamma- G subunits and chains. *J Immunol* 1965; **95:** 1034-1040
17 **Reist CJ**, Bigner DD, Zalutsky MR. Human IgG2 constant region enhances in vivo stability of anti-tenascin antibody 81C6 compared with its murine parent. *Clin Cancer Res* 1998; **4:** 2495-2502
18 **Colcher D**, Milenic D, Roselli M, Raubitschek A, Yarranton G, King D, Adair J, Whittle N, Bodmer M, Schlom J. Characterization and biodistribution of recombinant and recombinant/chimeric constructs of monoclonal antibody B72.3. *Cancer Res* 1989; **49:** 1738-1745
19 **Yata Y**, Otsuji E, Okamoto K, Tsuruta H, Kobayashi S, Toma A, Yamagishi H. Decreased production of anti-mouse antibody after administration of human/mouse chimeric monoclonal antibody-neocarzinostatin conjugate to human. *Hepatogastroenterology* 2003; **50:** 80-84
20 **Dimmock NJ.** Mechanisms of neutralization of animal viruses. *J Gen Virol* 1984; **65 (Pt 6):** 1015-1022
21 **Burton DR**, Williamson RA, Parren PW. Antibody and virus: binding and neutralization. *Virology* 2000; **270:** 1-3
22 **Cheung SC**, Dietzschold B, Koprowski H, Notkins AL, Rando RF. A recombinant human Fab expressed in Escherichia coli neutralizes rabies virus. *J Virol* 1992; **66:** 6714-6720
23 **Barbas CF 3rd,** Bjorling E, Chiodi F, Dunlop N, Cababa D, Jones TM, Zebedee SL, Persson MA, Nara PL, Norrby E. Recombinant human Fab fragments neutralize human type 1 immunodeficiency virus in vitro. *Proc Natl Acad Sci USA* 1992; **89:** 9339-9343
24 **Barbas CF 3rd,** Crowe JE Jr, Cababa D, Jones TM, Zebedee SL, Murphy BR, Chanock RM, Burton DR. Human monoclonal Fab fragments derived from a combinatorial library bind to respiratory syncytial virus F glycoprotein and neutralize infectivity. *Proc Natl Acad Sci USA* 1992; **89:** 10164-10168
25 **Lamarre A**, Talbot PJ. Protection from lethal coronavirus infection by immunoglobulin fragments. *J Immunol* 1995; **154:** 3975-3984
26 **Thullier P**, Lafaye P, Megret F, Deubel V, Jouan A, Mazie JC. A recombinant Fab neutralizes dengue virus in vitro. *J Biotechnol* 1999; **69:** 183-190
27 **Tada H**, Yanagida M, Mishina J, Fujii T, Baba K, Ishikawa S, Aihara S, Tsuda F, Miyakawa Y, Mayumi M. Combined passive and active immunization for preventing perinatal transmission of hepatitis B virus carrier state. *Pediatrics* 1982; **70:** 613-619
28 **Skerra A**. Bacterial expression of immunoglobulin fragments. *Curr Opin Immunol* 1993; **5:** 256-262
29 **Gram H**, Marconi LA, Barbas CF 3rd, Collet TA, Lerner RA, Kang AS. In vitro selection and affinity maturation of antibodies from a naive combinatorial immunoglobulin library. *Proc Natl Acad Sci USA* 1992; **89:** 3576-3580
30 **Rosok MJ**, Yelton DE, Harris LJ, Bajorath J, Hellstrom KE, Hellstrom I, Cruz GA, Kristensson K, Lin H, Huse WD, Glaser SM. A combinatorial library strategy for the rapid humanization of anticarcinoma BR96 Fab. *J Biol Chem* 1996; **271:** 22611-22618
31 **Ames RS**, Tornetta MA, Deen K, Jones CS, Swift AM, Ganguly S. Conversion of murine Fabs isolated from a combinatorial phage display library to full length immunoglobulins. *J Immunol Methods* 1995; **184:** 177-186
32 **Bender E**, Woof JM, Atkin JD, Barker MD, Bebbington CR, Burton DR. Recombinant human antibodies: linkage of an Fab fragment from a combinatorial library to an Fc fragment for expression in mammalian cell culture. *Hum Antibodies Hybridomas* 1993; **4:** 74-79
33 **Barbas CF 3rd**, Kang AS, Lerner RA, Benkovic SJ. Assembly of combinatorial antibody libraries on phage surfaces: the gene III site. *Proc Natl Acad Sci USA* 1991; **88**: 7978-7982
34 **Sambrook J**, Russell DW. Molecular Cloning: A Laboratory Manual. 3rd ed. Cold Spring Harbor, New York: Cold Spring Harbor Laboratory Press, 2001: 1.116-1.118
35 **Barbas CF 3rd**, Burton DR, Scott JK, Silverman GJ. Phage Display: A Laboratory Manual. 1st ed. Cold Spring Harbor, NY: Cold Spring Harbor Laboratory Press, 2001: 23.11-23.12
36 **Friguet B**, Chaffotte AF, Djavadi-Ohaniance L, Goldberg ME. Measurements of the true affinity constant in solution of antigen-antibody complexes by enzyme-linked immunosorbent assay. *J Immunol Methods* 1985; **77:** 305-319
37 **Bradford MM**. A rapid and sensitive method for the quantitation of microgram quantities of protein utilizing the principle of protein-dye binding. *Anal Biochem* 1976; **72:** 248-254
38 **Sakahara H**, Reynolds JC, Carrasquillo JA, Lora ME, Maloney PJ, Lotze MT, Larson SM, Neumann RD. In vitro complex formation and biodistribution of mouse antitumor monoclonal antibody in cancer patients. *J Nucl Med* 1989; **30:** 1311-1317
39 **Rettenbacher L**, Galvan G. [Anaphylactic shock after repeated injection of 99mTc-labeled CEA antibody] *Nuklearmedizin* 1994; **33**: 127-128
40 **Colcher D**, Goel A, Pavlinkova G, Beresford G, Booth B, Batra SK. Effects of genetic engineering on the pharmacokinetics of antibodies. *Q J Nucl Med* 1999; **43:** 132-139
41 **Clark MR**. IgG effector mechanisms. *Chem Immunol* 1997; **65:** 88-110
42 **Steplewski Z**, Sun LK, Shearman CW, Ghrayeb J, Daddona

P, Koprowski H. Biological activity of human-mouse IgG1, IgG2, IgG3, and IgG4 chimeric monoclonal antibodies with antitumor specificity. *Proc Natl Acad Sci USA* 1988; **85:** 4852-4856

43 **Rath S**, Devey ME. IgG subclass composition of antibodies to HBsAg in circulating immune complexes from patients with hepatitis B virus infections. *Clin Exp Immunol* 1988; **72:** 164-167

44 **Gregorek H**, Madalinski K, Woynarowski M, Mikolajewicz J, Syczewska M, Socha J. The IgG subclass profile of anti-HBs response in vaccinated children and children seroconverted after natural infection. *Vaccine* 2000; **18:** 1210-1217

45 **Honorati MC**, Borzi RM, Dolzani P, Toneguzzi S, Facchini A. Distribution of IgG subclasses after anti-hepatitis B virus immunization with a recombinant vaccine. *Int J Clin Lab Res* 1997; **27:** 202-206

46 **Cooper LJ**, Robertson D, Granzow R, Greenspan NS. Variable domain-identical antibodies exhibit IgG subclass-related differences in affinity and kinetic constants as determined by surface plasmon resonance. *Mol Immunol* 1994; **31:** 577-584

47 **Pritsch O**, Hudry-Clergeon G, Buckle M, Petillot Y, Bouvet JP, Gagnon J, Dighiero G. Can immunoglobulin C(H)1 constant region domain modulate antigen binding affinity of antibodies? *J Clin Invest* 1996; **98:** 2235-2243

48 **Adachi M**, Kurihara Y, Nojima H, Takeda-Shitaka M, Kamiya K, Umeyama H. Interaction between the antigen and antibody is controlled by the constant domains: normal mode dynamics of the HEL-HyHEL-10 complex. *Protein Sci* 2003; **12:** 2125-2131

49 **Strohal R**, Kroemer G, Wick G, Kofler R. Complete variable region sequence of a nonfunctionally rearranged kappa light chain transcribed in the nonsecretor P3-X63-Ag8.653 myeloma cell line. *Nucleic Acids Res* 1987; **15:** 2771

50 **Duan L**, Pomerantz RJ. Elimination of endogenous aberrant kappa chain transcripts from sp2/0-derived hybridoma cells by specific ribozyme cleavage: utility in genetic therapy of HIV-1 infections. *Nucleic Acids Res* 1994; **22:** 5433-5438

51 **Andersson SG**, Kurland CG. Codon preferences in free-living microorganisms. *Microbiol Rev* 1990; **54:** 198-210

52 **Jacques N**, Dreyfus M. Translation initiation in Escherichia coli: old and new questions. *Mol Microbiol* 1990; **4:** 1063-1067

53 **Stemmer WP**, Morris SK, Kautzer CR, Wilson BS. Increased antibody expression from Escherichia coli through wobble-base library mutagenesis by enzymatic inverse PCR. *Gene* 1993; **123:** 1-7

54 **Humphreys DP**, Carrington B, Bowering LC, Ganesh R, Sehdev M, Smith BJ, King LM, Reeks DG, Lawson A, Popplewell AG. A plasmid system for optimization of Fab' production in Escherichia coli: importance of balance of heavy chain and light chain synthesis. *Protein Expr Purif* 2002; **26:** 309-320

55 **Raffai R**, Vukmirica J, Weisgraber KH, Rassart E, Innerarity TL, Milne R. Bacterial expression and purification of the Fab fragment of a monoclonal antibody specific for the low-density lipoprotein receptor-binding site of human apolipoprotein E. *Protein Expr Purif* 1999; **16:** 84-90

56 **Fan JY**, Wang G, Li W, Wu YM, Liu YF. [Expression of human Fab antibody against keratin in E.coli and its renaturation] *Xi Bao Yu Fen Zi Mian Yi Xue Za Zhi* 2004; **20:** 441-443

57 **Wang C**, Hou LH, Zhang YM, Li JM, Liao ZL, Du GX, Chen W, Sun QH, Tong YG. Construction and expression of anti-human integrin alphavbeta3 scFv. *Xi Bao Yu Fen Zi Mian Yi Xue Za Zhi* 2004; **20:** 159-162

Science Editor Guo SY **Language Editor** Elsevier HK

PO Box 2345, Beijing 100023, China
www.wjgnet.com
wjg@wjgnet.com

ELSEVIER

World J Gastroenterol 2005;11(48):7579-7584
World Journal of Gastroenterology ISSN 1007-9327

Application of restriction display PCR technique in the preparation of cDNA microarray probes

Zhao-Hui Sun, Wen-Li Ma, Bao Zhang, Yi-Fei Peng, Wen-Ling Zheng

Zhao-Hui Sun, Wen-Li MA, Bao Zhang, Yi-Fei Peng, Institute of Genetic Engineering, Southern Medical University, Guangzhou 510515, Guangdong Province, China
Wen-Ling Zheng, Institute of Molecular Oncology, Guangzhou General Hospital of Guangzhou Military Area Command, Guangzhou 510010, Guangdong Province, China
Supported by the National Natural Science Foundation of China, No. 39880032; Major Programs for Science and Technology Development of Guangzhou, No. 01-Z-005-01
Co-first-authors: Wen-Li Ma and Zhao-Hui Sun
Correspondence to: Professor Wen-Li Ma, Institute of Genetic Engineering, Southern Medical University, Guangzhou 510515, Guangdong Province, China. wenli@fimmu.com
Telephone: +86-20-61648210 Fax: +86-20-61647755
Received: 2005-04-14 Accepted: 2005-07-15

Abstract

AIM: To develop a simplified and efficient method for the preparation of hepatitis C virus (HCV) cDNA microarray probes.

METHODS: With the technique of restriction display PCR (RD-PCR), restriction enzyme *Sau3A* I was chosen to digest the full-length HCV cDNAs. The products were classified and re-amplified by RD-PCR. We separated the differential genes by polyacrylamide gel electrophoresis and silver staining. Single bands cut out from the polyacrylamide gel were isolated. The third-round PCR was performed using the single bands as PCR template. The RD-PCR fragments were purified and cloned into the pMD18-T vector. The recombinant plasmids were extracted from positive clones, and the target gene fragments were sequenced. The cDNA microarray was prepared by spotting RD-PCR products to the surface of amino-modified glass slides using a robot. We validated the detection of microarray by hybridization and sequence analysis.

RESULTS: A total of 24 different cDNA fragments ranging from 200 to 800 bp were isolated and sequenced, which were the specific gene fragments of HCV. These fragments could be further used as probes in microarray preparation. The diagnostic capability of the microarray was evaluated after the washing and scanning steps. The results of hybridization and sequence analysis showed that the specificity, sensitivity, accuracy, reproducibility, and linearity in detecting HCV RNA were satisfactory.

CONCLUSION: The RD-PCR technique is of great value in obtaining a large number of size-comparable gene probes, which provides a speedy protocol in generating probes for the preparation of microarrays. Microarray prepared as such could be further optimized and applied in the clinical diagnosis of HCV.

Key words: Restriction display PCR; HCV; Microarray; Probes

Sun ZH, Ma WL, Zhang B, Peng YF, Zheng WL. Application of restriction display PCR technique in the preparation of cDNA microarray probes. *World J Gastroenterol* 2005; 11(48): 7579-7584
http://www.wjgnet.com/1007-9327/11/7579.asp

INTRODUCTION

Hepatitis C virus (HCV) is a RNA virus with a high rate of genetic mutation[1]. HCV has a linear genome approximately 10 kb in length, which consists of a positive sense single-stranded RNA (ssRNA)[2]. Consistent with related members of the family *Flaviviridae,* HCV demonstrates a high degree of sequence variation throughout its genome. Sequence analysis of multiple strains of HCV has demonstrated that the nucleotide sequence can differ by as high as 30%[3]. Infection with HCV has been identified as the major cause of post-transfusion non-A, non-B hepatitis, and is a major public health problem in most areas of the world, raising the issues of its diagnosis, treatment, and prevention[4-6].

In the present study, we utilized the technique of restriction display PCR (RD-PCR) to prepare HCV cDNA chip probes. Restriction enzyme *Sau3A* I was chosen to digest the full-length HCV cDNAs. The products were classified and re-amplified by RD-PCR. We separated the differential genes by polyacrylamide gel electrophoresis and silver staining. The cDNA microarray was prepared by spotting RD-PCR products to the surface of amino-modified glass slides using a robot. The specificity, sensitivity, accuracy, reproducibility, and linearity in detecting HCV RNA were evaluated.

MATERIALS AND METHODS

Probe template

The full-length plasmid of HCV pCV-J4L6S was presented

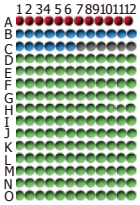

Figure 1 Arrangement of all spots on gene chip. Positive controls, negative controls, empty controls, HCV probes.

by Dr Jens Bukh of NIH (USA)[7].

Chemicals and reagents

Premix Taq, dNTP, *Eco*RI, *Not*I, *Xba*I, *Sau*3A I, pMD18-T vector, and T4 DNA ligase were obtained from Takara Corp. (Japan). Dimethyl sulfoxide (DMSO) was bought from Sangon (Shanghai, China). Plasmid Miniprep kits, 3S PCR purification kit V20 were purchased from Shen Neng Bo Cai Corp. (China). PCR primers of HCV and the primers in pMD18-T vector were synthesized by BioAsia Corp. (China). Universal primer (U) cy3-GTTTG GCTGGTGT GGATC, selective primers (similar with U but with one "nesting" base overhanging at 3'-end, UA, UT, UC, UG) and the adapter (SIP, SIR) were purchased from GIBCO Corp. (USA).

Instruments

GenePix 4000B scanner and ScanArray Lite were provided by GSI Lumonics (Billerica, USA). GS Gene Linker ultraviolet chamber was obtained from BioRad (Hercules, USA). PixSys 5500 gene chip printing machine was purchased from Cartesian Technologies (Irvine, USA). CMT-GAPSTM coated slides and Corning CMT-Hybridization™ chambers were ordered from Corning Microarray Technology (Acton, USA).

Bacterial strains

The *E. coli* strain XL-1 used in experiments was maintained in our laboratory.

Probe preparation

To isolate HCV genomes, plasmid pCV-J4L6S was digested with *Not*I and *Xba*I. The plasmid (1-2 μg) was added to a total volume of 20 μL mixture at 37 °C for 4 h. The target HCV gene was isolated and recovered with UNIQ-5 column DNA extraction kit (Sangon, China). RD-PCR was performed as previously described[8-10]. The recovered HCV cDNAs were digested with 2 μL *Sau*3A1 (5'↓ GATC3') (10 U/μL) in a total volume of 20 μL mixture at 37 °C for 3 h. The two ends of each *Sau*3AI-digested fragment were linked to an adapter that was prepared by annealing the 2 oligonucleotides containing the sequences of 5'-GATCCACACCAGCCAAACC CA (SIP) and 5' -GGTTTGGCTGGTGTG (SIR) in a ligation reaction containing 1 μL T4 DNA ligase (350 U/μL), 1 μL 10× DNA ligation buffer, 1 μL adapter (50 μmol/L), 20 pmol of digested HCV cDNA fragments of *Sau*3AI, and then UPW was added for a total of 10 μL. After 4 h of ligation at 16 °C, PCR was performed in a 9700 thermocycler with an initial denaturation at 94 °C for 5 min, followed by 35 cycles at 94 °C for 30 s, at 60 °C for 30 s, at 72 °C for 1 min, and a final extension at 72 °C for 7 min. PCR primers were designed to match the universal adapters, including the restriction site sequence, but with one "nesting" base overhanging at the 3'-end, and the reactions were divided into 10 subgroups. To check for positive PCR results, 7 μL of the PCR products was loaded onto 5% polyacrylamide (Takara, Japan) gel electrophoresis at 90 V for 5-6 h and the technique of DNA silver staining[11] was used to separate different target gene fragments.

DNA microarray printing

The final concentration of each probe was adjusted to 0.3 mg/mL with DMSO and water. The DMSO concentration was 50% (v/v). The probes were spotted onto a CMT-GAPS aminosilane-coated glass microscope slide at 25 °C and 60% relative humidity, using the ArrayIt ChipMaker2™ microspotting pins (TeleChem International, Sunnyvale, USA) and a Cartesian PixSys 5500 robot. A microarray of 12×15 spots was printed. The arrangement of all spots on the gene chip is shown in Figure 1. After printing, the slide was rehybridized and snap-dried in a plate at 80 °C for 5 min. A BioRad UV crosslinker was used to immobilize the DNAs onto the slide with 125 mJ of energy. The slide was treated with blocking solution (335 mL 1-methyl-2-pyrrolidinone, 6 g succinic anhydride and 15 mL 1 mol/L sodium borate, pH 8) and stored for later use.

Fluorescent labeling

The samples of HCV were digested at 37 °C with the restriction enzyme *Sau*3AI. T4 DNA ligase was used to link gene fragments with universal adapters (SIP, SIR). After 3 h of ligation at 16 °C, 25 μL 2×premix, 2 μL of linkage products, 2 μL of Cy3 labeled universal primer matched with the adapter, and 21 μL of water were added for a total volume of 50 μL. Reactions were performed in a GeneAmp PCR 9700 system with an initial denaturation at 94 °C for 10 min, and then subjected to 30 thermal cycles at 94 °C for 30 s, at 60 °C for 30 s, at 72 °C for 1 min, followed by a final incubation at 72 °C for 5 min. Finally, the reaction was stopped by cooling down the solution to 4 °C. After this labeling reaction, the sample DNA fragments of hundreds of base pairs were labeled with fluorescent Cy3. The labeled PCR products were further purified using a 3S PCR product purification kit V20. Of the 30 μL purified products, 5 μL was used for hybridization with the microarray probes.

Pre-hybridization and hybridization

The slide was incubated in 25% formamide, 5×SSC, 0.1% sodium dodecyl sulfate (SDS) in a jar for 45 min at 42 °C, rinsed 5 times in distilled water, immersed in isopropyl alcohol for 1 s, and then dried in the air. Five microliters of Cy3 labeled samples was mixed with 1 μL Cot-1 DNA (20 μg/μL, Life Technologies) and 6 μL 2×hybridization

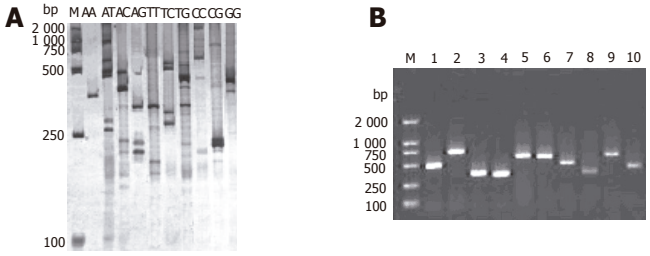

Figure 2 RD-PCR patterns of HCV genes (**A**) and 1.5% agarose gel electrophoresis of RD-PCR products from the white clones of HCV genomic fragments (**B**). M: MDL2 000 standard DNA ladder; lanes 1-10: PCR products of positive clones.

buffer (50% formamide, 10×SSC, 0.2% SDS) that was preheated at 42 °C, then heated to 95 °C for 5 min and centrifuged at 14 000 *g* for 2 min. This mixture was completely pipetted onto the pre-hybridized lambda phage DNA microarray slide and covered with a glass coverslip pretreated with Sigmacote® (Sigma, St. Louis, USA) to keep the sample from evaporating. The slide was put into a sealed hybridization box, 10 μL UPW was added to each well at the two ends of the chamber. The sealed chamber containing the DNA microarray slide was placed in a 42 °C water bath. After 4 h of incubation, the slide was taken out and washed in low-stringency washing buffer containing 1 ×SSC and 0.2% SDS at 42 °C for 5 min, in high-stringency washing buffer containing 0.1×SSC and 0.2% SDS at room temperature for 10 min, in 0.1×SSC and Milli Q water and ethanol, respectively. Finally, the air-dried slide was scanned using the ScanArray® Lite MicroArray Analysis System.

Scanning and analysis

The hybridized microarrays were scanned using GenePix 4000B scanner under the conditions of 90% laser power and 70% photo-multiplier tube (PMT). The results were analyzed using the QuantArray array analysis software. The criteria for positivity included the average fluorescence signal of Cy3 being three times as great as the value of the negative point, with a retro value of 2.7-3.3.

Probe optimization and printing

Ten HCV gene fragments were selected from the high value of the hybridized fluorescence signals to low fluorescence signals as microarray probes. The probes were spotted onto a CMT-GAPS aminosilane-coated glass microscope slide at 25 °C and 60% relative humidity, using the ArrayIt ChipMaker2™ microspotting pins and a Cartesian PixSys 5500 robot. A microarray of 12×8 spots was printed. The arrangement of all spots on the gene chip was similar to that shown in Figure 1. After printing, the slide was rehybridized and snap-dried in a plate at 80 °C for 5 min. A BioRad UV crosslinker was used to immobilize the DNAs onto the slide with 125 mJ of energy. The slide was treated with blocking solution and stored for later use.

Evaluation of microarray in sample detection

The specificity, sensitivity, accuracy, reproducibility, and linearity of this assay system were evaluated.

Identification of microarray probes and positive serum samples

After purification using the 3S PCR purification kit V20, the RD-PCR products (for probe preparation) and real-time RT-PCR products (for clinical serum sample detection) were inserted into the pMD18-T vector. The ligation mixture containing 4 μL of PCR products, 1 μL of pMD18-T vector (50 ng/μL) and 5 μL of loading buffer solution was incubated at 16 °C for 3 h, and then transferred into 100 μL of XL-1 *E. coli* competent cells treated with solutions containing Ca^{2+} ions (0.1 mol/L). To transform *E. coli*, the mixture of DNA formed in a ligation reaction was combined with a suspension of competent cells for 30 min, then heat-shocked at 42 °C for 1-2 min. The cells were then incubated in a growth medium and finally spread on an agar plate and incubated until single bacterial colonies were grown. Then the clones containing target fragments were selected and identified with the pMD18-T vector primer (primer A 5'-GTAAAACGACGGCC AGT-3', primer B 5'-CAGGAAACAGCTATGAC-3'). To check for positive PCR results, 5 μL of the PCR products was analyzed by 1.5% agarose (Takara, Japan) gel electrophoresis at 75 V for 45 min with a DNA marker DL2000 (Takara, Japan) as reference. Then the sequence was analyzed with ABI Prism™ 3730 DNA sequencer, and GenBank Blast sequence alignments were done.

RESULTS

Probe preparation

Twenty-four gene fragments of HCV were found in each subgroup by RD-PCR amplification with the expected size. The products were separated by electrophoresis on 5% polyacrylamide gel, and cDNA bands were stained with a silver solution (Figure 2A). Each subgroup produced 1-5 single cDNA bands with their length ranging from 200 to 800 bp. These bands could be used as probes for chip manufacture. Figure 2B shows the 1.5% agarose gel electrophoresis results of the clones.

Microarray design

The clinical diagnostic microarray was prepared by immobilizing the captured target genes of pathogens on a slide specifically treated. The DNA or RNA extracted from the patient's serum was labeled with fluorochrome and hybridized to the target DNA. In this study, the microarray was prepared by spotting RD-PCR products of HCV onto the surfaces of glass slides using a Cartesian 5500 MicroArrayer. Controls were immobilized at the same time. The control system was composed of empty controls which were DMSO without gene fragments, negative controls which were gene fragments of plants (rice) (B1-6) and an eukaryocyte (K562 cell) (B7-12) and a prokaryocyte (*E. coli*) (C1-6) not homologous with HCV, positive controls which were the reconstructed gene fragments.

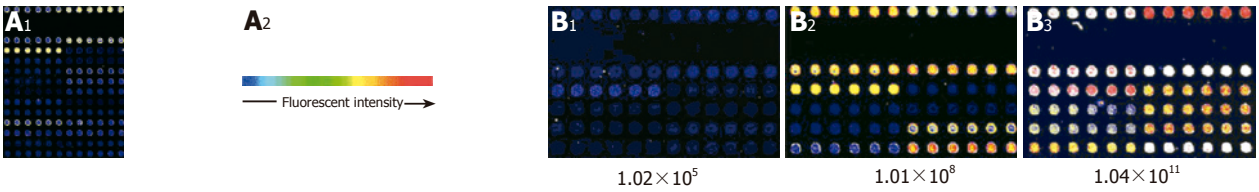

Figure 3 Scanning plots of hybridizing signals on gene chip of HCV (**A**) and modified gene chip (**B**). The samples were serially diluted (1.02×10^5, 1.01×10^8, 1.04×10^{11} copies/mL) and used in microarray analysis.

Eight of the 12×15 microarrays could be simultaneously immobilized on a glass slide.

Detection and analysis of hybridization

Based on the hybridizing signals under 90% laser energy and 70% GMT on the gene chip, the specificity and sensitivity in detecting HCV were satisfactory (Figure 3A). There was no signal on the empty control spots (printing 50% DMSO) and negative control spots (printing gene fragments of eukaryotic cells). The signal of spots hybridized to HCV positive controls and samples of HCV was strong and clear, but the analysis of variance showed that the density of signal was different in different probes (F = 8.325, P<0.001).

Optimization of microarray probes

Ten HCV gene fragments selected from the high- to low-density signals of hybridization were prepared for HCV gene chip probes. To obtain further information about the ten probes, we sequenced and analyzed the probes and found that nearly all of them had a similar length ranging 250-700 bp and a high GC content (≥40%) and T_m values (≥82 °C). The microarray was prepared by spotting the probes with Cartesian 5500 MicroArrayer. A microarray of 12×8 spots was printed. The arrangement of all spots on the gene chip is shown in Figure 1. The hybridization results indicated that the positive signal was strong compared to the hybridization signal (Figure 3B). There was no signal on the empty control spots and negative control spots.

Evaluation of microarray in sample detection

There was a strong linear relation between the concentrations of target cDNA and the fluorescence intensities obtained from microarray assay (r = 0.9819). The detection range of the microarray was 10^4-10^{11} copies/mL. The lower detection limit of HCV cDNA by microarray was 1.03×10^4 copies/mL, which was 2 log units lower than that by real-time RT-PCR. The reproducibility and accuracy of this assay system were evaluated by repeated measurement, and the within-run coefficient of validation was 6.6%, while the between-run coefficient of validation was 7.6%. Seventeen serum samples from hepatitis C patients (positive for anti-HCV, ALT≥80) were analyzed, and 15 patients (88.2%) were positive by microarray assay. Ten serum samples from healthy people were also evaluated and the results were all negative. The obtained sequences were verified and each sequenced PCR product was confirmed to be a HCV genome fragment using the basic local alignment search tool (BLAST) and the GenBank database.

DISCUSSION

HCV is the most important cause of transfusion-associated and community-acquired non-A, non-B hepatitis. Chronically infected individuals have a relatively high risk of developing chronic hepatitis, liver cirrhosis, and hepatocellular carcinoma. No effective vaccine therapy is available at present for HCV. Detection of HCV is essential for the correct diagnosis of HCV infection. Antibody-based methods have been considered as a practical way to detect infection of HCV. However, these methods cannot diagnose patients with hypoimmunity. Nucleic acid hybridization may have an excellent specificity, but its sensitivity is not satisfactory. In the protocol of PCR, cross contamination and false negative and positive incidents often occur. DNA microarray offers a solution to these problems and has the potential for the diagnosis of HCV infection. Compared to traditional diagnostic techniques, it has a number of advantages such as integration, micromation, and automatization[12,13]. The use of multiple independent gene fragments with a suitable size (ranging from 200 to 800 bp) for the probes to detect the same molecular targets can greatly enhance the signal-to-noise ratio and reduce the false-positive rate[14]. The gene chip also offers a dependable basis for the diagnosis and treatment of hepatotropic viral infections[15-17].

Probe preparation is a key step for microarray. One of the major difficulties in the development of microarray is to collect or prepare sufficient probes[18]. A few methods can be used to prepare microarray probes, including PCR amplification of DNA fragments with a molecular clone[19], artificial synthesis of oligonucleotide arrays by a DNA synthesizing machine[20] and light direction of *in situ* synthesis[21]. We prefer the first method because of its rapidity, simplicity, and effectiveness. However, conventional PCR is conducted with specific primers. RD-PCR provides an efficient and a simple way to obtain probes, since cDNA gene fragments digested by 4-cutter restriction endonuclease can be ligated with adapters at the same restriction site. In the present study, a PCR universal primer (U) was designed to match the sequence of both the adapters and the restriction site, but there were too many fragments amplified with universal primers (U). Using the selective primers with one or more

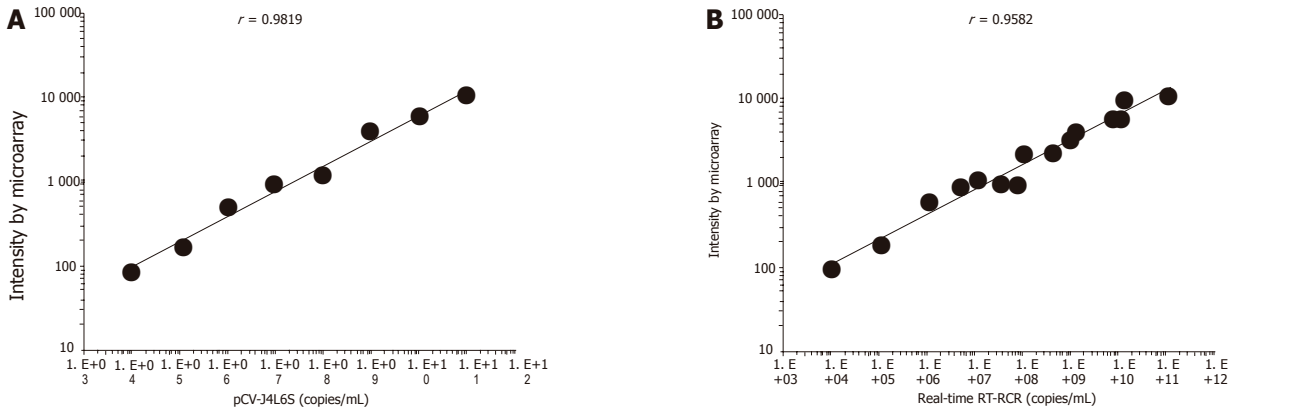

Figure 4 Fluorescence intensity from cDNA microarray analysis as a function of serial dilution from 10^4 to 10^{11} copies of plasmid pCV-J4L6S (r = 0.9819, ^bP<0.01)/mL (**A**) and comparison of the HCV RNA levels in 15 serum samples determined by cDNA microarray analysis and RT-PCR (Taqman) assays (**B**).

"nesting" bases at the 3'-end of universal primer, 10 or more subgroups of PCR reaction were performed for various single selective primers or primer combination, in which gene fragments were widely distributed in different groups and their isolation was achieved. We separated the differential genes by polyacrylamide gel electrophoresis and silver staining. Single bands cut out from polyacrylamide gel were isolated. Using the single bands as PCR template, we performed the third-round PCR and a total of 24 different cDNA fragments ranging from 200 to 800 bp were obtained and sequenced, which were the specific gene fragments of HCV. These fragments could be further used as probes in microarray preparation, suggesting that RD-PCR technique is of great value in obtaining a large number of size-comparable gene probes, thus providing a swift protocol in generating probes for the preparation of microarrays.

In general, the density of hybridization signal is correlative to the length of probes, GC contents and T_m value under the same experimental conditions. A further sequence analysis of the 10 probes, GC contents, and T_m value showed that these probes were 250-700 bp in length, and had a high GC content (≥40%) and T_m values (≥82 °C).The probes were widely distributed in the full HCV genome. The results of hybridization and sequence analysis showed that the specificity, sensitivity, accuracy, reproducibility, and linearity in detecting HCV RNA were satisfactory. There was a linear correlation between the concentrations of pCV-J4L6S target cDNA and the signal intensities (correlation coefficient = 0.9819). The detection range of the microarray was 10^4-10^{11} copies/mL. The lower detection limit of HCV RNA was 1.03×10^4 copies/mL, which was 2 log higher than that by RT-PCR (Taqman method). But the assay was as sensitive as the conventional RT-PCR in HCV detection. The chip we developed is cost-effective, and the procedure required to prepare the chip is straightforward and convenient. When results are verified by molecular hybridization, PCR cross contamination can be overcome. By incorporating negative and positive controls, the detection results can be reduced greatly using analytic software[22]. Seventeen serum samples from hepatitis C patients (positive for anti-HCV, ALT≥80) were analyzed, and fifteen patients (88.2%) were positive by microarray assay. Within the detection range of 10^4-10^{11} copies/mL, there was a good correlation between the two assay systems (n = 15, r = 0.9582) (Figure 4B). Ten serum samples from healthy people were also detected by this assay and no specific signal intensities were obtained from the samples. Finally, the reproducibility and accuracy of this assay system were evaluated by repeated measurement, and the within-run coefficient of validation was 6.6%, while the between-run coefficient of validation was 7.6%. However, further work should be done. It took about 10 h to complete our assay. Modifying the DNA extraction procedure could reduce this time. The sensitivity of the assay could be enhanced by increasing the amount of captured cDNA on the slide, or by pretreatment of the sample RNA. A large number of serum samples should be tested to verify the reliability of microarray assay in the detection of HCV.

In conclusion, cDNA microarray technology can be applied to other pathogens and is a useful diagnostic method for HCV infection.

ACKNOWLEDGMENTS

The authors thank Dr Jens Bukh for the presentation of HCV plasmid and Drs Zhang Bao and Shi Rong for critical technical assistance.

REFERENCES

1 **Ogata N**, Alter HJ, Miller RH, Purcell RH. Nucleotide sequence and mutation rate of the H strain of hepatitis C virus. *Proc Natl Acad Sci USA* 1991; **88:** 3392-3396

2 **Choo QL**, Kuo G, Weiner AJ, Overby LR, Bradley DW, Houghton M. Isolation of a cDNA clone derived from a blood-borne non-A, non-B viral hepatitis genome. *Science* 1989; **244:** 359-362

3 **Simmonds P**. Variability of hepatitis C virus. *Hepatology* 1995; **21:** 570-583

4 **Alter HJ**, Purcell RH, Shih JW, Melpolder JC, Houghton M, Choo QL, Kuo G. Detection of antibody to hepatitis C virus

in prospectively followed transfusion recipients with acute and chronic non-A, non-B hepatitis. *N Engl J Med* 1989; **321:** 1494-1500

5 **Hoofnagle JH**, di Bisceglie AM. The treatment of chronic viral hepatitis. *N Engl J Med* 1997; **336:** 347-356

6 **Cui J**, Dong BW, Liang P, Yu XL, Yu DJ. Construction and clinical significance of a predictive system for prognosis of hepatocellular carcinoma. *World J Gastroenterol* 2005; **11:** 3027-3033

7 **Yanagi M**, Purcell RH, Emerson SU, Bukh J. Hepatitis C virus: an infectious molecular clone of a second major genotype (2a) and lack of viability of intertypic 1a and 2a chimeras. *Virology* 1999; **262:** 250-263

8 **Ma WL**, Zheng WL. The research and development of DNA microarray technology. *Sci Found China* 1999; **13**: 270-273

9 **Ma WL**, Zheng WL, James FB. RD-PCR: A new technique of differential display.*In*:Sun yixian(ed).The development of biochemistry and molecular biology in PLA.vol.1. *Beijing: Uniform Medical Publishing*, 1998: 99-113

10 **Zheng WL**, Ma WL, Waes CV. The differential display of poly A polymerase in tumor cells of differential malignancy. *In:* Ye XS(ed). Investigation on cell modulation. vol.1. *Beijing: Uniform Medical Publishinghouse*, 1998: 73-79

11 **Zhao F**, Zhang SJ, Jiang SH. Modification of the technique of staining and the PAGE. *J Clin Exp Patho*l 1999; **15:** 401-402

12 **Sun ZH**, Ma WL, Zheng WL. Microarrays development in the diagnosis of HBV and HCV. *Med J Chin PLA* 2003; **28**: 375-376

13 **Sun ZH**, Zheng WL, Ma WL. The development of molecular diagnosis of viral hepatitis. *Guangdong med J* 2003; **24:** 440-442

14 **Lipshutz RJ**, Fodor SP, Gingeras TR, Lockhart DJ. High density synthetic oligonucleotide arrays. *Nat Genet* 1999; **21:** 20-24

15 **Petrik J**. Microarray technology: the future of blood testing? *Vox Sang* 2001; **80**: 1-11

16 **Zhaohui S**, Wenling Z, Bao Z, Rong S, Wenli M. Microarrays for the detection of HBV and HDV. *J Biochem Mol Biol* 2004; **37:** 546-551

17 **Livache T**, Fouque B, Roget A, Marchand J, Bidan G, Teoule R, Mathis G. Polypyrrole DNA chip on a silicon device: example of hepatitis C virus genotyping. *Anal Biochem* 1998; **255:** 188-194

18 **Stewart DJ**. Making and using DNA microarrays: a short course at Cold Spring Harbor Laboratory. *Genome Res* 2000; **10:** 1-3

19 **Sun ZH**, Zheng WL, Mao XM, Zhang B, Lu L, Ma XD, Shi R, Ma WL. Rapid preparation of DNA microarray using PCR for hepatitis B and D virus detection. *Di Yi Jun Yi Da Xue Xue Bao* 2003; **23:** 677-679

20 **Wang HY**, Malek RL, Kwitek AE, Greene AS, Luu TV, Behbahani B, Frank B, Quackenbush J, Lee NH. Assessing unmodified 70-mer oligonucleotide probe performancs. *Orv Hetil* 1998; **139:** 957-960

Science Editors Wang XL and Guo SY **Language Editor** Elsevier HK

PO Box 2345, Beijing 100023, China
www.wjgnet.com
wjg@wjgnet.com

ELSEVIER

World J Gastroenterol 2005;11(48):7585-7590
World Journal of Gastroenterology ISSN 1007-9327

Response of porcine hepatocytes in primary culture to plasma from severe viral hepatitis patients

Yong-Bo Cheng, Ying-Jie Wang, Shi-Chang Zhang, Jun Liu, Zhi Chen, Jia-Jia Li

Yong-Bo Cheng, Ying-Jie Wang, Shi-Chang Zhang, Jun Liu, Zhi Chen, Jia-Jia Li, Institute of Infectious Diseases, Southwest Hospital, Third Military Medical University, Chongqing 400038, China
Supported by National Natural Science Foundation of China, No. 30470458
Correspondence to: Ying-Jie Wang, MD, Institute of Infectious Diseases, Southwest Hospital, Third Military Medical University, Chongqing 400038, China. wangyj103@263.net
Telephone: +86-23-68754479-8062
Received: 2005-04-14 Accepted: 2005-06-24

Abstract

AIM: To observe the effects of plasma from patients with severe viral hepatitis (SVHP) on the growth and metabolism of porcine hepatocytes and the clinical efficiency of bioartificial liver device.

METHODS: Hepatocytes were isolated from male porcines by collagenase perfusion. The synthesis of DNA and total protein, leakages of AST and LDH, changes in glutathione (GSH), catalase and morphology of porcine hepatocytes exposed to SVHP were investigated to indicate the effect of plasma from patients with severe hepatitis on the growth, injury, detoxification, and morphology of porcine hepatocytes.

RESULTS: The synthesis of DNA and protein was inhibited in the medium containing 100% SVHP compared to the controls. The leakages of LDH and AST increased in porcine hepatocytes following exposure to 100% SVHP for 5 h. The difference between 100% SVHP and 10% newborn calf serum (NCS) was significant in t-test (LDH: t = 24.552, P = 0.001; AST: t = 4.169, P = 0.014). After exposure to SVHP for 24 h, alterations in GSH status were significant (F = 2.746, P<0.05) between porcine hepatocytes in 100% SVHP and 10% NCS, but no alteration occurred in the culture medium after 48 h (F = 4.378, P<0.05). A similar profile was observed in catalase activity. Many round vacuoles were observed in porcine hepatocytes cultured in SVHP. The membranes of these cells became indistinct and almost all the cells died on d 5.

CONCLUSION: Plasma from patients with severe hepatitis inhibits the growth, injures membrane, disturbs GSH homeostasis and induces morphological changes of porcine hepatocytes. It is suggested that SVHP should be pretreated to reduce the toxin load and improve the performance of porcine hepatocytes in extracorporeal liver-support devices.

Key words: Bioartificial liver; Porcine hepatocytes; Cell culture; Plasma toxicity

Cheng YB, Wang YJ, Zhang SC, Liu J, Chen Z, Li JJ. Response of porcine hepatocytes in primary culture to plasma from severe viral hepatitis patients. *World J Gastroenterol* 2005; 11(48):7585-7590
http://www.wjgnet.com/1007-9327/11/7585.asp

INTRODUCTION

A bioartificial liver (BAL) support system, composed of artificial materials and biological components such as hepatocytes, acts as a bridge to provide patients with prolonged time of survival until a donor organ becomes available for the transplantation or their own liver can regenerate[1]. The performance of a BAL depends on the viability and functional activities of hepatocytes in the system. Many laboratories are currently investigating the factors influencing the viability and functional activities of hepatocytes. It has been demonstrated that serum or plasma from liver failure patients interferes extensively with cellular metabolism[2-6]. When the patient's blood is detoxified by the BAL device, there is contact between the patient's plasma and cells in the device. It is thus important to assess the direct interactions between plasma and hepatocytes.

Porcine and human hepatocytes have similar physiological characteristics and metabolic functions and are considered to be the best candidate for use in a BAL[7-11]. They have been applied in clinical trials based on their easy source and excellent functions for the synthesis of protein, glucose, and urea as well as lower lactate dehydrogenase release. *In vitro*, porcine hepatocytes in the bioreactor can clear most conjugated bile acid species from pooled patient plasma[6]. Furthermore, it can be immobilized on a "hepatocyte/gold colloid" interface at which hepatocytes proliferate quickly[12].

In China, HBV infection rate has been estimated to be 10% or higher, and severe hepatitis caused by HBV is common[13,14]. BAL also provides temporary support for these patients when acute or chronic severe viral hepatitis (SVHP) develops. However, there are few reports on

how SVHP interferes with the growth and function of hepatocytes in primary culture. Therefore, we investigated the direct interactions between SVHP and porcine hepatocytes.

MATERIALS AND METHODS

Materials

Cell culture reagents, including RPMI-1640, sodium pyruvate, and L-glutamine were purchased from GIBCO, Life Technologies, Ltd. (Paisley, Scotland, UK). Type IV collagenase was a product of Sigma Chemical Co, Ltd (St. Louis, MO, USA). Reagents for the measurement of reduced glutathione (GSH), catalase (CAT) and total protein (TP) were from Nanjing Biological Technology Co, Ltd. Methyl thiazolyl tetrazolium (MTT) was from Fluka Chemic AG (Switzerland). TriPure isolation reagent was from Roche (Switzerland). Plasticware was from Nunc (Denmark). All solutions were prepared with twice-distilled water.

Hepatocyte preparation

Healthy Chinese experimental miniature male pigs aged 1-4 d were provided by Experimental Animal Center of Third Military Medical University. The research protocol was in compliance with Chinese guidelines for the humane care of experimental animals. Porcine hepatocytes were isolated by modified two-step *in situ* collagenase perfusion method[15,16]. The viability of freshly isolated suspensions determined by trypan blue exclusion was 85-95%. Porcine hepatocytes were cultured at 37 °C for 24 h in RPMI-1640 medium supplemented with 10% (vol/vol) newborn calf serum (NCS) at a density of 2×10^5 cells/mL in a 50 mL/L CO_2 incubator. The cultures were washed twice in warm phosphate-buffered saline (PBS) and cultured in a medium containing 10% (vol/vol) NCS, normal plasma (NP) anti-coagulated by heparin, and SVHP. Porcine hepatocytes were prepared for assay as described below.

Plasma from patients with severe virus hepatitis

Plasma was obtained from six patients with SVHP (3 females, 3 males, aged 34-60 years) at the onset of plasmapheresis and stored at -80 °C until use. Diagnosis of these patients was in accordance with the criteria of severe hepatitis described in the Viral Hepatitis Protection and Cure Guideline established by the Chinese Infection and Hepatology Association. In these six patients, total bilirubin (TB) averaged 611.8 μmol/L, prothrombin time (PT) averaged 32 s, total bile acids (TBA) averaged 309.8 μmol/L and PTa averaged 29%. Hepatitis B surface antigen (HBsAg) was positive and HBV-DNA was greater than 10^5 copies/mL in all the 6 patients. All patients suffered from hepatic encephalopathy, grade II in two patients, grade III in three patients, and grade IV in one patient. Normal serum was obtained from normal individuals.

Cell viability determination

Cells were seeded in 24-well plates in 500 μL medium. The viability was assessed by tetrazolium bromide assay (MTT) on d 0-5 after exposure to the culture medium containing 10% (vol/vol) NCS, 100% NP, and 100% SVHP.

DNA synthesis

After being cultured in six-well plates for 24 h, the media were discarded, and DNA was isolated as the procedures of TriPure isolation reagent description. DNA content was determined using a spectrophotometer (SmartSpec 3000, BioRad, USA).

Protein content

After being incubated for 24 and 48 h, monolayer cells were washed and dissolved. Total cellular protein was digested in 0.5 mol/L NaOH and measured by micromodification as previously described[17].

Leakage of LDH and AST

Porcine hepatocytes were exposed to 100% SVHP and 10% (vol/vol) NCS in RPMI-1640 for 5 h. The media were washed thrice with PBS and replaced with RPMI-1640 without plasma and serum. After 24 h of culture, the leakage of LDH and AST from hepatocytes into the supernatant was measured using an automated chemical analyzer (Model 7020 Hitachi Co., Tokyo, Japan)[18].

Oxidative status

After being incubated for 24 and 48 h, the medium containing 10% NCS, 100% NP, 100% SVHP was removed, the wells were washed with PBS, and GSH was added into 0.2 mL 10% (w/v) trichloroacetic acid for 10 min at room temperature. Samples were frozen at -20 °C until measurement of GSH by fluorimetry. CAT activity was measured.

Morphology

Cultured hepatocytes were observed daily under phase contrast microscope (IX70, Olympus, Tokyo, Japan), and the morphological changes were compared.

Statistical analysis

Data were expressed as mean±SD. Statistical analysis was carried out by analysis of variance and *t*-test. $P<0.05$ was considered statistically significant.

RESULTS

Viability of porcine hepatocytes cultured in SVHP

The viability of porcine hepatocytes cultured in 100% SVHP was significantly lower than that cultured in the medium containing 10% NCS ($F = 6.328$, $P<0.01$). The viability of porcine hepatocytes in 100% NP group was not higher than that in 10% NCS group. The viability of porcine hepatocytes in all the groups tended to decrease from the third day (Figure 1).

DNA content

After being cultured for 24 h, the DNA level in three

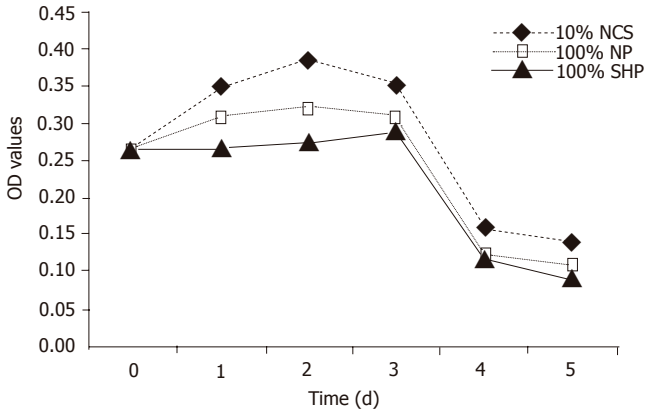

Figure 1 Viability of porcine hepatocytes cultured in ♦ medium containing 10% NCS, □ 100% NP, ▲ 100% SVHP. Results were expressed as mean±SD for six samples.

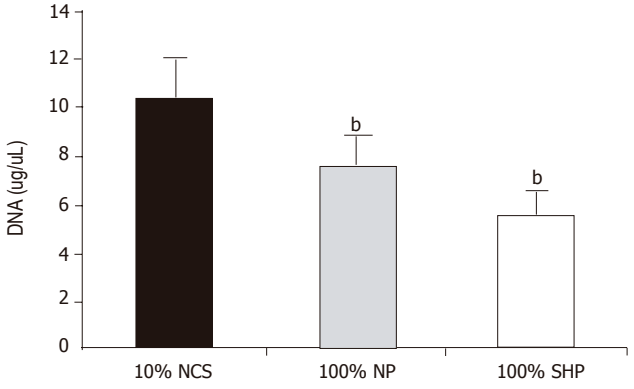

Figure 2 DNA content in porcine hepatocytes grown in three different media. DNA synthesis in 100% SVHP and normal plasma was compared to that in the medium containing 10% NCS (^bP<0.01 *vs* 10% NCS group, by ANOVA followed by multiple comparisons). Results were expressed as mean±SD for six samples Black oblique line: 10% NCS, black small point: 100% NP; black small square: 100% SVHP.

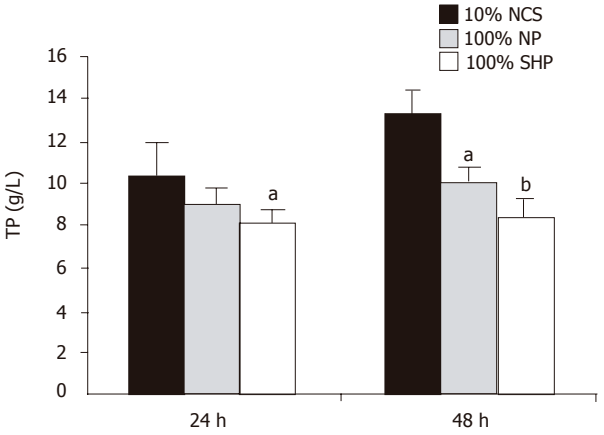

Figure 3 TP content in porcine hepatocytes grown in three different media. TP synthesis in 100% SVHP and NP was compared to that in the medium containing 10% NCS (^aP<0.05, ^bP<0.01 *vs* 10% NCS group, by two-way variance analysis). Results were expressed as mean±SD for six samples. Black bar: 10% NCS; gray bar: 100% NP; white bar: 100% SVHP.

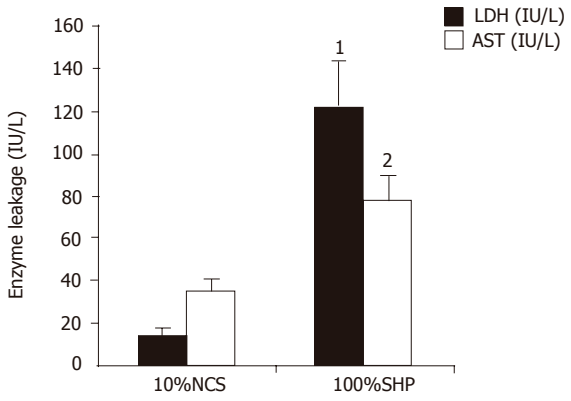

Figure 4 Leakage of LDH and AST after 5 h of culture (black bar: LDH; white bar: AST). The levels of LDH and AST in 100% SVHP were significantly higher than those in the medium containing 10% NCS. Results were expressed as mean±SD (1: t = 24.552, P = 0.001 and 2: t = 4.169, P = 0.014, compared to the10% NCS group, n = 6).

different media was significantly different (F = 20.107, P<0.01). The level was the lowest in 100% SVHP and lower in 100% NP than in 10% NCS. The inhibitory effect of porcine hepatocytes on DNA synthesis is shown in Figure 2.

Total protein synthesis

During the course of culture, the amount of TP in three different media was significantly different (F = 9.281, P<0.01, Figure 3). Multiple comparison showed that the TP level in 100% SVHP was lower than that in 10% NCS (P<0.01). The TP level in 100% NP was also significantly lower than that in 10% NCS (P<0.05).

Leakage of LDH and AST

LDH and AST elevations were observed in 100% SVHP group after 5 h of culture. The LDH level in 100% SVHP group was significantly higher than that in 10% NCS group (t = 24.552, P = 0.001). The AST level in 100% SVHP group was also significantly higher than that in 10% NCS group (t = 4.169, P = 0.014, Figure 4), indicating that hepatocytes cultured in plasma from patients with SVHP had damage in the cell membrane.

GSH content and CAT activity

GSH concentration in porcine hepatocytes decreased in SVHP and NP as compared to that in the culture medium containing 10% NCS (Figure 5A). A significant decrease in GSH content was observed in SVHP compared to that in the medium containing 10% NCS within 24 h (F = 2.746, P<0.05). After 48 h the GSH level declined slightly. There was no difference between 100% SVHP and 10% NCS (F = 4.378, P>0.05). A similar profile was observed in CAT levels following incubation with SVHP and NP (Figure 5B). The only difference between GSH and CAT was that the CAT content was dramatically decreased after being cultured for 48 h.

Morphological study

The dramatic change of porcine hepatocyte morphology

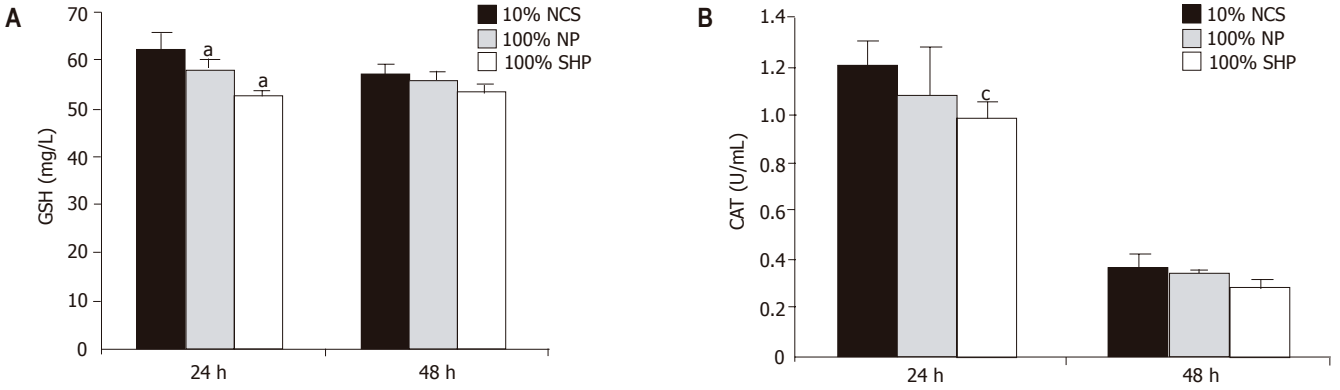

Figure 5 GSH content in porcine hepatocytes grown in three different cultures (**A**) ($^{a}P<0.05$ *vs* 10% NCS, by two-way variance analysis, compared to 10% NCS) and CAT activity of porcine hepatocytes grown in the three different cultures (**B**) ($^{c}P<0.05$ *vs* 10% NCS by two-way variance analysis, compared to 10% NCS). Black bar: 10% NCS, gray bar: 100% NP; white bar: 100% SVHP.

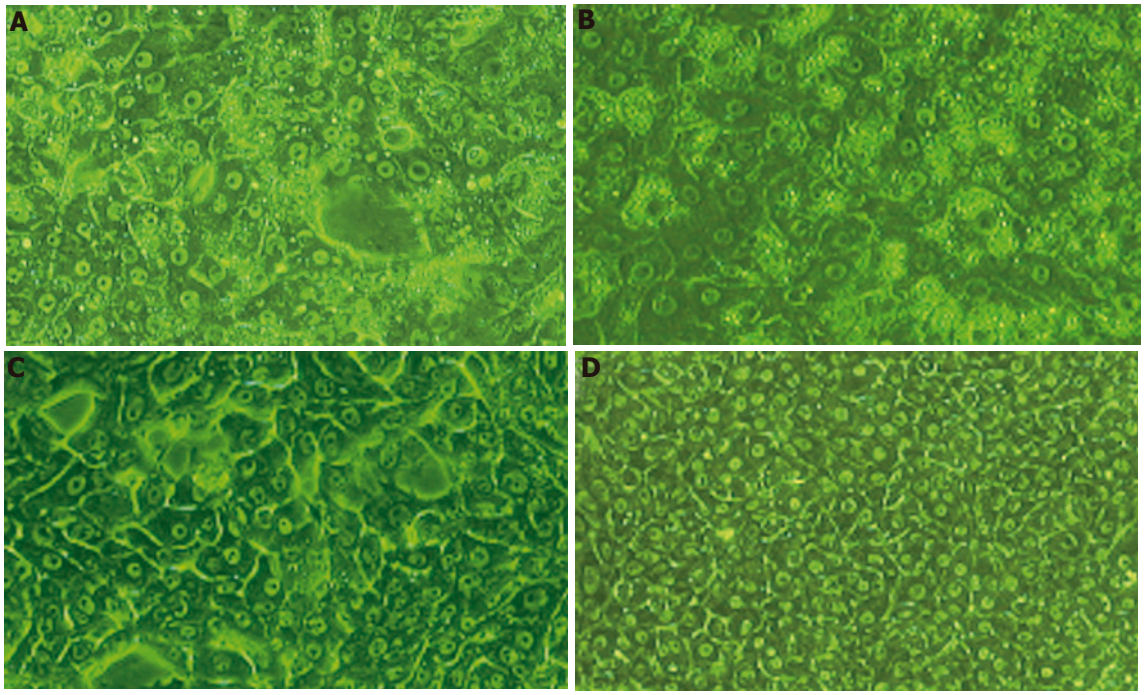

Figure 6 Morphological changes of porcine hepatocytes cultured in 100% SVHP **(A** and **B**) and media containing 10% NCS (**C** and **D**). After 24 h of culture, hepatocytes in the100% SVHP group were detached from the dishes, vacuolization in the cytoplasm and deformities were more commonly observed. The membranes of cells became indistinct (**A**); after 48 h of culture, vacuoles were more and mainly concentrated around cell nuclei (**B**); after 24 h of culture, hepatocytes in the 10% NCS group constituted confluent monolayers with an intact morphology throughout the culture (**C**); after 48 h of culture, hepatocytes in the 10% NCS group constituted confluent monolayers with an intact morphology throughout the culture (**D**).

after 24 h exposure to 100% SVHP was observed under phase contrast microscope. As shown in Figures 6A-D, most of the cells became detached and deformed. Vacuolization in cytoplasm and necrosis were more commonly observed. Membranes of the cells became indistinct. These morphological changes became marked after 48 h of culture. Vacuoles were mainly concentrated around cell nuclei and detached from their dishes. During the 48-h culture, hepatocytes in groups of 100% NP and 10% NCS spread and formed a clear confluent monolayer. Detachment, deformity, and vacuolization were not observed in the cytoplasm. There was no obvious difference between the two groups. After 5 d of culture, necrosis was observed in the two groups and almost all hepatocytes were dead in 100% SVHP group.

DISCUSSION

Experimental studies[3-5] have demonstrated that plasma from patients with fulminant hepatic failure (FHF) or liver failure (LF) can inhibit the growth of hepatocytes and synthesis of macromolecules in hepatocytes. McCloskey *et al*.[5] found that plasma from patients with liver failure could diminish DNA and protein synthesis.

Shi *et al*.[4] reported that serum from patients with FHF inhibits the growth rate and synthesis of DNA, RNA, and protein. In our study, the plasma was from patients with SVHP. Inhibition of growth and macromolecule synthesis, reduction of viability of porcine hepatocytes were demonstrated. The inhibition mechanism might be related to endogenic materials such as bile acids, growth factors, and cytokines in SVHP. There are more bile acids, hepatic growth factor (HGF) and tumor growth factor-β (TGF-β)[19] in SVHP. Accumulation of intracellular bile acids causes damage to intracellular organelles, such as mitochondria[20]. Bile acids in nuclei cause DNA injury by changing chromatin structure or by activating nuclear nuclease, thus resulting in conversion into a metabolite that could directly damage DNA[21,22]. HGF does not always accelerate the growth of hepatocytes. Sometimes there are converse results[23]. It was reported that HGF inhibits cell growth at a cell cycle phase and growth of cells is impaired with the increasing HGF concentration, while elevated serum TGF may lead to an increase in p21, a cyclin-dependent kinase inhibitor that can inhibit the activation of G1-associated cyclins such as Cdk2[24,25]. In this study, the viability of porcine hepatocytes cultured in 100% NP was decreased compared to that in 10% NCS, which may result from cytokine- and antibody-mediated damage.

Membrane damage and enzyme leakage have been detected in the culture medium[5,26,27]. McCloskey *et al*.[5] reported that after HHY41 hepatocytes are exposed to plasma from patients with LF containing $Na_2{}^{51}CrO_4$ for 16 h, the leakage of ^{51}Cr is about 20 times higher than that in controls. However, Uchino *et al*.[28] demonstrated that the function of pig hepatocytes does not deteriorate when they are exposed to the serum from the patients with FHF[28]. In this study, LDH and AST leakage from porcine hepatocytes cultured in SVHP was significantly higher than that from porcine hepatocytes cultured in 10% NCS. Morphological changes of hepatocytes also suggested severe cell membrane damage, indicating that SVHP can lead to hepatocellular membrane impairment. Endogenic toxins may originate either from cellular necrosis debris and breakdown products released into the blood stream or from accumulation of an agent that is normally eliminated by metabolism in hepatocytes. Bile acids play an important role in the toxicities and can form micelles with cholesterol and phospholipids on the surface of hepatocyte membranes, which produce apparent hepatocellular membrane injury[22]. Virus-mediated damage involves immune-mediated and direct viral cytopathic effects.

The highest cytotoxicity values have been found in the plasma from patients with FHF, indicating the utmost importance of detoxification by BAL. Intracellular GSH content often reflects the fate of potentially harmful substances, and examination of GSH status may provide information on the mechanisms of toxicity. Previous experimental studies revealed that exposure of hepatocytes to the serum from patient with FHF results in increase or decrease in GSH content. The changes are related to plasma concentration, culture time, hepatocyte type[4,5]. Previous studies have shown that Hep G2 cells respond to abnormal culture conditions and toxic concentrations of bile. GSH of HHY41 in plasma from patients with LF is decreased[5]. In our study, the pronounced decrease in GSH levels was observed following incubation with SVHP. As a main member of anti-oxidizing system, GSH plays an important role in relieving the tissue depression due to electrophilic reactive toxins or oxidative stress because it can react directly with reactive oxygen free-radicals and conjugate bile acids[29].These factors lead to a depletion of cellular GSH store. The activity of CAT changes as GSH, which requires further investigation.

REFERENCES

1 **Hui T**, Rozga J, Demetriou AA. Bioartificial liver support. *J Hepatobiliary Pancreat Surg* 2001; 8: 1-15

2 **Hughes RD**, Cochrane AM, Thomson AD, Murray-Lyon IM, Williams R. The cytotoxicity of plasma from patients with acute hepatic failure to isolated rabbit hepatocytes. *Br J Exp Pathol* 1976; **57:** 348 348-353

3 **Gove CD,** Hughes RD, Williams R. Rapid inhibition of DNA synthesis in hepatocytes from regenerating rat liver by serum from patients with fulminant hepatic failure. *Br J Exp Pathol* 1982; **63:** 547-553

4 **Shi Q,** Gaylor JD, Cousins R, Plevris J, Hayes PC, Grant MH. The effects of serum from patients with acute liver failure on the growth and metabolism of Hep G2 cells. *Artif Organs* 1998; **22:** 1023-1030

5 **McCloskey P**, Tootle R, Selden C, Larsen F, Roberts E, Hodgson HJ. Modulation of hepatocyte function in an immortalized human hepatocyte cell line following exposure to liver-failure plasma. *Artif Organs* 2002; **26:** 340-348

6 **Pazzi P**, Morsiani E, Vilei MT, Granato A, Rozga J, Demetriou AA, Muraca M. Serum bile acids in patients with liver failure supported with a bioartificial liver. *Aliment Pharmacol Ther* 2002; **16:** 1547-1554

7 **Rozga J**, Williams F, Ro MS, Neuzil DF, Giorgio TD, Backfisch G, Moscioni AD, Hakim R, Demetriou AA. Development of a bioarti.cial liver: properties and function of a hollow module inoculated with livers cells. *Hepatology* 1993; **17:** 258–265

8 **Watanabe FD**, Mullon CJ, Hewitt WR, Arkadopoulos N, Kahaku E, Eguchi S, Khalili T, Arnaout W, Shackleton CR, Rozga J, Solomon B, Demetriou AA. Clinical experience with a bioartificial liver in the treatment of severe liver failure. A phase I clinical trial. *Ann Surg* 1997; **225:** 484-91; discussion 491-494

9 **Khalili TM**, Navarro A, Ting P, Kamohara Y, Arkadopoulos N, Solomon BA, Demetriou AA, Rozga J. Bioarti.cial liver treatment prolongs survival and lowers incranial pressure in pigs with fulminant hepatic failure. *Artif Organs* 2001; **25:** 566–570

10 **Nagaki M**, Miki K, Kim YI, Ishiyama H, Hirahara I, Takahashi H, Sugiyama A, Muto Y, Moriwaki H. Development and characterization of a hybrid bioartificial liver using primary hepatocytes entrapped in a basement membrane matrix. *Dig Dis Sci* 2001; **46:** 1046-1056

11 **Mears DC**, Stewart G, Sun J, Woodman K, Bourne R, Wang L, Sheil AG. Experience with a porcine hepatocyte-based bioartificial liver support system. *Transplant Proc* 2003; **35:** 441 –442

12 **Gu HY**, Chen Z, Sa RX, Yuan SS, Chen HY, Ding YT, Yu AM. The immobilization of hepatocytes on 24 nm-sized gold colloid for enhanced hepatocytes proliferation. *Biomaterials* 2004; **25:** 3445-3451

13 **Merican I**, Guan R, Amarapuka D. Chronic hepatitis B virus infection in Asian countries. *J Gastroenterol Hepatol* 2000; **15:** 1356-1361

14 **Pokorski RJ**, Ohlmer U. Long-term morbidity and mortality

in Chinese insurance applicants infected with the hepatitis B virus. *J Insur Med* 2001; **33:** 143-164
15 **Chen Z**, Ding Y, Zhang H. Cryopreservation of suckling pig hepatocytes. *Ann Clin Lab Sci* 2001; **31:** 391-398
16 **Wang YJ**, Liu HL. Mass isolation and cryopreservation of hepatocytes. In: Wang YJ, eds. Bioartificial Liver. *Beijing-China: People's Health Publishing House* 2000: 207-2009.
17 **Lowry OH**, Rosebrough NJ, Farr AL, Randall RJ. Protein measurement with the Folin phenol reagent. *J Biol Chem* 1951; **193:** 265-275
18 **Flendrig LM**, la Soe JW, Jorning GG, Steenbeek A, Karlsen OT, Bovee WM, Ladiges NC, te Velde AA, Chamuleau RA. In vitro evaluation of a novel bioreactor based on an integral oxygenator and a spirally wound nonwoven polyester matrix for hepatocyte culture as small aggregates. *J Hepatol* 1997; **26:** 1379-1392
19 **Nozato E**, Shiraishi M, Nishimaki T. Up-regulation of hepatocyte growth factor caused by an over-expression of transforming growth factor beta, in the rat model of fulminant hepatic failure. *J Surg Res* 2003; **115:** 226-234
20 **Hoshino M**, Ohiwa T, Hayakawa T, Kamiya Y, Tanaka A, Hirano A, Kumai T, Katagiri K, Miyaji M, Takeuchi T. Effects of dibutyryl cyclic AMP and papaverine on intrahepatocytic bile acid transport. Role of vesicle transport. *Scand J Gastroenterol* 1993; **28:** 833-838
21 **Russo P**, Taningher M, Pala M, Pisano V, Pedemonte P, De Angeli MT, Carlone S, Santi L, Parodi S. Characterization of the effects induced on DNA in mouse and hamster cells by lithocholic acid. *Cancer Res* 1987; **47:** 2866-2874
22 **Kulkarni MS**, Cox BA, Yielding KL. Requirements for induction of DNA strand breaks by lithocholic acid. *Cancer Res* 1982; **42:** 2792-2795
23 **Drixler TA**, Vogten MJ, Ritchie ED. Liver regeneration is an angiogenesis associated phenomenon. *Ann Surg* 2002; **236:** 703-711
24 **Albrecht JH**, Meyer AH, Hu MY. Regulation of cyclin-dependent kinase inhibitor p21(WAF1/Cip1/Sdi1) gene expression in hepatic regeneration. *Hepatology* 1997; **25:** 557-563
25 **Sugiyama A**, Nagaki M, Shidoji Y, Moriwaki H, Muto Y. Regulation of cell cycle-related genes in rat hepatocytes by transforming growth factor beta1. *Biochem Biophys Res Commun* 1997; **238:** 539-543
26 **Ohiwa T**, Katagiri K, Hoshino M, Hayakawa T, Nakai T. Tauroursodeoxycholate and tauro-beta-muricholate exert cytoprotection by reducing intrahepatocyte taurochenodeoxycholate content. *Hepatology* 1993; **17:** 470-476
27 **Heuman DM**, Pandak WM, Hylemon PB, Vlahcevic ZR. Conjugates of ursodeoxycholate protect against cytotoxicity of more hydrophobic bile salts: in vitro studies in rat hepatocytes and human erythrocytes. *Hepatology* 1991; **14:** 920-926
28 **Uchino J**, Matsue H, Takahashi M, Nakajima Y, Matsushita M, Hamada T, Hashimura E. A hybrid artificial liver system. Function of cultured monolayer pig hepatocytes in plasma from hepatic failure patients. *ASAIO Trans* 1991; **37:** M337-M338
29 **Smirthwaite AD**, Gaylor JD, Cousins RB, Grant MH. Cytotoxicity of bile in human Hep G2 cells and in primary cultures of rat hepatocytes. *Artif Organs* 1998; **22:** 831-836

Science Editors Wang XL and Guo SY **Language Editor** Elsevier HK

PO Box 2345, Beijing 100023, China
www.wjgnet.com
wjg@wjgnet.com

ELSEVIER

World J Gastroenterol 2005;11(48):7591-7596
World Journal of Gastroenterology ISSN 1007-9327

Hepatitis C virus infection down-regulates the expression of peroxisome proliferator-activated receptor α and carnitine palmitoyl acyl-CoA transferase 1A

Yang Cheng, Sébastien Dharancy, Mathilde Malapel, Pierre Desreumaux

Yang Cheng, Sébastien Dharancy, Mathilde Malapel, Pierre Desreumaux, Equipe mixte INSERM 0114, Université de Lille, CHU, Lille 59037, France
Supported by the National Natural Science Foundation of China, No.30300458
Correspondence to: Yang Cheng, Institute of Liver Diseases, Shanghai University of TCM, Shanghai 201203, China. yangcheng@myrealbox.com
Telephone: +86-21-51322444 Fax: +86-21-51322445
Received: 2005-03-31 Accepted: 2005-04-18

Abstract

AIM: To elucidate the role of the peroxisome proliferator-activated receptor α (PPARα) and its target gene carnitine palmitoyl acyl-CoA transferase 1A (CPT1A) in the pathogenesis of hepatitis C virus (HCV) infection.

METHODS: Liver samples were collected from the patients with chronic HCV infection and controls. HepG2 cells were transfected with vector pEF352neo carrying. Two independent clones (clone N3 and N4) stably expressing HCV core protein were analyzed. Total RNA was extracted from cells and liver tissues. PPARα and CPT1A mRNAs were quantified by real-time polymerase chain reaction (PCR) using SYBR Green Master. Total extracted proteins were separated by polyacrylamide gel electrophoresis, and electroblotted. Membranes were incubated with the anti-PPARα antibody, then with a swine anti-rabbit IgG conjugated to horseradish peroxidase for PPARα. Protein bands were revealed by an enhanced chemiluminescence reaction for PPARα. For immunohistochemical staining of PPARα, sections were incubated with the primary goat polyclonal antibody directed against PPARα at room temperature.

RESULTS: Real-time PCR indicated that the PPARα level and expression level of CPT1A gene in hepatitis C patients lowered significantly as compared with the controls (1.8±2.8 *vs* 13±3.4, $P = 0.0002$; 1.1±1.5 *vs* 7.4±1, $P = 0.004$). Western blot results showed that the level of PPARα protein in the livers of hepatitis C patients was lower than that in controls (2.3±0.3 *vs* 3.6±0.2, $P = 0.009$). The immunohistochemical staining results in chronic hepatitis C patients indicated a decrease in PPARα staining in hepatocytes compared with those in the control livers. The *in vitro* studies found that in the N3 and N4 colon stably expressing HCV core protein, the PPARα mRNA levels were significantly lower than that in the controls.

CONCLUSION: The impaired intrahepatic PPARα expression is associated with the pathogenic mechanism in hepatic injury during chronic HCV infection. HCV infection reduced the expression of PPARα and CPT1A at the level of not only mRNAs but also proteins. PPARα plays an important role in the pathogenesis of chronic HCV infection, but the impaired function of this nuclear receptor in HCV infection needs further studies.

Key words: Hepatitis C virus; Infection; PPARα; CPT1A

Cheng Y, Dharancy S, Malapel M, Desreumaux P. Hepatitis C virus infection down-regulates the expression of peroxisome proliferator-activated receptor α and carnitine palmitoyl acyl-CoA transferase 1A. *World J Gastroenterol* 2005; 11(48): 7591-7596
http://www.wjgnet.com/1007-9327/11/7591.asp

INTRODUCTION

Hepatitis C virus (HCV) infection is a major health care problem around the world[1]. It is estimated that there are about 170 million chronic carriers worldwide with four million in the USA[2-4] and five million in the western Europe[5-6]. HCV infection accounts for 20% of cases of acute hepatitis, 70% of chronic hepatitis, 40% of end-stage cirrhosis, 60% of cases of hepatocellular carcinoma, and 30% of liver transplantation[7-10]. Liver lesions are thought to be mainly related to immune-mediated mechanisms[5] but the exact mechanisms during HCV infection are still unclear[8,9,11]. However, the HCV core protein is a major component of viral nucleocapsid and it is a multifunctional protein that affects transcription and cell growth[12]. HCV core protein plays an important role in the HCV pathogenesis[13].

The ability of peroxisome proliferators to activate a receptor in the steroid receptor superfamily was first discovered in 1990[14], and the cognate protein was designated as peroxisome proliferator-activated receptors (PPARs). The PPARs are soluble transcription factors that are activated by a diverse class of lipophilic compounds[15].

With the activation of PPAR, a concomitant induction of a number of genes that code for peroxisomal fatty acid metabolizing enzymes was observed in mouse liver. There are three PPAR subtypes: PPARα (NR1C1), PPARβ (NR1C2), and PPARγ (NR1C3); and each subtype is capable of binding to DNA after heterodimerizing with RXR (NR2B1). PPARα is highly expressed in the liver, kidney, and cardiac smooth muscles. Many of the genes regulated by PPARα are involved in fatty acid metabolism[16]. PPARα could influence fatty acid import into hepatocyte mitochondria by up-regulating the expression of the liver-predominant mitochondrial carnitine palmtoylacyl-CoA transferase 1 (CPT1) gene[17].

Three CPT1 isoforms with various tissue distributions and encoded by distinct genes have been identified: CPT1A or L-CPT1 (liver isoform), CPT1B or M-CPT1 (muscle isoform), and CPT1C (brain isoform). CPT1A is expressed in the liver, the neonatal heart, and a number of other tissues, and has been the most investigated member of the acyltransferase family. It is anchored in the mitochondrial outer membrane by two transmembrane segments (TM1 and TM2), its N terminus (residues 1-47) and C-terminal catalytic domain (residues 123-773) being located on the cytosolic face of mitochondria. The N-terminal domain (1-147 residues) was shown to be essential for mitochondrial import and for the maintenance of a folded active and malonyl-CoA-sensitive conformation[18].

Until now, the role of PPARα and its target gene CPT1A in liver diseases is still limited to animal studies. In order to elucidate the mechanism of PPARα during the pathogenesis of HCV infection, PPARα and CPT1A expression levels were studied *ex vivo* and *in vitro,* respectively in this study.

MATERIALS AND METHODS

Subjects and liver samples processing

Chronic hepatitis C infection was defined by increased serum alanine transaminase activity (>35 IU/L), positive serum HCV replication determined by polymerase chain reaction (PCR; Amplicor Monitor v2.0; Roche, Indianapolis, IN, USA), and histological hepatic injury quantified by the METAVIR score evaluating the intensity of fibrosis (F1-F4) and necroinflammatory activity (A1-A3)[19]. The subjects were excluded if their body mass index was greater than 30 or if they suffered from diabetes or dyslipidemia.

Patient liver samples were collected from 46 patients with chronic HCV infection (41 transcutaneous needle liver biopsy samples from chronic hepatitis C patients and 5 surgical liver samples from HCV-related cirrhotic patients when they underwent transplantation). Non-HCV-infected liver tissues as controls were collected from 40 patients (29 normal tissue samples from patients who underwent surgery because of hepatic carcinoma, 5 biopsy samples from patients with alcoholic cirrhosis, and 6 samples from patients with alcoholic hepatitis). Both patients and controls did not receive any therapy (antiviral therapy, hepatotoxic drugs, corticosteroids, or immunosuppressive drugs) before or during liver sample collection.

The liver samples collected from hepatitis C patients or controls were divided into two parts: one part was fixed in 4% paraformaldehyde/phosphate-buffered saline and embedded in paraffin wax, and routinely processed for pathological analysis and for immunostaining[20]. Specimen slides were incubated for 48 h at 37 °C and then deparaffinized by dimethylbenzene and rehydrated by graded alcohol series, then stained with H&E, safran, and Masson's trichrome. The other part was frozen immediately in the liquid nitrogen and stored at -80 °C for mRNA and protein analysis.

HepG2 cell culture and transfection

Human hepatocellular carcinoma cell line HepG2 was used for this study. Cells were maintained in Dulbecco's modified Eagle's medium (Sigma-Aldrich, St. Louis, MO, USA) supplemented with 10% heat-inactivated fetal bovine serum (Eurobio, Les Ulis, France) in a humidified atmosphere of 50 mL/L CO_2 in air at 37 °C.

In order to analyze the effect of the HCV core protein on PPARα expression, HepG2 cells were transfected with vector pEF352neo carrying, under the control of the elongation factor-1α promoter, an HCV complementary DNA including 1b HCV sequences from core to NS3 region as previously described[21]. Two independent clones (clone N3 and N4) stably expressing HCV core protein were analyzed. The clone transfected with the empty vector acted as negative control. Cells were resuspended in lysis buffer with 10% β-mercaptoethanol for RNA isolation[22]. All studies were performed in triplicate samples for three separate experiments.

RNA extraction and the real-time PCR analysis

Total RNA was extracted from cells and liver tissues by RNeasy kit (Macherey Nagel, Hoerdt, France) and TRIzol reagent (Life Technologies, Cergy Pontoise, France) following the protocols provided by the manufacturers with some modification[20]. RNA quantification was performed using spectrophotometry. After treatment at 37 °C for 30 min with 20-50 U of RNase-free DNase I (Roche Diagnostics Corporation), oligo-dT primers (Roche Diagnostics Corporation) were used to synthesize single-stranded complementary DNA. PPARα and CPT1A mRNAs were quantified using SYBR Green Master Mix (Applera, Courtaboeuf, France) with specific primers in a GeneAmp ABI prism 7000 (Applera). The primers used were as follows: PPARα anti-sense 5'-CCA CCA TCG CGA CCA GAT-3', PPARα sense 5'-GAC GTG CTT CCT GCT TCA TAG A-3'; CPT1A anti-sense 5'-TGT GCT GGA TGG TGT CTG TCT C-3', CPT1A sense 5' -CGT CTT TTG GGA TCC ACG ATT-3'; TBP anti-sense 5'-TTT TCT TGC TGC CAG TCT GGA C-3', TBP sense 5'-CAC GAA CCA CGG CAC TGA TT-3'. Calibrated and nontemplate controls were included in each assay. Each sample was run in triplicate. SYBR Green dye intensity was analyzed using the ABI prism 7000 SDS software (Applera). All results were normalized to the

TATA box-binding protein, an unaffected housekeeping gene[23]. All quantifications were performed in triplicate samples for three separate experiments.

Western blotting analysis

Protein preparation and immunoblotting were performed in liver specimens as described before. Total protein extracts were obtained by homogenization of tissues in an extraction buffer containing phosphate-buffered saline with 1% tergitol NP-40, 0.5% sodium desoxycholate, 0.1% sodium dodecyl sulfate, and a classic protease inhibitor cocktail. One hundred micrograms of total proteins were then separated by 10% polyacrylamide gel electrophoresis and electroblotted. Blots were blocked for 1 h at 4 °C with 5% milk Tris-Tween buffered saline 1×, and were incubated overnight at 1:1 000 with the anti-PPARα (Geneka Biotechnology Inc., Montreal, Canada). Membranes were incubated for 1 h with a swine anti-rabbit IgG conjugated to horseradish peroxidase for PPARα (dilution 1:1 000, Dako Laboratories, Trappes, France). Protein bands were revealed by an enhanced chemiluminescence reaction for PPARα. The results were expressed as units of optical density per quantity of total protein[20,24,25].

Immunohistochemical staining in liver tissues

Serial sections of paraffin embedded liver tissues were cut at 4 μm by Leica RM2145 rotary microtome (Leica Instruments GmbH, Germany). Glass slides were treated with poly-L-lysine in advance. Specimen slides were incubated for 48 h at 37 °C and then deparaffinized by xylene and rehydrated by graded alcohol series. An immunohistochemical staining was performed[20,24,25] for the detection of PPARγ expression. Liver sections were incubated in 3% H_2O_2 in methanol to deactivate endogenous peroxidase activity for 20 min. Then slides were incubated with 0.05% Saponin (ICN Biomedicals, OH, USA) for 30 min at room temperature to permeablize the tissues. After being washed, sections were pre-treated with Avidin D, followed by Biotin (Vector Laboratories) to block non-specific binding of Biotin/Avidin system reagents. Non-specific antibody binding was blocked with 1.5% goat serum in PBS for 15 min. Slides were incubated with 5% milk and 0.1% bovine serum albumin (BSA) in PBS for 15 min. Sections were incubated with the primary goat polyclonal antibody directed against PPARγ at room temperature (dilution 1:50, TEBU International) for 30 min, and were processed for peroxidase immunostaining using the Dako Laboratories system following the manufacturer's instructions. Sections were incubated for 30 min at room temperature in rabbit anti-goat IgG (dilution 1:100, Dako Laboratories), and then under the same conditions in an avidin-biotinylated peroxidase complex (Dako, Denmark) that was prepared at least 30 min before use. Staining was developed with 3,3'-diaminobenzidine in chromogen solution for 1 min, and the reaction was stopped in distilled water. Sections were counterstained with hematoxylin. As a negative control experiment, the primary antibody was omitted and replaced with a non-specific antibody[20].

Statistical analysis

All results were expressed as mean±SD. Comparisons were analyzed by the nonparametric Mann-Whitney *U* test. Differences were considered statistically significant, if the *P* value was less than 0.05.

RESULTS

Patients' ALT, HCV load, histological scores, and genotype

In this study, the body weights of the chronic hepatitis C patients were within the normal range and homogeneous. Before and during the study, they did not receive any treatment which could have influenced the results. Their mean serum alanine transaminase value was 119±27 IU/L, mean peripheral blood HCV RNA level was $747\pm267\times10^3$ IU/mL, and their histological lesions were consistent at the time of liver biopsy examination. Half of the patients had fibrosis scored F1, 24% F2, and 26% F3-F4. Seventy-two percent of the cases had an inflammatory activity scored A1 and 28% A2. Fifty-two percent of patients were genotype 1, 31% were genotype 3, 12% were genotype 2, and 5% were genotype 4.

HCV infection reduced the expression of PPARα and CPT1A

The real-time PCR analysis indicated that the housekeeping gene TATA box-binding protein concentrations were similar in patients and controls. But the level of PPARα in hepatitis C patient livers lowered by 86% compared with controls (1.8±2.8 *vs* 13±3.4, $P = 0.0002$) (Figure 1A). And the reduction in CPT1A mRNA was similar to the reduction in PPARα in the livers of patients in the study (Figure 1B). Compared with the 40 controls, the expression level of the CPT1A gene in the 46 hepatitis C patients lowered by more than 80% (1.1±1.5 *vs* 7.4±1, $P = 0.004$).

In a similar pattern, the Western blot also proved the results of real-time PCR analysis. Because of the limited amount of the liver biopsy samples, the Western blot analysis of PPARα was performed only in the surgically obtained liver specimens of patients with HCV infection ($n = 5$) and controls ($n = 7$). The analysis revealed a band with a molecular weight of approximately 55 ku corresponding to PPARα in all surgical liver specimens, and significantly lower levels of PPARα protein in HCV patients than in controls (2.3±0.3 *vs* 3.6±0.2 OD of PPARα protein/5 ng total protein, $P = 0.009$) (Figure 1C).

PPARα protein expression decreased in hepatocytes

The immunohistochemical staining was performed in all hepatitis C patients' and controls. Cell staining was positive for PPARα mainly in hepatocytes and by perinuclear staining (Figure 2, left). However, the results of stained cells in chronic hepatitis C patients indicated a decrease in PPARα staining in hepatocytes compared to those in control livers (Figure 2, right). Negative control staining was performed by omitting the primary antibody or the use of an irrelevant antibody. These results suggested that hepatocytes were the major sources of PPARα and they expressed low levels of PPARγ during HCV infection.

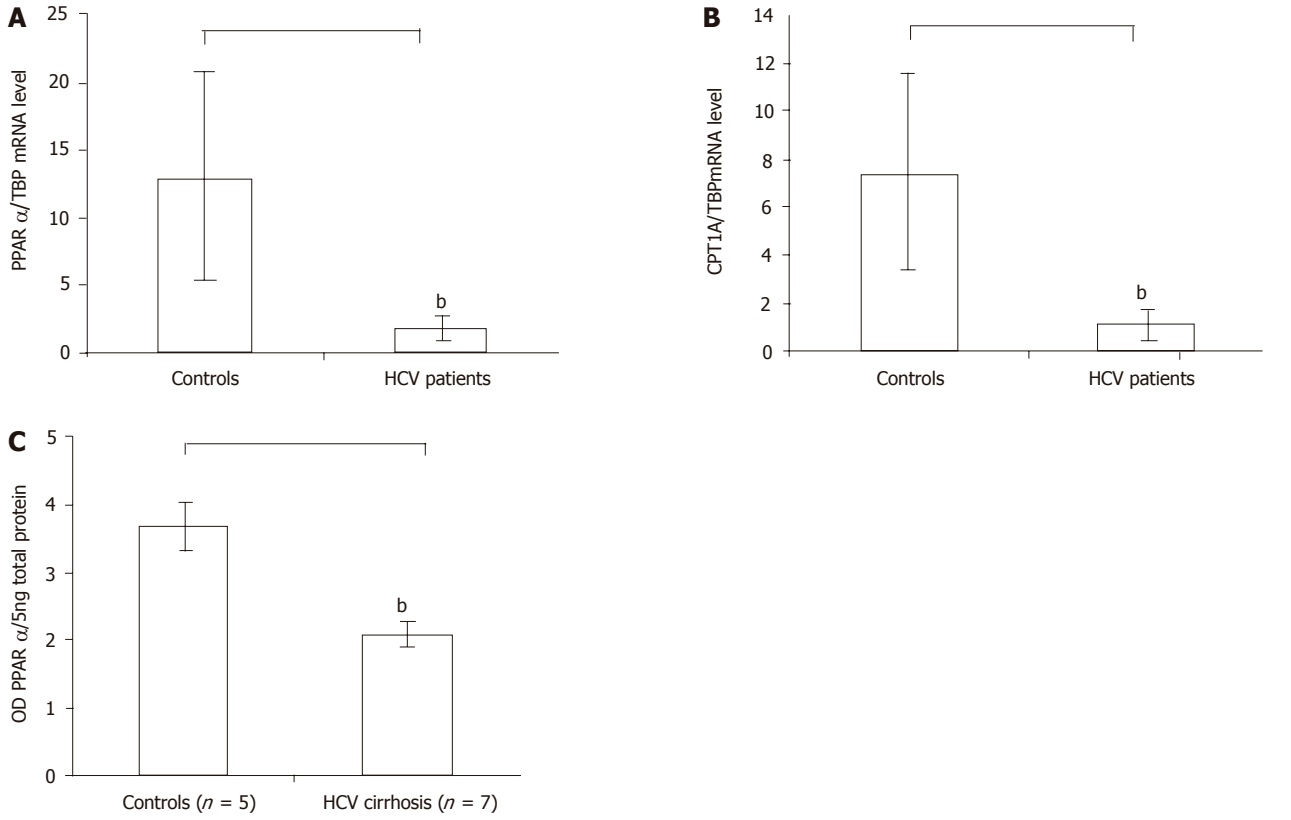

Figure 1 **A:** The PPARα mRNA level in the HCV patients reduced compared with controls by real-time RT-PCR, $^{b}P<0.01$ *vs* control; **B:** The PPARα target gene CPT1A mRNA level in the HCV patients also reduced compared with controls by real-time RT-PCR, $^{b}P<0.01$ *vs* control; **C:** The PPARα protein level in the HCV cirrhotic patients reduced compared with controls by Western blot. Results were expressed as mean±SD, $^{b}P<0.01$ *vs* control.

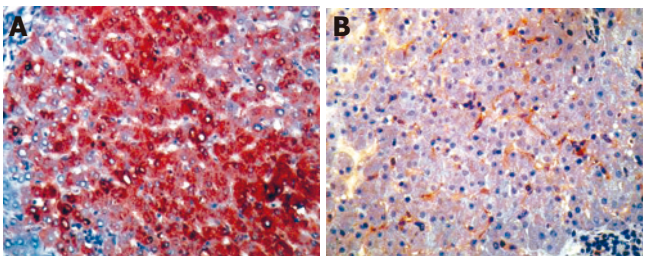

Figure 2 Representative PPARα immunostainings in liver specimens. The left: a control liver, PPARα staining was detected in the majority of hepatocytes (magnification ×160); The right: a severe hepatitis patient liver, the number of PPARα-stained hepatocytes was decreased markedly (magnification ×160).

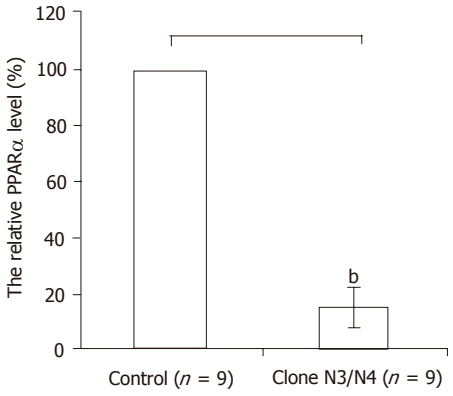

Figure 3 In the N3 colon and N4 colon which were stably expressing the HCV core protein PPARα mRNA levels decreased more than 80% compared with controls by real-time RT-PCR. Results were expressed as mean±SD, $^{b}P<0.01$ *vs* control.

HCV core protein reduced the expression of PPARα

Because hepatocytes were the parenchymal component in the liver that were prone to be infected by HCV, and HCV core protein regulated the transcriptional activity of several genes, the PPARα expression in HepG2 cells stably expressing HCV core protein were also quantified with the real-time PCR. In the N3 and N4 colons which were stably expressing the HCV core protein, PPARα mRNA levels were found to be similar, but decreased more than 80% compared with controls (Figure 3).

DISCUSSION

Because the morbidity and mortality of hepatitis C is high and the natural history is generally long and slow, many patients develop complications[6-8]. It is difficult to find an effective treatment if the exact mechanism of HCV is not clear, so it is a very important task to elucidate the pathogenesis of hepatitis C[2,4]. The results in this study demonstrated for the first time that the expression of PPARα was impaired in the livers of chronic hepatitis C patients. Both *in vitro* studies and the transgenic mouse model suggested that the HCV core protein is possibly responsible for lipid accumulation[12,26]. It was reported

that HCV core protein expression in transgenic mice could inhibit microsomal triglyceride transfer protein activity and very low density lipoprotein secretion causing steatosis[13]; and the mechanism postulated seemed to be related to mitochondrial toxicity with the production of reactive oxygen species. In this study, it was also found that in the N3 colon and N4 colon stably expressing the HCV core protein, the PPARα mRNA levels lowered significantly compared with controls. These results indicated the involvement of the HCV protein in the regulation of PPARα expression and activation.

PPARα plays a fundamental role in regulating energy homeostasis through controlling lipid metabolism[14]. PPARs belong to the type II steroid receptor family, including members such as RXR and thyroid hormone receptor[27]. These receptors are generally considered to localize to the nucleus and appear not to be bound to other proteins in inactive complexes, as has been extensively described for type I receptors (e.g. glucocorticoid receptor, progesterone receptor, androgen receptor). PPARα is a fatty acid-activated transcription factor that up-regulates the expression of a variety of genes encoding proteins involved in β-oxidation and lipoprotein metabolism[16]. PPARα plays a central role in fatty acid homeostasis by regulating the degradation of fatty acids by mitochondrial as well as by peroxisomal and microsomal fatty acid oxidation[28]. In addition, PPARα contributes to the maintenance of energy balance by regulating the expression of enzymes that participate in mitochondrial fatty acid oxidation and the formation of ketone bodies from fatty acids. Lack of this transcriptional factor in PPARα–/– mice results in the inability to up-regulate hepatic fatty acid oxidation and ketogenesis in the face of increased concentrations of free fatty acids in the circulation[15]. In this study, both the real-time PCR and Western blot analysis indicated that PPARα expression level was down-regulated in HCV infection; and the immunohistochemical staining also showed that the decreased expression was mainly in hepatocytes. So it suggests that HCV injures the liver partly through down-regulation of PPARα.

The PPARα-responsive human genes include CPT1A, the long chain fatty acyl-CoA synthase (ACS), and the mitochondrial HMG-CoA synthase (HMGCS2). Several aspects of fatty acid oxidation are disrupted in PPARα null mice that include a diminished, constitutive expression of several components of the mitochondrial fatty acid oxidation pathway. These results suggest that in mice, PPARα is a significant regulator of the mitochondrial capacity for fatty acid β-oxidation. The flux of long chain fatty acids through the mitochondrial γ-oxidation pathway is regulated by CPT1, a component of the long chain fatty acylcarnitine translocases. The activity of CPT1 is modulated by the concentration of malonyl-CoA, a potent inhibitor of the enzyme formed in the first committed step of fatty acid synthesis. Because CPT1 is induced by peroxisome proliferators in the liver, the target gene CPT1A of PPARα was also studied in order to understand the possible mechanisms of reduced expression of PPARα in the HCV infection. The human CPT1A gene is PPARα-responsive[17,18,29-31]. The fatty acyl-CoA substrates for CPT1 are formed by the esterification of free fatty acids to CoA by ACS. ACS is induced by peroxisome proliferators in rat liver, and PPRE has been identified in the promoter of the rat gene. In this study, the expression levels of the CPT1A gene in the livers of hepatitis C patients decreased significantly. It indicated that HCV core protein was possibly responsible for lipid accumulation by CPT1A, which was regulated by the transcriptional factor PPARα that was also the major isoform required for mediating the responses resulting from the actions of peroxisome proliferators in liver.

It was reported that human genes encoding key enzymes for mitochondrial fatty acid oxidation and ketogenesis could be regulated by human PPARα. In these tissues malonyl-CoA may act as a sensor or hormone and fuel through its ability to inhibit mitochondrial outer membrane CPT I[17]. This enzyme catalyzes the transesterification of long-chain fatty acyl-CoAs to long-chain acylcarnitines, which are carried into the mitochondrial matrix where acyl-CoA is regenerated for β-oxidation[18,30,31]. The role of PPARα in cell proliferation[32,33], tumor promotion[34,35] and in the prevention/reversal of liver injury has been studied by different researchers before[34-36].

To sum up, this report showed that the reduced intrahepatic PPARα expression level was associated with the HCV core protein. HCV infection down-regulated the expression of PPARα and CPT1A not only at mRNA level but also at the protein level. Correspondingly, the reduced PPARα level induced the low expression of CPT1A. The immunohistochemical analysis also proved that expression level of PPARα decreased in the hepatocytes. The function impairment of PPARα and CPT1A during the HCV infection still needs further investigation. The results in this study indicated that PPARα played an important role in the pathogenesis of chronic HCV infection, and this nuclear receptor could be a potential therapeutic target[34-36] in the treatment of HCV infection in the future.

REFERENCES

1 **Cohen J**. The scientific challenge of hepatitis C. *Science* 1999; **285**: 26-30

2 **Burroughs AK**, Groszmann R, Bosch J, Grace N, Garcia-Tsao G, Patch D, Garcia-Pagan J C, Dagher L. Assessment of therapeutic benefit of antiviral therapy in chronic hepatitis C: is hepatic venous pressure gradient a better end point? *Gut* 2002; **50**: 425-427

3 **Hickman IJ**, Clouston AD, Macdonald GA, Purdie DM, Prins JB, Ash S, Jonsson JR, Powell EE. Effect of weight reduction on liver histology and biochemistry in patients with chronic hepatitis C. *Gut* 2002; **51**: 89-94

4 **Siebert U**, Sroczynski G, Rossol S, Wasem J, Ravens-Sieberer U, Kurth BM, Manns MP, McHutchison JG, Wong JB. Cost effectiveness of peginterferon alpha-2b plus ribavirin versus interferon alpha-2b plus ribavirin for initial treatment of chronic hepatitis C. *Gut* 2003; **52:** 425-432

5 **Asselah T**, Boyer N, Guimont MC, Cazals-Hatem D, Tubach F, Nahon K, Daikha H, Vidaud D, Martinot M, Vidaud M, Degott C, Valla D, Marcellin P. Liver fibrosis is not associated

with steatosis but with necroinflammation in French patients with chronic hepatitis C. *Gut* 2003; **52**: 1638-1643
6 **Hoofnagle JH**. Hepatitis C: the clinical spectrum of disease. *Hepatology* 1997; **26**: 15S-20S
7 **Pagliaro L**, Peri V, Linea C, Camma C, Giunta M, Magrin S. Natural history of chronic hepatitis C. *Ital J Gastroenterol Hepatol* 1999; **31**: 28-44
8 **Desmet VJ**, Gerber M, Hoofnagle JH, Manns M, Scheuer PJ. Classification of chronic hepatitis: diagnosis, grading and staging. *Hepatology* 1994; **19**: 1513-1520
9 **Kage M**, Shimamatu K, Nakashima E, Kojiro M, Inoue O, Yano M. Long-term evolution of fibrosis from chronic hepatitis to cirrhosis in patients with hepatitis C: morphometric analysis of repeated biopsies. *Hepatology* 1997; **25**: 1028-1031
10 **Yano M**, Kumada H, Kage M, Ikeda K, Shimamatsu K, Inoue O, Hashimoto E, Lefkowitch JH, Ludwig J, Okuda K. The long-term pathological evolution of chronic hepatitis C. *Hepatology* 1996; **23**: 1334-1340
11 **Zaitoun AM**, Al Mardini H, Awad S, Ukabam S, Makadisi S, Record CO. Quantitative assessment of fibrosis and steatosis in liver biopsies from patients with chronic hepatitis C. *J Clin Pathol* 2001; **54**: 461-465
12 **Moriya K**, Fujie H, Shintani Y, Yotsuyanagi H, Tsutsumi T, Ishibashi K, Matsuura Y, Kimura S, Miyamura T, Koike K. The core protein of hepatitis C virus induces hepatocellular carcinoma in transgenic mice. *Nat Med* 1998; **4**: 1065-1067
13 **Perlemuter G**, Sabile A, Letteron P, Vona G, Topilco A, Chretien Y, Koike K, Pessayre D, Chapman J, Barba G, Brechot C. Hepatitis C virus core protein inhibits microsomal triglyceride transfer protein activity and very low density lipoprotein secretion: a model of viral-related steatosis. *FASEB J* 2002; **16**: 185-194
14 **Issemann I**, Green S. Activation of a member of the steroid hormone receptor superfamily by peroxisome proliferators. *Nature* 1990; **347:** 645-650
15 **Bandsma RH**, Van Dijk TH, Harmsel At A, Kok T, Reijngoud DJ, Staels B, Kuipers F. Hepatic de novo synthesis of glucose 6-phosphate is not affected in peroxisome proliferator-activated receptor alpha-deficient mice but is preferentially directed toward hepatic glycogen stores after a short term fast. *J Biol Chem* 2004; **279**: 8930-8937
16 **Gilde AJ**, van der Lee KA, Willemsen PH, Chinetti G, van der Leij FR, van der Vusse GJ, Staels B, van Bilsen M. Peroxisome proliferator-activated receptor (PPAR) alpha and PPARbeta/delta, but not PPARgamma, modulate the expression of genes involved in cardiac lipid metabolism. *Circ Res* 2003; **92:** 518-524
17 **van der Leij FR**, Cox KB, Jackson VN, Huijkman NC, Bartelds B, Kuipers JR, Dijkhuizen T, Terpstra P, Wood PA, Zammit VA, Price NT. Structural and functional genomics of the CPT1B gene for muscle-type carnitine palmitoyltransferase I in mammals. *J Biol Chem* 2002; **277:** 26994-27005
18 **Gobin S**, Thuillier L, Jogl G, Faye A, Tong L, Chi M, Bonnefont JP, Girard J, Prip-Buus C. Functional and structural basis of carnitine palmitoyltransferase 1A deficiency. *J Biol Chem* 2003; **278:** 50428-50434
19 **Bedossa P**, Poynard T. An algorithm for the grading of activity in chronic hepatitis C. The METAVIR Cooperative Study Group. *Hepatology* 1996; **24**: 289-293
20 **Desreumaux P**, Dubuquoy L, Nutten S, Peuchmaur M, Englaro W, Schoonjans K, Derijard B, Desvergne B, Wahli W, Chambon P, Leibowitz MD, Colombel JF, Auwerx J. Attenuation of colon inflammation through activators of the retinoid X receptor (RXR)/peroxisome proliferator-activated receptor gamma (PPARgamma) heterodimer. A basis for new therapeutic strategies. *J Exp Med* 2001; **193**: 827-838
21 **Barba G**, Harper F, Harada T, Kohara M, Goulinet S, Matsuura Y, Eder G, Schaff Z, Chapman MJ, Miyamura T, Brechot C. Hepatitis C virus core protein shows a cytoplasmic localization and associates to cellular lipid storage droplets. *Proc Natl Acad Sci USA* 1997; **94:** 1200-1205
22 **Martin G**, Schoonjans K, Lefebvre AM, Staels B, Auwerx J. Coordinate regulation of the expression of the fatty acid transport protein and acyl-CoA synthetase genes by PPARalpha and PPARgamma activators. *J Biol Chem* 1997; **272**: 28210-28217
23 **Bieche I**, Onody P, Laurendeau I, Olivi M, Vidaud D, Lidereau R, Vidaud M. Real-time reverse transcription-PCR assay for future management of ERBB2-based clinical applications. *Clin Chem* 1999; **45**: 1148-1156
24 **Dubuquoy L**, Jansson EA, Deeb S, Rakotobe S, Karoui M, Colombel JF, Auwerx J, Pettersson S, Desreumaux P. Impaired expression of peroxisome proliferator-activated receptor gamma in ulcerative colitis. *Gastroenterology* 2003; **124**: 1265-1276
25 **Philippe D**, Dubuquoy L, Groux H, Brun V, Chuoi-Mariot MT, Gaveriaux-Ruff C, Colombel JF, Kieffer BL, Desreumaux P. Anti-inflammatory properties of the mu opioid receptor support its use in the treatment of colon inflammation. *J Clin Invest* 2003; **111**: 1329-1338
26 **Otani K**, Korenaga M, Beard MR, Li K, Qian T, Showalter LA, Singh AK, Wang T, Weinman SA. Hepatitis C virus core protein, cytochrome P450 2E1, and alcohol produce combined mitochondrial injury and cytotoxicity in hepatoma cells. *Gastroenterology* 2005; **128**: 96-107
27 **McCarthy TC**, Pollak PT, Hanniman EA, Sinal CJ. Disruption of hepatic lipid homeostasis in mice after amiodarone treatment is associated with peroxisome proliferator-activated receptor-alpha target gene activation. *J Pharmacol Exp Ther* 2004; **311**: 864-873
28 **Mehendale HM**. PPAR-alpha: a key to the mechanism of hepatoprotection by clofibrate. *Toxicol Sci* 2000; **57**: 187-190
29 **Hsu MH**, Savas U, Griffin KJ, Johnson EF. Identification of peroxisome proliferator-responsive human genes by elevated expression of the peroxisome proliferator-activated receptor alpha in HepG2 cells. *J Biol Chem* 2001; **276**: 27950-27958
30 **Bonnefont JP**, Djouadi F, Prip-Buus C, Gobin S, Munnich A, Bastin J. Carnitine palmitoyltransferases 1 and 2: biochemical, molecular and medical aspects. *Mol Aspects Med* 2004; **25**: 495-520
31 **Price NT**, Jackson VN, van der Leij FR, Cameron JM, Travers MT, Bartelds B, Huijkman NC, Zammit VA. Cloning and expression of the liver and muscle isoforms of ovine carnitine palmitoyltransferase 1: residues within the N-terminus of the muscle isoform influence the kinetic properties of the enzyme. *Biochem J* 2003; **372**: 871-879
32 **Reddy JK**. Nonalcoholic steatosis and steatohepatitis. III. Peroxisomal beta-oxidation, PPAR alpha, and steatohepatitis. *Am J Physiol Gastrointest Liver Physiol* 2001; **281**: G1333- G1339
33 **Chakrabarti R**, Vikramadithyan RK, Misra P, Hiriyan J, Raichur S, Damarla RK, Gershome C, Suresh J, Rajagopalan R. Ragaglitazar: a novel PPAR alpha PPAR gamma agonist with potent lipid-lowering and insulin-sensitizing efficacy in animal models. *Br J Pharmacol* 2003; **140**: 527-537
34 **Rao MS**, Papreddy K, Musunuri S, Okonkwo A. Prevention/reversal of choline deficiency-induced steatohepatitis by a peroxisome proliferator-activated receptor alpha ligand in rats. *In Vivo* 2002; **16**: 145-152
35 **Karlic H**, Lohninger S, Koeck T, Lohninger A. Dietary l-carnitine stimulates carnitine acyltransferases in the liver of aged rats. *J Histochem Cytochem* 2002; **50**: 205-12
36 **Sumanasekera WK**, Tien ES, Turpey R, Vanden Heuvel JP, Perdew GH. Evidence that peroxisome proliferator-activated receptor alpha is complexed with the 90-kDa heat shock protein and the hepatitis virus B X-associated protein 2. *J Biol Chem* 2003; **278**: 4467-4473

Science Editors Ma JY and Guo SY **Language Editor** Elsevier HK

PO Box 2345, Beijing 100023, China
www.wjgnet.com
wjg@wjgnet.com

ELSEVIER

World J Gastroenterol 2005;11(48):7597-7601
World Journal of Gastroenterology ISSN 1007-9327

• *BASIC RESEARCH* •

Cytoskeleton reorganization and ultrastructural damage induced by gliadin in a three-dimensional *in vitro* model

Ersilia Dolfini, Leda Roncoroni, Luca Elli, Chiara Fumagalli, Roberto Colombo, Simona Ramponi, Fabio Forlani, Maria Teresa Bardella

Ersilia Dolfini, Leda Roncoroni, Chiara Fumagalli, Department of Biology and Genetics for Health Sciences, University of Milan, Milan, Italy
Luca Elli, Maria Teresa Bardella, Department of Digestive Diseases and Endocrinology, IRCCS Ospedale Maggiore di Milano, University of Milan, Milan, Italy
Roberto Colombo, Department of Biology, University of Milan, Milan, Italy
Simona Ramponi, Milan Research Imaging Centre, Bracco SpA, Milan, Italy
Fabio Forlani, Department of Agrifood Molecular Sciences, University of Milan, Milan, Italy
Supported by the "Fondazione San Paolo" grant to "Centro per lo Studio della Celiachia"
Correspondence to: Dr Ersilia Dolfini, Department of Biology and Genetics for Health Sciences, Via Viotti 3/5, 20131 Milano, Italy. ersilia.dolfini@unimi.it
Telephone: +39-02-50315837 Fax: +39-02-50315864
Received: 2005-03-01 Accepted: 2005-07-08

Abstract

AIM: To evaluate the interplay between gliadin and LoVo cells and the direct effect of gliadin on cytoskeletal patterns.

METHODS: We treated LoVo multicellular spheroids with digested bread wheat gliadin in order to investigate their morphology and ultrastructure (by means of light microscopy and scanning electron microscopy), and the effect of gliadin on actin (phalloidin fluorescence) and the tight-junction protein occludin and zonula occluden-1.

RESULTS: The treated spheroids had deep holes and surface blebs, whereas the controls were smoothly surfaced ovoids. The incubation of LoVo spheroids with gliadin decreased the number of intracellular actin filaments, impaired and disassembled the integrity of the tight-junction system.

CONCLUSION: Our data obtained from an "*in vivo*-like" polarized culture system confirm the direct noxious effect of gliadin on the cytoskeleton and tight junctions of epithelial cells. Unlike two-dimensional cell culture systems, the use of multicellular spheroids seems to provide a suitable model for studying cell-cell interactions.

Key words: Celiac disease; Gliadin; Cytoskeleton; Multicellular spheroids

Dolfini E, Roncoroni L, Elli L, Fumagalli C, Colombo R, Ramponi S, Forlani F, Bardella MT. Cytoskeleton reorganization and ultrastructural damage induced by gliadin in a three-dimensional *in vitro* model. *World J Gastroenterol* 2005; 11(48): 7597-7601
http://www.wjgnet.com/1007-9327/11/7597.asp

INTRODUCTION

Celiac disease (CD) is an immunomediated intestinal disorder that is triggered by dietary gluten and related cereal proteins in genetically susceptible individuals[1,2]. Gluten consists of a complex mixture of gliadin monomers and large polymeric glutenin polypetides. A number of *in vitro* studies of two-dimensional cell cultures have shown that gliadin has direct cytotoxic effects on epithelial cells[3], but the early steps allowing the start of the immunoreaction are largely unknown.

CD is characterized by enhanced paracellular permeability across the intestinal epithelium, a "leaky gut" condition that allows the passage of macromolecules through the paracellular spaces[4-6]. Moreover, it has also been demonstrated that cytoskeleton involved in the pathogenesis of CD as a gluten challenge rapidly causes the disappearance and disorganization of actin filaments in the intestinal mucosa of CD patients[7]. The actin filaments in epithelial cells are associated with tight junctions (TJs), appearing as a series of discrete sites of apparent membrane fusion (so called "kissing points") involving the outer leaflets of the plasma membranes of adjacent cells. The integrity of the barrier function is important for the separation of two different compartments, and TJs play a major role in controlling paracellular transport between the luminal and basolateral fluid compartments[8].

Almost all the proteins associated with TJs are peripheral membrane proteins that form part of the submembrane plaque (Figure 1). The first TJ-associated protein to be identified is zonula occluden-1 (ZO-1) whose C-terminal half contains an actin-binding site and mediates interactions between transmembrane proteins and cytoskeleton elements[9]. Occludin, a 60 ku integral membrane protein in TJ strands[10], is involved in TJ barrier and fence functions through its four transmembrane domains, three cytoplasmic domains and two extracellular

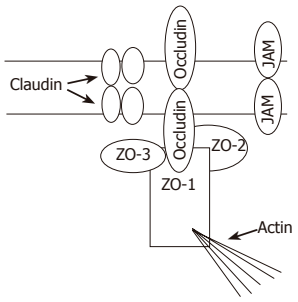

Figure 1 Tight junction (TJ) structure with emphasis on proteins of the TJ membrane domain: ZO family members and their interaction with actin filaments.

loops[8]. Claudin-1 and claudin-2 are 23 ku integral membrane proteins that function as major structural components of TJ strands[11]. Junctional adhesion molecules (JAMs) have only one putative transmembrane sequence. The intracellular domain consists of 45 residues, and the extracellular portion (215 residues) contains two domains with intra chain disulfide bonds[12].

The cytoskeletal network generates tension and transmits stress within and among the cells[13]. The formation of multicellular tumor spheroids (MCTSs) involves cell translocations and morphological changes that are indicative of the organization of the cytoskeleton. The cells grown in MCTSs are interconnected by the means of TJs that form a seal between adjacent cells, thus defining their apical and basolateral surfaces, and creating a model similar to *in vivo* tissue. This is very different from the organization of two-dimensional cell cultures[14,15].

The aim of this study was to evaluate the interplay between gliadin and LoVo MCTSs, with specific emphasis on the direct effect of gliadin on cytoskeleton patterns and reorganization.

MATERIALS AND METHODS

Cell line

Cells from the human colon adenocarcinoma cell line (LoVo, ATCC, Rockville, USA) were grown in T75 flasks (PBI, Italy) at 37 °C in an atmosphere containing 95% air and 50 mL/L CO_2. The medium consisted of Ham's F-12 medium (GIBCO, Italy), supplemented with 10% fetal bovine serum (GIBCO, Italy), 1% MEM vitamin solution 100× (GIBCO, Italy), and 3% L-glutamine 200 mmol/L (GIBCO, Italy).

After one week, the cells were removed using solution containing 0.25% (w/v) trypsin and 0.02% (w/v) EDTA (Sigma-Aldrich, Italy), and the cell suspensions were cultured again. Mycoplasma contamination was regularly searched for and excluded using the Hoechst method[16].

Gliadin digestion

Gliadin was purified from *Triticum aestivum* flour (Hereward Cultivar, UK) according to Capelli[17]. Pepsin (3.2-4.5 U/mg) was supplied by Sigma (Italy), and the pancreatin (0.1 mAnson/mg) by Merck (USA). All the chemicals were of analytical grade. Digestion was performed as previously described by our group[18]. Briefly, the gliadin was first incubated with pepsin at 37 °C for 24 h, and then with pancreatin at 37 °C for 3 h, adjusting to a pH of 8. The digested protein was analytically controlled by means of RP-HPLC, SE-HPLC, and SDS-PAGE, freeze-dried and stored.

Three-dimensional cell cultures and gliadin treatment

Three-dimensional cell cultures were initiated by seeding 4×10^5 cells/mL in 25 mL of complete medium supplemented with penicillin (100 U/mL) and streptomycin (100 Ug/mL) (GIBCO, Italy) in Erlenmeyer flasks (Corning, Italy), and incubated in a gyratory rotation incubator (60 rev/min) at 37 °C in air (Colaver, Italy). Homotypical aggregations were visible after 4 d of culture, and the MCTSs were usually complete within 7 d (average diameter±SD, 370±48.5 μm).

On the seventh day, the MCTSs were exposed to PT-digested gliadin (500 μg/mL) in a completely renewed medium for further 4 d and subsequently taken for microscopic examination. The PT-digested gliadin greatly inhibited cell growth (50% inhibitory concentration: 390 μg/mL) and the dose used was selected from four different concentrations (125, 500, 750, 1 000 μg/mL) on the basis of previous data obtained in our laboratory[18,19].

Scanning electron microscopy (SEM)

Three-dimensional cell cultures were washed twice in PBS, and then fixed in 2.5% glutaraldehyde in phosphate buffer at room temperature for 24 h at 4 °C. At the time of analysis, a representative sample of spheroids was recovered, immediately placed on a paper filter and observed in low vacuum modality at a high voltage of 10 kV. SEM analysis was performed using a Philips Scanning Electron Microscope (Mod. ×L20).

Confocal laser scanning microscopy of intracellular F-actin

LoVo MCTSs were washed twice in PBS, fixed in 4% paraformaldeyde for 1 h, permeabilized with 0.4% Triton X-100 (Sigma-Aldrich, Italy) for 20 min, washed thrice for 5 min in PBS and stained for immunocytochemistry by means of incubation with fluorescein TRITC-phalloidin (Sigma-Aldrich, Italy) (1:200 PBS) in a humid chamber at room temperature for 6 h. After washing thrice in PBS each for 5 min, 10 spheroids were transferred onto slides, and each slide was mounted with 90% glycerol in PBS. The results were analyzed using a confocal laser scanning microscope (Leica TCSNT, Germany).

Confocal laser scanning microscopy of occludin

LoVo MCTSs were washed twice in PBS and fixed in ethanol for 30 min at 4 °C. After the first incubation, the samples were incubated with acetone (previously stored at -20 °C) for an additional 3 min at room temperature. They were then blocked and incubated for immunocytochemistry overnight with anti-occludin-FITC (Zymed, CA, USA) before being analyzed by means of confocal laser scanning microscopy (Leica TCSNT, Germany).

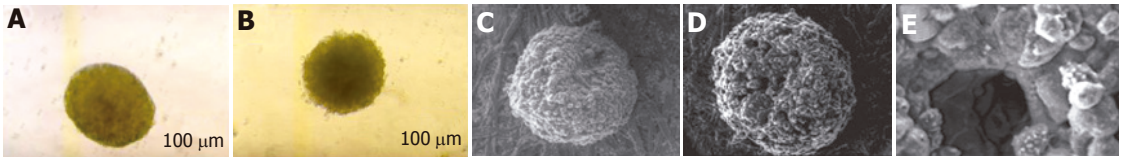

Figure 2 Phase-contrast micrographs (10×) showing control (**A**) and gliadin-treated multicellular tumor spheroids of the human colon adenocarcinoma LoVo cell line (**B**) after 11 d of culture; Scanning electron micrographs: showing the ovoid control spheroids (**C**) and their very compact, densely organized and tightly packed structure that they can be clearly distinguished from each other; The surface of gliadin-treated spheroids (**D**) focally interrupted by irregularly distributed holes, and loss of their structural thickness and organization (**E**).

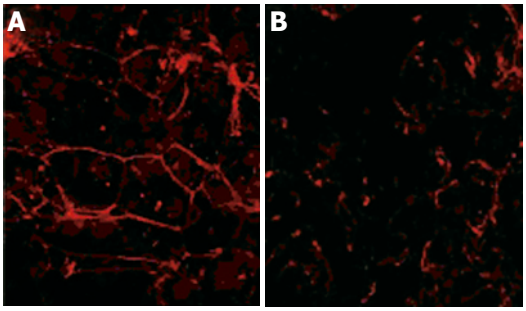

Figure 3 Confocal laser scanning micrograph in which TRICT-phalloidin highlights the organization of F-actin in multicellular tumor spheroids. The control spheroids (**A**) have a "chicken-wire" distribution under the plasma membrane, whereas the treated spheroids (**B**) show a reorganized actin cytoskeleton.

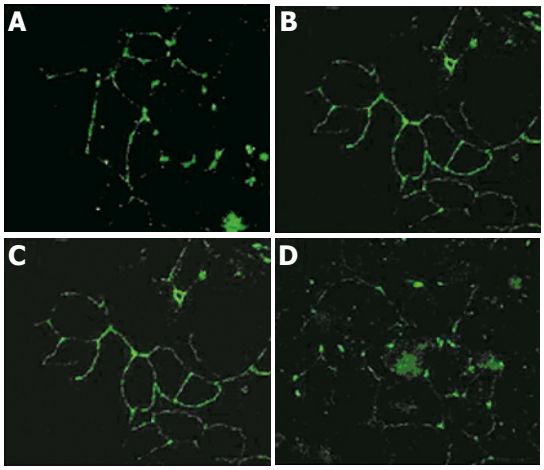

Figure 4 Confocal microscopy immunolocalization of occludin and zonula occluden-1 (ZO-1) in LoVo multicellular tumor spheroids. In the control spheroids, occludin and ZO-1 localized sharply in the apical region of the lateral membrane are visualized en face as a ring pattern (**A** and **C**), whereas the distribution of occludin and ZO-1 in the spheroids exposed to gliadin for 4 d is far from the lateral TJ membrane (**B** and **D**).

Confocal laser scanning microscopy of zonula occluden-1

LoVo MCTSs were washed twice in PBS and fixed in ethanol for 30 min at 4 °C. After the first incubation, the samples were incubated with acetone (previously stored at -20 °C) for an additional 3 min at room temperature. They were then blocked and incubated overnight with anti-ZO-1-FITC (Zymed, CA, USA) before being analyzed by means of confocal laser scanning microscopy (Leica TCSNT, Germany).

RESULTS

Light microscopy and SEM

The untreated MCTSs appeared bright and round at phase-contrast microscopy (Figure 2A). SEM showed that they were well-defined and compact, with smooth boundaries and a regular surface. Their structure was compact, densely organized and tightly packed (Figure 2C).

The MCTSs treated with PT-digested gliadin were loosely connected and irregularly shaped (Figure 2B). They were less bright than the controls and had frayed borders. SEM revealed an altered surface, with deep and irregularly distributed holes (Figures 2D and E).

Confocal laser scanning microscopy

The untreated MCTSs stained with TRITC-phalloidin had regular perijunctional actin rings and showed organized distribution at the cell boundaries (Figure 3A), whereas those treated with PT-digested gliadin had reorganized intracellular actin filaments and disassembled F-actin (Figure 3B).

In comparison with the normal subapical honeycomb pattern typical of TJs (Figures 4A and C), treatment with PT-digested gliadin led to their structural dissociation (Figures 4B and D). The morphologically characteristic ring structure of occludin and ZO-1 immunolocalization in the en face confocal images had sharp boundaries in the untreated spheroids, but was partially or completely lost in the treated spheroids.

DISCUSSION

CD is a chronic intestinal inflammatory disorder characterized by mucosal changes including lymphocyte infiltration, crypt hyperplasia and villous atrophy. Furthermore, intestinal permeability is increased and TJs appear open[20]. As TJs form a barrier against the diffusion of molecules from the lumen to the tissue parenchyma (barrier function), and restrict the diffusion of lipids and proteins between the apical and basolateral plasma membranes (fence function)[21], the loss of permeability allows the translocation of antigenic molecules from the intestinal lumen to the lamina propria, thus creating a condition for an immune response.

Traditional tissue culture methods have been based on growing cell lines as monolayers, but a new three-

dimensional culture system (Figure 2A) has been investigated as a mean of modeling a solid tumor under *in vitro* conditions that simulates its *in vivo* biological properties. Given the fundamental differences between monolayer and three-dimensional cultures, spheroids should become mandatory test systems in oncological therapeutic screening programs[22]. Furthermore, cells grown in three-dimensional cultures are oriented and polarized[23,24], and often express a gene repertoire that is different from that of the monolayer cultures[25]. Previous studies from our laboratory have confirmed the polarized structure, and the presence of microvilli and tightly connected epithelial junctional complexes[18].

The interaction between TJ proteins and actomyosin cytoskeleton in MCTSs is a primary target for physiological and pathological signals. Circumferential actomyosin contraction and cytoskeleton interaction modulate TJ permeability, thus contributing to the formation of the TJ fence[21]. Pizzuti *et al*.[26] have recently demonstrated that the intestinal mucosa of celiac patients has an altered TJ system during gluten exposure, and decreased ZO-1 expression is associated with a disrupted F-actin organization and the loss of normal distribution at cell-cell contact sites.

Our SEM morphological examinations confirmed that gliadin treatment could affect spheroid structure, causing a loss of cell thickness and organization, and the formation of hole-like surface structures (Figures 2C-E). Confocal laser scanning microscopy showed that gliadin could induce cytoskeleton reorganization (Figures 3A and B), and specifically act on TJ structural proteins.

Though our results have confirmed that the expression of occludin correlates with barrier properties, the decreased intensity or disappearance of occludin staining at cell–cell borders in gliadin-treated spheroids (Figures 4A and B) do not presuppose the absence of TJ structural integrity. Knockout experiments in mouse embryonic stem cells have demonstrated that occludin is not necessary to form functionally competent TJs[27], and ZO-1 has a wild-type localization in apical junctional regions of the outermost layer of epithelial cells in the absence of occludin[28]. We found that the immunolocalization of ZO-1 in TJ ring structures was severely disrupted by gliadin exposure, leading to almost complete lack of continuity, and *en face* confocal images showed a breakdown of junctional complexes (Figures 4C and D). Taken together, these findings suggest that ZO-1 lies at the centre of a network of protein–protein interactions and may be critical in recruiting the proteins necessary to establish TJs.

Our preliminary data showed that TJ permeability might be regulated directly as a result of TJ protein modifications, or indirectly as a result of the effects of xenobiotics on the cytoskeleton. New insights into the molecular architecture of TJs and their regulation have given rise to a new concept of TJ modulation based on peptides from the first extracellular domain of occludin[29]. We can speculate that gliadin peptides also act as modulators on the extracellular loops of TJ transmembrane proteins, mediating TJ opening and the consequent cytoskeletal redistribution. According to the "tensegrity model"[30,31], the cells are in prestressed structures in which cytoskeletal elements are major determinants of deformability, and so a local stress can cause global structural rearrangements. The cell response to xenobiotic exposure leads to the retraction of submembranous actin filaments from junctional complexes, thus determining the disappearance of organized TJs. Furthermore, this alteration of internal balance of tensile stress compromises the stability of cell shape: the cells become rounded and stimulate an apoptotic process. The correlation of apoptosis with a disrupted cytoskeleton and junctional system may explain the SEM images: the blebs and holes visible on the surface of treated spheroids are the results of an apoptotic process initiated by the deregulation of internal cell balance. Ojakian *et al*.[32] reported that gliadin has an apoptotic effect on Caco-2 colon carcinoma cells directly stimulated by digested gliadin.

Understanding the events of this process will throw light onto the changes in paracellular permeability caused by gliadin and identify novel therapeutic targets in celiac disease. Though the intricacies of this process *in vivo* have not yet been fully elucidated, our results indicate that a pivotal role is played by the disarrangement of the "belt-like" structure of perijunctional F-actin affiliated with TJs. This highlights the importance of the cytoskeleton network in the ultrastructural architecture of enterocytes, given that a gluten challenge in CD patients rapidly distorts the microvillous structure, thus disorganizing the actin network on the intestinal mucosa.

If the early steps of gliadin-induced mucosal damage in patients with CD concern intestinal permeability, which is directly altered by gliadin before the immunological response, MCTSs could become essential for testing the cytotoxic effects of new chemically, enzymatically or genetically modified gliadins studied as alternative therapies to a gluten-free diet.

ACKNOWLEDGMENTS

The authors would like to thank Kevin Smart (Link srl, Milan), "Centro per lo Studio della Celiachia" of the University of Milan, for his help in preparing the English version of the manuscript, Maria Letizia Falini and Rosita Caramanico for their help in preparing peptides, and San Paolo Bank for financial support.

The study was conceived and designed by E. Dolfini, R. Colombo, L. Roncoroni, C. Fumagalli, L. Elli, and M.T. Bardella. L. Roncoroni and C. Fumagalli were responsible for the cell cultures. V. Lorusso and S. Ramponi undertook the morphological investigations and F. Forlani prepared the digested gliadin.

REFERENCES

1 **Fasano A**, Catassi C. Current approaches to diagnosis and treatment of celiac disease: an evolving spectrum. *Gastroenterology* 2001; **120**: 636-651

2 **Green PH**, Jabri B. Coeliac disease. *Lancet* 2003; **362**: 383-391
3 **Elli L**, Dolfini E, Bardella MT. Gliadin cytotoxicity and in vitro cell cultures. *Toxicol Lett* 2003; **146**: 1-8
4 **Cooper BT.** Intestinal permeability in coeliac disease. *Lancet* 1983; **1**: 658-659
5 **Bjarnason I**, Peters TJ, Veall N. Intestinal permeability defect in coeliac disease. *Lancet* 1983; **1**: 1284-1285
6 **Schulzke JD**, Bentzel CJ, Schulzke I, Riecken EO, Fromm M. Epithelial tight junction structure in the jejunum of children with acute and treated celiac sprue. *Pediatr Res* 1998; **43:** 435-441
7 **Sjolander A**, Magnusson KE. Effects of wheat germ agglutinin on the cellular content of filamentous actin In intestine 407 cells. *Eur J Cell Biol* 1988; **47**: 32-35
8 **Tsukita S**, Furuse M. Occludin and claudins in tight-junction strands: leading or supporting players? *Trends Cell Biol* 1999; **9**: 268-273
9 **Stevenson BR**, Siliciano JD, Mooseker MS, Goodenough DA. Identification of ZO-1: a high molecular weight polypeptide associated with the tight junction (zonula occludens) in a variety of epithelia. *J Cell Biol* 1986; **103:** 755-766
10 **Furuse M**, Hirase T, Itoh M, Nagafuchi A, Yonemura S, Tsukita S, Tsukita S. Occludin: a novel integral membrane protein localizing at tight junctions. *J Cell Biol* 1993; **123**: 1777-1788
11 **Furuse M**, Fujita K, Hiiragi T, Fujimoto K, Tsukita S. Claudin-1 and -2: novel integral membrane proteins localizing at tight junctions with no sequence similarity to occludin. *J Cell Biol* 1998; **141**: 1539-1550
12 **Martin-Padura I**, Lostaglio S, Schneemann M, Williams L, Romano M, Fruscella P, Panzeri C, Stoppacciaro A, Ruco L, Villa A, Simmons D, Dejana E. Junctional adhesion molecule, a novel member of the immunoglobulin superfamily that distributes at intercellular junctions and modulates monocyte transmigration. *J Cell Biol* 1998; **142**: 117-127
13 **Bates RC**, Buret A, van Helden DF, Horton MA, Burns GF. Apoptosis induced by inhibition of intercellular contact. *J Cell Biol* 1994; **125:** 403-415
14 **Conforti G**, Codegoni AM, Scanziani E, Dolfini E, Dasdia T, Calza M, Caniatti M, Broggini M. Different vimentin expression in two clones derived from a human colocarcinoma cell line (LoVo) showing different sensitivity to doxorubicin. *Br J Cancer* 1995; **71:** 505-511
15 **Matsubara S**, Ozawa M. Expression of alpha-catenin in alpha-catenin-deficient cells results in a reduced proliferation in three-dimensional multicellular spheroids but not in two-dimensional monolayer cultures. *Oncogene* 2004; **23**: 2694-2702
16 **La Porta CA**, Dolfini E, Comolli R. Inhibition of protein kinase C-alpha isoform enhances the P-glycoprotein expression and the survival of LoVo human colon adenocarcinoma cells to doxorubicin exposure. *Br J Cancer* 1998; **78**: 1283-1287
17 **Capelli L**, Forlani F, Perini F, Guerrieri N, Cerletti P, Righetti PG. Wheat cultivar discrimination by capillary electrophoresis of gliadins in isoelectric buffers. *Electrophoresis* 1998; **19:** 311-318
18 **Dolfini E**, Elli L, Ferrero S, Braidotti P, Roncoroni L, Dasdia T, Falini ML, Forlani F, Bardella MT. Bread wheat gliadin cytotoxicity: a new three-dimensional cell model. *Scand J Clin Lab Invest* 2003; **63:** 135-141
19 **Dolfini E**, Elli L, Dasdia T, Bufardeci B, Colleoni MP, Costa B, Floriani I, Falini ML, Guerrieri N, Forlani F, Bardella MT. In vitro cytotoxic effect of bread wheat gliadin on the LoVo human adenocarcinoma cell line. *Toxicol In Vitro* 2002; **16**: 331-337
20 **Clemente MG**, De Virgiliis S, Kang JS, Macatagney R, Musu MP, Di Pierro MR, Drago S, Congia M, Fasano A. Early effects of gliadin on enterocyte intracellular signalling involved in intestinal barrier function. *Gut* 2003; **52**: 218-223
21 **Schneeberger EE**, Lynch RD. The tight junction: a multifunctional complex. *Am J Physiol Cell Physiol* 2004; **286**: C1213-C1228
22 **Desoize B.** Contribution of three-dimensional culture to cancer research. *Crit Rev Oncol Hematol* 2000; **36**: 59-60
23 **Ojakian GK**, Schwimmer R. Regulation of epithelial cell surface polarity reversal by β-1 integrins. *J Cell Sci* 1994; **107**: 561-576
24 **Laderoute KR**, Murphy BJ, Short SM, Grant TD, Knapp AM, Sutherland RM. Enhancement of transforming growth factor-alpha synthesis in multicellular tumour spheroids of A431 squamous carcinoma cells. *Br J Cancer* 1992; **65:** 157-162
25 **Murphy BJ**, Laderoute KR, Vreman HJ, Grant TD, Gill NS, Stevenson DK, Sutherland RM. Enhancement of heme oxygenase expression and activity in A431 squamous carcinoma multicellular tumor spheroids. *Cancer Res* 1993; **53:** 2700-2703
26 **Pizzuti D**, Bortolami M, Mazzon E, Buda A, Guariso G, D' Odorico A, Chiarelli S, D'Inca R, De Lazzari F, Martines D. Transcriptional downregulation of tight junction protein ZO-1 in active coeliac disease is reversed after a gluten-free diet. *Dig Liver Dis* 2004; **36**: 337-341
27 **Saitou M**, Ando-Akatsuka Y, Itoh M, Furuse M, Inazawa J, Fujimoto K, Tsukita S. Mammalian occludin in epithelial cells: its expression and subcellular distribution. *Eur J Cell Biol* 1997; **73**: 222-231
28 **Harhaj NS**, Antonetti DA. Regulation of tight junctions and loss of barrier function in pathophysiology. *Int J Biochem Cell Biol* 2004; **36**: 1206-1237
29 **Tavelin S**, Hashimoto K, Malkinson J, Lazorova L, Toth I, Artursson P. A new principle for tight junction modulation based on occludin peptides. *Mol Pharmacol* 2003; **64**: 1530-1540
30 **Ingber DE**. Tensegrity I. Cell structure and hierarchical systems biology. *J Cell Sci* 2003; **116:** 1157-1173
31 **Ingber DE.** Tensegrity II. How structural networks influence cellular information processing networks. *J Cell Sci* 2003; **116**: 1397-1408
32 **Ojakian GK**, Schwimmer R. Regulation of epithelial cell surface polarity reversal by beta 1 integrins. *J Cell Sci* 1994; **107 (Pt 3):** 63-71

Science Editor Wang XL and Guo SY **Language Editor** Elsevier HK

PO Box 2345, Beijing 100023, China
www.wjgnet.com
wjg@wjgnet.com

ELSEVIER

World J Gastroenterol 2005;11(48):7602-7605
World Journal of Gastroenterology ISSN 1007-9327

• *BASIC RESEARCH* •

Cyclosporine A, FK-506, 40-0-[2-hydroxyethyl]rapamycin and mycophenolate mofetil inhibit proliferation of human intrahepatic biliary epithelial cells *in vitro*

Chao Liu, Thomas Schreiter, Andrea Frilling, Uta Dahmen, Christoph E Broelsch, Guido Gerken, Ulrich Treichel

Chao Liu, Thomas Schreiter, Guido Gerken, Ulrich Treichel, Department of Gastroenterology and Hepatology, University Hospital Essen, Germany
Andrea Frilling, Uta Dahmen, Christoph E Broelsch, Department of General Surgery and Transplantation, University Hospital Essen, Germany
Chao Liu, Department of General Surgery, Sun Yat-Sen Memorial Hospital, Sun Yat-Sen University, No. 107 West Yan Jiang Road, 510120 Guangzhou, Guangdong Province, China. mdliuchao@hotmail.com,
Telephone: +86-20-3407-0891
Correspondence to: Ulrich Treichel, MD, Department of Gastroenterology and Hepatology, University Hospital Essen, Hufelandstr. 55, 45122 Essen, Germany. ulrich.treichel@uni-essen.de
Telephone: +49-201-723-3612 Fax: +49-201-723-5970
Received: 2004-12-30 Accepted: 2005-02-18

Abstract

AIM: To investigate the effect of cyclosporine A (CsA), FK-506, and mycophenolate mofetil (MMF) and 40-0-[2-hydroxyethyl]rapamycin (RAD) on proliferation of human intrahepatic biliary epithelial cells (BECs) *in vitro*.

METHODS: BECs were isolated from six human liver tissuespecimens with the immunomagnetic separation method and treated with different concentrations of CsA, FK-506, RAD, and MMF *in vitro*. Proliferation of the cells was measured by MTT assay at 24 and 48 h after treatment, respectively. One-way analysis of variance was used to analyze the results. Expression of CK 19 in BECs was monitored by flow cytometry and Western blot.

RESULTS: Six lines of BECs were established. They survived for 4-18 wk *in vitro*. Flow cytometry analysis showed that these cells always expressed CK19. CsA, FK-506, RAD, and MMF inhibited proliferation of BECs in a dose-dependent manner. The lowest concentration of CsA, FK-506, RAD, and MMF to inhibit proliferation of BECs ($P<0.05$) was 500, 100, 0.25, and 100 μg/L, respectively. However, the expression of CK19 by BECs was not changed.

CONCLUSION: CsA, FK-506, RAD, and MMF have an antiproliferative effect on human intrahepatic BECs *in vitro*, while RAD has the strongest growth-inhibitory effect. Their possible effects on liver regeneration and bile duct injury in transplant patients should be further investigated.

Key words: Cyclosporine A; FK-506, Rapamycin; Mycophenolate mofetil; Biliary epithelial cells

Liu C, Schreiter T, Frilling A, Dahmen U, Broelsch CE, Gerken G, Treichel U. Cyclosporine A, FK-506, 40-0-[2-hydroxyethyl]rapamycin and mycophenolate mofetil inhibit proliferation of human intrahepatic biliary epithelial cells *in vitro*. *World J Gastroenterol*; 2005: 11(48): 7602-7605
http://www.wjgnet.com/1007-9327/11/7602.asp

INTRODUCTION

Within the last decade, living donor liver transplantation (LDLT) has become an accepted treatment for adult patients with end-staged liver disease and it provides a viable alternative to many recipients who would otherwise die while on the waiting lists. Part of the donor liver used for adult LDLT is small in size when transplanted into the recipient. The liver has the unique ability to regenerate and adjust its size according to the requirement of the recipient. Therefore, liver regeneration is crucial for a successful LDLT. The volume and quality of the graft, ischemic time, portal flow, venous outflow, and immunosuppressive agents are among the factors affecting liver regeneration after adult LDLT.

Cyclosporine A (CsA), FK-506, and MMF can augment liver regeneration after hepatectomy or orthotopic liver transplantation in rats[1-6]. However, in vitro experiments indicate that CsA and FK-506 have an antiproliferative or cytotoxic effect on adult human hepatocytes[7,8]. During liver regeneration after partial hepatectomy, both mature hepatocytes and BECs are induced to proliferate. Human hepatocytes and intrahepatic BECs can be isolated from the liver tissue and maintained *in vitro* for a certain time. *In vitro*, mature hepatocytes have a very limited ability to replicate, while BECs have a great potential to proliferate[9,10]. In this study, the effect of CsA, FK-506, MMF, and 40-0-[2-hydroxyethyl]rapamycin (RAD) on the proliferation of human intrahepatic BECs *in vitro* was investigated.

MATERIALS AND METHODS

Liver tissue

All liver specimens were taken from the patients who

underwent hepatectomy or liver transplantation at University Hospital Essen, Germany. The procedure confirmed to the local ethical guidelines and followed the ethical guidelines of the 1975 Declaration of Helsinki. All patients or their relatives gave informed consents. Three diseased liver tissues were obtained from explanted livers, including one case of primary biliary cirrhosis (64 years old), one case of oxalosis (one year old) and one case of carbamoyl-phosphate-synthetase deficiency (one year old). Two normal liver tissues were obtained during hepatectomy, including one case of hepatoblastoma (1.5 years old) and one case of hepatocellular carcinoma (67 years old). Another normal liver tissue was obtained from a donor (10 years old) when the graft exceeded surgical requirement. All tissues were stored in Dulbecco' s minimum essential medium (PAA Laboratories, Coelbe, Germany) at 4 ºC and used within 36 h after hepatectomy.

Isolation and culture of human intrahepatic BECs

Human intrahepatic BECs were isolated with an immunomagnetic separation method employing an antibody against human epithelial antigen (HEA) as reported[11,12]. BECs were cultured with the plating medium in a 25-cm^2 flask (Greiner, Frickenhausen, Germany) pre-coated with collagen G (Biochrom KG, Berlin). The cell culture was maintained in a humidified atmosphere composed of 95% air and 50 mL/L CO_2. About 24-72 h after plating, the growth medium containing hepatocyte growth factor (HGF, R&D systems, UK) was used to culture the cells. The composition of the plating medium and growth medium was similar to the reported[13]. At confluence, BECs were detached with a solution containing 0.1 g/L trypsin and 1.0 g/L EDTA (Sigma, Taufkirchen, Germany) and maintained in a culture or used for the experiment.

Flow cytometry analysis of cytokeratin (CK) 19 expression

The expression of CK19 by BECs was investigated using flow cytometry with a FACS-Scan machine (Becton Dickinson, Heidelberg, Germany). Cells were pre-treated with the Fix & Perm cell permeabilization kit (Dianova, Hamburg, Germany). The monoclonal antibody against CK19 (IgG2b, Progen, Heidelberg, Germany) was used in a three times dilution according to the manufacturer's instructions. The FITC-labeled second antibody (Dianova, Hamburg, Germany) was diluted fifty times.

In vitro exposure to drugs

During passage, BECs were seeded at the density of 1×104 viable cells/well in 24-well plates with the plating medium. One day later, the medium was changed to the growth medium containing the drugs. CsA (MW 1203, Sandoz, Switzerland), FK 506 (MW 822, Fujisawa, Japan), RAD (MW 958.25, Sandoz, Switzerland) and MMF (MW 433.5, Sandoz, Switzerland) were diluted with a phosphate-buffered solution (PBS, PAA Laboratories, Coelbe, Germany). The concentrations of CsA, FK 506, RAD, and MMF in the medium ranged from 10 to 1 000 μg/L, 10 to 1 000 μg/L, 0.05 to 10 μg/L, 0.05 to 500 μg/L, respectively. Each concentration of the drug was determined in eight wells per experiment. The vigorously proliferating BECs derived from each liver tissue were used in the study and each drug was investigated eight times. Negative control cultures only received the growth medium.

MTT assay of cell growth

Dimethylthiazol-diphenyl-tetrazolium (MTT) assay was performed at 24 and 48 h after addition of the drugs, respectively. Fifty microliters of 4 mg/mL MTT (Sigma, Taufkirchen, Germany) was given to each well (containing 0.5 mL medium) in the 24-well plate. Four hours later, the medium was removed and 250 μL dimethyl sulfoxide (DMSO) was added into each well to solubilize the formazan dye converted from MTT by the cells. Five minutes later, the plates were shaken to make a homogenous dye solution and measured immediately with an ELISA reader (Lambda E, MWG-Biotech, Ebersberg, Germany) at a wavelength of 550 nm minus 690 nm. The cell number in each well was recorded in the form of optical density (OD).

Western blot analysis of CK19 expression

BECs were passaged into six-well plates pre-coated with collagen G. After 24 h, CsA or FK-506 was added into the growth medium and the cells were cultured for 48 h. The concentrations of both CsA and FK-506 in the medium were 500, 1 000 and 2 000 μg/L, respectively. BECs were detached by the use of 0.05% collagenase XI (Sigma, Taufkirchen, Germany), washed with PBS and stored at –20 °C. Protein amount was determined with the Bradford method (Biorad, Munich, Germany) after the cell pellet was boiled 10 times with 40 μL of 0.1% Triton/PBS. Extracted protein (1 μg/lane) was electrophoretically separated on a 10% SDS-PAGE and transferred to nitrocellulose. For the staining, blots were blocked with 1.2% gelatin in PBS and washed with 0.05% Tween 20 in PBS. First antibody against CK19 (IgG2b, Progen, Heidelberg, Germany) was diluted 1:80 in PBS and incubated for 1 h at room temperature. Anti-mouse Ig AP-conjugate as second antibody was diluted 1:1 000 in PBS and also incubated for 1 h at room temperature. Finally, the color was developed using BCIP and NBT (Gerbu, Gaiberg, Germany).

Statistical analysis

The average OD measured at different concentrations of each drug was compared using one-way analysis of variance (ANOVA) with the software SPSS 11.0 (SPSS, Inc., Chicago, IL, USA). Proliferation of the cells exposed to the drugs was compared to the negative control. $P<0.05$ was considered statistically significant.

RESULTS

Isolation and culture of intrahepatic BECs

The freshly isolated cells were small and round in shape and most of them formed clusters. Magnetic beads could

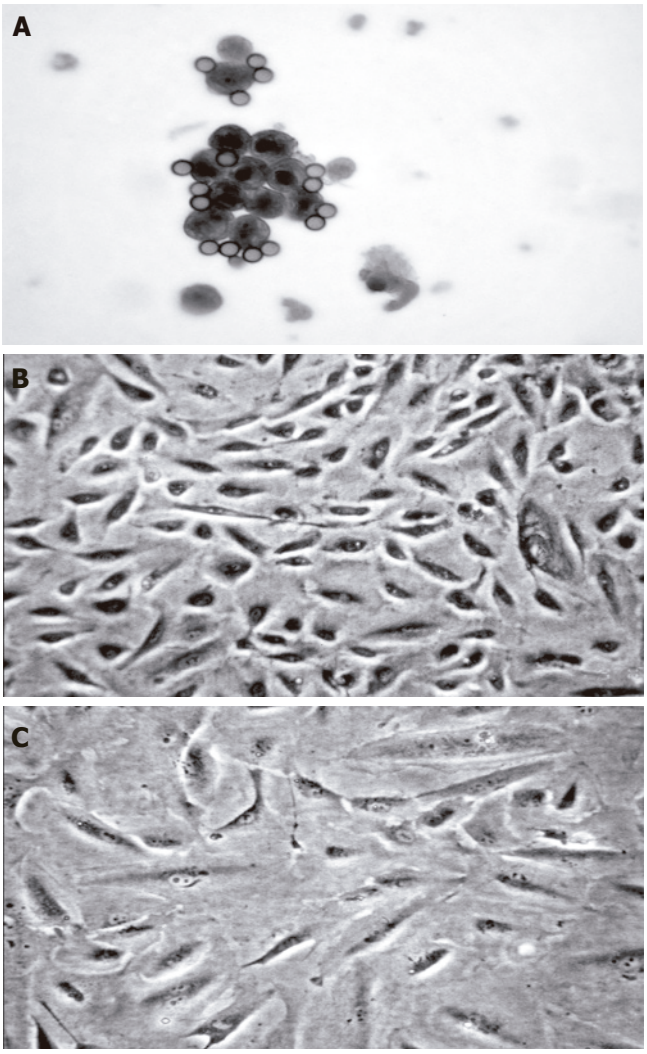

Figure 1 Freshly isolated (**A**) and proliferating human intrahepatic BECs (**B**) as well as BECs exposed to immunosuppressive agents (**C**).

be seen on the cell surface (Figure 1A). Intrahepatic BECs isolated from six liver tissues proliferated for 4-18 wk *in vitro* and were passaged 3-12 times. The proliferating BECs were small and oval in shape (Figure 1B). Flow cytometry analysis showed that the proliferating BECs consistently expressed CK19 (Figure 2).

Growth of intrahepatic BECs exposed to drugs

The vigorously proliferating BECs which represented passage (P) 1–6 BECs derived from different liver tissues, were exposed to the drugs. In this set of experiments, all the four immunosuppressive agents had no growth-promoting effect on BECs at any concentration *in vitro*. On the contrary, they inhibited the proliferation of BECs and this could be clearly shown at 48 h after the addition of the drugs (Figure 3A). All the four drugs inhibited the proliferation of BECs in a dose-dependent manner (Figure 3B) and this was repeatedly demonstrated with BECs derived from different liver tissues and in different passages. The lowest concentration for CsA, FK-506,

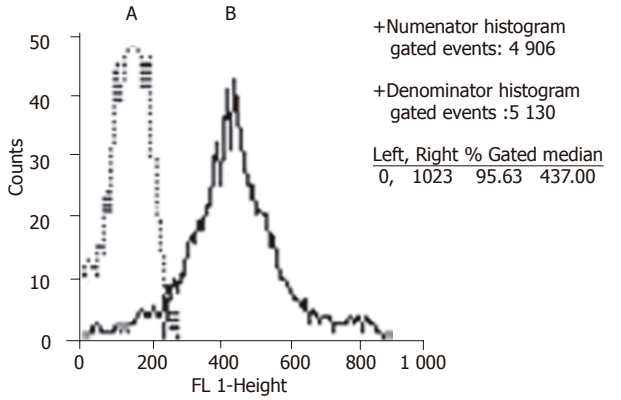

Figure 2 Flow cytometry analysis of CK19 expression. **A:** negative control. **B:** with antibody against CK19.

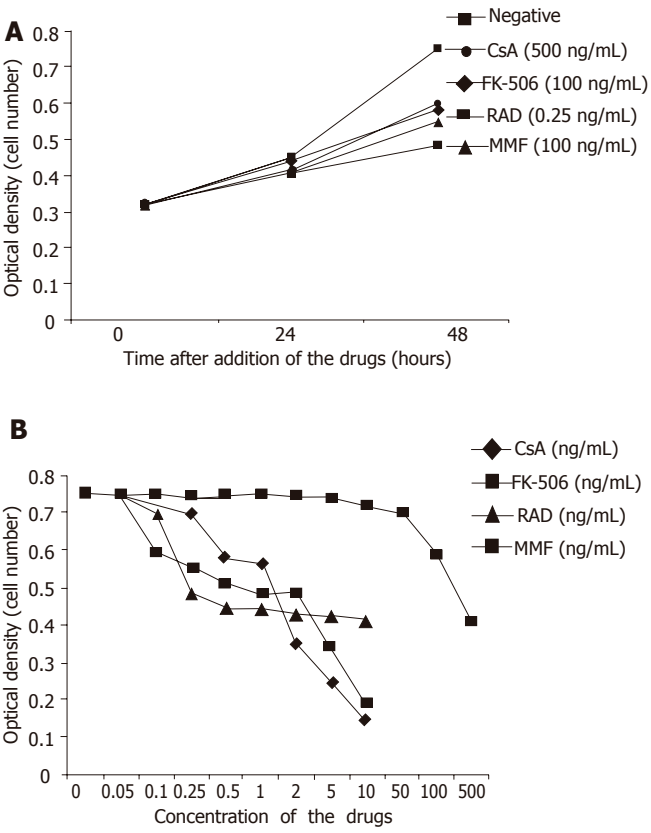

Figure 3 MTT analysis of proliferation of BECs exposed to drugs. **A:** BECs exposed to the drugs for 24 and 48 h. At 48 h, CsA (500 μg/L), FK-506 (100 μg/L), RAD (0.25 μg/L), and MMF (100 μg/L) inhibited proliferation of BECs (P<0.05). **B:** BECs exposed to the drugs for 48 h. CsA, FK-506, RAD, and MMF inhibited the proliferation of BECs in a dose-dependent manner.

RAD, and MMF to inhibit the proliferation of BECs (P<0.05) was 500, 100, 0.25, and 100 μg/L, respectively (Figures 3A and B). RAD had the strongest growth-inhibiting effect. Microscopically, the BECs treated with the drugs became larger than the cells in negative control (Figure 1C). However, Western blot analysis showed that CsA and FK-506 did not change CK19 protein expression by BECs (Figure 4).

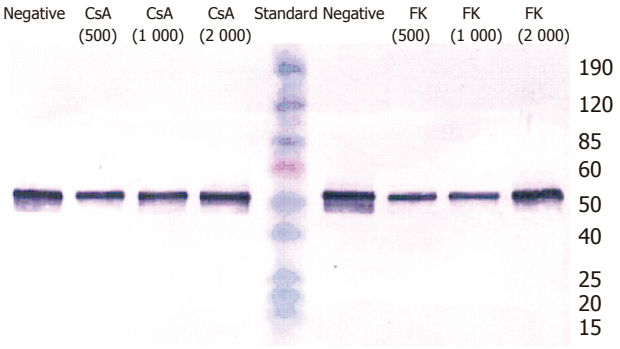

Figure 4 Western blot analysis of CK19 expression. BECs were treated with 500, 1 000, 2 000 μg/L CSA, and FK-506, respectively for 48 h. CsA and FK-506 did not change the protein expression of CK19 in BECs.

DISCUSSION

Intrahepatic BECs represent about 5% of total cell population in the liver. In the human liver, human epithelial antigen (HEA) is the cell surface antigen that only exists in intrahepatic BECs. With the immunomagnetic isolation technique employing anti-HEA monoclonal antibody, intrahepatic BECs can be purified after density-gradient centrifugation[11]. The purity of isolated human intrahepatic BECs is more than 99%[12]. The specific markers for biliary cells include CK7 and CK19. All the cells used in this experiment expressed CK19 (Figure 2), indicating that they are intrahepatic BECs.

In liver transplantation, the damaged liver cells caused by ischemia-reperfusion injury are repaired by liver regeneration. In adult LDLT, liver regeneration is of particular importance to meet the necessary metabolism requirement of the recipient. An immunosuppressive agent is one of the factors affecting liver regeneration after liver transplantation.

Generally speaking, CsA and FK-506 exert their immunosuppressive effect by blocking the production of interleukin-2 (IL-2) by T helper cells, while MMF and RAD exert their immunosuppressive effect by inhibiting proliferation of lymphocytes. CsA, FK-506, and MMF can enhance liver regeneration after hepatectomy or small-for-size liver transplantation in animals. The augmented liver regeneration might be an indirect effect, as CsA and FK-506 have anti-proliferative or cytotoxic effect on hepatocytes[7,8]. The possible mechanism for CsA and FK-506 on enhanced liver regeneration is through inhibition of production of IL-2 production and activation of natural killer (NK) cells[6]. The mechanism of MMF underlying accelerated liver regeneration is not fully understood.

In this study, all the four immunosuppressive agents inhibited human intrahepatic BECs in a dose-dependent manner *in vitro*, indicating that they have a direct inhibiting effect on liver regeneration and this direct effect should not be neglected, especially in adult LDLT. Our results showed that RAD had the strongest inhibiting effect on human intrahepatic BECs *in vitro*. The minimal concentration of RAD to inhibit proliferation of BECs (0.25 μg/L) *in vitro* was much lower than that of target serum through RAD level in patients undergoing immunosuppression (8-12 μg/L) after liver transplantation. Though the results obtained from an *in vitro* experiment were not identical to the results *in vivo*, it may indicate the importance of the direct effect of RAD on liver regeneration. Also, as an immunosuppressive agent, RAD has been reported to attenuate liver regeneration in a rat hepatectomy model[14]. Moreover, immunosuppressant-induced bile duct damage has been reported in azathioprine[15-18]. RAD and azathioprine share the similar immunosuppressive mechanism and it should be alerted that RAD might also cause bile duct damage in transplant patients.

In conclusion, CsA, FK-506, RAD, and MMF have an anti-proliferative effect on human intrahepatic BECs *in vitro*, while RAD has the strongest growth-inhibitory effect. Their possible effects on liver regeneration and bile duct injury in transplant patients should be further investigated.

REFERENCES

1 **Motale P,** Mall A, Spearman CW, Lotz Z, Tyler M, Shepherd E, Kahn D. The effect of mycophenolate mofetil on liver regeneration. *Transplant Proc* 2001; **33:** 1054-1055
2 **Mazzaferro V,** Porter KA, Scotti-Foglieni CL, Venkataramanan R, Makowka L, RossaroL, Francavilla A, Todo S, Van Thiel DH, Starzl TE. The hepatotropic influence of cyclosporine. *Surgery* 1990; **107:** 533-539
3 **Starzl TE,** Porter KA, Mazzaferro V, Todo S, Fung J, Francavilla A. Hepatotrophic effects of FK506 in dogs. *Transplantation* 1991; **51:** 67-70
4 **Kikuchi N,** Yamaguchi Y, Mori K, Takata N, Goto M, Makino Y, Hamaguchi H, Hisama N, Ogawa M. Effect of cyclosporine on liver regeneration after orthotopic reduced-size hepatic transplantation in the rat. *Dig Dis Sci* 1993; **38:** 1492-1499
5 **Kahn D,** Makowka L, Lai H, Eagon PK, Dindzans V, Starzl TE, Van Thiel DH.Cyclosporine augments hepatic regenerative response in rats. *Dig Dis Sci* 1990; **35:** 392-398
6 **Francavilla A,** Barone M, Todo S, Zeng Q, Porter KA, Starzl TE. Augmentation of rat liver regeneration by FK 506 compared with cyclosporin. *Lancet* 1989; **2:** 1248-1249
7 **Loreal O,** Fautrel A, Meunier B, Guyomard C, Guillouzo A, Launois B. FK 506 is less cytotoxic than cyclosporine to human and rat hepatocytes in vitro. *Transplant Proc* 1991; **23:** 2825-2828
8 **Blanc P,** Etienne H, Daujat M, Fabre I, Pichard L, Domergue J, Joyeux H, Fourtanier G, Maurel P. Antiproliferative effect of FK 506 and cyclosporine on adult humanhepatocytes in culture. *Transplant Proc* 1991; **23:** 2821-2824
9 **Strain AJ.** Isolated hepatocytes: use in experimental and clinical hepatology. *Gut* 1994; **35:** 433-436
10 **Joplin R.** Isolation and culture of biliary epithelial cells. *Gut* 1994; **35:** 875-878
11 **Joplin R,** Strain AJ, Neuberger JM. Immuno-isolation and culture of biliary epithelialcells from normal human liver. *In Vitro Cell Dev Biol* 1989; **25:** 1189-1192
12 **Joplin R,** Strain AJ, Neuberger JM. Biliary epithelial cells from the liver of patients withprimary biliary cirrhosis: isolation, characterization, and short-term culture. *J Pathol* 1990; **162:** 255-260
13 **Joplin R,** Hishida T, Tsubouchi H, Daikuhara Y, Ayres R, Neuberger JM, Strain AJ.Human intrahepatic biliary epithelial cells proliferate in vitro in response to human hepatocyte growth factor. *J Clin Invest* 1992; **90:** 1284-1289
14 **Chavez R,** Jamieson N, Takamori S, Nivatvongs S, Pino G, Metcalfe A, Watson C,14 Romero D, Metcalfe S. Hepatotrophic

effect of cyclosporine and FK 506 is not mimicked by rapamycin. *Transplant Proc* 1999; **31:** 2429

15 **Sobesky R,** Dusoleil A, Condat B, Bedossa P, Buffet C, Pelletier G. Azathioprine-induced destructive cholangitis. *Am J Gastroenterol* 2001; **96:** 616-617

16 **Horsmans Y,** Rahier J, Geubel AP. Reversible cholestasis with bile duct injury following azathioprine therapy. *A case report. Liver* 1991; **11:** 89-93

17 **DePinho RA,** Goldberg CS, Lefkowitch JH. Azathioprine and the liver. Evidence favoring idiosyncratic, mixed cholestatic-hepatocellular injury in humans. *Gastroenterology* 1984; **86:** 162-165

18 **Desmet VJ.** Vanishing bile duct syndrome in drug-induced liver disease. *J Hepatol* 1997; **26** Suppl 1: 31-35

Science Editor Wang XL and Guo SY **Language Editor** Elsevier HK

PO Box 2345, Beijing 100023, China
www.wjgnet.com
wjg@wjgnet.com

ELSEVIER

World J Gastroenterol 2005;11(48):7607-7614
World Journal of Gastroenterology ISSN 1007-9327

• *BASIC RESEARCH* •

Protective effects of Asian green vegetables against oxidant induced cytotoxicity

Peter Rose, Choon Nam Ong, Matt Whiteman

Peter Rose, Matt Whiteman, Department of Biochemistry, Faculty of Medicine, Yong Loo Lin School of Medicine, National University of Singapore, 8 Medical Drive, Singapore 117597, Singapore
Choon Nam Ong, Department of Community, Occupational and Family Medicine, Faculty of Medicine, Yong Loo Lin School of Medicine, National University of Singapore, 8 Medical Drive, Singapore 117597, Singapore
Correspondence to: Dr Peter Rose, Department of Biochemistry, National University of Singapore, 8 Medical Drive, 117597 Singapore. bchpcr@nus.edu.sg
Telephone: +65-6874-4996
Received: 2004-09-02 Accepted: 2005-02-01

Abstract

AIM: To evaluate the antioxidant and phase II detoxification enzyme inducing ability of green leaf vegetables consumed in Asia.

METHODS: The antioxidant properties of six commonly consumed Asian vegetables were determined using the ABTS, DPPH, deoxyribose, PR bleaching and iron-ascorbate induced lipid peroxidation assay. Induce of phase II detoxification enzymes was also determined for each respective vegetable extract. Protection against authentic ONOO- and HOCl mediated cytotoxicity in human colon HCT116 cells was determined using the MTT 3-(4,5-dimethylthiazol-2-yl)-2,5-diphenyl tetrasodium bromide) viability assay.

RESULTS: All of the extracts derived from green leaf vegetables exhibited antioxidant properties, while also having cytoprotective effects against ONOO- and HOCl mediated cytotoxicity. In addition, evaluation of the phase II enzyme inducing ability of each extract, as assessed by quinone reductase and glutathione-S-transferase activities, showed significant variation between the vegetables analyzed.

CONCLUSION: Green leaf vegetables are potential sources of antioxidants and phase II detoxification enzyme inducers in the Asian diet. It is likely that consumption of such vegetables is a major source of beneficial phytochemical constituents that may protect against colonic damage.

Key Words: Cruciferous vegetables; Lipid peroxidation; Free radicals; Isothiocyanates

Rose P, Ong CN, Whiteman M. Protective effects of Asian green vegetables against oxidant induced cytotoxicity. *World J Gastroenterol* 2005; 11(48): 7607-7614
http://www.wjgnet.com/1007-9327/11/7607.asp

INTRODUCTION

Reactive oxygen, nitrogen and chlorine species are generated *in vivo* by a diverse array of mechanisms including inflammatory responses, aerobic metabolism, and exposure to ionizing radiation. For example, the interaction of nitrogen monoxide (·NO) and superoxide ($O_2^{\cdot -}$) forms the cytotoxic product peroxynitrite, ($ONOO^-$) (Eq. 1)[1]. $NO + O_2^{\cdot -} \rightarrow ONOO^-$ (1)

Under physiological conditions ONOO- is converted to its protonated form peroxynitrous acid, ONOOH, which in turn decays to generate multiple toxic products with reactivities resembling those of the nitryl cation (NO_2^+), nitrogen dioxide radical ($^{\cdot}NO_2$), and hydroxyl radical (·OH). Similarly, at sites of chronic inflammation, neutrophils secrete hydrogen peroxide (H_2O_2) and the enzyme myeloperoxidase (MPO) which catalyzes the formation of hypochlorous acid (HOCl) (equation 2).

$H_2O_2 + Cl^- \rightarrow HOCl + OH^-$ (2)

Up to 80% of the H_2O_2 generated by activated neutrophils is used to form 20-400 μmol/L HOCl an hour[2-4]. Throughout this paper we use the term "hypochlorous acid" (pKa = 7.46) to refer to the approximately 50% ionized mixture of HOCl and OCl- species that exists at physiological pH 6[5]. Both peroxynitrite and HOCl and species derived from it can oxidize lipids, proteins, DNA, and carbohydrates[6-11]. Indeed, the addition of ONOO- or HOCl to biological fluids leads to the depletion of antioxidants including ascorbate, urate, and thiols. Depletion of *in vivo* antioxidant level by RS can initiate and promote cellular damage leading to genotoxicity and disease progression[12]. For example, RS may participate in the carcinogenesis by inducing genetic mutations. Therefore, due to the cytotoxicity of RS considerable interest in identifying chemical agents or dietary constituents that can interfere with RS mediated damage has been sought[13,14]. Plant derived antioxidants have been proposed to fulfill this role[15,16] and much research has focused on the potential antioxidant and cytoprotective or anti-carcinogenic properties of numerous phytochemical compounds[17,18]. These studies have been further supported by epidemiological investigations indicating that dietary habits

Table 1 Total phenolic content and inhibition of PR bleaching mediated by ONOO- and HOCl by green leaf vegetables used in this study.

Common name	Latin name	Total phenoliccontent (GAE mg/g Dwt)	% Inhibition of PR bleaching
Watercress "Rorripa"	*Rorripa nasturtium aquaticum*	133.6±15.1	75.6±3.2[a] 68.6±3.4
Broccoli	*Brassica oleracea var. italica*	61.03±13.1	85.7±10.36[a] 0.6±0.5
Choi Sum	*B.chinensis var. parachinensis*	163.7±2.11	104±6.6[a] 53.3±1.2
Pa Po	*B. chinensis var. parachinensis*	65.7±3.6	91.1±7.2[a] 50.1±1.6
Pheuy leng	*Amaranthus tricolor*	56.2±3.0	102±3.5[a] 50.7±0.2
SioPek	*B. chinensis*	111.0±11.9	76.9±7.8[a] 58.3±0.6

[a]$P<0.05$ *vs* others.

play a significant role in the risk of developing cancer[19]. High consumption of fruits and vegetables, reduced red meat intake and low alcohol consumption appears to be inversely correlated with colon cancer development. In Asia the lower prevalence of degenerative disease like cancer and heart disease are thought to be due to the high consumption of fruits and vegetables[20]. However, little information is available on the antioxidant properties of green vegetables that are widely consumed in Asia. These food stuffs are perhaps a major source of antioxidants and antioxidant like compounds in the Asian diet. Therefore, in this report, we determined the antioxidant properties and phase II enzyme inducing the ability of several green vegetables commonly consumed in Asia. In addition, each vegetable was evaluated for its protective effects against both authentic ONOO- and HOCl mediated cellular toxicity in human colon cells.

MATERIALS AND METHODS

Chemicals

Glutathione (GSH, reduced form), 4-nitrobenzaldehyde (4-NBA), h-nicotinamide adenine dinucleotide (NAD), NADP, NADPH, NADH, 1-chloro-2,4-dinitrobenzene (CDNB), flavin adenine dinucleotide (FAD), 2,6-dichloroindophenol (2,6-DCIP), were purchased from Sigma Chemical Co. (St. Louis, MO, USA). Protein assay kit was purchased from Bio-Rad labs (Hercules, CA, USA).

Plant material and extract preparation

Individual vegetables, broccoli (B), *Rorripa* (R), Sio Pek (SP), Pa Po (PP), Pheuy leng (PL) and Choi Sum (CS) were collected over a 3 mo period from the local supermarkets (Table 1). *Rorripa* and watercress are used interchangeably through the current text. All individual varieties were placed on dry ice and freeze dried immediately to preserve freshness. All individual representative vegetable samples were then pooled, this being conducted to eliminate variation. Extracts were then prepared using the procedure detailed[23,24]. In brief, 100 mg of freeze-dried tissue was weighed into a 50 mL polypropylene tube, hydrated with 2.0 mL of deionised water and homogenized for 15 s (Ultraturrax homogeniser) and left at room temperature for 1 h with occasional vortexing. Boiling 700 mL/L methanol (3.0 mL) was added to the mix and incubated for a further 15 min at +70 °C. The mixture was cooled to room temperature, and centrifuged at 3 000 r/min for 5 min. After centrifugation 1 mL aliquots were removed and vacuum condensed to 200 μL volumes. The resultant concentrates were filtered through sterile non-pyrogenic filters (0.2 μm; Millipore) and stored at -70 °C prior to testing. Extracts gave an equivalent concentration of 100 mg/mL for each sample. All extracts were analyzed for their respective ITC composition using a Finnigan- LCQ LC-MS system using the method previously described.

Cell culture and treatments

Human HCT116 cells were obtained from the American Type Culture Collection (ATCC, Manassas, VA, USA). Cells were grown in complete DMEM (containing 100 mL/L FBS, 100 000 U/L penicillin, 100 mg/L streptomycin, pH 7.4) in 75/cm^2 culture flasks at 37 °C in 50 mL/L CO_2. HOCl concentration was quantified immediately before use spectrophotometrically at 290 nm (pH 12, ε = 350 mol/L/cm). HOCl was diluted in ice cold EBSS to a concentration of 10 mmoL/L and stored on ice for no longer than 1 min. To expose the cells to HOCl, cells were washed twice with PBS and once with EBSS warmed to 37 °C. Fresh EBSS was then added followed by oxidant addition as described. The addition of HOCl did not significantly alter the pH of the reaction mixture. Hydrogen peroxide-free peroxynitrite (ONOO-) was synthesized as described[24], respectively. ONOO- solution was quantified immediately before use using a molar absorption coefficient of 1670/cm/mol/L[5].

ABTS assay

This was carried out as described in Ref.[25] 2,2'-Azinobis[3-ethylbenzothiazoline-6-sulfonate] (ABTS) in water (7 mmol/L final concentration) was oxidized using potassium persulfate (2.45 mmol/L final concentration) for at least 12 h in the dark. The ABTS$^+$ solution was diluted to an absorbance of 0.8±0.05 at 734 nm (Beckman UV-VIS spectrophotometer, Model DU640B) with phosphate-buffered saline (PBS). Absorbance was measured every 1 min for 5 min after initial mixing of extracts of different concentrations or Trolox standard with 1 mL of ABTS$^+$ solution. Trolox was used as a reference standard. Antioxidant properties of extracts were expressed as Trolox equivalent antioxidant capacity (TEAC).

Ascorbate-iron induced lipid peroxidation

Peroxidation of bovine brain extract was performed as described[26]. Briefly, bovine brain extract (BBE, 100 mg) was dissolved with PBS, and sonicated in an ice bath until dissolved. The BBE (0.2 mL) was preincubated with vegetable extracts in the presence of PBS and $FeCl_3$ (1 mmol/L). Lipid peroxidation was initiated by adding ascorbate (1 mmol/L), and the mixture was then incubated

for 1 h at 37 °C. The reaction was stopped by adding butylated hydroxytoluene (2 g/L in 950 mL/L ethanol), followed by the addition of trichloroacetic acid (28 g/L) and 2-thiobarbituric acid (TBA, 1 g/L). The mixture was heated at 80 °C for 20 min in a water bath. The (TBA) 2-MDA (malondialdehyde) chromogen formed was measured at 532 nm after extraction into 1-butanol using a SpectraMax190 microplate reader (Molecular Devices). Results were expressed as percentages of control.

Scavenging of 2,2-diphenyl-1-picrylhydrazyl

Scavenging activity was determined as described in Ref.[27]. DPPH solution (200 µmol/L in 800 mL/L ethanol) was mixed with an equal volume of extracts, and the absorbance at 520 nm was measured after 20 min at room temperature using the microplate reader. Results were expressed as percentages of control (100%).

Assessment of pyrogallol red bleaching by peroxynitrite

Bleaching of PR was performed as described in Ref.[28], respectively. PR (100 µmol/L final concentration) was dissolved in K_2HPO_4-KH_2PO_4 buffer. Compounds to be tested were added into the PR solution and incubated at room temperature for 10 min; addition of ONOO- (200 µmol/L) or HOCl (125 µmol/L) followed and the mixture was vortexed immediately for 10 s. The decrease in absorbance at 542 nm was determined using a microplate reader.

Total phenolic content

Total phenolic content of extracts was assessed approximately by using the Folin-Ciocalteu phenol reagent as described in Ref.[29]. The extracts (100 µL) were mixed with the Folin-Ciocalteu phenol reagent (0.2 mL), water (2 mL), and Na_2CO_3 (15 g/L, 1 mL), and absorbance at 765 nm was measured 2 h after incubation at room temperature using the microplate reader specified above. Gallic acid was used as a reference standard, and the total phenolics were expressed as milligrams per milliliter of gallic acid equivalents (GAEs).

Determination of phase II enzymatic induction and cellular glutathione

Glutathione-S-transferase and quinone reductase activities were determined as previously described[30]. Reduced glutathione levels in HCT116 cells were determined using the procedure described[31]. The formation of the GSH-phthalaldehyde conjugate was measured fluorometrically (excited at a wavelength of 350 nm, and the fluorescence measured at 420 nm).

Statistical analysis

All statistical analysis of data was conducted using MINITAB version 10.1 software package. ANOVA analysis was performed to determine the variation within and between selected populations.

RESULTS

Total phenolic content

The amounts of total phenolics varied widely in the vegetable extracts evaluated, these ranging between 56.2 to 163.7 mg GAE/g dry weight material (Table 1). Among the vegetable extracts, Choi Sum (*B. chinensis var. parachinensis*) contained the highest total amount of phenolics (163.2 mg GAE/g), whereas lower levels were found in Pa Po (*B. chinensis*), broccoli (*Brassica oleracea. var. italica*), and Pheuy leng (*Amaranthus tricolor*), (65.7, 61.0, and 56.2, respectively).

An additional assay, pyrogallol red (PR) bleaching, was used as an initial screening for the protective effects of each vegetable extract (10 mg/mL concentration) against ONOO- and HOCl induced PR bleaching. As shown in Table 1, all extracts showed some degree in preventing both ONOO- and HOCl mediated bleaching.

Radical scavenging by Asian green leaf vegetable extracts

The antioxidant activities of each vegetable extract were determined using four different chemical assays, ABTS, DPPH, deoxyribose and iron ascorbate lipid peroxidation assay. All the methods have been extensively used for the screening of antiradical activities of fruit and vegetable juices and extracts.

The antioxidant properties of each individual vegetable extract are represented in Figure 1A and F. Extracts of each vegetable were examined and compared for their free radical scavenging activities against radical cation ABTS+. The ABTS assay has been widely used to determine the radical scavenging ability of both synthetic chemicals and plant extracts. All extracts showed ABTS+ scavenging capacity as determined by the reduction in absorbance at 734 nm, as previously reported (Figures 1A and B). In addition, comparison with the water soluble analog Trolox allowed us to determine the total antioxidant capacity TEAC value for each extract, none of the extracts were more effective than Trolox alone (Figure 1C). Likewise, as demonstrated in Figure 1D, all vegetable extracts showed antioxidant scavenging potential in the DPPH assay. In additional assays, we also examined the effects of extracts on hydroxyl radicals and lipid peroxidation (Figures 1E and F). Again all extracts showed some positive inhibition in each assay however, we were unable to show any correlation between phenolic acid content and scavenging ability. Kahkonen *et al.* and Shahidi *et al.* reported that differences in antioxidant activities of plant extracts are a likely result of differences in the types of phenolic acids and flavonoid compounds and their derivatives present with in the plant extracts[32,33]. For example, the antioxidant activities of phenolic acids and their esters are dependant on the number of hydroxy groups in the molecules. Perhaps such limitations are also apparent in our study.

Protection Against ONOO- and HOCl mediated cytotoxicity in HCT116 cells by asian green leaf vegetables

Incubating HCT116 colon cells in the presence of each vegetable extract (0.2-10 mg/mL extract) for 1 h did not result in any significant cytotoxicity measured using the MTT assay (data not shown) whereas the addition of 200 µmol/L ONOO- or 125 µmol/L HOCl led to

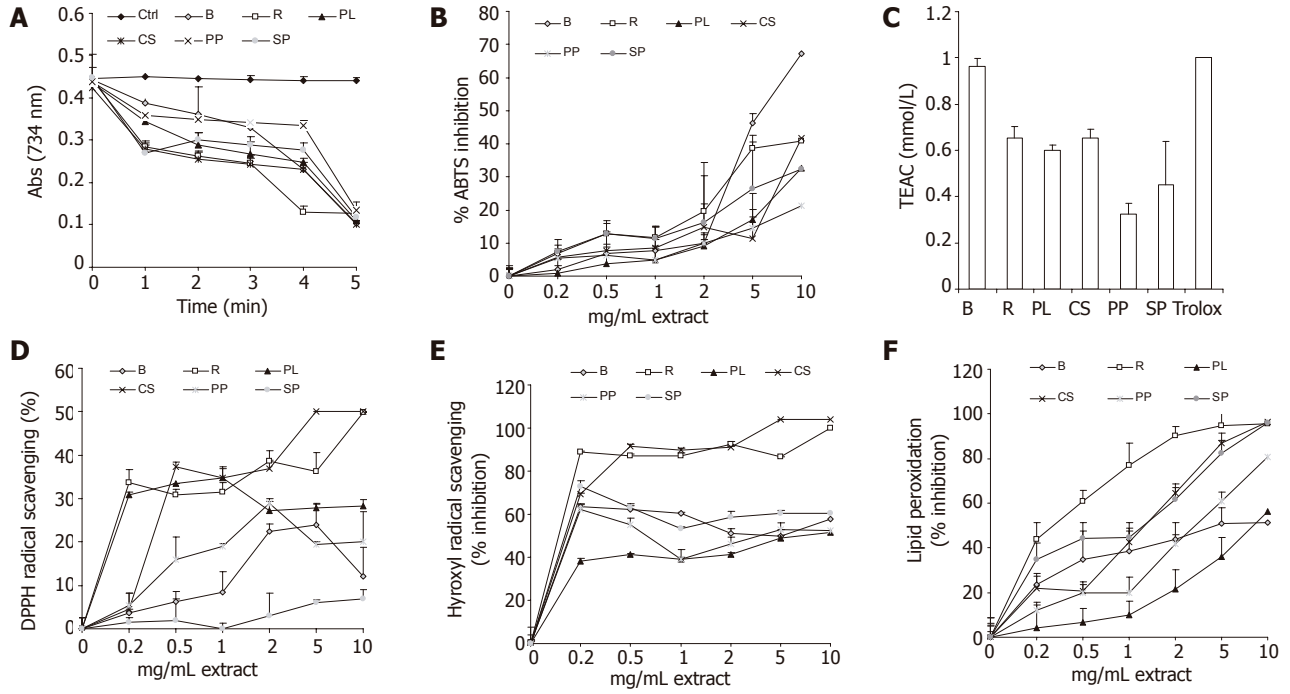

Figure 1 Kinetics of reactions of ABTS radicals in the presence of 10 mg/mL of each vegetable extract (**A**), (**B**) the effects of increased concentration of the vegetable extracts on the inhibition of the ABTS radical represented as % ABTS inhibition, (**C**) total antioxidant activity of extracts from green leaf vegetables as compared to trolox, (**D**) DPPH radical scavenging, (**E**) hydroxyl radical scavenging, and (**F**) iron-ascorbate induced lipid peroxidation. Values are presented as means±SD (n = 6).

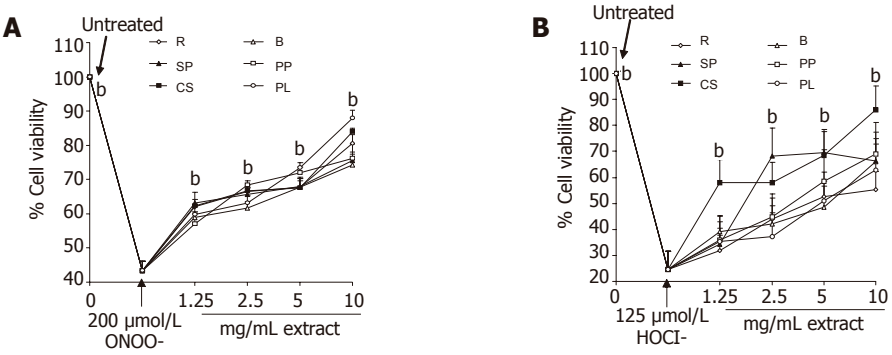

Figure 2 Concentration dependant inhibition of ONOO–- and HOCl mediated cytotoxicity by green leaf vegetable extracts. HCT116 cells were treated with each extract for 5 min and ONOO– or HOCl added. Cell viability was assayed using MTT and measurement of the solubilized formazan dye at Abs 595 nm. Experiments were conducted as described in Materials and methods and data are expressed as mean±SD (n = 6). ^{b}P<0.01 comparing extracts to ONOO– or HOCl treatment alone.

substantial decrease in viability (Figures 3A and B). All extracts significantly inhibited ONOO–- and HOCl mediated cytotoxicity in a concentration-dependent manner.

Induction of phase II detoxification enzymes by Asian green leaf vegetable extracts inhibits ONOO- and HOCl mediated cytotoxicity

The induction of phase II detoxification enzymes QR and GST varied widely among the vegetable extracts evaluated. As shown in Figures 3A and B, both the broccoli and watercress extracts, two species previously been shown as potent inducers of phase II enzymes, showed the most significant induction of QR and GST at 0.02-0.1 mg/mL extract in human HCT116 cells. In contrast, only extracts of Choi Sum (*B. chinensis var. parachinensis*) and Pheuy leng (*Amaranthus tricolor*), showed any potential in inducing QR and GSTs in the current study, all be it at a 10 fold higher concentration (0.1-10 mg/mL extract) than that of broccoli or watercress. Neither Pa Po (*B. chinensis var. parachinensis*) nor Sio Pek (*B. chinensis var. parachinensis*) showed any ability to induce QR or GST (Figure 3C and D). In addition, analysis of each vegetable extract using LC-MS, we were unable to find any putative ITCs present except in any extracts except for broccoli (4-methylsulfinylbutyl ITC) and *Rorripa* (7-methylsulfinylheptyl ITC), respectively. All LC-MS data corresponded to that previously published[23-24]. This may suggest that the other vegetable extracts did not contain any ITCs or that the levels were below the level of detection in our method (Figures 3E and F). To

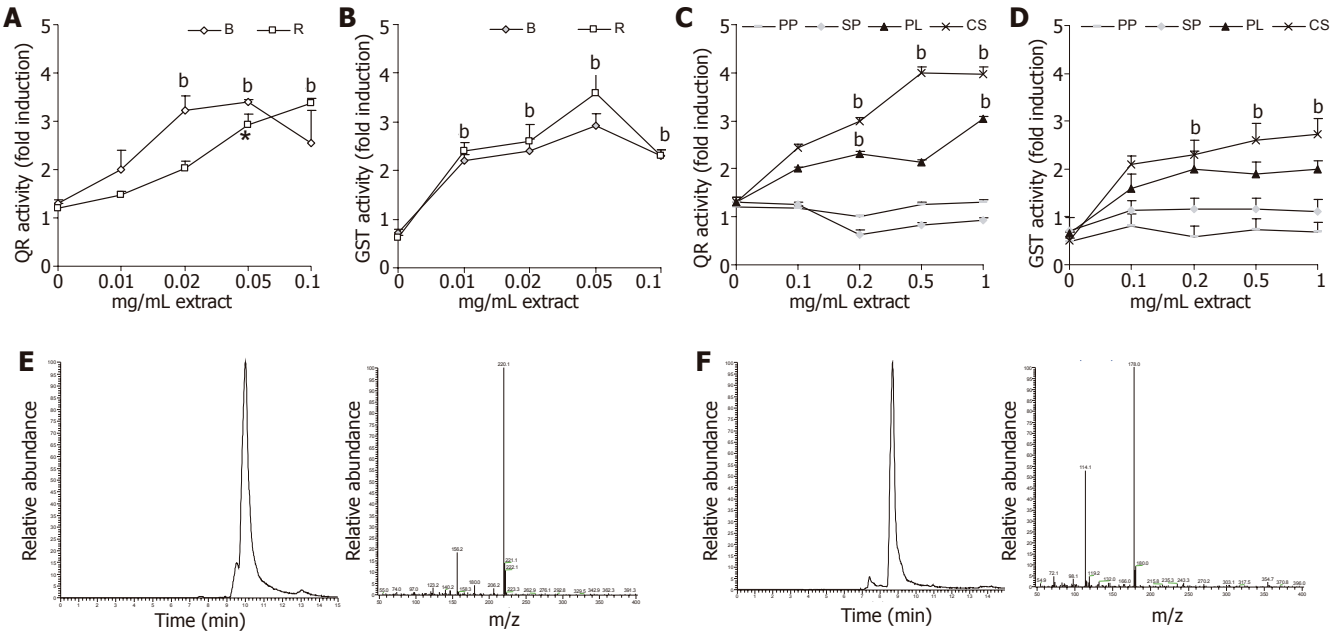

Figure 3 Effect of green vegetable extracts on QR and GST induction in the human colon HCT116 cell line. Cells were treated with each respective extract at 0.01-1 mg/mL (broccoli and *Rorripa*) and 1-10 mg/mL Choi Sum, Pa Po, Pheuy leng and Sio Pek for 24 h. (**A**) induction of QR and (**B**) GST induction by broccoli and *Rorripa*, (**C**) and (**D**) induction of QR and GST by Choi Sum, Pa Po, Pheuy leng and Sio Pek, (**E**) *Rorripa* ITC, 7-methylsulfinylheptyl ITC and (**F**) broccoli ITC, 4-methylsulfinylbutyl ITC as determined using LC-MS. Each data point represents the mean±SD for four separate experiments. $^{b}P<0.001$ *vs* the control cells.

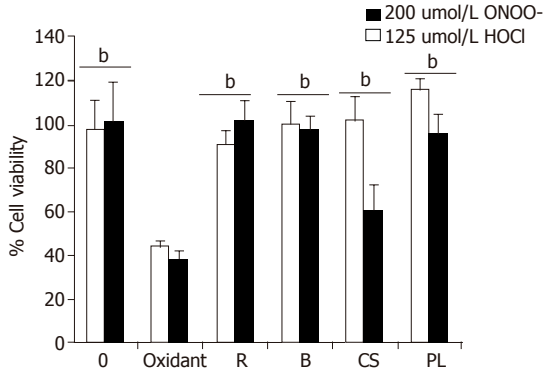

Figure 4 Protective effects of vegetable extracts on ONOO-- and HOCl mediated cytotoxicity in HCT116 cells. Cells were pre-treated with each extract for 24 h to induce phase II detoxification enzymes prior to the addition of ONOO- or HOCl for 30 min. Cell viability was assayed using MTT and measurement of the solubilized formazan dye at Abs 595 nm. Experiments were conducted as described in Materials and methods and data are expressed as mean±SD (n = 6). $^{b}P<0.001$ *vs* extracts to ONOO- or HOCl treatment alone.

examine whether the induction of phase II enzymes could protect against oxidative stress, human HCT116 cell were pre-incubated for 24 h with each respective extract at a concentration that induced a 2 fold induction of QR and GST [(0.01mg/mL) broccoli or *Rorripa* and 1 mg/mL for Pheuy leng, and Choi Sum)], respectively. Consequently, intracellular glutathione was determined prior to the addition of the oxidants ONOO- and HOCl. In all the treatment groups particularly broccoli, Rorripa and Choi Sum, intracellular GSH was elevated (Table 2). Moreover, pre-treated cells were more resistant against ONOO- and HOCl mediated toxicity (Figure 4A).

Table 2 Pre-treatment with green leaf vegetables increases intracellular glutathione levels in HCT116 cells. $^{b}P<0.01$ comparing treated to control cells (mean±SD).

Vegetable	Total GSH ($nmol^{-1}/mg^{-1}$protein)
Ctrl	15.2±0.4
Watercress "*Rorripa*"	33.2±2.7^{b}
Broccoli	28.7±0.5^{b}
Choi Sum	25.1±1.9^{b}
Pheuy leng	25.2±2.2^{b}

DISCUSSION

In the present investigation we evaluated green leaf vegetables that are commonly consumed in Singapore, this being a representative group of vegetables commonly consumed in the region. Recent epidemiological studies have highlighted a protective effect of vegetable consumption, particularly cruciferous vegetables, on colon cancer development[34-37]. Thus, knowledge of the antioxidant properties of local vegetables may partly explain their beneficial health effects.

The generation of $ONOO^{-}$ and HOCl *in vivo* is implicated in a wide range of human diseases ranging from cancer and cardiovascular diseases to chronic inflammation[12]. The *in vivo* formation of ONOO- in patients with colorectal cancer and a corresponding reduction in plasma antioxidant status has been reported[38]. While increased expression levels of inducible nitric oxide sythase and the formation of ONOO- is observed in patients with ulcerative colitis[39]. Similarly, HOCl produced by inflammatory phagocytic leukocytes reportedly contribute to gastrointestinal mucosal damage[40]. These data being suggestive that

oxidative stress contributes to the pathogenesis of colonic inflammation and cancers. Indeed, supplementation with antioxidants in numerous gastrointestinal model systems has been shown to reduce oxidant induced damage[41-45]. Therefore, agents that are able to protect against ONOO- and HOCl dependent damage may be particularly useful in the diet.

Till date, much is known about the dietary sources and antioxidant properties of vegetables commonly consumed in the Western diet however, much less is known about the antioxidant properties of green leaf vegetables consumed in Asia. In our study, we examined six local vegetables, five being members of the family Cruciferae, and an additional specimen being a spinach substitute used in the region, a member of the genus *Amaranthus* (Table 1). Analysis of total phenolic content using the Folin–Ciocalteu phenol reagent method showed considerable variation among the vegetables studied. Chye Sim had the highest total phenolic content (163.7±2.1 mg/g sample) whereas Pheuy leng had the lowest (56.2±3.0 mg/g sample). Dietary derived phenolic compounds like flavonoids, phenolic acids and condensed tannins are all reported to function as antioxidants. Indeed, in all the antioxidant assays used in the current study, PR bleaching, lipid peroxidation, ABTS, DPPH and hydroxyl radical scavenging; all vegetable extracts, to a varying degree, possessed antioxidant properties. Moreover, co-treatment of human colon cancer HCT116 cell line with individual vegetable extract inhibited both ONOO- and HOCl mediated toxicities in a concentration dependant manner. Several investigators have correlated the antioxidant potential of plant extracts with the content of individual compounds. As well as phenolic constituents many vegetables also contain fat-soluble vitamins and precursors, such as tocopherols and carotenoids, along with the water-soluble vitamin ascorbic acid that also poses antioxidant properties. Indeed, the antioxidant potential of Broccoli has been partially attributed to both flavonoid as well as hydroxycinnamic acid constituents[46]. Flavonoids along with other phenolic constituents are widely distributed in higher plants and exhibit diverse biological activities. For example, the antioxidant action of flavonoids in the GI tract could be mediated by the suppression of ROS formation either by inhibition of enzymes or chelating trace elements involved in free radical production, direct scavenging ROS or the upregulation of antioxidant defense system. Structure function analysis has revealed that the antioxidant properties are dependant upon the extent, type and position of functional group substitutions on the ring structures. In our study we were unable to find any correlation between the antioxidant potential of individual vegetable extracts and their total phenolic content. Our findings are in-agreement with that of Kurilich *et al.* 2002, who demonstrated that the antioxidant properties of different broccoli cultivars did not correlate with their respective ascorbic acid or flavonoid composition[47]. We propose that such discrepancies are a likely result of differences in the chemical composition of each vegetable and that such effects may influence the antioxidant properties as observed in the current study. Also, given that recent evidence suggests that many phenolic compounds such as flavonoids are not absorbed to any appreciable levels *in vivo*, perhaps the major site of action is in the lumen of the GI tract as has previously been suggested[48]. We assume that the observed variation in antioxidant properties and cytoprotective effects are perhaps due to the composition of phenolic compounds present in each vegetable, although this requires further study.

In contrast to direct antioxidant scavenging properties, a secondary mechanism that may protect against oxidative stress is the stimulation of cellular protective pathways. The co-ordinate induction of phase 2 detoxification enzymes provides protection against electrophilic and oxidant induced cellular damage. Interestingly, cruciferous vegetables contain phytochemicals known as glucosinolates that under the action of plant or bacterial myrosinases (thioglucoside glucohydrolase; EC 3.2.3.1) following tissue disruption, are converted to bioactive isothiocyanates (ITC)[49]. ITCs are potent inducers of phase II detoxification enzymes in mammals[23-52]. Indeed, induction of phase II enzymes by the ITC sulforaphane has recently been shown to protect human adult retinal pigment cells, epithelial keratinocytes and murine leukemia cells against oxidant induced damage[50]. Mechanistic studies have also indicated that, depending upon the specific structure of the ITC, these compounds can act at three stages of carcinogenesis. Firstly, they can prevent carcinogen activation through inhibition of phase I enzymes such as cytochrome P450s[51]. Secondly they can induce phase II enzymes such as quinone reductase (QR) [NAD(P)H: (quinone-acceptor) oxidoreductase, EC 1.6.99.2], glutathione S-transferases (GSTs) [EC 2.5.1.18] and UDP-glucuronosyltransferases [EC 2.4.1.17] , resulting ultimately in the excretion of the potential carcinogens[52]. Thirdly, they can induce apoptosis[53-56]. The putative anticarcinogenic activity of ITCs is consistent with the results of epidemiological studies, which have suggested a reduction in risk of cancer, particularly of the gastrointestinal tract, through the consumption of cruciferous vegetables[34,36]. In our, study, we found a 10 fold difference in the ability of the vegetables examined to induce both QR and GSTs in human colon HCT116 cells. Both broccoli and *Rorripa* were the strongest enzyme inducers, this previously being attributed to there ITC composition[23-24]. Of the local vegetables only Choi Sum and Pheuy leng induced any significant increase in QR and GST activity. We assume that such variation in phase II enzyme induction is likely to be a result of the composition and content of ITCs present within each vegetable. Jiao *et al.* 1998, previously demonstrated that considerable variation exists between local cruciferous asian vegetables (low ITC content) when compared to broccoli or *Rorripa* (High ITC content)[57]. Moreover, Hecht *et al.* 2004, also reported that cruciferous vegetables collected in Singapore contained high levels of glucobrassicins (70-90%) and relatively low levels of alkyl GSLs, the progenitor compounds of chemicals like sulforaphane[58]. Glucobrassicins, upon tissue disruption form indole-3-carbinols, these compounds have previously been shown to be poor inducers of phase II detoxification enzymes[59].

In summary, our data supports the finds that cruciferous vegetables can decrease *in vitro* and *in vivo* oxidant induced genotoxicity[60] by being potent source of antioxidants that may offer protection against oxidant induced damage in human beings. Moreover, we also found that the phase II enzyme inducing ability varied considerably among the vegetables analyzed, these data suggesting that biomarkers of exposure to cruciferous vegetables may be a more important inclusion into epidemiological studies than previously thought.

REFERENCES

1 **Beckman JS,** Chen J, Ischiropoulos H, Crow JP. Oxidative chemistry of peroxynitrite. *Methods Enzymol* 1994; **233**: 229-240
2 **Foote CS**, Goyne TE, Lehrer RI. Assessment of chlorination by human neutrophils. *Nature* 1983; **301:** 715-716
3 **Weiss SJ,** Klein R, Slivka A, Wei M. Chlorination of taurine by human neutrophils. Evidence for hypochlorous acid generation. *J Clin Invest* 1982; **70:** 598-607
4 **Babior BM.** Phagocytes and oxidative stress. *Am J Med* 2000; **109:** 33-44
5 **Morris JC.** The acid ionization constant of hypochlorous acid from 5 to 35 degrees. *J Phys Chem* 1966; **70:** 3798–3805.
6 **Schraufstatter IU,** Browne K, Harris A, Hyslop PA, Jackson JH, Quehenberger O, Cochrane CG. Mechanisms of hypochlorite injury of target cells. *J Clin Invest* 1990; **85:** 554-562
7 **Prutz WA.** Hypochlorous acid interactions with thiols, nucleotides, DNA, and other biological substrates. *Arch Biochem Biophys* 1996; **332:** 110-120
8 **Spickett CM,** Jerlich A, Panasenko OM, Arnhold J, Pitt AR, Stelmaszynska T, Schaur RJ. The reactions of hypochlorous acid, the reactive oxygen species produced by myeloperoxidase, with lipids. *Acta Biochim Pol* 2000; **47:** 889-899
9 **Radi R,** Beckman JS, Bush KM, Freeman BA. Peroxynitrite-induced membrane lipid peroxidation: the cytotoxic potential of superoxide and nitric oxide. *Arch Biochem Biophys* 1991; **288:** 481-487
10 **Ischiropoulos H,** al-Mehdi AB. Peroxynitrite-mediated oxidative protein modifications. *FEBS Lett* 1995; **364:** 279-282
11 **Beckman JS,** Beckman TW, Chen J, Marshall PA, Freeman BA. Apparent hydroxyl radical production by peroxynitrite: implications for endothelial injury from nitric oxide and superoxide. *Proc Natl Acad Sci USA* 1990; **87:** 1620-1624
12 **Halliwell B,** Gutteridge JMC. Free radicals in biology and medicine, 3rd ed., Oxford: Oxford Univ. Press; 1999
13 **Whiteman M,** Halliwell B. Protection against peroxynitrite dependent tyrosine nitration and alpha 1-antiproteinase inactivation by ascorbic acid A comparison with other biological antioxidants. *Free Radic Res* 1996; **25:** 275-283
14 **Hooper DC,** Spitsin S, Kean RB, Champion JM, Dickson GM, Chaudhry I, Koprowski H. Uric acid, a natural scavenger of peroxynitrite, in experimental allergic encephalomyelitis and multiple sclerosis. *Proc Natl Acad Sci USA* 1998; **95:** 675-680
15 **Choi JS,** Chung HY, Kang SS, Jung MJ, Kim JW, No JK, Jung HA. The structure-activity relationship of flavonoids as scavengers of peroxynitrite. *Phytother Res* 2002; **16:** 232-235
16 **Heijnen CG,** Haenen GR, van Acker FA, Van der Vijgh WJ, Bast A. Flavonoids as peroxynitrite scavengers: the role of the hydroxyl groups. *Toxicol In Vitro* 2001; **15:** 3-6
17 **Harborne JB,** Williams CA. Advances in flavonoid research since 1992. *Phytochemistry* 2000; **55:** 481-504
18 **Nijveldt RJ,** van Nood E, van Hoorn DE, Boelens PG, van Norren K, van Leeuwen PA. Flavonoids: a review of probable mechanisms of action and potential applications. *Am J Clin Nutr* 2001; **74:** 418-425
19 **Hertog MG,** Kromhout D, Aravanis C, Blackburn H, Buzina R, Fidanza F, Giampaoli S, Jansen A, Menotti A, Nedeljkovic S. Flavonoid intake and long-term risk of coronary heart disease and cancer in the seven countries study. *Arch Intern Med* 1995; **155:** 381-386
20 **Mason JB.** Nutritional chemoprevention of colon cancer. *Semin Gastrointest Dis* 2002; **13:** 143-153
21 **Miller AB,** Howe GR, Jain M, Craib KJ, Harrison L. Food items and food groups as risk factors in a case-control study of diet and colo-rectal cancer. *Int J Cancer* 1983; **32:** 155-161
22 **Tarwadi K,** Agte V. Potential of commonly consumed green leafy vegetables for their antioxidant capacity and its linkage with the micronutrient profile. *Int J Food Sci Nutr* 2003; **54:** 417-425
23 **Rose P,** Faulkner K, Williamson G, Mithen R. 7-Methylsulfinylheptyl and 8-methylsulfinyloctyl isothiocyanates from watercress are potent inducers of phase II enzymes. *Carcinogenesis* 2000; **21**: 1983-1988
24 **Mithen R,** Faulkner K, Magrath R, Rose P, Williamson G, Marquez J. Development of isothiocyanate-enriched broccoli, and its enhanced ability to induce phase 2 detoxification enzymes in mammalian cells. *Theor Appl Genet* 2003; **106:** 727-734
25 **Re R,** Pellegrini N, Proteggente A, Pannala A, Yang M, Rice-Evans C. Antioxidant activity applying an improved ABTS radical cation decolorization assay. *Free Radic Biol Med* 1999; **26:** 1231-1237
26 **Gutteridge JM,** Halliwell B. The measurement and mechanism of lipid peroxidation in biological systems. *Trends Biochem Sci* 1990; **15:** 129-135
27 **Gao X,** Ohlander M, Jeppsson N, Bjork L, Trajkovski V. Changes in antioxidant effects and their relationship to phytonutrients in fruits of sea buckthorn (*Hippophae rhamnoides L.*) during maturation. *J Agric Food Chem* 2000; **48:** 1485-1490
28 **Balavoine GG,** Geletii YV. Peroxynitrite scavenging by different antioxidants. Part I: convenient assay. *Nitric Oxide Biol Chem* 1999; **3:** 40- 54
29 **Singleton VL,** Orthofer R, Lamuela-Raventos RM. Analysis of total phenols and other oxidation substrates and antioxidants by means of Folin– Ciocalteu reagent. *Methods Enzymol* 1999; **299:** 152-178
30 **Jiang ZQ,** Chen C, Yang B, Hebbar V, Kong AN. Differential responses from seven mammalian cell lines to the treatments of detoxifying enzyme inducers. *Life Sci* 2003; **72:** 2243-2253
31 **Hissin PJ,** Hilf R. A fluorometric method for determination of oxidized and reduced glutathione in tissues. *Anal Biochem* 1976; **74:** 214-226
32 **Kahkonen MP,** Hopia AI, Heinonen M. Berry phenolics and their antioxidant activity. *J Agric Food Chem* 2001; **49:** 4076-4082
33 **Sahidi F.** Antioxidant factors in plant foods and selected oilseeds. *Biofactors* 2000; **13:** 179-185
34 **Lee HP,** Gourley L, Duffy SW, Esteve J, Lee J, Day NE. Colorectal cancer and diet in an Asian population--a case-control study among Singapore Chinese. *Int J Cancer* 1989; **43:** 1007-1016
35 **Voorrips LE,** Goldbohm RA, van Poppel G, Sturmans F, Hermus RJ, van den Brandt PA. Vegetable and fruit consumption and risks of colon and rectal cancer in a prospective cohort study: The Netherlands Cohort Study on Diet and Cancer. *Am J Epidemiol* 2000; **152:** 1081-1092
36 **Seow A,** Yuan JM, Sun CL, Van Den Berg D, Lee HP, Yu MC. Dietary isothiocyanates, glutathione S-transferase polymorphisms and colorectal cancer risk in the Singapore Chinese Health Study. *Carcinogenesis* 2002; **23:** 2055-2061
37 **Witte JS,** Longnecker MP, Bird CL, Lee ER, Frankl HD, Haile RW. Relation of vegetable, fruit, and grain consumption to colorectal adenomatous polyps. *Am J Epidemiol* 1996; **144:** 1015-1025
38 **Szaleczky E,** Pronai L, Nakazawa H, Tulassay Z. Evidence of in vivo peroxynitrite formation in patients with colorectal

carcinoma, higher plasma nitrate/nitrite levels, and lower protection against oxygen free radicals. *J Clin Gastroenterol* 2000; **30:** 47-51

39 **Kimura H,** Hokari R, Miura S, Shigematsu T, Hirokawa M, Akiba Y, Kurose I, Higuchi H, Fujimori H, Tsuzuki Y, Serizawa H, Ishii H. Increased expression of an inducible isoform of nitric oxide synthase and the formation of peroxynitrite in colonic mucosa of patients with active ulcerative colitis. *Gut* 1998; **42:** 180-187

40 **Yamada T**, Grisham MB. Role of neutrophil-derived oxidants in the pathogenesis of intestinal inflammation. *Klin Wochenschr* 1991; **69:** 988-994

41 **Martin AR,** Villegas I, La Casa C, de la Lastra CA. Resveratrol, a polyphenol found in grapes, suppresses oxidative damage and stimulates apoptosis during early colonic inflammation in rats. *Biochem Pharmacol* 2004; **67:** 1399-1410

42 **Loguercio C,** D'Argenio G, Delle Cave M, Cosenza V, Della Valle N, Mazzacca G, Del Vecchio Blanco C. Glutathione supplementation improves oxidative damage in experimental colitis. *Dig Liver Dis* 2003; **35:** 635-641

43 **Oliveira CP,** Kassab P, Lopasso FP, Souza HP, Janiszewski M, Laurindo FR, Iriya K, Laudanna AA. Protective effect of ascorbic acid in experimental gastric cancer: reduction of oxidative stress. *World J Gastroenterol* 2003; **9:** 446-448

44 **Rotting AK,** Freeman DE, Eurell JA, Constable PD, Wallig M. Effects of acetylcysteine and migration of resident eosinophils in an in vitro model of mucosal injury and restitution in equine right dorsal colon. *Am J Vet Res* 2003; **64:** 1205-1212

45 **Tamai H,** Kachur JF, Grisham MB, Gaginella TS. Scavenging effect of 5-aminosalicylic acid on neutrophil-derived oxidants. Possible contribution to the mechanism of action in inflammatory bowel disease. *Biochem Pharmacol* 1991; **41:** 1001-1006

46 **Plumb GW.** Price KR. Rhodes MJ. Williamson G. Antioxidant properties of the major polyphenolic compounds in broccoli. *Free Radic Res* 1997; **27:** 429-435

47 **Kurilich AC,** Jeffery EH, Juvik JA, Wallig MA, Klein BP. Antioxidant capacity of different broccoli (*Brassica oleracea*) genotypes using the oxygen radical absorbance capacity (ORAC) assay. *J Agric Food Chem* 2002; **50:** 5053-5057

48 **Halliwell B,** Zhao K, Whiteman M. The Gastrointestinal Tract: A Major Site of Antioxidant Action? *Free Radic Res* 2001; **33:** 819-830

49 **Rask L,** Andreasson E, Ekbom B, Eriksson S, Pontoppidan B, Meijer J. Myrosinase: gene family evolution and herbivore defense in Brassicaceae. *Plant Mol Biol* 2000; **42:** 93-113

50 **Gao X,** Dinkova-Kostova AT, Talalay P. Powerful and prolonged protection of human retinal pigment epithelial cells, keratinocytes, and mouse leukemia cells against oxidative damage: the indirect antioxidant effects of sulforaphane. *Proc Natl Acad Sci USA* 2001; **98:** 15221-15226

51 **Conaway CC,** Jiao D, Chung FL. Inhibition of rat liver cytochrome P450 isozymes by isothiocyanates and their conjugates: a structure-activity relationship study. *Carcinogenesis* 1996; **17:** 2423-2427

52 **Zhang Y,** Talalay P. Mechanism of differential potencies of isothiocyanates as inducers of anticarcinogenic Phase 2 enzymes. *Cancer Res* 1998; **58:** 4632-4639

53 **Gamet-Payrastre L,** Li P, Lumeau S, Cassar G, Dupont MA, Chevolleau S, Gasc N, Tulliez J, Terce F. Sulforaphane, a naturally occurring isothiocyanate, induces cell cycle arrest and apoptosis in HT29 human colon cancer cells. *Cancer Res* 2000; **60:** 1426-1433

54 **Rose P,** Whiteman M, Huang SH, Halliwell B, Ong CN. beta-Phenylethyl isothiocyanate-mediated apoptosis in hepatoma HepG2 cells. *Cell Mol Life Sci* 2003; **60:** 1489-1503

55 **Rose P,** Armstrong JS, Chua YL, Ong CN, and Whiteman M. Beta-phenylethyl isothiocyanate mediated apoptosis; contribution of Bax and the mitochondrial death pathway. *Int J Biochem Cell Biol* 2005; **37:** 100-119

56 **Xu K,** Thornalley PJ. Studies on the mechanism of the inhibition of human leukaemia cell growth by dietary isothiocyanates and their cysteine adducts in vitro. *Biochemical Pharmacol* 2000; **60:** 221-231

57 **Jiao D,** Yu MC, Hankin JH, Low SH, and Chung FL. Total Isothiocyanate Contents in Cooked Vegetables Frequently Consumed in Singapore. *J Agric Food Chem* 1998; **46:** 1055-1058

58 **Hecht SS,** Carmella SG, Kenney PM, Low SH, Arakawa K, Yu MC. Effects of cruciferous vegetable consumption on urinary metabolites of the tobacco-specific lung carcinogen 4-(methylnitrosamino)-1-(3-pyridyl)-1-butanone in singapore chinese. *Cancer Epidemiol Biomarkers Prev* 2004; **13:** 997-1004

59 **Chen YH,** Yang D. Differential effects of vegetable-derived indoles on the induction of quinone reductase in hepatoma cells. *J Nutr Sci Vitaminol* (Tokyo) 2002; **48:** 477-482

60 **Gill CI,** Haldar S, Porter S, Matthews S, Sullivan S, Coulter J, McGlynn H, Rowland I. The effect of cruciferous and leguminous sprouts on genotoxicity, in vitro and in vivo. *Cancer Epidemiol Biomarkers Prev* 2004; **13:** 1199-1205

Science Editor Li WZ **Language Editor** Elsevier HK

PO Box 2345, Beijing 100023, China
www.wjgnet.com
wjg@wjgnet.com

ELSEVIER

World J Gastroenterol 2005;11(48):7615-7619
World Journal of Gastroenterology ISSN 1007-9327

• *BASIC RESEARCH* •

Detection and identification of intestinal pathogenic bacteria by hybridization to oligonucleotide microarrays

Lian-Qun Jin, Jun-Wen Li, Sheng-Qi Wang, Fu-Huan Chao, Xin-Wei Wang, Zheng-Quan Yuan

Lian-Qun Jin, Zheng-Quan Yuan, PLA Center of Disease Control and Prevention, Beijing 100039, China
Jun-Wen Li, Fu-Huan Chao, Xin-Wei Wang, Tianjin Institute of Hygiene and Environmental Medicine, Tianjin 300050, China
Sheng-Qi Wang, Beijing Institute of Radiation Medicine, Beijing 100850, China
Supported by the National High Technology Research and Development Program of China (863 Program), No. 2002AA2Z2011
Correspondence to: Dr Jun-Wen Li, Tianjin Institute of Hygiene and Environmental Medicine, 1, Da Li Road, Tianjin 300050, China. jinlianqun@sina.com
Telephone: +86-22-84655345 Fax: +86-22-23328809
Received: 2005-01-14 Accepted: 2005-06-06

Abstract

AIM: To detect the common intestinal pathogenic bacteria quickly and accurately.

METHODS: A rapid (<3 h) experimental procedure was set up based upon the gene chip technology. Target genes were amplified and hybridized by oligonucleotide microarrays.

RESULTS: One hundred and seventy strains of bacteria in pure culture belonging to 11 genera were successfully discriminated under comparatively same conditions, and a series of specific hybridization maps corresponding to each kind of bacteria were obtained. When this method was applied to 26 divided cultures, 25 (96.2%) were identified.

CONCLUSION: *Salmonella sp*., *Escherichia coli*, *Shigella sp*., *Listeria monocytogenes*, *Vibrio parahaemolyticus*, *Staphylococcus aureus*, *Proteus* sp., *Bacillus cereus*, *Vibrio cholerae*, *Enterococcus faecalis*, *Yersinia enterocolitica*, and *Campylobacter jejuni* can be detected and identified by our microarrays. The accuracy, range, and discrimination power of this assay can be continually improved by adding further oligonucleotides to the arrays without any significant increase of complexity or cost.

Key words: Oligonucleotide array; Sequence analysis; Gene chip; Intestines; Microbiology

Jin LQ, Li JW, Wang SQ, Chao FH, Wang XW, Yuan ZQ. Detection and identification of intestinal pathogenic bacteria by hybridization to oligonucleotide microarrays. *World J Gastroenterol* 2005; 11(48): 7615-7619
http://www.wjgnet.com/1007-9327/11/7615.asp

INTRODUCTION

Intestinal pathogenic bacteria exert a great threat upon human health. It is still a challenge to detect and identify bacterial pathogens quickly and accurately from the samples. Since intestinal bacterial pathogens involve a wide range of genera and species, few existing methods can meet the requirement of quick and parallel detection of these bacterial pathogens. Classical diagnostic methods, including culture and biochemical identification, immunological assay, nucleotide probe hybridization, and PCR amplification, share a common shortcoming: only one or few kinds of bacteria can be identified in a complete cycle of experiment. These serial procedures are hard to use for quick and simultaneous detection of multiple pathogenic bacteria. To meet the demands of rapid and parallel detection and identification of many common pathogenic bacteria in one experiment, we present here a new approach based on the epoch-making gene-chip (microarray) technology.

Gene chip technology is based upon the reversed solid hybridization of oligonucleotides[1,2]. The major advantages of gene chip technology, including miniature, high performance, parallelism, automation, have expanded its application in this decade[3]. Since the efficacy of gene chip technology depends heavily upon the oligonucleotide probes, careful selection of target genes and wise design of oligonucleotide probes with variable kind, sequence and amount, are cardinal factors for a good gene chip. The target genes may be species-specific. For example, the pathogenic genes[4] can be easily identified by simple PCR. However, it is impractical to use different primers for different species in gene chip technology, especially in the case where a specimen of one or more possible bacteria is given. Either a complex PCR with a mixture of many primers or a series of PCRs performed in parallel or sequential are necessary to amplify the target genes. However, the time, complexity and expense of experiment will also increase. On the contrary, if a consensus gene among many pathogenic bacteria is chosen, a single pair of carefully designed universal primers may be used to amplify the conserved stretches of DNA, which are then detected and identified by the wisely designed oligonucleotide probes. The conserved consensus genes usually chosen by many researchers are 16S ribosomal DNA (rDNA),

Table 1 Standard strains used in the present study

Genus or species	Standard strain(s)[1]
Salmonella	50 001, 50 004, 50 009, 50 013, 50 014, 50 018, 50 019, 50 020, 50 021, 50 023, 50 029, 50 041, 50 042, 50 043, 50 047, 50 051, 50 073, 50 082, 50 083, 50 086, 50 093, 50 096, 50 098, 50 099, 50 100, 50 104, 50 105, 50 106, 50 109, 50 112, 50 115, 50 120, 50 124, 50 128, 50 145, 50 191, 50 200, 50 201, 50 220, 50 304, 50 306, 50 307, 50 309, 50 310, 50 313, 50 315, 50 320, 50 321, 50 322, 50 326, 50 327, 50 333, 50 335, 50 337, 50 338, 50 354, 50 355, 50 358, 50 360, 50 362, 50 402, 50 707, 50 708, 50 709, 50 710, 50 711, 50 712, 50 718, 50 719, 50 730, 50 731, 50 732, 50 733, 50 735, 50 736, 50 739, 50 746, 50 761, 50 774, 50 783, 50 825, 50 835, 50 846, 50 853, 50 854, 50 864, 50 913
Shigella	51 081, 51 100, 51 207, 51 227, 51 233, 51 252, 51 253, 51 255, 51 258, 51 259, 51 262, 51 307, 51 315, 51 334, 51 335, 51 336, 51 424, 51 464, 51 570, 51 571, 51 572, 51 573, 51 575, 51 582, 51 583, 51 584, 51 585, 51 610
Escherichia coli	44 102, 44 105, 44 109, 44 110, 44 113, 44 126, 44 127, 44 149, 44 155, 44 156, 44 186, 44 216, 44 336, 44 338, 44 344, 44 505, 44 710, 44 719, 44 752, 44 813, 44 824, 44 825
Proteus	49 027, 49 101, 49 102, 49 103
Staphylococcus	26 001, 26 003, 26 005, 26 101, 26 111, 26 113, 26 517
Yersinia enterocolitica	52 202, 52 203, 52 206, 52 207, 52 211, 52 215, 52 217, 52 219, 52 302
Listeria monocytogenes	54 003, 54 005, 54 006, 54 007
Vibrio	20 502, 20 506, 20 507, 20 511, 02-12
Enterococcus faecalis	32 221, 32 223
Campylobacter jejuni	26 277
Bacillus cereus	63 301

[1]Except that one strain of Vibrio sp. was obtained from the Beijing Institute of Microbiology and Epidemiology, all other strains used in the present study were purchased from the National Center for Medical Culture Collection.

23S rDNA[5,6], 16S-23S rDNA spacer region[7], ERIC, while 16S rDNA[8] is the most popular one. Among the eubacterial 16S rDNA genes, the highly conserved sequences compose the constant regions, and the relatively less conserved sequences compose the variable regions, both interlace along the linear genes. Therefore, the pair of universal primers was carefully designed based upon the constant regions of 16S rDNA, so that they were capable of amplifying the 16S rDNA genes of all bacteria under certain circumstances. Meanwhile, the oligonucleotide probes were wisely designed based upon the variable regions of 16S rDNA at the species or genera level.

MATERIALS AND METHODS

Materials

The standard strains used in this study including a wide range of species and many of the common organisms causing intestinal disease are listed in Table 1. These organisms were identified by conventional methods.

Extraction of bacterial DNA from standard cultures

One colony from a fresh culture was resuspended in 100 μL distilled water in Eppendorf tubes. Then the tubes were transferred to a thermal cycler (Techgene, Techne Ltd.) and heated to 95 °C for 10 min. Finally, they were spun at 10 000 *g* for 1 min in a microcentrifuge, and 2 μL of the supernatant was used in PCR described below.

Sample preparation

Strains divided from Hai River, Luan River, municipal sewage, and food samples from markets were used in this study. All the divided strains were identified by conventional methods and the VITEK test system (BioMerieux SA, France). Extraction of DNA from divided bacterial cultures was performed as above.

Design of primers to amply bacterial 16S rDNA

We downloaded 113 bacterial 16S rDNA sequences from the GenBank database. Then, we used the program ClustalW alignment of the software MacVector 6.5.1 to analyze these sequences and showed the conserved regions of 16S rDNA. The primers were based on the conserved regions 8 and 10 of the 16S rDNA. The sequences of forward primer 1169U20 (5'-AACTGGAGGAAGGTGGGGAT) and reverse primer 1521L19 (5'-AGGAGGTGATCCAACCGCA) were used to amply bacterial 16S rDNA. The forward primer 1169U20 was labeled with 5'-Cy3 fluorescence.

Design of primers to amply specific pathogenic genes of Salmonella and Shigella

Sequences of forward primer invA-139 (5'-GTGAAA TTATCGCCACGTTCGGGCAA) and reverse primer invA-141 (5'-TCATCGCACCGTCAAAGGAACC) were used to amplify the invA gene of *Salmonella*. Sequences of forward primer virA-1 (5'-CTGCATTCTGGCAATCTC TTCACATC) and reverse primer virA-2 (5'-TGATGAG CTAACTTCGTAAGCCCTCC) were used to amplify the virA gene of *Shigella*. The forward primers invA-139 and virA-1 were labeled with 5'-Cy3 fluorescence.

PCR amplification to get hybridization targets

Each 50 μL reaction contained 33 μL sterile water, 5 μL 10 ×buffer (Takara Biotechnology Co., Ltd.), 2 μL supernatant from the extraction of bacterial DNA, 200 μmol/L dNTP mixture (Takara), 0.02 U/μL Takara Taq (Takara, 5 U/mL) and 0.1 μmol/L each primer (1169U20, 1521L19, invA-139, invA-141, virA-1, and virA-2). The PCR mixtures were subjected to 95 °C for 5 min, followed by 35 cycles at 94 °C for 25 s, at 55 °C for 30 s, and at 72 °C for 25 s. The PCR products were checked using 2% agarose electrophoresis and visualized with ethidium bromide staining.

Making oligonucleotide microarrays

All the oligonucleotide probes were chosen based on the variable regions between PCR primers using the alignment information. They were synthesized and modified with

Table 2 Oligonucleotide probes used in the present study

No.	Sequence (5' to 3')	Target
1	gtacaaggcccgggaacgtattcacc	All known eubacteria (universal bacterial probe)
2	gacataaggggcatgatgatttgacgt	All Gram-positive bacteria
3	gtcgtaagggccatgatgacttgacgt	All Gram-negative bacteria
4	gtcatgaatcacaaagtggtaagcgc	All enteric bacterial
5	acgacgcactttatgaggtccgcttg	*Escherichia coli, Shigella sp.* and *Salmonella sp.*
6	gctcctaaaaggttactccaccggct	*Staphylococcus aureus*
7	cgacggctagctccaaatggttactg	Coagulase-negative *Staphylococcus*
9	tcacggtcttgcgtcttattgtacctac	*Clostridium botulinum*
11	gaactgagactggtttttaagtttggct	*Clostridium perfringens*
15	cgaactgggacatattttatagatttgc	*Campylobacter jejuni*
16	aggtcgccccttcgccgccctctgtatc	*Legionella pneumophila*
17	cgatccgaactgagaccggcttttaagg	*Mycobacterium tuberculosis*
18	tactcgtaagggccatgatacgacttaa	*Proteus sp.*
19	cgcggcttggcaacccttttgtaccgacc	*Pseudomonas aeruginosa*
20	actgagaatagttttatgggattagg	*Listeria monocytogenes*
21	gctccaccttcgcggtattcgctgccct	*Vibrio cholerae*
22	tcactttcgcaagttggccgccctctgt	*Vibrio fluvialis*
23	tggtaagcgtccccccgtagttgaaac	*Vibrio parahaemolyticus*
24	tacgacagactttatgtggtccgcttgc	*Yersinia enterocolitica*
25	cctcgcggtctagcagctcgttgtgctt	*Enterococcus faecalis*
26	ggattcgctcactatcgctagcttgcag	*Aeromonas hydrophila*
27	ccgacttcgggtgttacaaactctcg	*Bacillus cereus, P.*
28	gcttcatgcactcgagttgcagagtg	*cocovenenans subsp. farinofermentans*
30	atccccaccttcctccagtt	Positive control
31	cccccagaggcagagattgca	virA gene of *Shigella* sp.
32	cgccaataacgaattgcccga	invA gene of *Salmonella* sp.

3'-NH_2 in order to increase their binding to the glass slide surface and their hybridization intensity.

Before use, the glass slides for microscopy must be cleaned as described by Brown (http://cmgm.stanford.edu/pbrown/protocols.html). Then the oligonucleotide probes were bound to the slides as follows: 5 μL of 50 μmol/L oligonucleotide drop was spotted on the glass slide by an arrayer (PixSys 5500 Workstation, Cartesian Technologies), 5 mm between each oligonucleotide spot. When all the oligonucleotide probes were applied, the glass slides were left at room temperature for 24 h to permit thorough drying of the DNA on the slide surface. After drying, the slides were washed twice in 0.2% SDS for 5 min each and twice in distilled water for 5 min each. Subsequently, the slides were washed in sodium borohydride solution (1.3 g Na_2BH_4 was dissolved in 375 mL phosphate buffered saline, and then 125 mL pure ethanol was added) for 5 min, in 0.2% SDS for 2 min, and twice in distilled water for 2 min each.

Hybridization

The fluorescent-labeled amplicons were hybridized to the oligonucleotide microarrays using the following protocol: 1 μL of amplicons was added into a tube containing 4 μL hybridization solution (UniHyb™, TeleChem International, Inc.), and the tube was heated to 95 °C for 10 min and was put on ice immediately. Mixture in the tube was then transferred onto the microarray, kept at 50 °C for 1 h in a hybridization cassette (TeleChem International, Inc.). After hybridization, unbound fluorescent amplicons were washed with washing buffer A (1×SSC+0.2% SDS) for 1 min, B (0.1×SSC+0.2% SDS) for 1 min, C (0.1×SSC) for 1 min, respectively.

Scanning the microarray for fluorescent signals

We used the ScanArray 3000 (GSI Lumonics) to scan the area of the slide containing the microarray. The laser power and PMT were set at 80%.

Scoring hybridization results

The resolution of the ScanArray 3000 scanner is 10 μm, and the fluorescent density of each pixel is saved into the TIFF image file, facilitating further process and analysis of software. We uploaded the scanned image TIFF file into the ImaGene 4.0 software (BioDiscovery) to examine each feature for fluorescence intensity.

RESULTS

Under the same conditions for PCR amplification and hybridization, all the 170 strains produced PCR products, showing bands at approximately 370 bp, being equivalent to the fragment of 16s rDNA. Besides, strains belonging to *Salmonella* sp. produced another band of 285 bp, and strains belonging to *Shigella* sp. produced a 215-bp band. After the hybridization between PCR products and oligonucleotide probes, respective hybridization maps were built through the signal acquisition step using the ScanArray 3000 scanner. The original images generated by ScanArray 3000 scanner are shown in Figure 1. Monochrome fluorescent signals were mapped into pseudocolor spectrum according to their density in ascending order, e.g. black, dark blue, blue, green, yellow, red, white. Twelve typical hybridization maps corresponded to nine genera or species of bacteria, specifically.

The wisely designed oligonucleotide probes could be classified by their efficacy into six categories (Table 2).

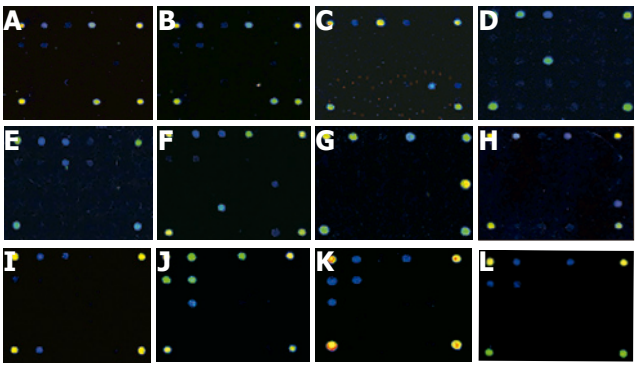

Figure 1 Typical hybridization results from *Vibrio parahaemolyticus* (**A**), *Yersinia enterocolitica* (**B**), *Listeria monocytogenes* (**C**), *Bacillus cereus* (D), *Staphylococcus aureus* (**E**), *Proteus sp.* (**F**), *Campylobacter jejuni* (**G**), *Vibrio cholerae* (**H**), *Enterococcus faecalis* (**I**), *Salmonella sp.* (**J**), *Shigella sp.* (**K**) and *Escherichia coli* (**L**).

	1	2	3	4	5	6
A	30	1	2	3	–[1]	30
B	4	5	6	7	28	9
C	31	32	27	11	26	15
D	16	17	18	19	20	21
E	30	25	22	23	24	30

[1]Negative control (3×SSC).

Figure 2 Layout of oligonucleotide probes.

Category one, including oligonucleotide probe 1, a universal probe targeting the portion of 16S rDNA shared by all known eubacteria, was used to detect all kinds of known eubacteria. Category two, including oligonucleotide probes 2 and 3, the specific probes targeting the portion of 16S rDNA shared by both Gram-positive (G^+) and negative (G^-) bacteria, was used to distinguish between G^+ and G^- bacteria. Category three, including oligonucleotide probes 4 and 5, targeting the portion of 16S rDNA shared by all enteric bacteria, was used to identify intestinal bacteria at the family level. Category four, including oligonucleotide probes 6, 7, 9, 11, and 15-28, a cluster of genus or species-specific probes targeting the portion of 16S rDNA shared by their respective bacteria, was used to identify bacteria at genus or species level. Category five, including oligonucleotide probes 31 and 32, targeting the portion of the specific pathogenic genes of *Shigella* and *Salmonella*, was used to discriminate between bacteria of these two genera. Category six, including oligonucleotide probe 30, a positive control probe, was used both as a gauge to reflect the effectiveness of this hybridization system and as a reference coordinate for scanning. From hybridization signals of the five categories of oligonucleotide probes, it was easy to identify the target pathogenic bacteria in a given specimen. For instance, strong hybridization signals at the sites corresponding to the oligonucleotide probes 1, 3, and 23 were found, so the pathogenic bacteria in the given specimen could be sequentially identified as eubacteria, G^- bacteria, and strains of *Vibrio parahaemolyticus* (Figure 1G). Some slightly weaker signals due to unspecific hybridization were also found. By means of multiple experiments, a hybridization signal was regarded as a specific signal if it meets the following criterion: the foreground fluorescent signal at an oligonucleotide probe spot was stronger than its background fluorescent signal with a signal-noise ratio larger than 100 calculated by ImaGene 4.0. Since the fluorescent signals of specific hybridization were three-fold stronger compared to those of unspecific hybridization, it was easy to identify the specific hybridization signals from the hybridization maps directly (Figure 2).

Twenty-six unselected divided cultures were also processed and hybridized as described above, and then identified according to the specific hybridization maps (Table 3). Among them, 25 strains were distinguished according to their hybridization maps, but only one strain was indistinguishable due to its weak signal. The comprehensive identification results by classical methods were regarded as the final standards. Except for sample 7, all other results were consistent with those detected by hybridization assay and conventional method, the consistency was 96.2% (25/26).

DISCUSSION

Our study showed that the gene chip-based method could identify a wide range of intestinal pathogenic bacterial species. The genus or species specific probes on the microarray are targeted at the 16S rDNA, while two discriminative probes are targeted at special pathogenic genes. Sample DNA was labeled with fluorescence by PCR, then hybridized to the probes on the chip, thus a couple of genus or species-specific hybridization patterns could be generated and used to discriminate the bacteria[9].

When the oligonucleotide probes for 16S rDNA were designed, we preferred a longer oligonucleotide segment with multiple mutation sites over a shorter one, which is also suitable for detecting single-nucleotide mutation[10-12]. The advantages are obvious: the amount of essential oligonucleotides is less, the cost of experiment is lower, and the identification of hybridization map is easier. However, the shortcoming is somewhat less discriminative to those sequences where only minor differences are present.

The 16S rDNA sequences of *Shigella*, *Salmonella,* and *Escherichia coli* are similar, and share almost identical sequences of the target 16S rDNA genes. Thus, these three genera can hardly be identified by only 16S rDNA[13,14].

Besides, intestinal pathogenic bacteria belonging to *Listeria monocytogenes*, *Vibrio parahaemolyticus*, *Proteus* sp., *Vibrio cholerae*, *Enterococcus faecalis*, *Yersinia enterocolitica,* and *Campylobacter jejuni*, could be detected and identified using the gene chip.

Compared to the classic microbial assay, immunological assay, PCR-based assay, the method based upon the gene chip technology could detect and identify a given strain of bacterium within 3 h. It is a fundamental start point to develop other methods for a large-scale assay. The target spectrum of this gene chip may be gradually expanded

Table 3 Comparison of identifications based on hybridization assay and conventional methods for 26 cultures

No.	Hybridization assay	Conventional methods	Consistency
1	*Staphylococcus aureus*	*Staphylococcus aureus*	Y[1]
2	Coagulase-negative *Staphylococcus*	*Staphylococcus epidermidis*	Y
3	*Staphylococcus aureus*	*Staphylococcus aureus*	Y
4	*Staphylococcus aureus*	*Staphylococcus aureus*	Y
5	*Staphylococcus aureus*	*Staphylococcus aureus*	Y
6	*Pseudomonas aeruginosa*	*Pseudomonas aeruginosa*	Y
7	-[3]	*Salmonella typhimurium*	-[2]
8	*Escherichia coli*	*Escherichia coli*	Y
9	*Staphylococcus aureus*	*Staphylococcus aureus*	Y
10	*Pseudomonas aeruginosa*	*Pseudomonas aeruginosa*	Y
11	*Shigella* sp.	*Shigella flexneri*	Y
12	*Shigella* sp.	*Shigella flexneri*	Y
13	*Shigella* sp.	*Shigella flexneri*	Y
14	*Shigella* sp.	*Shigella flexneri*	Y
15	*Vibrio parahaemolyticus*	*Vibrio parahaemolyticus*	Y
16	*Yersinia enterocolitica*	*Yersinia enterocolitica*	Y
17	*Pseudomonas aeruginosa*	*Pseudomonas aeruginosa*	Y
18	*Shigella* sp.	*Shigella flexneri*	Y
19	*Shigella* sp.	*Shigella flexneri*	Y
20	*Vibrio parahaemolyticus*	*Vibrio parahaemolyticus*	Y
21	*Escherichia coli*	*Escherichia coli*	Y
22	*Escherichia coli*	*Escherichia coli*	Y
23	*Salmonella* sp.	*Salmonella typhimurium*	Y
24	*Campylobacter jejuni*	*Campylobacter jejuni*	Y
25	*Salmonella* sp.	*Salmonella typhimurium*	Y
26	*Salmonella* sp.	*Salmonella typhimurium*	Y

[1]The results from hybridization assay and conventional methods are consistent. [2]The results are inconsistent. [3]No signal was detected.

by adding newly designed oligonucleotide probes into the oligonucleotide microarray, and the accuracy may also be improved by increasing and readjusting the oligonucleotide probes in the oligonucleotide microarray. The arrangement of the oligonucleotide microarray may be rearranged according to its end usage. This method for intestinal pathogen assay using gene chip technology can be used for the diagnosis of infectious diseases, environmental supervision, food quality surveillance, etc.

REFERENCES

1 **Cheung VG**, Morley M, Aguilar F, Massimi A, Kucherlapati R, Childs G. Making and reading microarrays. *Nat Genet* 1999; **21:** 15-19

2 **Bowtell DD**. Options available--from start to finish--for obtaining expression data by microarray. *Nat Genet* 1999; **21:** 25-32

3 **Holloway AJ**, van Laar RK, Tothill RW, Bowtell DD. Options available--from start to finish--for obtaining data from DNA microarrays II. *Nat Genet* 2002; **32 Suppl:** 481-489

4 **Chizhikov V**, Rasooly A, Chumakov K, Levy DD. Microarray analysis of microbial virulence factors. *Appl Environ Microbiol* 2001; **67:** 3258-3263

5 **Ludwig W**, Schleifer KH. Bacterial phylogeny based on 16S and 23S rRNA sequence analysis. *FEMS Microbiol Rev* 1994; **15:** 155-173

6 **Anthony RM**, Brown TJ, French GL. Rapid diagnosis of bacteremia by universal amplification of 23S ribosomal DNA followed by hybridization to an oligonucleotide array. *J Clin Microbiol* 2000; **38:** 781-788

7 **Sharples GJ**, Lloyd RG. A novel repeated DNA sequence located in the intergenic regions of bacterial chromosomes. *Nucleic Acids Res* 1990; **18:** 6503-6508

8 **Dams E**, Hendriks L, Van de Peer Y, Neefs JM, Smits G, Vandenbempt I, De Wachter R. Compilation of small ribosomal subunit RNA sequences. *Nucleic Acids Res* 1988; **16 Suppl:** r87-173

9 **Call DR**, Borucki MK, Loge FJ. Detection of bacterial pathogens in environmental samples using DNA microarrays. *J Microbiol Methods* 2003; **53:** 235-243

10 **Noller HF**, Green R, Heilek G, Hoffarth V, Huttenhofer A, Joseph S, Lee I, Lieberman K, Mankin A, Merryman C. Structure and function of ribosomal RNA. *Biochem Cell Biol* 1995; **73:** 997-1009

11 **Boyer SL**, Flechtner VR, Johansen JR. Is the 16S-23S rRNA internal transcribed spacer region a good tool for use in molecular systematics and population genetics? A case study in cyanobacteria. *Mol Biol Evol* 2001; **18:** 1057-1069

12 **Hacia JG**. Resequencing and mutational analysis using oligonucleotide microarrays. *Nat Genet* 1999; **21:** 42-47

13 **Villalobo E**, Torres A. PCR for detection of Shigella spp. in mayonnaise. *Appl Environ Microbiol* 1998; **64:** 1242-1245

14 **Rahn K**, De Grandis SA, Clarke RC, McEwen SA, Galan JE, Ginocchio C, Curtiss R 3rd, Gyles CL. Amplification of an invA gene sequence of Salmonella typhimurium by polymerase chain reaction as a specific method of detection of Salmonella. *Mol Cell Probes* 1992; **6:** 271-279

Science Editor Wang XL and Guo SY **Language Editor** Elsevier HK

PO Box 2345, Beijing 100023, China
www.wjgnet.com
wjg@wjgnet.com

ELSEVIER

World J Gastroenterol 2005;11(48):7620-7624
World Journal of Gastroenterology ISSN 1007-9327

• *BASIC RESEARCH* •

Morphological and serum hyaluronic acid, laminin and type IV collagen changes in dimethylnitrosamine-induced hepatic fibrosis of rats

Chun-Hui Li, Dong-Ming Piao, Wen-Xie Xu, Zheng-Ri Yin, Jing-Shun Jin, Zhe-Shi Shen

Chun-Hui Li, Dong-Ming Piao, Zheng-Ri Yin, Jing-Shun Jin, Zhe-Shi Shen, Department of Pathology, Affiliated Hospital of Yanbian University College of Medicine, Yanji 133000, Jilin Province, China
Wen-Xie Xu, Department of Physiology, College of Medicine, Shanghai Jiaotong University, Shanghai 200030, China
Chun-Hui Li, Affiliated Hospital of Chengde Medical College, Chengde 067000, Hebei Province, China
Correspondence to: Dong-Ming Piao, Department of Pathology, Affiliated Hospital of Yanbian University College of Medicine, Yanji 133000, Jilin Province,
China. pdm11172000@yahoo.con.cn
Telephone: +86-0433-2660203 Fax: +86-0433-2513610
Received: 2005-05-18 Accepted: 2005-06-18

Abstract

AIM: To study the morphological and serum hyaluronic acid (HA), laminin (LN), and type IV collagen changes in hepatic fibrosis of rats induced by dimethylnitrosamine (DMN).

METHODS: The rat model of liver fibrosis was induced by DMN. Serum HA, type IV collagen, and LN were measured by ELISA. The liver/weight index and morphological changes were examined under electron microscope on d 7, 14, 21, and 28 by immunohistochemical alpha smooth muscle actin α-SMA staining as well as Sirius-red and HE staining.

RESULTS: The levels of serum HA, type IV collagen and LN significantly increased from d 7 to d 28 (P = 0.043). The liver/weight index increased on d 7 and decreased on d 28. In the model group, the rat liver stained with HE and Sirius-red showed evident hemorrhage and necrosis in the central vein of hepatic 10 lobules on d 7. Thin fibrotic septa were formed joining central areas of the liver on d 14. The number of α-SMA positive cells was markedly increased in the model group. Transitional hepatic stellate cells were observed under electron microscope. All rats in the model group showed micronodular fibrosis in the hepatic parenchyma and a network of α-SMA positive cells. Typical myofibroblasts were embedded in the core of a fibrous septum. Compared to the control group, the area-density percentage of collagen fibrosis and pathologic grading were significantly different in the model group (P<0.05) on different d (7, 14, and 28). The area-density percentage of collagen fibrosis in hepatic tissue had a positive correlation with the levels of serum HA, LN, and type IV collagen.

CONCLUSION: The morphological and serum HA, type IV collagen, and LN are changed in DMN-induced liver fibrosis in rats.

Key words: Rat; Hepatic fibrosis; DMN; Morphological change; Serum; Experimental studies

Li CH, Piao DM, Xu WX, Yin ZR, Jin JS, Shen ZS. Morphological and serum hyaluronic acid, laminin and type IV collagen changes in dimethylnitrosamine-induced hepatic fibrosis of rats. *World J Gastroenterol* 2005; 11(48): 7620-7624
http://www.wjgnet.com/1007-9327/11/7620.asp

INTRODUCTION

In China, the incidence of liver cirrhosis is still high[1]. Hepatic cirrhosis results from fibrosis[2-4]. Many factors can lead to chronic liver disease and hepatic fibrosis[5-9]. Hepatic fibrosis is associated with a number of morphological and biochemical changes leading to structural and metabolic abnormalities in the liver. Hepatic stellate cells (HSCs) play a major role in various types of liver fibrosis through initial myofibroblast transformation. Transformed HSCs can actively synthesize extracellular matrix and then change morphology and function of the liver. Dimethylnitrosamine (DMN)-induced hepatic fibrosis in rats appears to be a good and reproducible model with decompensating features of human disease[10,11]. This study was to observe the morphological and serum hyaluronic acid (HA), laminin (LN), and type IV collagen changes in DMN-induced hepatic fibrosis of rats.

MATERIALS AND METHODS

Animals and experiment protocol

Male Wistar rats weighing 175-200 g were obtained from the Experimental Animal Center of Yanbian University College of Medicine. The rats were divided into two groups. The model group (n = 40) received 1% DMN (10 μL/kg

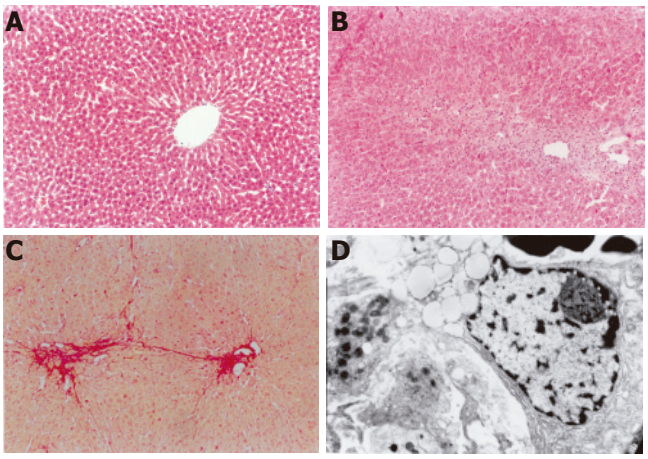

Figure 1 Changes after DMN treatment. **A:** Livers in the control group showed normal lobular architecture with central veins; **B:** after 7 d of DMN treatment, extensive necrosis was observed in portal areas; **C:** after 14 d of DMN treatment, thin fibrotic septa were formed joining central areas; **D:** after 21 or 28 d of DMN treatment, thick intralobular septa were evident.

body weight, i.p.) thrice a week for 4 wk, while the control group (n = 12) received an equivalent amount of saline. The animals were killed on d 7, 14, 21, and 28 (10 treated with DMN at each time interval). Blood was taken from the left ventricle. Serum samples obtained from all study subjects were frozen at -70 °C and aliquots were thawed when needed for specific tests. The liver was examined by light and electron microscopy.

Serum HA, type IV collagen, and LN levels testing

A quantitative ELISA was used to determine serum HA, type IV collagen, and LN levels according to the manufacturer's instructions.

Sirius-red and HE staining

Formalin-fixed tissues were paraffin-embedded and cut into 4-μm thick sections from the right lobe of rat's liver for HE and Sirius-red staining. HE staining was used to observe liver pathologic structures, Sirius-red staining was used to grade liver fibrosis from 0 to 4[16]: grade 0 = no fibrosis, grade 1 = portal area fibrosis, grade 2 = fibrotic septa between portal tracts, grade 3 = fibrosis septa and structure disturbance of hepatic lobule, grade 4 = cirrhosis. At the same time, Sirius-red staining and CMIAS image analysis system (Beijing, China) were used to determine the area-density percentage of collagen fibrosis in hepatic tissue. At least five high-power (×400 field) fields were chosen and positive collagen fibrosis (red staining) was determined. Area-density percentage of collagen fibrosis was calculated by dividing the number of positive collagen fibroses (positive optical density) over the total number of collagen fibroses (integrated optical density).

Immunohistochemical staining

α-SMA for the detection of activated HSCs was studied by immunohistochemical staining. Sections (5-μm) were deparaffinized, rehydrated and incubated with 0.3% hydrogen peroxidase in methanol for 15 min at room temperature to block endogenous peroxidase activity. After being washed twice with phosphate-buffered saline (PBS) for 5 min, tissue sections were incubated at 37 °C for 20 min with blocking solution, then incubated at 37 °C for 2 h with rabbit anti-rat α-SMA antibody (Dako, Denmark) at dilution 1:100. After being washed twice with PBS (0.01 mol/L, PH 7.4) for 10 min, tissue sections were incubated at 37 °C for 30 min with biotin-anti-rabbit IgG. After being washed twice with PBS for 5 min, the sections were incubated with streptavidin-HRP for 30 min. Then the sections were washed twice with PBS for 5 min and incubated with metal-enhanced 3, 3-diaminobenzidine solution for 15 min, washed twice in distilled waster and counterstained with hematoxylin. Negative control sections were incubated with normal rabbit serum instead of primary antibody. The positive staining for α-SMA positive cells was expressed as red brown granules and photomicrographed (Olympus PM-10AD).

Electron microscopy

Fresh fragments of 1 mm^3 liver tissue were fixed in 10% paraffin, dehydrated and embedded in Epon-812 resin. Sections were stained with uranyl acetate for 15 min and then lead citrate for 15 min. Transitional HSCs were observed under JEM-1200EX, 80 kV electron microscope (JEOL, Japan).

Statistical analysis

Data were expressed as mean±SD. The two-tailed χ^2 test was used to examine the correlation between the area-density percentage of collagen fibrosis in hepatic tissue and serum HA, LN, and type IV collagen levels. Statistical significance was estimated by t-test. $P<0.05$ was considered statistically significant. All calculations were made by SPSS 11.0 for Windows.

RESULTS

Serum HA, type IV collagen, and LN levels change

When compared to control values, a significant increase ($P<0.05$) was observed in serum levels of HA, LN, and type IV collagen on d 7, 14, 21, and 28 after administration of DMN. The maximum increase in serum levels of HA, LN, and type IV collagen was observed on d 28 after DMN treatment (Figure 3).

Change in the weight of body and liver as well as liver and body ratio

An increase in liver weight was observed on d 7 after DMN treatment, with a decreased liver weight on d 28. The maximum liver and body weight ratio increased on d 14 and decreased on d 28 (Table 1).

Changes after DMN treatment

The rat liver stained with Sirius-red and HE showed an extensive accumulation of collagens. Fibrotic septum increased from port to port and from port to central

Table 1 Changes in the weight of body and liver as well as liver/body ratio of rats during DMN treatment (mean±SD)

Group	*n*	Body weight	Liver weight	Liver/body ratio
Control	10 (0)	192.50±9.0446	6.2260±0.3848	3.2191±0.2829
Day 7	6 (4)	207.85±5.3293	7.8114±0.3869	3.7492±0.1195
Day 14	9 (1)	167.27±11.9157[a]	6.9164±0.6229[a]	4.1059±0.1636[a,c]
Day 21	9 (1)	181.11±13.3536[a]	6.5122±0.6200[a]	3.5671±0.1437[a]
Day 28	10 (0)	186.42±10.7301[a]	6.3657±0.5306[a]	3.3903±0.1096[a,c]

[a]*P*<0.05 *vs* control; [c]*P*<0.05 *vs* day 7; ( ): number of deaths.

Table 2 Pathologic grading of DMN-induced hepatic fibrosis in rats (mean±SD)

Groups	*n*	Grading of hepatic fibrosis				
		–	+	++	+++	++++
Control	10 (0)	10	0	0	0	0
Day 7	6 (4)	0	3	3	0	0
Day 14	9 (1)	0	2	4	3	0
Day 21	9 (1)	0	0	2	4	3
Day 28	10 (0)	0	0	2	4	4

P<0.001 *vs* control; *P*<0.001 *vs* d 7; ( ): number of deaths.

vein in some parts of lobules. The livers of the rats in the control group showed normal lobular architecture with central veins and radiating hepatic cords (Figure 1A). After 7 d of DMN treatment, extensive necrosis occurred in portal area and hemorrhage was prominent (Figure 1B). After 14 d, hemorrhagic necrosis and formation of thin fibrotic septa joining central areas were found (Figure 1C). After 21 d, thick intralobular septa were evident (Figure 1D). After 28 d, the pattern was similar with that after 21 d. At the same time, fibrotic septum increased the area-density percentage of collagen fibrosis in hepatic fibrosis. Compared to control values, a significant increase ($P<0.05$) was observed in area-density percentage of collagen fibrosis on d 7, 14, 21, and 28 after administration of DMN. The maximum increase in the levels of the area-density percentage of collagen fibrosis was observed on d 28 after DMN treatment (Figure 2). Liver fibrosis was graded from 0 to 4 (Table 2)

Distribution of α-SMA positive cells

Activated HSCs characterized by the expression of α-SMA increased in the liver of rats that received DMN. The distribution of α-SMA positive cells was similar to that of collagen in the liver. After 14 d, linear immunoreaction for α-SMA was scattered along the sinusoidal wall (Figure 4A). After 21 d, a network of α-SMA cells was evident (Figure 4B). After 28 d, a dense network of α-SMA cells was evident (Figure 4C). Transitional HSCs were observed under electron microscope, showing features of lipid-containing myofibroblasts and bundles of connective tissue after 14 d of DMN treatment (Figure 4D). Typical myofibroblasts were embedded in the core of fibrous septa after 21–28 d of DMN treatment. The elongated cell body contained a nucleus and numerous microfilaments outlined by a lamina-like structure. Collagen fibers of variable size were seen around the myofibroblasts (Figure 4E).

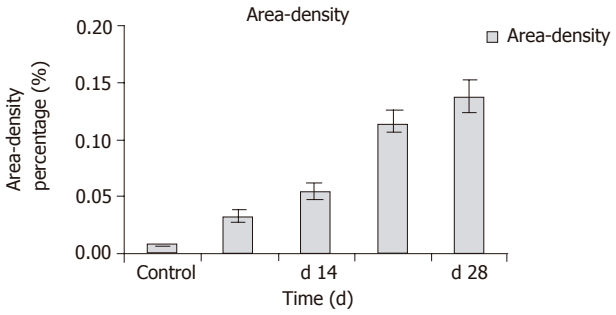

Figure 2 Area–density percentage of collagen fibrosis in hepatic tissue. *P*<0.05 *vs* control; *P*<0.05 *vs* d 7.

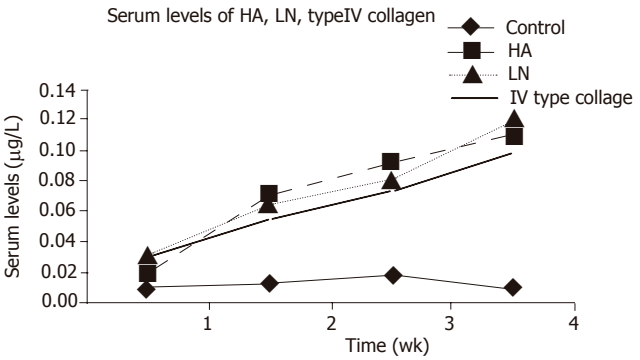

Figure 3 Serum levels of HA, LN, and Type IV collagen in DMN-induced fibrosis of rats and control, *P*<0.05 *vs* control.

Relationship between area-density percentage of collagen fibrosis and serum HA, type IV collagen, and LN levels

A positive correlation ($r = 0.707$, $P<0.01$) was noticed between the area-density percentage of collagen fibrosis and serum levels of HA, LN, and type IV collagen during the course of DMN administration.

DISCUSSION

Liver fibrosis is common in most chronic liver diseases regardless of their etiology[12-15]. The incidence rate of chronic liver disease in China is high[16]. Hepatic fibrosis is the intermediate and crucial stage of cirrhosis. If treated properly in this stage, cirrhosis could be successfully prevented[17], but it remains a problem to prevent cirrhosis or to control its progression in patients with chronic liver disease[18]. HSCs play a central role in the pathogenesis of liver fibrosis. After liver injury, HSCs become activated and express a wide variety of extracellular matrixes. It was reported that hepatic fibrosis is induced in rats by low doses of DMN and morphological changes of hepatic fibrosis are associated with cells bearing 'transitional' features of HSCs, myofibroblasts and fibroblasts[19]. Activated but not quiescent HSCs have a high level of collagen and express α-SMA. HSCs play a key role in the pathogenesis of hepatic fibrosis[20]. To evaluate the distribution of α-SMA positive cells in various liver diseases, Yu *et al*.[21] undertook an immunohistochemical

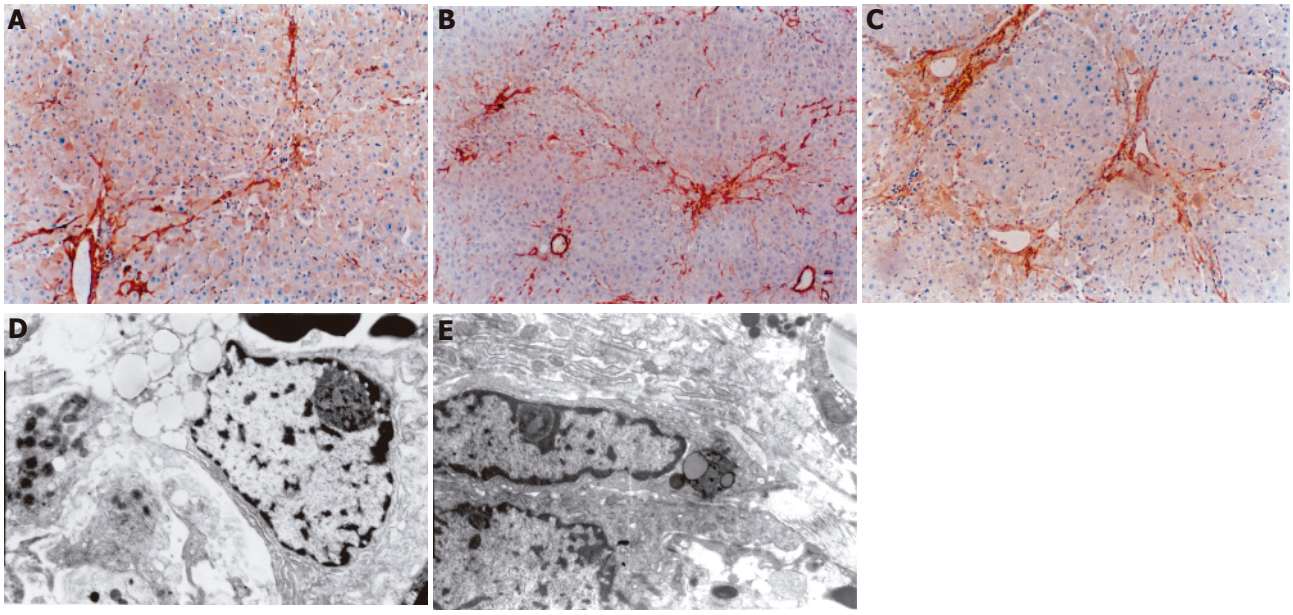

Figure 4 Distribution of α-SMA positive cells after DMN treatment. **A:** After 14 d, linear immunoreaction for α-SMA was scattered along the sinusoidal wall; **B:** after 21 d, a network of α-SMA cells was evident; **C:** after 28 d, a dense network of α-SMA cells was evident; **D:** after 14 d, transitional hepatic stellate cells were observed under electron microscope; **E:** after 21 or 28 d, typical myofibroblasts were embedded in the core of fibrous septa.

study of liver diseases including chronic persistent hepatitis, chronic active hepatitis, liver cirrhosis, intrahepatic cholelithiasis and hepatocellular carcinoma, and found that expression of α-SMA may be related to the fibrotic process[22]. DMN-induced experimental model may contribute to the understanding of the relationship between liver injury and hepatic fibrosis[23] and is used to detect different degrees of hepatic fibrosis[24,25]. In our study, serum levels of HA, LN, and type IV collagen increased significantly in hepatic fibrosis, suggesting that detection of HA, LN, and type IV collagen level is an optimal choice[26]. In this study, a positive correlation was noticed between the area-density percentage of collagen fibrosis and serum levels of LN, HA, and type IV collagen during the course of DMN administration, indicating that DMN is a potent hepatotoxin that can cause fibrosis of the liver. DMN can be administered to adult male albino rats in order to document sequential pathological and biochemical alterations[27].

In conclusion, HSCs play a central role in the pathogenesis of liver fibrosis and can regulate degradation of matrix in the liver.

REFERENCES

1 **Du WD**, Zhang YE, Zhai WR, Zhou XM. Dynamic changes of type I,III and IV collagen synthesis and distribution of collagen-producing cells in carbon tetrachloride-induced rat liver fibrosis. *World J Gastroenterol* 1999; **5:** 397-403

2 **Canturk NZ,** Canturk Z, Ozden M, Dalcik H, Yardimoglu M, Tulubas F. Protective effect of IGF-1 on experimental liver cirrhosis-induced common bile duct ligation. *Hepatogastroenterology* 2003; **50:** 2061-2066

3 **Xu LX**, Xie XC, Jin R, Ji ZH, Wu ZZ, Wang ZS. Protein deficiency and muscle damage in carbon tetrachloride induced liver cirrhosis. *Food Chem Toxicol* 2003; **41:** 1789-1797

4 **Pan NS**, Li ST, Wang Y, Li MF, Han Z. [Therapeutic effect of "anti-hepatic-fibrosis 268" on hepatic fibrosis in rats] *Sichuan Da Xue Xue Bao Yi Xue Ban* 2004; **35:** 528-531

5 **Kuroki T,** Seki S, Kawakita N, Nakatani K, Hisa T, Kitada T, Sakaguchi H.Expression of antigens related to apoptosis and cell proliferation in chronic nonsuppurative destructive cholangitis in primary biliary cirrhosis. *Virchows Arch* 1996; **429:** 119-129

6 **Jia JD.** Further systematize and standardize the diagnosis and treatment of liver cirrhosis. *Zhonghua Ganzangbing Zazhi* 2005; **13:** 401-402

7 **Jaster R**. Molecular regulation of pancreatic stellate cell function. *Mol Cancer* 2004; **3:** 26

8 **Breitkopf K**, Sawitza I, Gressner AM. Characterization of intracellular pathways leading to coinduction of thrombospondin-1 and TGF-beta1 expression in rat hepatic stellate cells. *Growth Factors* 2005; **23:** 77-85

9 **Tox U**, Goeser T. [Therapy of complications of hepatic cirrhosis] *Schweiz Rundsch Med Prax* 2005; **94:** 727-733

10 **Jenkins SA**, Grandison A, Baxter JN, Day DW, Taylor I, Shields R. A dimethylnitrosamine-induced model of cirrhosis and portal hypertension in the rat. *J Hepatol* 1985; **1:** 489-499

11 **Veal N**, Auduberteau H, Lemarie C, Oberti F, Cales P. Effects of octreotide on intestinal transit and bacterial translocation in conscious rats with portal hypertension and liver fibrosis. *Dig Dis Sci* 2001; **46:** 2367-2673

12 **McCaughan GW**, Gorrell MD, Bishop GA, Abbott CA, Shackel NA, McGuinness PH, Levy MT, Sharland AF, Bowen DG, Yu D, Slaitini L, Church WB, Napoli J. Molecular pathogenesis of liver disease: an approach to hepatic inflammation, cirrhosis and liver transplant tolerance. *Immunol Rev* 2000; **174:** 172-191

13 **Jung SA**, Chung YH, Park NH, Lee SS, Kim JA, Yang SH, Song IH, Lee YS, Suh DJ, Moon IH. Experimental model of hepatic fibrosis following repeated periportal necrosis induced by allylalcohol. *Scand J Gastroenterol* 2000; **35:** 969-975

14 **Plummer JL**, Ossowicz CJ, Whibley C, Ilsley AH, Hall PD. Influence of intestinal flora on the development of fibrosis and cirrhosis in a rat model. *J Gastroenterol Hepatol* 2000; **15:** 1307-1311

15 **Ramalho F**. Hepatitis C virus infection and liver steatosis. *Antiviral Res* 2003; **60:** 125-127

16 **Lamireau T**, Desmouliere A, Bioulac-Sage P, Rosenbaum J. Mechanisms of hepatic fibrogenesis. *Arch Pediatr* 2002; **9:** 392-405

17 **Riley TR 3rd**, Bhatti AM. Preventive strategies in chronic liver disease: part II. Cirrhosis. *Am Fam Physician* 2001; **64:** 1735-1740

18 **Murphy F**, Arthur M, Iredale J. Developing strategies for liver fibrosis treatment. *Expert Opin Investig Drugs* 2002; **11:** 1575-1585

19 **Jezequel AM,** Mancini R, Rinaldesi ML, Macarri G, Venturini C, Orlandi F. A morphological study of the early stages of hepatic fibrosis induced by low doses of dimethylnitrosamine in the rat**.** *J Hepatol* 1987; 5: 174-187

20 **Lee KS,** Lee SJ, Park HJ, Chung JP, Han KH, Chon CY, Lee SI, Moon YM. Oxidative stress effect on the activation of hepatic stellate cells. *Yonsei Med J* 2001; **42:** 1-8

21 **Yu E**, Choe G, Gong G, Lee I. Expression of alpha-smooth muscle actin in liver diseases. *J Korean Med Sci* 1993; **8:** 367-373

22 **Tanaka Y**, Nouchi T, Yamane M, Irie T, Miyakawa H, Sato C, Marumo F. Phenotypic modulation in lipocytes in experimental liver fibrosis. *J Pathol* 1991; **164:** 273-278

23 **Jezequel AM,** Mancini R, Rinaldesi ML, Ballardini G, Fallani M, Bianchi F, Orlandi F. Dimethylnitrosamine-induced cirrhosis. Evidence for an immunological mechanism**.** *J Hepatol* 1989 ; **8:** 42-52

24 **Lee MH,** Yoon S, Moon JO. The flavonoid naringenin inhibits dimethylnitrosamine-induced liver damage in rats**.** *Biol Pharm Bull* 2004; **27:** 72-76

25 **Hsu YC,** Chiu YT, Lee CY, Lin YL, Huang YT. Increases in fibrosis-related gene transcripts in livers of dimethylnitrosamine-intoxicated rats**.** *J Biomed Sci* 2004; **11:** 408-417

26 **Liang XH,** Zheng H. Value of simultaneous determination of serum hyaluronic acid, collagen type IV and the laminin level in diagnosing liver fibrosis. *Hunan Yike Daxue Xuebao* 2002; **27:** 67-68

27 **Madden JW**, Gertman PM, Peacock EE. Dimethylnitrosamine-induced hepatic cirrhosis:a new canine model of an ancient human disease. *Surgery* 1970; **68:** 260-268

Science Editor Wang XL and Guo SY **Language Editor** Elsevier HK

PO Box 2345, Beijing 100023, China
www.wjgnet.com
wjg@wjgnet.com

ELSEVIER

World J Gastroenterol 2005;11(48):7625-7630
World Journal of Gastroenterology ISSN 1007-9327

• *CLINICAL RESEARCH* •

Management of hilar cholangiocarcinoma in the North of England: Pathology, treatment, and outcome

SD Mansfield, O Barakat, RM Charnley, BC Jaques, CB O'Suilleabhain, PJ Atherton, D Manas

SD Mansfield, O Barakat, RM Charnley, BC Jaques, CB O' Suilleabhain, PJ Atherton, D Manas, Department of Hepato-Pancreatico-Biliary Surgery, Liver Transplantation, and Oncology, Freeman Hospital, Newcastle upon Tyne, United kingdom
Correspondence to: Derek Manas, Hepato-Pancreatico-Biliary Surgery Unit, Freeman Hospital, High Heaton, Newcastle upon Tyne, Tyne and Wear NE7 7DN,
United kingdom. derek.manas@nuth.northy.nhs.uk
Telephone: +44-191-2336161 Fax: +44-191-2231483
Received: 2004-04-30 Accepted: 2004-07-15

Key words: Hilar cholangiocarcinoma; Pathology; Treatment; Outcome; England

Mansfield SD, Barakat O, Charnley RM, Jaques BC, O' Suilleabhain CB, Atherton PJ, Manas D. Management of hilar cholangiocarcinoma in the North of England: Pathology, treatment, and outcome. *World J Gastroenterol* 2005; 11(48): 7625-7630
http://www.wignet.com/1007-9327/11/7625.asp

Abstract

AIM: To assess the management and outcome of hilar cholangiocarcinoma (Klatskin tumor) in a single tertiary referral center.

METHODS: The notes of all patients with a diagnosis of hilar cholangiocarcinoma referred to our unit for over an 8-year period were identified and retrospectively reviewed. Presentation, management and outcome were assessed.

RESULTS: Seventy-five patients were identified. The median age was 64 years (range 34-84 years). Male to female ratio was 1:1. Eighty-nine percent of patients presented with jaundice. Most patients referred were under Bismuth classification 3a, 3b or 4. Seventy patients required biliary drainage, 65 patients required 152 percutaneous drainage procedures, and 25 had other complications. Forty-one patients had 51 endoscopic drainage procedures performed (15 failed). Of these, 36 subsequently required percutaneous drainage. The median number of drainage procedures for all patients was three, 18 patients underwent resection (24%), nine had major complications and three died post-operatively. The 5-year survival rate was 4.2% for all patients, 21% for resected patients and 0% for those who did not undergo resection (P = 0.0021). The median number of admissions after diagnosis in resected patients was two and three in non-resected patients (P<0.05). Twelve patients had external-beam radiotherapy, seven brachytherapy, and eight chemotherapy. There was no significant benefit in terms of survival (P = 0.46) or hospital admissions.

CONCLUSION: Resection increases survival but carries the risk of significant morbidity and mortality. Percutaneous biliary drainage is almost always necessary and endoscopic drainage should be avoided if possible.

INTRODUCTION

Cholangiocarcinoma is a relatively rare tumor, accounting for approximately 2% of all diagnosed cancers. Its prevalence in England and Wales is approximately 2.0/100 000; however, the mortality rate has risen sharply in the past 30 years[1]. Upper third or perihilar (Klatskin) tumors make up 40-60% of cases[2,3] and are the main subjects of this paper. Klatskin tumors may be categorized as suggested by Bismuth classification into:

- Type I: tumors below the bifurcation of the common hepatic duct;
- Type II: tumors involving the bifurcation, but not extending into the main right or left duct;
- Type III: tumors infiltrating the right (IIIa) or the left (IIIb) hepatic duct;
- Type IV: tumors involving both the right and left hepatic ducts.

Cholangiocarcinoma is a slowly growing tumor and tends to spread longitudinally along the bile ducts with neural, perineural, and subepithelial extensions[4]. Lymph node invasion, particularly to the portal and peripancreatic regions, can be found in 46% of patients at the time of diagnosis[5]. Blood-born metastasis is rare and occurs at later stages of the disease. The prognosis for patients with unresectable tumors is poor and the majority of them die within 6 mo to a year of diagnosis[3].

Most patients present with obstructive jaundice. Preoperative investigations help establish the cause of obstruction, determine the extent of local disease and any evidence of distant metastasis, and evaluate the hepatic vasculature.

Treatment options for Klatskin tumors may be primarily surgical - either curative resection or palliative bypass, or non-surgical using modalities such as chemotherapy,

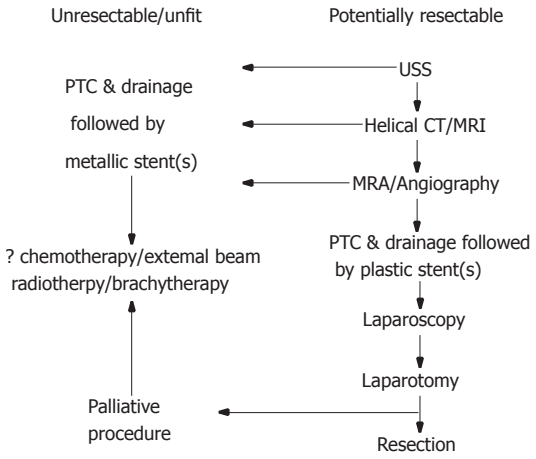

Figure 1 Flow chart demonstrating management options for hilar cholangiocarcinoma. USS, ultrasound scan; CT, computed tomography; MRI, magnetic resonance imaging; MRA, magnetic resonance angiography; PTC, percutaneous transhepatic cholangiography.

radiotherapy (external or endoluminal), a combination of the two or more recently photodynamic therapy and gene therapy. The use of biliary endoprosthesis is common either as the primary modality in palliation or for relieving jaundice or sepsis prior to more definitive treatment.

The aim of our study was to assess the management and outcome of hilar cholangiocarcinoma in a single tertiary referral center in the United Kingdom.

MATERIALS AND METHODS

Patients

Our unit is a cancer center recognized for the treatment of hepatobiliary malignancy and covers a population of approximately 3.5 million people across the North of England. The notes of all patients with hilar cholangiocarcinoma presenting to our unit during an 8-year period from June 1995 to June 2003 were identified and assessed retrospectively. Seventy-five patients were identified. Male to female ratio was 1:1 with a median age of 64 years (range 34-84 years). Thirty-seven patients had confirmed histological diagnoses with the remainder being diagnosed on strong radiological evidence. In each case, tumors were categorized using the Bismuth classification. A schematic representation for the treatment of these patients is shown in Figure 1.

Investigations

All patients were assessed using triple phase helical CT or magnetic resonance imaging. Scans performed at referring hospitals were repeated, if deemed to be of insufficient quality. Vascular involvement of hilar vessels by tumors was assessed using magnetic resonance angiography (MRA) or transfemoral angiography if MRA could not be performed or was inadequate for accurate assessment. No percutaneous or endoscopic cholangiography was performed for purely diagnostic reasons. Further imaging and laparoscopic assessment were performed if clinically indicated. Staging procedures were completed, wherever possible, before biliary drainage.

Biliary drainage

It is our policy, to drain all obstructed segments of the bile ducts in all jaundiced patients with hilar cholangiocarcinoma wherever possible. Many patients referred from other units attempted endoscopic stenting of hilar strictures. In our experience, this is often inadequate and therefore staged percutaneous drainage was performed in the majority of cases with the initial placement of internal/external or external biliary catheters being followed by the placement of single or multiple stents. When the possibility of resection was excluded, self-expanding metallic stents were used, otherwise plastic stents were inserted.

Surgical procedures

Tumors were deemed to be unresectable on pre-operative staging in the presence of extra-hepatic metastases, occlusion of main hepatic vessels, or bilateral invasion of secondary biliary radicals into the liver parenchyma. On laparotomy or laparoscopic assessment, evidence of extensive lymph node involvement and peritoneal deposits were also taken to indicate unresectability. Curative resections involved complete removal of all gross and microscopic diseases to achieve negative histological margins with eradication of all metastatic lymph nodes restricted to the scope of dissection (Ro) and restoration of bilio-enteric continuity. Caudate lobectomy was also performed in the majority of cases. For all surgical procedures, duration, blood loss, utilization of critical care beds, and complications were recorded.

Other treatment modalities

Palliative chemotherapy, external beam radiotherapy, and brachytherapy were utilized in selected cases after consultation with clinical oncologists.

Follow-up

For all patients, the last consultation date as well as dates and causes of death were recovered from patient records. For those who lost their follow-up, data were completed by consulting the patients' general practitioners or collected from the local health authority records.

Statistical analysis

Data were analyzed using Minitab statistical software. Numbers of admissions and drainage procedures were compared using the Student's *t*-test and Bismuth classification. Breakdown was made using the χ^2 test. Survival analysis was made using the log-rank test. In all cases, $P<0.05$ was considered statistically significant.

RESULTS

Management for the 75 patients is shown in Figure 2. Of these, 67 (89%) patients presented with obstructive jaundice. Although there was an incidence of type IV tumors in the non-resected group, there was no significant difference in Bismuth classification between resected and

Table 1 Bismuth classification

Bismuth classification	All patients	Resected	Not resected
1	5	0	5
2	14	4	10
3a	12	6	6
3b	13	4	9
4	24	4	20
Not recorded	6	0	6

Table 2 Surgical procedures

Procedure	*n*
Extend right hemihepatectomy and excision of extrahepatic biliary tree	7
Right hemihepatectomy and excision of extrahepatic biliary tree	4
Left hemihepatectomy and excision of extrahepatic biliary tree	6
Segment 4 resection and excision of extrahepatic biliary tree	1
Roux-en-Y segment 2,3,5 bypass	1
Roux-en-Y hepaticojejunostomy and U-tube insertion	1
U-tube insertion	1
Choledochojejunostomy	3
Laparoscopy and lateral segmentectomy (due to hemorrhage)	1
Open/close	2

non-resected groups (χ^2 test, Table 1).

Investigations

All patients received transcutaneous ultrasonography, of them 72 patients (96%) underwent assessment with CT scanning, 42 (56%) had MRI scans, and 18 (24%) received transfemoral angiography.

Biliary drainage

Biliary drainage was necessary in 70 patients, of them 65 (93%) required percutaneous drainage. A total of 51 endoscopic biliary drainages were performed in 41 patients, of which 15 (29%) failed. Percutaneous drainage was subsequently required in 36 of the 41 patients who underwent ERCP, due to failure or inadequate drainage or stent occlusion. Of the 199 drainage procedures performed, 49 (24.6%) had complications including 20 failures, 20 episodes of biliary sepsis, and 3 cases of pancreatitis. The median number of drainage procedures for all patients was three.

Surgical procedures and complications

A total of 27 surgical procedures were performed in 26 patients (Table 2). Eighteen patients underwent resection (24%) and three underwent portal vein resection. Major complications occurred in nine (50%) including three post-operative deaths (16.7%). The breakdown of complications is shown in Table 3. The median blood loss (range) in resected cases was 2.4 L (range 1-12 L), the median duration of procedure was 8 h (6-18) and the median critical care stay was 6 d (range 2-40d).

Follow-up

The median follow-up time was 9 mo. The 5-year survival rate was 4.2% for all patients, 21% for resected patients and 0% for those who did not undergo resection (P = 0.0021, log-rank test, Figure 2). The number of admissions after diagnosis was significantly lower (P<0.05, Student's t-test) in resected patients (median = 2) than in non-resected patients (median = 3).

Table 3 Complications of resection

Complication	*n*
Death	3 (17%)
Sepsis	9 (50%)
Bile leak	6 (33%)
Collection	6 (33%)
Chest infection	5 (28%)
Liver failure	5 (28%)
Wound infection	4 (22%)
Bleeding	3 (17%)
ARDS	1 (6%)
Hepatic artery thrombosis	1 (6%)
GI obstruction	1 (6%)
Pleural effusion	1 (6%)
Renal failure	1 (6%)
Respiratory arrest	1 (6%)
Wound dehiscence	1 (6%)

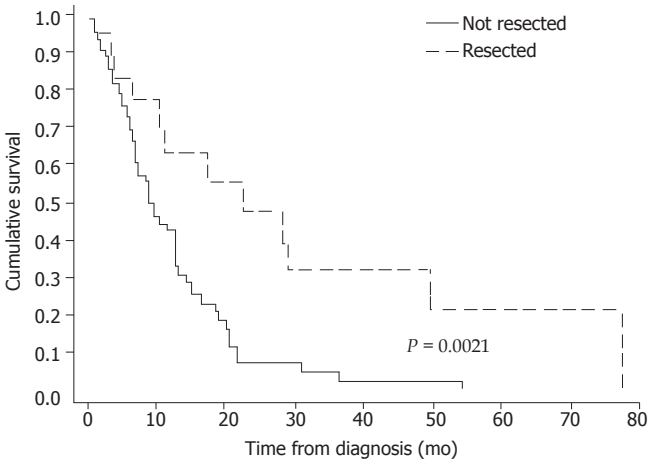

Figure 3 Kaplan–Meier survival plots for all patients with breakdown in resected and non-resected groups.

Other treatment modalities

In 23 patients who did not undergo resection, radiotherapy or chemotherapy was employed (Figure 3). These conferred no significant benefit in terms of survival (P = 0.46, log-rank test) (Figure 4), number of drainage procedures, or total hospital admissions.

Resected specimen pathology and staging

R0 resections were reported in 13 of 18 resected cases (72%). The pathological breakdown of resected cases by

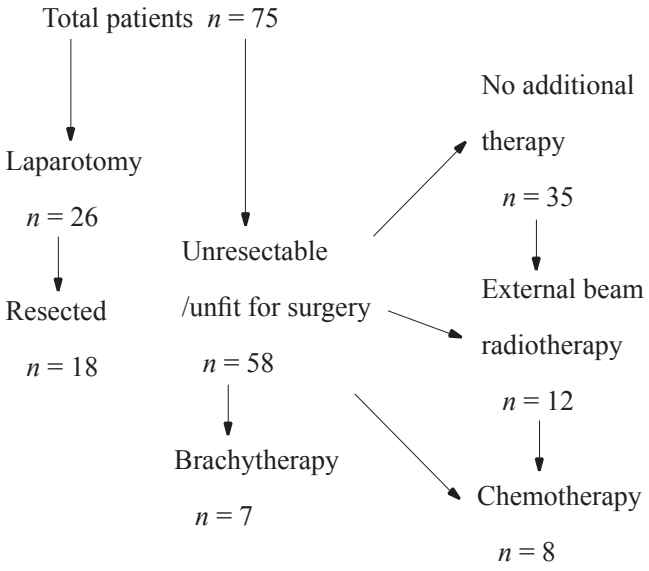

Figure 2 Flow chart showing management outcomes.

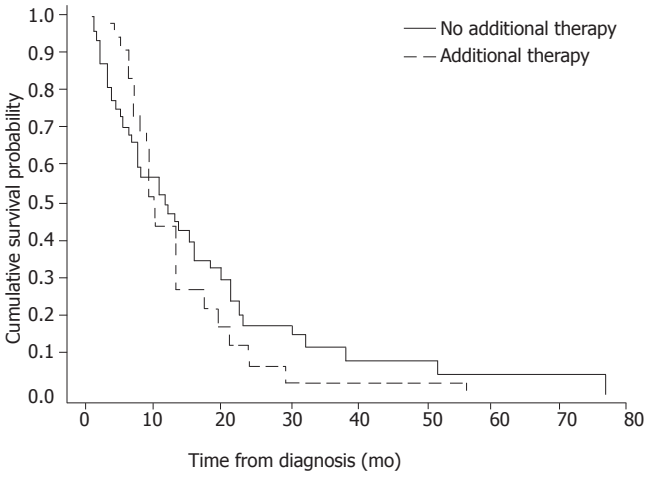

Figure 4 Kaplan-Meier survival plots for non-surgical therapeutic modalities in non-resected patients.

TNM classification is shown in Table 4. Vascular invasion was present in 9 cases (50%), perineural invasion in 13 cases (72%) and lymphatic invasion in 7 cases (39%). Patients who had node-negative resections tended to have a better survival than those who had node-positive resections (Figure 5) but this did not reach statistical significance ($P = 0.1$, log-rank test).

DISCUSSION

Our study is one of the few UK studies, documenting experienc-es in the management of hilar cholangiocarcinoma. The disease generally has a dismal prognosis; however, our findings demonstrate that an aggressive approach to the resection of these tumors results in prolonged survival. Resection is the only potentially curative treatment, and many patients do develop recurrence; however, these still benefit in terms of survival, fewer hospital admissions and decreased necessity for

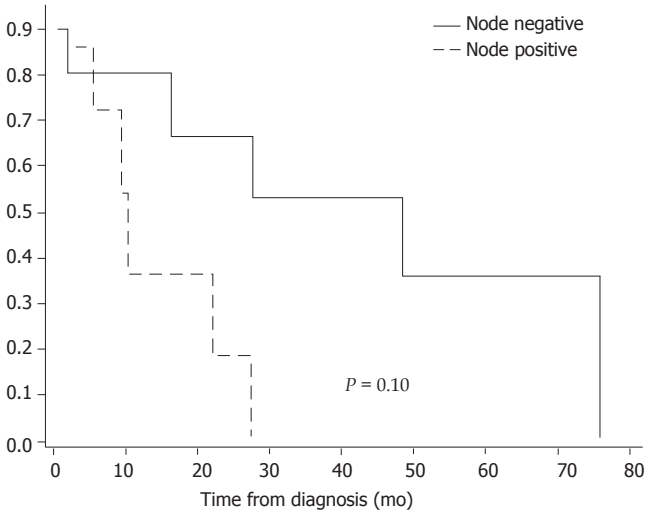

Figure 5 Kaplan-Meier survival plots for node positive and node negative resections.

Table 4 Pathological breakdown for resected cases

TNM classification	*n*
T1 N0	0
T1 N1	1
T2 N0	7
T2 N1	3
T3 N0	3
T3 N1	2
T3 N2	1
T4 N1	1

biliary drainage. Our results are comparable with several reported series of surgical resections for Klatskin tumors, with 5-year survival of 8-56%, in-hospital mortality of 6-17% and morbidity of 30-50%[2,3,6-11]. Negative resection margins have been shown to be important in prolonging survival although this could not be independently assessed in our study due to small numbers[3,8,12-14].

Major resection of a cholestatic liver is associated with an increased risk of serious complications due to impairment of liver function, including reticuloendothelial cells, mitochondrial and microsomal functions, impaired protein synthesis, wound healing and cell medicated immunity. All obstructed segments of the bile ducts in all patients undergoing preoperative assessment for surgical resection are therefore drained in our center. This facilitates not only the relief of jaundice, but also provides valuable information regarding the proximal extent of the tumor. In addition, it identifies the most common organisms isolated from the bile cultures to formulate the most appropriate perioperative antibiotic regimen.

In our study, endoscopic biliary drainage of hilar lesions had a high failure rate and almost all patients had to have subsequent percutaneous procedures in order to achieve adequate drainage. This is comparable with previously published data. Success rates for adequate endoscopic

biliary drainage for hilar tumors has been reported to be between 55% and 81%[15-18]. Even in studies supporting this modality, stent occlusion requiring further drainage procedures has been reported between 33% and 94% with morbidity of 22% and 44%[15,20]. Rerknimitr[15] describes an 81% rate for successful endoscopic drainage for Bismuth type II, III or IV tumors; however, 54% developed cholangitis and 30 of the 32 who did not undergo resection required further procedures within a mean of 47 d from initial drainage. Liu[18]describes a cohort of 55 patients undergoing endoscopic biliary drainage. Of these, only 73% had successful prosthesis insertion (16% required multiple procedures) with only 20 having satisfactory drainage. Of the 16 patients treated with palliative intent only, only 3 were successfully palliated by endoscopic means with the remainder requiring percutaneous drainage. Finally, Nomura[20]describes a significantly higher risk of cholangitis in patients treated endoscopically when compared to percutaneous drainage. Biliary obstruction due to hilar cholangiocarcinoma should therefore be ideally managed with percutaneous biliary drainage. Plastic internal-external catheters are placed initially and are then internalized. The majority of patients present with unresectable disease and in these cases, effective and reliable relief of the primary symptom - usually obstructive jaundice is paramount. For these patients also, percutaneous drainage is the method of choice. Self-expanding metallic Wallstents are preferred over plastic stents that have been shown to have longer duration of patency (6-8 mo), are more cost-effective, and are associated with a shorter hospital stay[21-23].

The use of palliative non-surgical treatment modalities conferred no benefit in our study. To date, there is no chemotherapeutic regimen that markedly improves survival in patients with advanced Klatskin tumors. Almost all phase II trials using single agents failed to demonstrate any beneficial effects with partial response rate of less than 10%[24-27]. Using combination therapy, however, the overall response rate has generally been shown to be slightly better at around 27%[28-32]. Radiotherapy may be delivered as an external beam irradiation using linear accelerator or by intraluminal brachytherapy. Trials assessing the palliative radiotherapy have generally been disappointing although a few have shown promising results. Shinchi *et al*. have shown in a retrospective review of 51 patients that external radiotherapy combined with metallic stents can offer a mean survival rate of 10.6% mo, which was significantly longer than stenting alone (4-6 mo), with a much improved quality of life[33]. Kuvshinoff *et al*. also reported similar encouraging results in 12 patients managed with intra-ductal brachytherapy and external beam radiation; the mean survival being 14.5 mo[34].

In conclusion, resection of hilar cholangiocarcinoma, when possible, increases survival although it carries the risk of significant morbidity and mortality. Percutaneous biliary drainage is almost always necessary and ERCP should be avoided. There is no evidence of benefit from chemotherapy or radiotherapy in non-resected patients, although there is data from other studies suggesting some beneficial effects.

REFERENCES

1 **Taylor-Robison SD,** Toledano MB, Arora S, Keegan TJ,Hargreaves S, Beck A, Khan SA, Elliott P, Thomas HC. Increase in mortality rates from intrahepatic cholangiocarcinoma in England and Wales 1968-1998. *Gut* 2001; **48**: 816-820

2 **Nakeeb A,** Pitt HA, Sohn TA, Coleman J, Abrams RA, Piantadosi S, Hruban RH, Lillemoe KD, Yeo CJ, Cameron JL. Cholangiocarcinoma A spectrum of intrahepatic, perihilar, and distal tumours. *Ann Surg* 1996. **224**: 463-447

3 **Burke EC,** Jarnagin WR, Hochwald SN, Pisters PW, Fong Y, Blumgart LH. Hilar Cholangiocarcinoma: patterns of spread, the importance of hepatic resection for curative operation, and a pre-surgical clinical staging system. *Ann Surg* 1998; **228**: 385-394

4 **Weinbren K,** Mutum SS. Pathological aspects of cholangiocarcinoma. *J Pathol* 1983; **139**: 217-238

5 **Chamberlain RS,** Blumgart LH. Hilar cholangiocarcinoma: a review and commentary. *Ann Surg Oncol* 2000; **7**: 55-66

6 **Lee SG,** Lee YJ, Park KM, Hwang S, Min PC. One hundred and eleven liver resections for hilar bile duct cancer. *J Hepatobiliary Pancreat Surg* 2000; **7**: 135-141

7 **Gazzaniga GM,** Filauro M, Bagarolo C, Mori L. Surgery for hilar cholangiocarcinoma: an Italian experience. *J Hepatobiliary Pancreat Surg* 2000; **7**: 122-127

8 **Pichlmayr R,** Weimann A, Ringe B. Indications for liver transplantation in hepatobiliary malignancy. *Hepatology* 1994; **20**: 33S-40S

9 **Madariaga JR,** Iwatsuki S, Todo S, Lee RG, Irish W, Starzl TE.Liver resection for hilar and peripheral cholangiocarcinomas: a study of 62 cases. *Ann Surg* 1998; **227**: 70-79

10 **Launois B, Reding R,** Lebeau G, Buard JL. Surgery for hilar cholangiocarcinoma: French experience in a collective surveyof 552 extrahepatic bile duct cancers. *J Hepatobiliary Pancreat Surg* 2000; **7**: 128-134

11 **Klempnauer J,** Ridder GJ, Werner M, Weimann A, Pichlmayr R. What constitutes long-term survival after surgery for hilar cholangiocarcinoma? *Cancer* 1997; **79**: 26-34

12 **Tabata M,** Kawarada Y, Yokoi H, Higashiguchi T, IsajiS. Surgical treatment for hilar cholangiocarcinoma. *J Hepatobiliary Pancreat Surg* 2000; **7**: 148-154

13 **Lillemoe KD,** Cameron JL. Surgery for hilar cholangiocarcinoma: the Johns Hopkins approach. *J Hepatobiliary Pancreat Surg* 2000; **7**: 115-121

14 **Tsao JI,** Nimura Y, Kamiya J, Hayakawa N, Kondo S, Nagino M, Miyachi M, Kanai M, Uesaka K, Oda K, Rossi RL, Braasch JW, Dugan JM. Management of hilar cholangiocarcinoma: comparison of an American and a Japanese experience. *Ann Surg* 2000; **232**: 166-174

15 **Rerknimitr R,** Kladcharoen N, Mahachai V, Kullavanijaya P. Result of endoscopic biliary drainage in hilar cholangiocarcinoma. *J Clin Gastroenterol* 2004; **38**: 518-523

16 **Born P,** Rosch T, Bruhl K, Sandschin W, Weigert N, Ott R,Frimberger E, Allescher HD, Hoffmann W, Neuhaus H, Classen M. Long-term outcome in patients with advanced hilar bile duct tumors undergoing palliative endoscopic or percutaneous drainage. *Z Gastroentero l* 2000; **38**: 483-489

17 **Lai EC,** Mok FP, Fan ST, Lo CM, Chu KM, Liu CL, Wong J. Preoperative endoscopic drainage for malignant obstructive jaundice *Br J Surg* 1994; **81**: 1195-1198

18 **Liu CL,** Lo CM, Lai EC, Fan ST. Endoscopic retrogra-de cholangiopancreatography and endoscopic endoprosthesis insertion in patients with Klatskin tumors. *Arch Surg* 1998; **133**: 293-296

19 **De Palma GD,** Galloro, G, Siciliano S, IovinoP, Catanzano C. Unilateral versus bilateral endoscopic hepatic duct drainage in patients with malignant hilar biliary obstruction: results of a prospective, randomized, and controlled study. *Gastrointest*

Endosc 2001; **53**: 547-553

20 **Nomura T,** Shirai Y, Hatakeyama K. Cholangitisafter endoscopic biliary drainage for hilar lesions. *Hepatogastroenterology* 1997; **44**: 1267-1270

21 **Jarngian WR,** Burke E, Powers C, Fong Y, Blumgart LH. Intrahepatic biliary enteric bypass provides effective palliation in selected patients with malignant obstruction at the hepatic duct confluence. *Am J Surg* 1998; **175**: 453-460

22 **Prat F,** Chapat O, Ducot B, Ponchon T, Pelletier G, Fritsch J, Choury AD, Buffet C. A randomized trial of endoscopic drainage methods for inoperable malignant strictures of the common bile duct. *Gastrointest Endosc* 1998; **47**: 1-7

23 **Lammer J,** Hausegger KA, Fluckiger F, Winkelbauer FW, Wildling R, Klein GE, Thurnher SA, Havelec L. Common bile duct obstruction due to malignancy: treatment with plastic versus metal stents. *Radiology* 1996; **201**: 167-172

24 **Falkson G,** MacIntyre JM, Moertel CG. Eastern CooperativeOncology Group experience with chemotherapy for inoperable gallbladder and bile duct cancer. *Cancer* 1984; **54:** 965-969

25 **Taal BG,** Audiso RA, Bleiberg H, Blijham GH, Neijt JP, Veenhof CH, Duez N, Sahmoud T. Phase II trial of mitomycin C (MMC) in advanced gallbladder and biliary tree carcinoma. An EORTC Gastrointestinal Tract Cancer CooperativeGroup Study. *Ann Oncol* 1993; **4**: 607-609

26 **Sali A,** McQuillan T, Read A, Kune G. Rifampicin as cytotoxic agent for cholangiocarcinoma: preliminary report of seven cases. *J Cancer Res Clin Oncol* 1991; **11**: 7: 503-504

27 **Jones DV Jr,** Lozano R, Hoque A, Markowitz A, Patt YZ. PhaseII study of paclitaxel therapy for unresectable biliary tree carcinomas. *J Clin Oncol* 1996; **14**: 2306-2310

28 **Ekstrom K,** Hoffman K, Linne T, Eriksson B, Glimelius B.Single-dose etoposide in advanced pancreatic and biliary cancer, a phase II study. *Oncol Rep* 1998; **5**: 931-934

29 **Ellis PA,** Hill NA, O'Brien ME, Nicolson M, Hickish T, Cunningham D. Epirubicin, Cisplatin and infusional 5-fluorouracil (5-FU) (ECF) in hepatobiliary tumour. *Eur J Cancer* 1995; **31A**: 1594-1598

30 **Kajanti M,** Pyrhonen S. Epirubicin-sequential methotrexate-5fluorouracil-leucovorin treatment in advanced cancer of the extrahepatic biliary system. A phase II sturdy. *Am J Clin Oncol* 1994; **17**: 223-226

31 **Patt YZ,** Jones DV Jr, Hoque A, Lozano R, Markowitz A, Raijman I, Lynch P, Charnsangavej C. Phase II trial of intravenous fluorouracil and subcutaneous interferon alfa-2b for biliary tract cancer. *J Clin Oncol* 1996; **14**: 2311-2315

32 **Sanz-Altamira PM,** Ferrante K, Jenkins RL, Lewis WD, Huberman MS, Stuart KE. A phase II trial of 5-fluorouracil, leucovorin, and carboplatin in patients with unresectable biliary tree carcinoma. *Cancer* 1998; **82**: 2321-2325

33 **Shinchi H,** Takao S, Nishida H, Aikou T. Length and quality of survival following external beam radiotherapy combined with expandable metallic stent for unresectable hilar cholangiocarcinoma. *J Surg Oncol* 2000; **75**: 89-94

34 **Kuvshinoff BW,** Armstrong JG, Fong Y, Schupak K, Getradjman G, Heffernan N, Blumgart LH. Palliation of irresectable hilar cholangiocarcinoma with biliary drainage and radiotherapy. *Br J Surg* 1995; **82**: 1522-1525

Science Editor Wang XL and Guo SY **Language Editor** Elsevier HK

PO Box 2345, Beijing 100023, China
www.wjgnet.com
wjg@wjgnet.com

ELSEVIER

World J Gastroenterol 2005;11(48):7631-7638
World Journal of Gastroenterology ISSN 1007-9327

• *CLINICAL RESEARCH* •

Distribution and effects of polymorphic RANTES gene alleles in HIV/HCV coinfection – A prospective cross-sectional study

Golo Ahlenstiel, Agathe Iwan, Jacob Nattermann, Karin Bueren, Jürgen K Rockstroh, Hans H Brackmann, Bernd Kupfer, Olfert Landt, Amnon Peled, Tilman Sauerbruch, Ulrich Spengler, Rainer P Woitas

Golo Ahlenstiel, Agathe Iwan, Jacob Nattermann, Karin Bueren, Jürgen K Rockstroh, Tilman Sauerbruch, Ulrich Spengler, Rainer P Woitas, Department of Internal Medicine 1, University of Bonn, 53105 Bonn, Germany
Hans H Brackmann, Institute of Experimental Hematology, University of Bonn, 53105 Bonn, Germany
Bernd Kupfer, Institute of Medical Microbiology and Immunology, University of Bonn, 53105 Bonn, Germany
Olfert Landt, TIB MOLBIOL Synthesis Laboratory, 12103 Berlin, Germany
Amnon Peled, Goldyne Savad Institute of Gene Therapy, Hadassah University Hospital, Jerusalem 91120, Israel
Correspondence to: RP Woitas, Medizinische Klinik u Poliklinik 1, Universitätsklinikum Bonn, Sigmund-Freud-Straße 25, D-53105 Bonn, Germany. rainer.woitas@ukb.uni-bonn.de
Telephone: +49-228-2875507 Fax: +49-228-287-6643
Received: 2005-04-01 Accepted: 2005-06-18

Abstract

AIM: Chemokines and their receptors are crucial for immune responses in HCV and HIV infection. RANTES gene polymorphisms lead to altered gene expression and influence the natural course of HIV infection. Therefore, these mutations may also affect the course of HIV/HCV coinfection.

METHODS: We determined allele frequencies of RANTES-403 (G→A), RANTES-28 (C→G) and RANTES-IN1.1 (T→C) polymorphisms using real-time PCR and hybridization probes in patients with HIV (n = 85), HCV (n = 112), HIV/HCV coinfection (n = 121), and 109 healthy controls. Furthermore, HIV and HCV loads as well as CD4+ and CD8+ cell counts were compared between different RANTES genotypes.

RESULTS: Frequencies of RANTES-403 A, RANTES-28 G and RANTES-IN1.1 C alleles were higher in HIV infected patients than in healthy controls (-403: 28.2% *vs* 15.1%, P = 0.002; -28: 5.4% *vs* 2.8%, not significant; IN1.1: 19.0% *vs* 11.0%, P = 0.038). In HIV/HCV coinfected patients, these RANTES alleles were less frequent than in patients with HIV infection alone (15.4% P = 0.002; 1.7%; P = 0.048; 12.0%; not significant). Frequencies of these alleles were not significantly different between HIV/HCV positive patients, HCV positive patients and healthy controls.

CONCLUSION: All three RANTES polymorphisms showed increased frequencies of the variant allele exclusively in patients with HIV monoinfection. The finding that the frequencies of these alleles remained unaltered in HIV/HCV coinfected patients suggests that HCV coinfection interferes with selection processes associated with these alleles in HIV infection.

Key words: RANTES polymorphism; HIV/HCV-coinfection; HCV

Ahlenstiel G, Iwan A, Nattermann J, Bueren K, Rockstroh JK, Brackmann HH, Kupfer B, Landt O, Peled A, Sauerbruch T, Spengler U, Woitas RP. Distribution and effects of polymorphic RANTES gene alleles in HIV/HCV coinfection – A prospective cross-sectional study. *World J Gastroenterol* 2005; 11(48): 7631-7638
http://www.wjgnet.com/1007-9327/11/7631.asp

INTRODUCTION

Coinfection with human immunodeficiency virus (HIV) and hepatitis C virus (HCV) is common among certain risk groups such as hemophiliacs and intravenous drug abusers (IVDA)[1]. Unfortunately, HIV/HCV coinfection is associated with an accelerated course of HCV infection leading to progressive liver disease, cirrhosis, and hepatic failure[2,3].

Chemokines and their receptors play a central role in HIV infection. During the initial steps of viral infection chemokine receptors, such as the chemokine receptor 5 (CCR5), are used as co-receptors by HIV to enter monocytes and CD4 positive T-helper cells. A mutation in the encoding region of CCR5, CCR5-△32, abrogates HIV cell entry of m-tropic HIV strains, and thus prevents HIV infection in CCR5-△32 homozygous patients[4]. Heterozygosity for the CCR5-△32 mutation is associated with delayed progression of HIV infection to AIDS[4]. Recently, we have reported that the CCR5-△32 mutation was more prevalent in hemophiliac patients with chronic hepatitis C virus infection and was associated with increased hepatitis C viral loads[5]. A study on liver biopsies of patients with chronic hepatitis C revealed that this mutation may be associated with reduced portal inflammation and fibrosis[6]. Furthermore, we have found epidemiological evidence that the CCR5-△32 mutation is a predictor of treatment failure in interferon-α monotherapy

of chronic HCV infection, possibly indicating that the CCR5 receptor may also play an important role in the immune response to HCV infection[7].

The natural ligands of CCR5 are the chemokines RANTES (regulated on activation normal T cell expressed and secreted; CCL5), MIP-1α (macrophage inhibitory protein-1α; CCL3) and MIP-1β (macrophage inhibitory protein-1β; CCL4), all of which are potent inhibitors of HIV-1 cell entry[8]. Importantly, RANTES blocks the CCR5 receptor via receptor binding and down-regulation of CCR5 on T cells and macrophages. Furthermore, RANTES was reported to be critically involved in the recruitment of T cells to the liver[9]. Several single nucleotide polymorphisms in the RANTES gene have been reported to influence the natural course of HIV infection by up- or down-regulating RANTES gene activity. The most frequent of those polymorphic sites comprise RANTES-403 (G→A) and RANTES-28 (C→G) in the promoter region and RANTES-IN1.1 (T→C) in the first intron region[10,11]. Both promoter polymorphisms increase RANTES transcription and may delay HIV disease progression[11,12]. Conversely, the RANTES-IN1.1 C allele seems to decrease RANTES transcriptional activity and is probably associated with an increased risk for HIV infection and progression to AIDS[10].

Since RANTES seems to be involved in the pathogenesis of both HIV and HCV infection, we studied the effects of the RANTES gene polymorphisms in patients with HIV/HCV coinfection as compared to patients with HIV infection. To exclude that HCV infection or allele frequency in the background population contributed to our results we also included patients with HCV monoinfection as well as a group of healthy blood donors into the study.

MATERIALS AND METHODS

Design and study populations

All anti-HCV or anti-HIV positive patients of Caucasian descent attending our outpatient department between May 1999 and August 2000 were enrolled into one of the three study groups (HCV monoinfection = group I, HIV monoinfection = group II, HIV/HCV double infection = group III). None of the anti-HCV positive and anti-HIV/HCV positive patients had received interferon therapy at the time of the study. Type and duration of antiretroviral therapy and risk factors for infection were recorded in groups II and III. One hundred and nine healthy Caucasian blood donors of the Bonn University transfusion center (females 37, males 72, median age 27 years, range: 12-58 years) served as a reference group. In this reference group, HIV and HCV infection had been excluded by serology and PCR.

EDTA blood samples were obtained from each patient for genotyping of RANTES-403, -28 and -IN1.1 alleles. HCV genotype, HCV, and HIV viral loads, aminotransferase serum levels, CD4+ and CD8+ cell counts were determined in HIV, HCV, and HIV/HCV coinfected patients, respectively.

Serum aminotransferase levels were determined by routine biochemical procedures. Serologic markers of hepatitis B virus infection (HBs antigen, anti-HBs, and anti-HBc) were assessed by commercially available assays according to the manufacturer's instructions (Abbott, Wiesbaden, Germany). CD4 and CD8 cell counts were analyzed on a FACSort™ (Becton Dickinson, Heidelberg, Germany) flow cytometer using the Simulset™ test kit (Becton Dickinson, Heidelberg, Germany). The study conformed to the ethical guidelines of the Helsinki declaration as approved by the local ethics committee.

Diagnosis of HIV infection

Serum samples were analyzed for anti-HIV antibodies and p24 antigen with commercially available test kits (Abbott, Wiesbaden and Coulter, Hamburg, Germany) according to the manufacturer's instructions. A positive ELISA result was confirmed by immunoblot (Biorad, Munich, Germany).

HIV DNA was amplified from peripheral blood leukocytes by nested PCR according to Saiki *et al*.[13]. Amplification of the HIV-1 proviral DNA was carried out as nested PCR with the following primers for the first PCR (sense: 5-ATTTGTCATCCATCCTATTTGTTCCTGAA GGGT-3, antisense: 5-AGTGGGGGGGACATCAAGC AGCCATGCAAAT-3) and with the following primers for the second PCR (sense: 5-TGCTATGTCACTTCCCCTT GGTTCTCT-3, antisense: 5-GAGACTATCAATGAGGA AGCTGCAGAATGGGAT-3). The amplified product was detected by agarose gel electrophoresis.

HIV load was determined quantitatively using the NucliSens HIV-QT assay (Organon Teknika, Boxtel, the Netherlands). Amplified patient and calibrator RNA were quantified with different electrochemiluminescent probes in the NASBA QR system (Organon Teknika, Boxtel, the Netherlands) based on competitive internal linear standard curves[14]. This assay had a detection limit of 80 copies/mL.

Diagnosis of HCV infection

HCV antibodies were detected with a microparticle enzyme immunoassay (MEIA, Axsym, Abbott, Wiesbaden, Germany). Positive results were confirmed by dot immunoassay (Matrix, Abbott, Wiesbaden, Germany). HCV RNA was detected after nucleic acid purification kit (Viral Kit, Qiagen, Hilden, Germany) followed by reverse transcription and nested polymerase chain reaction as described elsewhere[15]. The detection limit was 100 copies/mL. Quantitative determination of HCV load was done via branched DNA technology (Quantiplex HCV RNA 2.0 assay, Chiron, Emeryville, CA, USA), which has good linearity for all genotypes above its detection limit of 200 000 copies/mL serum. HCV genotypes were determined by the Innolipa II line probe assay (Innogenetics, Zwijndrecht, Belgium) according to the manufacturer's instructions.

Genotyping of the RANTES-403, -IN1.1, and -28 single nucleotide polymorphisms

Genomic DNA was extracted from 200 μL EDTA-

treated blood samples using the QIAamp Blood Mini Kit (Qiagen, Hilden, Germany) according to the manufacturer's protocol.

Light Cycler PCR and hybridization probes: RANTES genotyping was performed using lightcycler and "fluorescence resonance energy transfer" (FRET) technology[16,17]. For amplification 2 μL light cycler-DNA master hybridization probes (Roche Diagnostics, Mannheim, Germany), 2 μL $MgCl_2$ (25 mmol/L), 8 μL PCR-grade water were used. For genotyping of the amplified DNA, 4 pmol of each hybridization probe (TIB MolBiol, Germany) was added to the reaction mixture. Sequences of oligonucleotide primers and hybridization probes for RANTES-403 were: sense *CACCTCCTTTGGGGACTGTA* and antisense *CCTCCGGAAATTCGAGTCTC*, anchor *GAGTCACTG AGTCTTCAAAGTTCCTGCTTA-F* and sensor *LC640-CATTACAgATCTTACCTCCTTTCCp*. The sensor hybridization probe was specific for the RANTES-403G allele at a melting temperature of 62.5 ℃.

Sequences of oligonucleotide primers and hybridization probes for RANTES-28 were: sense *CACCTCCTTTGGGGACTgTA* and antisense *TGGGATGGGGTAGGCATTCTA*, anchor probe *GTTGCTATTTTGGAAACTCCCCTTAGG-F* and sensor probe *LC705-ATGCCCCTGAACTGGCCp*. The sensor hybridization probe was specific for the RANTES-28G allele at a melting temperature of 60.0 ℃. Sequences of oligonucleotide primers and hybridization probes for RANTES-IN1.1 were: sense *CCTGGTCTTGACCACCACA* and antisense *GCTGACAGGCATGAGTCAGA*, anchor probe *LC640-CCCTCAAGGCCTACAGGTGTTCACp* and sensor probe *TCAGTTTTTCTGTCTTCAAGTCTAC-F*. The sensor probe was specific for the C allele at a melting temperature of 65 ℃.

An initial denaturation step at 95 ℃ (60 s, ramp rate 20 ℃/s) was followed by amplification for 40 cycles of denaturation (95 ℃, 0 s, ramp rate 20 ℃/s), annealing (63 ℃, 10 s, ramp rate 20 ℃/s) and extension (72 ℃, 15 s, ramp rate 20 ℃/s). For RANTES-IN1.1, the annealing temperature was lowered to 55 ℃. After DNA amplification a melting curve was generated at 95 ℃ (5 s, ramp rate 20 ℃/s) followed by 45 ℃ (15 s, ramp rate 20 ℃/s) and 75 ℃ (0 s, ramp rate 0.1 ℃/s, acquisition mode: continuous) for RANTES-403 and RANTES-IN1.1 and 95 ℃, 35 ℃, and 70 ℃ for RANTES-28. After a final cooling step for 30 s at 40 ℃ melting curve analysis could be performed. Representative genotyping results are given in Figures 1A-C.

Statistical analysis

RANTES genotypes and allele frequencies were compared to the healthy reference population via contingency tables using χ^2 statistics and Fisher's exact test where appropriate. Based on gene frequencies, the expected phenotype frequencies were calculated according to the Hardy–Weinberg equation and compared to the observed frequencies using χ^2statistics[18]. Haplotype analysis for combined RANTES-403 and -28 genotypes as in Table 3 was performed according to Gonzalez *et al*.[19]. In each group, different genotypes of each RANTES polymorphism were compared with respect to HIV and HCV loads, CD4+ and CD8+ cell counts using parametric (unifactorial ANOVA with Bonferroni's correction) or non-parametric statistical analysis as appropriate (Kruskal-Wallis test followed by the Mann-Whitney test for pairwise comparison of the groups), if the number of patients with the particular genotype exceeded five. Results are given as median and range unless indicated otherwise.

In all statistical tests, $P<0.05$ were regarded as significant. All calculations were performed on a personal computer with SPSS 11.0 software (SPSS, Chicago, IL, USA).

RESULTS

Patient groups

One hundred and twelve anti-HCV positive, 85 anti-HIV positive, and 121 anti-HIV/HCV double-positive Caucasian patients were recruited into this study. The characteristics of these patient groups are summarized in Table 1. Hemophilia was the major risk factor for infection in HCV and HIV/HCV coinfected patients, whereas sexual transmission was the main risk factor in HIV infected patients. Rates of persistent HBs antigenemia was low in each study group (<5%), although the high prevalence of anti-HBc antibodies in the anti-HCV and the double infected groups indicated significant exposure to HBV (Table 1).

Distribution of RANTES-403, -28, and -IN1.1 genotypes

The distribution of RANTES-403, -28, and -IN1.1 alleles is shown in Table 2. The RANTES-403 A, RANTES-28 G, and RANTES-IN1.1 C alleles were more frequent in HIV monoinfected patients than in healthy controls as has been previously described[10]. The distribution of RANTES-403 genotypes in HIV infected patients differed significantly from controls ($P = 0.004$), whereas the RANTES-28 and RANTES-IN1.1 genotypes did not differ between the groups.

Unexpectedly, these higher frequencies of distinct RANTES alleles and genotypes were not observed in patients with HIV/HCV coinfection. RANTES-403 A, RANTES-28 G, and RANTES-IN1.1 C alleles were significantly less frequent than in HIV monoinfected patients ($P = 0.002$; $P = 0.048$; not significant). In contrast, the frequencies of the different RANTES alleles did not differ between HIV/HCV coinfected and HCV infected patients or healthy controls. This also held true for RANTES-403, -28, and IN1.1 genotype distribution ($P = 0.005$; $P = 0.045$; not significant). There was no deviation from the Hardy-Weinberg equilibrium in any of the groups.

Interestingly, the frequency of the combined RANTES wildtype (-403 G/G; -28 C/C; IN1.1 T/T) was lowest in HIV infected patients (49.4%) compared to healthy

Table 1 Patient Characteristics [data given as number (%) or median (range)]

	HCV-infection (Group I)	HIV-infection (Group II)	HCV/HIV-coinfection (Group III)	Statistical significance
Number	112	85	121	
Sex (Male / female)	108 / 4	73 / 12	117 / 4	Group I *vs* II $P = 0.009$*; group II *vs* III $P = 0.007$*
Age (median, range)	39 (13 - 77)	38 (23 - 70)	37 (21 - 62)	
Risk factors (%)				
Sexual	- - -	62 (72.9)	1 (0.8)	Group I *vs* II and II *vs* III $P < 0.001$*
Endemic	- - -	5 (5.9)	- - -	Group I *vs* II $P = 0.009$*; group II *vs* III $P = 0.011$*
I.V. drugs	- - -	4 (4.7)	3 (2.4)	Group I *vs* II $P = 0.023$*
Blood transfusion	- - -	1 (1.2)	- - -	
Hemophilia	110 (98.2)	- - -	115 (95.0)	Group I *vs* II $P < 0.001$*; group II *vs* III $P < 0.001$*
Unknown	2 (1.8)	13 (15.3)	2 (1.7)	Group I *vs* II $P < 0.001$*; group II *vs* III $P < 0.001$*
Aminotransferase activities				
ALT U/L (median, range)	34.0 (5.2 - 226.0)	17.0 (7.0 - 84.0)	38.5 (1.0 - 214.0)	Group I *vs* II and II *vs* III $P < 0.001$
AST U/L (median, range)	19.0 (5.8 - 157.0)	12.0 (4.3 - 106.0)	26.1 (7.8 - 168.0)	Group I *vs* II $P = 0.002$; group I *vs* III $P = 0.030$; Group II *vs* III $P < 0.001$
GGT U/L (median, range)	25.2 (5.2 - 350.9)	17.0 (6.2 - 149.0)	42.0 (2.9 - 254.6)	Group II *vs* III $P < 0.001$
HIV-status				
CD4 count (median, range)	668 (171 - 2 039)/μL	350 (5 - 1 142)/μL	292.5 (6 - 1 219)/μL	Group I *vs* II and I *vs* III $P < 0.001$
CD8 count (median, range)	499 (62 - 1 653)/μL	931 (88 - 2 152)/μL	804 (39 - 3 056)/μL	Group I *vs* II and I *vs* III $P < 0.001$
HIV load (median, range)	- - -	300 (<80 - 830 000)	725 (<80 - 210,000)	
HIV-viremia < 80 copies/mL	- - -	47 (55.3%)	80 (66.1%)	
Type of antiretroviral Therapy (%)				
Protease inhibitor-based HAART	- - -	62 (72.9)	58 (47.9)	Group II *vs* III $P = 0.001$
NNRTI-based HAART	- - -	11 (12.9)	25 (20.7)	
Total	- - -	73 (85.9)	83 (68.6)	Group II *vs* III $P = 0.007$
HCV-status				
HCV load (copies/mL)	8 888 000 (n.d.-126,500,000)	- - -	13 535 000 (n.d.-178 900 000)	Group I *vs* III $P = 0.012$
HCV load (IU/mL)	1 410 794 (n.d.-20,079,365)	- - -	2 148 413 (n.d.-28 396 825)	
HCV-genotypes (%)				
Genotype 1	70 (62.5)	- - -	76 (62.8)	
Genotype 2	14 (12.5)	- - -	11 (9.1)	
Genotype 3	8 (7.1)	- - -	21 (17.4)	Goups I *vs* III $P = 0.028$*
Genotype 4	6 (5.4)	- - -	5 (4.1)	
Multiple genotypes	1 (0.9)	- - -	1 (0.8)	
Undeterminded genotype	13 (11.6)	- - -	7 (5.8)	
HBV-status (%)				
Anti-HBs+ and anti-HBc+	52 (46.4)	15 (17.6)	43 (35.5)	Group I *vs* II $P < 0.001$; group II *vs* III $P = 0.008$
Anti-HBc+ alone	10 (8.9)	5 (5.9)	34 (28.1)	Group I *vs* III $P < 0.001$; group II *vs* III $P < 0.001$*
HBs-Ag+	1 (0.9)	3 (3.5)	6 (5.0)	

* Fisher´s exact test; n.d. = not detected.

controls (69.9%; $P = 0.007$), but also compared to HCV (63.4%; not significant) and HIV/HCV coinfected patients (70.4%; $P = 0.004$). The [-403 G/A; -28 C/G; IN1.1 T/C] combination genotype had the highest prevalence in HIV infected patients (9.6%) differing significantly from HCV (0.9%; $P = 0.005$) and HIV/HCV coinfected patients (1.7%; $P = 0.015$) as well as controls (4.9%; not significant).

When haplotype analysis for RANTES promoter polymorphisms was performed as described previously by Gonzalez *et al*.[19], the RANTES high producer haplotype (-403A, -28G) was most frequent in HIV monoinfected patients, whereas in HIV/HCV coinfected patients the frequency of this haplotype was similar in HCV infected patients and healthy controls (Table 3). The same finding also applies when the frequency of the (-403A, -28G) haplotype was compared between HIV and HIV/HCV infected patients ($P = 0.006$), between HIV and HCV infected patients ($P = 0.002$) and between HIV infected patients and controls ($P = 0.019$).

Effects of the RANTES-403, -28 and -IN1.1 mutations on parameters of HIV and HCV infection

HCV and HIV viral loads as well as the numbers of CD4+ and CD8+ cell counts are given in Table 4 stratified according to RANTES genotypes. There was a trend towards higher HIV loads in HIV infected patients with the RANTES-403 G/G genotype (wildtype) compared to subjects with the G/A and A/A genotype. Furthermore, HIV infected patients with the RANTES-28 C/G genotype tended to have lower HIV loads than patients with the C/C genotype (wildtype), whereas the RANTES-IN1.1 polymorphism did not affect HIV or HCV viral loads. However, statistical analysis could not be performed for RANTES-403 A/A and RANTES-IN1.1 C/C genotypes in HCV and HCV/HIV coinfection, because these genotypes were rare in each of the groups. CD4+ and CD8+ cell counts were not affected by any of the different RANTES genotypes. Finally, HIV and HCV viral loads did not differ significantly between the different haplotypes (Figure 1).

Table 2 Distribution of RANTES-403, RANTES-28 and RANTES IN1.1 genotypes and allele frequencies

RANTES-403 (%)	G/G	G/A	A/A	Statistics	[A]-allele frequency (%)	Statistics
HCV (n = 112)	71 (63.4)	39 (34.8)	2 (1.8)	*vs* HIV P = 0.077	19.2	*vs* HIV P = 0.047
HIV (n = 85)	42 (49.4)	38 (44.7)	5 (5.9)		28.2	
HCV/HIV (n = 120)	86 (71.7)	31 (25.8)	3 (2.5)	*vs* HIV P = 0.005	15.4	*vs* HIV P = 0.002
Controls (n = 109)	77 (70.6)	31 (28.4)	1 (0.9)	*vs* HIV P = 0.004	15.1	*vs* HIV P = 0.002
RANTES-28 (%)	**C/C**	**C/G**	**G/G**	**Statistics**	**[G]-allele frequency**	**Statistics**
HCV (n = 112)	108 (96.4)	4 (3.6)	0 (0.0)	*vs* HIV P = 0.078	1.8	*vs* HIV P = 0.083
HIV (n = 83)	74 (89.2)	9 (10.8)	0 (0.0)		5.4	
HCV/HIV (n = 116)	112 (96.6)	4 (3.4)	0 (0.0)	*vs* HIV P = 0.045	1.7	*vs* HIV P = 0.048
Controls (n = 109)	103 (94.5)	6 (5.5)	0 (0.0)	*vs* HIV P = 0.186	2.8	*vs* HIV P = 0.195
RANTES-In1.1 (%)	**T/T**	**T/C**	**C/C**	**Statistics**	**[C]-allele frequency**	**Statistics**
HCV (n = 112)	87 (77.7)	25 (22.3)	0 (0.0)	*vs* HIV P = 0.054	12.6	*vs* HIV P = 0.041
HIV (n = 84)	53 (63.1)	30 (35.7)	1 (1.2)		19	
HCV/HIV (n = 121)	93 (76.9)	27 (22.3)	1 (0.8)	*vs* HIV P = 0.101	12	*vs* HIV P = 0.066
Controls (n = 109)	86 (78.9)	22 (20.2)	1 (0.9)	*vs* HIV P = 0.052	11	*vs* HIV P = 0.038

Table 3 Distribution of RANTES-403/-28 haplotypes

Haplotype 403	28	HIV	HIV/HCV	HCV	Controls
G	C	71.7%	84.0%	80.8%	84.2%
A	G	5.4%	1.3%	1.8%	2.9%
A	C	22.9%	14.2%	17.4%	12.9%
G	G	- - -	0.5%	- - -	- - -

Haplotype pair (-403/-28)		HIV[1,2,3]	HIV/HCV	HCV	Controls
G/C	G/C	41 (49.4%)	82 (70.7%)	71 (63.4%)	73 (69.5%)
G/C	G/G	- - -	1 (0.9%)	- - -	- - -
G/C	A/C	28 (33.7%)	28 (24.1%)	37 (33.0%)	25 (23.8%)
G/C	A/G	9 (10.8%)	2 (1.7%)	2 (1.8%)	6 (5.7%)
A/C	A/C	5 (6.0%)	2 (1.7%)	- - -	1 (1.0%)
A/C	A/G	- - -	1 (0.9%)	2 (1.8%)	- - -

[1] *vs* HIV P = 0.002; [2] *vs* HIV/HCV P = 0.006; [3] *vs* controls P = 0.019.

DISCUSSION

RANTES polymorphisms have been proposed to modify susceptibility to HIV infection and progression to AIDS[10,11,19]. In this study, the prevalence of all three polymorphic RANTES alleles (RANTES-403 A, RANTES-28 G, and RANTES-IN1.1 C) was higher in HIV monoinfected patients compared to healthy blood donors. In contrast, in HIV/HCV coinfection the frequency of the studied RANTES alleles did not differ from HCV monoinfection or healthy controls. Since we included patients with HCV monoinfection as well as a cohort of healthy blood donors into the study to exclude biased results as a consequence of HCV infection or allele frequency of the background population, the influence of RANTES alleles on HIV infection seems to be neutralized by concomitant HCV infection.

The increased frequency of distinct polymorphic RANTES alleles in HIV infection is in line with McDermott *et al*., who observed increased susceptibility to HIV infection in patients with RANTES-403 G/A -28 C/C haplotypes[20]. The prevalence of the RANTES-28 G allele in all groups was as low as previously described by An *et al*.[10], and none of our patients was homozygous for the RANTES-28 G allele[11].

The RANTES-IN1.1 C allele has been reported to be associated with an increased susceptibility for infection with HIV, which would explain the significantly increased frequency of the C allele in our HIV monoinfected patients[10]. However, none of the different RANTES alleles was significantly associated with altered HIV viral loads or CD4+ cells counts. In this context, we cannot rule out that we have missed an association between viral loads or CD4 counts and the polymorphic RANTES alleles, because our study group was rather small and not well balanced for antiviral therapy. To exclude that the presence of the CCR5-△32 allele which probably also affects susceptibility to HCV infection has influenced our findings, we tested whether any of the RANTES polymorphisms was associated or in linkage disequilibirum with CCR5-△32[5]. However, we could not find any associations between CCR5-△32 and the RANTES alleles.

The low frequency of the RANTES alleles -403A and -28G in our HCV infected patients is in accordance with Promrat *et al*., who also could not find any association of RANTES-403 and –28 polymorphisms with susceptibility to HCV infection or laboratory parameters of chronic

Table 4 Viral loads and immunological data in different RANTES-403, RANTES-28 and RANTES-IN1.1 genoytpes. Data are given as [median (range)]. Statistically significant differences are indicated by index numbers

	HCV-Infection			HIV-Infection			HIV/HCV-Infection		
RANTES-403	G/G	G/A	A/A	G/G	G/A	A/A	G/G	G/A	A/A
	(*N* = 71)	(*N* = 39)	(*N*= 2)	(*N*= 42)	(*N* = 38)	(*N* = 5)	(*N* = 86)	(*N* = 31)	(*N* = 3)
HCV-Load	10.8	4.2	39.0	- - -	- - -	- - -	13.8	14.0	1.6
x 10^6 copies/mL	(n.d.-126.5)	(n.d.-56.6)	(n.d.-39.8)				(0.2-178.9)	(0.6-150.5)	(0.4-6.8)
HIV-Load	- - -	- - -	- - -	455	380	<80	550	770	9900
x 10^3 copies/mL				(<80-830 000)	(<80-50 000)	(<80-990)	(<80-210 000)	(<80-50 000)	(2 400-27 000)
CD4 count	683	621	916	353.5	348.5	300	302	279	293
cells/μL	(171-2 039)	(282-1 544)	(787-1 045)	(51-1 111)	(5-1 142)	(28-629)	(6-1 219)	(106-651)	(149-331)
CD8 count	496.5	499	581.5	918.5	927	1 099	792	968.5	675
cells/μL	(62-1 653)	(185-1 183)	(425-738)	(202-1 717)	(88-2 152)	(382-1 421)	(39-2 466)	(319-3 056)	(465-895)
RANTES-28	C/C	C/G	G/G	C/C	C/G	G/G	C/C	C/G	G/G
	(*N* = 108)	(*N* = 4)	(*N* = 0)	(*N* = 74)	(*N* = 9)	(*N* = 0)	(*N* = 112)	(*N* = 4)	(*N* = 0)
HCV-Load	8.4	38.3	- - -	- - -	- - -	- - -	13.5	22.3	- - -
x 10^6 copies/mL	(n.d.-126.5)	(29.9-39.8)					(0.2-178.9)	(0.4-45.8)	
HIV-Load	- - -	- - -	- - -	310	<80	- - -	560	2 150	- - -
x 10^3 copies/mL				(<80-830 000)	(<80-3 700)		(<80-210 000)	(400-91 000)	
CD4 count	662	916	- - -	355	330	- - -	293	220	- - -
cells/μL	(171-2 039)	(443-1 305)		(10-1 142)	(141-637)		(13-1 219)	(149-651)	
CD8 count	499	581.5	- - -	942.5	636	- - -	828	602.5	- - -
cells/μL	(62-1 653)	(338-739)		(202-2 152)	(362-1 997)		(39-3 056)	(397-2 401)	
RANTES-IN1.1	T/T	T/C	C/C	T/T	T/C	C/C	T/T	T/C	C/C
	(*N* = 87)	(*N* = 25)	(*N* = 0)	(*N* = 53)	(*N* = 30)	(*N* = 1)	(*N* = 93)	(*N* = 27)	(*N* = 1)
HCV-Load	9.6	6.2	- - -	- - -	- - -	- - -	13.5	14.2	1.6
x 10^6 copies/mL	(n.d.-126.5)	(0.4-56.6)					(0.2-178.9)	(0.4-150.5)	
HIV-Load	- - -	- - -	- - -	600	<80	990	735	560	9 900
x 10^3 copies/mL				(<80-830 000)	(<80-38 000)		(<80-210 000)	(<80-91 000)	
CD4 count	662	702	- - -	353	342	629	294	242	331
cells/μL	(171-2 039)	(392-1 305)		(51-1 142)	(10-1 028)		(6-1 219)	(110-651)	
CD8 count	501	497	- - -	936.5	927	1 421	792	1 034	675
cells/μL	(62-1 653)	(191-1 119)		(202-1 717)	(362-2 152)		(39-2 466)	(319-3 056)	

n.d. = not detectable

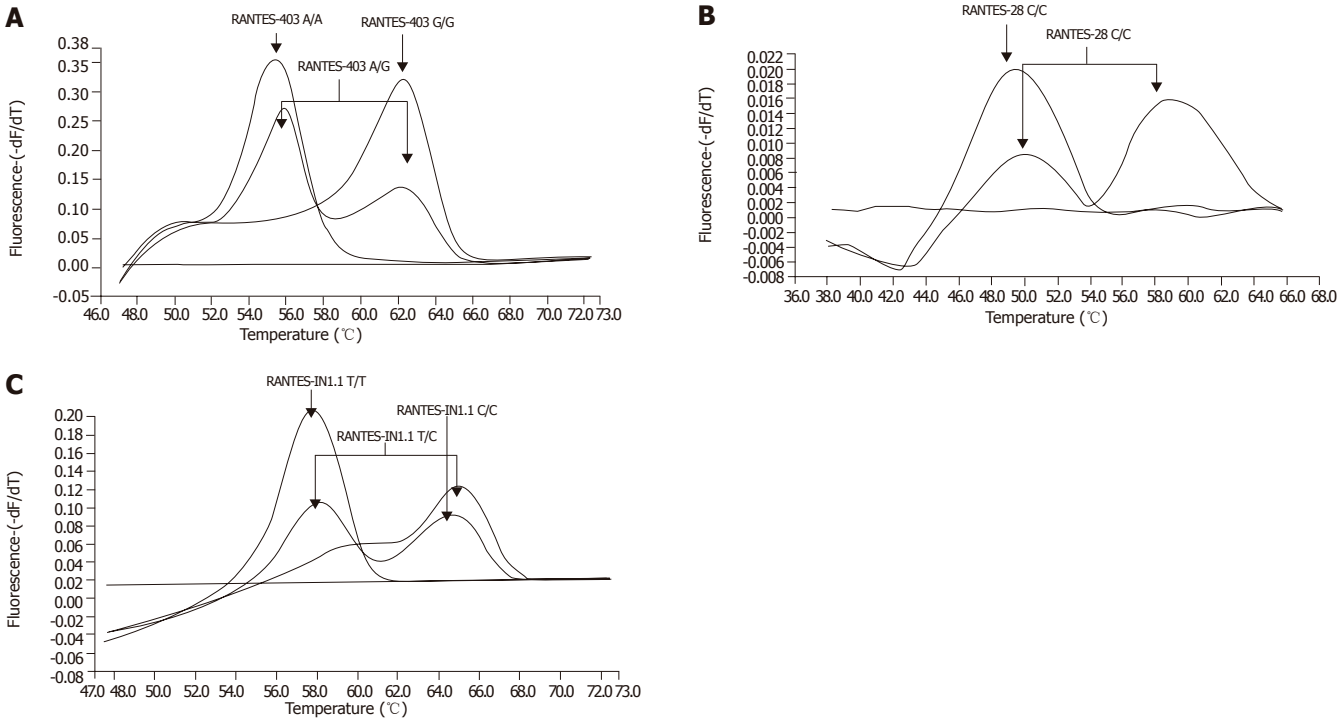

Figure 1 Shows the melting curve analysis (first order derivate) for different genotypes of the RANTES-403 (**A**), RANTES-28 (**B**), and RANTES-IN1.1 (**C**) polymorphisms. When the PCR product is melted, the probe-DNA binding will break up at a hybridization probe-specific temperature, which causes a loss in emitted fluorescence energy. This can be seen as a peak in the first order derivate of the melting curve. As the sensor probe is specific for only one of the two possible alleles in each PCR, binding of the probe to the other allele will cause a mismatch and therefore a weaker coupling and disengagement of probe and DNA at lower temperatures.

hepatitis C[21]. In contrast, Hellier *et al*. reported the RANTES-403 A/A genotype to be associated with mild portal inflammation[6]. However, the frequency of the A/A genotype in the study of Hellier (1.9%) was not different from the frequency in our patients[6]. Therefore, it was unexpected that the prevalence of RANTES alleles known to be increased in patients with HIV monoinfection was significantly lower in our HIV/HCV coinfected patients. Additionally, prevalence of these alleles was similar to HCV monoinfected patients and controls.

Several explanations may account for these divergent results: First, none of the studies so far was controlled for differences in transmission routes. Therefore, it is unclear whether disease modifying effects of the RANTES polymorphisms are equally operative in patients with sexual transmission *vs* parenteral transmission.

Alternatively, our patients with HIV/HCV coinfection could represent long time survivors: The RANTES-IN1.1 C allele has been described to be associated with rapid progression to AIDS, whereas both the RANTES-403 A and the RANTES-28 G allele have been reported to delay HIV disease progression[10,11,19]. However, frequency of these polymorphic RANTES alleles did not differ from our background population. Finally, differences in genotype and allele frequencies between HIV and HIV/HCV coinfected patients might reflect differences in the physiological roles of the single polymorphisms. RANTES-403 A and RANTES-28 G alleles have been shown to up-regulate RANTES transcription, whereas RANTES-IN1.1 C has been reported to be associated with the down-regulation of RANTES promoter activity[10-12]. Thus, RANTES expression should be characterized in terms of haplotypes, defined by the combination of the various alleles, giving the possibility to explain selection effects on the course of HIV infection[10]. However, only haplotypes AC and AG were more prevalent in patients with HIV infection, whereas their frequencies in patients with HCV and HIV/HCV coinfection were identical to the healthy background population.

The selection effect of the RANTES alleles in HIV infection may be lost in patients with HCV coinfection, because interactions of HCV-specific proteins such as core and NS5A may interact with host genes to augment RANTES promotor activity[22]. Binding of the HCV-specific protein E2 to CD81 is associated with increased RANTES serum levels resulting in CCR5 internalization[23]. Therefore, HCV infection is likely to trigger increased RANTES serum levels, which in turn decrease CCR5 expression on the cell surface due to receptor internalization. This hypothesis is further supported by a recent study that shows reduced CCR1 and CCR5 surface expression on peripheral blood cells in chronic HCV infection[24]. Thus, it is intriguing to speculate that the effects of RANTES polymorphisms on RANTES expression in HIV infection are abrogated in HIV/HCV coinfection due to induction of RANTES by HCV-specific proteins. In line with this assumption, we observed reduced frequencies of patients carrying the putatively up-regulating (RANTES-403 and RANTES-28) as well as down-regulating RANTES polymorphisms (RANTES-IN1.1) in our patients with HCV and HIV/HCV coinfection.

In summary, deviations in polymorphic RANTES allele frequencies seen in HIV infection could not be confirmed in HIV/HCV coinfection. Functional studies will be required to further analyze the differences in RANTES regulation between HIV and HIV/HCV coinfection at a molecular level.

REFERENCES

1 **Rockstroh JK**, Spengler U. HIV and hepatitis C virus co-infection. *Lancet Infect Dis* 2004; **4:** 437-444

2 **Soto B**, Sanchez-Quijano A, Rodrigo L, del Olmo JA, Garcia-Bengoechea M, Hernandez-Quero J, Rey C, Abad MA, Rodriguez M, Sales Gilabert M, Gonzalez F, Miron P, Caruz A, Relimpio F, Torronteras R, Leal M, Lissen E. Human immunodeficiency virus infection modifies the natural history of chronic parenterally-acquired hepatitis C with an unusually rapid progression to cirrhosis. *J Hepatol* 1997; **26:** 1-5

3 **Telfer P**, Sabin C, Devereux H, Scott F, Dusheiko G, Lee C. The progression of HCV-associated liver disease in a cohort of haemophilic patients. *Br J Haematol* 1994; **87:** 555-561

4 **Dean M**, Carrington M, Winkler C, Huttley GA, Smith MW, Allikmets R, Goedert JJ, Buchbinder SP, Vittinghoff E, Gomperts E, Donfield S, Vlahov D, Kaslow R, Saah A, Rinaldo C, Detels R, O'Brien SJ. Genetic restriction of HIV-1 infection and progression to AIDS by a deletion allele of the CKR5 structural gene. Hemophilia Growth and Development Study, Multicenter AIDS Cohort Study, Multicenter Hemophilia Cohort Study, San Francisco City Cohort, ALIVE Study. *Science* 1996; **273:** 1856-1862

5 **Woitas RP**, Ahlenstiel G, Iwan A, Rockstroh JK, Brackmann HH, Kupfer B, Matz B, Offergeld R, Sauerbruch T, Spengler U. Frequency of the HIV-protective CC chemokine receptor 5-Delta32/Delta32 genotype is increased in hepatitis C. *Gastroenterology* 2002; **122:** 1721-1728

6 **Hellier S**, Frodsham AJ, Hennig BJ, Klenerman P, Knapp S, Ramaley P, Satsangi J, Wright M, Zhang L, Thomas HC, Thursz M, Hill AV. Association of genetic variants of the chemokine receptor CCR5 and its ligands, RANTES and MCP-2, with outcome of HCV infection. *Hepatology* 2003; **38:** 1468-1476

7 **Ahlenstiel G**, Berg T, Woitas RP, Grunhage F, Iwan A, Hess L, Brackmann HH, Kupfer B, Schernick A, Sauerbruch T, Spengler U. Effects of the CCR5-Delta32 mutation on antiviral treatment in chronic hepatitis C. *J Hepatol* 2003; **39:** 245-252

8 **Berger EA**, Murphy PM, Farber JM. Chemokine receptors as HIV-1 coreceptors: roles in viral entry, tropism, and disease. *Annu Rev Immunol* 1999; **17:** 657-700

9 **Apolinario A**, Majano PL, Alvarez-Perez E, Saez A, Lozano C, Vargas J, Garcia-Monzon C. Increased expression of T cell chemokines and their receptors in chronic hepatitis C: relationship with the histological activity of liver disease. *Am J Gastroenterol* 2002; **97:** 2861-2870

10 **An P**, Nelson GW, Wang L, Donfield S, Goedert JJ, Phair J, Vlahov D, Buchbinder S, Farrar WL, Modi W, O'Brien SJ, Winkler CA. Modulating influence on HIV/AIDS by interacting RANTES gene variants. *Proc Natl Acad Sci USA* 2002; **99:** 10002-10007

11 **Liu H**, Chao D, Nakayama EE, Taguchi H, Goto M, Xin X, Takamatsu JK, Saito H, Ishikawa Y, Akaza T, Juji T, Takebe Y, Ohishi T, Fukutake K, Maruyama Y, Yashiki S, Sonoda S, Nakamura T, Nagai Y, Iwamoto A, Shioda T. Polymorphism

in RANTES chemokine promoter affects HIV-1 disease progression. *Proc Natl Acad Sci USA* 1999; **96:** 4581-4585

12 **Nickel RG**, Casolaro V, Wahn U, Beyer K, Barnes KC, Plunkett BS, Freidhoff LR, Sengler C, Plitt JR, Schleimer RP, Caraballo L, Naidu RP, Levett PN, Beaty TH, Huang SK. Atopic dermatitis is associated with a functional mutation in the promoter of the C-C chemokine RANTES. *J Immunol* 2000; **164:** 1612-1616

13 **Saiki RK**, Gelfand DH, Stoffel S, Scharf SJ, Higuchi R, Horn GT, Mullis KB, Erlich HA. Primer-directed enzymatic amplification of DNA with a thermostable DNA polymerase. *Science* 1988; **239:** 487-491

14 **van Gemen B**, Kievits T, Schukkink R, van Strijp D, Malek LT, Sooknanan R, Huisman HG, Lens P. Quantification of HIV-1 RNA in plasma using NASBA during HIV-1 primary infection. *J Virol Methods* 1993; **43:** 177-187

15 **Imberti L**, Cariani E, Bettinardi A, Zonaro A, Albertini A, Primi D. An immunoassay for specific amplified HCV sequences. *J Virol Methods* 1991; **34:** 233-243

16 **Morrison LE**, Halder TC, Stols LM. Solution-phase detection of polynucleotides using interacting fluorescent labels and competitive hybridization. *Anal Biochem* 1989; **183:** 231-244.

17 **Morrison LE**, Stols LM. Sensitive fluorescence-based thermodynamic and kinetic measurements of DNA hybridization in solution. *Biochemistry* 1993; **32:** 3095-3104

18 **Emery AEH**. An Introduction to Statistical Methods. Methodology in medical genetics. 2nd ed. London, New York: *Churchill Livingstone* 1986

19 **Gonzalez E**, Dhanda R, Bamshad M, Mummidi S, Geevarghese R, Catano G, Anderson SA, Walter EA, Stephan KT, Hammer MF, Mangano A, Sen L, Clark RA, Ahuja SS, Dolan MJ, Ahuja SK. Global survey of genetic variation in CCR5, RANTES, and MIP-1alpha: impact on the epidemiology of the HIV-1 pandemic. *Proc Natl Acad Sci USA* 2001; **98:** 5199-5204

20 **McDermott DH**, Beecroft MJ, Kleeberger CA, Al-Sharif FM, Ollier WE, Zimmerman PA, Boatin BA, Leitman SF, Detels R, Hajeer AH, Murphy PM. Chemokine RANTES promoter polymorphism affects risk of both HIV infection and disease progression in the Multicenter AIDS Cohort Study. *AIDS* 2000; **14:** 2671-2678

21 **Promrat K**, McDermott DH, Gonzalez CM, Kleiner DE, Koziol DE, Lessie M, Merrell M, Soza A, Heller T, Ghany M, Park Y, Alter HJ, Hoofnagle JH, Murphy PM, Liang TJ. Associations of chemokine system polymorphisms with clinical outcomes and treatment responses of chronic hepatitis C. *Gastroenterology* 2003; **124:** 352-360

22 **Soo HM**, Garzino-Demo A, Hong W, Tan YH, Tan YJ, Goh PY, Lim SG, Lim SP. Expression of a full-length hepatitis C virus cDNA up-regulates the expression of CC chemokines MCP-1 and RANTES. *Virology* 2002; **303:** 253-277

23 **Nattermann J**, Nischalke HD, Feldmann G, Ahlenstiel G, Sauerbruch T, Spengler U. Binding of HCV E2 to CD81 induces RANTES secretion and internalization of CC chemokine receptor 5. *J Viral Hepat* 2004; **11:** 519-526

24 **Lichterfeld M**, Leifeld L, Nischalke HD, Rockstroh JK, Hess L, Sauerbruch T, Spengler U. Reduced CC chemokine receptor (CCR) 1 and CCR5 surface expression on peripheral blood T lymphocytes from patients with chronic hepatitis C infection. *J Infect Dis* 2002; **185:** 1803-1807

Science Editor Guo SY **Language Editor** Elsevier HK

PO Box 2345, Beijing 100023, China
www.wjgnet.com
wjg@wjgnet.com

ELSEVIER

World J Gastroenterol 2005;11(48):7639-7645
World Journal of Gastroenterology ISSN 1007-9327

• *CLINICAL RESEARCH* •

Elevated plasma von Willebrand factor levels in patients with active ulcerative colitis reflect endothelial perturbation due to systemic inflammation

Petros Zezos, Georgia Papaioannou, Nikolaos Nikolaidis, Themistoclis Vasiliadis, Olga Giouleme, Nikolaos Evgenidis

Petros Zezos, Nikolaos Nikolaidis, Themistoclis Vasiliadis, Olga Giouleme, Nikolaos Evgenidis, Division of Gastroenterology, 2nd Propaedeutic Department of Internal Medicine, Hippokration General Hospital, Aristotle University of Thessaloniki, Greece
Georgia Papaioannou, Department of Haematology, Papageorgiou General Hospital of Thessaloniki, Greece
Correspondence to: Associate Professor Nikolaos Evgenidis, Division of Gastroenterology, 2nd Propaedeutic Department of Internal Medicine, Aristotle University of Thessaloniki, Hippokration General Hospital, 49 Konstantinoupoleos Str., 54642 Thessaloniki, Greece. zezosp@hol.gr
Telephone: +302310892073 Fax: +302310848354
Received: 2005-01-22 Accepted: 2005-04-09

Abstract

AIM: To evaluate the plasma von Willebrand factor (vWF) levels in patients with ulcerative colitis (UC) and to investigate their relationship with disease activity, systemic inflammation and coagulation activation.

METHODS: In 46 patients with ulcerative colitis (active in 34 patients), clinical data were gathered and plasma vWF levels, markers of inflammation (ESR, CRP, and fibrinogen) and thrombin generation (TAT, F1+2, and D-dimers) were measured at baseline and after 12 wk of treatment. Plasma vWF levels were also determined in 52 healthy controls (HC). The relationship of plasma vWF levels with disease activity, disease extent, response to therapy, acute-phase reactants (APRs) and coagulation markers (COAGs) was assessed.

RESULTS: The mean plasma vWF concentrations were significantly higher in active UC patients (143.38 ±63.73%) than in HC (100.75±29.65%, P = 0.001) and inactive UC patients (98.92±43.6%, P = 0.031). ESR, CRP and fibrinogen mean levels were significantly higher in active UC patients than in inactive UC patients, whereas there were no significant differences in plasma levels of D-dimers, F1+2, and TAT. UC patients with raised APRs had significantly higher mean plasma vWF levels than those with normal APRs (144.3% *vs* 96.2%, P = 0.019), regardless of disease activity. Although the mean plasma vWF levels were higher in UC patients with raised COAGs than in those with normal COAGs, irrespective of disease activity, the difference was not significant (141.3% *vs* 118.2%, P = 0.216). No correlation was noted between plasma vWF levels and disease extent. After 12 wk of treatment, significant decreases of fibrinogen, ESR, F1+2, D-dimers and vWF levels were noted only in UC patients with clinical and endoscopic improvement.

CONCLUSION: Our data indicate that increased plasma vWF levels correlate with active ulcerative colitis and increased acute-phase proteins. Elevated plasma vWF levels in ulcerative colitis possibly reflect an acute-phase response of the perturbed endothelium due to inflammation. In UC patients, plasma vWF levels may be another useful marker of disease activity or response to therapy.

Key words: Coagulation; Endothelial injury; Inflammation; Inflammatory bowel disease; Ulcerative colitis; von Willebrand factor

Zezos P, Papaioannou G, Nikolaidis N, Vasiliadis T, Giouleme O, Evgenidis N. Elevated plasma von Willebrand factor levels in patients with active ulcerative colitis reflect endothelial perturbation due to systemic inflammation. *World J Gastroenterol* 2005; 11(48): 7639-7645
http://www.wjgnet.com/1007-9327/11/7639.asp

INTRODUCTION

The etiology and pathogenesis of inflammatory bowel diseases (IBD), ulcerative colitis (UC) and Crohn's disease (CD), are still unclear[1]. "Vascular" theory supports that intestinal vascular injury is involved in CD and UC pathogenesis[2,3].

There is evidence that a hypercoagulable state exists in IBD, which might play a role in IBD pathogenesis[3-5]. This theory is further supported by the observation of Gaffney *et al*.[6] that patients with hemophilia and von Willebrand's disease have a lower risk in developing IBD and by the beneficial effects of heparin in the treatment of refractory ulcerative colitis[7,8]. The hypercoagulable state has been found to exist both in active and in inactive disease[9-15]. Furthermore, endothelial dysfunction, due to effects of

increased proinflammatory cytokines (IL-1, TNF-α), seems to play a central role in the hypercoagulant state production in IBD and also provides an evidence of interrelation between coagulation and inflammation pathways[16-18].

von Willebrand factor (vWF) is a large glycoprotein which circulates in human plasma or is deposited into the vascular subendothelium. Approximately 85% of circulating vWF is synthesized by the vascular endothelial cells, which are the main source of synthesis and secretion of this coagulation factor. vWF is also synthesized by megakaryocytes and is contained in platelets, which derive the remaining 15% of the circulating protein in blood. vWF serves as a stabilizing carrier protein of the coagulation factor VIII in circulation. vWF also mediates platelet to platelet interactions and platelet adhesion to the subendothelium in response to endothelial injury during the first step of thrombus formation[19]. Increased circulating levels of vWF in serum are considered as a marker of endothelial dysfunction or injury[19,20]. Increased levels of vWF are also observed as an acute-phase response in various inflammatory conditions[21].

vWF serum levels have been reported to be increased in patients with IBD, but it is not clear whether they reflect primary endothelial damage[17,22–25] or they are a manifestation of acute-phase response due to inflammation[22,23,26].

In this study, in order to clarify the meaning of elevated vWF levels in ulcerative colitis, we measured the circulating plasma vWF levels in a group of patients with ulcerative colitis and investigated their relationship with clinical activity and endoscopic severity of disease, markers of systemic inflammation and thrombin generation. We also monitored the changes of these variables during 12 wk of therapy and estimated their relationship with the clinical outcome.

MATERIALS AND METHODS

Patients and controls

Forty-six patients with ulcerative colitis (30 males and 16 females, mean age 41.8 years, range 17-73 years) and 52 healthy individuals (healthy controls, HC) (30 males and 22 females, mean age 40.9 years, range 19-65 years) were consecutively included in the study. All patients and controls were from the same geographical area (Northern Greece) and had a Greek ancestry.

Methods

The diagnosis of UC was based on the standard clinical, endoscopic and histological criteria. A complete medical history was obtained and physical examination was performed in all UC patients. During baseline evaluation, disease activity in patients with UC (active or inactive) was assessed with the simple clinical colitis activity index (SCCAI), taking into account five clinical criteria: day and night stool frequency, urgency of defecation, blood in the stool, general well being and presence of extracolonic manifestations[27]. A SCCAI score of ≤2 points was defined as clinical remission. Baseline colonoscopy with biopsy sampling was performed in all patients with UC, in order to assess the endoscopic severity and extent of disease. Endoscopic severity was measured by a modified endoscopic score with an 18-point scale[28] involving nine parameters: erythema, vascular pattern, friability, granularity, spontaneous bleeding, occurrence and severity of ulcers, extent of ulcerated surface, and presence of mucopurulent exudates. All parameters were scored from 0 to 2 points. Four grades of activity were considered according to the sum of all parameters: inactive disease (0-3), mild disease (4-7), moderate disease (8-12), and severe disease (13-18). Grading of endoscopic severity was done from the most inflamed part of the bowel. The extent of disease was recorded as rectosigmoiditis, left-sided colitis, and pancolitis. Patients with severe hepatic, renal and cardiac disease were excluded from the study.

Healthy control subjects were visitors in the outpatient clinic of Haematology Department and had no known diseases, or clinical or laboratory evidence of metabolic, neoplastic or inflammatory disease. They also had no history of thromboembolic disease.

All patients and control subjects gave their informed consent to participate in the study, which was approved by the Hospital's Scientific Committee.

Laboratory studies

Blood samples were collected at baseline from UC patients and control subjects for the quantitative determination of von Willebrand factor antigen (vWFAg) in plasma with an immuno-turbidimetric assay (STA-Liatest vWF, Diagnostica Stago, France; normal values 50-160%). Additional blood samples were obtained from UC patients in order to determine variables of inflammation (ESR, CRP and fibrinogen) and parameters reflecting thrombin generation (thrombin–antithrombin complex [TAT], prothrombin fragments 1+2 [F1+2], and D-dimers [D-Di]).

ESR was measured by standard laboratory technique (normal values <20 mm/h) and CRP was measured with ELISA (normal values <5 mg/L). Plasma fibrinogen concentration was measured by the Claus method using bovine thrombin (bioMerieux sa, France) on OPTION coagulation analyzer (normal values 2-4 g/L).

TAT levels in plasma were measured by sandwich enzyme immunoassay (Enzygnost TAT micro, Dade Behring, Marburg, Germany; normal values 1-4.1 μg/L). F1+2 levels in plasma were measured by sandwich enzyme immunoassay (Enzygnost F1+2 micro, Dade Behring, Marburg, Germany; normal values 0.4-1.1 nmol/L). D-dimers levels in plasma were measured by immuno-turbidimetric assay (STA-Liatest D-Di, Diagnostica Stago, France; normal values <500 μg/L).

All venipunctures were performed using a butterfly 18-gauge needle between 08:00 and 10:00 a.m. The first 10 mL of blood was not used for determination of hemostatic variables. Venous blood samples for hemostatic variables were collected in trisodium citrate tubes and platelet-poor plasma was prepared by one-stage centrifugation at 2 000 r/min for 20 min at 4 °C. Plasma was removed and assayed immediately for fibrinogen and stored at -20 °C until assayed, within one month, for vWF, TAT, F1+2, and D-dimers.

All UC patients were considered to have increased acute-phase reactants (APRs) if an increase in at least one of the two inflammation variables (ESR, CRP) was noted, as previously described[26]. Likewise, all UC patients were considered to have increased coagulation markers (COAGs) if an increase in at least one of the three hemostatic variables (TAT, F1+2, and D-dimers) was noted.

Treatment and course

Patients with active UC were treated for attenuation of disease activity with high-dose corticosteroids and mesalazine orally and rectally. Azathioprine was continued if already used. Patients were set into a follow-up program with regular visits every 2nd wk for 12 wk. Corticosteroids were tapered off with a weekly based schedule throughout the study period. At the end of the study (12th wk), complete clinical, endoscopic and laboratory evaluation, similar to baseline week, was performed in all patients with active colitis. Complete response to therapy (remission) was considered, if a SCCAI score of ≤2 and endoscopic remission was achieved after 12 wk of therapy. Partial response was considered if a 50% reduction of SCCAI score was noted together with a reduction of endoscopic activity by at least one grade.

Statistical analysis

Statistical analysis was performed using the SPSS for Windows package (version 11.0, SPSS, Chicago, IL, USA). Data were presented as mean±SD. Baseline comparisons were performed between the three main groups (healthy controls, patients with inactive UC and patients with active UC). A detailed analysis and multiple comparisons were performed between different subgroups of patients with UC according to disease activity, raised APRs or raised COAGs. Comparisons between groups were performed with Student's *t* test or ANOVA when appropriate. Student's *t* test for paired samples was used to compare baseline and follow-up measurements in patients with active disease. Associations between continuous variables were tested with Pearson's correlation. Differences in frequencies were studied with Fisher's exact test. $P<0.05$ was considered statistically significant.

RESULTS

During baseline evaluation, 12 patients with ulcerative colitis were found to be in remission and 34 patients had active disease. Demographic and clinical data of patients are shown in Table 1. There were no significant differences in sex, age and extent of disease between patients with active and inactive disease.

Table 1 Demographic and clinical data of ulcerative colitis patients (mean±SD)

	Active UC (n = 34)	Inactive UC (n = 12)
Male/female	22/12	8/4
Age (yr)	41.5±14.6 (17–73)	42.8±15.2 (18–65)
Extent of disease		
Rectosigmoiditis	6	3
Left-sided colitis	20	6
Pancolitis	8	3
SCCAI score	8±3 (3–12)	0±1 (0–2)
Endoscopic score	16±2 (12–18)	2±1 (0–3)
Treatment		
Oral steroids	15	0
5-ASA compounds	30	12
Azathioprine	11	2
None	2	0
Smoking	7	5

SCCAI: simple clinical colitis activity index; 5-ASA: 5-aminosalicylates.

Elevated plasma vWF concentrations were found in 1 patient with ulcerative colitis in remission and in 11 patients with active disease. None of the healthy subjects had an elevated value of plasma vWF. Mean plasma vWF concentrations were significantly higher in active ulcerative colitis patients (143.38±63.73%) than in healthy controls (100.75±29.65%, $P = 0.001$) and inactive UC patients (98.92 ±43.6%, $P = 0.031$). There was no difference in mean plasma vWF concentrations between HC and inactive UC patients (Table 2).

Mean levels of ESR, CRP and fibrinogen were significantly higher in active UC patients than in inactive UC patients. There were no significant differences in plasma levels of coagulation markers (D-dimers, F1+2 and TAT) between patients with active and inactive UC (Table 2).

UC patients with raised APRs (n = 34), irrespective of disease activity, had significantly higher mean plasma vWF levels than those with normal APRs (n = 12) (144.3 ±62.4% *vs* 96.2±45.8%, $P = 0.019$). Mean plasma vWF levels were also higher in UC patients with raised COAGs (n = 27), irrespective of disease activity, than in those with normal COAGs (n = 19), but did not reach statistical significance (141.3±64.8% *vs* 118.2±56.3%, $P = 0.216$). However, when all UC patients were divided into four subgroups according to raised or normal APRs and COAGs,

Table 2 Acute phase reactants and coagulation factors in patients with ulcerative colitis and healthy controls (mean±SD)

	Active UC (n = 34)	Inactive UC (n = 12)	Healthy controls (n = 52)
vWF (%)	143.38±63.73 (49-278)	98.92±43.6[a] (25-188)	100.75±29.65[b] (51–160)
ESR (mm/h)	40±21 (10-97)	16±12[a] (4-40)	
CRP (mg/L)	24.7±40.2 (3.1-175.5)	4.1±1.7[a] (3.1-7.3)	
Fibrinogen (g/L)	4.86±1.21 (2.93-7.3)	3.48±1.14[a] (1.25-5.61)	
D-dimers (μg/L)	873±1 308 (32-3 993)	608±1 149 (19-4 038)	
F1+2 (nmol/L)	3.71±6.09 (0.21–22.53)	3.72±6.41 (0.28-21.52)	
TAT (μg/L)	6.91±15.18 (0.09–85.9)	3.99±4.2 (0.85-13.2)	

vWF: von Willebrand factor; ESR: erythrocyte sedimentation rate; CRP: C-reactive protein; F1+2: prothrombin fragments 1+2; TAT: thrombin–antithrombin complexes. [a]$P<0.05$ active UC *vs* inactive UC. [b]$P<0.001$ active UC *vs* HC.

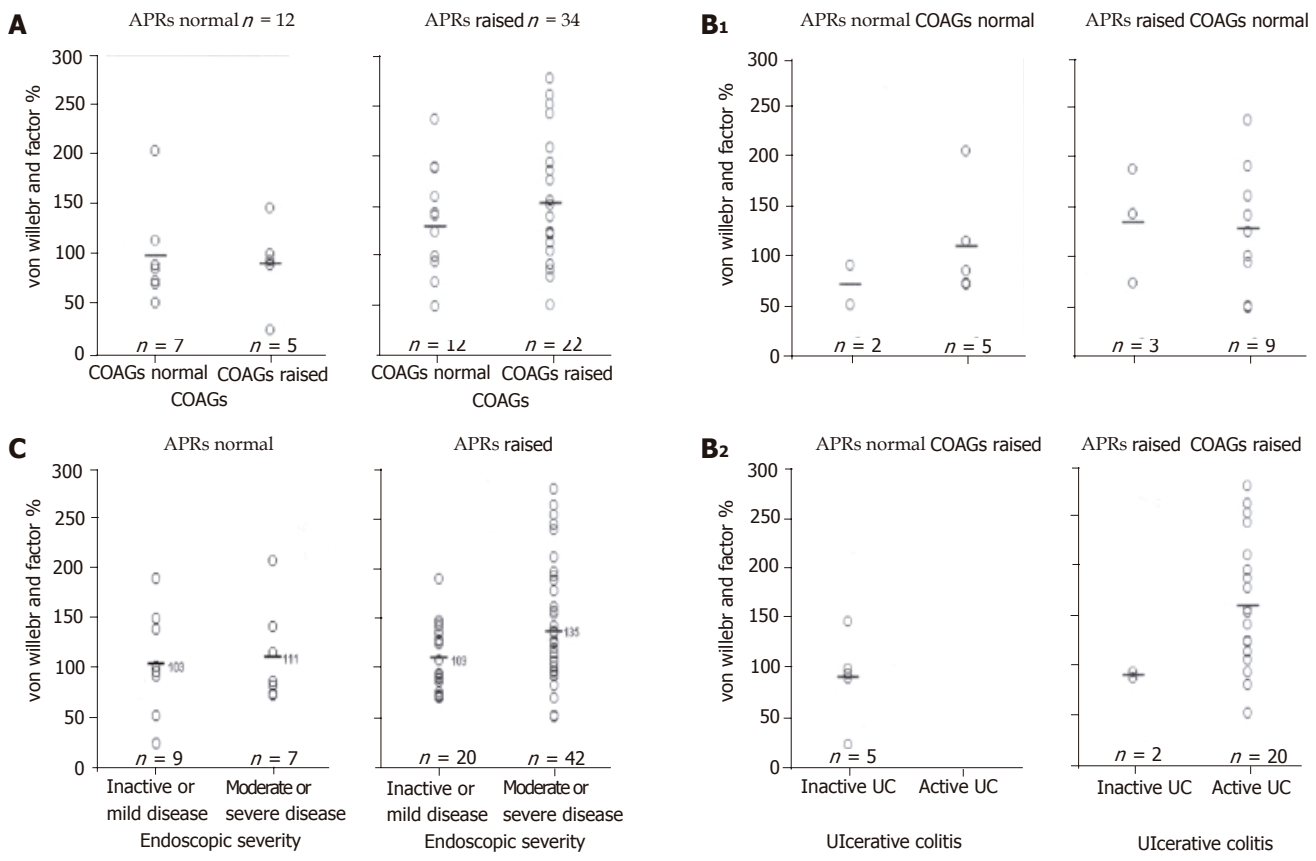

Figure 1 Mean plasma von Willebrand factor (vWF) levels in UC patients (**A**), their subgroups were divided according to disease activity, APRs and COAGs (**B1**, **B2**), as well as according to endoscopic severity and APRs(**C**). Open circle black dots (o) represent individual values and horizontal black lines (-) represent mean values. APRs: acute-phase reactants; COAGs: thrombin generation coagulation markers.

irrespective of disease activity, it was noted that patients with raised APRs had significantly higher mean plasma vWF levels than those with normal APRs, regardless of COAGs status (Figure 1A).

Furthermore, when UC patients were divided into subgroups according to disease activity and raised or not APRs and COAGs, there was a trend towards higher mean plasma vWF levels in almost all subgroups of patients with raised APRs (especially to those with active disease) compared to the patients with normal APRs. However, there were no significant differences between subgroups (Figure 1B1, B2).

In patients with ulcerative colitis (active and inactive), Pearson's correlation analysis revealed that there was a significant positive correlation of plasma vWF levels with clinical activity index (SCCAI) (r = 0.41, P = 0.004), endoscopic score (r = 0.3, P = 0.041), ESR (r = 0.39, P = 0.006), fibrinogen (r = 0.42, P = 0.003) and D-dimers (r = 0.36, P = 0.015). No correlation was noted between plasma vWF levels and extent of the disease or smoking status.

In all patients with UC, analysis of the percentages of high plasma vWF levels between subgroups revealed that raised APRs were the main factors influencing the plasma vWF levels (data not shown).

Thirty-two patients with active UC completed the study after 12 wk of treatment. Two patients did not show up at the final date of the follow-up schedule (12th week). There were no complications of the disease or adverse events from the treatment during the study period. Twenty-two patients showed response to therapy (complete or partial) and 10 patients were non-responders. A significant decrease of the inflammatory parameters (fibrinogen and ESR), the coagulation markers (F1+2 and D-dimers) and von Willebrand factor levels was noted only in the "responders" group (Table 3).

We pooled all patients in respect of endoscopic severity, before and after the therapy for active disease plus patients in remission at baseline week, and found that mean plasma vWF levels in patients with active disease at endoscopy (n = 54, 131.2±56.2%) were significantly higher than those in patients with endoscopic remission (n = 24, 103.1±36.7%, P = 0.028). There were no significant differences in plasma vWF levels between the groups of endoscopic severity grades (mild to severe) in patients with active disease. However, when we divided the patients in respect of APR status, we found that patients with raised APRs and moderate or severe endoscopic activity had significantly higher mean plasma vWF levels than the other subgroups (Figure 1C).

DISCUSSION

This study showed that mean plasma vWF levels were significantly raised in patients with active UC compared

Table 3 Laboratory parameters at baseline and after 12 wk of therapy in active UC patients who completed the study (*n* = 32) (mean±SD)

	Weeks of follow-up	Responders	Non-responders
	Paired samples *t* test	*n* = 22	*n* = 10
ESR (mm/h)	Baseline	43±24	34±13
	12th week	32±18	27±12
	P	0.055	0.206
CRP (mg/L)	Baseline	27.21±42.13	22.24±41.2
	12th week	11.11±25.57	11.42±13.29
	P	0.106	0.460
Fibrinogen (g/L)	Baseline	4.9±1.13	4.98±1.48
	12th week	4.05±0.68	4.55±0.82
	P	0.001	0.372
vWF (%)	Baseline	153.91±69.53	129.3±50.35
	12th week	111.14±30.65	105.4±32.87
	P	0.005	0.153
F1+2 (nmol/L)	Baseline	3.73±5.73	4.21±7.26
	12th week	1.23±1.12	0.71±0.26
	P	0.043	0.186
D-dimers (μg/L)	Baseline	1 202±1 522	302±329
	12th week	251±288	683±1 286
	P	0.005	0.381
TAT (μg/L)	Baseline	4.39±4.6	13.43±26.94
	12th week	5.41±13.1	1.97±1.57
	P	0.733	0.211

vWF: von Willebrand factor; ESR: erythrocyte sedimentation rate; CRP: C-reactive protein; F1+2: prothrombin fragments 1+2; TAT: thrombin–antithrombin complexes.

to healthy controls and patients with UC in remission. Since elevated circulating von Willebrand factor levels are regarded as markers of both endothelial dysfunction and acute phase response to inflammation, we tried to investigate the relationship between vWF and markers of inflammation and coagulation, in order to clarify the meaning of elevated vWF levels in our patients with active ulcerative colitis. APRs were significantly higher in patients with active UC than in those with inactive disease. On the other hand, there were no significant differences in markers of thrombin generation between patients with active and inactive UC (Table 2). These observations are in accordance with previous studies, suggesting that a hypercoagulable state exists in both active and inactive UC[29-31]. In contrast, intense inflammatory response to elevated APRs is a prominent feature of active UC[32,33].

In our study, UC patients were divided into subgroups according to disease activity (active and inactive) and APRs or COAGs status (raised or not). The analysis of data revealed two main findings. The mean plasma vWF levels were significantly higher in patients with active disease (Table 2) and higher in patients with raised APRs irrespective of disease activity or COAGs status (Figure 1).

In a recent study, Meucci *et al*.[26] reported that elevated vWF levels in a group of patients with IBD are related to increased APRs, regardless of disease activity and concluded that elevated plasma vWF levels are a secondary manifestation due to systemic inflammation. In our study, we had similar findings with Meucci *et al*.[26], suggesting that elevated plasma vWF levels in patients with UC correlate mainly with the inflammatory response and to a lesser degree with hypercoagulability. However, in the most recent study, Xu *et al*.[25] had the opposite findings in a group of patients with UC, reporting that plasma vWF levels are significantly higher in patients with ulcerative colitis than in controls, with no differences between active and inactive disease. They also reported that D-dimers levels are higher in patients with active disease than in those in remission and D-dimers levels are positively correlated with vWF levels. The authors concluded that elevated vWF levels both in active and inactive UC reflect the fact that endothelial cell damage is a feature of UC and that D-dimers levels can be used as a marker of inflammation to distinguish active from inactive UC.

Inflammation, coagulation and endothelial dysfunction correlations have been studied in many other clinical conditions[34-37]. Inflammation as measured by CRP has been found to be associated with prothrombotic status and endothelial dysfunction as reflected by elevated vWF in acute coronary syndromes[38]. Plasma vWF has been reported as an APR in patients with acute infectious diseases which parallels CRP levels during illness and recovery phase[21]. The inflammatory and coagulation abnormalities observed in patients with ulcerative colitis possibly represent combined and cross-linked manifestations of the inflammation and coagulation systems, which are interrelated in a bidirectional way with the endothelium being the interface between inflammation and coagulation[18].

Inflammation is undoubtedly a key component in the pathogenesis of ulcerative colitis[39] and proinflammatory cytokines (IL-1, IL-6, IL-8, TNF-α, and IFN-γ) operate as a cascade and network in stimulating the production of acute-phase proteins and induction of acute-phase manifestations[40]. Inflammation can also lead to activation of coagulation system with the endothelium playing a central role in all major pathways involved in the pathogenesis of hemostatic derangement[18]. Proinflammatory cytokines induce a procoagulant profile with thrombin production,

through their effects on the vascular endothelial cells[18] and can also stimulate vWF secretion from Weibel-Palade storage granules of the endothelial cells[19,41,42]. A small fraction of the elevated plasma vWF levels can also be derived from platelets, since reactive thrombocytosis and *in vivo* activation of platelets are observed in active ulcerative colitis[15], consisting acute-phase phenomena due to systemic inflammation[40], but it seems that the contribution of platelet-derived vWF to elevated plasma levels is minor[23]. We can assume that, like other coagulation factors which are synthesized in liver cells and behave as acute-phase proteins (fibrinogen, factor VIII) during inflammation, elevated plasma vWF concentrations represent an endothelial component of the acute-phase response[23].

Glucocorticoids are known to increase plasma concentrations of factor VIII (FVIII) and von Willebrand factor (vWF), and their administration is associated with an increased thrombotic tendency[43,44]. In our study, patients with active ulcerative colitis were treated with high doses of corticosteroids for attenuation of disease activity and had no thromboembolic complications during the study period. Follow-up measurements after 12 wk of treatment showed that patients who responded to therapy had a significant improvement of all the variables of inflammation and hemostasis, including von Willebrand factor. Inflammation is undoubtedly the main feature of UC and the attenuation of inflammatory process due to the potent anti-inflammatory properties of corticosteroids is the principal mechanism that contributes to the improvement of disease severity and its clinical or laboratory manifestations. It is likely that hepatic and endothelial acute-phase responses have a parallel course during inflammatory process since they may be regulated in a similar manner by the same cytokines.

In our study, we investigated the relationship of plasma vWF levels with disease activity, parameters of inflammation and hemostasis in a group of patients with ulcerative colitis (active and inactive), before and after therapy. It is the first study to our knowledge which combines the assessment of all these variables in a time course manner and represents an extension of the two most recent studies[25,26]. The small number of patients in our study did not allow us to generalize our findings and give a possible explanation for any discrepancies of data among all relative studies. However, the general trend from the data is that plasma vWF levels are correlated with systemic inflammation.

In conclusion, increased plasma vWF levels in ulcerative colitis patients correlate with disease activity and increased acute-phase proteins. It seems that elevated plasma vWF levels in active ulcerative colitis patients reflect an acute-phase response of the perturbed endothelium due to inflammation and von Willebrand factor can be regarded as an endothelial APR. Further and larger studies are needed to show if plasma von Willebrand factor levels can be a useful and sensitive marker of disease activity or response to therapy.

REFERENCES

1 **Oliva-Hemker M,** Fiocchi C. Etiopathogenesis of inflammatory bowel disease: the importance of the pediatric perspective. *Inflamm Bowel Dis* 2002; **8:** 112-128
2 **Hamilton MI**, Dick R, Crawford L, Thompson NP, Pounder RE, Wakefield AJ. Is proximal demarcation of ulcerative colitis determined by the territory of the inferior mesenteric artery? *Lancet* 1995; **345:** 688-690
3 **Wakefield AJ**, Sawyerr AM, Dhillon AP, Pittilo RM, Rowles PM, Lewis AA, Pounder RE. Pathogenesis of Crohn's disease: multifocal gastrointestinal infarction. *Lancet* 1989; **2:** 1057-1062
4 **Juhlin L**, Krause U, Shelley WB. Endotoxin-induced microclots in ulcerative colitis and Crohn's disease. *Scand J Gastroenterol* 1980; **15:** 311-314
5 **Dhillon AP**, Anthony A, Sim R, Wakefield AJ, Sankey EA, Hudson M, Allison MC, Pounder RE. Mucosal capillary thrombi in rectal biopsies. *Histopathology* 1992; **21:** 127-133
6 **Thompson NP,** Wakefield AJ, Pounder RE. Inherited disorders of coagulation appear to protect against inflammatory bowel disease. *Gastroenterology* 1995; **108**: 1011-1015
7 **Gaffney PR**, Doyle CT, Gaffney A, Hogan J, Heys DP, Annis P. Paradoxical response to heparin in 10 patients with ulcerative colitis. *Am J Gastronterol* 1995; **90:** 220-223
8 **Torkvist L**, Thorlacius H, Sjoqvist U, Bohman L, Lapidus A, Flood L, Agren B, Raud J, Lofberg R. Low molecular weight heparin as adjuvant therapy in active ulcerative colitis. *Aliment Pharmacol Ther* 1999; **13:** 1323-1328
9 **Lee LC**, Spittell JA Jr, Sauer WG, Owen CA Jr, Thompson JH Jr. Hypercoagulability associated with chronic ulcerative colitis: changes in blood coagulation factors. *Gastroenterology* 1968; **54:** 76-85
10 **Lam A**, Borda IT, Inwood MJ, Thomson S. Coagulation studies in ulcerative colitis and Crohn's disease. *Gastroenterology* 1975; **68:** 245-251
11 **de Jong E**, Porte RJ, Knot EA, Verheijen JH, Dees J. Disturbed fibrinolysis in patients with inflammatory bowel disease. A study in blood plasma, colon mucosa, and faeces. *Gut* 1989; **30:** 188-194
12 **Conlan MG**, Haire WD, Burnett DA. Prothrombotic abnormalities in inflammatory bowel disease. *Dig Dis Sci* 1989; **34:** 1089-1093
13 **Vecchi M**, Cattaneo M, de Franchis R, Mannucci PM. Risk of thromboembolic complications in patients with inflammatory bowel disease. Study of hemostasis measurements. *Int J Clin Lab Res* 1991; **21:** 165-170
14 **Hudson M**, Hutton RA, Wakefield AJ, Sawyerr AM, Pounder RE. Evidence for activation of coagulation in Crohn's disease. *Blood Coagul Fibrinolysis* 1992; **3:** 773-778
15 **Collins CE**, Cahill MR, Newland AC, Rampton DS. Platelets circulate in an activated state in inflammatory bowel disease. *Gastroenterology* 1994; **106:** 840-845
16 **Bevilacqua MP**, Gimbrone MA Jr. Inducible endothelial functions in inflammation and coagulation. *Semin Thromb Hemost* 1987; **13:** 425-433
17 **Souto JC**, Martinez E, Roca M, Mateo J, Pujol J, Gonzalez D, Fontcuberta J. Prothrombotic state and signs of endothelial lesion in plasma of patients with inflammatory bowel disease. *Dig Dis Sci* 1995; **40:** 1883-1889
18 **Levi M**, ten Cate H, van der Poll T. Endothelium: interface between coagulation and inflammation. *Crit Care Med* 2002; **30:** S220- S224
19 **Mannucci PM**. von Willebrand factor: a marker of endothelial damage? *Arterioscler Thromb Vasc Biol* 1998; **18:** 1359-1362
20 **Goldsmith I**, Kumar P, Carter P, Blann AD, Patel RL, Lip GY. Atrial endocardial changes in mitral valve disease: a scanning electron microscopy study. *Am Heart J* 2000; **140:** 777-784
21 **Pottinger BE**, Read RC, Paleolog EM, Higgins PG, Pearson JD. von Willebrand factor is an acute phase reactant in man. *Thromb Res* 1989; **5:** 387-394
22 **Stevens TR**, James JP, Simmonds NJ, McCarthy DA, Lauren-

son IF, Maddison PJ, Rampton DS. Circulating von Willebrand factor in inflammatory bowel disease. *Gut* 1992; **33:** 502-506
23 **Sawyerr AM**, Smith MS, Hall A, Hudson M, Hay CR, Wakefield AJ, Brook MG, Tomura H, Pounder RE. Serum concentrations of von Willebrand factor and soluble thrombomodulin indicate alteration of the endothelial function in inflammatory bowel disease. *Dig Dis Sci* 1995; **40:** 793–799
24 **Stevens TR**, Harley SL, Groom JS, Cambridge G, Leaker B, Blake DR, Rampton DS. Anti-endothelial cell antibodies in inflammatory bowel disease. *Dig Dis Sci* 1993; **38:** 426-432
25 **Xu G**, Tian KL, Liu GP, Zhong XJ, Tang SL, Sun YP. Clinical significance of plasma D-dimer and von Willebrand factor levels in patients with ulcer colitis. *World J Gastroenterol* 2002; **8:** 575-576
26 **Meucci G**, Pareti F, Vecchi M, Saibeni S, Bressi C, de Franchis R. Serum von Willebrand factor levels in patients with inflammatory bowel disease are related to systemic inflammation. *Scand J Gastroenterol* 1999; **34:** 287-290
27 **Walmsley RS**, Ayres RC, Pounder RE, Allan RN. A simple clinical colitis activity index. *Gut* 1998; **43:** 29-32
28 **van der Heide H**, van der Brandt-Gradel V, Tytgat GN, Endert E, Wiltink EH, Schipper ME, Dekker W. Comparison of beclomethasone diproprionate and pednisolone 21-phosphate enemas in the treatment of ulcerative colitis. *J Clin Gastroenterol* 1988; **10:** 169-172
29 **van Bodegraven AA**, Schoorl M, Baak JPA, Linskens RK, Bartels PC, Tuynman HA. Hemostatic imbalance in active and quiescent ulcerative colitis. *Am J Gastroenterol* 2001; **96:** 487-493
30 **van Bodegraven AA**, Schoorl M, Linskens RK, Bartels PC, Tuynman HA. Persistent activation of coagulation and fibrinolysis after treatment of active ulcerative colitis. *Eur J Gastroenterol Hepatol* 2002; **14:** 413-418
31 **Kjeldsen J**, Lassen JF, Brandslund I, Schaffalitzky de Muckadell OB. Markers of coagulation and fibrinolysis as measures of disease activity in inflammatory bowel disease. *Scand J Gastroenterol* 1998; **33:** 637-643
32 **Niederau C**, Backmerhoff F, Schumacher B, Niederau C. Inflammatory mediators and acute phase proteins in patients with Crohn's disease and ulcerative colitis. *Hepatogastroenterology* 1997; **44:** 90-107
33 **Vermeire S**, Van Assche G, Rutgeerts P. C-reactive protein as a marker for inflammatory bowel disease. *Inflamm Bowel Dis* 2004; **10:** 661-665
34 **Thor M**, Yu A, Swedenborg J. Markers of inflammation and hypercoagulability in diabetic and nondiabetic patients with lower extremity ischemia. *Thromb Res* 2002; **105:** 379-383
35 **Conway DS**, Buggins P, Hughes E, Lip GY. Predictive value of indexes of inflammation and hypercoagulability on success of cardioversion of persistent atrial fibrillation. *Am J Cardiol* 2004; **94:** 508–510
36 **Paisley KE**, Beaman M, Tooke JE, Mohamed-Ali V, Lowe GD, Shore AC. Endothelial dysfunction and inflammation in asymptomatic proteinuria. *Kidney Int* 2003; **63:** 624-633
37 **Hurlimann D**, Enseleit F, Ruschitzka F. Rheumatoid arthritis, inflammation, and atherosclerosis. *Herz* 2004; **29:** 760-768
38 **Apetrei E**, Ciobanu-Jurcut R, Rugina M, Gavrila A, Uscatescu V. C-reactive protein, prothrombotic imbalance and endothelial dysfunction in acute coronary syndromes without ST elevation. *Rom J Intern Med* 2004; **42:** 95-102
39 **Podolsky DK**. Inflammatory bowel disease. *N Engl J Med* 2002; **347:** 417-429
40 **Gabay C**, Kushner I. Acute-phase proteins and other systemic responses to inflammation. *N Engl J Med* 1999; **340:** 448-54
41 **van der Poll T**, van Deventer SJ, Pasterkamp G, van Mourik JA, Buller HR, tenCate JW. Tumor necrosis factor induces von Willebrand factor release in healthy humans. *Thromb Haemost* 1992; **67:** 623-626
42 **Paleolog EM**, Crossman DC, McVey JH, Pearson JD. Differential regulation by cytokines of constitutive and stimulated secretion of von Willebrand factor from endothelial cells. *Blood* 1990; **75:** 688-695
43 **Casonato A**, Pontara E, Boscaro M, Sonino N, Sartorello F, Ferasin S, Girolami A. Abmormalities of von Willebrand factor are also part of the prothrombotic state of Cushing's syndrome. *Blood Coagul Fibrinolysis* 1999; **10:** 145-151
44 **Boscaro M**, Sonino N, Scarda A, Barzon L, Fallo F, Sartori MT, Patrassi GM, Girolami A. Anticoagulant prophylaxis markedly reduces thromboembolic complications in Cushing's syndrome. *J Clin Endocrinol Metab* 2002; **87:** 3662-3666

Science Editor Wang XL and Guo SY **Language Editor** Elsevier HK

PO Box 2345, Beijing 100023, China
www.wjgnet.com
wjg@wjgnet.com

ELSEVIER

World J Gastroenterol 2005;11(48):7646-7650
World Journal of Gastroenterology ISSN 1007-9327

• *CLINICAL RESEARCH* •

Involvement of serum retinoids and Leiden mutation in patients with esophageal, gastric, liver, pancreatic, and colorectal cancers in Hungary

Gyula Mózsik, György Rumi, András Dömötör, Mária Figler, Beáta Gasztonyi, Előd Papp, Alajos Pár, Gabriella Pár, József Belágyi, Zoltán Matus, Béla Melegh

Gyula Mózsik, György Rumi, András Dömötör, Beáta Gasztonyi, Előd Papp, Alajos Pár, Gabriella Pár, First Department of Medicine, Medical Faculty, Medical and Health Centre, University of Pécs, Hungary
Zoltán Matus, Department of Biochemistry and Medical Chemistry, Medical Faculty, Medical and Health Centre, University of Pécs, Hungary
Béla Melegh, Department of Medical Genetics and Child Development, Medical Faculty, Medical and Health Centre, University of Pécs, Hungary
József Belágyi, Department of Bioanalysis, Medical Faculty, Medical and Health Centre, University of Pécs, Hungary
Mária Figler, Department of Human Clinical Nutrition and Dietetics, Faculty of Health Sciences, Medical and Health Centre, University of Pécs, Hungary
Supported by the grant from the Hungarian Ministry of Health (ETT 595/2003)
Correspondence to: Professor. Gyula Mózsik, MD, First Department of Medicine, Medical and Health Centre, University of Pécs, Hungary. gyula.mozsik@aok.pte.hu
Telephone: +36-72-536-494 Fax: +36-72-536-495
Received: 2005-03-10 Accepted: 2005-08-03

Abstract

AIM: To analyze the serum levels of retinoids and Leiden mutation in patients with esophageal, gastric, liver, pancreatic, and colorectal cancers.

METHODS: The changes in serum levels of retinoids (vitamin A, α- and β-carotene, α- and β-cryptoxanthin, zeaxanthin, lutein) and Leiden mutation were measured by high liquid performance chromatography (HPLC) and polymerase chain reaction (PCR) in 107 patients (70 males/37 females) with esophageal (0/8), gastric (16/5), liver (8/7), pancreatic (6/4), and colorectal (30/21 including 9 patients suffering from *in situ* colon cancer) cancer. Fifty-seven healthy subjects (in matched groups) for controls of serum retinoids and 600 healthy blood donors for Leiden mutation were used.

RESULTS: The serum levels of vitamin A and zeaxanthin were decreased significantly in all groups of patients with gastrointestinal (GI) tumors except for vitamin A in patients with pancreatic cancer. No changes were obtained in the serum levels of α- and β-carotene, α- and β-cryptoxanthin, zeaxanthin, lutein in patients with GI cancer. The prevalence of Leiden mutation significantly increased in all groups of patients with GI cancer.

CONCLUSION: Retinoids (as environmental factors) are decreased significantly with increased prevalence of Leiden mutation (as a genetic factor) in patients before the clinical manifestation of histologically different (planocellular and hepatocellular carcinoma, and adenocarcinoma) GI cancer.

Key words: Human gastrointestinal cancer; Leiden mutation; Retinoids; Vitamin A; Zeaxanthin

Mózsik G, Rumi G, Dömötör A, Figler M, Gasztonyi B, Papp E, Pár A, Pár G, Belágyi J, Matus Z, Melegh B. Involvement of serum retinoids and Leiden mutation in patients with esophageal, gastric, liver, pancreatic, and colorectal cancers in Hungary. *World J Gastroenterol* 2005; 11(48): 7646-7650
http://www.wjgnet.com/1007-9327/11/7646.asp

INTRODUCTION

The number of patients with different gastrointestinal (esophageal, gastric, liver, pancreatic, and colorectal) cancer has increased about two- to threefolds in the last decades (except for gastric cancer which has decreased 50%) in Hungary. The number of patients who died of these malignant diseases represents the second highest population of the total mortality of patients in Hungary. The second highest mortality rate of gastrointestinal (GI) tumor takes place at the second place in our country.

The causes of GI tumors are not known. However, different genetic and environmental factors play a role in the development of GI cancer. It is generally accepted that different diseases such as acute and chronic inflammatory diseases, polyposis, can be taken as precancerous states of GI cancer.

Since the year of l980, we have studied the role of retinoids in protecting gastrointestinal mucosa in animal experiments and human observations[1-4]. Retinoids are chemical compounds of color materials from plants and are built up from C-20 and four isoprene units, while carotenoids are built up from C-40 and eight isoprene units located in about 600 plants, and about 50 from 600

Table 1 Patients with different gastrointestinal tumors

	Number of patients			
Types of tumors	Male	Female	Total	Histology
Esophageal	8 (60±10 yr)[1]	–	8	Planocellular carcinoma
Gastric	16 (64±12 yr)[1]	5 (68±10 yr)[1]	21	Adenocarcinoma
Liver	8 (60±8 yr)[1]	7 (57±13 yr)[1]	15	Hepatocellular carcinoma
Pancreas	6 (56±11 yr)[1]	4 (63±9 yr)[1]	10	Adenocarcinoma
Colorectal	30 (66±10 yr)[1]	23 (65±11 yr)[1]	53	Adenocarcinoma
In situ carcinoma in colon polyps	4 (60±5 yr)[1]	5 (61±5 yr)[1]	9	Adenocarcinoma
Total	70	37	107	
Healthy subjects	29 (50±12 yr)[1]	28 (49±10 yr)[1]	57	

600 blood donors (healthy controls) for Leiden mutation study. [1]Age of patients (mean±SD).

isolated compounds are precursors of vitamin A.

Vitamin A and β-carotene (and other retinoids) have gastric mucosal protective effects in rats provoked by intragastric administration of 1 mL from 0.6 mol/L HCl, 25% NaCl, 0.2 NaOH, and 960 mL/L ethanol, without the presence of any inhibition of gastric acid secretion[1]. Vitamin A has a higher ulcer healing effect than atropine, cimetidine DE-NOL (tripotassio–dicitrato) in patients with gastric ulcer[2-4] .The serum level of retinoids is decreased in patients with inflammatory bowel disease[5-8]. It was also demonstrated that the serum levels of vitamin A and zeaxanthin are also decreased in patients with GI cancer[9], but the possible correlation between the changes in other serum retinoids and the prevalence of Leiden mutation has not been studied.

The presence of Leiden mutation (replacement of Arg by Glu of residue 506 in the factor V molecule, FVR, 506 Q) has been proven in thrombophylia[10-13] as well as in Crohn's disease and ulcerative colitis[14-18], meanwhile no higher prevalence of Leiden mutation has been obtained in patients with acute gastritis and hepatitis[17]. The significant presence of Leiden mutation (APC) is responsible for blood coagulation abnormality in thrombophylia.

The aims of our present study were to evaluate the changes in serum levels of retinoids (as nutritional components of vitamin A, β-carotene, α-carotene, α- and β-cryptoxanthin, zeaxanthin, lutein) in patients with different gastrointestinal (esophageal, gastric, liver, pancreatic, and colorectal) cancer, to study the prevalence of Leiden mutation in the above mentioned patients, to find some correlation between the changes in Leiden mutation and serum level of vitamin A and zeaxanthin in GI cancer patients as well as between GI cancer development and chemical structure of retinoids, to obtain some correlation between serum levels of vitamin A and zeaxanthin in patients with different GI tumors.

MATERIALS AND METHODS

Observations were carried in 107 patients with esophageal (n = 8), gastric (n = 21), liver (n = 15), pancreatic (n = 10), colorectal (n = 53), and *in situ* colon (n = 9) cancer, including 70 males (50±12 years) and 37 females (49± 10 years). Fifty-seven healthy persons (in matched group) were used as control, and 600 healthy blood donors were used for the control of Leiden mutation (Table 1). A total of 764 patients with gastrointestinal cancer and healthy subjects were included in this study. The studies were approved by the Ethical Committee of University of Pécs, Hungary. Written informed consent was obtained from all participants and the nature of the study was fully explained (Table 1).

Physical, laboratory, iconographic, and histological examinations were carried out in the patients with gastrointestinal tumor. The diagnostic histology indicated planocellular carcinoma in esophagus, hepatocellular carcinoma in liver and adenocarcinoma in stomach, pancreas and colorectum. The control (healthy subjects) persons received physical and laboratory screening, and the medical histories were found to be negative (including the genetic backgrounds).

Measurement of serum retinoid levels

The serum levels of retinoids were measured by high performance liquid chromatography (HPLC). The serum levels of vitamin A, α- and β-carotene, α- and β-cryptoxanthin, zeaxanthin and lutein both in the control (healthy subjects) and in patients with GI tumors were measured. Blood samples were prepared for HPLC measurements: 2 mL of serum sample was shaken with 2 mL/L ethanol for 2 min, and extracted with 3 mL hexane for 2 min. The mixture was centrifuged for 5 min. As an internal standard, canthaxanthin was added to the removed homogenous organic phase, evaporated in vacuum. The residue was dissolved in 0.2 mL 1:4 dichloromethane/methanol and 0.125 mL of this solution was injected. The chromatographic system consists of a gradient former Model 250 B Glenco injector (Glycotec, Germany) and a time programmable UV-vis detector Model 166-2, equipped with Gold chromatography software (Beckmann, USA).The column is 150 mm× 4.6 mm in size packed with Chromsil-C 0.186 mm. The eluent was 30 mL/L water in methanol (A), methanol (B) and 20 v/v dichloromethane in methanol. The flow rate was 1.5 mL/min. The gradient program was 100% A for 30 s, 100% B for 3 min, to 100% for 4 min (linear steps). The time program of wavelength was 323 mm for 3.5 min (detecting vitamin A), then 450 mm (detecting other retinoids). The chromatograms were evaluated quantitatively by relating the peak areas of the individual components to canthaxanthin used as internal standard. The ratio of the molar extinctions of the authentic

Table 2 Serum retinoid level in patients with different gastrointestinal cancer (mean±SE, μmol/L)

Retinoids	Healthy subjects	Esophageal cancer	Gastric cancer	Liver cancer	Pancreatic cancer	Colon cancer	*In situ* colon cancer
Vitamin A	2.07±0.12	0.14±0.04[b]	1.02±0.10[b]	0.75±0.07[c]	1.68±0.10[NS]	0.35±0.02[c]	0.30±002[c]
α-Carotene	3.93±0.40	3.81±0.50[NS]	3.85±0.60[NS]	3.82±0.50[NS]	3.90±0.40[NS]	3.80±0.70[NS]	3.80±0.70[NS]
β-Carotene	8.59±0.40	7.50±0.30[NS]	8.01±0.35[NS]	8.10±0.30[NS]	8.40±0.40[NS]	6.80±0.40[NS]	7.90±0.30[NS]
α-Cryptoxanthin	4.10±0.50	4.00±0.60[NS]	3.90±0.50[NS]	4.00±0.40[NS]	3.90±0.40[NS]	4.00±0.30[NS]	4.00±0.30[NS]
β-Cryptoxanthin	6.00±0.60	5.90±0.40[NS]	6.00±0.50[NS]	5.90±0.40[NS]	5.90±0.50[NS]	4.95±0.40[NS]	4.90±0.30[NS]
Zeaxanthin	0.14±0.01	0.074±0.007[b]	0.08±0.004[a]	0.05±0.005[c]	0.03±0.002[c]	0.07±0.004[c]	0.03±0.002[c]
Lutein	0.11±0.007	0.10±0.04[NS]	0.10±0.02[NS]	0.08±0.007[NS]	0.06±0.004[b]	0.010±0.04[NS]	0.10±0.04[NS]

NS: not significant, [a]P<0.05, [b]P<0.01, [c]P<0.001 *vs* each group.

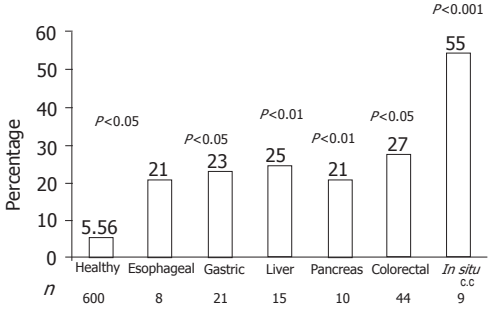

Figure 1 Prevalence of Leiden mutation in patients with different gastrointestinal tumors. The number in abscissa indicates the number of patients (600 healthy blood donors used as control).

samples to that of canthaxanthin was employed as a correction factor of the detector signals. The results were given in μmol/L, and expressed as mean±SE.

Determination of Leiden mutation

Leiden mutation was detected by polymerase-chain reaction (PCR)[12]. The DNA was isolated from 3 mL EDTA blood.

Statistical analysis

The changes in serum levels of retinoids were detected by the method of ANOVA. The prevalence of Leiden mutation was statistically analyzed by χ^2 test. P<0.05 (in the changes of serum retinoids and prevalence of Leiden mutation) was considered statistically significant.

RESULTS

The serum levels of vitamin A were decreased in all groups of patients with esophageal, gastric, hepatocellular and colorectal cancer meanwhile its level remained normal in patients with pancreatic cancer. The serum levels of α- and β-carotene, as provitamins of vitamin A, were normal in different groups of patients with GI cancer. Zeaxanthin level (without presence of any vitamin A property) was decreased significantly in patients with esophageal, gastric, hepatocellular, pancreatic, and colorectal cancer. No changes were obtained in the serum levels of α- and β-cryptoxanthin and lutein in the studied cancer patients (Table 2).

Prevalence of Leiden mutation accounted for 5.56% in 600 healthy blood donors, which was significantly higher in patients with esophageal (P<0.05), gastric (P<0.01), liver (P<0.01), pancreatic (P<0.05), colorectal (P<0.001) cancer. The higher prevalence of Leiden mutation (55%) was found *in situ* colorectal cancer (P<0.001, Figures 1 and 2).

DISCUSSION

Retinoids are chemical compounds of color materials from plants. Increased intake of plant foods can prevent different types of GI cancer. We studied the possible role of different retinoids (vitamin A, α- and β-carotene, α- and β-cryptoxanthin, zeaxanthin, and lutein) in patients with different GI cancer based on previous studies[5–9,19,20]. The location of GI tumor differed in organs (esophagus, stomach, pancreas, liver, and colon), suggesting that different etiological factors are involved in the development of different GI cancer (Barrett's esophageal metaplasia, chronic atrophic gastritis, viral infection in liver, chronic inflammatory bowel disease) in our everyday medical practice.

The serum levels of vitamin A and zeaxanthin were decreased significantly in all groups of GI cancer patients (not in patients with pancreatic cancer). Surprisingly the serum levels of provitamins were normal in patients with different GI tumor. These results indicate that transformation of provitamins into vitamin A is impaired by some factors at the level of liver, suggesting that the liver plays a key role in the development of tumor. Similar changes were observed in the serum levels of retinoids in patients with hepatocellular cancer, which offers a further proof for this hypothesis.

It is also interesting to evaluate the possible correlation between the terminal chemical structure, vitamin A activity and GI mucosal protection. Our results have clearly proved that there is no close correlation between the terminal chemical structure, vitamin A activity and GI mucosal protection (Table 3).

Similar results have been obtained in animal experiments[1,21-24] (Table 4). At present, no information is available on the correlation between the serum and tissue levels of retinoids in patients with different GI tumor. These observations cannot be done due to the obligatory necessity of histological evaluation of tumor tissues.

In animal experiments, β-carotene has been found in gastric mucosa of indomethacin-treated rats after

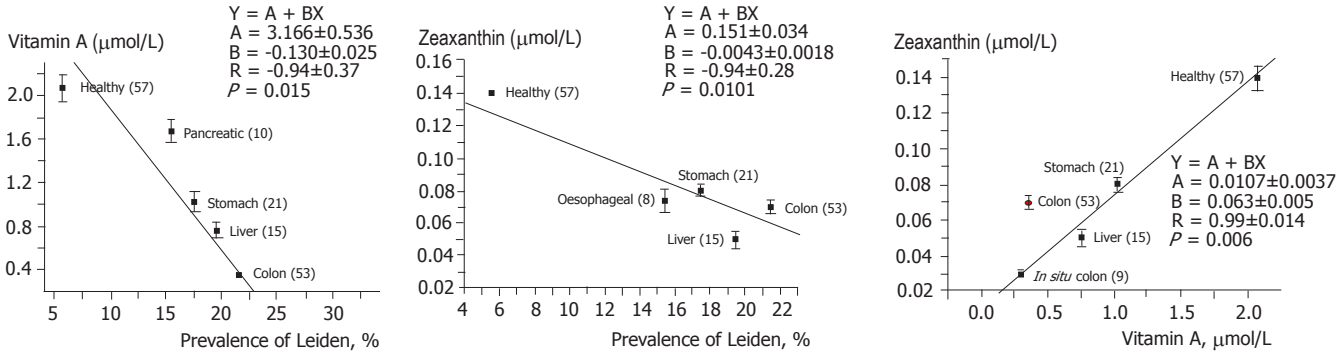

Figure 2 Correlation between the prevalence of Leiden mutation and serum level of vitamin A (**A**) and zeaxanthin (**B**) as well as between serum levels of vitamin A and zeaxanthin (**C**) in patients with different GI tumors. *n* indicates the number (in parenthesis) of examined patients.

Table 3 Changes of serum level of retinoids in patients with different gastrointestinal cancer

	Esophageal cancer	Gastric cancer	Hepatocellular cancer	Pancreatic cancer	Colorectal cancer	*In situ* colon cancer
Patients	8	21	15	10	44	9
Vitamin A	↓↓	↓↓	↓↓↓	NS	↓↓↓	↓↓↓
α-Carotene	NS	NS	NS	NS	NS	NS
β-Carotene	NS	NS	NS	NS	NS	NS
α-Cryptoxantin	NS	NS	NS	NS	NS	NS
β-Cryptoxantin	NS	NS	NS	NS	NS	NS
Zeaxantin	↓↓	↓	↓↓↓	↓↓↓	↓↓↓	↓↓↓
Lutein	NS	NS	NS	↓↓	NS	NS

P values: between healthy controls *vs* each group; ↓= $P<0.05$ ↓↓ = $P<0.01$ ↓↓↓ = $P<0.01$.

Table 4 Correlation between gastric cytoprotective effects of retinoids, their chemical structure and vitamin A activity in rats

Retinoids	Terminal chemical structure	Vitamin A activity	Gastric mucosal prevention
Vitamin A	*R* = *a*	Yes	Yes
β-Carotene	*X* = *Y* = *a*	Yes	Yes
β-Cryptoxanthin	*X* = a, *Y* = b	Yes	Yes
Zeaxanthin	*X* = *Y* = b	None	Yes
Lutein	*X* = b, *Y* = c	None	Yes
Capsorubin	*X* = *Y* = d	None	None
Capsanthin	*X* = b, *Y* = d	None	None
Capsanthol	*X* = b, *Y* = e	None	None
Lycopene	*X* = *Y* = f	None	None

acute surgical vagatomy[25,26], however no gastric mucosal protection is found, indicating that intact vagal nerve is necessary for the development of β-carotene-induced gastric cytoprotection[26]. The mechanism of retinoids is very complex. Our earlier observations indicate that the GI mucosal protective effect of retinoids depends on intact vagal nerve and adrenals as well as on gastric mucosal biochemical changes (retinoids produce a dose-dependent inhibition on the extent of ATP-transformation into ADP in association with a simultaneous increase in the transformation of ATP into cAMP), intact function of sulfhydryl groups and scavenger properties[9,19-28].

Retinoid-induced GI mucosal protection does not depend on the inhibition of gastric acid secretory responses, vitamin A activity, number of unsaturated double bonds, presence of a characteristic chemical structure of their terminal components and modification of vascular permeability[20]. These results clearly indicate that the beneficial effect of retinoids is much more complex than that of their scavengers. The results of biochemical observations suggest that different cAMP-dependent cellular regulatory mechanisms exist (including the functions of retinoid receptors, gene expressions)[7,20,27].

The involvement of vascular events is suggested in the development of different acute inflammatory processes in the GI tract[20]. That is the reason why we studied the potential role of Leiden mutation in acute and chronic gastrointestinal inflammatory processes (*Helicobacter pylori*-induced gastritis, viral hepatitis, Crohn's disease, ulcerative colitis). The prevalence of Leiden mutation increased in chronic inflammatory bowel diseases, but no changes were obtained in gastritis and hepatitis. The prevalence of Leiden mutation was also significantly higher in patients with esophageal, gastric, hepatocellular, pancreatic, and colorectal cancer. These results indicate that only the increased prevalence of Leiden mutation does not take place directly in the tumor genesis of human GI cancer. We compared the different results in the examined parameters in patients with acute and chronic gastrointestinal inflammatory diseases, and found a time-sequence process between the inflammatory diseases and GI cancer in patients, suggesting that retinoids play a key role in the development of precancerous state to cancerous state[5,8,20].

In conclusion, the prevalence of Leiden mutation is significantly correlated with decrease in serum levels of vitamin A and zeaxanthin, suggesting that retinoids play a role in the human GI tumor genesis.

ACKNOWLEDGMENTS

The authors express their thanks to Ms. Katalin Vincze and Ms. Erika Kispap for the careful preparation of the manuscript.

REFERENCES

1 **Javor T**, Bata M, Lovasz L, Moron F, Nagy L, Patty I, Szabolcs J, Tarnok F, Toth G, Mozsik G. Gastric cytoprotective effects of vitamin A and other carotenoids. *Int J Tissue React* 1983; **5:** 89-296

2 **Patty I**, Benedek S, Deak G, Javor T, Kenez P, Nagy L, Simon L, Tarnok F, Mozsik G. Controlled trial of vitamin A therapy in gastric ulcer. *Lancet* 1982; **2:** 876

3 **Patty I**, Benedek S, Deak G, Javor T, Kenez P, Moron F, Nagy L, Simon L, Tarnok F, Mozsik G. Cytoprotective effect of vitamin A and its clinical importance in the treatment of patients with chronic gastric ulcer. *Int J Tissue React* 1983; **5:** 301-307

4 **Patty I**, Tarnok F, Simon L, Javor T, Deak G, Benedek S, Kenez P, Nagy L, Mozsik G. A comparative dynamic study of the effectiveness of gastric cytoprotection by vitamin A, De-Nol, sucralfate and ulcer healing by pirenzepine in patients with chronic gastric ulcer (a multiclinical and randomized study). *Acta Physiol Hung* 1984; **64:** 379-384

5 **Rumi G Jr,** Szabo I, Vincze A, Matus Z, Toth G, Rumi G, Mozsik G. Decrease in serum levels of vitamin A and zeaxanthin in patients with colorectal polyp. *Eur J Gastroenterol Hepatol* 1999; **11:** 305-308

6 **Rumi Gy,** Szabó I, Matus Z, Vincze Á, Tóth Gy, Rumi Gy, Mózsik Gy Decrease of serum carotenoids in Crohn's disease. *J Physiol (Paris)* 2000; **94:** 159-161

7 **Mózsik Gy,** Bódis B, Karádi O, Király Á, Rumi Gy, Sütő G, Szabó I, Vincze Á Cellular Mechanisms of ß-carotene induced gastric cytoprotection in indomethacine treated rats. *Inflammopharmacology* 1998; **6**: 27-40

8 **Mozsik G**, Nagy Z, Nagy A, Rumi G, Karadi O, Czimmer J, Matus Z, Toth G, Par A. Leiden mutation (as genetic) and environmental (retinoids) sequences in the acute and chronic inflammatory and premalignant colon disease in human gastrointestinal tract. *J Physiol Paris* 2001; **95:** 489-494

9 **Rumi Gy,** Pár A, Matus Z, Rumi Gy, Mózsik Gy The Defensive Effects of Retinoids in the Gastrointestinal Tract (Animal Experiments and Human Observations). *Budapest, Akadémiai Kiadó* 2001: 1-79

10 **Bargen JA,** Barker NW Extensive arterial and venous thrombosis complicating chronic ulcerative colitis. *Arch Intern Med* 1936; **58:** 17-31

11 **Dahlback B,** Carlsson M, Svensson PJ. Familial thrombophilia due to a previously unrecognized mechanism characterized by poor anticoagulant response to activated protein C: prediction of a cofactor to activated protein C. *Proc Natl Acad Sci USA* 1993; **90:** 1004-1008

12 **Bertina RM,** Koeleman BP Koster T, Rosendaal FR, Dirven RJ, Ronde de H, Velden van der PA. Reitsma PH. Mutation in blood coagulation factor V associated with resistance to activated protein C resistance resistance. *Nature* 1994; **369**: 64-67

13 **Dahlback B**. New molecular insights into the genetics of thrombophilia. Resistance to activated protein C caused by Arg506 to Gln mutation in factor V as a pathogenic risk factor for venous thrombosis. *Thromb Haemost* 1995; **74:** 139-148

14 **Talbot RW**, Heppell J, Dozois RR, Beart RW Jr. Vascular complications of inflammatory bowel disease. *Mayo Clin Proc* 1986; 61: 140-145

15 **Best WR**, Becktel JM, Singleton JW, Kern F Jr. Development of a Crohn's disease activity index. National Cooperative Crohn's Disease Study. *Gastroenterology* 1976; **70:** 439-444

16 **Nagy Z,** Nagy A, Karadi O, Par A, Mozsik G. The high prevalence of the factor V Leiden mutation in central European inflammatory bowel disease patients. *Am J Gastroenterol* 2000; **95:** 3013-3014

17 **Nagy Z**, Nagy A, Karadi O, Figler M, Rumi G Jr, Suto G, Vincze A, Par A, Mozsik G. Prevalence of the factor V Leiden mutation in human inflammatory bowel disease with different activity. *J Physiol Paris* 2001; **95:** 483-487

18 **Papa A**, Danese S, Grillo A, Gasbarrini G, Gasbarrini A. Review article: inherited thrombophilia in inflammatory bowel disease. *Am J Gastroenterol* 2003; **98:** 1247-1251

19 **Mózsik Gy,** Pár A, Pár G, Gasztonyi B, Figler M Nutritional gastrointestinal mucosal protection: an update overview. In: Sikiric P, Seiwerth S., *Mózsik Gy., Arakava T., Takeuchi K.,* Ulcer Research, *Bologna Monduzzi Editore,* 1994: 155-162

20 **Mózsik Gy,** Neural, hormonal and pharmacological regulations of retinoids-induced gastrointestinal musocal protection. *Recent Res Develop in Life Sci* 2005; **3:** 131-202

21 **Mózsik Gy,** Garamszegi M, Jávor T, Sütő G, Vincze Á, Tóth Gy, Zsoldos T Correlations between the oxygen free radicals, membrane-bound ATP-dependent energy systems in relation of development of ethanol- and HCl- induced gastric mucosal damage and of β-carotene-induced gastric cytorprotection. In: Tsuchiya M, Kawai K, Kondo M, Yoshikawa T, eds. Free Radicals in Digestive Diseases. *Amsterdam: Elsevier Science Publisher Co., Inc,* 1988: 111-116

22 **Mózsik Gy,** Figler M, Garamszegi M, Jávor T, Nagy L, Sütő G, Vincze Á, Zsoldos T Mechanism of gastric mucosal cytoprotection. I. Time-sequence analysis of gastric mucosal membrane-bound ATP-dependent energy systems, oxygen free radicals and macroscopically appearance of gastric cytoprotection by PGI_2 and β-carotene in HCL- model of rats. In: Hayashi E, Niki M, Kondo M, Yoshikawa T eds. Medical, Biochemical, and Chemical Aspects of Free Radicals. *Amsterdam: Elsevier Science Publishers Co, Inc,* 1989: 1421 -1425

23 **Mózsik Gy,** Figler M, Garamszegi M, Jávor T, Nagy L, Sütő G, Vincze Á, Zsoldos T Mechanism of gastric mucosal cytoprotection. II. Time-sequence analysis of gastric mucosal membrane-bound ATP-dependent energy systems, oxygen free radicals and appearance of gastric mucosal damage. In: Hayashi E, Niki M, Kondo M, Yoshikawa T eds. Medical, Biochemical, and Chemical Aspects of Free Radicals. *Amsterdam Elsevier Science Publishers, Co, Inc* 1989: 1427-1431

24 **Mózsik Gy,**. Jávor T Therapy of ulcers with sulfhydryl and nonsulfhydryl antioxidants. In: Swabb A, Szabo S eds. Ulcer Disease. Investigation and Basis for Therapy. *New York, Basel, Hong Kong Marcel Dekker Inc,* 1991: 321-341

25 **Mozsik G**, Kiraly A, Garamszegi M, Javor T, Nagy L, Suto G, Toth G, Vincze A. Failure of prostacyclin, beta-carotene, atropine and cimetidine to produce gastric cyto- and general mucosal protection in surgically vagotomized rats. *Life Sci* 1991; **49:** 1383-1389

26 **Mozsik G**, Nagy Z, Nagy A, Rumi G, Karadi O, Czimmer J, Matus Z, Toth G, Par A. Leiden mutation (as genetic) and environmental (retinoids) sequences in the acute and chronic inflammatory and premalignant colon disease in human gastrointestinal tract. *J Physiol Paris* 2001; **95:** 229-239

27 **Mozsik G,** Bodis B, Figler M, Kiraly A, Karadi O, Par A, Rumi G, Suto G, Toth G, Vincze A. Mechanisms of action of retinoids in gastrointestinal mucosal protection in animals, human healthy subjects and patients. *Life Sci* 2001; **69:** 3103-3112

28 **Mózsik Gy,** Bódis B, Garamszegi M, Karádi O, Király Á, Nagy L, Sütő G, Tóth Gy, Vincze Á Role of vagal nerve in the development of gastric mucosal injury and its prevention by atropine, cimetidine, β-carotene and prostacyclin in rats. In: Szabo S, Tache Y, Neuroendocrinology of Gastrointestinal Ulceration. *New York Plenum Press,* 1995: 175-190

Science Editor Wang XL and Guo SY **Language Editor** Elsevier HK

PO Box 2345, Beijing 100023, China
www.wjgnet.com
wjg@wjgnet.com

ELSEVIER

World J Gastroenterol 2005;11(48):7651-7656
World Journal of Gastroenterology ISSN 1007-9327

• *RAPID COMMUNICATION* •

Helicobacter pylori upregulates prion protein expression in gastric mucosa: A possible link to prion disease

Peter C Konturek, Karolina Bazela, Vitaliy Kukharskyy, Michael Bauer, Eckhart G Hahn, Detlef Schuppan

Peter C Konturek, Karolina Bazela, Vitaliy Kukharskyy, Michael Bauer, Eckhart G Hahn, Detlef Schuppan, Department of Medicine, University of Erlangen-Nuernberg, 91054 Erlangen, Germany
Supported by Bavarian Ministry of Health, Germany
Co-correspondents: Eckhart G Hahn
Correspondence to: Assistant Professor Dr Peter C Konturek, Department of Medicine I, University Erlangen-Nuremberg, Germany. peter.konturek@med1.imed.uni-erlangen.de
Telephone: +49-9131-8535210 Fax: +49-9131-8535212
Received: 2005-01-18 Accepted: 2005-07-08

Abstract

AIM: Pathological prion protein (PrP^{sc}) is responsible for the development of transmissible spongiform encephalopathies (TSE). While PrPc enters the organism via the oral route, less data is available to know about its uptake and the role of gastrointestinal inflammation on the expression of prion precursor PrPc, which is constitutively expressed in the gastric mucosa.

METHODS: We studied PrPc expression in the gastric mucosa of 10 *Helicobacter pylori*-positive patients before and after successful *H pylori* eradication compared to non-infected controls using RT-PCR and Western blotting. The effect of central mediators of gastric inflammation, i.e., gastrin, prostaglandin E_2 (PGE_2), tumor necrosis factor alpha (TNF-α) and interleukin 1 beta (IL-1β) on PrPc expression was analyzed in gastric cell lines.

RESULTS: PrPc expression was increased in *H pylori*-infection compared with non-infected controls and decreased to normal after successful eradication. Gastrin, PGE_2, and IL-1β dose-dependently upregulated PrPc in gastric cells, while TNF-α had no effect.

CONCLUSION: *H pylori* infection leads to the upregulation of gastric PrPc expression. This can be linked to *H pylori* induced hypergastrinemia and increased mucosal PGE_2 and IL-1β synthesis. *H pylori* creates a milieu for enhanced propagation of prions in the gastrointestinal tract.

Key words: Prions; *Helicobacter pylori*; Gastrin; Pro-inflammatory cytokines

Konturek PC, Bazela K, Kukharskyy V, Bauer M, Hahn EG, Schuppan D. *Helicobacter pylori* upregulates prion protein expression in gastric mucosa: A possible link to prion disease. *World J Gastroenterol* 2005; 11(48): 7651-7656
http://www.wjgnet.com/1007-9327/11/7651.asp

INTRODUCTION

Transmissible spongiform encephalopathies (TSE) are fatal neurodegenerative diseases affecting both animals and human beings[1]. They are characterized by typical cerebral histopathological findings such as amyloid deposition, neuronal loss, and spongiform changes. The prion protein (PrP) can exist in the normal cellular form (PrPc) or in an "infectious" form (PrP^{sc}) that causes disease by converting apathogenic PrPc into pathogenic PrP^{sc}[2]. Previous studies have demonstrated that PrPc is required for prion infection propagation and infectivity has been suggested to be a consequence of conformational modification of PrPc by the infectious PrP^{sc}. Experiment on animals shows that animals lacking the PrPc gene are not able to propagate prion infectivity and are not able to develop the disease[3]. Both the prion isoforms differ dramatically in their physicochemical properties. Whereas PrPc is soluble and easily digested by proteinase K, PrP^{sc} is rich in β-sheet structure, aggregates into fibrils, and is resistant to proteinase K.

The main entry for prions is the gastrointestinal tract. Recent animal studies have shown that after oral exposure to pathogenic prions, PrP^{sc} accumulates in gut lymphoid tissues or in the enteric nervous system prior to its appearance in the central nervous system[4,5]. It has been postulated that prions then propagate from the enteric nervous system along the nerve pathways to ventral and dorsal root ganglia and further through the spinal cord into the brain cortex[4-6].

However, the mechanisms of propagation of prions from the gut lumen, before they reach intestinal lymph follicles or the enteric nervous system remain unexplained. Recently, the 67-ku laminin, binding protein, which can act as a PrP^{sc} receptor was demonstrated on small intestinal epithelial cells[7-9], suggesting that individuals with a high expression of this receptor could be at greater risk of developing TSE after oral challenge with PrP^{sc}. There is also evidence of transepithelial transport of pathogenic prions via intestinal M cells to adjacent lymph follicles (Peyer's patches)[10]. However, it is unknown if and how far gastrointestinal inflammation may influence PrPc expression

and thus potentially PrP^{sc} propagation in the GI tract.

MATERIALS AND METHODS

Patients

Ten *H pylori* positive patients with non-ulcer dyspepsia (mean age 47 years, range 20-79 years) were included in this study. All patients underwent upper gastrointestinal endoscopy during which four biopsies from the antrum and corpus were obtained. Patients with *H pylori* gastritis were graded according to the updated Sydney classification[11]. All patients underwent a second endoscopy 4 wk after completing successful eradication therapy consisting of clarithromycine 500 mg twice daily, amoxicillin 1 000 mg twice daily and omeprazole 40 mg twice daily for 1 wk. *H pylori* was considered to be successfully eradicated, if histology was normal and silver stainable organisms were not detected anymore in the follow-up endoscopy, during which again four biopsies from the antrum and corpus were obtained.

Cell culture

MKN45 and KATO III cell lines were obtained from the American Type Culture Collection. Cells were cultured in RPMI medium containing 10% of fetal calf serum (FCS), 2 mmol/L L-glutamine and antibiotics (1% penicillin-streptomycin, 0.5% gentamycin) at 37 ℃ in a water-saturated atmosphere of 95% air and 50 mL/L CO_2. Subconfluent MKN45 cells were incubated in RPMI without FCS and antibiotics for 24 h. Following serum starvation, cells were exposed to the increasing amounts of gastrin (Clinalfa, Switzerland, C-210), prostaglandin E_2 (PGE_2), interleukin 1 beta (IL-1β) or tumor necrosis factor alpha (TNF-α) (all from Calbiochem, Bad Soden, Germany).

Extraction of mRNA and RT-PCR analysis

Total RNA was extracted from biopsy specimens and cultured cells using TRIzol reagent (Gibco, Karlsruhe, Germany). Single stranded cDNA was generated from 5 μg RNA using Moloney murine leukemia virus reverse transcriptase (MMLV-RT) and oligo-(dT)-primers (both Stratagene, Heidelberg, Germany). Briefly, 5 μg of total RNA was uncoiled by heating (65 ℃ for 5 min) and then reverse transcribed (37 ℃ for 1 h) into complementary DNA (cDNA) in a 50 μL reaction mixture that contained 50 U MMLV-RT, 0.3 μg oligo-(dT)-primer, 40 U RNase Block Ribonuclease Inhibitor, 2 μL of a 100 mmol/L mixture of dNTPs, and 5 μL of buffer (10 mmol/L Tris-HCl, 50 mmol/L KCl, 5 mmol/L $MgCl_2$, pH 8.3). The resultant cDNA (2 μL) was amplified in a 50 μL reaction volume containing 2 U Taq polymerase, dNTP (200 μmol/L each), 1.5 mmol/L $MgCl_2$, 5 μL 10× PCR buffer (50 mmol/L KCl, 10 mmol/L Tris-HCl, pH 8.3) and specific primers at a final concentration of 1 mmol/L (all reagents from Takara, Shiga, Japan). Reactions were carried out at the following conditions: denaturation at 94 ℃ for 45 s, annealing at 60 °C (for GAPDH) and 67 ℃ (for PrPc) for 45 s and extension at 72 ℃ for 2 min. Polymerase chain reaction (PCR) products were detected by electrophoresis on a 1.5% agarose gel containing ethidium bromide. Product size was confirmed by using a 100-bp ladder (Takara, Shiga, Japan) as standard. The gel was photographed under UV transillumination and the intensity of PCR products were measured using a video image analysis system (Kodak Digital Science). The signal for PrPc mRNAs was standardized against that of the GAPDH mRNA from each sample and the results were expressed as PrPc/GAPDH mRNA ratio. The following PCR primers were used based on published sequences: PrPc (sense) 5`- GGCAGTG ACTATGAGGACCGTTAC-3´; PrPc (antisense) 5´-GG CTTGACCAGCATCTCAGGTCTA-3´; GAPDH (sense) 5´-GTCTTCACCACCATGGAGAAGGCT-3´; GAPDH (antisense) 5´-CATGCCAGTGAGCTTCCCGTTCA-3´. Expected product lengths were 528 bp for PrPc and 392 bp for GAPDH. All primer sequences were based on the sequences of the published cDNAs[12,13] and synthesized by GIBCO BRL/Life Technologies (Eggenstein, Germany).

Real-time RT-PCR

PrPc transcript levels were quantified by real-time RT-PCR. Using the Primer Express software (Perkin Elmer, Tokyo, Japan) TaqMan probe and primer set were designed based on published sequences of human PrPc (GenBank accession no.: GI 11079225); PrPc sense (5´ -CGCGAGCTTCTCCTCTCCTC-3´), PrPc antisense (5´ -GCCCAGGTCACTCCATGT-3´) and beta-2-microglobulin (β2M, GenBank accession no.: XM_007650), β2M sense 5 ´-TGACTTTGT-CACAGCCCAAGATA-3´, β2M antisense primer 5´-AATCCA-AATGCGGCATCTTC-3´. Probes for PrPc (5´-TCGCCATAA-TGACTGCTCTGCCTCGGT-3´) and β2M (5´-TGATGCTG-CTTACAT GTCTCGATCCCA-3´) were synthesized and labeled with a reporter dye (FAM) at the 5' end and quencher dye (TAMRA) at the 3´-end at MWG Biotech AG (Ebersberg, Germany). For normalization of differences in RNA amounts and efficiencies in the reverse transcription reactions, the housekeeping gene β2M was amplified under the same conditions as PrPc. Real-time RT-PCR was performed on a LightCycler (Roche, Mannheim, Germany) in a reaction volume of 15 μL using the LightCycler FastStart DNA Master Hybridization Probes Kit (Roche Molecular Biochemicals, Mannheim, Germany). The reaction mix included FastStart Taq DNA-Polymerase, dNTP-mix, reaction buffer, $MgCl_2$ (3.0 mmol/L), primers (2 μmol/L of each) and probe (0.5 μmol/L). After pippeting 13.5 μL of this mixture into LC-capillaries and 1.5 μL template cDNA was added. The capillaries were sealed and placed into the thermal chamber of the LightCycler. Samples were amplified with a pre-cycling step at 95 ℃ for 10 min, followed by 40 cycles of denaturation at 95 ℃ for 10 s, annealing at 60 ℃ for 15 s and extension at 72 ℃ for 6 s.

Immunoblot

MKN45 cells were incubated with Gastrin 1-1 000 nmol/L, PGE_2 1-100 nmol/L, TNF-α 1-10 ng/mL or IL-1β 1-10 ng/mL) for 24 h. Cells were collected, washed

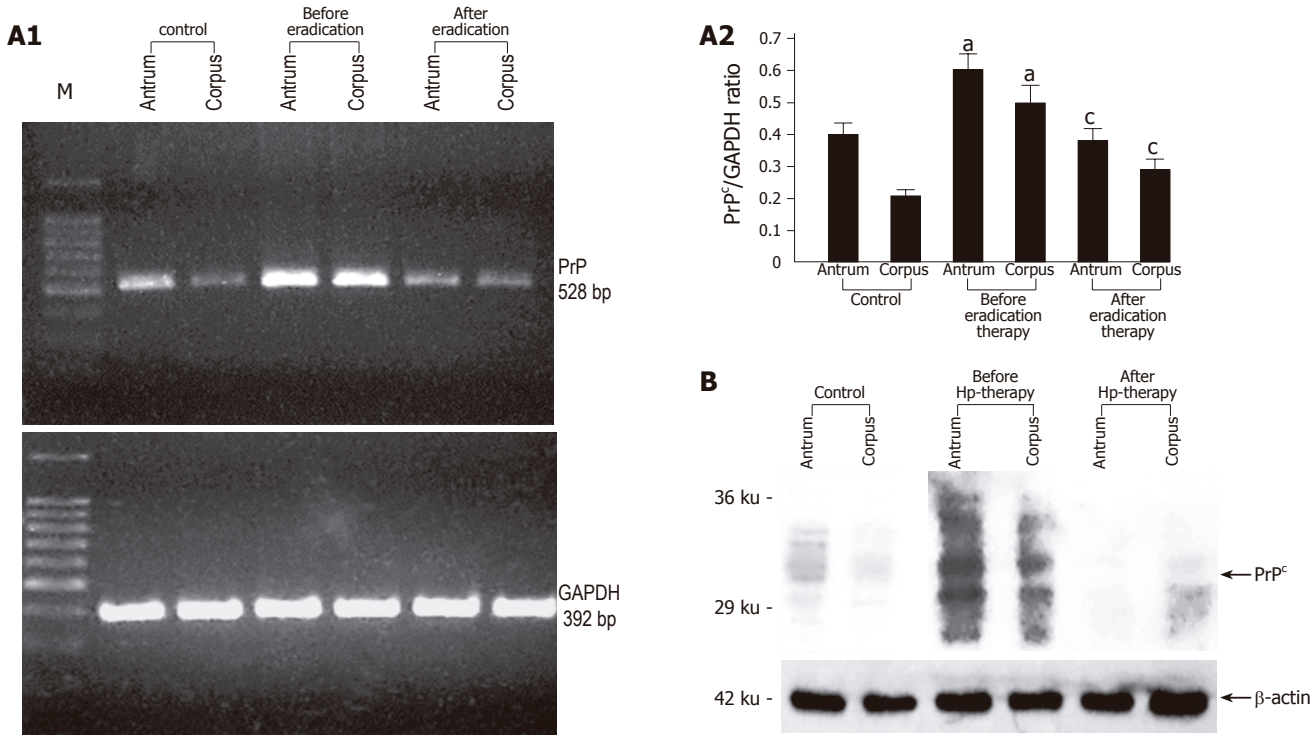

Figure 1 A: Representative RT-PCR and densitometric analysis showing PrPc mRNA expression in the gastric mucosa colonized with *H pylori* before and after successful eradication therapy (n = 10). Data are expressed as means ± SE. $^{a}P<0.05$ *vs* the control group, $^{c}P<0.05$ *vs* the expression before eradication therapy; **B**: Representative immunoblot analysis showing PrPc protein expression in the gastric mucosa colonized with *H pylori* before and after successful eradication therapy.

twice with PBS, and lysed in 0.4 mL of lysis buffer (0.06 mol/L Tris-HCl, pH 6.8, 10% glycerol, 2% SDS, 5% beta-mercaptoethanol, 0.0025% bromophenol blue). DNA was sheared by a needle, the solution heated at 95 ℃ for 5 min and centrifuged at 15 000 *g* for 2 min at 4 ℃. Twenty-five micrograms of the total protein was loaded on SDS-polyacrylamide gel, run at 40 mA and transferred to nitrocellulose (Protran, Schleicher&Schuell, Germany) by electroblotting. Filters were blocked with 3% bovine serum albumin (BSA, Sigma Aldrich, Germany) in TBS/Tween-20 buffer (137 mmol NaCl, 20 mmol Tris-HCl, pH 7.4, 0.1% Tween-20) before incubation with antibodies against PrPc (mouse monoclonal anti-PrP antibody 6H4, 1:2 000 dilution; Prionics, Switzerland), or β-actin (mouse monoclonal, dilution 1:5 000; Sigma Aldrich, Germany), followed by horseradish peroxidase-conjugated anti-mouse or anti-rabbit-IgG secondary antibody (dilution 1:20.000; Promega, WI, USA) dissolved in 1% non-fat milk in TBS/Tween-20. Immune complexes were detected by the SuperSignal West Pico Chemiluminescent Kit (Pierce, USA) and exposed to an X-ray film (Kodak, Wiesbaden, Germany).

Statistical analysis

Statistical analysis was performed using the Mann-Whitney Wilcoxon's test. The level of significance was set at $P<0.05$.

RESULTS

Analysis of gastric biopsy samples obtained endoscopically from patients infected with *H pylori*, which is found in approximately 50% of the world's population[14] and which causes gastric inflammation and ulceration[15] demonstrated highly increased PrPc expression compared to uninfected controls. After treatment with antibiotics which usually lead to *H pylori* eradication, PrPc mRNA and protein expression decreased to control levels (Figures 1A and B).

Using RT-PCR and immunoblotting we demonstrated the expression of PrPc mRNA and protein in two different gastric cell lines (MKN45 and KATO III) (Figure 2). In order to assess possible mechanisms responsible for the upregulation of PrPc during chronic *H pylori* gastritis, we analyzed the effect of increasing doses of key physiological modulators of the gastric mucosa on PrPc expression in these gastric cell lines. These modulators included gastrin (hypergastrinemia is a hallmark of chronic *H pylori* infection[16,17], PGE_2 chronic *H pylori* infection is accompanied by an increased mucosal production of PGE_2[18], and the pro-inflammatory cytokines TNF-α and IL-1β, which are implicated as key promoters of *H pylori*-induced gastritis and ulceration. When exposed to gastrin, cellular PrPc expression increased in a dose-dependent manner, reaching a peak value of 100 nmol/L (Figure 3A). Similarly, PGE_2 induced maximal PrPc mRNA and protein expression at 10 μmol/L (Figure 3B). While IL-1β increased PrPc expression in a dose-dependent manner at the mRNA and protein level (Figures 3C and D), TNF-α showed no effect (Figure 3E).

DISCUSSION

Considering the importance of the human gastrointestinal

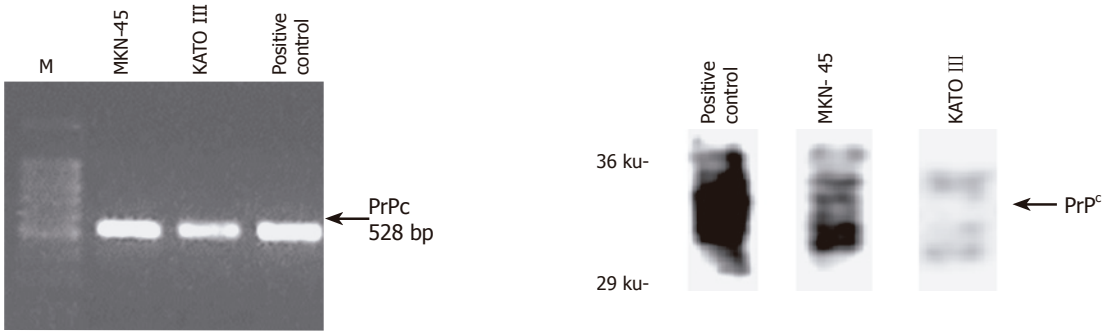

Figure 2 Protein expression of PrPc in two gastric cell lines (MKN45 and KATO III); the positive control is from bovine brain.

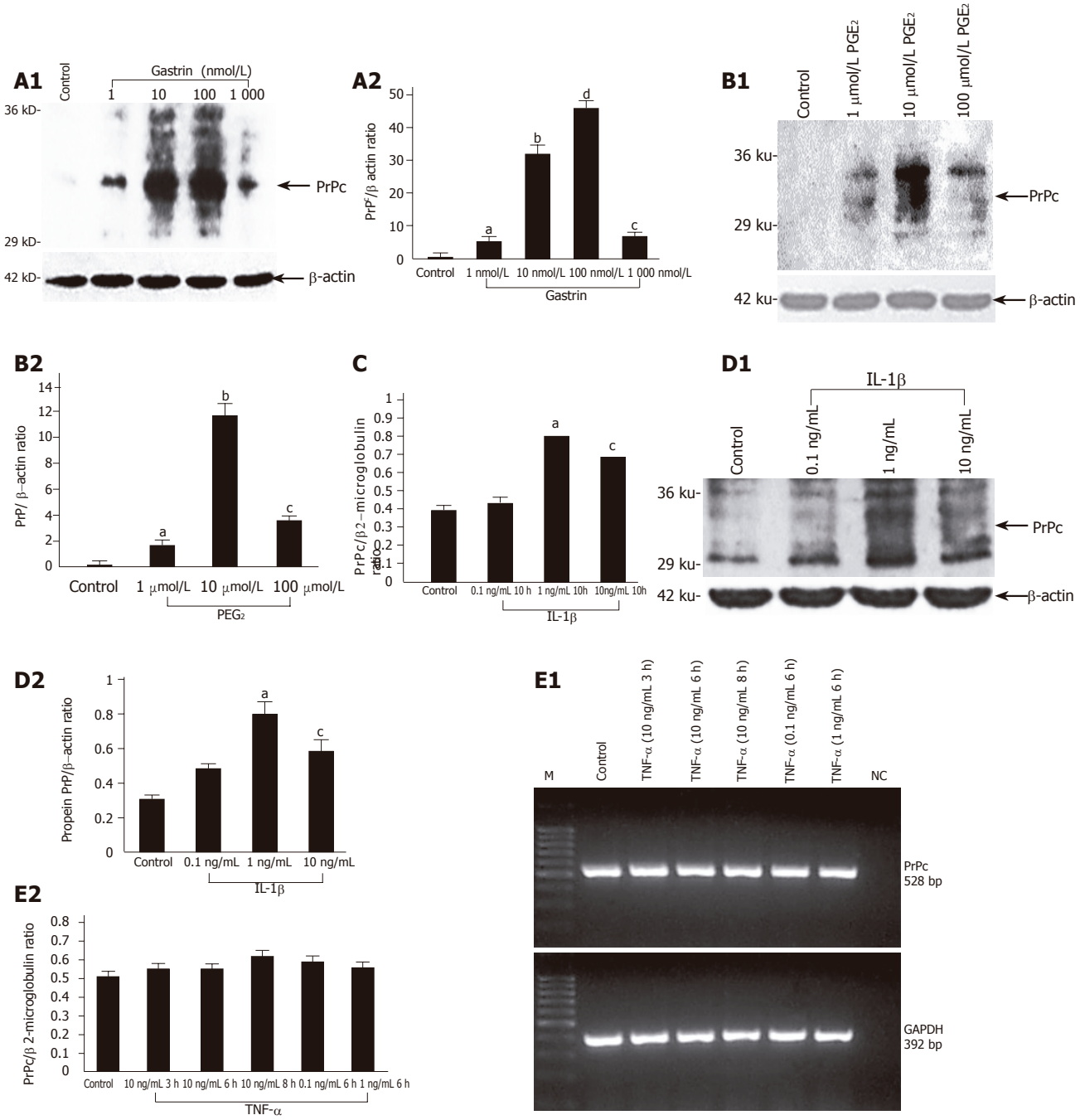

Figure 3 PrPc protein and mRNA expression in MKN45 cells incubated with increasing doses of gastrin (1-1 000 nmol/L) (**A**), PGE_2 (1-100 μmol/L) [a]*P*<0.05 *vs* control, [b]*P*<0.001 *vs* control, [c]*P*<0.05 *vs* control, [d]*P*<0.001 *vs* control (**B**), interleukin 1β (0.1-10 ng/mL) (**C** and **D**) or TNF-α (0.1-10 ng/mL) [a]*P*<0.05 *vs* control, [b]*P*<0.001 *vs* control, [c]*P*<0.05 *vs* control (**E**). Data represent means±SE of three independent experiments. At the mRNA level, the expression of PrPc was normalized to β2-microglobulin and at the protein level to β-actin.

tract for the propagation of prions from the gut to the central nervous system, we analyzed the expression of PrPc in human beings with *H pylori* infection (determined by histology) before and after eradication therapy. This study provides the first *in vitro* and *in vivo* evidence that *H pylori* infection is accompanied by a dramatic upregulation of PrPc expression in the gastric mucosa. The physiological importance of the observed PrPc overexpression in *H pylori* infected gastric mucosa remains elusive. However, multiple physiological functions of PrPc were identified only recently. Thus, PrPc is involved in signal transduction, from the extracellular space to cells, participates in intracellular signaling and regulation of cell survival, protects against oxidative stress, and interacts preferentially with some of the heat-shock-proteins[19-20]. Therefore, the main role of increased PrPc expression in the stomach appears to be the protection of the gastric mucosa against oxidative stress induced, for example by chronic *H pylori* infection[21]. This assumption is further supported by a previous study demonstrating that PrPc upregulates antioxidant enzyme activities[22]. Another possible role of PrPc in the gastric mucosa could be the modulation of apoptosis induced by *H pylori*[23], since PrPc was shown to protect cells against Bax-mediated cell death[24,25]. But this issue remains controversial, as other investigators demonstrated that PrPc may sensitize cells to apoptosis[26,27]. An explanation could be the preferential use of various neuronal cell lines[28] *in vitro* which necessitates further *in vitro* and *in vivo* studies on modulation of apoptosis gastric epithelial cells by PrPc.

In the present study, using quantitative RT-PCR and Western blot analysis we demonstrated an increased PrPc expression in the *H pylori* infected mucosa which significantly decreased after a successful eradication therapy. The mechanisms behind this phenomenon appears to be linked to the hypergastrinemia observed during *H pylori* infection which is supported by our *in vitro* data showing a dose-dependent increase in PrPc expression in gastric epithelial MKN45 cells after incubation with gastrin. According to previous studies, this finding shows that PrPc expression may be modulated by different growth factors[29,30].

Since *H pylori* infection is associated with an increased generation of prostaglandins in the gastric mucosa[18], we analyzed the effect of prostaglandin PGE_2 on PrPc expression in MKN45 cells. At the protein level, we observed a dose-dependent increase in PrPc expression which reached its maximum at the physiological concentration of 10 μmol/L. This could represent another mechanism by which the *H pylori*-induced inflammatory response triggers protective mechanisms in the gastric mucosa.

According to previous studies, chronic infection with *H pylori* is accompanied by a significantly increased generation of pro-inflammatory cytokines, especially IL-1β and TNF-α, in the gastric mucosa. Thus, both cytokines could be responsible for the upregulation of PrPc in the gastric mucosa colonized by *H pylori*. Here we have demonstrated a significant dose-dependent increase of PrPc expression in MKN45 cells incubated with IL-1β, while in contrast, TNF-α showed no effect. We did not further analyze the difference in the action of these two cytokines, but it has been shown by others that these two cytokines evoke different signaling cascades in gastric epithelial cells[31,32].

Gastrin, IL-1β and prostaglandins are not the sole candidates for stimulation of PrPc expression in *H pylori* infected gastric mucosa. Although not investigated in this study, heat shock proteins could represent additional important factors responsible for the upregulation of PrPc. Previous studies demonstrated that exposure of the gastric mucosa to *H pylori* lipopolysaccharide leads to a strong upregulation of heat shock proteins which could in turn stimulate the PrPc expression in gastric epithelial cells[33]. In a previous study, it was found that cellular stress upregulates PrPc expression through its interaction with the heat shock elements (HSE) on the PrPc gene promoter[34]. Together these findings suggest a regulation of PrPc expression by heat shock proteins. All these findings demonstrate the complexicity of the regulation PrPc expression and underscore the need to further analyze the precise link between *H pylori* infection and PrPc expression.

In conclusion, our results indicate that (1) *H pylori* infection is accompanied by a dramatic upregulation of PrPc expression in the gastric mucosa; (2) this is linked to *H pylori*-induced hypergastrinemia, increased mucosal prostaglandin synthesis and enhanced mucosal generation of IL-1β; (3) Thus, *H pylori* infection may promote uptake and propagation of alimentary prions from the gastrointestinal tract by upregulation of PrPc expression.

REFERENCES

1 **Prusiner SB.** Prions. *Proc Natl Acad Sci USA* 1998; **95**: 13363-13383
2 **Raeber AJ,** Brandner S, Klein MA, Benninger Y, Musahl C, Frigg R, Roeckl C, Fischer MB, Weissmann C, Aguzzi A. Transgenic and knockout mice in research on prion diseases. *Brain Pathol* 2002; **98**: 715-733
3 **Weissmann C,** Bueler H, Fischer M, Sailer A, Aguzzi A, Aguet M. PrP-deficient mice are resistant to scrapie. *Ann NY Acad Sci* 1994; **724**: 235-240
4 **Beekes M,** McBride PA. Early accumulation of pathological PrP in the enteric nervous system and gut-associated lymphoid tissue of hamsters orally infected with scrapie. *Neurosci Lett* 2000; **278**: 181-184
5 **Shmakov AN,** Ghosh S. Prion proteins and the gut: une liaison dangereuse? *Gut* 2001; **48**: 443-447
6 **Shmakov AN,** McLennan NF, McBride P, Farquhar CF, Bode J, Rennison KA, Ghosh S. Cellular prion protein is expressed in the human enteric nervous system. *Nat Med* 2000; **6**: 840-841
7 **Gauczynski S,** Peyrin JM, Haik S, Leucht C, Hundt C, Rieger R, Krasemann S, Deslys JP, Dormont D, Lasmezas CI, Weiss S. The 37-kDa/67-kDa laminin receptor acts as the cell surface receptor for the cellular prion protein. *EMBO J* 2001; **20**: 5863-5875
8 **Rieger R,** Edenhofer F, Lasmezas CI , Weiss S. The human 37-kDa laminin receptor precursor interacts with the prion protein in eucaryotic cells. *Nature Med* 1997; **3**: 383-1388
9 **Shmakov AN,** Bode J, Kilshaw PJ, Ghosh S. Diverse patterns of expression of the 67-kD laminin receptor in human small intestinal mucosa: potential binding sites for prion proteins? *J Pathol* 2000; **191**: 318-322
10 **Heppner FL,** C.A., Klein MA, Prinz M, Fried M, Kraehenbuhl

JP, Aguzzi A. Transepithelial prion transport by M cells. *Nature Med* 2001; **7**: 976-977

11 **Dixon MF,** Genta RM, Yardley JH , Correa P. Classification and grading of gastritis. The updated Sydney System. International Workshop on the Histopathology of Gastritis, Houston 1994. *Am J Surg Pathol* 1996; **20**: 1161-1181

12 **Burthem J,** Urban B, Pain A, Roberts DJ. The normal cellular prion protein is strongly expressed by myeloid dendritic cells. *Blood* 2001; **98**: 3733-3738

13 **Konturek PC,** Konturek SJ, Sulekova Z, Meixner H, Bielanski W, Starzynska T, Karczewska E, Marlicz K, Stachura J, Hahn EG. Expression of hepatocyte growth factor, transforming growth factor alpha, apoptosis related proteins Bax and Bcl-2, and gastrin in human gastric cancer. *Aliment Pharmacol Ther* 2001; **15**: 989-999

14 **Brown LM.** Helicobacter pylori: epidemiology and routes of transmission. *Epidemiol Rev* 2002; ***200***: 283-297

15 **Marshall BJ,** Warren JR. Unidentified curved bacilli in the stomach of patients with gastritis and peptic ulceration. *Lancet* 1984; **1**: 1311-1315

16 **Levi S,** Beardshall K, Swift I, Foulkes W, Playford R, Ghosh P, Calam J. Antral Helicobacter pylori, hypergastrinaemia, and duodenal ulcers: effect of eradicating the organism. *BMJ* 1989; **299**: 1504-1505

17 **Smith JT,** Pounder RE, Nwokolo CU. Inappropriate hypergastrinaemia in asymptomatic healthy subjects infected with Helicobacter pylori. *Gut* 1990; **28**, 522-525

18 **Hudson N,** Balsitis M, Filipowicz F, Hawkey CJ. Effect of Helicobacter pylori colonisation on gastric mucosal eicosanoid synthesis in patients taking non-steroidal anti-inflammatory drugs. *Gut* 1993; **34**: 748-7512

19 **Lasmezas CI.** Putative functions of PrPc. *Br Med Bull* 2003; **66**: 61-70

20 **Derrington EA,** Darlix JL. The Enigmatic Multifunctionality of the Prion Protein. *Drug News Perspect* 2002; **15**: 206-219

21 **Felley CP,** Pignatelli B, Van Melle GD, Crabtree JE, Stolte M, Diezi J, Corthesy-Theulaz I, Michetti P, Bancel B, Patricot LM, Ohshima H, Felley-Bosco E. Oxidative stress in gastric mucosa of asymptomatic humans infected with Helicobacter pylori: effect of bacterial eradication. *Helicobacter* 2002; **7**: 342-348

22 **Rachidi W,** Vilette D, Guiraud P, Arlotto M, Riondel J, Laude H, Lehmann S, Favier A . Expression of prion protein increases cellular copper binding and antioxidant enzyme activities but not copper delivery. *J Biol Chem* 2003; **278**: 9064-9072

23 **Konturek PC,** Pierzchalski P, Konturek SJ, Meixner H, Faller G, Kirchner T, Hahn EG. *Helicobacter pylori* induces apoptosis in gastric mucosa through an upregulation of Bax expression in humans. *Scand J Gastroenterol* 1999; **34**: 375-383

24 **Kuwahara C,** Takeuchi AM, Nishimura T , Haraguchi K, Kubosaki A, Matsumoto Y, Saeki K, Matsumoto Y, Yokoyama T, Itohara S, Onodera T. Prions prevent neuronal cell-line death. *Nature* 1999; **400**: 225-226

25 **Bounhar Y,** Zhang Y, Goodyer CG, LeBlanc A. Prion protein protects human neurons against Bax-mediated apoptosis. *J Biol Chem* 2001; **276**: 39145-39149

26 **Paitel E,** Alves da Costa C, Vilette D, Grassi J, Checler F. Overexpression of PrPc triggers caspase 3 activation: potentiation by proteasome inhibitors and blockade by anti-PrP antibodies. *J Neurochem* 2002; **83**: 1208.1214

27 **Paitel E,** Fahraeus R, Checler F. Cellular prion protein sensitizes neurons to apoptotic stimuli through Mdm2-regulated and p53-dependent caspase 3-like activation. *J Biol Chem* 2003; **278**: 10061-10066

28 **Satoh J,** Kurohara K, Yukitake M, Kuroda Y. Constitutive and cytokine-inducible expression of prion protein gene in human neural cell lines. *J Neuropathol Exp Neurol* 1998; **57**: 131-139

29 **Sauer H,** Wefer K, Vetrugno V, Pocchiari M, Gissel C, Sachinidis A, Hescheler J, Wartenberg M. Regulation of intrinsic prion protein by growth factors and TNF-alpha: the role of intracellular reactive oxygen species. *Free Radic Biol Med* 2003; **35**: 586-594

30 **Kuwahara C,** Kubosaki A, Nishimura T, Nasu Y, Nakamura Y, Saeki K, Matsumoto Y, Onodera T. Enhanced expression of cellular prion protein gene by insulin or nerve growth factor in immortalized mouse neuronal precursor cell lines. *Biochem Biophys Res Commun* 2000; **268**: 763-766

31 **Clerk A,** Harrison JG, Long CS, Sugden PH. Pro-inflammatory cytokines stimulate mitogen-activated protein kinase subfamilies, increase phosphorylation of c-Jun and ATF2 and upregulate c-Jun protein in neonatal rat ventricular myocytes. *J Mol Cell Cardiol* 1999; **31**: 2087-2099

32 **Wang H,** Xu L, Venkatachalam S, Trzaskos JM, Friedman SM, Feuerstein GZ, Wang X. Differential regulation of IL-1beta and TNF-alpha RNA expression by MEK1 inhibitor after focal cerebral ischemia in mice. *Biochem Biophys Res Commun* 2001; **286**: 869-874

33 **Brzozowski T,** Konturek PC, Moran AP, et al. Enhanced expression of gastric mucosa to damaging agents in the rat stomach adapted to Helicobacter pylori lipopolysaccharide. *Digestion* 2003; **67**: 195-208

34 **Shyu WC,** Harn HJ, Saeki K, Kubosaki A, Matsumoto Y, Onodera T, Chen CJ, Hsu YD, Chiang YH. Molecular modulation of expression of prion proteins by heat shock. *Mol Neurobiol* 2002; **26**; 1-12

Science Editor Xia HHX and Guo SY **Language Editor** Elsevier HK

PO Box 2345, Beijing 100023, China
www.wjgnet.com
wjg@wjgnet.com

ELSEVIER

World J Gastroenterol 2005;11(48):7657-7660
World Journal of Gastroenterology ISSN 1007-9327

• *RAPID COMMUNICATION* •

Asthma and gastroesophageal reflux disease: Effect of long-term pantoprazole therapy

Calabrese Carlo, Fabbri Anna, Areni Alessandra, Scialpi Carlo, Zahlane Desiree, Di Febo Giulio

Calabrese Carlo, Fabbri Anna, Areni Alessandra, Scialpi Carlo, Zahlane Desiree, Di Febo Giulio, Department of Internal Medicine and Gastroenterology, University of Bologna, Italy
Supported by grants from Altana-Pharma Italia
Correspondence to: Carlo Calabrese, Department of Internal Medicine and Gastroenterology, Policlinico S. Orsola-Malpighi, Via Massarenti 9, 40138 Bologna, Italy. calabrese.c@med.unibo.it
Telephone: +390516364191 Fax: +390516364138
Received: 2005-03-01 Accepted: 2005-08-03

Abstract

AIM: To define the prevalence of gastroesophageal reflux disease (GERD) in mild persistent asthma and to value the effect of pantoprazole therapy on asthmatic symptoms.

METHODS: Seven of thirty-four asthmatic patients without GERD served as the non-GERD control group. Twenty-seven of thirty-four asthmatic patients had GERD (7/27 also had erosive esophagitis, sixteen of them presented GERD symptoms. An upper gastrointestinal endoscopy was performed in all the subjects to obtain five biopsy specimens from the lower 5 cm of the esophagus. Patients were considered to have GERD when they had a dilation of intercellular space (DIS)>0.74 μm at transmission electron microscopy. Patients with GERD were treated with pantoprazole, 80 mg/day. Forced expiratory volume in one second (FEV1) was performed at entry and after 6 mo of treatment. Asthmatic symptoms were recorded. The required frequency of inhaling rapid acting β2-agonists was self-recorded in the patients' diaries.

RESULTS: Seven symptomatic patients presented erosive esophagitis. Among the 18 asymptomatic patients, 11 presented DIS, while all symptomatic patients showed ultrastructural esophageal damage. Seven asymptomatic patients did not present DIS. At entry the mean of FEV_1 was 1.91 L in symptomatic GERD patients and 1.88 L in asymptomatic GERD patients. After the treatment, 25 patients had a complete recovery of DIS and reflux symptoms. Twenty-three patients presented a regression of asthmatic symptoms with normalization of FEV1. Four patients reported a significant improvement of symptoms and their FEV1 was over 80%.

CONCLUSION: GERD is a highly prevalent condition in asthma patients. Treatment with pantoprazole (80 mg/day) determines their improvement and complete regression.

Key words: Asthma; Gastroesophageal reflux disease; Pantoprazole; NERD; ERD; Dilated intercellular spaces; TEM

Carlo C, Anna F, Alessandra A, Carlo S, Desiree Z, Giulio DF. Asthma and gastroesophageal reflux disease: Effect of long term pantoprazole therapy. *World J Gastroenterol* 2005; 11(48): 7657-7660
http://www.wjgnet.com/1007-9327/11/7657.asp

INTRODUCTION

The association of asthma with GERD has attracted particular attention because about half of the patients with asthma also have GERD[1–3]. Mechanisms by which esophageal reflux triggers asthma include acid aspiration, direct acid stimulation of the esophagus, or stimulation of vagal nerves which heightens bronchial responsiveness to extrinsic allergens. Clinicians are advised to treat GERD to improve and control asthma[1]. Endoscopic findings of the esophageal erosions (ERD) confirm the diagnosis of GERD. However, absence of macroscopic signs of damage does not rule out an endoscopy negative esophagitis (NERD) that may also be associated with asthma[4]. Recently, we have shown the presence of a highly sensitive and specific marker of damage, the dilation of intercellular spaces (DIS) in GERD with or without erosions, which permits us to define NERD with a strong accuracy[5].

The prevalence of GERD and effects of proton pump inhibitor (PPI) treatment on the decors of asthma are still uncertain and results obtained are often conflicting[6,7]. Bias in the selection of asthma patients or during PPI treatment and absence of highly sensitive parameters of morphology to define the presence of esophageal mucosa damage, may affect the reported results of studies. Moreover, several studies have a non-randomized poor quality design which leads to a further potential error on definition of treatment effects[8,9].

For this reason, the aim of the present study was to define the prevalence of GERD in patients with mild persistent intrinsic asthma and to estimate the effect of pantoprazole in relation with GERD, asthmatic symptoms and respiratory function in this subset of patients.

Table 1 Demographic data of 34 asthmatic patients with or without GERD symptoms

	Symptomatic	Asymptomatic	
		GERD	Non-GERD
Number	16	11	7
Male/female	6/10	5/6	4/3
ERD	7	0	0
NERD	9	11	7
Age (mean±SD) (yrs)	33.75±10	38.27±5.68	36.14±8.76
DIS (mean±SD) (μm)	2.105±0.262	2.08±0.24	0.5±0.08
FEV1 (mean±SD) (L)	1.87±0.05	1.95±0.04	1.88±0.02

Table 2 Comparison of background characteristics of asthmatic patients with GERD and controls

	GERD (27)	Controls (7)	*t*-Test
Age (yrs) (mean±SD)	35.59±8.67	36.14±8.76	NS
Male/female	11/16	4/3	NS
QUEST score	8.8±4.5	0.12±0.8	$P<0.0001$
Erosive esophagitis	7 (4B, 2C, 1D)	0	$P<0.05$
DIS (mean±SD) (μm)	2.09±0.24	0.5±0.08	$P<0.001$
FEV_1 (L)	1.91±0.045	1.88±0.02	NS

MATERIALS AND METHODS

Among the 301 asthma patients, 34 consecutive asthma patients with intrinsic, mild persistent asthma[10] were enrolled and their diagnosis was made according to the diagnostic criteria recommended by American Thoracic Society (ATS). Patients were excluded if they had any of the following: past or present smoker, unequivocally extrinsic and/or occupational asthma, acids suppression therapy within 4 wk prior to recruitment, previous gastroesophageal surgery, professional voice users, previous glottal surgery or radiotherapy or malignancy, immune suppression therapy, age above 50 years.

For evaluation of ventilation function, FEV_1 was performed using the Jaeger Masterlab spirometer based on the guidelines of ATS[14]. Symptoms were recorded in each patient to rate the frequency and severity of asthmatic episodes. Symptom severity was rated on a scale of 0 (none) to 6 (severe). The required frequency of inhaling rapid acting β2-agonists was self-recorded in the patients' diaries. All the patients did not use systemic bronchodilators or corticosteroids.

For the diagnosis of GERD, the patients underwent gastrointestinal endoscopic (GE) examination and interviews according to the QUEST questionnaire[11]. Reflux esophagitis was graded according to the Los Angeles classification[12,13]. During endoscopy, five biopsy specimens were taken from the lower 5 cm of esophagus for ultrastructural evaluation. At transmission electron microscopy (TEM), ultrastructural signs of mucosal damage were considered to be the DIS>0.74 μm[5]. To obtain this measure, 10 photomicrographs of biopsy specimens of the supra-basal layer of the esophageal mucosa from each patient were taken. At least 10 randomly selected perpendicular trans-sections to adjacent membranes were drawn and measured in each image for a total of 100 measurements in each case. Measurements obtained were used to calculate the mean DIS score.

The endoscopists, pneumologists and pathologists were unaware of the clinical history of the patients. Data were collected separately by another physician (DZ) who assigned patients to different groups and established the therapy. Symptomatic and asymptomatic patients with or without endoscopic signs, were considered to have GERD when they had ultrastructural evidence of esophageal damage. Patients so defined with GERD were treated with pantoprazole, 80 mg once daily for 6 mo. After 6 mo, a new endoscopy with biopsies was performed and DIS was evaluated. Improvements in GERD symptoms according to the QUEST questionnaire were recorded. FEV_1 was valued.

Asthma patients without GERD were followed up for 6 mo and the use of anti-asthmatic treatment (inhaled glucocorticosteroid 200–1 000 μg BDP or rapid acting β_2-agonists) and symptoms were recorded. We considered them as the control group for the evaluation of asthmatic symptoms, respiratory function and drug assumption with time.

The study was conducted in accordance with the guidelines of the Declaration of Helsinki. The local research ethical committee approved the study protocol in 2002. The objective of the study was explained to each patient and written informed consent was obtained from each one.

For statistical analysis, one-way analysis of variance, paired and unpaired *t* test were performed. The results of the treatment were compared by χ^2 test or Fisher' s exact test. All statistical analyses were two-tailed. Data were analyzed with SPSS software. $P<0.05$ was considered statistically significant.

RESULTS

Among the 34 patients evaluated, 16 presented GERD symptoms (heartburn and/or acid regurgitation) and 18 were asymptomatic for reflux disease. At endoscopy, all asymptomatic subjects had no macroscopic signs of esophagitis. Seven symptomatic patients (43.75%) presented erosive esophagitis (ERD).

Among the 18 asymptomatic patients, 11 (61%) presented DIS, while all symptomatic patients showed ultrastructural esophageal damage. Seven asymptomatic patients (38.9%) did not present DIS (Table 1). At entry the mean of FEV_1 was 1.91 L in symptomatic GERD patients and 1.88 L in asymptomatic GERD patients. The two groups at baseline were not significantly different (P = NS) (Table 2).

All the 27 patients with GERD (79.4%) completed the study. They were treated for 6 mo with pantoprazole. At the end of this period erosive esophagitis was healed in seven patients with ERD. Among the 25 patients (92.6%), 6 with ERD and 19 with NERD, had a complete recovery of DIS and reflux symptoms (Table 3 and Figure 1A).

Twenty-three patients (85.18%) presented a regression of asthmatic symptoms (Table 4 and Figure 1B), including nocturnal asthma and FEV_1 (2.75 L, $P<0.01$), but there

Table 3 Effect of treatment on dilation of intercellular space (DIS) in 25 responders to pantoprazole (mean±SD)

		Value (μm)	*t*-Test
Symptomatic	Baseline	2.105±0.261	*P*<0.001
	After therapy	0.592±0.194	
Asymptomatic	Baseline	2.081±0.242	*P*<0.001
	After therapy	0.517±0.072	

Table 4 Effect of therapy on asthma symptom score in GERD patients (mean±SD)

		Baseline	After therapy	*t*-test
Patients	GERD	4.37±0.97	0.33±0.83	*P*<0.001
	Controls	4.57±0.79	4.14±0.38	*P* = NS

was no statistical difference in respiratory parameters between patients with ERD and those with NERD. After 3 wk of treatment no more asthmatic symptoms occurred and no inhaler was needed.

Four patients (14.8%) reported a significant improvement in symptoms, including dyspnea, cough, wheeze, and expectoration with a significant reduction in the consumption of inhalers and FEV_1 over 80%.

DISCUSSION

Physicians mostly focus on the effects induced by gastroesophageal reflux into the esophagus. The anatomic proximity of the esophagus to the respiratory tract in some patients also leads to his involvement. Thus, the spectrum of symptoms of GERD includes also respiratory complications like chronic cough, laryngeal disorders, chest pain, and asthma. In this contest, GERD gains an additional fraction of significance and has been reported to occur in 30-89% of asthma patients[13,15-18].

Treatment with PPI can relieve the symptoms of GERD in up to 90% of patients. It has been tempted to investigate if treatment of GERD with PPI could improve also the respiratory symptoms of asthma patients[19].

It seems obvious that to achieve improvement in asthma symptoms and lung function, the treatment needs to be effective in controlling reflux as well as reducing acidity. However, this has been only objectively confirmed in few studies using high doses of omeprazole[19]. An optimal study design would establish if the esophageal damage is adequately treated as a prerequisite to assess the effects on asthma.

In this study, we analyzed the esophageal specimens from 31 consecutive asthmatic patients, 16 of them were symptomatic for GERD. We found that all symptomatic patients presented an ultrastructural pattern of damage and 73% of asymptomatic GERD patients had esophageal signs of ultrastructural damage, suggesting that GERD is a highly prevalent condition even in asymptomatic patients. Acid stress might initiate or exacerbate asthma in this contest. Electron microscopy is able to find out esophageal damage, especially in asymptomatic patients with NERD.

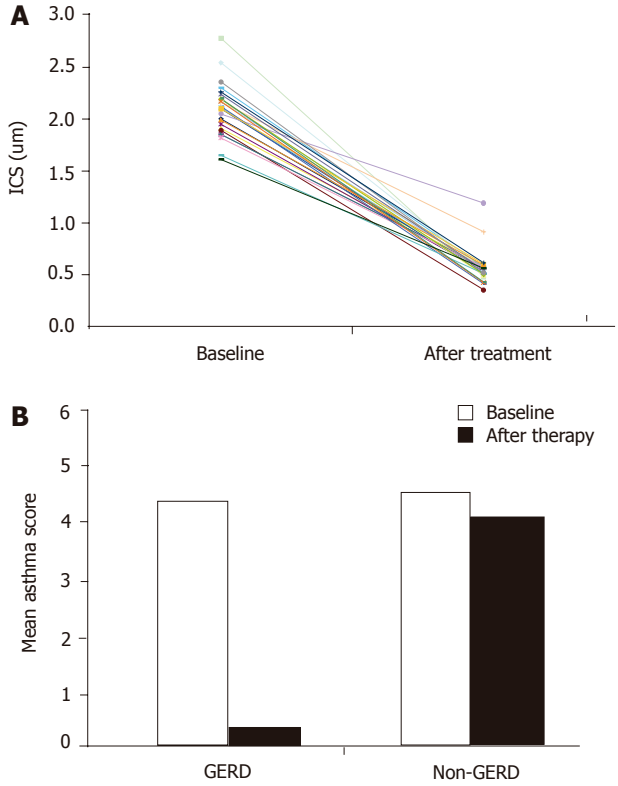

Figure 1 Effect of pantoprazole treatment on dilation of DIS (**A**) and asthma symptom scores (**B**) in GERD patients. The dashed line in Figure 1A corresponds to the mean score of DIS; its cut-off (0.74 μm) represents the presence of damage. Graphic is based on the data analyzed as mean value.

All patients with GERD so defined in our study were treated with a high dosage of pantoprazole for 6 mo. We observed that 93% of patients recovered DIS, 85% of them presented a regression of asthmatic symptoms with normalization of FEV_1, with no statistical difference in respiratory parameters between patients with ERD or NERD. Other patients improved markedly their symptoms and pulmonary function but sporadically presented asthmatic episodes.

We believe that the strong efficacy of PPI treatment in these patients is related to the characteristics of the carefully defined population. The young age of subjects and the mild-moderate asthma let us suppose the existence of an early "action" of treatment before the chronicity of the illness or the worsening to a severe status of asthma. In other words, PPI can suppress or delay the potential development of pulmonary tissue injury.

In conclusion, GERD-related asthma complications are highly prevalent in patients with mild-moderate intrinsic asthma. Treatment with pantoprazole (80 mg once daily for 6 mo) determines the improvement and complete regression of asthmatic symptoms and respiratory function in most patients.

REFERENCES

1 **Harding SM**, Richter JE. The role of gastroesophageal reflux

in chronic cough and asthma. *Chest* 1997; **111:** 1389-1402
2 **Field SK**, Sutherland LR. Does medical antireflux therapy improve asthma in asthmatics with gastroesophageal reflux? *Chest* 1998; **114:** 275-283
3 **Harding SM**, Guzzo MR, Richter JE. 24-h esophageal pH testing in asthmatics: respiratory symptom correlation with esophageal acid events. *Chest* 1999; **115:** 654-659
4 **Jaspersen D**, Kulig M, Labenz J, Leodolter A, Lind T, Meyer-Sabellek W, Vieth M, Willich SN, Lindner D, Stolte M, Malfertheiner P. Prevalence of extra-oesophageal manifestations in gastro-oesophageal reflux disease: an analysis based on the ProGERD Study. *Aliment Pharmacol Ther* 2003; **17:** 1515-1520
5 **Calabrese C**, Fabbri A, Bortolotti M, Cenacchi G, Areni A, Scialpi C, Miglioli M, Di Febo G. Dilated intercellular spaces as a marker of oesophageal damage: comparative results in gastro-oesophageal reflux disease with or without bile reflux. *Aliment Pharmacol Ther* 2003; **18:** 525-532
6 **Harding SM**, Sontag SJ. Asthma and gastroesophageal reflux. *Am J Gastroenterol* 2000; **95:** S23 - S32
7 **Hogan WJ,** Shaker R. Medical treatment of supraesophageal complications of gastroesophageal reflux disease. *Am J Med* 2001; **111 Suppl 8A:** 197S-201S
8 **Levin TR**, Sperling RM, McQuaid KR. Omeprazole improves peak expiratory flow rate and quality of life in asthmatics with gastroesophageal reflux. *Am J Gastroenterol* 1998; **93:** 1060-1063
9 **Teichtahl H**, Kronborg IJ, Yeomans ND, Robinson P. Adult asthma and gastro-oesophageal reflux: the effects of omeprazole therapy on asthma. *Aust NZJ Med* 1996; **26:** 671-676
10 National Institute of Health NHLBI. Burden of asthma. In: Global Strategy for Asthma Management and Prevention. *NIH Publication*, 2002: 11-27
11 **Carlsson R**, Dent J, Bolling-Sternevald E, Johnsson F, Junghard O, Lauritsen K, Riley S, Lundell L. The usefulness of a structured questionnaire in the assessment of symptomatic gastroesophageal reflux disease. *Scand J Gastroenterol* 1998; **33:** 1023-1029
12 **Armstrong D**, Bennett JR, Blum AL, Dent J, De Dombal FT, Galmiche JP, Lundell L, Margulies M, Richter JE, Spechler SJ, Tytgat GN, Wallin L. The endoscopic assessment of esophagitis: a progress report on observer agreement. *Gastroenterology* 1996; **111:** 85-92
13 **Lundell LR**, Dent J, Bennett JR, Blum AL, Armstrong D, Galmiche JP, Johnson F, Hongo M, Richter JE, Spechler SJ, Tytgat GN, Wallin L. Endoscopic assessment of oesophagitis: clinical and functional correlates and further validation of the Los Angeles classification. *Gut* 1999; **45:** 172-180
14 Standardization of Spirometry, 1994 Update. American Thoracic Society. *Am J Respir Crit Care Med* 1995; **152:** 1107-1136
15 **Buts JP**, Barudi C, Moulin D, Claus D, Cornu G, Otte JB. Prevalence and treatment of silent gastro-oesophageal reflux in children with recurrent respiratory disorders. *Eur J Pediatr* 1986; **145:** 396-400
16 **Ducolone A**, Vandevenne A, Jouin H, Grob JC, Coumaros D, Meyer C, Burghard G, Methlin G, Hollender L. Gastroesophageal reflux in patients with asthma and chronic bronchitis. *Am Rev Respir Dis* 1987; **135:** 327-332
17 **Perrin-Fayolle M**, Bel A, Braillon G, Lombard-Platet R, Kofman J, Harf R, Montagnon B, Pacheco Y, Perpoint B. [Asthma and gastro-esophagal reflux (GER). Results of surgical treatment of reflux in 50 patients (author's transl)] *Poumon Coeur* 1980; **36:** 231-237
18 **Sontag SJ,** O'Connell S, Miller TQ, Bernsen M, Seidel J. Asthmatics have more nocturnal gasping and reflux symptoms than nonasthmatics, and they are related to bedtime eating. *Am J Gastroenterol* 2004; **99:** 789-796
19 **Sontag S**, O'Connell S, Khandelwal S, et al. Most asthmatics have gastroesophageal reflux with or without bronchodilator therapy. *Gastroenterology* 1990; **99:** 613-620
20 **Kiljander TO**. The role of proton pump inhibitors in the management of gastroesophageal reflux disease-related asthma and chronic cough. *Am J Med* 2003; **115 Suppl 3A:** 65S-71S
21 **Chiba N**, De Gara CJ, Wilkinson JM, Hunt RH. Speed of healing and symptom relief in grade II to IV gastroesophageal reflux disease: a meta-analysis. *Gastroenterology* 1997; **112:** 1798-1810

Science Editor Wang XL and Guo SY **Language Editor** Elsevier HK

PO Box 2345, Beijing 100023, China
www.wjgnet.com
wjg@wjgnet.com

ELSEVIER

World J Gastroenterol 2005;11(48):7661-7665
World Journal of Gastroenterology ISSN 1007-9327

• *RAPID COMMUNICATION* •

Phagocytic and oxidative burst activity of neutrophils in the end stage of liver cirrhosis

Anatol Panasiuk, Jolanta Wysocka, Elzbieta Maciorkowska, Bozena Panasiuk, Danuta Prokopowicz, Janusz Zak, Karol Radomski

Anatol Panasiuk, Bozena Panasiuk, Danuta Prokopowicz, Department of Infectious Diseases, Medical University of Bialystok, Poland
Jolanta Wysocka, Janusz Zak, Karol Radomski, Department of Pediatrics Diagnostics, Medical University of Bialystok, Poland
Elzbieta Maciorkowska, Department of Pediatric Nursing, Medical University of Bialystok, Poland
Correspondence to: Anatol Panasiuk, MD, Department of Infectious Diseases, Medical University of Bialystok, Zurawia Str, 14, 15-540 Bialystok, Poland. anatol@panasiuk.pl
Telephone: +4885-7416-921 Fax: +4885-7416-921
Received: 2005-03-01 Accepted: 2005-04-18

Abstract

AIM: To evaluate the phagocytic activity and neutrophil oxidative burst in liver cirrhosis.

METHODS: In 45 patients with advanced postalcoholic liver cirrhosis (aged 45±14 years) and in 25 healthy volunteers (aged 38±5 years), the percentage of phagocytizing cells after *in vitro* incubation with *E. coli* (Phagotest Kit), phagocytic activity (mean intensity of fluorescence, MIF) and the percentage of neutrophil oxidative burst (Bursttest Kit), and the level of free oxygen radical production (MIF of Rodamine 123) were analyzed by flow cytometry. The levels of soluble sICAM-1, sVCAM-1, sP-selectin, sE-selectin, sL-selectin, and TNF-α were determined in blood serum.

RESULTS: The percentage of *E. coli* phagocytizing neutrophils in liver cirrhosis patients was comparable to that in healthy subjects. MIF of neutrophil - ingested *E. coli* was higher in patients with liver cirrhosis. The oxidative burst in *E. coli* phagocytizing neutrophils generated less amount of active oxygen compounds in liver cirrhosis patients (MIF of R123: 24.7±7.1 and 29.7±6.6 in healthy, $P<0.01$). Phorbol myristate acetate (PMA) - stimulated neutrophilsproduced less reactive oxidants in liver cirrhosis patients than in healthy subjects (MIF of R123: 42.7± 14.6 *vs* 50.2±13.3, $P<0.01$). A negative correlation was observed between oxidative burst MIF of PMA-stimulated neutrophils and ALT and AST levels (r -0.35, $P<0.05$; r-0.4, $P<0.03$). sVCAM-1, sICAM-1, sE-selectin concentrations correlated negatively with the oxygen free radical production (MIF of R123) in neutrophils after PMA stimulation in liver cirrhosis patients (r-0.45, $P<0.05$; r-0.41, $P<0.05$; r-0.39, $P<0.05$, respectively).

CONCLUSION: Neutrophil metabolic activity diminishes together with the intensification of liver failure. The metabolic potential of phagocytizing neutrophils is significantly lower in liver cirrhosis patients, which can be one of the causes of immune mechanism damage. The evaluation of oxygen metabolism of *E. coli*-stimulated neutrophils reveals that the amount of released oxygen metabolites is smaller in liver cirrhosis patients than in healthy subjects.

Key words: Neutrophil; Phagocytosis; Oxidative burst; Liver cirrhosis; Flow cytometry

Panasiuk A, Wysocka J, Maciorkowska E, Panasiuk B, Prokopowicz D, Zak J, Radomski K. Phagocytic and oxidative burst activity of neutrophils in the end stage of liver cirrhosis. *World J Gastroenterol* 2005; 11(48): 7661-7665
http://www.wjgnet.com/1007-9327/11/7661.asp

INTRODUCTION

Neutrophils play an important role in non-specific immune response and organism resistance, specifically in anti-bacterial resistance as effectors, inducing and regulating cells[1,2]. They reveal many features which are crucial in organism immunity: to produce and adhere towards vascular endothelial cells, migrate to inflammatory sites through the vessel walls, recognize and phagocytize opsonized molecules, and degradate and release proteins from granules[3,4]. These features are possible due to the presence of receptors distributed on the surface and inside of the cells such as cytokine-, neuromediator-, autocoid-, hormone receptors. Neutrophil chemotaxis occurs towards stimulus gradient, in response to chemotactic factors (chemotaxins) produced at the inflammatory site. Moreover, chemotaxins increase neutrophil metabolism, aggregation, and bactericidal abilities[5-7].

Phagocytosis is facilitated by specific (immunoglobulins IgG) and non-specific (complement components) opsonins, circulating in the plasma. On their surface, granulocytes have receptors that bind to Fc fragment of IgG1 and IgG2 immunoglobulins, and complement C3b fragment receptors[8]. Absorbed opsonized microorganisms are killed through both oxygen-dependent and independent mechanisms. Free oxygen radicals kill

absorbed bacteria in phagosomes and partially are released into the environment, intensifying killing microorganisms and simultaneously injuring the surrounding tissues. It is specifically intensified in acute inflammation, less in chronic course of the disease[1]. Microorganism killing is also possible by proteins present in azurophil granules, such as cathepsin G, lysozyme, interferons, and others.

Inflammatory mediators, cytokines (e.g. TNFα) and selectins increase the ability of granulocytes to localize at the site of inflammation. Phagocytic ability is elevated by intensification of hydroxylic radical production and lysosomal enzyme release[9,10]. TNFα is an important factor strengthening granulocyte phagocytic and cytotoxic activity. Activated granulocytes secrete cytokines. IL-1, which stimulates monocytes, endothelial cells, and fibroblasts to secrete IL-8, in turn increases the expression of CD11b/CD18 adhesive molecules and granulocyte oxygen metabolism[11]. Interferon gamma is a strong cytokine, which intensifies Fc receptor expression, stimulates oxygen changes, and strengthens granulocytic granule release.

The aim of the study was to evaluate the metabolic activity of oxidative burst *in vitro* and the production of active oxygen compounds stimulated by *E. coli* and phorbol myristate acetate (PMA). Determination of the percentage of phagocytizing cells and their ability to phagocytize opsonized bacteria is of great importance in the estimation of neutrophil functioning. We evaluated the neutrophil ability to phagocytize *E. coli in vitro* in advanced liver cirrhosis. We also tried to establish the relationship between the neutrophil ability and the concentration of soluble adhesive molecules in peripheral blood.

MATERIALS AND METHODS

Patients

The studies were conducted in the group of 45 patients with advanced postalcoholic liver cirrhosis (30 men and 15 women, aged 45±14 years) (Table 1). Liver cirrhosis was confirmed clinically and histologically. Patients with acute viral or bacterial disease and those in the course of corticosteroid therapy who did not drink alcohol for at least 6 mo were excluded from the study. Patients with liver cirrhosis were divided into groups B and C in accordance with the classification of liver failure according to Child-Pugh[12]. The control group consisted of 25 healthy volunteers (12 women and 13 men, aged 38±5 years), who had never suffered from liver diseases and those without registered immunity disorders. Ethical approval for research was obtained from local Ethics Committee in the Medical University.

Methods

Blood was collected in plastic testing tubes with EDTA K2 and the absolute number of leukocytes and neutrophils was evaluated. The blood was collected in lithium heparin plastic testing tubes for the evaluation of phagocytizing cells and phagocytic activity and the percentage of bursting cells as well as neutrophil oxygen metabolism.

Table 1 Clinical characteristics of patients with liver cirrhosis (mean±SD)

	Child–Pugh B	Child–Pugh C
Age, year	43±12	46±13
Male/female	15/10	15/5
Albumin, g/dL	3.2±0.3	2.8±0.6
AST/ALT, IU/mL	98±65/87±98	110±45/97±45
Bilirubin, mg/dL	4.5±3.8	9.7±6.5

The assessment of phagocytosis was performed using the Phagotest Kit (ORPEGEN Pharma, Germany) containing fluorescein-labeled opsonized Escherichia coli (*E. coli* - FITC). Samples of 100 μL of blood with heparin were cooled in an ice bath for 15 min mixed with 2×10^7 FITC-labeled *E. coli* and then put in a chamber thermostat at 37 °C for 10 min. Simultaneously, the control samples were put into an ice bath to inhibit phagocytosis. Afterwards, 100 μL of brilliant blue (Quenching solution) was added in order to suppress the fluorescence of bacteria connected to the leukocyte surface. After two washing steps (with 2 mL of washing solution, centrifuged at 2 000 r/min, supernatant was pumped out), erythrocytes were lysed using lysis fluid for 20 min at room temperature. At the end, 50 μL propidyne iodide was added to stain leukocytes and bacterial DNA.

Oxidative burst

Granulocyte oxidative burst was determined quantitatively with Bursttest Kit (ORPEGEN Pharma, Germany). Fresh heparinized blood was put in a water bath for 15 min. Then, four testing tubes were filled with 100 μL of blood each and 2×10^7 unlabeled opsonized bacteria *E. coli*, 20 μL of substrate solution (negative control), 20 μL fMLP (peptide *N*-formyl-MetLeuPhe) as chemotactic low physiological stimulus (low control) and 20. μL phorbol 12-myristate 13-acetate (PMA), a strong non-receptor activator (high control). All the samples were incubated for 10 min at 37.0 °C in a water bath, dihydrorhodamine (DHR) 123 as a fluorogenic substrate was added and incubated again in the same conditions. The oxidative burst occurred with the production of reactive oxygen substrates (ROS) (superoxide anion, hydrogen peroxide) in granulocytes stimulated *in vitro*. In ROS-stimulated granulocytes, nonfluorescent DHR 123 underwent conversion to fluorescent rhodamine (R) 123 registered in the flow cytometer. Erythrocytes were removed using lysing solution for 20 min at room temperature, centrifuged (5 min, 250 r/min, 4 °C), and supernatant was discarded. Samples were washed again (washing solution), centrifuged (5 min, 250 r/min, 4 °C) and the supernatant was decanted. An amount of 200 μL of DNA staining solution (centrifuged and incubated for 10 min at 0 °C in a dark place) was added to discriminate and exclude aggregation artifacts of bacteria and/or cells in cytometric flow analysis.

Cytometric analysis

The flow cytometer EPICS XL (Coulter, USA) equipped

with 488 nm argon-ion laser was used. The apparatus was calibrated every day using DNA check. Neutrophil populations were identified by the use of forward and right angle light scatter, and the fluorescence emission of 10^4 cells per sample was recorded on a logarithmic scale. Fluorescent measurements were conducted with identical settings as for the standard determination of cell phenotype with fluorochrome-stained mAb.

Phagocytic activity was determined as the percentage of phagocytizing neutrophils (one or more bacteria ingestion) and as the mean intensity of fluorescence (MIF) value, which equaled the mean number of bacteria phagocytized by the cells.

Granulocyte oxygen metabolism was determined with the percentage of cells phagocytizing *E. coli* producing reactive oxidants (cells undergoing bursts, the change from DHR 123 to R 123), and with the evaluation of granulocyte enzymatic activity (the amount of released active oxygen compounds – the amount of MIF R 123 per cell).

Adhesive molecules and TNFα

ELISA tests were used to determine the level of sICAM-1 (Human sICAM-1, R&D, UK), sVCAM-1 (Human sVCAM-1, R&D), and the level of tumor necrosis factor alpha (Human TNFα, R&D) in blood serum. Soluble forms of P- (Human soluble P-Selectin, R&D), E- (Human sE-Selectin, R&D), and L-selectins (Human sL-Selectin, R&D) were determined by ELISA tests simultaneously in blood serum.

Statistical analysis

The results were presented as mean±SD. Statistical analysis was performed by non-parametrical *U* (Mann-Whitney) test. The result of correlation was calculated by Spearman's correlation test. $P<0.05$ was considered statistically significant.

RESULTS

Phagocytic activity of neutrophils

The ability of neutrophils to phagocytize opsonized *E. coli* was assessed. No significant differences were found in phagocytizing neutrophils both in liver cirrhosis patients and in healthy subjects (Table 2). The MIF of absorbed *E. coli* was slightly higher in patients with liver cirrhosis (differences being statistically insignificant). A positive correlation was observed between the percentage of neutrophils-phagocytized *E. coli* and the percentage of neutrophils with oxidative burst after *E. coli* stimulation *in vitro* ($r = 0.37$, $P<0.05$, Table 3).

Neutrophil oxidative burst

Stimulation *in vitro* with a strong activator PMA causes a markedly lower production of reactive oxidants in neutrophils in liver cirrhosis patients than in healthy individuals (MIF 42.7±14.6 *vs* 50.2±13.3, $P<0.01$, Table 2). Incubation of neutrophils with non-opsonized *E. coli* induced oxidative burst in more neutrophils in patients with liver cirrhosis than in the control group. However, neutrophils phagocytizing *E. coli* showed markedly lower metabolic potential in liver cirrhosis patients than that in healthy subjects. The oxidative burst in neutrophils phagocytizing *E. coli* caused generation of smaller amounts of active oxygen compounds in the cells of patients with liver cirrhosis. Neutrophils with oxidative burst (MIF of rhodamine 123) were statistically lower in liver cirrhosis patients (24.7±7.1) than in healthy subjects (29.7±6.6, $P<0.01$). PMA neutrophil stimulation *in vitro* was more effective than a direct contact with *E. coli*.

The decrease in neutrophil metabolic and phagocytic activities was observed together with the intensification of liver damage. We noted a negative correlation of MIF of neutrophil oxidative burst after PMA stimulation and ALT and AST, which was $r = -0.35$, $P<0.05$ and $r = -0.4$, $P<0.03$, respectively.

Adhesive molecules and TNFα

The concentrations of adhesive molecules sVCAM-1 and sICAM-1 in blood serum were several times higher in patients with liver cirrhosis ($P<0.01$, Table 2). Soluble E-selectin concentrations in liver cirrhosis patients were also significantly higher than in healthy subjects ($P<0.01$). However, significant differences of sL-selectin concentrations were not present, while sP-selectin concentrations were lower in liver cirrhosis patients. The level of sVCAM-1, sICAM-1, sE-selectin correlated negatively with the activity of oxygen radical production (MIF) after PMA neutrophil simulation ($r = -0.45$, $P<0.05$, $r = -0.41$, $P<0.05$, $r = -0.39$, $P<0.05$, respectively). The concentration of TNFα was markedly higher in liver cirrhosis patients than in healthy individuals ($P<0.01$). No correlation was observed between neutrophil metabolic and phagocytic activities and TNFα concentration. On the other hand, there was a positive correlation between sVCAM-1 and sE-selectin concentration ($r = 0.4$, $P<0.05$) and between sL-selectin concentration and the production of free oxygen radicals in neutrophils (MIF of R123) ($r = 0.35$, $P< 0.05$).

DISCUSSION

Infectious and toxic factors and over reactivity of the immune system are crucial in the pathogenesis of chronic liver diseases. The essence of the disease is accumulation of natural killer cells and inflammatory cells as well as intensified fibrosis in the liver. Chronic failure of endothelial cells of hepatic vessels increases expression and concentration of adhesive molecules. It facilitates inflammatory cell activation, margination and accumulation of leukocytes in the liver[4,13-15]. Neutrophils are professionally phagocytizing cells, which play an important role in immunological processes of the organism. They participate mainly in non-specific response as they do not possess the properties for precise recognition of antigens. Chemotactic factors and cytokines (IL-1, IL-8, TNFα, TGF-β) induce migration of granulocytes and other cells to the inflammatory site.

Table 2 Phagocytic and oxidative burst activity of neutrophils, level of soluble form of adhesive molecules and TNFα in liver cirrhosis patients (mean±SD)

		Liver cirrhosis		Healthy
	Total	Child–Pugh B	Child–Pugh C	
Oxidative burst				
Percentage of neutrophils with oxidative burst after PMA stimulation (%)	98.3±1.2	98.4±1.5	98.2±1.6	98.8±2.8
MIF oxidative burst after PMA stimulation	42.7±14.6[b]	44.3±10.1[b]	41.1±12.6[b]	50.2±13.3
Percentage of neutrophils with oxidative burst after *E. coli* stimulation (%)	94.0±4.8	93.0±4.1	94.0±3.8	92.2±3.7
MIF oxidative burst after *E. coli* stimulation	24.7±7.1[b]	25.1±8.1[b]	22.2±5.1[b]	29.7±6.6
Phagocytic activity				
Percentage of neutrophils phagocytizing of *E. coli*	93.0±3.3	92.9±4.3	93.8±2.3	92.5±4.3
MIF phagocytosis *E. coli*	20.0±3.9	19.8±4.1	21.0±2.8	19.0±5.8
Soluble form of adhesion molecules and TNFα				
sICAM-1 (ng/mL)	852±331[b]	788±343[b]	892±293[b]	254±74
sVCAM-1 (ng/mL)	2 937±1 591[b]	2 637±1 291[b]	3 297±1 490[b]	510±248
sP-selectin (ng/mL)	101±180[b]	98±140[b]	104±162[b]	124±58
sE-selectin (ng/mL)	136±89[b]	120±68[b]	148±58[b]	49±21
sL-selectin (ng/mL)	1 209±364	1 206±314	1 211±344	1 209±291
TNFα (pg/mL)	2.94±1.43[b]	2.64±1.33[b]	2.99±1.02[b]	1.58±0.22

[b]$P<0.01$ *vs* healthy subjects (Mann–Whitney *U* test).

Table 3 Correlation (*r*) of phagocytic activity of neutrophils with their oxidative burst level and biochemical tests of liver dysfunction (Spearman test)

Correlations	*r*	*P*
MIF oxidative burst neutrophils after PMA stimulation with ALT level	-035	0.05
MIF phagocytizing *E. coli* with prothrombin time	-0.47	0.03
Percentage of neutrophils phagocytizing *E. coli* with leukocyte number	0.35	0.05
Percentage of oxidative burst neutrophils after *E. coli* stimulation with MIF phagocytosis *E. coli*	0.37	0.05

The study showed a significant impairment of neutrophil immune mechanisms in liver cirrhosis as well as oxidative burst damage with diminished amount of generated free oxygen form in neutrophils. Stimulation *in vitro* with the strong stimulant PMA and non-opsonized *E. coli* induces less amount of released active oxygen compounds in neutrophils in liver cirrhosis patients than in healthy subjects. It should be assumed that it is a result of permanent stimulation of neutrophils by inflammatory factors or lipopolysaccarides (LPS). Observed disorders can be treated as dysfunctions of exhausted neutrophils, and oxygen exchange impairment (processes being important in the maintenance of organism immunity) has been confirmed in other studies[16,17]. The higher release of oxygen metabolites observed after PMA is probably due to different stimulation mechanisms. The neutrophil phagocytic activity in both groups was comparable. Cytometric examinations of the percentage of phagocytizing neutrophils and MIF of absorbed opsonized *E. coli* did not show differences in both groups.

Vascular endothelium has many important functions, and is a barrier against pathogens as well as the site of immunological and inflammatory process initiation with participating neutrophils[18]. Neutrophil accumulation at the site of inflammation depends on the adhesive molecule expression in endothelial cells. Neutrophil stimulation leads to activation of L-selectin and other molecules (β2-integrines) that participate in adhesion to the endothelium. In addition, increase in adhesive molecule expression directly activates antibacterial mechanisms, granule secretion and neutrophil oxygen metabolism. Activation of neutrophils (the main generators of free oxygen radicals in inflammatory processes) leads to elevation of active oxygen metabolites responsible for killing microorganisms[19]. In patients with end-stage liver disease, the ability of neutrophils to migrate to the inflammatory sites is impaired. It was observed that neutrophils present there have their phagocytizing activity reduced[16].

Adhesive molecules (ICAM-1, VCAM-1, selectins) play an important role in keeping neutrophils in liver sinusoids. Antibodies against anti-ICAM-1 and anti-VCAM-1 inhibit neutrophil accumulation in liver tissues and diminish their damage[9,20]. P- and E-selectin expressions in endothelial cells and L-selectin – in leukocytes – lead to slower flow of leukocytes and blood platelets in bloodstream, activation, rolling, and adhesion of these cells. In liver cirrhosis patients, adhesive molecule expression increases due to tissue hypoxia, deposits of immunological complexes, endogenic toxic compounds, LPS, bacteria, and viruses[21-23].

Fiuza *et al.*[16] have suggested that, in the end-stage liver disease, neutrophils have injured ability to migrate to the inflammatory sites and their phagocytic activity is diminished, which in turn, correlates with the severity of liver disease. It has been shown that chronic intravascular peripheral neutrophil activation occurs in vessels. Their results point to the fact that antibacterial early inflammatory immune response is damaged in liver cirrhosis. The increase in bacterial translocation and endotoxin absorption from the bowel is a stimulus for the reticuloendothelial system to produce proinflammatory cytokines[24,25]. Neutrophil activity and phagocytic ability failure may result in ascitic fluid microinfection and

subclinical SBP. On the other hand, a persistent stimulation of neutrophils by inflammatory factors can lead to the exhaustion of their functional potential. Proinflammatory factor elimination from peripheral blood is impaired in liver cirrhosis which facilitates persistent stimulation of peripheral blood neutrophils[25].

We observed high concentrations of soluble adhesive molecules VCAM-1, ICAM-1, and E-selectin, which can account for a marked vascular endothelium damage in liver cirrhosis. Endothelial cell failure or stimulation can occur due to high levels of proinflammatory cytokines (e.g. TNFα). Chronic endotoxemia may also stimulate adhesive molecule expression. High concentrations of VCAM-1, ICAM-1 and E-selectin stimulate inflammatory site to accumulate in terminal capillaries of the liver and other organs. In our studies, the increased expression and concentration of soluble adhesive molecules might result in exhaustion of oxygen metabolism of neutrophils in liver cirrhosis.

Neutrophils are an important host immune barrier against bacterial infections. A persistent stimulation of leukocytes that flow through the liver affected by inflammation leads to the exhaustion of mechanisms responsible for their immune properties.

REFERENCES

1 **Chishti AD,** Shenton BK, Kirby JA, Baudouin SV. Neutrophil chemotaxis and receptor expression in clinical septic shock. *Intensive Care Med* 2004; **30**: 605-611

2 **Tanji-Matsuba K,** van Eeden SF, Saito Y, Okazawa M, Klut ME, Hayashi S, Hogg JC. Functional changes in aging polymorphonuclear leukocytes. *Circulation* 1998; **97**: 91-98

3 **Gregory SH,** Sagnimeni AJ, Wing EJ. Bacteria in the bloodstream are trapped in the liver and killed by immigrating neutrophils. *J Immunol* 1996; **157:** 2514-2520

4 **Jaeschke H,** Smith CW. Cell adhesion and migration. III. Leukocyte adhesion and transmigration in the liver vasculature. *Am J Physiol* 1997; **273:** G1169-G1173

5 **Charo IF,** Taubman MB. Chemokines in the pathogenesis of vascular disease. *Circ Res* 2004; **95**: 858-866

6 **Liu L,** Cara DC, Kaur J, Raharjo E, Mullaly SC, Jongstra-Bilen J, Jongstra J, Kubes P. LSP1 is an endothelial gatekeeper of leukocyte transendothelial migration. *J Exp Med* 2005; **201**: 409-418

7 **Speyer CL,** Gao H, Rancilio NJ, Neff TA, Huffnagle GB, Sarma JV, Ward PA. Novel chemokine responsiveness and mobilization of neutrophils during sepsis. *Am J Pathol* 2004; **165**: 2187-2196

8 **Gomez F,** Ruiz P, Schreiber AD. Impaired function of macrophage Fc gamma receptors and bacterial infection in alcoholic cirrhosis. *N Engl J Med* 1994; **331**: 1122-1128

9 **Jaeschke H,** Farhood A, Fisher MA, Smith CW. Sequestration of neutrophils in the hepatic vasculature during endotoxemia is independent of beta 2 integrins and intercellular adhesion molecule-1. *Shock* 1996; **6***:* 351-356

10 **Laffi G,** Foschi M, Masini E, Simoni A, Mugnai L, La Villa G, Barletta G, Mannaioni PF, Gentilini P. Increased production of nitric oxide by neutrophils and monocytes from cirrhotic patients with ascites and hyperdynamic circulation. *Hepatology* 1995; **22**: 1666-1673

11 **Li CP,** Lee FY, Tsai YT, Lin HC, Lu RH, Hou MC, Wang TF, Chen LS, Wang SS, Lee SD. Plasma interleukin-8 levels in patients with post-hepatitic cirrhosis: relationship to severity of liver disease, portal hypertension and hyperdynamic circulation. *J Gastroenterol Hepatol* 1996; 11: 635-640

12 **Pugh RN,** Murray-Lyon IM, Dawson JL, Pietroni MC, Williams R. Transection of the oesophagus for bleeding oesophageal varices. *Br J Surg* 1973; **60:** 646-649

13 **Chosay JG,** Essani NA, Dunn CJ, Jaeschke H. Neutrophil margination and extravastaion in sinusoids and venules of liver during endotoxin-induced injury. *Am J Physiol 1997;* **272***:* G1195-G1200

14 **Moulin F,** Copple BL, Ganey PE, Roth RA. Hepatic and extrahepatic factors critical for liver injury during lipopolysaccharide exposure. *Am J Physiol Gastrointest Liver Physiol* 2001; **281:** G1423-G1431

15 **Rosenbloom AJ,** Pinsky MR, Bryant JL, Shin A, Tran T, Whiteside T. Leukocyte activation in the peripheral blood of patients with cirrhosis of the liver and SIRS. Correlation with serum interleukin-6 levels and organ dysfunction. *JAMA* 1995; **274**: 58-65

16 **Fiuza C,** Salcedo M, Clemente G, Tellado JM. In vivo neutrophil dysfunction in cirrhotic patients with advanced liver disease. *J Infect Dis* 2000; **182**: 526-533

17 **Rajkovic IA,** Williams R. Abnormalities of neutrophil phagocytosis, intracellular killing and metabolic activity in alcoholic cirrhosis and hepatitis. *Hepatology* 1986; **6**: 252-262

18 **Hippenstiel S,** Suttorp N. Interaction of pathogens with the endothelium. *Thromb Haemost* 2003; **89:** 18-24

19 **Aratani Y,** Kura F, Watanabe H, Akagawa H, Takano Y, Suzuki K, Dinauer MC, Maeda N, Koyama H. In vivo role of myeloperoxidase for the host defense. *Jpn J Infect Dis* 2004; **57**: S15

20 **Essani NA,** Bajt ML, Farhood A, Vonderfecht SL, Jaeschke H. Transcriptional activation of vascular cell adhesion molecule-1 gene in vivo and its role in the pathophysiology of neutrophil-induced liver injury in murine endotoxin shock. *J Immunol* 1997; **158:** 5941-5948

21 **Lautenschlager I,** Hockerstedt K, Taskinen E, von Willebrand E. Expression of adhesion molecules and their ligands in liver allografts during cytomegalovirus (CMV) infection and acute rejection. *Transpl Int* 1996; **9** Suppl 1: S213-S215

22 **Panasiuk A,** Prokopowicz D, Zak J, Matowicka-Karna J, Osada J, Wysocka J. Activation of blood platelets in chronic hepatitis and liver cirrhosis P-selectin expression on blood platelets and secretory activity of beta-thromboglobulin and platelet factor-4. *Hepatogastroenterology* 2001; **48**: 818-822

23 **Pata C,** Yazar A, Altintas E, Polat G, Aydin O, Tiftik N, Konca K. Serum levels of intercellular adhesion molecule-1 and nitric oxide in patients with chronic hepatitis related to hepatitis C virus: connection fibrosis. *Hepatogastroenterology* 2003; **50:** 794-797

24 **Runyon BA,** Squier S, Borzio M. Translocation of gut bacteria in rats with cirrhosis to mesenteric lymph nodes partially explains the pathogenesis of spontaneous bacterial peritonitis. *J Hepatol* 1994; **21***:* 792-796

25 **Saitoh O,** Sugi K, Lojima K, Matsumoto H, Nakagawa K, Kayazawa M, Tanaka S, Teranishi T, Hirata I, Katsu Ki K. Increased prevalence of intestinal inflammation in patients with liver cirrhosis. *World J Gastroenterol* 1999; **5**: 391-396

Science Editor Wang XL and Guo SY **Language Editor** Elsevier HK

PO Box 2345, Beijing 100023, China
www.wjgnet.com
wjg@wjgnet.com

ELSEVIER

World J Gastroenterol 2005;11(48):7666-7670
World Journal of Gastroenterology ISSN 1007-9327

• *RAPID COMMUNICATION* •

Possible involvement of leptin and leptin receptor in developing gastric adenocarcinoma

Liang Zhao, Zhi-Xiang Shen, He-Sheng Luo, Lei Shen

Liang Zhao, Zhi-Xiang Shen, He-Sheng Luo, Lei Shen, Department of Gastroenterology, Renmin Hospital, Wuhan University, Wuhan 430060, Hubei Province, China
Correspondence to: Liang Zhao, MD, Department of Gastroenterology, Renmin Hospital, Wuhan University, Wuhan 430060, Hubei Province, China. airman-zhao@tom.com
Telephone: +86-27-88041919-2135
Received: 2005-01-31 Accepted: 2005-04-11

Abstract

AIM: To investigate the expression of leptin and leptin receptor (ob-R) in intestinal-type gastric cancer and precancerous lesions, and to explore the possible mechanism and role of the leptin system in developing intestinal-type gastric adenocarcinoma.

METHODS: Immunohistochemistry was performed to examine the expression of leptin and leptin receptor in archival samples of gastric adenocarcinoma and preneoplastic lesions, including intestinal metaplasia and mild to severe gastric epithelial dysplasia. Positive staining was identified and percentage of positive staining was graded.

RESULTS: Dual expression of leptin and leptin receptor were detected in 80% (16/20) intestinal metaplasia, 86.3% (25/30) mild gastric epithelial dysplasia, 86.7% (26/30) moderate gastric epithelial dysplasia, 93.3% (28/30) severe gastric epithelial dysplasia, 91.3% (55/60) intestinal-type gastric adenocarcinoma and 30.0% (9/30) diffuse-type gastric carcinoma. The percentage of dual expression of leptin and leptin receptor in intestinal-type gastric adenocarcinoma was significantly higher than that in diffuse-type gastric adenocarcinoma ($\chi^2 = 37.022$, $P<0.01$).

CONCLUSION: Our results indicate the presence of an autocrine loop of leptin system in the development of intestinal-type gastric adenocarcinoma.

Key words: Leptin; Leptin receptor (ob-R); Intestinal-type gastric adenocarcinoma; Intestinal metaplasia; Gastric epithelial dysplasia

Zhao L, Shen ZX, Luo HS, Shen L. Possible involvement of leptin and leptin receptor in developing gastric adenocarcinoma. *World J Gastroenterol* 2005; 11(48): 7666-7670
http://www.wjgnet.com/1007-9327/11/7666.asp

INTRODUCTION

Leptin, the product of the obesity gene (ob gene), is a cytokine-like peptide capable of signal transduction via interaction with its specific receptor (ob-R). It was initially found to be synthesized by adipocytes and act centrally in the hypothalamus to regulate food intake and energy expenditure[1]. Subsequently, expressions of leptin or ob-R were detected in a wide variety of tissues with multiple role in hematopoiesis, reproductive control, angiogenesis, cardiovascular medication, immunomodulation and carcinogenesis[2–6]. Recently, the presence of leptin has also been demonstrated in stomach and thought to be stomach-derived. This endogenous gastric leptin acts as a gastrointestinal hormone via autocrine and/or paracrine pathway in gastrointestinal tract and plays an important role in digestive physiological activities, including short-term meal size control, gastric mucosal cytoprotection and nutrition, regulation of gastric acid and gastric hormone secretion, and modulation of intestinal transport[7].

According to Lauren, gastric cancer can be divided into two histological types: diffuse and intestinal[8]. During the carcinogenesis of intestinal-type gastric adenocarcinoma, a stepwise process proposed by Correa has been widely accepted, which suggested that prolonged *H pylori* infection leads to atrophic gastritis, then with further mutational events leads to the development of intestinal metaplasia, epithelial dysplasia and finally intestinal-type gastric adenocarcinoma[9]. Gastrointestinal hormones and cytokines, including gastrin, epithelial growth factor, vasoactive intestinal peptide and IL-6, seem to play important roles in this transformation processes[10–16]. However, whether leptin, a cytokine-like gastrointestinal hormone that share similarity with aforementioned hormones or cytokines, is involved in the development of intestinal-type gastric adenocarcinoma remains unclear. In the present study, using immunohistochemistry, we examined the expression of leptin and ob-R protein in the tissues of intestinal metaplasia, gastric epithelial dysplasia and intestinal-type gastric adenocarcinoma. Their presence may suggest an autocrine/paracrine pathway of leptin system in gastric carcinogenesis.

MATERIALS AND METHODS

Samples

Formalin-fixed samples of 30 cases of intestinal

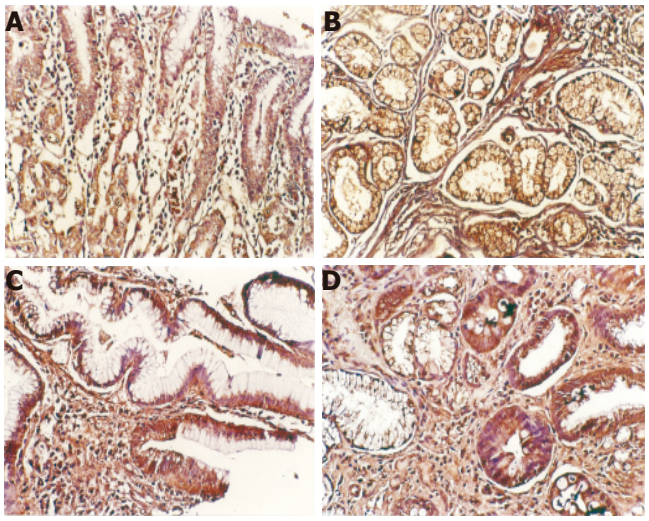

Figure 1 Immunohistochemical stainings of leptin located in cytoplasm (×200). **A:** Normal gastric mucosa; **B:** intestinal metaplasia; **C:** gastric dysplasia; **D:** intestinal-type gastric adenocarcinoma.

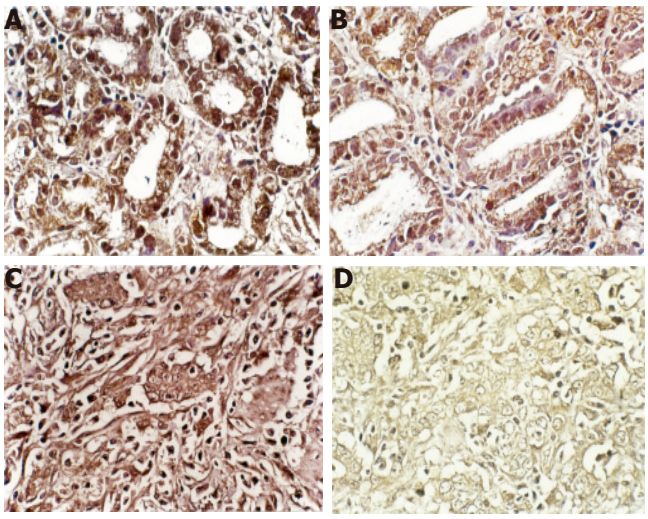

Figure 2 Immunohistochemical stainings of leptin receptor located at cell membrane (×200). **A:** Normal gastric mucosa; **B:** intestinal metaplasia; **C:** gastric dysplasia; **D:** intestinal-type gastric adenocarcinoma.

metaplasia, 90 cases of epithelial dysplasia (mild dysplasia, moderate dysplasia and severe dysplasia, each 30 cases), and 90 cases of gastric adenocarcinoma (60 intestinal-type, 30 diffuse-type) were obtained from pathology archives during 1995-2004 from Renmin Hospital, Wuhan University, Wuhan, China. Those patients had never received chemotherapy, radiation therapy or *H pylori* eradiation. For each case, a paraffin-embedded section with hematoxylin-eosin-safran staining was subjected to pathological identification by a consultant histopathologist on the basis of the Lauren's classification and WHO classification.

Immunohistochemistry

For immunohistochemistry analysis, paraffin-embedded tissue blocks were serially sectioned (4-μm thickness) and mounted onto histostick-coated slides and kept in an oven at 72 °C for 2 h. Sections were deparaffinized in xylene and rehydrated before analysis. Endogenous peroxides was quenched with 30 mL/L hydrogen peroxide in methanol for 10 min. Antigen retrieval was performed by means of microwave irradiation for 15 min and blocked for 15 min with normal goat serum, followed by incubation overnight at 4 °C with a rabbit polyclonal antibody (SC-842) against human leptin (Santa Cruz Biotechnology) and a rabbit polyclonal antibody (SC-1834) against human leptin receptor (Santa Cruz Biotechnology) both at a dilution of 1:70. Replacement of the primary antibodies by PBS solution was used as a negative control. Sections of normal gastric fundus mucosa that had previously shown expression of leptin and ob-R were used as positive

Table 1 Expression of leptin and ob-R in gastric cancer and precancerous lesions

	n	Leptin						Ob-R						Dual expression of leptinand ob-R	
		–	+	+ +	++ +	++ ++		–	+	++	++ +	+++ +		*n*	(%)
Intestinal metaplasia	30	5	4	5	17	0		4	5	7	14	0		25	(83.3)
Gastric dysolasia	90	6	12	28	39	0		9	15	25	35	4		79	(87.7)
Gastric cancer	90	25	9	16	16	24		24	9	22	12	25		75	(83.3)

For comparison of positive percentage for dusl expression of loptin and ob-R among (1) intestinal metaplsia (2) gastric dysplasia (3) gastric carcinoma, (1) *vs* (2) $\chi^2 = 0.3864$, P=0.5351; (1) *vs* (3) $\chi^2 = 0.3864$, $P = 1.000$; (2) *vs* (3) $\chi^2 = 0.7193$, $P = 0.3964$

Table 2 Expression of leptin and ob-R in mild, moderate, and severe gastric

	n	Leptin						Ob-R						Dual expression of leptinand ob-R	
		–	+	+ +	++ +	++ ++		–	+	++	++ +	+++ +		*n*	(%)
Mild dysplasia	30	3	6	9	12	0		4	8	9	9	0		25	(83.3)
Moderate dysplasia	30	3	2	12	10	3		3	3	9	13	2		26	(86.7)
Severe dysplasia	30	0	4	7	17	2		2	4	7	15	2		28	(93.3)

For comparison of positive percentage for dusl expression of loptin and ob-R among (1) mild gastric dysplasia (2) moderate gastric dysplasia (3) severe gastric dysplasia, (1) *vs* (2) $\chi^2 = 0.1307$, $P = 0.7177$; (1) *vs* (3) $\chi^2 = 1.456$, $P = 0.2276$; (2) *vs* (3) $\chi^2 = 0.7407$, $P = 0.3894$

Table 3 Expression of leptin and ob-R in intestinal-type and diffuse-type gastric cancer

	n	Leptin					Ob-R					Dual expression of leptinand ob-R	
		-	+	++	++	++	-	+	++	++	+++	*n*	(%)
				+	+	++				+	+		
Intestinal-type GC[1]	60	4	6	11	15	24	5	7	15	10	25	55	(91.7)
Diffuse-type GC[1]	30	21	3	5	1	0	19	2	7	2	0	9	(30)

[1]GC-gastric cancer for comparison of positive percentage for dual expression of leptin and ob-R between intestinal-type gastric carcinoma and diffuse-type gastric carcinoma, $\chi^2 = 37.022$, $P<0.001$.

controls. Sections were washed thrice with PBS for 2 min each and incubated with biotin-labeled anti-rabbit IgG at room temperature for 1 h. After washing thrice with PBS for 2 min each, sections were stained by streptavidin-peroxidase detection system. Antibody binding was visualized using the diaminobenzidine as chromogen and counterstained with hematoxylin. The positive cells were counted in ten randomly selected fields under ×200 or × 400 microscopic magnification for each specimen and the mean positive percentage was calculated as the density of positive cells. Immunoreactivity was performed by two experienced histopathologists without knowledge of the background features. The abundance of positive stains was graded as follows: -, no cell stained; +, <25% of cells stained; ++, 25–50% of cells stained; +++, 50–75% of cells stained; and ++++, >75% of cells stained.

Statistical analysis

Data were analyzed using SPSS 10.0 software. The χ^2 test was used to compare binomial proportions. A P value less than 0.05 was considered statistically significant.

RESULTS

Immunostainings of leptin and ob-R in normal gastric mucosa, intestinal metaplasia, gastric epithelial dysplasia, intestinal-type gastric adenocarcinoma, diffuse-type gastric carcinoma are shown in Figures 1 and 2. Positive staining of leptin was identified as brownish-yellow granules in cytoplasm. Positive staining of ob-R was identified as brownish-yellow granule at cell membrane.

DISCUSSION

In the present study, the expressions of leptin and ob-R in intestinal metaplasia, gastric epithelial dysplasia, intestinal-type gastric adenocarcinoma and diffuse-type gastric cancer were determined using immunohistochemistry. Our results demonstrated that dual expressions of leptin and leptin receptor were detected in 83.3% (25/30) intestinal metaplasia, 87.7% (79/90) gastric epithelial dysplasia, and 83.3% (75/90) intestinal-type gastric adenocarcinoma without statistically significant difference among those groups. Moreover, no obvious difference among mild gastric dysplasia (83.3%, 25/30), moderate gastric dysplasia (86.7%, 26/30) and severe gastric dysplasia (93.3%, 28/30) was observed. The percentage of dual expression in intestinal-type gastric adenocarcinoma (91.7%, 55/60) was significantly higher than that in diffuse-type gastric carcinoma (30.0%, 9/30). These results indicated that dual expression of leptin and ob-R might be a tumor-specific phenomenon in the transformation from intestinal metaplasia to intestinal-type gastric adenocarcinoma. To the best of our knowledge, our study may be the first study demonstrating dual expression of leptin and ob-R in intestinal metaplasia, gastric epithelial dysplasia and intestinal-type gastric adenocarcinoma, which may play important roles in this transformation process.

As a growth factor, leptin exhibited simulative effect on the proliferation of a variety of malignant cell lines, including leukemia, breast cancer, esophagus adenocarcinoma, prostate cancer, colon cancer, and pituitary adenomas[6,17–21]. In addition, there had been increasing evidence that leptin plays an important role in tumor invasion, metastases, angiogenesis and resistance to chemotherapy[22–26]. Based on these results, leptin is considered to serve as a multi-functional growth factor in tumorigenesis and is capable of promoting an aggressive cancer phenotype. Recently, it has been shown that leptin induced the proliferation of human gastric adenocarcinoma AGS cell line in a dose-dependent fashion[27]. Therefore, it is reasonable to speculate that dual expression of leptin and ob-R may form an autocrine/paracrine stimulatory loop based on intestinal-type gastric adenocarcinoma and precancerous lesions, and play an important role in gastric carcinogenesis.

As a member of the class I cytokine receptor family, ob-R is identified as a single membrane-spanning protein with multiple isoforms (ob-Ra, ob-Rb, ob-Rc, ob-Rd). ob-Rb contains sequence motifs of janus-kinase (JAK)/signal transduction and activation of transcription signal transduction pathways. In addition, leptin activates mitogen-activated protein kinase (MAPK) signal transduction pathways through the ob-Rb receptor and also through the ob-Ra receptor in some cases[18,28]. Those downstream signal pathways of leptin system were verified to be implicated in the formation and progression of tumor. Proliferation of prostate cancer cells appeared to be working through the PI3K and MAPK leptin receptor-activated pathways, depending on cell type[21]. In colon cancer cell line, leptin was demonstrated to stimulate proliferation via P42/44 MAPK signal pathway and induce invasion via JAK/PI3K signal pathway[18,23]. Recently, Schneilder et al.[27] have also reported that leptin caused a moderate, significant proliferative effect on gastric adenocarcinoma cell line AGS proliferation through MAPK signal pathways.

On the other hand, the expression of leptin protein in intestinal-type gastric adenocarcinoma and precancerous lesions in our study can be viewed as "ectopic secretion"

of gastric leptin in those tissues. Similar "ectopic secretion" of gastrointestinal hormone such as gastrin, epithelial growth factor, cholecystokinin, vasoactive intestinal peptide in gastrointestinal tumors has been well documented in previous studies[13–16]. Those "ectopic secretion" of gastrointestinal hormone acted as a growth factor and promoter of angiogenesis in gastrointestinal tumors via interaction with its specific receptor in tumors. Taking into account that those ectopic-secreting gastrointestinal hormones exert similar function in gastrointestinal tumors to their physiological functions to normal gastrointestinal tract, we hypothesized that the ectopic-secreting leptin in intestinal-type gastric adenocarcinoma and precancerous lesions may have similar function with gastric leptin[13–16]. As gastric leptin has been found to mediate gastric cytoprotection and increase mucosal blood flow via overexpression of growth factors, such as EGF, TGF-α and VEGF[29,30], it can be anticipated that leptin may enhance growth and angiogenesis of intestinal-type gastric cancer via similar mechanism mentioned above.

What activates leptin expression in gastric adenocarcinoma remains unclear. Recently, it has been reported that *H pylori* infection significantly increases gastric leptin expression[31]. In addition, leptin expression and secretion were induced by chronic inflammation of inflammatory bowel disease in colonic epithelial cells that were unable to express leptin physiologically[32]. Therefore, we postulated that leptin might be induced as a pro-inflammatory mediator in chronic gastrointestinal inflammation, including *H pylori*-associated chronic gastritis. In addition, previous reports demonstrated that K-ras mutation or amplification of chromosome 17q12-q21 induced the amplification of gastrin gene in colon or gastric cancer[33,34]. Whether *H pylori* infection and chronic gastritis might induce some special biomolecular alterations to amplify leptin expression and its downstream signal pathways during gastric carcinogenesis needs further investigation.

In conclusion, our study demonstrates constitutive dual expression of leptin and ob-R in intestinal-type gastric adenocarcinoma and precancerous lesions. Based on these results, we suggest that leptin system might act as a growth factor and angiogenesis promoter via autocrine and/or paracrine pathway in gastric carcinogenesis. Further investigations are warranted to identify the exact role of leptin system and exact mechanism of its activation in gastric carcinogenesis.

REFERENCES

1 **Zhang YR,** Proenca M, Maffei M, Barone M, Leopold L, Friedman JM. Positional cloning of the mouse ob gene and its human homlogue. *Nature* 1994; **372:** 425-432
2 **Wauters M,** Van Gaal L. Gender differences in leptin levels and physiology: a role for leptin in human reproduction. *J Gend Specif Med* 1999; **2:** 46-51
3 **Baratta M.** Leptin--from a signal of adiposity to a hormonal mediator in peripheral tissues. Med Sci Monit 2002; **8:** 282-292
4 **Fantuzzi G,** Faggioni R. Leptin in the regulation of immunity, inflammation, and hematopoiesis. *J Leukoc Biol* 2000; **68:** 437-446
5 **Rahmouni K,** Haynes WG. Leptin and the cardiovascular system. *Recent Prog Horm Res* 2004; **59:** 225-244
6 **Somasundar P,** McFadden DW, Hileman SM, Vona-Davis L. Leptin is a growth factor in cancer. *J Surg Res* 2004; **116:** 337-349
7 **Lewin MJ,** Bado A. Gastric leptin. *Microsc Res Tech* 2001; **53:** 372-376
8 **Lauren P.** The two histological main types of gastric carcinoma: diffuse and so-called intestinal-type carcinoma. *Acta pathol Microbiol Sacnd* 1965; **64:** 31-49
9 **Correa P.** A human model of gastric carcinogenesis. *Cancer Res* 1988; **48:** 3354-3360
10 **Tanahashi T,** Kita M, Kodama T, Yamaoka Y, Sawai N, Ohno T, Mitsufuji S, Wei YP, Kashima K, Imanishi J. Cytokine expression and production by purified Helicobacter pylori urease in human gastric epithelial cells. *Infect Immun* 2000; **68:** 664-671
11 **Coyle WJ,** Sedlack RE, Nemec R, Peterson R, Duntemann T, Murphy M, Lawson JM. Eradication of Helicobacter pylori normalizes elevated mucosal levels of epidermal growth factor and its receptor. *Am J Gastroenterol* 1999; **94:** 2885-2889
12 **Jonjic N,** Kovac K, Krasevic M, Valkovic T, Ernjak N, Sasso F, Melato M. Epidermal growth factor-receptor expression correlates with tumor cell proliferation and prognosis in gastric cancer. *Anticancer Res* 1997; **17:** 3883-3888
13 **Zhou JJ,** Chen ML, Zhang QZ, Hu JK, Wang WL. Coexpression of cholecystokinin-B/gastrin receptor and gastrin gene in human gastric tissues and gastric cancer cell line. *World J Gastroenterol*. 2004; **10:** 791-794
14 **Okada N,** Kubota A, Imamura T, Suwa H, Kawaguchi Y, Ohshio G, Seino Y, Imamura M. Evaluation of cholecystokinin, gastrin, CCK-A receptor, and CCK-B/gastrin receptor gene expressions in gastric cancer. *Cancer Lett*. 1996; **106:** 257-262
15 **Heasley LE.** Autocrine and paracrine signaling through neuropeptide receptors in human cancer. *Oncogene* 2001; **20:** 1563-1569
16 **Reubi JC,** Laderach U, Waser B, Gebbers JO, Robberecht P, Laissue JA. Vasoactive intestinal peptide/pituitary adenylate cyclase-activating peptide receptor subtypes in human tumors and their tissues of origin. *Cancer Res* 2000; **60:** 3105-3112
17 **Hu X,** Juneja SC, Maihle MJ, Cleary MP. Leptin-a growth factor in normal and malignant breast cells and for normal mammary gland development. *J Natl Cancer Inst* 2002; **94:** 1704-1711
18 **Isono M,** Inoue R, Kamida T ,Kobayashi H, Matsuyama J. Significance of leptin expression in invasive potential of pituitary adenomas. *Clin Neurol Neurosurg* 2003; **105:** 111-116
19 **Hardwick JC,**VanDen Brink GR, Offerhaus GJ, Van Deventer SJ, Peppelenbosch MP. Leptin is a growth factor for colonic epithelial cells. *Gastroenterology* 2001; **121:** 79-90
20 **Somasundar P,** Riggs D, Jackson B, Vona-Davis L, McFadden DW. Leptin stimulates esophageal adenocarcinoma growth by nonapoptotic mechanisms. *Am J Surg* 2003; **186:** 575-578
21 **Somasundar P,** Frankenberry KA, Skinner H, Vedula G, McFadden DW, Riggs D, Jackson B, Vangilder R, Hileman SM, Vona-Davis LC. Prostate cancer cell proliferation is influenced by leptin. *J Surg Res* 2004; **118 :** 71-82
22 **Mareel M,** Leroy A. Clinical, cellular, and molecular aspects of cancer invasion. *Physiol Rev* 2003; **83:** 337-376
23 **Attoub S,** Noe V, Pirola L, Bruyneel E, Chastre E, Mareel M, Wymann MP, Gespach C. Leptin promotes invasiveness of kidney and colonic epithelial cells via phosphoinositide 3-kinase-, rho-, and rac-dependent signaling pathways. *FASEB J* 2000; **14:** 2329-2338
24 **Beecken WD,** Kramer W, Jonas D. New molecular mediators in tumor angiogenesis. *J Cell Mol Med* 2000; **4:** 262-269
25 **Iversen PO,** Drevon CA, Reseland JE. Prevention of leptin binding to its receptor suppresses rat leukemic cell growth by

inhibiting angiogenesis. *Blood* 2002; **100:** 4123-4128

26 **Efferth T,** Fabry U, Osieka R. Leptin contributes to the protection of human leukemic cells from cisplatinum cytoxicity. *Anticancer Res* 2000; **20:** 2541-2546

27 **Schneilder R,** Bomstein SR, Chrousos GP, Boxberger S, Ehninger G, Breidert M. leptin mediates a proliferative response in human gastric mucosa cells with functonal receptor. *Horm Metab Res* 2001; **33:** 1-6

28 **Hegyi K,** Fulop K, Kovacs K, Toth S, Falus A. Leptin-induced signal transduction pathways. *Cell Biol Int* 2004; **28:** 159-169

29 **Konturek SJ,** Bielanski W ,Karcze wska E,Pierzchalski P, Hahn EG, Hartwich A. Role of gastrin in gastric cancerogenesis in Helicobacter pylori infecsed humans . *J Physiol Pharmacol* 1999; **50:** 857-873

30 **Konturek PC,** Brzozowski T, Sulekova Z, Meixner H, Hahn EG, Konturek SJ. Enhanced expression of leptin following acute gastric injury in rat. 1999; **50:** 587-595

31 **Azuma T,** Suto H, Ito Y, Ohtani M, Dojo M, Kuriyama M, Kato T. Gastric leptin and *Helicobacter pylori* infection. *Gut* 2001; **49:** 324-329

32 **Sitaraman S,** Liu X, Charrier L, Ziegler TR, Gewirtz A, Merlin D. Colonic leptin: source of a novel proinflammatory cytokine involved in IBD. *FASEB J* 2004; **18:** 696-69833

33 **Nakata H,** Wang Sl, Chung DC ,Westwick JK, Tilotson LG. Oncogenic ras induces gastrin gene expression in colon cancer. *Gastroentrology* 1998; **115:** 1144-1153

34 **Vidgren V,** Varis A, Kokkola A, Monni O, PurlakkainenP, Nordling S, Fonzan F, Kallioniemi A, Vakkari ML, Kirilaakso E, Knmntilas. Concomitant gastrin and ERBB2 gene amplifications at 17q12-q21 in the intestinal type of gastric cancer. : *Genes Chromosomes Cancer* 1999; **24:** 24-29

Science Editor Kumar M and Guo SY **Language Editor** Elsevier HK

PO Box 2345, Beijing 100023, China
www.wjgnet.com
wjg@wjgnet.com

ELSEVIER

World J Gastroenterol 2005;11(48):7671-7675
World Journal of Gastroenterology ISSN 1007-9327

• *RAPID COMMUNICATION* •

New tumor-associated antigen SC6 in pancreatic cancer

Min-Pei Liu, Xiao-Zhong Guo, Jian-Hua Xu, Di Wang, Hong-Yu Li, Zhong-Min Cui, Jia-Jun Zhao, Li-Nan Ren

Min-Pei Liu, Xiao-Zhong Guo, Jian-Hua Xu, Di Wang, Hong-Yu Li, Zhong-Min Cui, Jia-Jun Zhao, Li-Nan Ren, Department of Experimental Medicine, Northern Hospital, Shenyang, Liaoning Province, China
Correspondence to: Dr. Min-Pei Liu, Department of Experimental Medicine, Northern Hospital, No. 83, Wenhua Road, Shenhe District, Shenyang 110016, Liaoning Province, China. liuminp@yahoo.com.cn
Telephone: +86-24-2305-6274 Fax: +86-24-2450-8052
Received: 2005-01-28 Accepted: 2005-04-30

Abstract

AIM: To examine the concentration of a new antigen SC6 (SC6-Ag) recognized by monoclonal antibody (MAb) in patients with pancreatic cancer and other malignant or benign diseases and to understand whether SC6-Ag has any clinical significance in distinguishing pancreatic cancer from other gastrointestinal diseases.

METHODS: Six hundred and ninety-five serum specimens obtained from 115 patients with pancreatic cancer, 154 patients with digestive cancer and 95 patients with non-digestive cancer were used and classified in this study. Serum specimens obtained from 140 patients with benign digestive disease and 89 patients with non-benign digestive disease served as controls. Ascites was tapped from 16 pancreatic cancer patients, 19 hepatic cancer patients, 16 colonic cancer patients, 10 gastric cancer and 6 severe necrotic pancreatitis patients. The samples were quantitated by solid-phase radioimmunoassay. The cut-off values (CV) of 41, 80, and 118 U/mL were used.

RESULTS: The average intra- and interassay CV detected by immunoradiometric assay of SC6-Ag was 5.4% and 8.7%, respectively. The sensitivity and specificity were 73.0% and 90.9% respectively. The levels in most malignant and benign cases were within the normal upper limit. Among the 16 pancreatic cancer cases, the concentration of SC6-Ag in ascites was over the normal range in 93.8% patients. There was no significant difference in the concentration of SC6-Ag. Decreased expression of SC6-Ag in sera was significantly related to tumor differentiation. The concentration of SC6-Ag was higher in patients before surgery than after surgery. The specificity of SC6-Ag and CA19-9 was significantly higher than that of ultrasound and computer tomography (CT) in pancreatic cancer patients. Higher positive predictive values were indicated in 92.3% SC6-Ag and 88.5% CA19-9, but lower in 73.8% ultrasound and 76.2% CT.

CONCLUSION: The combined test of SC6-Ag and CA19-9 may improve the diagnostic rate of primary cancer. The detection of SC6-Ag is valuable in the diagnosis of pancreatic cancer before and after surgery.

Key words: Tumor antigen SC6; Pancreatic neoplasm; Immunoradiometric assay

Liu MP, Guo XZ, Xu JH, Wang D, Li HY, Cui ZM, Zhao JJ, Ren LN. New tumor-associated antigen SC6 in pancreatic cancer. *World J Gastroenterol* 2005; 11(48): 7671-7675
http://www.wjgnet.com/1007-9327/11/7671.asp

INTRODUCTION

Pancreatic cancer is the fourth or the fifth leading cause of cancer-related deaths in the Western world[1,2]. Approximately 50% of pancreatic cancer patients have metastatic disease at the time of diagnosis with a median survival of 3-6 mo[2,3]. However, even 70-80% of patients, whose tumor could be completely removed, suffer from an incurable local relapse, distant metastases, or peritoneal carcinosis[4,5]. The overall 5-year survival rate of pancreatic cancer patients is only 1%[6,7]. Ultrasound, computer tomography (CT), magnetic resonance imaging and other methods have made it easier to define the late-stage disease and to establish its diagnosis. Unfortunately, these imaging and diagnostic methods cannot detect the early-stage disease[8-11].

In recent years, there has been an increasing clinical attention to the role of tumor markers in the pathogenesis of pancreatic cancer[12-14]. The most widely used marker for pancreatic cancer is CA19-9[15-18]. CA19-9 has a mean sensitivity of 81% and a mean specificity of 90% for pancreatic cancer[19-23]. Other mucin-type markers such as CA50, CA242, DU-PAN2, CA195 and CAM17.1/WGA have also been described for pancreatic cancer[24-28]. These markers have been investigated less widely than CA19-9 but available evidence appears to provide similar data[29-33]. CA19-9 remains as the "gold standard marker"[10] against which tumor markers for pancreatic cancer are evaluated.

Antigen SC6 (SC6-Ag) recognized by monoclonal antibody SC6 (MAb SC6) against human colonic cancer is a relatively new marker compared with CA19-9, CA242, CEA, AFP, DU-PAN-2 and β_2-MG[34-36]. The antigen was purified by immunoaffinity chromatography using the MAb SC6 at our laboratory. The results of SDS-

PAGE, Western blotting and amino acid analysis indicate that SC6-Ag is a glycoprotein with a molecular weight of 67 kμ and contains 18 amino acids. An immunoradiometric sandwich assay of SC6-Ag has been established by us[37]. The diagnostic value of SC6-Ag was evaluated in patients with pancreatic cancer. The sensitivity and specificity of SC6Ag for patients with pancreatic cancer are similar to those of CA 19-9 detected by radioimmunodetection[38]. Therefore, in the present study, we analyzed and compared the pattern of SC6Ag expression in pancreatic cancer and other gastrointestinal cancers to evaluate whether it might be also of high biological strategy in the diagnosis of pancreatic cancer.

MATERIALS AND METHODS

Patients

Serum specimens were obtained from 115 patients with pancreatic cancer (41 females and 74 males, mean age 61 years, with a range of 39-80 years). Among them, 39 had well-and moderately-differentiated tumor, 55 had poorly-differentiated tumor and 21 had differentiated tumor with unknown reason. According to International Union Against Cancer criteria, 9 patients had stage I disease, 33 stage II, 46 stage III and 6 stage IV. Fifteen primary esophageal cancer specimens, 43 gastric cancers specimens, 11 specimens of cancer of papilla of Vater, 39 hepatocellular carcinoma specimens and 46 colonic cancer specimens were classified. Fifteen esophagitis patients (5 females and 10 males; mean age 41 years), 27 gastritis patients (11 females and 16 males; mean age 38 years), 16 papilla of Vater cancer patients (7 females and 9 males; mean age 43 years), 28 pancreatitis patients (15 females and 13 males; mean age 35 years), 23 cirrhosis patients (10 females and 13 males; mean age 44 years) and 31 colitis patients (17 females and 14 males; mean age 35 years) were obtained. The diagnosis of pancreatic cancer was made based on histology and clinical and radiological findings. We noted weight loss, duration of symptoms and tumor position. Other cancers were diagnosed by abdominal ultrasound and CT scan, surgery and pathology. Ninety-five cancers involving lung and bladder were determined. Fifteen out of 42 suspicious patients before surgery were diagnosed having pancreatic cancer after surgery. CA 19-9 was examined in the same samples. Ascites was tapped from 16 pancreatic cancer patients, 19 hepatic cancer patients, 16 colonic cancer patients, 10 gastric cancer and 6 severe necrotic pancreatitis patients.

Sample collection

Blood samples were obtained from all the subjects after an overnight fast. The plasma was immediately separated by centrifugation. The samples were frozen and stored at -20 °C until assay.

Radiolabeling of MAb SC6

MAb SC6 is a murine MAb of the IgG1 isotype against purified antigen SC6 from human colonic cancer tissues as described previously[34-36]. MAb SC6 was isolated from the ascitic fluid of BALB/C mice in which hybridoma cell line SC6 was injected intraperitoneally and purified by protein A-Sepharose 4B columns (Bioinstitute, Shanghai, China). Normal murine immunoglobulin (IgG1, Bioinstitute, Beijing, China) was used as nonspecific control antibody. The MAb was labeled with $Na^{125}I$ by the iodogen method. The average intra- and interassay CV of the method was 5.4% and 8.7% respectively. The recovery rate was 96.5-108.0%, average 102.3%.

Sandwich measurement by radioimmunoassay

After the MAb SC6 was labeled, ^{125}I uncombined with MAb SC6 was separated from bound iodine by gel filtration on a Sephadex G-25 column. Microtiterplates (96-well) were coated with MAb SC6 (20 ng/mL, 100 μL/well) overnight and then incubated with 100 μL/well of 3% bovine albumin in phosphate-buffered saline at 37 °C for 2.5 h. Standard SC6-Ag, various sera, quantity control sera and nonspecific control were incubated at 37 °C for 1 h. ^{125}I-MAb SC6 (25 ng/mL, 100 μL/well) was coated at 37 °C for 3 h and the radioactivity of each well was determined with a Gamma counter (Instrument Factory, Xian, China). After each step, the wells were washed four times with phosphate-buffered saline.

The cut-off values (CV) of SC6-Ag were determined and expressed as mean±SD. The SC6-Ag concentration in sera of controls was lower than CV. The CV of 41 U was mean±2SD, 80 U was mean±3SD, 118 U was mean±4SD. CA 19-9 kit (Abbott Diagnostics, USA) was quantitated by solid-phase radioimmunoassay, CV of 37 U/mL were used.

Statistical analysis

Analysis was performed using SPSS 10.0 software package. For the comparison of various tumor markers, CV representing 90% and 95% specificity levels in patients with relevant benign diseases were determined. The correlation between SC6-Ag and CA 19-9 concentrations was calculated by linear regression using the logarithms of the serum levels. The statistical comparison of multifactors was made and results were significant ($P<0.05$).

RESULTS

SC6-Ag levels in pancreatic cancer and other diseases

The characteristics of the 695 patients are presented in Table 1. Low concentration SC6-Ag was found in the sera from 102 healthy individuals and the cut-off of its normal upper limit was 41 U/mL (20.7±9.8). Among the 115 patients with pancreatic cancer, the cut-off was over the normal range in 73.3% patients, more than 118 U/mL in 48.7% patients and over 41 U/mL in 29.9% patients. The SC6-Ag level was mainly elevated in colonic cancer, hepatic carcinoma and gall bladder tract/bile duct cancers. Non-digestive cancers were mainly non-small cell lung cancer and renal carcinoma. Lower levels of SC6-Ag were observed in benign digestive and non-digestive diseases

Table 1 SC6-Ag levels in patients with malignant and benign disease

Groups	Cases	>41 U/mL	>80 U/mL	>118 U/mL
		n (%)	*n* (%)	*n* (%)
Control	102	7 (6.9)	2 (2.0)	0 (0.0)
Pancreatic Ca	115	84 (73.0)	68 (59.1)	56 (48.7)
Digestive Ca	154	46 (29.9)	24 (15.6)	11 (7.1)
Non-digestive Ca	95	11 (11.6)	8 (8.4)	4 (4.2)
Benign digestive Diseases	140	13 (9.3)	9 (6.4)	2 (1.4)
Non-benign digestive Diseases	89	8 (9.0)	4 (4.5)	0 (0.0)

Table 2 SC6-Ag concentration in ascites from patients with different digestive diseases (mean±SD)

Groups	Cases	SC6-Ag (U/mL) Concentration	>41	>80	>118
			n (%)	*n* (%)	*n* (%)
Pancreatic Ca	16	120.9±109.1	15 (93.8)	11 (68.8)	7 (43.8)
Hepatic Ca	19	55.7±33.4	10 (52.6)	3 (15.8)	1 (5.3)
Colonic Ca	16	54.9±36.7	9 (56.3)	4 (25.0)	1 (6.3)
Gastric Ca	10	38.1±23.4	3 (30.0)	1 (10.0)	0 (0.0)
Several pancreatitis	6	30.9±26.3	2 (33.3)	0 (0.0)	0 (0.0)

mainly including acute pancreatitis and obstruction of gall bladder/bile duct and acute renal impairment.

Relationship between SC6-Ag and clinicopathological factors

SC6-Ag was not significantly related with clinicopathological factors in patients with pancreatic cancer. Decrease of SC6-Ag in the pancreatic head was compared with that in its body and tail. However, the difference failed to reach statistical significance ($P>0.05$).

SC6-Ag concentration in ascites from patients with different digestive diseases

Among the 16 patients with pancreatic cancer, the concentration of SC6-Ag in ascites was over the normal range in 93.8% patients, over 41 U/mL in 33.3-52.6% patients and more than 118 U/mL in 43.8% patients (Table 2).

Parameters for SC6-Ag, CA19-9, ultrasound and CT in patients with pancreatic cancer

The sensitivity of SC6-Ag and CA19-9 was similar to that of ultrasound and CT, while the specificity of SC6-Ag and CA19-9 was significantly higher than that of ultrasound and CT in patients with pancreatic cancer. Higher positive predictive values were found in 92.3% SC6-Ag and 88.5% CA19-9, but lower positive predictive values were found in 73.8% ultrasound and 76.2% CT (Table 3).

Table 3 Comparison of parameters for SC6-Ag, CA19-9, ultrasound and CT in patients with pancreatic cancer

	SC6-Ag (%)	CA19-9 (%)	Ultrasound (%)	CT (%)
Sensitivity	73.0 (84/115)	84.3 (97/115)	82.6 (95/115)	83.5 (96/115)
Specificity	90.9 (70/77)	84.4 (65/77)	55.8 (43/77)	59.7 (46/77)
Positive predictive value	92.3 (84/91)	88.5 (92/104)	73.8 (96/130)	76.2 (99/130)
Negative predictive value	69.3 (70/101)	73.9 (65/88)	69.4 (43/62)	74.2 (46/62)

DISCUSSION

It is obvious that early diagnosis has the greatest impact on the survival of patients with pancreatic cancer. Clinically, fast spiral CT using dynamic intravenous contrast and the potential for improved MRI can provide high-resolution images of small masses[9-13]. Endoscopic retrograde cholangiopancreatography with improved cytology, brushes, and biopsy forceps should enhance preoperative diagnosis of this malignancy. Endoscopic ultrasound also may help detect small lesions and determine the depth of invasion and vascular involvement. Tumor markers are normally produced in low quantities by cells in the body. Detection of a higher serum level of tumor markers by radioimmunoassay or immunohistochemical techniques usually indicates the presence of a certain type of cancer. In some types of cancer, tumor marker levels may reflect the extent or stage of the disease and can be useful in its diagnosis. Recently, the most widely used marker for pancreatic carcinoma is CA19-9, but SC6-Ag has also been found in China[34-38].

In the present study, high levels of SC6-Ag over the normal upper limit (41 U/mL) were found in 73.0% patients with pancreatic cancer, and in 29.8% patients with other digestive tumors. Using a cut-off point of 80 U/mL, the proportion of patients with elevated levels was 59.2%. But over 118 U/mL SC6-Ag was detected in 48.7% patients with pancreatic cancer, in 5.8% patients with digestive cancers, in 4.2% patients with non-digestive carcinoma and in 2% patients with benign digestive diseases. Furthermore, patients with certain benign diseases such as jaundice and pancreatitis, may present with elevated levels of CA19-9[12-14], suggesting that SC6-Ag and CA19-9 may have similar value in the diagnosis of pancreatic cancer.

Increased SC6-Ag concentrations in ascites are not specific for adenocarcinoma of the pancreas when the CV is 41 U/mL, which was evaluated in other digestive tumors and pancreatitis in our study (Table 2). With a cut-off point of 118 U/mL, the respective specificities for patients with pancreatic cancer were high compared to patients with gastric cancer or pancreatitis, indicating that high SC6-Ag level can be used to distinguish pancreatic cancer from benign disorders. However, decreased level of SC-Ag in pancreatic head compared to that in its body and tail failed to reach statistical significance, and there was no relationship between SC-Ag and tumor stage, size and duration ($P>0.05$).

Up to now, it is difficult to diagnose pancreatic cancer using one of the tumor markers because tumor marker levels can be elevated in patients with benign conditions.

In the recent study, the sensitivity, specificity and positive predictive value of SC6-Ag were found to be 73.0%, 90.9% and 92.3%, respectively. By analyzing the four factors, we found that the sensitivity of SC6 and CA19-9 was lower than that of ultrasound and CT, but their specificity was significantly higher (Table 3). Positive predictive values in SC6-Ag and CA19-9 were 92.3% and 88.5%, which were distinctly higher than those of ultrasound (73.8%) and CT (76.2%). The lack of sensitivity and specificity also limits the diagnosis of pancreatic cancer although CA19-9 and SC6-Ag may be useful in differentiating benign from malignant pancreatic disease in non-jaundiced patients. However, combined measures are more useful in the diagnosis of pancreatic cancer.

In conclusion, detection of SC6-Ag is valuable in the diagnosis of pancreatic cancer before and after surgery. The combined test of SC6-Ag and CA19-9 may improve the diagnostic rate of primary cancer.

REFERENCES

1 **Jemal A,** Thomas A, Murray T, Thun M. Cancer statistics, 2002. *CA Cancer J Clin* 2002; **52:** 23-47
2 **Liu MP,** Ma JY, Pan BR, Ma LS, Study of pancreatic cancer in China. *Shijie Huaren Xiaohua Zazhi* 2001; **9:** 1103-1109
3 **Rocha Lima CM,** Centeno B. Update on pancreatic cancer. *Curr Opin Oncol* 2002; **14:** 424-430
4 **Sawabu N,** Watanabe H, Yamaguchi Y, Ohtsubo K, Motoo Y. Serum tumor markers and molecular biological diagnosis in pancreatic cancer. *Pancreas* 2004; **28:** 263-267
5 **Iacobuzio-Donahue CA,** Hruban RH. Gene expression in neoplasms of the pancreas: applications to diagnostic pathology. *Adv Anat Pathol* 2003; **10:** 125-134
6 **Coppola D.** Molecular prognostic markers in pancreatic cancer. *Cancer Control* 2000; **7:** 421-427
7 **Schlieman MG,** Ho HS, Bold RJ. Utility of tumor markers in determining resectability of pancreatic cancer. *Arch Surg* 2003; **138:** 951-955; discussion 955-956
8 **Cohen-Scali F,** Vilgrain V, Brancatelli G, Hammel P, Vullierme MP, Sauvanet A, Menu Y. Discrimination of unilocular macrocystic serous cystadenoma from pancreatic pseudocyst and mucinous cystadenoma with CT: initial observations. *Radiology* 2003; **228:** 727-733
9 **Zhao XY,** Yu SY, Da SP, Bai L, Guo XZ, Dai XJ, Wang YM. A clinical evaluation of serological diagnosis for pancreatic cancer. *World J Gastroenterol* 1998; **4:** 147-149
10 **Rosty C,** Goggins M. Early detection of pancreatic carcinoma. *Hematol Oncol Clin North Am* 2002; **16:** 37-52
11 **Furukawa H.** Diagnostic clues for early pancreatic cancer. *Jpn J Clin Oncol* 2002; **32:** 391-392
12 **Bassi C,** Salvia R, Gumbs AA, Butturini G, Falconi M, Pederzoli P. The value of standard serum tumor markers in differentiating mucinous from serous cystic tumors of the pancreas: CEA, Ca 19-9, Ca 125, Ca 15-3. *Langenbecks Arch Surg* 2002; **387:** 281-285
13 **Carpelan-Holmstrom M,** Louhimo J, Stenman UH, Alfthan H, Haglund C. CEA, CA 19-9 and CA 72-4 improve the diagnostic accuracy in gastrointestinal cancers. *Anticancer Res* 2002; **22:** 2311-2316
14 **Schneider J,** Schulze G. Comparison of tumor M2-pyruvate kinase (tumor M2-PK), carcinoembryonic antigen (CEA), carbohydrate antigens CA 19-9 and CA 72-4 in the diagnosis of gastrointestinal cancer. *Anticancer Res* 2003; **23:** 5089-5093
15 **Crnogorac-Jurcevic T,** Missiaglia E, Blaveri E, Gangeswaran R, Jones M, Terris B, Costello E, Neoptolemos JP, Lemoine NR. Molecular alterations in pancreatic carcinoma: expression profiling shows that dysregulated expression of S100 genes is highly prevalent. *J Pathol* 2003; **201:** 63-74
16 **Kuwahara K,** Sasaki T, Kuwada Y, Murakami M, Yamasaki S, Chayama K. Expressions of angiogenic factors in pancreatic ductal carcinoma: a correlative study with clinicopathologic parameters and patient survival. *Pancreas* 2003; **26:** 344-349
17 **Akashi T,** Oimomi H, Nishiyama K, Nakashima M, Arita Y, Sumii T, Kimura T, Ito T, Nawata H, Watanabe T. Expression and diagnostic evaluation of the human tumor-associated antigen RCAS1 in pancreatic cancer. *Pancreas* 2003; **26:** 49-55
18 **Ji H,** Isacson C, Seidman JD, Kurman RJ, Ronnett BM. Cytokeratins 7 and 20, Dpc4, and MUC5AC in the distinction of metastatic mucinous carcinomas in the ovary from primary ovarian mucinous tumors: Dpc4 assists in identifying metastatic pancreatic carcinomas. *Int J Gynecol Pathol* 2002; **21:** 391-400
19 **Palumbo KS,** Wands JR, Safran H, King T, Carlson RI, de la Monte SM. Human aspartyl (asparaginyl) beta-hydroxylase monoclonal antibodies: potential biomarkers for pancreatic carcinoma. *Pancreas* 2002; **25:** 39-44
20 **Mizumoto K,** Tanaka M. Genetic diagnosis of pancreatic cancer. *J Hepatobiliary Pancreat Surg* 2002; **9:** 39-44
21 **Ghaneh P,** Kawesha A, Evans JD, Neoptolemos JP. Molecular prognostic markers in pancreatic cancer. *J Hepatobiliary Pancreat Surg* 2002; **9:** 1-11
22 **Boltze C,** Schneider-Stock R, Aust G, Mawrin C, Dralle H, Roessner A, Hoang-Vu C. CD97, CD95 and Fas-L clearly discriminate between chronic pancreatitis and pancreatic ductal adenocarcinoma in perioperative evaluation of cryocut sections. *Pathol Int* 2002; **52:** 83-88
23 **Maacke H,** Hundertmark C, Miska S, Voss M, Kalthoff H, Sturzbecher HW. Autoantibodies in sera of pancreatic cancer patients identify recombination factor Rad51 as a tumour-associated antigen. *J Cancer Res Clin Oncol* 2002; **128:** 219-222
24 **Tempia-Caliera AA,** Horvath LZ, Zimmermann A, Tihanyi TT, Korc M, Friess H, Buchler MW. Adhesion molecules in human pancreatic cancer. *J Surg Oncol* 2002; **79:** 93-100
25 **Kunzli BM,** Berberat PO, Zhu ZW, Martignoni M, Kleeff J, Tempia-Caliera AA, Fukuda M, Zimmermann A, Friess H, Buchler MW. Influences of the lysosomal associated membrane proteins (Lamp-1, Lamp-2) and Mac-2 binding protein (Mac-2-BP) on the prognosis of pancreatic carcinoma. *Cancer* 2002; **94:** 228-239
26 **Gerdes B,** Ramaswamy A, Ziegler A, Lang SA, Kersting M, Baumann R, Wild A, Moll R, Rothmund M, Bartsch DK. p16INK4a is a prognostic marker in resected ductal pancreatic cancer: an analysis of p16INK4a, p53, MDM2, an Rb. *Ann Surg* 2002; **235**: 51-59
27 **Kim GE,** Bae HI, Park HU, Kuan SF, Crawley SC, Ho JJ, Kim YS. Aberrant expression of MUC5AC and MUC6 gastric mucins and sialyl Tn antigen in intraepithelial neoplasms of the pancreas. *Gastroenterology* 2002; **123**: 1052-1060
28 **Hamanaka Y**, Suehiro Y, Fukui M, Shikichi K, Imai K, Hinoda Y. Circulating anti-MUC1 IgG antibodies as a favorable prognostic factor for pancreatic cancer. *Int J Cancer* 2003; **103**: 97-100
29 **Yiannakou JY,** Newland P, Calder F, Kingsnorth AN, Rhodes JM. Prospective study of CAM 17.1/WGA mucin assay for serological diagnosis of pancreatic cancer. *Lancet* 1997; **349:** 389-392
30 **Levi E,** Klimstra DS, Andea A, Basturk O, Adsay NV. MUC1 and MUC2 in pancreatic neoplasia. *J Clin Pathol* 2004; **57**: 456-462
31 **Swierczynski SL,** Maitra A, Abraham SC, Iacobuzio-Donahue CA, Ashfaq R, Cameron JL, Schulick RD, Yeo CJ, Rahman A, Hinkle DA, Hruban RH, Argani P. Analysis of novel tumor markers in pancreatic and biliary carcinomas using tissue microarrays. *Hum Pathol* 2004; **35:** 357-366
32 **Koopmann J,** Fedarko NS, Jain A, Maitra A, Iacobuzio-Donahue C, Rahman A, Hruban RH, Yeo CJ, Goggins M. Evaluation of osteopontin as biomarker for pancreatic

adenocarcinoma. *Cancer Epidemiol Biomarkers Prev* 2004; **13:** 487-491

33 **Grutzmann R,** Luttges J, Sipos B, Ammerpohl O, Dobrowolski F, Alldinger I, Kersting S, Ockert D, Koch R, Kalthoff H, Schackert HK, Saeger HD, Kloppel G, Pilarsky C. ADAM9 expression in pancreatic cancer is associated with tumour type and is a prognostic factor in ductal adenocarcinoma. *Br J Cancer* 2004; **90:** 1053-1058

34 **Liu MP**,Characteristics and reactivities of a panel of monoclonal antibodies (McAbs) recognizing human colon cancer associated antigens. *Zhonghua Zhongliu Zazhi* 1992; **14:** 91-93

35 **Liu MP,** Immunohistochemical analysis of physicochemical properties of target antigens with anti-tumor monoclonal antibodies. *Zhonghua Zhongliu Zazhi* 1992; **14:** 6-9

36 **Liu MP**, Zhou JC, Guo XZ, Chen W, Dai B,An TY, Ma SY. Purification and charaterization of antigen SC6 for pancreatic cancer. *Shijie Huaren Xiaohua Zazhi* 1999; **7:** 593-595

37 **Guo XZ**, Liu MP, Li XX, An R, Ma SY, Liu ZF, Zhao XL, Li RP. Evaluation of serum antigen SC6 using immunoradiomrtric assay for diagnosis of pancreatic cancer. *Zhonghua Neike Zazhi* 1992; **31:** 84-86

38 **Guo XZ,** Liu ZF, An R, Zhao XL, Li FH, Wang KG.antigen SC6 for the dia gnosis of pancreatic cancer before operation. *Zhonghua Yixue Zazhi* 1993; **73:** 26-28

Science Editor Wang XL and Guo SY **Language Editor** Elsevier HK

PO Box 2345, Beijing 100023, China
www.wjgnet.com
wjg@wjgnet.com

ELSEVIER

World J Gastroenterol 2005;11(48):7676-7683
World Journal of Gastroenterology ISSN 1007-9327

• *CASE REPORT* •

Liver transplantation for metastatic neuroendocrine tumor: A case report and review of the literature

Wojciech C Blonski, K Rajender Reddy, Abraham Shaked, Evan Siegelman, David C Metz

Wojciech C Blonski, Department of Gastroenterology and Hepatology, Wroclaw Medical University, Wroclaw, Poland
Wojciech C Blonski, the Kosciuszko Foundation Awardee in the Division of Gastroenterology at the University of Pennsylvania, Philadelphia, United States
K Rajender Reddy, Division of Gastroenterology, University of Pennsylvania, Philadelphia, PA, United States
Abraham Shaked, Department of Surgery, University of Pennsylvania, Philadelphia, PA, United States
Evan Siegelman, Department of Magnetic Resonance Imaging Division, University of Pennsylvania, Philadelphia, PA, United States
David C Metz, Division of Gastroenterology, University of Pennsylvania, Philadelphia, PA, United States
Correspondence to: Dr. David C. Metz, 3400 Spruce Street, 3 Ravdin Building, Gastroenterology Division, University of Pennsylvania Health System, Philadelphia, PA 19104, United States. david.metz@uphs.upenn.edu
Telephone: +1-215-662-3541 Fax: +1-215-349-5815
Received: 2005-04-09 Accepted: 2005-04-30

Abstract

Neuroendocrine tumors are divided into gastrointestinal carcinoids and pancreatic neuroendocrine tumors. The WHO has updated the classification of these lesions and has abandoned the term "carcinoid". Both types of tumors are divided into functional and non-functional tumors. They are characterized by slow growth and frequent metastasis to the liver and may be limited to the liver for long periods. The therapeutic approach to hepatic metastases should consider the number and distribution of the liver metastases as well as the severity of symptoms related to hormone production and tumor bulk. Surgery is generally considered as the first line therapy. In patients with unresectable liver metastases, alternative treatments are dependent on the type and the growth rate. Initial treatments consist of long acting somatostatin analogs and/or interferon. Streptozocin-based chemotherapy is usually reserved for symptomatic patients with rapidly advancing disease, but generally the therapy is poorly tolerated and its effects are short-lived. Locoregional therapy directed such as hepatic-artery embolization and chemoembolization, radiofrequency thermal ablation and cryosurgery, is often used instead of systemic therapy, if the disease is limited to the liver. However, liver transplantation should be considered in patients with neuroendocrine metastases to the liver that are not accessible to curative or cytoreductive surgery and if medical or locoregional treatment has failed and if there are life threatening hormonal symptoms. We report a case of liver transplantation for metastatic neuroendocrine tumor of unknown primary source and provide a detailed review of the world literature on this controversial topic.

Key words: Liver metastases; Neuroendocrine tumors; Liver transplantation

Blonski WC, Reddy KR, Shaked A, Siegelman E, Metz DC. Liver transplantation for metastatic neuroendocrine tumor: A case report and review of the literature. *World J Gastroenterol* 2005;11(48): 7676-7683
http://www.wjgnet.com/1007-9327/11/7676.asp

INTRODUCTION

Neuroendocrine tumors are divided into gastrointestinal carcinoids and pancreatic neuroendocrine tumors[1]. However, it is suggested that they may be grouped together and be categorized into functional and non-functional tumors[2] to indicate the clinical manifestations of syndromes caused by hypersecretion of neuropeptides and biogenic amines at supraphysiologic levels[2,3]. These tumors are very rare and occur with an incidence of 2 per 100 000/year (with a slight female predominance) for carcinoids[4-6] and 1-1.5 per 100 000/year for pancreatic neuroendocrine tumors[7].

Gastrointestinal carcinoid tumors originate from cells of the diffuse neuroendocrine system, which is composed of amine-and peptide-producing cells[1]. These cells are scattered throughout the body and predominantly occur in the submucosa of the large and small intestine, stomach and larger bronchi[1]. In 85% of all cases they arise in the lung, stomach, ileum, appendix and rectum[1]. Although the majority of these tumors are nonfunctional, certain primary site locations, such as the ileum and bronchi, have a predilection for producing the carcinoid syndrome[1]. This syndrome is characterized by flushing, diarrhea, abdominal pain and less often by wheezing and heart disease and is predominantly caused by the production of serotonin[1,8]. Other biological substances, produced by carcinoid tumors, such as kalikrein and prostaglandins also take part in the pathogenesis of the carcinoid syndrome[1]. Overall, the carcinoid syndrome develops in only 5% of all carcinoid tumor patients, but this figure rises to approximately 60% in cases with liver metastases[1]. Prior to metastasizing to the liver, carcinoid tumors are usually

silent because their secretory products are inactivated in the liver[1,8,9].

Pancreatic endocrine tumors arise from pleuropotential stem cells within the pancreas[9,10] and those that are functional produce biologically active peptides such as gastrin, insulin, glucagon, vasoactive intestinal polypeptide, somatostatin, growth hormone releasing factor, and pancreatic polypeptide which are responsible for distinct clinical syndromes[1,11]. Gastrinomas and the insulinomas are the most common functional pancreatic endocrine tumors whereas all others are rare[1,11]. Non-functional pancreatic neuroendocrine tumors (45-50% of all pancreatic neuroendocrine tumors) exhibit no specific syndromes; such tumors present only with symptoms due to tumor mass[3,11].

Liver metastases develop in 46-93% of patients with neuroendocrine tumors and can involve large portions of the liver before becoming symptomatic[12]. They exhibit a slow growth despite their multilocular and bilateral occurrence in most cases[13] and may be limited to the liver for long periods[14]. Surgery is generally the first line therapy for patients with liver metastases due to neuroendocrine tumors[15-17]. Potentially curative resection is considered in patients with solitary or unilobar hepatic metastases and without radiological evidence of systemic disease[18]. However, curative resection is possible only in approximately 20% of patients[19], because liver metastases frequently diffuse at the time of diagnosis[8]. In patients with bulky disease, preoperative hepatic artery embolization is recommended in order to decrease the blood flow and shrink tumors[18]. In patients with previously resected or resectable primary tumors, regional nodal disease and metastases confined to the liver, cytoreductive surgery is recommended, provided that preoperative imaging confirms that the primary and regional diseases are controlled or controllable and 90% or more of the bulk of the tumor can be removed[14]. In patients with unresectable liver metastases alternative treatments that can be considered include immunotherapy (somatostatin analogs and/or alpha-interferon) and chemotherapy (usually streptozocin-based). Additional therapy such as hepatic-artery embolization or chemoembolization, radiofrequency ablation and cryosurgery are pursued as needed[8,11,18,20]. Some studies report a tumoristatic effect of somatostatin analogs such as octreotide and lanreotide in 36.5-75% of treated patients lasting for 3-12 months[21-24]. Furthermore, treatment with high-dose somatostatin analogs may induce apoptosis in neuroendocrine tumors[25]. In addition, small liver metastases (diameter less than 1-2 cm) may respond to radiopharmaceutical agents such as Y (90)- and In (131)-labeled octreotide which involve insertion of radiotherapeutic agents directly into the tumor[26]. A recent study suggested that the administration of combinations of Y (90)- and Lu (177)-labeled octreotide in patients with tumors of different sizes may allow wider tumor penetration[27]. In patients with bilobar hepatic tumors, hepatic artery embolization combined with octreotide treatment has also been proposed[28].

Liver transplantation is considered in patients with neuroendocrine metastases to the liver which are not accessible to curative or cytoreductive surgery, tumors which do not respond to medical or interventional treatment and in tumors causing uncontrollable life-threatening hormonal symptoms (severe hypoglycemia, gastrointestinal hemorrhage, severe diarrhea, valvulopathy)[29,30] providing the disease has not extended beyond the liver, although certain hormonal symptoms (e.g. insulinoma) may be less amenable to transplantation than others.

We report herein a case of liver transplantation due to metastatic neuroendocrine tumor of unknown primary source. In addition, we present a comprehensive review of liver transplantation in patients with metastatic neuroendocrine tumors.

CASE REPORT

A 61-year-old white male with a prior history of hypertension and arteriosclerotic heart disease was referred in May 1999 for evaluation of multiple liver metastases from an unclear primary source. In the 4-5 years prior to referral, he described that he had flushing and cough. The flushing was primarily on his face, lasted for about an hour at a time and was precipitated by heat. In the few months prior to referral he developed episodes of fevers, chills and lassitude and had been treated briefly with antibiotics with a good response. The patient had lost about 16 pounds, which was attributed to dieting and anxiety. Physical examination revealed hepatomegaly. Ultrasound of the right upper quadrant and CT scanning of the chest and abdomen revealed multiple metastases in the liver but no other obvious primary tumor (Figure 1A). Laboratory data included a urinalysis which was negative, a serum albumin of 2.9 gm/dL (n.: 3.5-5.0), an elevated alkaline phosphatase of 197 IU/L (n.: 42-121), an ALT of 96 IU/L (n.: 10-60), an AST of 57 IU/L (n.: 10-42), a BUN of 18 mg/dL (n.: 6-20), a normal serum calcium and normal chloride and electrolytes. His total bilirubin was 1.0 mg/dL (n.: 0.2-1.0) and his total protein was 6.7 gm/dL (n.: 6.4-8.2). His CBC was within normal limits.

His serum gastrin level was 38 pg/mL (n.: 0-100), serum chromogranin A level was 275 ng/mL (n.<50) and serum pancreatic polypeptide was 258 pg/mL (n.<312). 24-h urine analysis for 5-hydroxydinoloacetic acid was normal. A transcutaneous liver biopsy was positive for neuroendocrine tumor. The tumor was strongly positive for neuron specific enolase, synaptophysin, insulin, S100 and chromogranin. An OctreoScan showed liver and midline abdominal foci of increased radiotracer uptake compatible with neuroendocrine lesions. There were no neuroendocrine lesions within the lungs and mediastinum. His small bowel enema was normal. An upper endoscopy revealed a few small prepyloric ulcers with no evidence of *Helicobacter pylori*. In addition, there was evidence of extrinsic antral compression from the left lobe of the liver. An echocardiogram was performed which showed a thickened and calcified aortic valve and mitral valve with mild mitral regurgitation. A diagnosis of metastatic

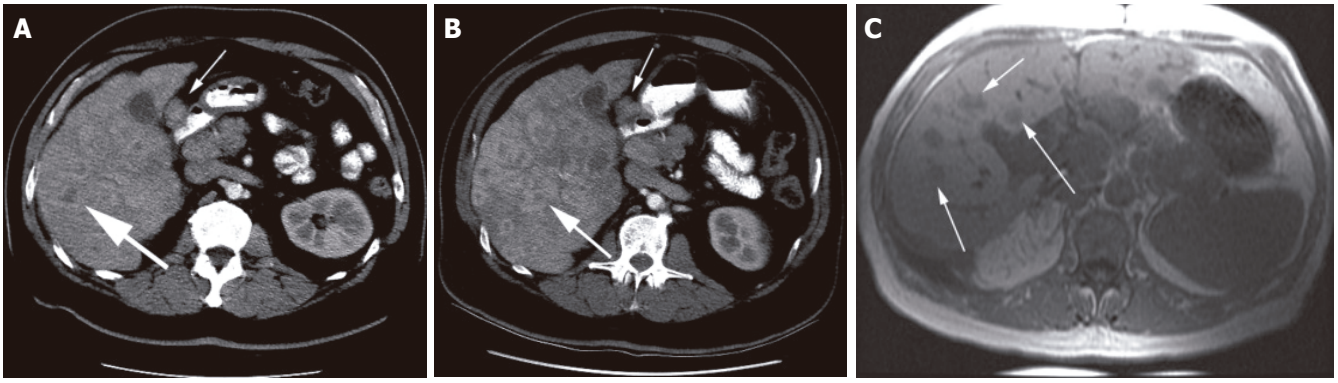

Figure 1 (A) Enhanced CT of the abdomen shows multiple hepatic metastases (big arrow) and lymphadenopathy of the gastrohepatic ligament (small arrow). **(B)** Follow-up CT, 2 mo later reveals an increase in size and number of liver metastases (big arrow) and persistent gastrohepatic ligament adenopathy (small arrow). **(C)** T1-weighed MR image performed 9 mo after transplantation shows the interval development of multiple liver metastases (arrows).

nonfunctional neuroendocrine tumor was eventually made. For the next six months the patient received somatostatin maintenance therapy at which point recurrent upper respiratory symptoms and severe abdominal discomfort developed. There were no carcinoid symptoms and the patient continued to work. A follow up CT scan of the abdomen revealed innumerable metastases throughout the liver (which had coalesced when compared to an examination performed 2 mo earlier) and increasing adenopathy within the gastrohepatic ligament (Figure 1B). Six months later, while on depot octreotide maintenance, he presented with bleeding esophageal varices, and frank hepatic encephalopathy. A metastatic work-up at that time revealed disease predominantly in the liver with additional sites of involvement in the pancreas (possibly an enlarging primary site) and questionable lesions in the chest.

His most recent MRI scan showed no change in tumor size although possibly there was more inferior vena cava obstruction.

The patient underwent orthotopic liver transplantation (OLT) without a pancreatic resection. His explant revealed a liver diffusely involved (approximately 60%) by low grade, neuroendocrine carcinoma with metastasis involving perihilar lymph nodes and cirrhosis. The patient was placed on Prograf and Ganciclovir. Octreotide was discontinued. The patient remained healthy for several months after the transplant and a follow up MRI at 3 mo did not reveal any malignancy until 12 mo later when he presented with pruritus, generalized fatigue and profound diminution in stamina. MRI of the liver confirmed metastasis (Figure 1C) as well as multiple pulmonary nodules and spinal lesions. He was retreated with somatostatin, initially subcutaneously and later by depot injections. However over the next 12 mo his condition deteriorated and despite treatment with Ytrium octreotide in an experimental protocol he ultimately expired 27 mo after liver transplantation.

DISCUSSION

Neuroendocrine tumors represent an unusual group of rare tumors due to their slow growth and ability to produce and secrete a multitude of peptide hormones and amines[30,31]. These substances give rise to different clinical syndromes related to the peptide production, such as the carcinoid syndrome, insulinoma syndrome, Zollinger-Ellison syndrome, glucagonoma syndrome, WDHA syndrome and somatostatinoma syndrome[31]. However, as in this case, many patients have nonfunctional tumors and present with hepatic metastases[30]. In most cases neuroendocrine metastases to the liver are located in both lobes. Gastrointestinal carcinoid tumors, especially those located in the small intestine or ascending colon, are the most common neuroendocrine tumors presenting with liver metastases. Gastrointestinal carcinoids and pancreatic neuroendocrine tumors have different degrees of malignant potential and frequency of liver metastases[32].

The therapeutic approach to hepatic metastases should consider the natural history of the disease and the progression and severity of symptoms caused by both hormone production and tumor mass[33]. In contrast to nonendocrine tumors, therapy for hepatic metastases from neuroendocrine tumors with liver transplantation is reasonable because the disease may be confined to the liver for extended periods and the growth is slow[13,34-36]. The presence of liver metastases from neuroendocrine tumors is a very important prognostic factor for decreased survival[37]. The 5-year survival rate in untreated patients is approximately 30%[38,39] and chemotherapy only prolongs life by a mean of 12-24 mo[40,41].

There have been several single-center (Table1) retrospective analyses and three multicenter restrospective studies[43,46,49] of liver transplantation in patients with liver metastases from neuroendocrine tumors. They are summarized in Table 1. However closer review of these reports reveals that some of the patients were part of more than one publication. Several tumor and patient characteristics influence the outcome following liver transplantation. A large retrospective study of 637 patients who underwent OLT between 1968 and 1991, observed that 67% of patients with carcinoid tumors had recurrence[42]. The authors concluded that patients with slowly growing metastatic neuroendocrine tumors might be suitable candidates for liver transplantation[42].

Table 1 Liver transplantation for metastatic neuroendocrine tumors

Author	Year	Number of patients	Actuarial survival (%)					Comments	Ref. no
			1 (yr)	2 (yr)	3 (yr)	4 (yr)	5 (yr)		
O'Grady	1987	2	nr	nr	nr	nr	nr	2 carcinoids, 1 death at 7 mo, 1 symptom free at 12 mo after LT	53
Makowka	1989	5	nr	nr	nr	nr	nr	3 alive 7, 16 and 34 mo after LT	35
Arnold	1989	4	nr	nr	nr	nr	nr	2 no recurrence 20, 38 moths after LT, 2 deaths 7, 8 mo (chronic rejection)	54
Bramley	1990	1	nr	nr	nr	nr	nr	VIP-oma, no tumor 12 mo after LT	55
Alsina	1990	2	nr	nr	nr	nr	nr	1 carcinoid and 1 PNT no symptoms 5, 13 mo after LT	56
Penn	1991	13	nr	nr	nr	nr	nr	9 carcinoids, 4PNT; 67%recurrence for carcinoids	42
Bechstein	1994	30	52	52	52	nr	nr	multicenter study; at the time of report: 57% alive, 43% dead, 30% recurrence, 70% no evidence of disease	43
Allessiani	1995	14	nr	nr	64	nr	nr	cluster transplantation, recurrence rate 45.5%	44
Routley	1995	11	82	nr	nr	nr	57	7 carcinoids, 2 PNT, 2 ET-primary unknown;6 alive (2 carcinoids) 8–106 mo after LT; 5 deaths(3 carcinoids) in 8–67 mo after LT	45
Curtiss	1995	3	nr	nr	nr	nr	nr	3 alive 12, 20, 30 mo after LT	57
Anthuber	1996	4	nr	nr	nr	nr	nr	4 deaths 10 days and 4, 8, 33 mo after LT	58
Dousset	1996	9	nr	nr	nr	nr	nr	4 carcinoids, 5 PNT; 3 (carcinoids) alive 15, 24, 62 mo after LT, 6 deaths 6, 7, 12, 83 days and 7, 8 mo after LT	59
Le Treut	1997	31	58	51	47	36	36	multicenter study, 11 centers in Europe; disease free survival: 45% at 1 yr, 29% at 3 yr, 17% at 5 yr after LT; higher survival for carcinoids (69% at 5 yr) than for non-carcinoids (8% at 4 yr)	46
Le Treut	1997	37	66	56	46	46	46	literature review, 14 centers, higher survival for non-carcinoids (83% at 2 yr) than carcinoids (34% at 2 yr)	46
Lang	1997	12	nr	nr	nr	nr	nr	9 alive-median survival 55 mo (4 no recurrence 2, 57, 58, 103.5 mo after LT)	47
Lehnert	1998	103	68	60	53	47	47	multicenter study; disease-free survival:60% at 1 yr, 48% at 2 yr, 42% at 3 yr, 42% at 3 yr,33% at 4 yr, 24% at 5 yr. favorable prognostic factors: age>50yr, limited operation (survival 65% at 5 yr).	48
Pilchmayr	1998	15	nr	nr	nr	nr	86.7	11 alive, 4 with no recurrence, the longest survival 10 yr after LT	49
Gottwald	1998	1	nr	nr	nr	nr	nr	Gastrinoma, alive with good liver function after LT	60
Frilling	1998	4	nr	nr	nr	nr	nr	3 carcinoids (2 alive,1 dead 32 d after LT), 1PNT(death 4 days after LT); 1 recurrence-free	61
Pascher	2000	4	nr	nr	nr	nr	nr	4 carcinoids; 2 deaths 14, 42 mo after LT, 2 alive 36, 76 mo after LT	62
Claure	2000	1	nr	nr	nr	nr	nr	1 carcinoid	63
Coppa	2001	9	100	100	100	70	70	Disease-free survival 53% at 5 yr	19
Ringe	2001	5	nr	nr	nr	nr	nr	4 alive (2 tumor-free survivals 4–25 mo after LT); 1 death 0.2 month after LT	64
Olausson	2002	9	89	nr	nr	nr	nr	5 PNT, 4 carcinoids; 7 OLT,2 MVT; 8 alive, 6 no evidence of disease, 4 recurrent tumors 9–36 mo after LT	29
Rosenau	2002	19	89	nr	nr	nr	80	Survival at 10 yr 50%;recurrence free survival 56% at 1 yr, 21% at 5 and 10 yr; survival 100% at 7 yr with Ki67<5% and regular E-cadherin staining; survival 0% at 7 yr with Ki67>5% and E-cadherin aberrant staining	50
Fernandez	2003	5	nr	nr	nr	nr	nr	2 alive and recurrence free 3, 6 yr after LT; 3 deaths 4, 10, 17 mo after LT	65
Amarapurkar	2003	14	nr	nr	nr	nr	nr	MIB-1 index >5%: recurrence at median 11 mo, survival median 13 mo MIB-1 index <5%: recurrence at median 69 mo, survival median 80.5 mo	66
Cahlin	2003	10	nr	80	nr	nr	nr	7 OLT, 3 MVT; 2 yr survival 100% for carcinoids; 67% for PNT; 2 yr disease-free survival 75% for carcinoids and 33% for PNT	51
Florman	2004	11	73	nr	nr	nr	36	1 patients disease-free at 5 yr after LT	52
Ahlman	2004	12	nr	nr	nr	nr	nr	8 after OLT alive at time of study, 2 after MVT died 4 mo after LT; other 2 after MVT with no recurrence at 8, 36 mo.	14

LT: liver transplantation; OLT: orthotopic liver transplantation; MVT: multivisceral transplantation; PNT: pancreatic endocrine tumors, nr: results not reported

These data were further supported by another experience on 30 patients from 14 centers who underwent OLT for metastatic neuroendocrine tumors[43]. It was noted that the actuarial survival, often combined with other upper abdominal resective procedures, for the entire group of patients was 52% after 1 year and remained stable for another 24 mo[43]. Overall, mortality during the first year after transplantation due to recurrent tumor was 17%[43]. The longest survival, 42 mo, was in a patient who died from recurrent carcinoid tumor[43]. Overall, at the time of this study 57% of patients were alive, 30% had developed recurrence, 43% had died and 70% did not have evidence of disease recurrence. Based on their observations they proposed that extrapancreatic primary neuroendocrine tumors be treated with radical hepatic resection followed by medical therapy and that the tumor response should be evaluated before considering liver transplantation[43]. Even the primary pancreatic primary tumors with slow growth that do not respond to medical therapy can be considered for liver transplantation but with a combination of a pancreatic resection procedure[43].

The role of abdominal cluster transplantation was best described in 57 patients presenting with primary or metastatic liver tumors[44]. Abdominal cluster transplantation for metastatic neuroendocrine liver tumors had a better 3-year survival rate (64%) than for patients who underwent this procedure due to sarcoma (44%), hepatocellular carcinoma (25%), cholangiocarcinoma (20%) and other adenocarcinomas (20%)[44]. OLT was found to be effective in controlling symptoms that were caused by carcinoid metastases to the liver[45]. The tumor recurrence was not necessarily associated with early recurrence of symptoms[45]. The patients with non-carcinoid tumors were found to have a higher likelihood of prolonged disease-free survival than those with carcinoid tumors[45]. On the other hand Le Treut *et al.* found significantly higher survival in patients with metastatic carcinoid tumors (80% after 1 year and 69% after 5 years) than in patients with non-carcinoid neuroendocrine tumors who underwent OLT (38% after 1 year and 8% after 4 years)[46]. However additional analysis of 37 cases of OLT for metastatic neuroendocrine tumors presented in the literature revealed significantly higher survival rates in patients with non carcinoid apudomas (83% after 2 years) than in patients with carcinoids (34% after 2 years)[46].

When liver transplantation was done only in cases with unresectable liver tumor, untreatable hormonal symptoms or massive tumor bulk[47] and without extrahepatic tumors at the time of transplantation, patients were observed to derive benefit from OLT[47]. A characteristic of the patients who did not have recurrence during follow up was that they had less than 40–50% tumor bulk in the explant. Thus, it has been suggested that OLT may be also regarded as curative treatment in some patients with neuroendocrine metastases who have relatively low tumor burden[47]. In contrast, Florman found only 1 rare case of 5-year disease free survival among 11 transplanted patients. Moreover, it was claimed that due to only few reports in the literature of 5-year disease free survival (4.6%), OLT cannot be considered as a curative procedure[48].

Other prognostic indicators that have been suggested include a limited operation and age of <50 years. Patients with such features had an overall 5-year survival of 65% and median survival of more than 8 years[49]. On the other hand, patients who underwent extended operations including upper abdominal exenteration or Whipple's operation had 1-year survival of 50% and 5-year survival of 31%[49]. Therefore, an extended operation (Whipple's operation, abdominal exenteration) and age≥50 years were considered as independent indicators of poor outcome and thus extensive surgery does not translate into better outcomes perhaps because of the high rate of post operative morbidity and mortality (10 of 11 patients with such features died after a median of 7 mo)[49]. Interestingly, location of the primary tumor, tumor histology and treatment with somatostatin were not found to be prognostic factors, although patients with primary tumors located in the pancreas or gastrinoma seemed to have poorer outcomes[49]. The outcome of liver transplantation showed a highly significant survival difference between patients with metastases from neuroendocrine tumors and other tumors such as colorectal carcinoma, melanoma, choriocarcinoma or pancreatic carcinoma[50]. The 5-year survival was 86.7% in patients with neuroendocrine metastases and 0% in patients with other malignancies[50].

Little is known about tumor markers as prognostic factors. It has been demonstrated that low tumor expression of the immunohistochemical marker, Ki67(<5%), and the adhesion molecule, E-cadherin, might be associated with a favorable outcome after liver transplantation for metastatic neuroendocrine tumors[51]. Patients (n = 12) with an increased expression of the markers, (Ki67≥5% positive cells and/or E-cadherin staining) showed decreased survival (median 46 mo) whereas patients (n = 5) with low expression of these markers showed increased survival (median 90 mo)[51]. It was also suggested that the combination of these two markers had an excellent specificity and sensitivity to predict a survival of 7 years after liver transplantation[51]. Further study showed that liver transplantation for metastatic well-differentiated neuroendocrine tumors with a low expression of protein Ki67 (Ki67<10%) resulted in relief of hormonal symptoms and long disease-free periods[14]. Another study suggested that MIB-1 antibody expression might have prognostic value in patients undergoing liver transplantation for metastatic carcinoid tumors[66]. The authors assessed the cell proliferative activity by MIB-1 antibody labeling in 14 patients with metastatic neuroendocrine liver tumors (7 carcinoids, 7 non-carcinoids) who underwent liver transplantation[66]. In this group, two patients remained alive and disease-free at 96 and 192 mo after liver transplantation[66]. MIB-1 index was calculated by dividing the number of tumor cells with positive staining for MIB-1 antibody by the total number of tumor cells[66]. It was shown that patients with a MIB-1 index of greater than 5% showed early tumor recurrence (median 11 mo) and shorter survival (median 13 mo)

whereas patients with a MIB-1 index of less than 5% showed late tumor recurrence (median 69 mo) and longer survival (median 80.5 mo)[66]. The low MIB-1 index (<5%) was found to have a sensitivity of 71% and a specificity of 83% for predicting survival of greater than 2 years[66].

Current knowledge about the role of liver transplantation for patients with neuroendocrine liver metastases indicates that liver transplantation should be considered only in selected individuals. Coppa *et al*. proposed that selection of patients with non-resectable metastatic neuroendocrine tumors for liver transplantation should be based on the Milan criteria: young patients (less than 50 years) with carcinoids confirmed by histology, with less than 50% of the liver replaced by metastases, with a primary tumor (originating from the gastrointestinal tract) drained by the portal venous system, an absence of extrahepatic disease and stable disease during the pretransplantation period[19]. In a group of nine patients who underwent liver transplantation based on these criteria the 5-year survival was 70% and the 5-year disease-free survival was 53%[19]. On the other hand, in the group of 20 patients who were treated by liver resection due to less advanced liver metastases, the 5-year survival was 67% and the 5 year disease-free survival was 29%[19]. Our patient had a 27 mo survival and the less than ideal outcome may have been because of some of the poor prognostic factors of age>50, tumor bulk exceeding 50%, and regional metastasis. Furthermore, whether immunosuppression after OLT has any effect on the rate of tumor recurrence or not is pure speculation. Thus, given the shortage of donor organs and the high rate of tumor recurrence, we currently believe that OLT should only be undertaken, when other therapeutic approaches including combinations of regional or systemic chemotherapy and hormone inhibitors together with partial hepatectomy have failed[64]. There is a need for prospective studies in large numbers of patients to fully evaluate the role of liver transplantation in patients with metastatic neuroendocrine tumors who may gain many years of effective palliation with careful selection. However, suboptimal outcomes may occur if case selection is compromised.

REFERENCES

1 **Metz DC,** Jensen RT. Endocrine tumors of the gastrointestinal tract and pancreas. In: Rustgi AK, ed. Gastrointestinal cancers. A companion to Sleisenger and Fordtran's Gastrointestinal and Liver Disease. *Edinburgh: Elsevier Science Ltd* 2003; 681-719

2 **Kloppel G,** Perren A, Heitz PU. The gastroenteropancreatic neuroendocrine cell system and its tumors: the WHO classification. *Ann N Y Acad Sci* 2004; **1014:** 13-27

3 **Oberg K,** Kvols L, Caplin M, Delle Fave G, de Herder W, Rindi G, Ruszniewski P, Woltering EA, Wiedenmann B. Consensus report on the use of somatostatin analogs for the management of neuroendocrine tumors of the gastroenteropancreatic system. *Ann Oncol* 2004; **15:** 966-973

4 **Modlin IM,** Sandor A. An analysis of 8305 cases of carcinoid tumors. *Cancer* 1997; **79:** 813-829

5 **Levi F,** Te VC, Randimbison L, Rindi G, La Vecchia C. Epidemiology of carcinoid neoplasms in Vaud, Switzerland, 1974-97. *Br J Cancer* 2000; **83:** 952-955

6 **Quaedvlieg PF,** Visser O, Lamers CB, Janssen-Heijen ML, Taal BG. Epidemiology and survival in patients with carcinoid disease in The Netherlands. An epidemiological study with 2391 patients. *Ann Oncol* 2001; **12:** 1295-1300

7 **Delcore R,** Friesen SR. Gastrointestinal neuroendocrine tumors. *J Am Coll Surg* 1994; **178:** 187-211

8 **McStay MKG,** Caplin ME: Carcinoid tumor. *Minerva Med* 2002; **93:** 389-401

9 **Norheim I,** Oberg K, Theodorsson-Norheim E, Lindgren PG, Lundqvist G, Magnusson A, Wide L, Wilander E. Malignant carcinoid tumors. An analysis of 103 patients with regard to tumor localization, hormone production, and survival. *Ann Surg* 1987; **206:** 115-125

10 **Jensen RT,** Norton JA. Pancreatic endocrine tumors. In: Feldman M, Friedman LS, Sleisenger MH, eds. Sleisenger and Fordtran's Gastrointestinal and liver disease. 7th ed. *Philadelphia: Saunders,* 2002: 988-1016

11 **McLoughlin JM,** Kuhn JA, Lamont JT. Neuroendocrine tumors of the pancreas. *Curr Treat Opin in Gastroenterol* 2004; **7:** 355-364

12 **Chamberlain RS,** Canes D, Brown KT, Saltz L, Jarnagin W, Fong Y, Blumgart LH. Hepatic neuroendocrine metastases: does intervention alter outcomes? *J Am Coll Surg* 2000; **190:** 432-445

13 **Frilling A,** Rogiers X, Malago M, Liedke O, Kaun M, Broelsch CE. Liver transplantation in patients with liver metastases of neuroendocrine tumors. *Transplant Proc* 1998; **30:** 3298-3300

14 **Ahlman H,** Friman S, Cahlin C, Nilsson O, Jansson S, Wangberg B, Olausson M. Liver transplantation for treatment of metastatic neuroendocrine tumors. *Ann N.Y Acad Sci* 2004; **1014:** 265-269

15 **Que F,** Nagorney DM, Batts KP, Linz LJ, Kvols LK. Hepatic resection for metastatic neuroendocrine carcinomas. *Am J Surg* 1995; **169:** 36-43

16 **Benevento A,** Boni L, Frediani L, Ferrari A, Dionigi R. Results of liver resection as treatment for metastases from noncolorectal cancer. *J Surg Oncol* 2000; **74:** 24-29

17 **Norton JA,** Warren RS, Kelly MC, Zuraek MB, Jensen RT. Aggresive surgery for metastatic neuroendocrine tumors. *Surgery* 2003; **134:** 1057-1065

18 **Sutcliffe R,** Maguire D, Ramage J, Rela M, Heaton N. Management of neuroendocrine liver metastases. *Am J Surg* 2004; **187**: 39-46

19 **Coppa J,** Pulvirent A, Schiavio M, Romito R, Collini P, Di Bartolomeo M, Fabbri A, Regalia E, Mazzaferro V. Resection versus transplantation for liver metastases from neuroendocrine tumors. *Transpl Proc* 2001; **33:** 1537-1539

20 **Miller CA,** Ellison EC. Therapeutic alternatives in metastatic neuroendocrine tumors. *Surg Oncol Clin N Am* 1998; **7:** 863-879

21 **Eriksson B,** Renstrup J, Imam H, Oberg K. High-dose treatment with lanreotide of patients with advanced neuroendocrine gastrointestinal tumors: clinical and biological effects. *Ann Oncol* 1997; **8:** 1041-1044

22 **Saltz L,** Trochanowski B, Buckley M, Heffernan B, Niedzwiecki D, Tao Y, Kelsen D. Octreotide as an antineoplastic agent in the treatment of functional and nonfunctional neuroendocrine tumors. *Cancer* 1993; **72:** 244-248

23 **Welin SV,** Janson ET, Sundin A, Stridsberg M, Lavenius E, Granberg D, Skogseid B, Oberg KE, Eriksson BK High-dose treatment with a long-acting somatostatin analogue in patients with advanced midgut carcinoid tumours. *Eur J Endocrinol* 2004; **151:** 107-112

24 **Arnold R,** Trautmann ME, Creutzfeldt W, Benning R, Benning M, Neuhaus C, Jurgensen R, Stein K, Schafer H, Bruns C, Dennler HJ. Somatostatin analogue octreotide and inhibition of tumour growth in metastatic endocrine gastroenteropancreatic tumours. *Gut* 1996; **38:** 430-438

25 **Imam H,** Eriksson B, Lukinius A, Janson ET, Lindgren PG, Wilander E, Oberg K. Induction of apoptosis in neuroendocrine tumors of the digestive system during treatment with somatostatin analogs.*Acta Oncol* 1997; **36:**

607-614
26 **Chatal JF,** Le Bodic MF, Kraeber-Bodere F, Rousseau C, Resche I. Nuclear medicine applications for neuroendocrine tumors. *World J Surg* 2000; **24:** 1285-1289
27 **De Jong M,** Valkema R, Jamar F, Kvols LK, Kwekkeboom DJ, Breeman WA, Bakker WH, Smith C, Pauwels S, Krenning EP. Somatostatin receptor-targeted radionuclide therapy of tumors: preclinical and clinical findings. *Semin Nucl Med* 2002; **32:** 133-140
28 **Wangberg B,** Wetsberg G, Tylen U, Tisell LE, Jansson S, Nilsson O, Johansson V, Schersten T, Ahlman H. Survival of patients with disseminated midgut carcinoid tumors after aggressive tumor reduction. *World J Surg* 1996; **20:** 892-896
29 **Olausson M,** Friman S, Cahlin C, Nilsson O, Jansson S, Wangberg B, Ahlman H: Indications and resuls of liver transplantation in patients with neuroendocrine tumors. *World J Surg* 2002; **26:** 998-1004
30 **Sarmiento JM,** Que FG. Hepatic surgery for metastases from neuroendocrine tumors. *Surg Oncol Clin N Am* 2003; **12:** 231-242
31 **Eriksson B,** Oberg K, Stridsberg M. Tumor markers in neuroendocrine tumors. *Digestion* 2000; **62**(suppl1):33-38
32 **Ihse I,** Persson B, Tibblin S: Neuroendocrine metastases of the liver. *World J Surg* 1995; **19:** 76-82
33 **Lang H,** Schlitt HJ, Schmidt H, Flemming P, Nashan B, Scheumann GFW, Oldhafer KJ, Manns MP, Raab R. Total hepatectomy and liver transplantation for metastatic neuroendocrine tumors of the pancreas- a single center experience with ten patients. *Langenbecks Arch Surg* 1999; **384:** 370-377
34 **Rosado B,** Gores GJ. Liver transplantation for neuroendocrine tumors:progress and uncertainty. *Liver Transplantation* 2004; **10:** 712-713
35 **Makowka L,** Tzakis AG, Mazzaferro V, Teperman L, Demetris J, Iwatsuki S, Starzl TE. Transplantation of the liver for metastatic endocrine tumors of the intestine and pancreas. *Surg Gynec Obst* 1989; **168:** 107-111
36 **El Rassi ZS,** Ferdinand L, Mohsine RM, Berger F, Lombard-Bohas C, Boillot O, Partensky CCM. Primary and secondary liver endocrine tumors:clinical presentation, surgical approach and outcome. *Hepato-Gastroenterology* 2002; **49:** 1340-1346
37 **Weber C,** Venzon DJ, Lin JT, Fishbein VA, Orbuch M, Strader DB, Gibril F, Metz DC, Fraker DL, Norton JA, Jensen RT. Determinants of metastatic rate and survival in patients with Zollinger-Ellison syndrome: a propsective long-term study. *Gastroenterology* 1995; **108:** 1637-1649
38 **Moertel CG.** Karnofsky memorial lecture. An odyssey in the land of small tumors. *J Clin Oncol* 1987; **5:** 1503-1522
39 **Soreide O,** Berstad T, Bakka A, Schrumpf E, Hanssen LE, Engh V, Bergan A, Flatmark A. Surgical treatment as a principle in patients with advanced abdominal carcinoid tumors. *Surgery* 1992; **111:** 48-54
40 **Moertel CG,** Kvols LK, O'Connell MJ, Rubin J. Treatment of neuroendocrine carcinomas with combined etoposide and cisplatin. Evidence of major therapeutic activity in the anaplastic variants of these neoplasms. *Cancer* 1991; **68:** 227-232
41 **Moertel CG,** Lefkopoulo M, Lipsitz S, Hahn RG, Klaassen D. Streptozocin-doxorubicin, streptozocin-fluorouracil or chlorozotocin in the treatment of advanced islet-cell carcinoma. *N Engl J Med* 1992; **326:** 519-523
42 **Penn I.** Hepatic transplantation for primary and metastatic cancers of the liver. *Surgery* 1991; **110:** 726-734
43 **Bechstein WO,** Neuhaus P. Liver transplantation for hepatic metastases of neuroendocrine tumors. *Ann N Y Ac Sci* 1994; **733:** 507-514
44 **Alessiani M,** Tzakis A, Todo S, Demetris AJ, Fung JJ, Starzl TE.Assessment of five-year experience with abdominal organ cluster transplantation. *J Am Coll Surg* 1995; **180:** 1-9
45 **Routley D,** Ramage JK, McPeake J, Tan KC, Williams R. Orthotopic liver transplantation in the treatment of metastatic neuroendocrine tumors of the liver. *Liver Transpl Surg* 1995; **1:** 118-121
46 **Le Treut YP,** Delpero JR, Dousset B, Cherqui D, Segol P, Mantion G, Hannoun L, Benhamou G, Launois B, Boillot O, Domergue J, Bismuth H. Results of liver transplantation in the treatment of metastatic neuroendocrine tumors. A 31-case French multicenter report. *Ann Surg* 1997; **225:** 355-364
47 **Lang H,** Oldhafer KJ, Weimann A,Schlitt HJ, Scheumann GFW, Flemming P, Ringe B, Pichlmayr R. Liver transplantation for metastatic neuroendocrine tumors. *Ann Surg* 1997; **225:** 347-354
48 **Florman S,** Toure B, Kim L, Gondolesi G, Roayaie S, Krieger N, Fishhein T, Emre S, Miller C, Schwartz M. Liver transplantation for neuroendocrine tumors. *J Gastrointest Surg* 2004; **8:** 208-212
49 ***Lehnert T.*** Liver transplantation for metastatic neuroendocrine carcinoma: An analysis of 103 patients. *Transplantation* 1998; **66:** 1307-1312
50 **Pichlmayr R,** Weimann A, Oldhafer KJ, Schlitt HJ, Tusch G, Raab R. Appraisal of transplantation for malignant tumors of the liver with special reference to early stage hepatocellular carcinoma. *Eur J Surg Oncol* 1998; **24:** 60-67
51 **Rosenau J,** Bahr MJ, von Wasielewski R, Mengel M, Schmidt HHJ, Nashan B, Lang H, Klempnauer J, Manns MP, Boeker KH. Ki67, e-cadherin, and p53 as prognostic indicators of long-term outcome after liver transplantation for metastatic neuroendocrine tumors. *Transplantation* 2002; **73:** 386-394
52 **Cahlin C,** Friman S, Ahlman H, Backman L, Mjornstedt L, Lindner P, Herlenius G, Olausson M. Liver transplantation for metastatic neuroendocrine tumor disease. *Transplant Proc* 2003; **35:** 809-810
53 **O'Grady JG,** Polson RJ, Rolles K, Calne RY, Williams R. Liver transplantation for malignant disease. Results in 93 consecutive patients. *Ann Surg* 1988; **207:** 373-379
54 **Arnold JC,** O'Grady JG, Bird GL, Calne RY, Williams R. Liver transplantation for primary and secondary hepatic apudomas. *Br J Surg* 1989; **76:** 248-249
55 **Bramley PN,** Lodge JP, Losowsky MS, Giles GR. Treatment of metastatic Vipoma by liver transplantation. *Clin Transplant* 1990; **4:** 276-278
56 **Alsina AE,** Bartus S, Hull D, Rosson R, Schweizer RT. Liver transplant for metastatic neuroendocrine tumor. *J Clin Gastroenterol* 1990; **12:** 533-537
57 **Curtiss SI,** Mor E, Schwartz ME, Sung MW, Hytiroglou P, Thung SN, Sheiner PA, Emre S, Miller CM. A rational approach to the use of hepatic transplantation in the treatment of metastatic neuroendocrine tumors. *J Am Coll Surg* 1995; **180:** 184-187
58 **Anthuber M,** Jauch KW, Briegel J, Groh J, Schildberg FW. Results of liver transplantation for gastroenteropancreatic tumor metastases. *World J Surg* 1996; **20:** 73-76
59 **Dousset B,** Saint-Marc O, Pitre J, Soubrane O, Houssin D, Chapuis Y. Metastatic endocrine tumors: medical treatment, surgical resection, or liver transplantation. *World J Surg* 1996; **20:** 908-914
60 **Gottwald T,** Koveker G, Busing M, Lauchart W, Becker HD. Diagnosis and management of metastatic gastrinoma by multimodality treatment including liver transplantation: report of a case. *Surg Today* 1998; **28:** 551-558
61 **Frilling A,** Rogiers X, Malago M, Liedke O, Kaun M, Broelsch CE. Liver transplantation in patients with liver metastases of neuroendocrine tumors. *Transplant Proc* 1998; **30:** 3298-3300
62 **Pascher A,** Steinmuller T, Radke C, Hosten N, Wiedenmann B, Neuhaus P, Bechstein WO. Primary and secondary hepatic manifestation of neuroendocrine tumors. *Langenbecks Arch Surg* 2000; **385:** 265-270
63 **Claure RE,** Drover DD, Haddow GR, Esquivel CO, Angst MS. Orthotopic liver transplantation for carcinoid tumour

metastatic to the liver: anesthetic management. *Can J Anaesth* 2000; **47:** 334-337

64 **Ringe B, Lorf T,** Dopkens K, Canelo R. Treatment of hepatic metastases from gastroenteropancreatic neuroendocrine tumors: Role of liver transplantation. *World J Surg* 2001; **25:** 697-699

65 **Fernandez JA,** Robles R, Marin C, Hernandez Q, Sanchez Bueno F, Ramirez P, Rodriguez JM, Lujan JA, Navalon JC, Parrilla P. Role of liver transplantation in the management of metastatic neuroendocrine tumors.*Transplant Proc* 2003; **35:** 1832-1833

66 **Amarapurkar AD,** Davies A, Ramage JK, Stangou AJ, Wight DGD, Portmann BD. Proliferation of antigen MIB-1 in metastatic carcinoid tumours removed at liver transplantation: revelance to prognosis. *Eur J Gastroenterol Hepatol* 2003; **15:** 139-143

Science Editor Guo SY **Language Editor** ELsevier HK

PO Box 2345, Beijing 100023, China
www.wjgnet.com
wjg@wjgnet.com

ELSEVIER

World J Gastroenterol 2005;11(48):7684-7685
World Journal of Gastroenterology ISSN 1007-9327

• *CASE REPORT* •

Successful outcome following resection of a pancreatic liposarcoma with solitary metastasis

IM Dodo, JA Adamthwaite, P Jain, A Roy, PJ Guillou, KV Menon

IM Dodo, JA Adamthwaite, P Jain, A Roy, PJ Guillou, KV Menon, Department of Academic Surgery, St James's University Hospital, Leeds, West Yorkshire LS9 7TF, United Kingdom
Correspondence to: Mr KV Menon, Consultant Hepatobiliary Surgeon, St James's University Hospital, Leeds LS9 7TF, United Kingdom. kvmenon@aol.com
Telephone: +44-113-2064036 Fax: +44-113-2066416
Received: 2004-12-30 Accepted: 2005-02-18

Abstract

Liposarcomas are rare soft tissue tumors, commonly affecting the lower limbs and less commonly the retroperitoneum. Although other organs can be affected, the pancreas is one of the rarest, and metastasis at presentation has never been reported. We describe the case of a 76-year-old gentleman presenting with abdominal pain and an abdominal mass. Imaging confirmed a primary tumor in the body and tail of the pancreas, with a metastatic deposit in the mesentery adjacent to the second part of the duodenum. Biopsy confirmed a liposarcoma, and subsequently a complete surgical excision was achieved. He then received adjuvant radiotherapy and has remained disease free for the next 26 mo.

Key words: Pancreas; Liposarcoma; Metastasis

Dodo IM, Adamthwaite JA, Jain P, Roy A, Guillou PJ, Menon KV. Successful outcome following resection of a pancreatic liposarcoma with solitary metastasis. *World J Gastroenterol* 2005; 11(48): 7684-7685
http://www.wjgnet.com/1007-9327/11/7684.asp

INTRODUCTION

Primary retroperitoneal neoplasms account for only 0.1-0.2% of all malignancies. Liposarcoma is a rare mesenchymal tumor that occurs most commonly in the soft tissues of the extremities, but other sites such as the retroperitoneum can also be involved. Retroperitoneal liposarcomas grow slowly and silently. Prognosis is poor due to relapse, so only complete excision, which is often difficult, produces a 'cure'[1]. There are only four cases of pancreatic liposarcoma in the literature. To our knowledge, this is the first reported case of metastatic pancreatic liposarcoma at the time of presentation, with successful outcome following surgery.

CASE REPORT

A 76-year-old retired civil engineer presented with a 1-mo history of abdominal pain. He had anorexia associated with significant weight loss. His medical history was unremarkable. He was a smoker and drank a moderate amount of alcohol. On examination he was cachectic and had a large, firm, but non-tender, upper abdominal mass. All blood results including tumor markers (CEA, CA 19.9, AFP, CA125) were within the normal limits. Abdominal ultrasound showed two large masses adjacent to the pancreas. CT scan revealed a 20-cm mass in the mesentery adjacent to the second part of the duodenum, and an 8-cm tumor of the body and tail of the pancreas (Figure 1). The appearances were suggestive of liposarcoma, and this was confirmed by CT-guided core biopsy.

At laparotomy, he had a primary tumor (9 cm×6 cm ×2.5 cm) (Figure 2A) in the distal body and tail of the pancreas attached to the spleen and a further tumor (27 cm ×20 cm×10 cm) (Figure 2B) adjacent to the second part of the duodenum, not infiltrating the bowel or the pancreas. He underwent distal pancreatectomy with splenectomy and the second lesion, which was encapsulated, was completely enucleated. His post-operative recovery was slow with the development of sepsis and a pancreatic fistula, which was managed conservatively with drainage.

Histology of both masses demonstrated a well differentiated sclerosing liposarcoma (Figure 3A) with an area within the primary mass of dedifferentiation (Trojani grade 3) (Figure 3B). The patient received adjuvant radiotherapy and was under follow-up with abdominal CT every 6 mo. At 26 mo, there was no evidence of recurrence and he remained asymptomatic.

DISCUSSION

Liposarcomas are intermediate (locally aggressive) malignant mesenchymal tumor comprising 16-18% of all malignant soft tissue tumors in adults[2]. The incidence is the same in the USA and Europe, with a slight male preponderance[2]. These tumors can grow slowly by direct invasion and can metastasize to the lungs, liver and other viscera[3]. Histologically they can be classified into well differentiated (WD), myxoid, round cell poorly differentiated myxoid and pleomorphic[4,5].

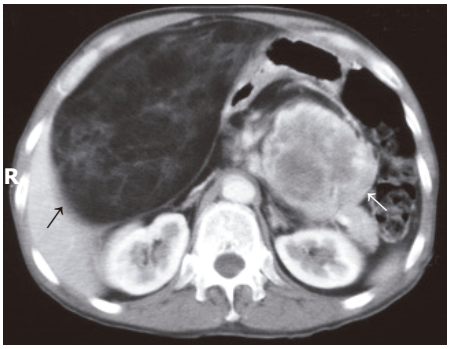

Figure 1 Abdominal CT showing the primary tumor in the body and tail of the pancreas (white arrow) and the solitary metastasis in the mesentery adjacent to the duodenum (black arrow).

Figure 2 The primary tumor (right) and its solitary metastasis (left) after removal.

WD liposarcomas are the commonest, accounting for approximately 40-45%[6]. WD liposarcomas can in turn be subdivided morphologically into four main subtypes: adipocytic, sclerosing, inflammatory and spindle cell. This case was a WD sclerosing liposarcoma, which ranks second in frequency, and is most often seen in retroperitoneal and paratesticular lesions[6].

WD liposarcomas show no potential for metastasis unless they undergo dedifferentiation. Dedifferentiation occurs in up to 10%, with 90% arising *de novo* and the rest in recurrences. Risk of dedifferentiation appears higher with deep-seated (particularly retroperitoneal) lesions and is markedly less in the limbs. This is probably a time-dependant phenomenon. However, it is often impossible to obtain a wide surgical resection margin and local recurrence is almost inevitable and often leads to death[6].

Retroperitoneal liposarcomas produce non-specific symptoms and are often extensive on diagnosis[1]. Most tumors occur at 40-60 years of age, though they may appear at any time. The etiology of these tumors is unknown, although trauma or radiation exposure has been suggested. CT scan is good at characterizing the lesions and aspiration cytology is recommended to differentiate from other pancreatic neoplasms[2]. Pancreatic liposarcomas are very rare with eventual metastases reported in 30-60% of cases[3]. Regardless of cell type, aggressive surgical excision offers the best chance of cure[3]. Some patients may benefit from adjuvant radiotherapy and less commonly chemotherapy. This patient had successful resection of the primary tumor and a giant metastasis followed by adjuvant radiotherapy, and had remained disease free. Prognosis depends on tumor location and histological type[2]. Reported 5-year survival following surgical excision varies from 41%[3] to 50%[4]. Radiotherapy can increase the duration of remission after incomplete excision and possibly achieve clinical cure[3].

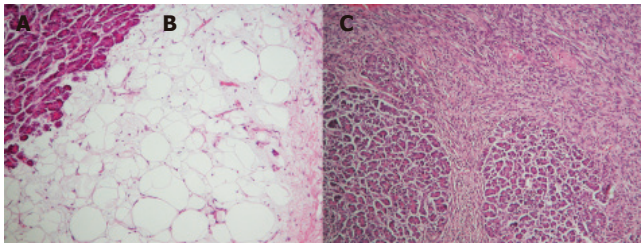

Figure 3 Microphotographs of the primary tumor. **A:** Normal pancreatic tissue; **B:** well-differentiated sclerosing liposarcoma; **C:** area of dedifferentiation.

CONCLUSION

Aggressive resection combined with adjuvant radiotherapy should be considered for metastatic pancreatic liposarcomas when feasible as this offers the best chance of cure and follow-up is essential.

REFERENCES

1 **Osmanagaoglu MA,** Bozkaya H, Ozeren M, Cobanoglu U. Primary retroperitoneal liposarcoma. *Eur J Obstet Gynecol Reprod Biol* 2003; **109:** 228-230
2 **Amano H,** Harima K, Aibe T, Nagatomi Y, Kawashima M, Maetani N, Azuma M, Ariyama S, Fuji T, Kawamura S, Takemoto T. A case of pancreatic liposarcoma (author's transl). *Nippon Shokakibyo Gakkai Zasshi* 1981; **78:** 1475-1479
3 **Elliott TE,** Albertazzi VJ, Danto LA. Pancreatic liposarcoma: case report with review of retroperitoneal liposarcomas. *Cancer* 1980; **45:** 1720-1723
4 **Milano C,** Colombato LA, Fleischer I, Boffi A. Liposarcoma of the pancreas. Report of a clinical case and review of the literature. *Acta Gastroenterol Latinoam* 1988; **18:** 133-138
5 **Choux R,** Andrac L, Rodriguez M, Masselot R, Hassoun J. Liposarcoma of the pancreas. Study of a case including ultrastructure. *Ann Anat Pathol (Paris)* 1979; **24:** 251-259
6 **Dei Tos AP, Pedeutour F.** Atypical lipomatous tumor/Well differentiated liposarcoma and Dedifferentiated liposarcoma. In: Fletcher CDM, Unni K, Mertens K eds. *Pathology and genetics of tumors of soft tissue and bone*. Lyon: IARC Press 2000: 35-39

Science Editor Wang XL and Guo SY **Language Editor** Elsevier HK

PO Box 2345, Beijing 100023, China
www.wjgnet.com
wjg@wjgnet.com

ELSEVIER

World J Gastroenterol 2005;11(48):7686-7687
World Journal of Gastroenterology ISSN 1007-9327

• *CASE REPORT* •

Recurrent severe gastrointestinal bleeding and malabsorption due to extensive habitual megacolon

Ingo Mecklenburg, Markus Leibig, Christof Weber, Stefan Schmidbauer, Christian Folwaczny

Ingo Mecklenburg, Christian Folwaczny, Department of Gastroenterology and Endoscopy, Medizinische Poliklinik, Ludwig-Maximilians-University, Munich, Germany
Markus Leibig, Department of Cardiology, Medizinische Poliklinik, Ludwig-Maximilians-University, Munich, Germany
Christof Weber, Institute for Clinical Radiology, Klinikum Innenstadt, Ludwig-Maximilians-University, Munich, Germany
Stefan Schmidbauer, Department of Surgery, Klinikum Innenstadt, Ludwig-Maximilians-University, Munich, Germany
Correspondence to: Dr. Christian Folwaczny, Medizinische Poliklinik, Klinikum Innenstadt, Ludwig-Maximilians-University, Pettenkoferstr. 8a, 80336 Munich, Germany. christian.folwaczny@med.uni-muenchen.de
Telephone: +49-89-5160-2625 Fax: +49-89-5160-4187
Received: 2005-03-01 Accepted: 2005-08-03

Abstract

Dilatation of the colon and the rectum, which is not attributable to aganglionosis, is a rare finding and can be the result of intractable chronic constipation. We report a rare case of a 29-year-old male patient with impressive megacolon, in whom Hirschsprung's or Chagas disease was ruled out. In the present case, dilatation of the colon was most likely due to a behavioral disorder with habitual failure of defecation. Chronic stool retention led to a bizarre bulging of the large bowel with displacement of the other abdominal organs and severe occult blood loss. Because of two episodes of life-threatening gastrointestinal bleeding despite conventional treatment of constipation, a surgical approach for bowel restoration was necessary. Temporary loop ileostomy had to be performed for depressurization of the large bowel and the subsequent possibility for effective antegrade colonic lavage to remove impacted stools. Shortly after the operation, the patient was healthy and could easily manage the handling of the ileostomy. However, the course of the megacolon in this young adult cannot be predicted and the follow-up will have to reveal if regression of this extreme colonic distension with reestablishment of regular rectal perception will occur.

Key words: Gastrointestinal bleeding; Malabsorption; Habitual megacolon

Mecklenburg I, Leibig M, Weber C, Schmidbauer S, Folwaczny C. Recurrent severe gastrointestinal bleeding and malabsorption due to extensive habitual megacolon. *World J Gastroenterol* 2005; 11(48): 7686-7687
http://www.wjgnet.com/1007-9327/11/7686.asp

INTRODUCTION

Occult gastrointestinal bleeding is a frequent actuality in human beings, likewise is a temporary absence after drinking beer on the "Oktoberfest" in Munich. We report the case of a young male with the unusual combination of both conditions.

CASE REPORT

A 29-year-old male patient collapsed at the "Oktoberfest" after consumption of a small beer and was admitted to our emergency department. The patient was pale and displayed hemoglobin of 30 g/L despite normal blood pressure and heart rate. On clinical examination, cachexia and an obvious distension of the abdomen with slight pain in the epigastrium and the periumbilical region were noted. The digital rectal exam revealed black stools with positive guaiac testing, but the patient denied gross rectal bleeding in the past. The patient has seldom bowel movements (every third day) and denotes the absence of the urge for defecation. He has recently lost his job as a janitor because of permanent fatigue and decreasing tolerance to work. Furthermore, he reported an unclassified "bowel disease" since early childhood and a "dilatation" of the colon which had been performed during infancy. Two years ago, iron deficiency anemia had been treated at another hospital but repeated attempts for colonoscopy had failed because of stool residues in the colon despite lavage for several days at that time.

After transfusion, a diagnostic procedure was performed in addition to the severe anemia and the laboratory tests revealed significant iron deficiency with a ferritin level of 6 μg/L and transferrin saturation of 4.5%. Serum potassium and albumin were decreased to 2.13 mmol/L and 28 g/L, respectively. The abdominal CT scan showed massive dilatation of the rectum and the left-sided colon (Figures 1A and B) with displacement of the other organs. A colonoscopy could not be performed because of persistent masses of stools in the colon even after prolonged bowel lavage. An upper gastrointestinal endoscopy demonstrated regular mucosa without evidence for celiac disease or a bleeding source in the proximal gastrointestinal tract. A radionuclide bleeding

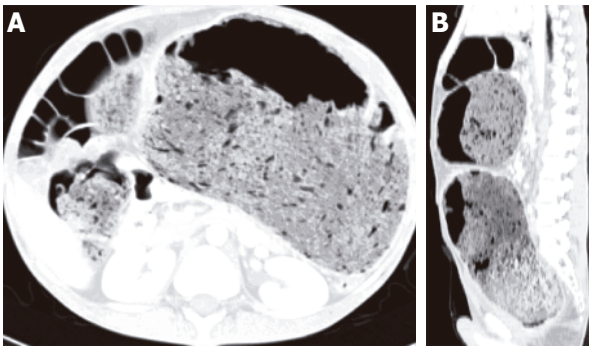

Figure 1 A: Axial CT image of the abdomen; **B:** Saggital CT reconstruction of the abdomen.

scan was negative for an apparent bleeding source. Rectal manometry demonstrated regular arbitrary contraction and a normal reflectory relaxation of the anal sphincter. A dynamic MR defecography revealed again a massive dilatation of the distal colon with complete failure of emptying on command. The histological examination of a rectal biopsy demonstrated chronic proctitis with pseudomelanosis and explicit verification of submucous ganglions excluding Hirschsprung's disease (aganglionosis). Chagas' disease was ruled out by serology. A pathological H2-glucose breath test showed signs for a bacterial overgrowth of the small bowel and significant osteopenia was documented by measurement of the bone density by dual X-ray densitometry.

Initially, we aimed at relieving the chronic constipation by regular administration of polyethylene glycol. However, distention of the colon was even progressive and gastrointestinal bleeding continued. Therefore, a temporary loop ileostomy was performed and about 12 kg of stools could be removed by antegrade colonic lavage. A CT scan 3 wk after surgery demonstrated declining of the colonic dilatation with a marked decrease of abdominal distension. The postoperative course was uneventful and the patient's fitness improved significantly. He received intravenous iron and vitamin supplementation and due to the bacterial overgrowth antibiotic treatment with metronidazole was initiated. Subsequently lower gastrointestinal bleeding subsided and a repeat colonoscopy showed regular mucosa in the right colon with atrophic appearance of the mucosa in the left colon. The patient was motivated to perform stool training aiming at the establishment of a normal rectal perception.

DISCUSSION

Dilatation of the colon and the rectum, which is not attributable to aganglionosis[1] is a rare finding and can be the result of intractable chronic constipation[2]. Herein we report a rare case of a young adult with impressive megacolon, in whom Hirschsprung's or Chagas disease was ruled out. In the present case dilatation of the colon is likely to be due to a behavioral disorder with habitual failure of defecation. Chronic stool retention led to a bizarre bulging of the large bowel with displacement of the other abdominal organs. Occult gastrointestinal bleeding has not been described in patients with megacolon, but in our patient dilation of the colonic wall presumably resulted in occult blood loss. The exact bleeding source could not be localized by a radionuclide bleeding scan, thus the intensity of bleeding was supposed to be low. The low hemoglobin value was well tolerated by the patient; therefore, the anemia was most likely due to a chronic blood loss. However, the patient had previously experienced two episodes of life-threatening gastrointestinal bleeding despite conventional treatment of constipation; consequently, a surgical approach for bowel restoration appeared feasible.

A further concern in this patient was the apparent malabsorption with low levels of albumin, severe iron deficiency and osteoporosis. Distension of the colon with subsequent stasis can lead to small bowel bacterial overgrowth, as demonstrated in patients with megacolon due to Chagas disease[3]. Restoration of the small bowel by antibiotic treatment would be a futile approach as long as the underlying stasis of the bowel is not corrected. Therefore, a temporary loop ileostomy was performed for depressurization of the large bowel and the subsequent possibility for effective antegrade colonic lavage to remove impacted stools[4].

In the present case, the indication for surgical intervention was delicate, because ileostomy does not affect the underlying behavioral disorder and includes the risk for a complete unlearning of defecation. Furthermore, the development of a diversion colitis is a possible sequelae[5]. Nevertheless, shortly after the operation the patient was healthy and could easily manage the handling of the ileostomy. However, the course of the megacolon in this young adult cannot be predicted and the follow-up will have to reveal if regression of this extreme colonic distension with re-establishment of regular rectal perception will occur.

REFERENCES

1 **Puri P**, Shinkai T. Pathogenesis of Hirschsprung's disease and its variants: recent progress. *Semin Pediatr Surg* 2004; **13:** 18-24
2 **Rajagopal A**, Martin J. Giant fecaloma with idiopathic sigmoid megacolon: report of a case and review of the literature. *Dis Colon Rectum* 2002; **45**: 833-835
3 **Guimaraes Quintanilha AG**, Azevedo dos Santos MA, Avila-Campos MJ, Saad WA, Pinotti HW, Zilberstein B. Chagasic megacolon and proximal jejunum microbiota. *Scand J Gastroenterol* 2000; **35**: 632-636
4 **Stabile G**, Kamm MA, Hawley PR, Lennard-Jones JE. Results of stoma formation for idiopathic megarectum and megacolon. *Int J Colorectal Dis* 1992; **7:** 82-84
5 **Edwards CM**, George B, Warren B. Diversion colitis--new light through old windows. *Histopathology* 1999; **34:** 1-5

Science Editor Guo SY **Language Editor** Elsevier HK

PO Box 2345, Beijing 100023, China
www.wjgnet.com
wjg@wjgnet.com

ELSEVIER

World J Gastroenterol 2005;11(48):7688-7689
World Journal of Gastroenterology ISSN 1007-9327

• *CASE REPORT* •

Does *Fasciola hepatica* infection modify the response of acute hepatitis C virus infection to IFN-α treatment?

Mehmet Sahin, Mehmet Isler, Altug Senol, Mustafa Demirci, Zeynep Dilek Aydın

Mehmet Sahin, Altug Senol, Zeynep Dilek Aydın, Department of Internal Medicine, Suleyman Demirel University, School of Medicine, Isparta, Turkey
Mehmet Isler, Department of Internal Medicine, Division of Gastroenterology, Suleyman Demirel University, School of Medicine, Isparta, Turkey
Mustafa Demirci, Department of Microbiology and Parasitology, Suleyman Demirel University, School of Medicine, Isparta, Turkey
Correspondence to: Mehmet Sahin, MD, SDU Tıp Fakultesi, Ic Hastalıkları BD, Isparta, Turkey. mehmetsahin66@hotmail.com
Telephone: +90-246-211-26-13 Fax: +90-246-237-02-40
Received: 2004-09-21 Accepted: 2004-12-01

Abstract

Immunologic response to acute hepatitis C is mainly a Th1 response, whereas fasciolopsiasis is associated with a diverse T-cell response. Interferon-alpha has immunomodulatory effects and enhances Th1 immune response. Fasciola infection could theoretically interfere with the Th1 immune response, even when acquired after an initial response to interferon-alpha treatment for acute hepatitis C virus (HCV) infection. We report here the case of a male patient who acquired *Fasciola hepatica* infection after an initial response to IFN-alpha therapy with a favorable outcome

Key words: Hepatitis C; Interferon; *Fasciola hepatica*

Sahin M, Isler M, Senol A, Demirci M, Aydın ZD. Does *Fasciola hepatica* infection modify the response of acute hepatitis C virus infection to IFN-α treatment? *World J Gastroenterol* 2005; 11(48): 7688-7689
http://www.wjgnet.com/1007-9327/11/7688.asp

INTRODUCTION

Hepatitis C virus (HCV) infection is a common cause of hepatocellular injury associated with complex immunologic mechanisms including both humoral and cell-mediated responses. Acute hepatitis C infection especially produces a Th1 response[1]. Fasciolopsiasis, like other helminth infections, is associated with the induction of T-cell responses particularly the Th2 subtype[2]. Enhanced induction of Th2 cytokines and downregulation of Th1 responses during infection with *Fasciola hepatica* could be expected to interfere with the natural course of and the response to the treatment of acute viral hepatitis C. The concurrence of HCV and *F. hepatica* infection is uncommon and whether *F. hepatica* infection acquired during IFN-α therapy has any effect on HCV replication is unknown.

CASE REPORT

A 50-year-old male patient, with chronic renal failure began hemodialysis 3 mo ago. Prior to initiation of hemodialysis, liver function tests were normal and serological tests for hepatitis B and C were negative. During the 3rd mo of hemodialysis, laboratory evaluation showed elevations of 183 IU/L AST (normal, 5-45 IU/L), 394 IU/L ALT (normal, 5-45 IU/L), 141 IU/L GGT (normal, 0-50 IU/L), and 90 IU/L ALP (normal, 53-128 IU/L). Physical examination was normal. Abdominal ultrasonography showed normal liver size with grade II heterogeneity, normal portal vein size and no ascites. Anti-HCV antibody and HCV RNA were positive. Anti-HAV IgM, HBs Ag, and anti HIV were negative.

The patient was diagnosed with acute viral hepatitis C. IFN-α 2b (Intron A; Schering Plough Corporation, Kenilworth, NJ, USA) was started 3 MU thrice weekly subcutaneously for 12 mo. ALT levels normalized during the 4th wk of the therapy. HCV RNA was negative after 6 mo.

After 6 mo of treatment with IFN-α, the patient reported marked malaise and right upper quadrant abdominal pain. Physical examination revealed right hypochondrium tenderness. Repeated liver function tests showed elevations of ALT (51 IU/L), ALP (196 IU/L), and GGT (272 IU/L). WBC were 6 800/mm^3 with marked eosinophilia (20%). Abdominal ultrasonography showed hepatomegaly and a well-defined 9-mm hyperechoic round mass in the anterior–superior segment of the right hepatic lobe which raised the suspicion of hemangioma and the possibility of *F. hepatica*. The causes of eosinophilia were investigated in the 9th mo of IFN-α therapy. Serology for fasciolopsiasis revealed positivity by enzyme-linked immunosorbent assay (ELISA) prepared against a secretory antigen according to Carnevale *et al*.[3]. The assay was reported to have 100% sensitivity and 100% specificity. ELISA absorbance value of the patient's sera was 2 900 units, while the cut-off value was 380. Stool specimens were negative for ova and parasites of *F. hepatica*. Oral triclabendazole (10 mg/kg), twice daily

doses was initiated for fasciolopsiasis. One week after the initiation of triclabendazole (10th mo of IFN therapy), the patient reported to have right upper abdominal pain and was hospitalized. Physical examination showed abdominal tenderness on the upper right quadrant and a positive Murphy's sign. Laboratory tests showed elevations of serum total and direct bilirubin which were 2.28 mg/L (normal, 0.2-1 mg/L) and 2.24 mg/L (normal, 0.1-0.5 mg/L), respectively in addition to elevations of ALT (58 IU/L), AST (53 IU/L), GGT (333 IU/L), and ALP (399 IU/L). WBC were 11 700/mm^3 with 10% eosinophilia. Abdominal ultrasonography revealed no intraparenchymal lesion in the liver, thickening of gallbladder wall and a hyperechoic round mass measured 10 mm in the gallbladder. Intra and extrahepatic bile ducts were normal. The patient's condition improved after 48 h of intravenous fluids and antibiotics.

Twenty-four months after the initiation of IFN-α treatment, liver function tests and complete blood count were normal with 2% eosinophilia. Stool specimen for fasciola was negative. HCV RNA was negative. The patient continued his regular hemodialysis schedule.

DISCUSSION

An effective host response against a viral infection requires coordinated efforts by both nonspecific and antigen-specific immune responses. Cytokines play a key role in the cell-to-cell communication necessary for this process. Immediately after viral infection, several antigen nonspecific effector mechanisms are activated[4].

Among the individuals who recover from acute HCV infection, Th1 subtype responses predominate and are necessary for complete recovery in acute HCV infection[5,6]. Lechmann *et al*.[7] found that cellular immune responses against a panel of HCV core-derived peptides are stronger than humoral immune responses in individuals who have recovered from acute HCV infection. Also, experimental models reveal that rats with resolved acute hepatitis C have a higher proportion of cells producing Th1 subtype cytokines. Parasitic infections are frequently accompanied with a downregulation of cell-mediated immunity. Parasitic infections can exert bystander suppression of protective Th1 responses to infection and liver flukes may secrete molecules that down-regulate Th1 responses[2]. In an experimental model, Miriam *et al*.[8] showed that Th1 response to *Bordetella pertussis* antigens is markedly suppressed following infection with *F. hepatica*. Kamal *et al*.[9] showed that patients with acute hepatitis C and schistosomiasis coinfection cannot clear viremia and show rapid progression once chronic infection is established. In contrast, in the present case, the clinical and serological response marked by the clearance of HCV-RNA was maintained though the acquisition of *F. Hepatica*. This favorable outcome may be related to immunomodulatory effects of IFN-α therapy. IFN-α induces the production of certain cytokines and has been recognized as a cytokine promoting Th1 differentiation[10,11]. In addition, it increases cytotoxic activity of natural killer cells, cytotoxic T lymphocytes and macrophages[12]. Recent data suggest that early treatment of acute HCV infection with IFN-α may be highly effective in preventing chronic hepatitis C infection[13].

In conclusion, the present case illustrates that acute hepatitis C is responsive to the treatment even in the coexistence of fasciolopsiasis.

REFERENCES

1 **Jacobson Brown PM**, Neuman MG. Immunopathogenesis of hepatitis C viral infection: Th1/Th2 responses and the role of cytokines. *Clin Biochem* 2001; **34:** 167-171

2 **O'Neill SM**, Brady MT, Callanan JJ, Mulcahy G, Joyce P, Mills KH, Dalton JP. Fasciola hepatica infection downregulates Th1 responses in mice. *Parasite Immunol* 2000; **22:** 147-155

3 **Carnevale S**, Rodriguez MI, Santillan G, Labbe JH, Cabrera MG, Bellegarde EJ, Velasquez JN, Trgovcic JE, Guarnera EA. Immunodiagnosis of human fascioliasis by an enzyme-linked immunosorbent assay (ELISA) and a micro-ELISA. *Clin Diagn Lab Immunol* 2001; **8:** 174-177

4 **Foster GR**. Interferons in host defense. *Semin Liver Dis* 1997; **17**: 287-295

5 **Koziel MJ**. The role of immune responses in the pathogenesis of hepatitis C virus infection. *J Viral Hepat* 1997; **4 Suppl 2:** 31-41

6 **Woitas RP**, Lechmann M, Jung G, Kaiser R, Sauerbruch T, Spengler U. CD30 induction and cytokine profiles in hepatitis C virus core-specific peripheral blood T lymphocytes. *J Immunol* 1997; **159**: 1012-1018

7 **Lechmann M**, Ihlenfeldt HG, Braunschweiger I, Giers G, Jung G, Matz B, Kaiser R, Sauerbruch T, Spengler U. T- and B-cell responses to different hepatitis C virus antigens in patients with chronic hepatitis C infection and in healthy anti-hepatitis C virus--positive blood donors without viremia. *Hepatology* 1996; **24:** 790-795

8 **Brady MT**, O'Neill SM, Dalton JP, Mills KH. Fasciola hepatica suppresses a protective Th1 response against Bordetella pertussis. *Infect Immun* 1999; **67:** 5372-5378

9 **Kamal SM**, Rasenack JW, Bianchi L, Al Tawil A, El Sayed Khalifa K, Peter T, Mansour H, Ezzat W, Koziel M. Acute hepatitis C without and with schistosomiasis: correlation with hepatitis C-specific CD4(+) T-cell and cytokine response. *Gastroenterology* 2001; **121**: 646-656

10 **Dianzani F**. Biological basis for the clinical use of interferon. *Gut* 1993; **34**: 74-76

11 **Eui-Young So**, Hyun-Hee Park and Choong-Eun Lee. IFN-gamma and IFN-α posttranscriptionally down-regulate the IL-4 induced IL-4 receptor gen expression. *J Immunol* 2000; **165**: 5472-5479

12 **Rook G**. Immunity to viruses, bacteria and fungi. In:Roitt I, Brostoff J, Male D, eds. *Immunology. London: Mosby* 1993; **3**: 15-22

13 **Jaeckel E**, Cornberg M, Wedemeyer H, Santantonio T, Mayer J, Zankel M, Pastore G, Dietrich M, Trautwein C, Manns MP. Treatment of acute hepatitis C with interferon alfa-2b. *N Engl J Med* 2001; **345:** 1452-1457

Science Editor Wang XL and Guo SY **Language Editor** Elsevier HK

PO Box 2345, Beijing 100023, China
www.wjgnet.com
wjg@wjgnet.com

ELSEVIER

World J Gastroenterol 2005;11(48):7690-7693
World Journal of Gastroenterology ISSN 1007-9327

• *CASE REPORT* •

Autosomal dominant polycystic liver disease in a family without polycystic kidney disease associated with a novel missense protein kinase C substrate 80K-H mutation

Ramón Peces, Joost PH Drenth, Rene HM te Morsche, Pedro González, Carlos Peces

Ramón Peces, Section of Nephrology, Hospital General La Mancha-Centro, Alcázar de San Juan, Ciudad Real and Service of Nephrology, Hospital Universitario La Paz, Madrid, Spain
Joost PH Drenth, Rene HM te Morsche, Department of Medicine, Division of Gastroenterology and Hepatology, Radboud University Nijmegen Medical Center, Nijmegen, The Netherlands
Pedro González, Section of Digestive Hospital General La Mancha-Centro, Alcázar de San Juan, Ciudad Real, Spain
Carlos Peces, Computer Science Superior School, Castilla La Mancha University and Technology Area of the Castilla La Mancha Health Service (SESCAM), Ciudad Real, Spain
Supported by a grant from the Instituto de Ciencias de la Salud, Consejería de Sanidad de Castilla La Mancha (Grant EQ03016). Joost PH Drenth is a recipient of a NOW-VIDI grant
Correspondence to: Dr Ramón Peces, Servicio de Nefrología, Hospital Universitario La Paz, Paseo de la Castellana 261, 28046 Madrid, Spain. cpeces@varnet.com
Telephone: +34-917277224 Fax: +34-917277133
Received: 2004-12-12 Accepted: 2005-06-16

Abstract

Polycystic liver disease (PLD) is characterized by the presence of multiple bile duct-derived epithelial cysts scattered in the liver parenchyma. PLD can manifest itself in patients with severe autosomal dominant polycystic kidney disease (ADPKD). Isolated autosomal dominant polycystic liver disease (ADPLD) is genetically distinct from PLD associated with ADPKD, although it may have similar pathogenesis and clinical manifestations. Recently, mutations in two causative genes for ADPLD, independently from ADPKD, have been identified. We report here a family (a mother and her daughter) with a severe form of ADPLD not associated with ADPKD produced by a novel missense protein kinase C substrate 80K-H (PRKCSH) mutation (R281W). This mutation causes a severe phenotype, since the two affected subjects manifested signs of portal hypertension. Doppler sonography, computed tomography (CT) and magnetic resonance (MR) imaging are effective in documenting the underlying lesions in a non-invasive way.

Key words: ADPLD; Hepatic cysts; Hepatocystin; Inferior vena cava compression; Polycystic liver disease; Portal hypertension

Peces R, Drenth JPH, te Morsche RHM, González P, Peces C. Autosomal dominant polycystic liver disease in a family without polycystic kidney disease associated with a novel missense protein kinase C substrate 80K-H mutation. *World J Gastroenterol* 2005; 11(48): 7690-7693
http://www.wjgnet.com/1007-9327/11/7690.asp

INTRODUCTION

Proof of existence of autosomal dominant polycystic liver disease (ADPLD) as a distinct genetic entity, independently from autosomal dominant polycystic kidney disease (ADPKD), stems from three studies in which isolated familial polycystic liver disease (PLD) was shown to be unlinked to the PKD1 or PKD2 loci[1-3]. In 2000, Reynolds *et al*.[4] identified a locus for ADPLD on chromosome 19p13.2-13.1. In 2003, two independent groups demonstrated that mutations in *PRKCSH*, encoding the β-subunit of glucosidase II, a N-linked glycan-processing enzyme in the endoplasmic reticulum, cause isolated ADPLD[5,6]. Given its role in the pathogenesis of ADPLD, this protein has been renamed as hepatocystin[5]. Very recently, Davila *et al*.[7] found that mutations in *SEC63* (chromosome 6q21), encoding a component of the protein translocation machinery in the endoplasmic reticulum, also cause ADPLD. Mutations in *PRKCSH* and *SEC63* probably account for less than one-third of ADPLD cases, indicating that there is at least one more locus associated with this disease[7,8].

We have reported here the first Spanish family with a severe form of ADPLD not associated with ADPKD. The proband manifested displacement of abdominal structures by a massively enlarged liver causing portal hypertension and inferior vena cava compression.

CASE REPORT

A 36-year-old woman presented with a long history of abdominal enlargement. She had two pregnancies and live births at 29 and 34 years of age, respectively. Physical examination showed a bulging abdomen with a palpable mass extending from the right hemiabdomen to the left quadrant reaching 10 cm below the umbilicus. Laboratory data showed 0.9 mg/dL creatinine (normal range 0.6-1.2 mg/dL), 7.2 g/dL total proteins (normal range 6-8 g/dL), 137 mg/dL total cholesterol (normal range 140-220 mg/dL), 30 mg/dL triglycerides (normal range 50-128 mg/dL), 29 IU/L aspartate

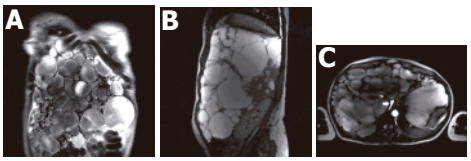

Figure 1 Massive polycystic liver disease on coronal MR imaging (**A**), caudal and posterior displacement of abdominal organs by the massively enlarged liver on sagittal MR imaging (**B**), and compression of the inferior vena cava (arrow) produced by the massively enlarged liver (**C**) on MR angiograph.

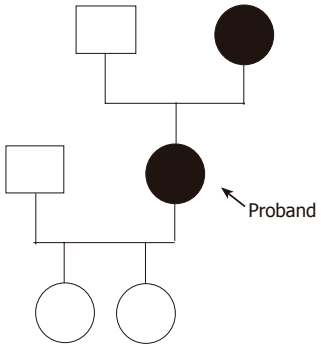

Figure 2 Family pedigree of the patient.

aminotransferase (normal range 10-40 IU/L), 22 IU/L alanine aminotransferase (normal range 10-40 IU/L), 135 IU/L gamma glutamyl transpeptidase (normal range 10-40 IU/L), 117 IU/L alkaline phosphatase (normal range 40-105 IU/L), 1.1 mg/dL total bilirubin (normal range 0.1-1.0 mg/dL), 82% prothrombin time and 394 mg/dL fibrinogen (normal range 200-400 mg/dL). Sonography and computed tomography (CT) of the abdomen were compatible with an increased liver volume caused by numerous hepatic cysts of various sizes. Magnetic resonance (MR) imaging of the abdomen revealed a massive polycystic liver with caudal and posterior displacement of the abdominal organs (Figures 1A and B). Doppler sonography and MR angiography demonstrated displacement of the kidneys and their vascular structures by the massively enlarged polycystic liver. The celiac axis was also displaced and the portal vein and a segment of the inferior vena cava below the hepatic veins were compressed by the hepatic cysts (Figure 1C). The kidneys were normal except for two small cortical cysts on the left kidney. There were signs of moderate portal hypertension with varices in the hepatic hilum. Seven years after the diagnosis, the patient was healthy and free of complications. Currently she is awaiting a liver transplantation.

Family history revealed that the patient's mother also had PLD without kidney disease. The father was not known to suffer from liver or kidney disease. The proband's daughters had no renal or hepatic cysts. The family pedigree is represented in Figure 2. The proband's mother (age 72 years) had a history of cholecystectomy in 1983 (performed in another hospital) and a diagnosis of heterozygous beta thalassemia minor in 1990. She had one daughter. Laboratory data showed 37% hematocrit (normal range 36-46%), 12.2 g/dL hemoglobin (normal range

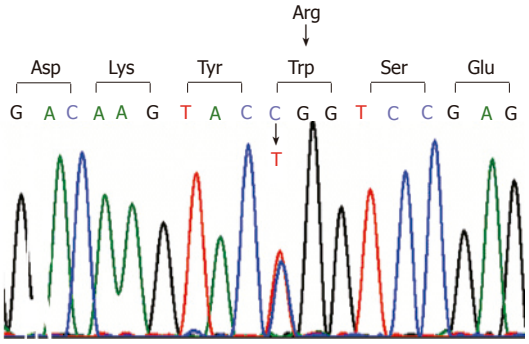

Figure 3 Sequence identification of the C>T changes in exon 10. This mutation, C841T which is predicted to change the amino acid composition of hepatocystin, changes arginine to tryptophan at codon 281 (R281W).

12-16 g/dL), 66.6 fL MCV (80-100 fL), 21.8 pg MCH (normal range 26-34 pg), 5.9% hemoglobin A2 (normal range 2-3.5%), 3 500/μL white blood cell with normal differentiation, 105 000/mm^3 platelet count, 0.6 mg/dL creatinine, 6.9 g/dL total proteins, 177 mg/dL total cholesterol, 101 mg/dL triglycerides, 31 IU/L aspartate aminotransferase, 19 IU/L alanine aminotransferase, 14 IU/L gamma glutamyl transpeptidase, 109 IU/L alkaline phosphatase, 2.1 mg/dL total bilirubin, 79% prothrombin time and 362 mg/dL fibrinogen. Ultrasonography and CT of the abdomen demonstrated PLD. There were signs of portal hypertension with varices in the hepatic hilum, gastrohepatic ligament, and lower esophagus. The spleen was enlarged, measuring 17.6 cm in length. The kidneys were normal. The patient was healthy and had no variceal bleeding. She refused any invasive procedure.

DNA sequencing and mutation detection

DNA was isolated from peripheral blood leukocytes by standard procedures. We performed polymerase chain reaction amplification using specific primer sets for all the 18 exons that constitute the open reading frame of *PRKCSH*. We determined the nucleotide sequences of the amplified fragments by fluorescence sequencing with dye-terminator chemistry on an ABI3700 capillary sequencer (Perkin-Elmer Applied Biosystems).

RESULTS

Sequence analysis of PRKCSH gene from DNA isolated from the proband demonstrated a base pair change (C>T) on one allele at position 841 (Figure 3). This mutation located in exon 10 resulted in a change of the amino acid composition of hepatocystin with the replacement of arginine to tryptophan at codon (R281W). The missense mutation was also present in the affected mother of the proband but not in her two children. Within hepatocystin, the mutation was located between the EF-hand calcium-binding domain, ending at codon 234 and the glutamic acid-rich region which starts at codon 299 (Figure 4). Hepatocystin, the protein product of PRKCSH, comprises 528 amino acid residues and has a predicted molecular mass of approximately 59 ku. This protein contains a signal peptide for translocation across the endoplasmic

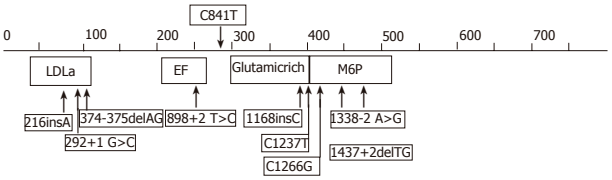

Figure 4 Schematic representation of hepatocystin. The position of *PRKCSH* mutations that have been associated with PCLD are superimposed on the structure of hepatocystin. The new mutation detected in our family is indicated on top. The numbers reflect the amino acid numbering of hepatocystin. LDLa: low-density lipoprotein receptor domain A; EF: EF-hand calcium-binding domains; MPR: mannose 6-phosphate receptor domain.

Table 1 Missense PRKCSH mutation detected in our family

	278			279			280			281		
Species	Asp			Lys			Tyr			Arg		
HS	G	A	C	A	A	G	T	A	C	C	G	G
BT	G	A	C	A	A	G	T	A	C	C	G	G
MM	G	A	C	A	A	G	T	A	C	C	G	C
RN	G	A	C	A	A	G	T	A	C	C	G	C
Patients	G	A	C	A	A	G	T	A	C	**T**	G	G

HS: *Homo sapiens*; BT: *Bos Taurus*; MM: *Mus musculus*, RN: *Rattus norvegicus*. The C841T *PRKCSH* mutation detected in this study is indicated in bold, and for comparison the corresponding nucleotides from various species are included. The numbers on top correspond with the codon numbering of hepatocystin, while Asp is aspartic acid; Lys is lysine; Tyr is tyrosine; Arg is arginine. Note that the C at position 841 is highly conserved among the species.

reticulum membrane, a low-density lipoprotein receptor domain class A (LDLa) domain, two EF-hand domains, a glutamic-acid-rich region, a mannose-6-phosphate receptor domain and a conserved C-terminal HDEL amino acid sequence for endoplasmic reticulum retention. Hepatocystin is an endoplasmic reticulum-resident enzyme that is involved in carbohydrate processing and quality control of newly synthesized glycoproteins.

DISCUSSION

ADPLD is a rare autosomal dominant disorder that has been described in fewer than 50 families from Finnish[8], Dutch[5], American[4], Belgian[2], and Spanish-Belgian[3] ancestry. The pathology of ADPLD consists of numerous cysts of biliary epithelial origin spread throughout the liver parenchyma. This disease is distinct from ADPKD1 and ADPKD2, in which affected individuals develop bilateral renal cysts and liver and pancreatic cysts in advanced cases[9-11]. Cystic liver disease occurs in a substantial portion of patients with ADPKD and end-stage renal disease. Factors influencing the prevalence of PLD in ADPKD include female sex, age (prevalence of PLD is 10% in the third decade, but 60% in patients older than 60 years), and pregnancy (multiparity is associated with increased size and number of cysts in ADPKD)[12].

The recent cloning of the gene involved in ADPLD has greatly facilitated the possibility of a firm molecular diagnosis in our family. Up to now, a total of nine different *PRKCSH* mutations have been described[13,14]. We detected a novel missense *PRKCSH* mutation (R281W) in our family. Several lines of evidence suggest that the R281W represents a bona fide disease causing mutation. First, there is segregation of the mutation with the disease in our family. Second, arginine, a positively charged amino acid is replaced by tryptophan which is neutral. Lastly, the C at position 841 is highly conserved among the species (Table 1).

As is the case for ADPKD, ADPLD is clinically and genetically heterogeneous[8-14]. Although isolated PLD is genetically distinct from PLD associated with ADPKD, both diseases may have similar pathogenesis and clinical manifestations. If ADPLD, like ADPKD[15], occurs by a cellular recessive, two-hit mechanism, then mutations in either *PRKCSH* or *SEC63* will result in loss of proper folding of integral membrane or secreted glycoproteins in bile duct cells that have undergone somatic second hits[7,13,14]. However, the two-hit model has not been investigated in isolated PLD.

The clinical profile of PLD has been defined by Qian *et al*.[16] who on the basis of a small series concluded that extra hepatic manifestations are infrequent but may include simple renal cysts, intracranial aneurysms, and mitral valve abnormalities. Genotype-phenotype relations remain speculative at this point. Liver cysts are usually asymptomatic, and as a consequence, the disease may go undetected and is likely to be underdiagnosed in the general population[17]. Symptoms occurred are caused by the mass effect of the cysts, or the development of complications such as hemorrhage, infection, or rupture of cysts. Symptoms caused by the mass effect of the cysts include vague abdominal distension, early satiety, dyspnea, and back pain. Rarely, ascites can form because of hepatic venous outflow obstruction by cysts. Lower extremity edema is secondary to extrinsic compression of the inferior vena cava, hepatic veins, or portal vein by large or by many small or medium size hepatic cysts. Compression of the bile ducts can cause jaundice. The symptoms of compression or thrombosis of the inferior vena cava may be obscure and a high index of suspicion is required for the diagnosis[18]. Liver metabolic and synthetic functions remain normal, although an increase in serum levels of alkaline phosphatase, bilirubin and gamma glutamyl transpeptidase, and a decrease in serum levels of total cholesterol and triglycerides have been described in some cases[16]. The factors that affect disease progression are unclear. However, some risk factors for the progression of the disease are age, sex, number of pregnancies, and use of estrogen[14,16].

The proband manifested a massively enlarged liver, which caused abdominal heaviness and progressive hemodynamic changes. She presented displacement of abdominal structures by the massively enlarged liver and hepatic cysts not only caused extrinsic compression of the inferior vena cava, but also were responsible for portal hypertension. Whereas laboratory studies in the proband disclosed a slight increase in the serum levels of alkaline phosphatase and gamma glutamyl transpeptidase, and a decrease in serum levels of total cholesterol and triglycerides, the proband's mother presented thrombocytopenia and a slight increase in total bilirubin.

As the proband's history shows, the disease may become highly symptomatic in young women. The more severe extensive development of the condition in the proband than in her affected mother contrasts with the reported greater severity of the liver involvement with age. The increased severity of the disease in the proband could be in relation, at least in part, with repeated pregnancies in this patient. However, other possible factors for the progression of the disease remain unknown. Screening of the at-risk members of the families of other affected patients could help to answer this question.

The presence of (few) renal cysts, as demonstrated in our proband who had 2 renal cysts does not preclude the diagnosis ADPLD. This is in accord with the data from another study that demonstrated *PRKCSH* mutations in four patients with polycystic livers who possessed at least one renal cyst[14].

Most patients with PLD require no treatment. In highly symptomatic patients, percutaneous cyst aspiration, sclerosis and cyst fenestration may be indicated[16]. In patients with diffuse cystic liver, hepatic resection[19] is often the only possibility but entails a high mortality rate. Stent placement in the inferior vena cava has been successfully applied in a few well-selected patients with only inferior vena cava compression. In patients with severe phenotype, liver transplantation should be considered[20]. In our patients, due to the size of their liver, resection of the lobes of their livers for decompression was deemed to be problematic and liver transplantation was considered as the better option in the proband.

In summary, we have described here a family with a severe form of ADPLD not associated with ADPKD, and a novel *PRKCSH* mutation that was vertically transmitted. The two affected subjects manifested signs of portal hypertension. This family underlines the need for a careful investigation of patients with otherwise unexplained liver cystic disease, focusing on whether other organ systems are involved. It also stresses the importance of accurate family investigation whenever possible. Doppler sonography, CT, and MR are effective in documenting the underlying lesions non-invasively.

ACKNOWLEDGMENTS

We thank the family members for their great cooperation.

REFERENCES

1 **Somlo S**, Torres VE, Reynolds D, King BF, Nagorney DM. Autosomal dominant polycystic liver disease without polycystic kidney disease is not linked to either the PKD1 or PKD2 gene loci [abstract]. *J Am Soc Nephrol* 1995; **6:** 727A

2 **Pirson Y**, Lannoy N, Peters D, Geubel A, Gigot JF, Breuning M, Verellen-Dumoulin C. Isolated polycystic liver disease as a distinct genetic disease, unlinked to polycystic kidney disease 1 and polycystic kidney disease 2. *Hepatology* 1996; **23:** 249-252

3 **Iglesias DM**, Palmitano JA, Arrizurieta E, Kornblihtt AR, Herrera M, Bernath V, Martin RS. Isolated polycystic liver disease not linked to polycystic kidney disease 1 and 2. *Dig Dis Sci* 1999; **44:** 385-388

4 **Reynolds DM**, Falk CT, Li A, King BF, Kamath PS, Huston J 3rd, Shub C, Iglesias DM, Martin RS, Pirson Y, Torres VE, Somlo S. Identification of a locus for autosomal dominant polycystic liver disease, on chromosome 19p13.2-13.1. *Am J Hum Genet* 2000; **67:** 1598-1604

5 **Drenth JP**, te Morsche RH, Smink R, Bonifacino JS, Jansen JB. Germline mutations in PRKCSH are associated with autosomal dominant polycystic liver disease. *Nat Genet* 2003; **33:** 345-347

6 **Li A**, Davila S, Furu L, Qian Q, Tian X, Kamath PS, King BF, Torres VE, Somlo S. Mutations in PRKCSH cause isolated autosomal dominant polycystic liver disease. *Am J Hum Genet* 2003; **72:** 691-703

7 **Davila S**, Furu L, Gharavi AG, Tian X, Onoe T, Qian Q, Li A, Cai Y, Kamath PS, King BF, Azurmendi PJ, Tahvanainen P, Kaariainen H, Hockerstedt K, Devuyst O, Pirson Y, Martin RS, Lifton RP, Tahvanainen E, Torres VE, Somlo S. Mutations in SEC63 cause autosomal dominant polycystic liver disease. *Nat Genet* 2004; **36:** 575-577

8 **Tahvanainen P**, Tahvanainen E, Reijonen H, Halme L, Kaariainen H, Hockerstedt K. Polycystic liver disease is genetically heterogeneous: clinical and linkage studies in eight Finnish families. *J Hepatol* 2003; **38:** 39-43

9 **Coto E**, Sanz de Castro S, Aguado S, Alvarez J, Arias M, Menendez MJ, Lopez-Larrea C. DNA microsatellite analysis of families with autosomal dominant polycystic kidney disease types 1 and 2: evaluation of clinical heterogeneity between both forms of the disease. *J Med Genet* 1995; **32:** 442-445

10 **Ariza M**, Alvarez V, Marin R, Aguado S, Lopez-Larrea C, Alvarez J, Menendez MJ, Coto E. A family with a milder form of adult dominant polycystic kidney disease not linked to the PKD1 (16p) or PKD2 (4q) genes. *J Med Genet* 1997; **34:** 587-589

11 **Torres VE**, Harris PC. Autosomal dominant polycystic kidney disease. *Nefrologia* 2003; **23 Suppl 1:** 14-22

12 **Everson GT**, Taylor MR, Doctor RB. Polycystic disease of the liver. *Hepatology* 2004; **40:** 774-782

13 **Drenth JP**, Martina JA, Te Morsche RH, Jansen JB, Bonifacino JS. Molecular characterization of hepatocystin, the protein that is defective in autosomal dominant polycystic liver disease. *Gastroenterology* 2004; **126:** 1819-1827

14 **Drenth JP**, Tahvanainen E, te Morsche RH, Tahvanainen P, Kaariainen H, Hockerstedt K, van de Kamp JM, Breuning MH, Jansen JB. Abnormal hepatocystin caused by truncating PRKCSH mutations leads to autosomal dominant polycystic liver disease. *Hepatology* 2004; **39:** 924-931

15 **Watnick TJ**, Torres VE, Gandolph MA, Qian F, Onuchic LF, Klinger KW, Landes G, Germino GG. Somatic mutation in individual liver cysts supports a two-hit model of cystogenesis in autosomal dominant polycystic kidney disease. *Mol Cell* 1998; **2:** 247-251

16 **Qian Q**, Li A, King BF, Kamath PS, Lager DJ, Huston J 3rd, Shub C, Davila S, Somlo S, Torres VE. Clinical profile of autosomal dominant polycystic liver disease. *Hepatology* 2003; **37:** 164-171

17 **Peces R**, González P, Venegas JL. Enfermedad poliquística hepática no asociada a poliquistosis renal autosómica dominante. *Nefrología* 2003; **23:** 454-458

18 **Peces R**, Gil F, Costero O, Pobes A. Trombosis masiva de la vena cava inferior secundaria a compresión por quistes hepáticos en un paciente con poliquistosis renal autosómica dominante. *Nefrología* 2002; **22:** 75-78

19 **Yang GS**, Li QG, Lu JH, Yang N, Zhang HB, Zhou XP. Combined hepatic resection with fenestration for highly symptomatic polycystic liver disease: A report on seven patients. *World J Gastroenterol* 2004; **10:** 2598-2601

20 **Gustafsson BI**, Friman S, Mjornstedt L, Olausson M, Backman L. Liver transplantation for polycystic liver disease--indications and outcome. *Transplant Proc* 2003; **35:** 813-814

Science Editor Wang XL and Guo SY **Language Editor** Elsevier HK

PO Box 2345, Beijing 100023, China
www.wjgnet.com
wjg@wjgnet.com

ELSEVIER

World J Gastroenterol 2005;11(48):7694-7696
World Journal of Gastroenterology ISSN 1007-9327

• *CASE REPORT* •

Robotic-assisted laparoscopic resection of ectopic pancreas in the posterior wall of gastric high body: Case report and review of the literature

Sheng-Der Hsu, Hurng-Sheng Wu, Chien-Long Kuo, Yueh-Tsung Lee

Sheng-Der Hsu, Division of General Surgery, Department of Surgery, Tri-Service General Hospital, National Defense Medical Center, Taipei, Taiwan, China
Chien-Long Kuo, Department of Pathology, Show-Chwan Memorial Hospital, Changhua, Taiwan, China
Hurng-Sheng Wu, Division of General Surgery, Department of Surgery, Tri-Service General Hospital, National Defense Medical Center, Taipei, Taiwan; Division of General Surgery, Department of Surgery, Show-Chwan Memorial Hospital, Changhua, Taiwan, China
Yueh-Tsung Lee, Division of General Surgery, Department of Surgery, Show-Chwan Memorial Hospital, Changhua, Taiwan, China
Correspondence to: Dr Yueh-Tsung Lee, Division of General Surgery, Department of Surgery, Show-Chwan Memorial Hospital, No. 325, Sec. 2, Cheng-Kung Road, Neihu 114, Taipei, Taiwan, China. f1233j@yahoo.com.tw
Telephone: +886-2-8792-7191
Received: 2005-01-24 Accepted: 2005-06-18

Abstract

Minimally invasive surgery has revolutionized the treatment of gastrointestinal tumors. Submucosal tumors of the stomach can be resected using laparoscopic techniques. We report here a case of ectopic pancreas tissue in the gastric wall that was removed using robotic-assisted laparoscopic resection. The patient was a 15-year-old female who presented with abdominal discomfort and tarry stools. Laboratory analysis showed iron deficiency anemia. Preoperative endoscopy revealed a submucosal lesion in the posterior wall of the gastric high body. Intraoperative upper endoscopy clearly located the lesion. A robotic-assisted laparoscopic wedge resection of the putative gastric submucosal tumor was performed. The pathology results showed an ectopic pancreas. The patient had an uneventful recovery and we believe that this is a valid treatment option for this benign condition.

Key words: Robotic surgery; Ectopic pancreas

Hsu SD, Wu HS, Kuo CL, Lee YT. Robotic-assisted laparoscopic resection of ectopic pancreas in the posterior wall of gastric high body: Case report and review of the literature. *World J Gastroenterol* 2005; 11(48): 7694-7696
http://www.wjgnet.com/1007-9327/11/7694.asp

INTRODUCTION

Ectopic pancreas is relatively rare and is definite as abnormally situated pancreatic tissue has no contact with the normal pancreas, and has its own ductal system and blood supply[1]. It is a rare entity and is usually an incidental finding in clinical practice. Most patients with an ectopic pancreas are asymptomatic, and if present, symptoms are nonspecific and depend upon the site of the lesion and different complications are encountered. Heterotopic pancreatic tissue has been found in several abdominal and intrathoracic locations, most frequently in the stomach (25-60%) or duodenum (25-35%)[2]. We report here a successful robotic-assisted laparoscopic wedge resection of a putative gastric submucosal tumor in a 15-year-old female.

CASE REPORT

A 15-year-old adolescent girl presented with intermittent epigastric pain with tarry stools for about 10 mo. She did not have any history of gastrointestinal cancer. The familial and personal history was nothing special. Laboratory findings showed iron deficiency anemia that prompted further gastrointestinal evaluation. The results of abdominal sonography and colonoscopy were negative. Panendoscopy revealed a submucosal lesion in the posterior wall of the gastric high body (Figure 1). The submucosal lesion measured about 1.5 cm in diameter. Pathological evaluation of a biopsy sample revealed chronic gastritis and mucosal hyperplasia. Biopsies collected with endoscopic techniques often do not provide the representative histologic sample needed for further therapeutic decisions. Because a malignant etiology could not be ruled out, a laparoscopic-endoscopic approach was considered to be appropriate for a curative and definitive diagnosis and minimally invasive for the resection of a localized gastric submucosal tumor.

The initial trocar was inserted at the umbilicus, using the Hasson technique. A pneumoperitoneum was created with carbon dioxide. In total, four trocars were inserted in the upper abdomen. The abdominal cavity was fully explored, during which robotic-assisted laparoscopic procedures were performed using the Zeus robot system. The greater omentum was detached from the greater curvature of the stomach with a harmonic scalpel, and the lesser sac was entered (Figure 2).

A clearly localized tumor mass was identified with

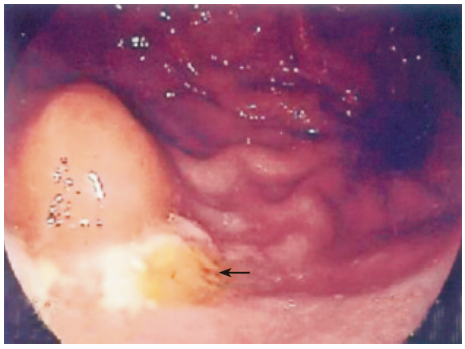

Figure 1 One submucosal lesion about 1.5 cm in diameter with a round surface on the area of the posterior wall of gastric high body with mucosal ulceration (arrow).

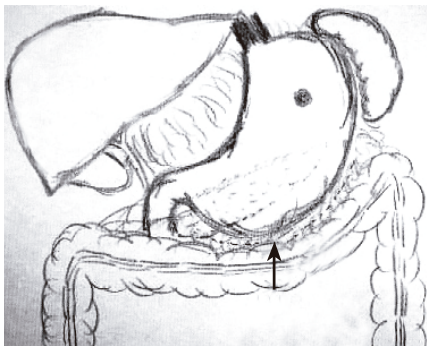

Figure 2 Detachment of greater omentum from the greater curvature of the stomach with a harmonic scalpel.

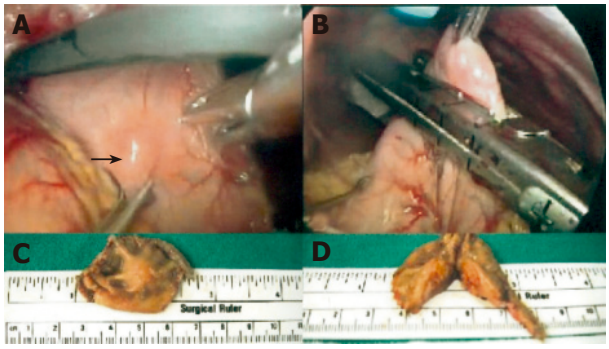

Figure 3 Localization of the tumor mass by intra-operative upper tract endoscopy. **A:** Tumor lesion in the posterior wall of gastric high body; **B:** robotic-assisted laparoscopic wedge resection of the gastric high body; **C:** submucosal tumor with tumor-free margin; **D:** cutting surface with firm, yellow, well-circumscribed, lobulated nodules.

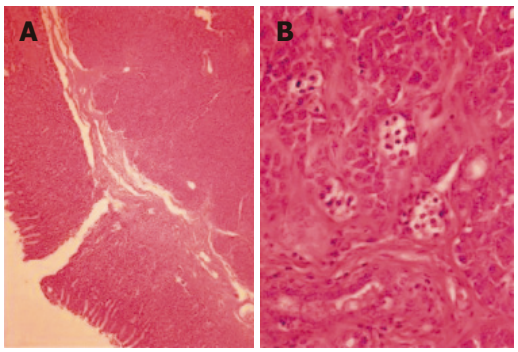

Figure 4 Pancreatic acinar cells and ducts shown in the low power view of gastric submucosal tumor (**A**) and in the high power view of ectopic pancreas (**B**).

the assistance of intraoperative upper-tract endoscopy. A robotic-assisted laparoscopic wedge resection of the gastric high body was performed using the Endo-GIA roticulator (Figure 3). The resection margins were clear and the specimen was sent for pathological analysis. A layer of interrupted silk sutures was placed in the serosa surface to ensure the integrity of the staple line. A nasogastric tube was inserted into the stomach and a drain tube was placed near the staple line. The abdominal cavity was deflated and the trocar sites were closed.

The final pathology report revealed that the resected specimen was an ectopic pancreas (Figure 4). The patient was discharged on postoperative d 6, with no complications and normal gastrointestinal motility. She had an uneventful recovery.

DISCUSSION

Ectopic pancreas is a rare entity and is usually an incidental finding in clinical practice. Most patients with an ectopic pancreas are asymptomatic, and if present, symptoms are nonspecific and depend on the site of the lesion and the different complications are encountered[3-5]. About 75% of all pancreatic rests are located in the stomach, duodenum, or jejunum[6]. However, they have also been found in the ileum, Meckel's diverticulum, gall bladder, common bile duct, splenic hilum, umbilicus, lung, and in perigastric and periduodenal tissues[7]. In autopsy series, the frequency of ectopic pancreas is between 1% and 2%. The rate of recognition at the time of laparotomy is 0.2%.

A preoperative diagnosis of ectopic pancreas in the gastric wall is not easy. Although a radiological diagnosis of gastric ectopic pancreatic tissue is difficult, double-contrast barium meal may show a characteristic focally raised mucosal area with associated superficial ulceration. The role of endoscopic biopsies in identifying ectopic pancreas remains questionable because normal gastric mucosa covers the lesion. Recently, endoscopic ultrasound combined with fine-needle aspiration cytology has been reported to facilitate a definitive diagnosis by histological examination[8]. Surgical excision, either endoscopically or laparoscopically, provides symptomatic relief and is recommended if the diagnosis remains uncertain. Laparoscopic wedge resection of a presumed gastric submucosal tumor appears to have been a suitable treatment for our patient. This approach is more advantageous over a laparotomy because recovery is easier and morbidity is less.

With the advent of laparoscopy at the end of the 1980s, surgery has entered the computer age[9]. More recently, robotic-assisted laparoscopy has joined the general surgeon's armory to address some of the shortcomings of laparoscopic surgery. Magnified and computer-enhanced

video images provide surgeons with much better access to and visualization of the abdomen. The main advantages of robot-assisted laparoscopic surgery are the availability of three-dimensional visibility and easier instrument manipulation compared to standard laparoscopy. Initially, robotic-assisted laparoscopic cholecystectomy was deemed safe, and has been proved to be safe in foregut procedures.

In conclusion, ectopic pancreas in the posterior wall of gastric high body can be resected by robotic-assisted laparotomy. This procedure is minimally invasive for such benign lesions.

REFERENCES

1 **Guillou L**, Nordback P, Gerber C, Schneider RP. Ductal adenocarcinoma arising in a heterotopic pancreas situated in a hiatal hernia. *Arch Pathol Lab Med* 1994; **118**: 568-571

2 **Moen J**, Mack E. Small-bowel obstruction caused by heterotopic pancreas in an adult. *Am Surg* 1989; **55**: 503-504

3 **Mulholland MW**, Simeone DM. Pancreas: Anatomy and structural anomalies: Congenital anomalies: Heterotopic pancreas. In: Yamada T, Alpers DH, Laine L, Owyang CH, Powell DW (eds): Textbook of Gastroenterology, ed 3. Philadelphia: Lippincott Williams & Wilkins, 1999; 2115-2119

4 **Abrahams JI**. Heterotopic pancreas simulating peptic ulceration. *Arch Surg* 1966; **93**: 589-592

5 **Armstrong CP**, King PM, Dixon JM, Macleod IB. The clinical significance of heterotopic pancreas in the gastrointestinal tract. *Br J Surg* 1981; **68**: 384-387

6 **Grendell JH**, Ermak TH. Anatomy, Histology, Embriology, and Developmental Anomalies of the Pancreas. In: Sleisenger & Fordtran's Gastrointestinal and Liver Disease, Philadelphia: WBSaunders, 1998: 761-771

7 **Kopelman HR**. The pancreas: Congenital anomalies. In: Walker WA¸ Durie PR¸ Hamilton RJ¸ Walker-Smith JW¸ Watkins JB. Pediatric Gastrointestinal Disease. St.Lous: Mosb, 1996; 1426-1427

8 **Riyaz A**, Cohen H. Ectopic pancreas presenting as a submucosal gastric antral tumor that was cystic on EUS. *Gastrointest Endosc* 2001; **53**: 675-677

9 **Chapman WH 3rd**, Albrecht RJ, Kim VB, Young JA, Chitwood WR Jr. Computer-assisted laparoscopic splenectomy with the da Vinci surgical robot. *J Laparoendosc Adv Surg Tech A* 2002; **12**: 155-159

Science Editors Wang XL and Guo SY **Language Editor** Elsevier HK

PO Box 2345, Beijing 100023, China
www.wjgnet.com
wjg@wjgnet.com

ELSEVIER

World J Gastroenterol 2005;11(48):7697-7699
World Journal of Gastroenterology ISSN 1007-9327

• *CASE REPORT* •

Isolated rectal diverticulum complicating with rectal prolapse and outlet obstruction: Case report

Chuang-Wei Chen, Shu-Wen Jao, Huang-Jen Lai, Ying-Chun Chiu, Jung-Cheng Kang

Chuang-Wei Chen, Shu-Wen Jao, Huang-Jen Lai, Ying-Chun Chiu, Jung-Cheng Kang, Division of Colon and Rectal Surgery, Department of Surgery; Department of Radiology, Tri-Service General Hospital, Taipei, Taiwan, China
Correspondence to: Dr Jung-Cheng Kang, Division of Colon and Rectal Surgery, Department of Surgery, Tri-Service General Hospital, No. 325, Cheng-Gong Road, Section 2, Taipei, Taiwan, China. docallen.tw@yahoo.com.tw
Telephone: +886-2-87923311-16049 Fax: +886-2-87927411
Received: 2005-04-12 Accepted: 2005-07-28

Abstract

The occurrence of rectal diverticula is very rare, with only sporadic reports in the literature since 1911. Symptomatic rectal diverticula are encountered even less frequently. Treatments of these complicated events range from conservative treatments to major surgical interventions. We present a hitherto unreported occurrence of isolated rectal diverticulum complicated with rectal prolapse and outlet obstruction. Delorme's procedure resulted in subsidence of symptoms and resolution of the diverticulum. It provides a minimal invasive surgical technique to successfully address the reported malady.

Key words: Rectal diverticula; Rectal prolapse; Delorme's procedure

Chen CW, Jao SW, Lai HJ, Chiu YC, Kang JC. Isolated rectal diverticulum complicating with rectal prolapse and outlet obstruction: Case report. *World J Gastroenterol* 2005; 11(48): 7697-7699
http://www.wjgnet.com/1007-9327/11/7697.asp

INTRODUCTION

Cases involving complicated rectal diverticula are extremely rare[1]. But when they occur, they usually present with rectal pain and bleeding, or inflammatory lesions such as abscess formation[3,4]. The following report documents a patient who experienced outlet obstruction during defecation and episodic rectal prolapse as the initial presentation. Eventual diagnosis was complication arising from a rectal diverticulum. Surgical intervention utilizing Delorme's procedure was successful, and is novel for the treatment of this rare and complicated event.

CASE REPORT

A 71-year-old female was admitted with a chief complaint of the sudden onset of a prolapsed mucosa through the anus during defecation on the night before admission. The protruding mucosa was reduced manually. She was nulliparous and had undergone surgical intervention for a benign tumor of unknown origin within the pelvis by a gynecologist 35 years before. Records had been lost during the subsequent postoperative period. She had experienced chronic constipation for 20 years, primarily involving an outlet obstruction for the passage of stools. She had to push her left buttock manually with her fingers to let the stool pass through the anal canal.

Upon admission, the patient was normal in general appearance except for a longitudinal surgical scar at the lower abdomen courtesy of the previous surgery. Results of physical examination were essentially normal except for the rectum. A large out-pouched pocket situated at the left lateral aspect of the rectal wall approximately 3 cm from the anal verge was digitally palpable. Sigmoidoscopy was negative. Barium enema examination showed a marked solitary 5 cm diameter diverticulum with wide-orifice neck arising from the rectal wall (Figure 1). Thus, we considered that the rectal diverticulum resulted in the accumulation of stools, causing the symptom of outlet obstruction, and subsequently had appeared as a prolapsed rectum due to the inverted rectal diverticulum protruding through the anus after excessive straining during defecation. The diagnosis of rectal diverticulum complicating with rectal prolapse and outlet obstruction was made.

The patient underwent a 50-min Delorme's procedure under intravenous anesthesia. A circumferential incision was made through the mucosa near the dentate line. Using electrocautery, the mucosa was stripped to the apex of the prolapsed lump and excised. The denuded prolapsed muscle was then pleated with 2-0 prolene sutures and reefed up. The transected edges of the mucosa were sutured together using 3-0 chromic catgut (Ethicon, Johnson & Johnson, Medical Taiwan). The excised specimen consisted of the resected rectal mucosa with an out-pouched sacculation measuring 50 mm×70 mm in size.

Postoperatively, bowel movements occurred more than 10 times a day initially but rapidly improved to 3-4 times per day in the following days. She recovered uneventfully and obtained relief from the outlet obstruction. Repeated

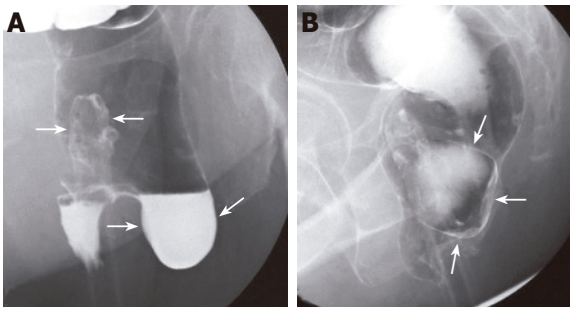

Figure 1 A and **B**. Double-contrast barium enema examination demonstrates a large diverticulum with wide-orifice arising from the left lateral rectal wall (large arrows). The rectal catheter is also seen (small arrows).

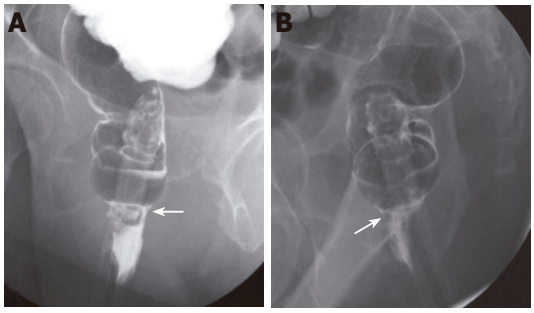

Figure 2 A and **B**. Postoperative barium study revealed the subsidence of the rectal diverticulum (arrows).

rectal examination revealed that the wide-orifice neck of the diverticular out-pouching had been tightly closed. She was discharged 6 d after the operation. A barium enema was repeated 2 mo later. (Figure 2) She defecated normally with 1–2 bowel movements per day during the 12 mo following the operation.

DISCUSSION

Diverticular disease occurs in the colon with great frequency. However, rectal involvement is very rare; being estimated to occur in less than 0.1% of cases[1,2]. Most patients with rectal diverticula are diagnosed by accident, as the malady is asymptomatic. Such uncomplicated rectal diverticula are clinically insignificant. However, complications associated with rectal diverticula can include rectal diverticulitis with perforation and abscess formation, diverticulitis of the midrectum, and a prolapsed rectum from an inverted rectal diverticulum[3-5]. Postinflammatory stenosis of the rectum, a rectal-vesical fistula, and an enormous fecaloma within a rectal diverticulum have also been reported as complications of rectal diverticula[6,7]. Erroneous diagnosis of carcinoma can prompt abdominal perineal resection[8].

Diverticulosis of the rectum typically occurs in the presence of colonic diverticula, especially the sigmoid segment. The factors that may contribute to rectal diverticula are still not completely understood. Possible predisposing factors include congenital anomalies such as weakness in the circumferential muscle that surrounds the rectum, primary muscle atrophy, or the absence of supporting structures such as the coccyx. Other acquired causes include relaxed rectal-vaginal septum, recurrent fecal impactions that exert pressure and cause distension of the rectum and pelvic trauma or infections leading to the weakening of the rectal wall[8,9]. In addition, Plavsic *et al*.[2] reported in 1995 that 2 of 27 patients with scleroderma had rectal diverticulosis without other diverticula in the rest of the colon. Loss of colonic haustrations has been reported in scleroderma and likely results in the development of colonic diverticula[10]. To our knowledge, the case we present is only the third reported case of isolated rectal diverticulum.

Rectal diverticula are typically situated along the lateral aspects of the rectum, since the complete longitudinal muscular layer of the rectum is thicker anteriorly and posteriorly compared to the lateral aspects of the wall[9]. Additionally, most rectal diverticula thus far described include all layers of the colonic wall as opposed to the more pseudodiverticula of the colon, suggesting the possibility that they occur at areas of focal weakness in the rectal wall caused by congenital or acquired origin[11]. The number of rectal diverticula per patient ranges from one to three with a diameter of 20 mm or greater compared with the remaining colonic diverticula, which typically measures less than 15 mm[9]. Rectal diverticula may also vary greatly in size with changes in intra-abdominal pressure[11].

Surgical treatments of the complicated rectal diverticula include drainage of the abscess, diverting colostomy, resection of the diverticular mass or abdominal perineal resection of the rectum. However, the Delorme's procedure has never been reported for these complicated events. This procedure is often used for small rectal prolapse but may also be used for large ones. Our case presented with rectal prolapse, which was considered to be the result of an inverted rectal diverticulum protruding through the anal canal. Delorme's procedure carries the advantage of a less invasive procedure that shortens the hospital stay. The patient recovered rapidly and uneventfully. Recurrence is the most common complication of this operation with an average incidence of 12% in different series[12]. Other complications such as hemorrhage, suture line dehiscence, stricture, and incontinence had ever been reported[13].

In conclusion, rectal diverticula are rare and can be easily missed by proctoscopy. They typically require no treatment because they are asymptomatic in most patients. Surgical intervention is only necessary in such patients with complicated events. Various approaches had been described in the management of different complications. Correct diagnosis preoperatively is required to prevent unnecessary surgery. In our presenting case, solitary rectal diverticulum was diagnosed by digital examination and barium enema preoperatively. Delorme's procedure provides a minimal invasive surgery and produces excellent results.

REFERENCES

1 **Walstad PM**, Sahibzada AR. Diverticula of the rectum. *Am J Surg* 1968; **116:** 937-939
2 **Plavsic BM**, Raider L, Drnovsek VH, Kogutt MS. Association of rectal diverticula and scleroderma. *Acta Radiol* 1995; **36:** 96-99
3 **Giustra PE**, Root JA, Killoran PJ. Rectal diverticulitis with perforation. *Radiology* 1972; **105**: 23-24
4 **Chiu TC**, Bailey HR, Hernandez AJ Jr. Diverticulitis of the midrectum. *Dis Colon Rectum* 1983; **26:** 59-60
5 **Edwards VH**, Chen MY, Ott DJ, King GT. Rectal diverticulum appearing as a prolapsed rectum. *J Clin Gastroenterol* 1994; **18**: 254-255
6 **Wilson LB**. Diverticula of the lower bowel: their development and relationship to carcinoma. *Ann Surg* 1911; **53**: 223-231
7 **Govoni AF**, Smulewicz JJ. Large diverticulum of the anal canal: case report and review of the literature on anal canal and rectal diverticula. *Am J Roentgenol* 1974; **121**: 344-7
8 **Weston SD**, Schlachter IS. Diverticulum of the rectum. *Dis Colon Rectum* 1959; **2:** 458-464
9 **Damron JR**, Lieber A, Simmons T. Rectal diverticula. *Radiology* 1975; **115**: 599-601
10 **Martel W**, Chang SF, Abell MR. Loss of colonic haustration in progressive systemic sclerosis. *Am J Roentgenol* 1976; **126**: 704
11 **Halpert RD**, Crnkovich FM, Schreiber MH. Rectal diverticulosis: a case report and review of the literature. *Gastrointest Radiol* 1989; **14:** 274-276
12 **Nay HR**, Blair CR. Perineal surgical repair of rectal prolapse. *Am J Surg* 1972; **123**: 577-579
13 **Senapati A**, Nicholls RJ, Thomson JP, Phillips RK. Results of Delorme's procedure for rectal prolapse. *Dis Colon Rectum* 1994; **37:** 456-460

Science Editor Guo SY **Language Editor** Elsevier HK

PO Box 2345, Beijing 100023, China
www.wjgnet.com
wjg@wjgnet.com

ELSEVIER

World J Gastroenterol 2005;11(48):7700-7701
World Journal of Gastroenterology ISSN 1007-9327

Mesenteric and portal vein thrombosis associated with hyperhomocysteinemia and heterozygosity for factor V Leiden mutation

Giuseppe Famularo, Giovanni Minisola, Giulio Cesare Nicotra, Claudio De Simone

Giuseppe Famularo, Giovanni Minisola, Giulio Cesare Nicotra, Department of Internal Medicine, San Camillo Hospital, Rome
Claudio De Simone, Department of Experimental Medicine, University of L'Aquila, L'Aquila, Italy
Correspondence to: Dr. Giuseppe Famularo, Department of Internal Medicine, San Camillo Hospital, Circonvallazione Gianicoense, 00152 Rome,
Italy. gfamularo@scamilloforlanini.rm.it
Telephone: + 39-6-58704325 Fax: + 39-6-58704325
Received: 2005-04-21 Accepted: 2005-07-14

Key words: Portal; Mesenteric; Thrombosis hyperhomocysteinemia; Factor V Leiden heterozygosity

Famularo G, Minisola G, Nicotra GC, Simone CD. Mesenteric and portal vein thrombosis associated with hyperhomocysteinemia and heterozygosity for factor V Leiden mutation. *World J Gastroenterol* 2005; 11(48): 7700-7701
http://www.wjgnet.com/1007-9327/11/7700.asp

TO THE EDITOR

A 79-year-old man was hospitalized because of worsening upper abdominal pain which started two days before admission and was continuously present. His personal and family history was uneventful, he did not smoke and denied toxic habits or using any medications, including over-the-counter medications, herbal remedies or any vitamin supplements.

At admission, the patient was fully alert and oriented, afebrile, but distressed due to severe abdominal pain; his vital parameters were normal. On physical examination, there was abdominal guarding and rebound with hypoactive bowel sounds, rectal examination revealed no masses, liver and spleen were normal, and a stool sample was guaiac negative. The remaining physical examination was unrevealing.

Laboratory tests showed a leukocyte count of 12×10^9 cells/L, 90% of which were neutrophils; electrolytes, amylase, lipase, and liver and renal function tests were normal. An electrocardiogram and a chest X-ray were also normal. A color Doppler ultrasonography and an emergency contrast-enhanced computed tomography disclosed thrombosis with complete occlusion of both intra- and extra-hepatic branches of the portal vein and partial obstruction of the superior mesenteric vein; abundant intraperitoneal fluid was observed with no collateral venous vessels or any direct or indirect evidence of transmural intestinal infarction. Endoscopy of both the upper and lower gastrointestinal tract was negative.

A thrombophilic screening showed extremely elevated blood levels of homocysteine (91 and 88 μmol/L on the 1st and 5th d of hospital stay; normal values < 15); search for antiphospholipid antibody and lupus anticoagulant was negative and blood levels of antithrombin and protein C and S were normal. Circulating vitamin B_6, B_{12}, and folate concentrations were also normal.

The patient was treated with bowel rest, intravenous fluids, antibiotics, and enoxaparin (100 IU/kg twice daily) and he reported complete recovery from abdominal pain on the 2nd d after admission. We added folate and vitamin B_6 to his regimen and the patient was discharged free of symptoms on the 15th d; at this time blood homocysteine was 75 μmol/L. At a follow-up visit 2 mo later, while still on enoxaparin and folate, he was doing well with no clinical or laboratory evidence of active thrombosis. We received the results of molecular studies performed on blood samples taken at admission, which showed heterozygosity for factor V Leiden mutation; search for prothrombin G20210A and MTHFR C677T mutations was negative. Blood homocysteine concentration was < 15 μmol/L and imaging studies showed normal flow in the superior mesenteric vein along with a complete occlusion of the portal vein, which was unchanged; there were venous collaterals in the hilar area of the liver. Anticoagulant therapy was shifted to warfarin with a targeted international normalized ratio (INR) 2-3 and, when last seen six months after discharge, the patient was asymptomatic with INR 2.6, normal blood homocysteine and no active thrombosis.

Combined thrombosis involving one mesenteric vein and the portal vein is rare, difficult to diagnose and can be fatal, with diffuse abdominal pain, distension and tenderness being the most common symptoms and physical findings[1,2]. Stricture and bowel necrosis with peritonitis due to transmural intestinal infarction may complicate the course and are important causes of mortality among those patients[1,2]. The early initiation of anticoagulation using unfractionated heparin or low

molecular weight heparin has been shown to minimize the risk of serious complications [1,2], nonetheless spontaneous resolution of extensive superior mesenteric and portal vein thrombosis has been also reported [3]. Common causes include liver disease, pancreatitis, inflammatory bowel disease, cancer, sepsis, an underlying myeloproliferative disorder, surgery or trauma, and systemic thrombophilia [4,5].

The association of hyperhomocysteinemia with extremely elevated blood levels of homocysteine and heterozygosity for factor V Leiden mutation was the cause of such a severe abdominal venous thrombosis in the case we report on. No precipitating events of venous thromboembolism were recognized and the patient had none of the abdominal disorders that may trigger thrombosis of the mesenteric veins or the portal vein or any other inherited or acquired prothrombotic condition. Available data consistently suggest a moderate, positive, and dose-related relationship between blood levels of homocysteine and the risk of portal or mesenteric venous thrombosis [6]. However, almost all the patients so far described in whom portal or mesenteric venous thrombosis was linked with hyperhomocysteinemia also had at least one additional prothrombotic disorder [7-10]. Our Medline search yielded no case of combined mesenteric-portal vein thrombosis associated only with hyperhomocysteinemia and no other risk factors for venous thromboembolism. It is not surprising in our opinion that, despite being heterozygous for factor V Leiden mutation, our patient did not experience any thrombotic disorders until severe hyperhomocysteinemia developed. This adds weight to the relevance of hyperhomocysteinemia in the pathophysiological mechanisms as a trigger of venous thrombosis in this case.

The mechanisms of hyperhomocysteinemia in our patient remain unclear. The patient was not exposed before presentation to any folate or vitamin B_6 antagonists, i.e. methotrexate, phenytoin, estrogens, or theophylline, and we ruled out upon history and clinical examination atherosclerosis, smoking or elevated blood pressure, which are also associated with raised circulating concentrations of homocysteine [11]. An acquired nutritional deficiency of folate also sounds a non reliable cause. Even though blood levels of folate, vitamin B6 and vitamin B12 were normal, homocysteine concentrations returned to the normal range after eight weeks of treatment with folate and vitamin supplements. This apparent discrepancy is difficult to explain, however we could reasonably speculate that the exogenous supplementation of folate and vitamins did ultimately correct a subtle age-dependent impairment of folate metabolism.

We claim that patients with apparently unexplained combined thrombosis involving both one mesenteric vein and the portal vein should be screened for hyperhomocysteinemia. Outcome could be favorable, even in those carrying other prothrombotic conditions such as factor V Leiden mutation, with a complete recovery if appropriate treatment with anticoagulants, folate and vitamin supplements is timely started.

REFERENCES

1 **Acosta S**, Ogren M, Sternby NH, Bergqvist D, Bjorck M. Mesenteric venous thrombosis with transmural intestinal infarction: a population-based study. *J Vasc Surg* 2005; **41**: 59-63

2 **Joh JH**, Kim DI. Mesenteric and portal vein thrombosis: treated with early initiation of anticoagulation. *Eur J Vasc Endovasc Surg* 2005; **29**: 204-208

3 **Fernandez-Marcote Menor EM**, Opio Maestro VA. [Spontaneous resolution of extensive superior mesenteric and portal vein thrombosis. A case report] *Gastroenterol Hepatol* 2004; **27:** 470-472

4 **Valla DC**, Condat B. Portal vein thrombosis in adults: pathophysiology, pathogenesis and management. *J Hepatol* 2000; **32**: 865-871

5 **Kumar S**, Kamath PS. Acute superior mesenteric venous thrombosis: one disease or two? *Am J Gastroenterol* 2003; **98**: 1299-1304

6 **Primignani M**, Martinelli I, Bucciarelli P, Battaglioli T, Reati R, Fabris F, Dell'era A, Pappalardo E, Mannucci PM. Risk factors for thrombophilia in extrahepatic portal vein obstruction. *Hepatology* 2005; **41:** 603-608

7 **Elhajj II**, Salem ZM, Birjawi GA, Taher AT, Soweid AM. Heterozygous prothrombin 20210G/A mutation, associated with hyperhomocysteinemia, and homozygous methylenete trahydrofolate reductase 677C/T mutation, in a patient with portal and mesenteric venous thrombosis. *Hematol J* 2004; **5:** 540-542

8 **Silingardi M**, Ghirarduzzi A, Galimberti D, Iorio A, Iori I. Mesenteric-portal vein thrombosis in a patient with hyperhomocysteinemia and heterozygous for 20210A prothrombin allele. *Thromb Haemost* 2000; **84**: 358-359

9 **Audemar F**, Denis B, Blaison G, Mazurier I, Peter A, Serbout R. Left branch portal vein thrombosis associated with hyperhomocysteinemia. *Gastroenterol Clin Biol* 1999; **23:** 1388-1391

10 **Spanier BW**, Frederiks J. Aetiology of extrahepatic portal vein thrombosis. *Gut* 2002; **51:** 755-756; author reply 756

11 **Hankey GJ**, Eikelboom JW. Homocysteine and vascular disease. *Lancet* 1999; **354**: 407-413

Science Editor Guo SY **Language Editor** ELsevier HK

PO Box 2345, Beijing 100023, China
www.wjgnet.com
wjg@wjgnet.com

ELSEVIER

World J Gastroenterol 2005;11(48):7702-7703
World Journal of Gastroenterology ISSN 1007-9327

Fenofibrate-induced liver injury

Kazufumi Dohmen, Chun Yang Wen, Shinya Nagaoka, Koji Yano, Seigo Abiru, Toshihito Ueki, Atsumasa Komori, Manabu Daikoku, Hiroshi Yatsuhashi, Hiromi Ishibashi

Kazufumi Dohmen, Internal Medicine, Okabe Hospital, 1-2-1 Myojinzaka Umi-machi Kasuya-gun Fukuoka 811-2122, Japan
Chun Yang Wen, Shinya Nagaoka, Koji Yano, Seigo Abiru, Toshihito Ueki, Atsumasa Komori, Manabu Daikoku, Hiroshi Yatsuhashi, Hiromi Ishibashi, Clinical Research Center, National Nagasaki Medical Center, Omura 856-8562, Japan
Correspondence to: Dr. Kazufumi Dohmen, Internal Medicine, Okabe Hospital, 1-2-1 Myojinzaka Umi-machi Kasuya-gun Fukuoka 811-2122,
Japan. dohmenk@par.odn.ne.jp
Telephone: +81-92-9322-0025 Fax: +81-92-933-7253
Received: 2005-04-12 Accepted: 2005-04-25

Dohmen K, Wen CY, Nagaoka S, Yano K, Abiru S, Ueki T, Komori A, Daikoku M, Yatsuhashi H, Ishibashi H. Fenofibrate-induced liver injury. *World J Gastroenterol* 2005; 11(48):7702-7703
http://www.wjgnet.com/1007-9327/11/7702.asp

TO THE EDITOR

Fenofibrate is a member of such fibrate class agents as bezafibrate and it work as a ligand of PPARα, and also shows a potent triglyceride-lowering effect. The elevation of aminotransferase levels has been frequently observed after the administration of fenofibrate and this phenomenon is considered to be non-pathological because fenofibrate activates the gene expression of the aminotransferases. Recently, fenofibrate has been used not only for hypercholesterolemia but also for primary biliary cirrhosis (PBC)[1, 2]. However, the occurrence of liver injury induced by fenofibrate has not yet been reported written in the English literature. We herein report a rare case of liver injury due to the oral use of this drug.

A 66-year-old Japanese female patient was admitted to undergo a further examination with a nearly 20-year history of liver dysfunction. She had been previously treated with 600 mg of ursodeoxycholic acid (UDCA) for nearly 6 mo at another clinic. On admission her conjunctiva was neither anemic nor icteric. The laboratory data revealed white blood cell counts of 6 600/μL with a differential of neutrophils 50%, lymphocyte 38%, monocytes 6%, basophils 1%, eosinophils 5%. The C reactive protein level was less than 0.3 mg/dL. The hepatic function profiles showed the total bilirubin to be 0.8 mg/dL, aspartate aminotransferase (AST) 40 IU/L, alanine aminotransferase (ALT) 29 IU/L, lactate dehydrogenase (LDH) 183 IU/L, alkaline phosphatase (ALP) 367 IU/L and gamma-glutamil transpeptidase (γ-GTP) 272 IU/L. Regarding the hepatitis virus, hepatitis B virus surface antigen and hepatitis C virus antibody were both negative. Serology revealed a high level of IgM of 393 mg/dL, and the antinuclear antibody of 80-fold and antimitochondrial antibody (AMA) of 320-fold each and antibody of 176 U/mL were positive for pyruvate dehydrogenase complex-E2. Histopathologically, a damaged bile duct with aggregates of lymphocytes with a nonsuppurative inflammatory destruction of the small bile duct and granuloma was seen in the portal area, which was compatible with those of Scheuer's stage 1 of primary biliary cirrhosis.

Based on the diagnosis of primary biliary cirrhosis, the administration of fenofibrate 150 mg per day was initiated in addition to 600 mg of UDCA. A fever of over 37.5 ℃, anorexia and discomfort in the right hypochondrium appeared 11 d after the administration of fenofibrate. Liver injury such as elevations of total bilirubin of 1.8 mg/dL, AST 268, ALT 216, ALP 537, and γ-GTP 660 IU/L was confirmed, and both the CRP level and the ratio of eosinophils in the peripheral blood increased to 5.14 mg/dL and 14.4 %, respectively. She was diagnosed to have fenofibrate-induced liver injury based on the laboratory data and the clinical course. Therefore, fenofibrate was discontinued, however, UDCA continued to be administered continuously. Thereafter, the serum concentrations of AST, ALT, ALP, γ-GTP, CRP, and the rate of eosinophils rapidly returned to the pretreatment levels of 30, 27, 457, 399 IU/L, less than 0.3 mg/dL and 4.6 %, respectively, 12 d after the discontinuation of fenofibrate (Figure 1). Later, the lymphocyte stimulation index for fenofibrate for this patient was found to be positive, while showing a stimulation index of 212 % in comparison to normal samples.

Several clinical studies on lipoprotein-lowering agents such as simvastatin[3] and bezafibrate[4-7] on PBC patients who failed to respond to UDCA have so far been conducted, and the results have been found to be of value. In addition, fenofibrate, a member of such fibrate class agents as bezafibrate, has also recently been found to be a likely agent for PBC because of its stronger anti-inflammatory effect via PPARα, and its greater ability to reduce the levels of TG and LDL-C than that of bezafibrate. We previously found fenofibrate to effectively treat UDCA-resistant PBC in nine cases without any adverse effect[2].

Regarding the adverse effect of fenofibrate, a Diabetes Arteriosclerosis Intervention Study (DAIS) showed that micronized fenofibrate at 200 mg (equivalent to 300 mg of

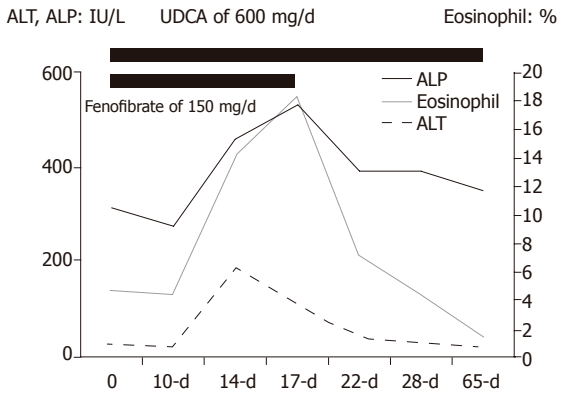

Figure 1 Clinical course.

the standard formulation) was administered for 3 years to type 2 diabetic patients in order to observe the inhibitory effect in the progression of coronary arterial stenosis. As a result, no difference in the safety between fenofibrate and placebo was observed[8]. In addition, studies of human first-generation cultured cells and HepG2 cells suggested the serum aminotransferase levels to be transiently elevated and normalized or returned to pretreatment levels[9]. The increase in the aminotransferase level which occurs after treatment with fenofibrate is not considered to be clinically significant although fenofibrate activates the aminotransferase gene expression, thus leading to a mild and transient elevation of aminotransferase via PPARα through mechanisms involving increased levels of reactive oxygen species and intracellular glutathion depletion, thus leading to mitochondrial dysfunction and a perturbation of intracellular Ca^{++} homeostasis and also cell death[9].

Since fenofibrate is a widely prescribed therapeutic agent world-wide for patients with hypercholesterolemia and recently for those with PBC[1, 2], the early recognition of any possible liver dysfunction especially in the case of PBC, and the immediate cessation of its administration, when positively identified are thus called for to avoid any dangerous clinical complications. Furthermore, our case shows that fenofibrate-induced liver injury might occur in addition to the transient elevations in the AST and ALT levels via PPARα.

REFERENCES

1 **Ohira H,** Sato Y, Ueno T, Sata M. Fenofibrate treatment in patients with primary biliary cirrhosis. *Am J Gastroenterol* 2002; **97:** 2147-2149
2 **Dohmen K,** Mizuta T, Nakamuta M, Shimohashi N, Ishibashi H, Yamamoto K. Fenofibrate for patients with asymptomatic primary biliary cirrhosis. *World J Gastroenterol* 2004; **10:** 894-898
3 **Ritzel U,** Leonhardt U, Nather M, Schafer G, Armstrong VW, Ramadori G. Simvastatin in primary biliary cirrhosis: effects on serum lipids and distinct disease markers. *J Hepatol* 2002; **36:** 454-458
4 **Nakai S,** Masaki T, Kurokohchi K, Deguchi A, Nishioka M. Combination therapy of bezafibrate and ursodeoxycholic acid in primary biliary cirrhosis: a preliminary study. *Am J Gastroenterol* 2000; **95:** 326-327
5 **Miyaguchi S,** Ebinuma H, Imaeda H, Nitta Y, Watanabe T, Saito H, Ishii H. A novel treatment for refractory primary biliary cirrhosis? *Hepatogastroenterology* 2000; **47:** 1518-1521
6 **Kurihara T,** Niimi A, Maeda A, Shigemoto M, Yamashita K. Bezafibrate in the treatment of primary biliary cirrhosis: comparison with ursodeoxycholic acid. *Am J Gastroenterol* 2000; **95:** 2990-2992
7 **Yano K,** Kato H, Morita S, Takahara O, Ishibashi H, Furukawa R. Is bezafibrate histologically effective for primary biliary cirrhosis? *Am J Gastroenterol* 2002; **97:** 1075-1077
8 Diabetes Arteriosclerosis Intervention Study Investigators. Effect of fenofibrate on progression of coronary–artery disease in type 2 diabetes: the Diabetes Arteriosclerosis Intervention Study, a randomized study. *Lancet* 2001; **357:** 905–910
9 **Edgar AD,** Tomkiewicz C, Costet P, Legendre C, Aggerbeck M, Bouguet J, Staels B, Guyomard C, Pineau T, Barouki R. Fenofibrate modifies transaminase gene expression via a peroxisome proliferator activated receptor alpha-dependent pathway. *Toxicol Lett* 1998; **98:** 13-23

Science Editor Guo SY **Language Editor** Elsevier HK

PO Box 2345, Beijing 100023, China
www.wjgnet.com
wjg@wjgnet.com

ELSEVIER

World J Gastroenterol 2005;11(48):7704-7714
World Journal of Gastroenterology ISSN 1007-9327

Acknowledgments to Reviewers of *World Journal of Gastroenterology*

Many reviewers have contributed their expertise and time to the peer review, a critical process to ensure the quality of *World Journal of Gastroenterology*. The editors and authors of the articles submitted to the journal are grateful to the following reviewers for evaluating the articles (including those were published and those were rejected in this issue) during the last editing period of time. Arabic number in parenthesis stands for the number of the reviewer have reviewed this year.

1 **Christian Cormac Abnet, PhD, MPH**
Investigator, tritional Epidemiology Branch Division of Cancer Epidemiology and Genetics, 6120 Executive Blvd, EPS/320, MSC 7232 Rockville, MD 20852, United States

2 **Kyoichi Adachi, MD (12)**
Department of Gastroenterology and Hepatology, Shimane University, School of Medicine Shimane, 89-1 Enya-cho, Izumo-shi Shimane 693-8501, Japan

3 **Yasushi Adachi, Dr**
First Department of Internal Medicine, Sapporo Medical University, South-1, West-16, Chuo-ku, Sapporo, 060-8543, Japan

4 **Taiji Akamatsu, Associate Professor (6)**
Department of Endoscopy, Shinshu University Hospital, 3-1-1 Asahi, Matsumoto 390-8621, Japan

5 **Gianfranco D Alpini, Professor (4)**
Internao Medicine and Medical Physiology, Scoh Whot Hospital, 702 SW H.K. dod genloop MRB rm316B, Temple 76504, United States

6 **Domenico Alvaro, MD (2)**
Division of Gastroenterology, Department of Clinical MedicineUniversity of Rome La Sapienza, Viale Università 37, Rome 00185, Italy

7 **Takafumi Ando, MD (5)**
Nagoya University Graduate School of Medicine, Therapeutic Medicine, 65 Tsurumai-cho, Showa-ku, Nagoya 466-8550, Japan

8 **Hisataka S Moriwaki, Professor**
Department Of Medicine, Gifu University, 1-1 Yanagido, Gifu 501-1194, Japan

9 **Akira Andoh, MD (5)**
Department of Internal Medicine, Shiga University of Medical Science, Seta Tukinowa, Otsu 520-2192, Japan

10 **Vito Annese, MD (2)**
Department of Internal Medicine, Unit of Gastroenterology, Hospital, Viale Cappuccini, 1, San Giovanni Rotondo 71013, Italy

11 **Bruno Annibale, Professor (2)**
Digestive and Liver Disease Unit, University " La Sapienza" II School of Medicine, Via di Grottarossa 1035, Roma 00189, Italy

12 **Taku Aoki, MD (5)**
Division of Hepato-Biliary-Pancreatic and Transplantation Surgery, Department of Surgery, Graduate School of Medicine, University of Tokyo,7-3-1 Hongo, Bunkyo-ku, Tokyo, 113-8655, Japan

13 **Masahiro Arai, MD, PhD (11)**
Department of Gastroenterology, Toshiba General Hospital, 6-3-22 Higashi-ooi, Shinagawa-ku,Tokyo 140-8522, Japan

14 **Tetsuo Arakawa, Professor**
Department of Gastroenterology, Osaka City University Medical School,1-4-3, Asahi-machi, Abeno-ku, Osaka 545-8585, Japan

15 **Yasuji Arase, MD (5)**
Department of Gastroenterology, Toranomon Hospital, 2-2-2Toranomonminato-ku, Tokyo 105-8470, Japan

16 **Rudolf Arnold, Professor**
Department of Internal Medicine, Philipps University Marburg, Baldingerstraße, Marburg D-35043, Germany

17 **Hitoshi Asakura, Director**
Emeritus Professor (2), International Medical Information Center, Shinanomachi Renga BLDG.35, Shinanomachi, Shinjukuku, Tokyo 160-0016, Japan

18 **Fernando Azpiroz, MD**
Digestive System Research Unit, University Hospital Vall d' Hebron, Paseo Vall d'Hebron, 119-129, Barcelona 08035, Spain

19 **Takeshi Azuma, Associate Professor**
Second Department of Internal Medicine, University of Fukui, Faculty of Medical Sciences, Matsuoka-cho, YoshIDa-gun, Fukui 910-1193, Japan

20 **Jasmohan Singh Bajaj, Assistant Professor**
Division of Gastroenterology and Hepatology, Medical College of Wisconsin, 9200 W Wisconsin Ave, Milwaukee WI 53212, United States

21 **Giovanni Barbara, Professor**
Internal Medicine and Gastroenterology, University of Bologna, St.Orsola Hospital - Building No. 5Via Massarenti, 9 -40138, Bologna 40138

22 **Jamie S Barkin, MD (2)**
Professor of Medicine, Chief, Sinai Medical Center Division of Gastroenterology, Mt. Sinai Medical Center, University of Miami, School of Medicine, 4300 Alton Road, Miami Beach, FL 33140, United States

23 **Kim Elaine Barrett, Professor (6)**
Department of Medicine, UCSD School of Medicine, UCSD Medical Center 8414, 200 West Arbor Drive, San Diego CA 92103, United States

24 Gabrio Bassotti, MD (2)
Department of Clinical and Experimental Medicine, University of Perugia, Via Enrico dal Pozzo, Padiglione W, Perugia 06100, Italy

25 **Ramon Bataller, MD, (4)**,
Liver Unit, Hospital Clinic,Villarroel 170, Barcelona 08036, Spain

26 **Daniel C Baumgart, MD, PhD, FEBG**
Division of Hepatology and Gastroenterology, Department of

Medicine, Charité Medical School，Humboldt-University of Berlin , Virchow Hospital, Berlin D-13344, Germany

27 **Yusuf Bayraktar, Professor (3)**
Department of Gastroenterology, School of Medicine, Hacettepe University, Ankara 06100, Turkey

28 **Christoph Beglinger, Professor**
University Hospital, Division of Gastroenterology, University of Basel, Petersgraben 4, Basel CH-4031, Switzerland

29 **Antomio Benedetti, Professor (2)**
epartment of Gastroenterology, University of Politecnica Melle Marche, Via Conca 71, Ancona 60020, Italy

30 **Trond Berg, Professor (2)**
Department of Molecular Biosciences, University of Oslo, PO Box 1041 Blindern, Oslo 0316, Norway

31 **Mauro Bernardi, Professor**
Internal Medicine,Cardioangiology,Hepatology, University of Bologna, Semeiotica Medica - Policlinico S. Orsola-Malpighi - Via Massarenti, 9, Bologna 40138, Italy

32 **Jennifer D Black, MD (2)**
Roswell Park Cancer Institute, Department of Pharmacology and Therapeutics, Roswell Park Cancer Institute, Elm and Carlton Streets, Buffalo 14263, United States

33 **Hubert Blum, Professor**
University of Freiburg, Hugastetter Strasse 55, Freiburg L-79106, Germany

34 **Luigi Bonavina, Professor**
Department of Surgery, Policlinico San Donato, University of Milano, via Morandi 30, Milano 20097, Italy

35 **Joseph Daoud Boujaoude, Assistant Professor**
Department of Gastroenterology, Hotel-Dieu de FranceHospital, aint-Joseph University, Beirut 961, Lebanon

36 **Lee Bouwman, Dr** Leiden University Medical Centre, department of surgery, Albinusdreef 2 PO Box 9600, 230 RC Leiden, The Netherlands

37 **Filip Braet, Associate Professor (3)**
Australian Key Centre for Microscopy and Microanalysis, Madsen Building (F09), The University of Sydney, Sydney NSW 2006, Australia

38 **Reinhard Buettner Professor** Institute of Pathology
University Hospital Bonn, Sigmund-Freud-Str. 25, D-53127 Bonn, Germany

39 **Michael F Byrne , MD**
Clinical Associate Professor, Division of Gastroenterology Vancouver General Hospital, 100-2647 Willow Street Vancouver BC V5Z 3P1, Canada

40 **Giovanni Cammarota, MD**
Department of Internal Medicine and Gastroent, Catholic University of Medicine and Surgery, Rome, Policlinico A. Gemelli; Istituto di Medicina Interna; Largo A. Gemlli, 8, Roma 00168, Italy

41 **Elke Cario, MD**
Division of Gastroenterology and Hepatology, University Hospital of Essen, Institutsgruppe I, Virchowstr. 171, Essen D-45147, Germany

42 **Julio Horacio Carri, Professor**
Internal Medicine – Gastroenterology, Universidad Nacional de Córdoba, Av.Estrada 160-P 5-Department D, Córdoba 5000, Argentina

43 **David L Carr-Locke, MD**
Director of Endoscopy, Brigham and Women's Hospital, Endoscopy Center, Brigham and Women's Hospital, 75 Francis St, Boston MA 02115, United States

44 **Antoni Castells, MD (3)**
Gastroenterology Department, Hospital Clínic, University of Barcelona, Villarroel 170, Barcelona 08036, Spain

45 **Yogesh K Chawla, Dr, Professor (2)**
Department of Hepatology, Postgraduate Institute of Medical Education and Research, Chandigarh 160012, India

46 **Wang-Xue Chen, Dr (3)**
Institute for Biological Sciences, National Research Concil Canada, 100 Sussex Drive, Room 3100, Ottawa, Ontario K1A 0R6, Canada

47 **Xian-Ming Chen, MD (3)**
Center for Basic Research in Digestive Diseases, Division of Gastroenterology and Hepatology, Mayo Clinic College of Medicine, 200 First Street, SW, Rochester, MN 55905, United States

48 **Xiao-Ping Chen, Professor (5)**
Institute of Hepato-Pancreato-Biliary Surgery, Tongji Hospital, 1095# Jie-fang Da-dao, Wuhan 430030, China

49 **Jun Cheng, Professor,**
Dean Assistant, Beijing Earth Altar Hospital Dean 13 Earth Altar Park, Anwai Avenue, East District, Beijing 100011, China

50 **Giuseppe Chiarioni, Dr (2)**
Gastroenterological Rehabilitation Division of the University of Verona, Valeggio sul Mincio Hospital, Azienda Ospedale di Valeggio s/M, Valeggio s/M 37067, Italy

51 **Yoichi Chida, Assistant professor (2)**
Department of Psychosomatic Medicine, Graduate School of Medical Sciences, Kyushu University, 3-1-1 Maidashi, Higashi-ku, Fukuoka 812-8582, Japan

52 **Andrew Seng Boon Chua, MD**
Department of Gastroenterology, Gastro Centre Ipoh, 1, lorong Rani, 31, lebuhraya Tmn Ipoh, Ipoh Garden South, IPOH 30350, Malaysia

53 **James M Church, MD**
Colorectal Surgery, Cleveland Clinic Foundation, Desk A 30, 9500 EuclID Ave, Cleveland 44195, United States

54 **Paul Jonathan Ciclitira, Professor (2)**
The Rayne Institute (GKT), St Thomas' hospital, London NW32QG, United Kingdom

55 **Andrew D Clouston, Associate Professor**
Histopath Laboratories, Suite 4, Level 9, Strathfield Plaza, Strathfield, Sydney, 2135, Australia

56 **Dario Conte, Professor (3)**
GI Unit - IRCCS Osp. Maggiore, Chair of Gastroenterology, Via F. Sforza, 35, Milano 20122, Italy

57 **Gino Roberto Corazza, Professor (5)**
Department of Internal Medicine, University of Pavia, Gastroenterology Unit - I.R.C.C.S. Policlinico San Matteo - Piazzale Golgi n.5, Pavia 27100, Italy

58 **Chi-Hin Cho, Chair and Professor**

90 Karel Geboes, Professor
Laboratory of Histo- and Cytochemistry; University Hospital K.U.Leuven, Capucienenvoer 33, 3000 Leuven, Belgium

91 John P Geibel, MD
Professor of Surgery and Cellular and Molecular Physiology, Director of Surgical Research, Yale University School of Medicine, BML 265, New Haven, CT 06520, United States

92 Alexander L Gerbes, Professor (3)
Medizinische Klinik II, Munich, Germany, Marchioninistr 15, Munich D-81377, Germany

93 Subrata Ghosh, Professor (2)
Department of Gastroenterology, Imperial College London, Hammersmith Hospital, 9 Lady Aylesford Avenue, Stanmore, Middlesex, London HA7 4FG, United Kingdom

94 Edoardo G Giannini, Assistant Professor (3)
Department of Internal Medicine, Gastroenterology Unit, Viale Benedetto XV, no. 6, Genoa, 16132, Italy

95 Ignacio Gil-Bazo, MD, PhD (2)
Cancer Biology and Genetics Program, Memorial-Sloan Kettering Cancer Center, 1275 York Avenue. Box 241, New York 10021, United States

96 Roberto De Giorgio, MD
Department of Internal Medicine and Gastroenterology, University of Bologna, St.Orsola-Malpighi Hospital, Via Massarenti, 9, Bologna 40138, Italy

97 Dieter Glebe, PhD
Institute for Medical Virology, Justus Liebig University Giessen, Frankfurter Str. 107, Giessen 35392, Germany

98 David Y Graham, Professor (6)
Department of Medicine, Michael E. DeBakey VAMC, Rm 3A-320 (111D), 2002 Holcombe Blvd, Houston, TX 77030, United States

99 William Greenhalf, PhD Division of Surgery and Oncology, University of Liverpool, UCD Building, 5th Floor, Royal Liverpool University Hospital, Daulby Street, Liverpool, L69 3GA, United Kingdom

100 Hans Gregersen, Professor
The Research Administration, Aalborg Hospital, Hobrovej 42 A, Aalborg 9000, Denmark

101 Axel M Gressner, Professor (4)
Institut für Klinische Chemie und Pathobiochemie sowie Klinisch-Chemisches Zentrallaboratorium, Universitätsklinikum Aachen, Pauwelsstr. 30, Aachen 52074, Germany

102 Rick Greupink, Dr (2)
University of Groningen, A. Deusinglaan 1, Groningen 9713AV, The Netherlands

103 Jin Gu, Professor (2)
Peking University School of Oncology, Beijing Cancer Hospital, Beijing 100036, China

104 Hallgrimur Gudjonsson, MD
Gastroenterolog, University Hospital, University Hospital, Landspitali,Hringbraut, Reykjavik 101, Iceland

105 Anna S Gukovskaya, Professor (2)
VA Greater Los Angeles Health Care System ,University of California, Los Angeles, 11301 Wilshire Blvd, Los Angeles 91301, United States

106 De-Wu Han, Professor (4)
Institute of Hepatology, Shanxi Medical University, 86 Xinjian South Road, Taiyuan 030001, China

107 Kazuhiro Hanazaki, MD, (11)
Department of Surgery, Shinonoi General Hospital, 666-1 Ai, Shinonoi, Nagano 388-8004, Japan

108 Naohiko Harada, PhD
Department of Gastroenterology, Fukuoka Higashi Medical Center, Chidori 1-1-1, Koga, Fukuoka 811-3195, Japan

109 Tetsuo Hayakawa, Emeritus Professor (3)
Director general, Meijo Hospital, Meijo Hospital, Sannomaru 1-3-1, Naka-ku, Nagoya 460-0001, Japan

110 Peter Clive Hayes, Professor
Liver Unit, Royal Infirmary, Si Little France Crescent, EH16 4SA, United Kingdom

111 Ming-Liang He, Associate Professsor (2)
Faculty of Medicine , The Center for Emerging Infectious Diseases, The Chinese University of Hong Kong, Hong Kong, China

112 Stephan Hellmig, Dr (2)
Department of General Internal Medicine, University Hospital Schleswig-Holstein, Campus Kiel, Schittenhelmstra 12, Kiel 24105, Germany

113 Alan W Hemming MD, MSc, FRCSC, FACS
Professor of Surgery, Director of Hepatobiliary Surgery, Department of Surgery, Division of Transplantation, PO Box 100286, University of Florida,Gainesville, FL, 32610
United States

114 Kazuhide Higuchi, Associate Professor (2)
Department of Gastroenterology, Graduate School of Medicine, Osaka City University, 1-4-3 Asahi-machi, Abeno-ku, Osaka 545-8585, Japan

115 Keiji Hirata, MD
Surgery 1, University of Occupational and Environmental Health, 1-1 Iseigaoka, Yahatanishi-ku, Kitakyushu 807-8555, Japan

116 Yik-Hong Ho, Professor (3)
Department of Surgery, School of Medicine, James Cook University, Townsville 4811, Australia

117 Anthony R Hobson, Dr (2)
Section of Gastrointestinal Sciences, University of Manchester, Eccles Old Road, Hope Hospital, Clinical Sciences Building, Salford M6 8HD, United Kingdom

118 Werner Hohenberger, Professor,
Chirurgische Klinik und Poliklinik, Krankenhausstrasse 12, Erlangen D-91054, Germany

119 Joerg C Hoffmann, Dr
Medizinische Klinik I, Charité - Universitätsmedizin Berlin, Campus Benjamin Franklin, Hindenburgdamm 30, Berlin D12200, Germany

120 Michael Horowitz, Professor (2)
Department of Medicine, University of Adelaide and Director, Endocrine and Metabolic Unit, Royal Adelaide Hospital, Level 6, Eleanor Harrald Bullding, North Terrace, Adelaide 5000, Australia

121 Yves J Horsmans, Professor

153 Jin-Hong Kim, Professor
Department of Gastroenterology, Ajou University Hospital, San 5, Wonchon-dong, Yeongtong-gu, Suwon 442-721, South Korea

154 Myung-Hwan Kim, Professor (10)
College of Medicine, Asan Medical Center, 388-1 Pungnap-dong, Songpa-gu, Seoul 138-736, South Korea

155 Tsuneo Kitamura, Associate Professor (5)
Department of Gastroenterology, Juntendo University Urayasu Hospital, Juntendo University School of Medicine, 2-1-1 Tomioka, Urayasu-shi, Chiba 279-0021, Japan

156 Seigo Kitano, Professor (5)
Department of Surgery I, Oita University Faculty of Medicine, 1-1 Idaigaoka Hasama-machi, Oita 879-5593, Japan

157 Burton I Korelitz, MD
Department of Gastroenterology, Lenox Hill Hospital, 100 East 77th Street, 3 Achelis, New York, N.Y 10032, United States

158 Robert J Korst, MD (3)
Department of Cardiothoracic Surgery, Weill Medical College of Cornell University, Room M404, 525 East 68th Street, New York 10032, United States

159 Elias A Kouroumalis, Professor (2)
Department of Gastroenterology, University of Crete, Medical School, Department of Gastroenterology, University Hospital, PO Box 1352, Heraklion, Crete 71110, Greece

160 Shoji Kubo, MD (3)
Hepato-Billiary-Pancreatic Surgery, Osaka City University Graduate School of Medicine, 1-4-3 Asahimachi, Abeno-ku, Osaka 545-8585, Japan

161 Gerd A Kullak-Ublick, Professor
Laboratory of Molecular Gastroenterology and Hepatology, Department of Internal Medicine, University Hospital Zurich, Zurich CH-8091, Switzerland

162 Shiu-Ming Kuo, MD (3)
University at Buffalo, 15 Farber Hall, 3435 Main Street, Buffalo 14214, United States

163 Shigeki Kuriyama, MD
Kagawa University School of Medicine, Third Department of InternalMedicine, 1750-1 Ikenobe, Miki-cho, Kita-gun, Kagawa 761-0793, Japan

164 Masato Kusunoki, Professor and Chairman (2)
Second Department of Surgery, Mie University School of Medicine, Mie, 2-174 Edobashi, Tsu MIE 514-8507, Japan

165 Joachim Labenz, Associate Professor (2)
Jung-Stilling Hospital, Wichernstr. 40, Siegen 57074, Germany

166 Giacomo Laffi, Professor (2)
University of Florence, Viale Morgagni 85, Firenze I-50134, Italy

167 Kam Chuen Lai, MD (2)
Department of Medicine, The University of Hong Kong, Queen Mary Hospital, Hong Kong, China

168 Peter Laszlo Lakatos, MD, PhD, Assistant Professor (4)
1st Department of Medicine, Semmelweis University, Koranyi S 2A, Budapest H1083, Hungary

169 Rene Lambert, Professor (8)
International Agency for Research on Cancer, 150 Cours Albert Thomas, Lyon 69372 cedex 8, France

170 Angel Lanas, Professor
Service of Gastroenterology, Hospital Clinico Universitario, Service of GastroenterologyUniversity HospitalC/ San Juan Bosco 15, Zaragoza 50009, Spain

171 Samuel S Lee, Professor
Department of Medicine, University of Calgary, Health Science Centre, Rm 1721, 3330 Hospital Dr NW, Calgary, AB, T2N 4N1, Canada

172 Jong Kyun Lee, Associate Professor (2)
Department of Gastroenterology, Sungkyunkwan University School of Medicine, Ilwom-Dong 50,Gangnam-GU, Seoul 135-710, South Korea

173 Samuel S Lee, Professor
Department of Medicine, University of Calgary, Health Science Centre, Rm 1721, 3330 Hospital Dr NW, Calgary, AB, T2N 4N1, Canada

174 Lee Shou-Dong Lee, Professor (6)
Department of Medicine, Taipei Veterans General Hospital, 201 Shih-Pai Road, Sec. 2. Taipei 112, Taiwan, China

175 Yuk Tong Lee, MD
Department of Medicine and Therapeutics, Prince of Wales Hospital, Shatin, New Territories, Hong Kong, China

176 Kurt Lenz, Professor
Department of Internal Medicine, Konventhospital Barmherzige Brueder, A-4020 Linz, Austria

177 Andreas Leodolter, Professor (10)
Department of Gastroenterology, Otto-von-Guericke University, c/o The Burnham Institute, Caner Genetics and Epigentics, 10901 N. Torrey Pines Road, La Jolla 92037, United States

178 Gene LeSage, Dr
Medicine, University of Texas Houston Medical School, 6431 Fannin Street, MSB 4.234, Houston, TX 77030, United States

179 Ming Li, Associate Professor
Tulane University Health Sciences Center, 1430 Tulane Ave Sl-83, New Orleans 70112, United States

180 Geng-Tao Liu, Professor
Department of Pharmacology, Institute of Materia Medica, Chinese Academy of Medical Sciences and Peking Union Medical College, Beijing 100050, China

181 Hong-Xiang Liu, PhD (2)
Department of Pathology, Division of Molecular Histopathology, University of Cambridge, Box 231, Level 3, Lab Block, Addenbrooke's Hospital, Hills Road, Cambridge CB2 2QQ, United Kingdom

182 Zhi-Hua Liu, Professor (2)
Cancer Institute, Chinese Academy of Medical Sciences, 17 Panjiayuan Nanli, Beijing 100021, China

183 Walter Edwin Longo, Professor
Department of Surgery, Yale University School of Medicine, 205 Cedar Street, New Haven 06510, United States

184 María Isabel Torres López, Professor (2)
Experimental Biology, University of Jaen, araje de las Lagunillas s/n, Jaén 23071, Spain

185 Robin G Lorenz, Associate Professor (6)
Department of Pathology, University of Alabama at Birmingham, 845 19th Street South BBRB 730, Birmingham, AL 35294-2170, United States

Minato-ku, Tokyo 105-8461, Japan

219 Hisato Nakajima, MD
Department of Gastroenterology and Hepatology, The Jikei University School of Medicine, 3-25-8, Nishi-Shinbashi, Minato-ku, Tokyo 105-8461, Japan

220 Hiroki Nakamura, MD (2)
Department of Gastroenterology and Hepatology, 1-1-1, Minami Kogushi, Ube, Yamaguchi 755-8505, Japan

221 Shotaro Nakamura, MD (6)
Department of Medicine and Clinical Science, Kyushu University, Maidashi 3-1-1, Higashi-ku, Fukuoka 812-8582, Japan

222 Nikolai V Naoumov, Professor
Department of Medicine, Institute of Hepatology University College London, 69-75 Chenies Mews, London WC1E 6HX, United Kingdom

223 John P Neoptolemos, Professor (2)
Divison of Surgery and Oncology, University of Liverpool, Royal Liverpool University Hospital, Daulby Street, Liverpool, L69 3GA, United Kingdom

224 James Neuberger, Professor (9)
Liver Unit, Queen Elizabeth Hospital, Birmingham B15 2TH, United Kingdom

225 Yaron Niv, Professor (3)
Department of Gastroenterology, Rabin Medical Center, Beilinson Campus, Tel Aviv University, 2 Hadekel St., Pardesia 42815, Israel

226 Masayuki Ohta, MD (7)
Department of Surgery I, Oita University Faculty of Medicine, 1-1 Idaigaoka, Hasama-machi, Oita 879-5593, Japan

227 Tetsuo Ohta, MD (2)
Department of Gastroenterologic Surgery, Kanazawa University Hospital, Takara-machi 13-1, Kanazawa 920-0934, Japan

228 Katsuhisa Omagari, MD (3)
Second Department of Internal Medicine, Nagasaki University School of Medicine, 1-7-1 Sakamoto, Nagasaki-city 852-8501, Japan

229 Giovanni D De Palma, Professor
Department of Surgery and Advanced Technologies, University of Naples Federico II, School of Medicine, Naples 80131, Italy

230 Bo-Rong Pan, Professor (2)
Departmant of Oncology, Xijing Hospital, Fourth Military Medical University, No.1, F. 8, Bldg 10, 97 Changying East Road, Xi'an 710032, Shaanxi Province, China

231 Julian Panes, Professor (2)
Department of Gastroenterology, Hospital Clinic of Barcelona, Villarroel 170, Barcelona 08036, Spain

232 Fabrizio R Parente, MD (2)
Department of Gastroenterology, L.Sacco University Hospital Via GB Grassi, 74, Milan 20157, Italy

233 Jae-Gahb Park, Professor (4)
Seoul National University College of Medicine, 28 Yongon-dong, Chongno-gu, Seoul 110-744, South Korea

234 Zhiheng Pei, Assistant Professor (3)
Department of Pathology and Medicine, New York University School of Medicine, Department of Veterans Affairs, New York Harbor Healthcare System, 6001W, 423 East 23rd street, New York NY 10010, United States

235 Amado Salvador Peña, Professor (2)
Department of Pathology, Immunogenetics, VU University Medical Centre, De Boelelaan 1117, PO Box 7057, Amsterdam 1007 MB, The Netherlands

236 Miguel Perez-Mateo, Professor (4)
Liver Unit, Hospital General Universitario Alicante, Pintor Baeza s/n, Alicante 03004, Spain

237 Raffaele Pezzilli, MD (6)
Department of Internal Medicine and Gastroenterology, Sant' Orsola-Malpighi Hospital, Via Massarenti, 9, Bologna 40138, Italy

238 Josep M Pique, MD
Department of Gastroenterology, Hospital Clínic of Barcelona, Villarroel, 170, Barcelona 08036, Spain

239 Gabriele Bianchi Porro, Professor
Gastroenterology Unit, "L. Sacco" University Hospital, Via G.B. Grassi 74, Milano 20157, Italy

240 Piero Portincasa, Professor
Internal Medicine – DIMIMP, University of Bari Medical School, Hospital Policlinico Piazza G. Cesare 11, Bari 70124, Italy

241 Jesus Prieto, Professor (5)
Clinica Universitaria, University of Navarra, Avda, Pio XII, 36, Pamplona 31080, Spain

242 Lun-Xiu Qin, Professor (3)
Liver Cancer Institute and Zhongshan Hospital, Fudan University, 180 Feng Lin Road, Shanghai 200032, China

243 Eamonn M Quigley, Professor (2)
Department of Medicine National University of Ireland, Cork, Cork University Hospital Clinical Sciences Building Wilton, Cork, Ireland

244 Massimo Raimondo, Dr
Division of Gastroenterology and Hepatology, Mayo Clinic, 4500 San Pablo Road, Jacksonville, FL 32224, United States

245 Bernardino Rampone, Dr
Department of General Surgery and Surgical Oncology, University of Siena, viale Bracci, Siena 53100, Italy

246 David S Rampton, Professor
Centre for Gastroenterology, Institute of Cell and Molecular Science, Queen Mary School of Medicine and Dentistry, London E1 2AD, United Kingdom

247 Vasiliy Ivanovich Reshetnyak, Professor (3)
Institute of General Reanimatology, 25-2, Petrovka Str., Moscow 107031, Russian

248 Sabino Riestra, Servicio Aparato Digestivo
Hospital Universitario Central de Asturias, Hermanos Felgueroso 4-3?b., Pola De Siero 33510, Spain

249 Enrico Roda, Professor
Director of Digestive Disease, Metabolism and Infectious Diseases, University of Bologna, Policlinico S.Orsola-Malpighi, Via Massarenti 9, 40138 Bologna, Italy

250 Luis Rodrigo, Professor (4)
Gastroenterology Service, Hospital Central de Asturias, c/ Celestino Villamil, s.n., Oviedo 33.006, Spain

Surgery, Graduate School of Medicine University of Tokyo, Tokyo, Japan

286 Hidekazu Suzuki, Assistant Professor (2)
Department of Internal Medicine, Keio University School of Medicine, 35 Shinanomachi, Shinjuku-ku, Tokyo 160-8582, Japan

287 Yvette Taché, PhD
Digestive Diseases Research Center and Center for Neurovisceral Sciences and Women's Health, Division of Digestive Diseases, Department of Medicine, David Geffen School of Medicine at UCLA, University of California, Los Angeles and VA Greater Los Angeles Healthcare System; 11301 Wilshire Boulevard, CURE Building 115, Room 117, Los Angeles, CA, 90073, United States

288 Seyed Alireza Taghavi, Associate Professor
Department of Internal Medicine, Nemazee Hospital, No.23, 59th Alley, Ghasrodasht St., Shiraz 71838-95453, Iran

289 Tadatoshi Takayama, Professor (2)
Department of Digestive Surgery, Nihon University School of Medicine, 30-1 Oyaguchikami-machi, Itabashi-ku, Tokyo 173-8610, Japan

290 Tadashi Takeda, MD (3)
Department of Hepatology, Osaka City University, 1-4-3 Asahimachi, Abeno-ku, Osaka 545-8585, Japan

291 Nicholas J Talley, MD, PhD, Professor of Medicine
Division of Gastroenterology and Hepatology, Mayo Clinic College of Medicine, 200 First Street S.W., PL-6-56, Rochester, MN 55905, United States

292 Kiichi Tamada, MD (4)
Department of Gastroenterology, Jichi Medical Shool, 3311-1 Yakushiji,Minamikawachi,Kawachigun, Tochigi 329-0498, Japan

293 Tanaka Noriaki Tanaka, Professor (3)
Department of Gastroenterological Surgery, Transplant and Surgical Oncology, Okayama University Graduate School of Medicine and Dentistry, 2-5-1, Shikata-cho, Okayama 700-8558, Japan

294 Shinji Tanaka, Director (5)
Department of Endoscopy, Hiroshima University Hospital, 1-2-3 Kasumi, Minami-ku, Hiroshima 734-8551, Japan

295 Wei Tang, MD, EngD, Assistant Professor (5)
H-B-P Surgery Division, Artificial Organ and Transplantation Division, Department of surgery, Graduate School of Medicine, The University of Tokyo, Tokyo 113-8655, Japan

296 Kyuichi Tanikawa, Professor
International Institute for Liver Research, 1-1 Hyakunen Kouen, Kurume 839-0864, Japan

297 Simon D Taylor-Robinson, MD
Department of Medicine A, Imperial College London, Hammersmith Hospital, Du Cane Road, London W12 0HS, United Kingdom

298 Simon D Taylor-Robinson, MD (4)
Department of Medicine A, Imperial College London, Hammersmith Hospital, Du Cane Road, London W12 0HS, United Kingdom

299 Akira Terano, Professor
Dokkyo University School of Medicine, Mibu, Shimotsugagun Tochigi 321-0293, Japan

300 Roberto Testa, Professor
Department of Internal Medicine, University of Genoa, Viale Benedetto XV 6, Genoa 16132, Italy

301 Paul Joseph Thuluvath, Professor
Department of Gastroenterology and Hepatology, The Johns Hopkins Hospital, 1830 E. Monument St, Baltimore MD 21205, United States

302 Swan Nio Thung, Professor
Department of Pathology, Mount Sinai School of Medicine, One Gustave L. Levy Place, New York 10029, United States

303 Hans Ludger Tillmann, Professor (4)
Medizinische Klinik und Poliklinik II, University Leipzig, Philipp Rosenthal, Str. 27, Leipzig 04103, Germany

304 Michael Trauner, Professor
Medical University Graz, Auenbruggerplatz 15, Graz A-8036, Austria

305 Chung-Jyi Tsai, MD
Division of Digestive Diseases and Nutrition, University of Kentucky Medical Center, 800 Rose Street, Lexington 40536-0298, Kentucky, United States

306 Akihito Tsubota, Assistant Professor (5)
Institute of Clinical Medicine and Research , Jikei University School of Medicine, 163-1 Kashiwa-shita, Kashiwa, Chiba 277-8567, Japan

307 Tung-Yu Tsui, Dr
Department of Surgery, University of Regensburg Medical Centre, Franz-Josef-Strauss-Allee 11, 93053 Regensburg, Germany

308 Shingo Tsuji, Professor
Department of Internal Medicine and Therapeutics, Osaka University Graduate School of Medicine(A8), 2-2 Yamadaoka, Suita, Osaka 565-0871, Japan

309 Ueno Takato Ueno, Professor (3)
Research Center for Innovative Cancer Therapy, Kurume University, 67 Asahi-machi, Kurume 830-0011, Japan

310 Yvan Vandenplas, Professor (5)
Department of Pediatrics, AZ-VUB, Laarbeeklaan 101, Brussels 1090, Belgium

311 Hugo E Vargas, Associate Professor of Medicine
Division of Transplantation Medicine, Mayo Clinic, 5777 E. Mayo Blvd, 5E, Scottsdale AZ 85054, United States

312 Patrick Veit, MD
Department of Diagnostic an Interventional Radiology and Neuroradiology University Hospital Essen Hufelandstrasse 55 45121 Essen, Germany

313 Saúl Villa-Trevi?o, MD, PhD
Departamento de Biología Celular, Centro de Investigación y de Estudios Avanzados del IPN (Cinvestav), Ave. IPN No. 2508. Col. San Pedro, Zacatenco, C.P. 07360, México, DF, Mexico

314 Shinichi Wada, MD (6)
Department of Gastroenterology, Jichi Medical School, Minamikawachimachi,Kwachi-gun, Tochigi-ken, Tochigi 329-0498, Japan

315 Siegfried Wagner, Professor (3)
Medizinische Klinik II, Klinikum Deggendorf, Perlasberger Str. 41, Deggendorf 94469, Germany

PO Box 2345, Beijing 100023, China
www.wjgnet.com
wjg@wjgnet.com

ELSEVIER

World J Gastroenterol 2005;11(48):7715
World Journal of Gastroenterology ISSN 1007-9327

Meetings

MAJOR MEETINGS COMING UP

American College of Gastroenterology Annual Scientific Meeting
October 28 -November 2, 2005
annualmeeting@acg.gi.org
www.acg.gi.org

EVENTS AND MEETINGS IN THE UPCOMING 6 MONTHS

ISGCON2005
November 11-15, 2005
isgcon2005@yahoo.co.in
isgcon2005.com

II Latvian Gastroenterology Congress
November 29, 2005
gec@stradini.lv
www.gastroenterologs.lv

70th ACG Annual Scientific Meeting and Postgraduate Course
October 28-November 2, 2005

Advanced Capsule Endoscopy Users Course
November 18-19, 2005
www.asge.org/education

2005 CCFA National Research and Clinical Conference - 4th Annual Advances in the Inflammatory Bowel Diseases
December 1-3, 2005
c.chase@imedex.com
www.imedex.com/calendars/therapeutic.htm

EVENTS AND MEETINGS IN 2005

XIII Argentine Hepatology Congress
XIII Congreso Argentino de HepatologÃa
June 10-13, 2005
mci@mcimeetings.com
www.hepatologia.org

9th Annual Coolum Update in Gastroenterology & Hepatology
June 11-13, 2005
info@e-Kiddna.com.au

Canadian Digestive Disease Week Conference
February 26-March 6, 2005
www.cag-acg.org

2005 World Congress of Gastroenterology
September 12-14, 2005
wcog2005@congrex.nl

International Colorectal Disease Symposium 2005
February 3-5, 2005
info@icds-hk.org

15th World Congress of the International Association of Surgeons and Gastroenterologists
September 7-10, 2005
iasg2005@guarant.cz
www.iasg2005.cz

7th International Workshop on Therapeutic Endoscopy
September 10-12, 2005
alfa@alfamedical.com
www.alfamedical.com

EASL 2005 the 40th annual meeting
April 13-17, 2005
www.easl.ch/easl2005/

ISGCON2005
November 11-15, 2005
isgcon2005@yahoo.co.in
isgcon2005.com

Pediatric Gastroenterology, Hepatology and Nutrition
March 13, 2005

II Latvian Gastroenterology Congress
November 29, 2005
gec@stradini.lv
www.gastroenterologs.lv

21st annual international congress of Pakistan society of Gastroenterology & GI Endoscopy
March 25-27, 2005
psgc05@hotmail.com
www.psgc2005.com

8th Congress of the Asian Society of HepatoBiliary Pancreatic Surgery
February 10-13, 2005

1º Workshop de Gastrenterologia para Clínica Geral
April 29, 2005
luis.m.lopes@sapo.pt

APDW 2005 - Asia Pacific Digestive Week 2005
September 25-28, 2005
asiapdw@kornet.net
www.apdw2005.org

World Congress on Gastrointestinal Cancer
June 15-18, 2005
meetings@imedex.com

British Society of Gastroenterology Conference
March 14-17, 2005
www.bsg.org.uk

Training Director's Workshop:Developing and Teaching Principles in the New Era of GI Training
February 4-6, 2005
www.asge.org/education

The Pharmacological, Surgical and Endoscopic Management of GERD
April 8-9, 2005
www.asge.org/education

Digestive Disease Week
DDW 106th Annual Meeting
May 15-18, 2005
ddwadmin@gastr.org
www.ddw.org

ASGE Advanced Endscopy Skills Hands-on Sessions
May 15, 2005
www.asge.org/education

ASGE GERD Hands-on Session
May 17, 2005
www.asge.org/education

Annual Postgraduate Course
May 18-19, 2005
www.asge.org/education

Advanced Capsule Endoscopy Users Course
June 4-5, 2005
www.asge.org/education

Advanced Capsule Endoscopy Users Course
August 12-13, 2005
www.asge.org/education

GI Practice Management Symposium: Solutions for a Successful Practice
August 18, 2005
www.asge.org/education

70th ACG Annual Scientific Meeting and Postgraduate Course
October 28-November 2, 2005

Advanced Capsule Endoscopy Users Course
November 18-19, 2005
www.asge.org/education

2005 CCFA National Research and Clinical Conference - 4th Annual Advances in the Inflammatory Bowel Diseases
December 1-3, 2005
c.chase@imedex.com
www.imedex.com/calendars/therapeutic.htm

EVENTS AND MEETINGS IN 2006

10th World Congress of the International Society for Diseases of the Esophagus
February 22-25, 2006
isde@sapmea.asn.au
www.isde.net

Easl 2006 - The 41st Annual Meeting
April 26-30, 2006

Canadian Digestive Disease Week Conference
March 4-12, 2006
www.cag-acg.org

XXX pan-american congress of digestive diseases
XXX congreso panamericano de anfermedades digestivas
November 25-December 1, 2006
amg@gastro.org.mx
www.gastro.org.mx

World Congress on Gastrointestinal Cancer
June 14-17, 2006
c.chase@imedex.com

7th World Congress of the International Hepato-Pancreato-Biliary Association
September 3-7, 2006
convention@edinburgh.org
www.edinburgh.org/conference

Annual Postgraduate Course
May 25-26, 2006
www.asge.org/education

71st ACG Annual Scientific Meeting and Postgraduate Course
October 20-25, 2006

PO Box 2345, Beijing 100023, China
www.wjgnet.com
wjg@wjgnet.com

ELSEVIER

World J Gastroenterol 2005;11(48):7716-7717
World Journal of Gastroenterology ISSN 1007-9327

Instructions to authors

GENERAL INFORMATION

World Journal of Gastroenterology (*WJG,* ISSN 1007-9327 CN 14-1219/R) is a weekly journal of more than 48 000 circulation, published on the 7th, 14th, 21st and 28th of every month.

Original Research, Clinical Trials, Reviews, Comments, and Case Reports in esophageal cancer, gastric cancer, colon cancer, liver cancer, viral liver diseases, *etc*., from all over the world are welcome on the condition that they have not been published previously and have not been submitted simultaneously elsewhere.

Published jointly by
The WJG Press and Elsevier Inc.

SUBMISSION OF MANUSCRIPTS

Manuscripts should be typed double-spaced on A4 (297×210 mm) white paper with outer margins of 2.5 cm. Number all pages consecutively, and start each of the following sections on a new page: Title Page , Abstract, Introduction, Materials and Methods, Results, Discussion, Acknowledgements, References, Tables, Figures and Figure Legends. Neither the Editors nor the Publisher is responsible for the opinions expressed by contributors. Manuscripts formally accepted for publication become the permanent property of The WJG Press and Elsevier Inc., and may not be reproduced by any means, in whole or in part without the written permission of both the Authors and the Publisher. We reserve the right to put onto our website and copy-edit accepted manuscripts. Authors should also follow the guidelines for the care and use of laboratory animals of their institution or national animal welfare committee.

Authors should retain one copy of the text, tables, photographs and illustrations, as rejected manuscripts will not be returned to the author(s) and the editors will not be responsible for the loss or damage to photographs and illustrations.

Online submission
Online submission is strongly advised. Manuscripts should be submitted through the Online Submission System at: http://www.wjgnet.com/index.jsp. Authors are highly recommended to consult the ONLINE INSTRUCTIONS TO AUTHORS (http://www.wjgnet.com/wjg/help/instructions.jsp) before attempting to submit online. Authors encountering problems with the Online Submission System may send an email describing the problem to wjg@wjgnet.com for assistance. If you submit manuscript online, do not make a postal contribution. A repeated online submission for the same manuscript is strictly prohibited.

Postal submission
Send 3 duplicate hard copies of the full-text manuscript typed double-spaced on A4(297×210 mm) white paper together with any original photographs or illustrations and a 3.5 inch computer diskette or CD-ROM containing an electronic copy of the manuscript including all the figures, graphs and tables in native Microsoft Word format or *.rtf format to:

World Journal of Gastroenterology
Apartment 1066 Yishou Garden,
58 North Langxinzhuang Road,
PO Box 2345, Beijing 100023, China
E-mail: wjg@wjgnet.com
http: //www.wjgnet.com

MANUSCRIPT PREPARATION

All contributions should be written in English. All articles must be submitted using a word-processing software. All submissions must be typed in 1.5 line spacing and in word size 12 with ample margins. The letter font is Tahoma. For authors originating from China, one copy of the Chinese translation of the manuscript is also required (excluding references). Style should conform to our house format. Required information for each of the manuscript sections is as follows:

Title page
Full manuscript title, running title, all author(s) name(s), affiliations, institution(s) and/or department(s) where the work was accomplished, disclosure of any financial support for the research, and the name, full address, telephone and fax numbers and email address of the corresponding author should be involved. Titles should be concise and informative (removing all unnecessary words), emphasize what is NEW, and avoid abbreviations. A short running title of less than 40 letters should be provided. List the author(s)' name(s) as follows: initials and/or first name, middle name or initial(s) and full family name.

Abstract
An informative, structured abstract of no more than 250 words should accompany each manuscript. Abstracts for original contributions should be structured into the following sections: AIM: Only the purpose should be included. METHODS: The materials, techniques, instruments and equipments, and the experimental procedures should be included. RESULTS: The observatory and experimental results, including data, effects, outcome, *etc*. should be included. Authors should present *P* value where necessary, and the significant data should accompany. CONCLUSION: Accurate view and the value of the results should be included.

The format of structured abstracts is at: http://www.wjgnet.com/wjg/help/11.doc

Key words
Please list 3-10 key words that could reflect content of the study.

Text
For most article types, the main text should be structured into the following sections: INTRODUCTION, MATERIALS AND METHODS, RESULTS and DISCUSSION, and should include appropriate Figures and Tables. Data should be presented in the body text or Figures and Tables, not both.

Illustrations
Figures should be numbered as 1, 2, 3 and so on, and mentioned clearly in the main text. Provide a brief title for each figure on a separate page. No detailed legend should be involved under the figures. This part should add into the text where the figures are applicable. Digital images: black and white photographs should be scanned and saved in TIFF format at a resolution of 300 dpi; color images should be saved as CMYK (print files) and not RGB (screen-viewing files). Place each photograph in a separate file. Print images: supply images of size no smaller than 126× 76 mm printed on smooth surface paper; label the image by writing the Figure number and orientation using an arrow. Photomicrographs: indicate the original magnification and stain in the legend. Digital Drawings: supply files in EPS if created by Freehand and Illustrator, or TIFF from Photoshop. EPS files must be accompanied by a version in native file format for editing purposes. Scans of existing line drawings should be scanned at a resolution of 1200 dpi and as close as possible to the size at which they will appear when printed, not smaller. Please use uniform legends for the same subjects. For example: Figure 1 Pathological changes of atrophic gastritis after treatment. A: ...; B: ...;C: ...; D: ...; E: ...; F: ...; G: ...

Tables
Three-line tables should be numbered as 1, 2, 3 and so on, and mentioned clearly in the main text. Provide a brief title for each table. No detailed legend should be involved under the tables. This part should add into the text where the tables are applicable. The information should complement but not duplicate that contained in the text. Use one horizontal line under the title, a second under the column heads, and a third below the Table, above any footnotes. Vertical and italic lines should be omitted.

Notes in tables and illustrations
Data which is not statistically significant should not be noted. $^{a}P<0.05$, $^{b}P<0.01$ ($P>0.05$ should not be noted). If there are other series of *P* values, $^{c}P<0.05$ and $^{d}P<0.01$ are used; Third series of *P* values can be expressed as $^{e}P<0.05$ and $^{f}P<0.01$. Other notes in tables or under illustrations should be expressed as ^{1}F, ^{2}F, ^{3}F; or some other symbols with a superscript (Arabic

numerals) in the upper left corner. In a multi-curve illustration, each curve should be labeled with ●, ○, ■, □, ▲, △, *etc*. in a certain sequence.

Acknowledgments

Brief acknowledgments of persons who have made genuine contributions to the manuscripts and who endorse the data and conclusions are included. Authors are responsible for obtaining written permission to use any copyrighted text and/or illustrations.

References

Cited references should mainly be drawn from journals covered in the Science Citation Index (http://www.isinet.com) and/or Index Medicus (http://www.ncbi.nlm.nih.gov/PubMed) databases. Mention all references in the text, tables and figure legends, and set off by consecutive, superscripted Arabic numerals. References should be numbered consecutively in the order in which they appear in the text. Abbreviate journal title names according to the Index Medicus style (http://www.ncbi.nlm.nih.gov/entrez/query.fcgi?db=journals). Unpublished observations and personal communications are not listed as references. The style and punctuation of the references conform to ISO standard and the Vancouver style (5th edition); see examples below. Reference lists not conforming to this style could lead to delayed or even rejected publication status. Examples:

Standard jounal article (list all authors and include the PubMed ID [PMID] where applicable)

1 **Das KM,** Farag SA. Current medical therapy of inflammatory bowel disease. *World J Gastroenterol* 2000; 6: 483-489 [PMID: 11819634]

2 **Pan BR**, Hodgson HJF, Kalsi J. Hyperglobulinemia in chronic liver disease: Relationships between *in vitro* immunoglobulin synthesis, short lived suppressor cell activity and serum immunoglobulin levels. *Clin Exp Immunol* 1984; 55: 546-551 [PMID: 6231144]

3 **Lin GZ,** Wang XZ, Wang P, Lin J, Yang FD. Immunologic effect of Jianpi Yishen decoction in treatment of Pixu-diarrhoea. *Shijie Huaren Xiaohua Zazhi* 1999; 7: 285-287 [CMFAID:1082371101835979]

Books and other monographs (list all authors)

4 **Sherlock S,** Dooley J. Diseases of the liver and billiary system. 9th ed. Oxford: Blackwell Sci Pub, 1993: 258-296

Chapter in a book (list all authors)

5 **Lam SK.** Academic investigator's perspectives of medical treatment for peptic ulcer. In: Swabb EA, Azabo S. Ulcer disease: investigation and basis for therapy. New York: Marcel Dekker, 1991: 431-450

Electronic journal (list all authors)

6 **Morse SS.** Factors in the emergence of infectious diseases. Emerg Infect Dis serial online, 1995-01-03, cited 1996-06-05; 1(1):24 screens. Available from: URL: http//www.cdc.gov/ncidod/EID/eid.htm

PMID requirement

From the full reference list, please submit a separate list of those references embodied in PubMed, keeping the same order as in the full reference list, with the following information only: (1) abbreviated journal name and citation (e.g. *World J Gastroenterol* 2003;9(11):2400-2403; (2) article title (e.g. Epidemiology of gastroenterologic cancer in Henan Province, China; (3) full author list (e.g. Lu JB, Sun XB, Dai DX, Zhu SK, Chang QL, Liu SZ, Duan WJ; (4) PMID (e.g. 14606064). Provide the full abstracts of these references, as quoted from PubMed on a 3.5 inch disk or CD-ROM in Microsoft Word format and send by post to The *WJG* Press. For those references taken from journals not indexed by *Index Medicus*, a printed copy of the first page of the full reference should be submitted. Attach these references to the end of the manuscript in their order of appearance in the text.

Inappropriate references

Authors should always cite references that are relevant to their article, and avoid any inappropriate references. Inappropriate references include those that are linked with a hyphen and the difference between the two numbers at two sides of the hyphen is more than 5. For example, [1-6], [2-14] and [1, 3, 4-10, 22] are all considered as inappropriate references. Authors should not cite their own unrelated published articles.

Statistical data

Present as mean±SD and mean±SE.

Statistical expression

Express *t* test as *t*(in italics), *F* test as *F*(in italics), chi square test as χ^2(in Greek), related coefficient as *r*(in italics), degree of freedom as γ (in Greek), sample number as *n*(in italics), and probability as *P*(in italics).

Units

Use SI units. For example: body mass, m(B) = 78 kg; blood pressure, p(B)=16.2/12.3 kPa; incubation time, t(incubation)=96 h, blood glucose concentration, c(glucose) 6.4±2.1 mmol/L; blood CEA mass concentration, p(CEA) = 8.6 24.5 μg/L; CO_2 volume fraction, 50 mL/L CO_2 not 5% CO_2; likewise for 40 g/L formaldehyde, not 10% formalin; and mass fraction, 8 ng/g, *etc*. Arabic numerals such as 23,243,641 should be read 23 243 641.

The format about how to accurately write common units and quantum is at: http://www.wjgnet.com/wjg/help/15.doc

Abbreviations

Standard abbreviations should be defined in the abstract and on first mention in the text. In general, terms should not be abbreviated unless they are used repeatedly and the abbreviation is helpful to the reader. Permissible abbreviations are listed in Units, Symbols and Abbreviations: A Guide for Biological and Medical Editors and Authors (Ed. Baron DN, 1988) published by The Royal Society of Medicine, London. Certain commonly used abbreviations, such as DNA, RNA, HIV, LD50, PCR, HBV, ECG, WBC, RBC, CT, ESR, CSF, IgG, ELISA, PBS, ATP, EDTA, mAb, can be used directly without further mention.

Italicization

Quantities: *t* time or temperature, *c* concentration, *A* area, *l* length, *m* mass, *V* volume.

Genotypes: *gyr*A, *arg* 1, *c myc*, *c fos*, *etc*.

Restriction enzymes: *Eco*RI, *Hin*dI, *Bam*HI, *Kbo* I, *Kpn* I, *etc*.

Biology: *Helicobacter pylori, H pylori, E coli, etc*.

SUBMISSION OF THE REVISED MANUSCRIPTS AFTER ACCEPTED

Please revise your article according to the revision policies of *WJG*. The revised version including manuscript and high-resolution image figures (if any) should be copied on a floppy or compact disk. Author should send the revised manuscript, along with printed high-resolution color or black and white photos, copyright transfer letter, the final check list for authors, and responses to reviewers by a courier (such as EMS) (submission of revised manuscript by e-mail or on the WJG Editorial Office Online System is NOT available at present).

Language evaluation

The language of a manuscript will be graded before sending for revision. (1) Grade A: priority publishing; (2) Grade B: minor language polishing; (3) Grade C: a great deal of language polishing; (4) Grade D: rejected. The revised articles should be in grade B or grade A.

Copyright assignment form

It is the policy of WJG to acquire copyright in all contributions. Papers accepted for publication become the copyright of WJG and authors will be asked to sign a transfer of copyright form. All authors must read and agree to the conditions outlined in the Copyright Assignment Form (which can be downloaded from http://www.wjgnet.com/wjg/help/9.doc).

Final check list for authors

The format is at: http://www.wjgnet.com/wjg/help/13.doc

Responses to reviewers

Please revise your article according to the comments/suggestions of reviewers. The format for responses to the reviewers' comments is at: http://www.wjgnet.com/wjg/help/10.doc

Proof of financial support

For paper supported by a foundation, authors should provide a copy of the document and serial number of the foundation.

Publication fee

Authors of accepted articles must pay publication fee.

PO Box 2345, Beijing 100023, China
www.wjgnet.com
wjg@wjgnet.com

ELSEVIER

World J Gastroenterol 2005;11(48):7718
World Journal of Gastroenterology ISSN 1007-9327

World Journal of Gastroenterology standard of quantities and units

Number	Nonstandard	Standard	Notice
1	4 days	4 d	In figures, tables and numerical narration
2	4 days	four days	In text narration
3	day	d	After Arabic numerals
4	Four d	Four days	At the beginning of a sentence
5	2 hours	2 h	After Arabic numerals
6	2 hs	2 h	After Arabic numerals
7	hr, hrs,	h	After Arabic numerals
8	10 seconds	10 s	After Arabic numerals
9	10 year	10 years	In text narration
10	Ten yr	Ten years	At the beginning of a sentence
11	0,1,2 years	0,1,2 yr	In figures and tables
12	0,1,2 year	0,1,2 yr	In figures and tables
13	4 weeks	4 wk	
14	Four wk	Four weeks	At the beginning of a sentence
15	2 months	2 mo	In figures and tables
16	Two mo	Two months	At the beginning of a sentence
17	10 minutes	10 min	
18	Ten min	Ten minutes	At the beginning of a sentence
19	50% (*V/V*)	500 mL/L	
20	50% (m/*V*)	500 g/L	
21	1 M	1 mol/L	
22	10 μM	10 μmol/L	
23	1N HCl	1 mol/L HCl	
24	1N H_2SO_4	0.5 mol/L H_2SO_4	
25	4rd edition	4^{th} edition	
26	15 year experience	15- year experience	
27	18.5 kDa	18.5 ku,18 500u or M_r18 500	
28	25 $g.kg^{-1}/d^{-1}$	25 g/(kg·d) or 25 g/kg per day	
29	6900	6 900	
30	1000 rpm	1 000 r/min	
31	sec	s	After Arabic numerals
32	1 pg $\cdot L^{-1}$	1 pg/L	
33	10 kilograms	10 kg	
34	13 000 rpm	13 000 *g*	High speed; *g* should be in italic and suitable conversion.
35	1000 *g*	1 000 r/min	Low speed. *g* cannot be used.
36	Gene bank	GenBank	International classified genetic materials collection bank
37	Ten L	Ten liters	At the beginning of a sentence
38	Ten mL	Ten milliliters	At the beginning of a sentence
39	umol	μmol	
40	30 sec	30 s	
41	1 g/dl	10 g/L	10-fold conversion
42	OD_{260}	A_{260}	"OD" has been abandoned.
43	One g/L	One microgram per liter	At the beginning of a sentence
44	*A*260 nm	A_{260} nm	*A* should be in italic.
	$^bP<0.05$	$^aP<0.05$	In Table, no note is needed if there is no significance in statistics: $^aP<0.05$, $^bP<0.01$ (no note if $P>0.05$). If there is a second set of *P* value in the same table, $^cP<0.05$ and $^dP<0.01$ are used for a third set: $^eP<0.05$, $^fP<0.01$.
45	**F*=9.87, $^§F$=25.9, $^{\#}F$=67.4	^1F=9.87,^2F=25.9, ^3F=67.4	Notices in or under a table
46	KM	km	kilometer
47	CM	cm	centimeter
48	MM	mm	millimeter
49	Kg, KG	kg	kilogram
50	Gm, gr	g	gram
51	nt	N	newton
52	l	L	liter
53	db	dB	decibel
54	rpm	r/min	rotation per minute
55	bq	Bq	becquerel, a unit symbol
56	amp	A	ampere
57	coul	C	coulomb
58	HZ	Hz	
59	w	W	watt
60	KPa	kPa	kilo-pascal
61	p	Pa	pascal
62	ev	EV	volt (electronic unit)
63	Jonle	J	joule
64	J/mmol	kJ/mol	kilojoule per mole
65	10×10×10cm^3	10 cm×10 cm×10 cm	
66	N·km	KN·m	moment
67	$\bar{x}\pm s$	mean±SD	In figures, tables or text narration
68	– Mean±SEM	mean±SE	In figures, tables or text narration
69	*im*	im	intramuscular injection
70	*iv*	iv	intravenous injection
71	Wang et al	Wang *et al.*	
72	EcoRI	*Eco*RI	*Eco* in italic and RI in positive. Restriction endonuclease has its prescript form of writing.
73	Ecoli	*E.coli*	Bacteria and other biologic terms have their specific expression.
74	Hp	*H pylori*	
75	Iga	*Iga*	writing form of genes
76	*igA*	IgA	writing form of proteins
77	-70 kDa	~70 ku	